Ollscoil na hÉireann, Corcaigh

National University of Ireland, Cork



Modelling the ecology, dynamics and assessment of *Nephrops norvegicus (Linnaeus, 1758)* in the waters around Ireland

Thesis presented by

Hocine Amine Benchikh

108222871

for the degree of

Doctor of Philosophy

University College Cork

School of Biological, Earth and Environmental Sciences

23rd of June 2022

External Examiner: Dr Spyros Fifas (Ifremer)

Internal Examiner: Dr Tom Doyle

Supervisors: Prof. Emer Rogan

Dr Colm Lordan

Prof. Edward A. Codling

Head of School/Department: Prof. Astrid Wingler

General Contents

General Introduction.....1

Introduction.....3

Objectives of the study.....22

Chapter 1 Time series analysis of *Nephrops norvegicus* landings off the coast of Ireland.....28

Abstract.....31

Introduction.....32

Aims of this Chapter.....35

Materials and Methods.....37

Results.....48

Discussion.....94

Conclusion.....103

Chapter 2 Spatial Analysis of the Aran grounds stock of *Nephrops norvegicus*….104

Abstract.....106

Introduction.....107

Aims of this chapter.....109

Materials and Methods.....111

Results.....121

Discussion.....171

Conclusion.....177

Chapter 3 Evaluation of the Aran grounds *Nephrops norvegicus* stock status.....178

Abstract.....180

Introduction.....181

Aims of this chapter.....185

Methods and Materials.....187

Results.....195

Discussion.....233

Conclusion.....245

General Discussion.....246

Introduction.....248

(A) Resilience of the Aran grounds population.....249

(B) Towards an ecosystem approach of fisheries management.....253

(C) The spatial dimensions of *Nephrops*.....256

(D) Climate strands: recruitment in jeopardy?.....259

(E) Fishery induced selection.....264
Conclusion.....269
Annexes A.....273
Annexes B.....294
Annexes C.....313
References.....330

Declaration

This is to certify that the work I am submitting is my own and has not been submitted for another degree, either at University College Cork or elsewhere. All external references and sources are clearly acknowledged and identified within the contents. I have read and understood the regulations of University College Cork concerning plagiarism and intellectual property.

Hocine Amine BENCHIKH

To my daughter EMI

"Si me caí es porque estaba caminando,
y caminar vale la pena aunque te caigas"
Eduardo Galeano

"Un arbre secoué par le rire lâche ses fruits et ses oiseaux"
Jean Cocteau

no god no master

Funding Information

This work was carried out under the Sea Change strategy scheme with the support of Marine Institute (Grant Aid Agreement No. PHD/FS/07/005) and the Marine Research Sub-programme of the National Development Plan 2007–2013, Ireland.

Acknowledgements

I am grateful to my supervisors, Prof. Emer Rogan, Prof. Edward Codling and Dr Colm Lordan for all their help and advice with this PhD.
I would like to thank the Marine Institute and the Marine Research Sub-programme of the National Development Plan 2007–2013 for the funding opportunity to undertake this thesis at the Department of Biological Earth & Environmental Sciences, University College Cork. In many aspects, a place where I truly learned and progressed.

I would like to extend my sincere thanks to all unknown, nevertheless real, men and women in their respective positions in those administrations that addressed awkward situations I faced (fees, visa...etc). Without your quality, many of us would be crushed by the rules.

When I came to Ireland I found people angry about an acute economic crisis resulting from the gross mismanagement of a corrupt political and economic ruling class*. And, during this dark and difficult period for many of them, I met men and women with an incredible joie de vivre and just as much heart. A lesson in living!
My gratitude to you Ireland! Strolling through your streets and paths is a joy!

* James Connolly (1868-1919): "Ireland, as distinct from her people, is nothing to me; and the man who is bubbling over with love and enthusiasm for "Ireland", and can yet pass unmoved through our streets and witness all the wrong and the suffering, shame and degradation wrought upon the people of Ireland-yea, wrought by Irishmen upon Irish men and women, without burning to end it, is, in my opinion, a fraud and a liar in his heart, no matter how he loves that combination of chemical elements he is pleased to call Ireland."

General abstract

Nephrops norvegicus is a valuable market species in the North-East Atlantic and it is of economic importance to Ireland. The present study investigated the status of the Aran ground stock, frequently ranked within the top two commercially valuable "fish" landed. Since 2002, under water TV surveys have been developed to provide a fishery independent estimate of burrow abundance in areas that exhibited a steady decrease in *Nephrops* over two decades contrasting with the increasing landings. In order to identify stock status and provide reliable information to management, we used a number of different approaches in the fields of time series analysis, spatial analysis and fisheries stock assessment.

We examined the temporal fluctuations in a 16 year time series of landings in Aran grounds and found fluctuating cycles within an overall decreasing trend. This stock dynamic was also compared with the other main areas of harvest off the coast of Ireland (Smalls ground, Porcupine Bank, and the west Irish Sea) disclosing a regional common trend in the pattern of the stocks for connecting areas.

Regional climatic influences (*e.g* NAO, AO and AMO) have been detected on various time scales ranging from month to years and the time series analysis method appears effective for detecting changes in fishing behaviours.

Spatial analysis of the burrow density over the stock area revealed patchy distribution varying in size and intensity over the years with a spatio-temporal trend marked by a depletion of abundance in midfield with noticeable consequences for fishing vessel activity at a regional level. This spatial approach enabled the evaluation of the influence of the mud content of the seabed on the density of burrows and to explore the potential impact of the prevailing current circulation pattern during the planktonic stage of *Nephrops* on the level of recruitment by using remote sensing data.

For an optimal fisheries management strategy, demographic information for the exploited species is necessary and for *Nephrops*, effective stock assessment is hampered because of the difficulty in age determination. A biomass model with a Schaefer surplus yield component and a data limited CMSY method were chosen to address the lack of age data and to predict biomass and related key fisheries reference points. Both approaches underline the ongoing decline of *Nephrops* abundance and reveal warning signals of unsustainable fishing exploitation.

General Introduction

Contents

General Introduction.....1
Introduction.....3
(I) *Nephrops norvegicus*.....5
(I.1) Conspicuous features.....5
(I.1.a) Superposition eyes.....5
(I.1.b) Sexual dimorphism.....6
(I.1.c) A sensory animal: sensilla.....6
(I.1.d) Burrow dwellers.....7
(I.2) "Misty blue".....9
(I.2a) Marked variations in catches.....10
(I.2.b) Seasonal peaks: exposure and withdrawal of females.....11
(I.3) Diet.....11
(I.4) Pelagic life stage.....12
(I.4.a) A critical period.....12
(I.4.b) Advection and diel movement.....12
(II) Snapshots of a profitable fishery.....13
(II.1) "Horses" for crustaceans: fleets involved during 1995-2014.....14
(II.2) Current management advice.....19
(II.2.a) Under water TV (UWTV) basis for total allowable catch (TAC).....19
(II.2.b) Structural fragilities.....21
(II.2.b.1) Ageing.....21
(II.2.b.2) Dubious data.....21
(II.2.b.3) Tracking the effort.....21
(II.2.c) ICES assessment framework.....21
Objectives of the study.....22

Introduction

Dublin Bay prawns (*Nephrops norvegicus*) is the second most valuable species (after mackerel, *Scomber scombrus*, €83M with 86,400 tonnes) with landings of 8,000 tonnes worth €55 million, more than all other whitefish species combined. *Nephrops* ranks fourth in terms of value of the exported fish species (€40M) equivalent to 4,200 tonnes with exports to the United Kingdom, Spain and Italy among the main recipients in Europe (BIM, 2017a, b).

In 2016, the total landings of *Nephrops* recorded from the 34 functional units of the European Union (EU) waters were about 58,958 tonnes, of which 15% were from Ireland (**Figure 1**; FAO FishstatJ, 2018). The EU landings rose sharply from 1950 to 1985 but since then have been very variable at around 60,000 tonnes.

In European waters, *Nephrops* is harvested from a wide geographical range in variable water depths. It is exploited from Iceland in the North to the Mediterranean and Canaries in the South, occurring at depths ranging from 20 m to 800 m and even shallower in some Scottish sea lochs. The life history characteristics of *Nephrops* also vary across its range, *e.g*. in relation to the time of spawning, duration of egg incubation, timing of larval release, duration of planktonic phase, whether eggs are spawned annually or biennially, timing of moulting and mating.

For Ireland, the main *Nephrops* populations and fishing grounds are located in the Aran grounds (FU17), Porcupine Bank (FU16), West Irish Sea (FU15), the Smalls grounds (FU22), the Labadie and Jone's Bank (FU20-21).

However, within the same stock unit, its distribution can be very heterogeneous and a stock may thus be divided into a (large) number of smaller "stocklets", with different population densities, size and sex compositions, and biological features (Tully and Hillis, 1995; Maynou and Sardà, 1997; Bell et al, 2006).

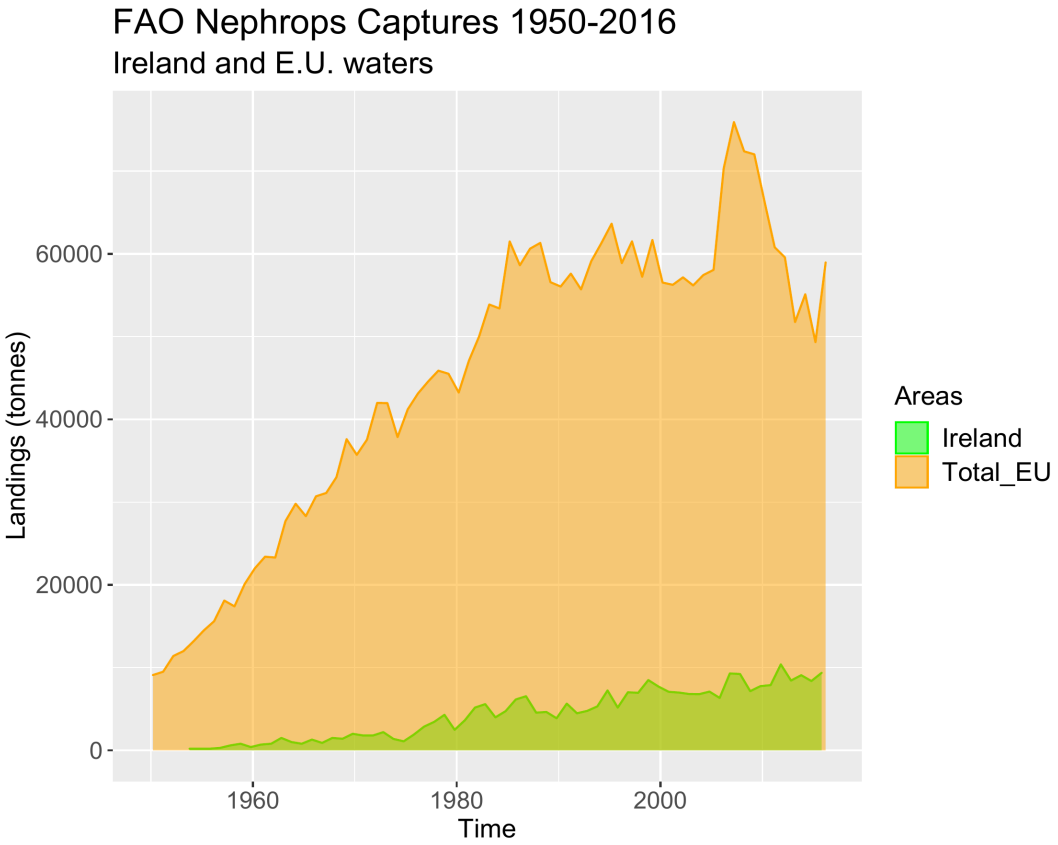


Figure 1: *Nephrops* landing trends for Ireland and the total European Union from 1950 to 2016 as reported by the Fisheries and Aquaculture Department of the Food Agriculture Organisation of the United Nations (Data source: FAO and FishstatJ, 2018).

In relation to the aforementioned economic values, it is clear that this species is of economic importance for the Republic of Ireland. It is therefore important that such a valuable fishery should be managed sustainably, particularly against a background of "overfishing, fleet overcapacity, heavy subsides, low economic resilience and decline in the volume of fish caught by European fishermen where "the current Common Fisheries Policy has not worked well enough to prevent those problems" as formally asserted by the European commission (EC, 2009).

Thus, the present introduction, is an attempt to gather the available knowledge of the species concerning many life history traits, population dynamics, exploitation and management that are deemed relevant to contextualise the following investigations into the status of one of the most yielding *Nephrops norvegicus* stock of this island, namely the Aran grounds.

(I) *Nephrops norvegicus*

Nephrops is a marine crustacean (Phylum *Arthropoda*, subphylum *Crustacea*) mainly targeted in the North Eastern Atlantic ocean and Mediterranean sea parts of the European waters where it is known by many different names, including Norway lobster, Dublin (Bay) prawn (English), Scampo (Italian), Escamarlà (Catalan), Cigala (Spanish) Langoustine (French) and Kaisergranat (Deutsch). In spite of the fact that the shell is only soft immediately after moulting but usually hard, the species belongs to the Class of the Malacostraca[1]. Its members are characterised by the presence of three specialised groupings of multiple segments (tagmata): the head, the thorax and the abdomen terminated by a telson. In the case of *Nephrops norvegicus*, partial cephalon-thoracic segments are fused to form a cephalotorax bearing 5 pairs of walking legs or pereiopods (P1 to P5) typical of the Order of Decapoda. With a clear demarcation, the following abdomen is composed of 5 segments, each endowed with a pair of pleopods (PL1 to PL5) + 1 typically flattened into uropod that, together with the terminal telson, makes up the "tail fan".

(I.1) Conspicuous features

The relative size of the nephridial form-like of the eye that gave the name to the genus is certainly the most striking aspect of the anatomy with also the prominent pair of claws (P1) in comparison to the body size.

(I.1.a) Superposition eyes

Cigala has a compound eye consisting of thousands of individual photoreceptor units (*i.e.* ommatidia) with a reflecting superposition eye, that is to say, in which the optical elements are not lenses but mirrors (*i.e.* reflectors) and with a layer of square corneal facets (*i.e.* superposition) arranged in a lattice and a distinct clear zone between the photoreceptive rhabdom layer and the lenses apparatus (*i.e.* dioptric).
Thus, the light beams from one direction are brought to converge at a light-receptive zone (*i.e.* target rhabdom) via a large number of square facets and this "corner-reflector" configuration (*i.e.* always two mirrors at right angles) makes it possible for the eye to form an image over a wide field of view inducing a better sensitivity to the low light

1 from the ancient Greek malakós for "soft" and óstrakon for "shell".

environment. The image formed is brighter but not as sharp as the pixels image formed by the apposition eye (Gaten et al., 2013).

Superposition eyes are more commonly found in nocturnal insects and deep-water crustaceans.

This adaptation is important given the range of depths of the Aran ground population, day and night transition as well as the seasonal fluctuations in the light intensity (Aguzzi et al., 2008). The presence of pigments similar to the eye and located at the caudal part of the body have also been reported.

(I.1.b) Sexual dimorphism

Nephrops is also a dioecious[2] animal with distinguishable external sexual dimorphism. The most obvious dimorphic feature is the first pairs of pleopodes (PL1) which are longer and stouter for males contrasting with the thin female ones seemingly atrophied. In addition, females have a genital aperture located at the basal segment of the 3rd pereiopods or P3 while it is present in the last walking leg or P5 for males. In addition, the females possess a "Y" shaped spermatheca situated between the P4 and P5.

(I.1.c) A sensory animal: sensilla

As *Nephrops* is an aquatic animal the detection of water-borne molecules is crucial for its existence and in fact, numerous sensillum are distributed over the body (Goodall, 1988; Katoh et al., 2013) exhibiting a variety of cuticular structures shown to have sensory functions covering a range of modalities.

Olfactory detection permits individuals to sense the chemical constituents of the predators, the prey, the congeners and of course the edible organic matter since they are reputed to be scavengers and not thought to move away too far from their burrow in general and for food prospection in particular.

In addition, *Nephrops* are also receptive to mechanical stimuli (tactile and hydrological) through mechanoreceptors of different forms and types (*e.g.* serrate setae, plumose setae, smooth setae) associated with different body parts. In addition, a balance sensory receptor called a statocyst is located in the basal segment of the antennules (Goodall, 1988; Katoh et al., 2013).

2 from the ancient Greek di for "double" and oikos for "dwelling", plus the Latin osus for "full of".

Regarding the type of signal involved (olfactory or not olfactory) these receptors are connected to the olfactory lobe or non-olfactory receptive zone. Similar to most arthropods, it has a nervous system made up of a series of ganglia. There is one ganglion per segment and each receives sensory and movement information via nerves coming from the muscles, hard structures, appendages, eyes, and mouthparts.

(I.1.d) Burrow dwellers

Nephrops shelter inside burrows built beneath the seabed (**Figure 2**).

An assemblage/matrix of silt and clay seems to constitute the most suitable substrate for excavating tunnels (Campbell et al., 2009) although, in some areas sand is present in varying proportions (Chapman et al., 1971). As the animal transitions from a pelagic phase to a benthic life, the strict sediment type and size preferences of the post-larval animals determines the quantitative level of juvenile recruitment.

Resin casts of surveyed burrows in shallow shelf (~10–30 metres) waters off England featured very specific formations defined as a burrow complex (**Figure 2a**) composed of conspicuous domes with a crescent shape entrance located in a depression side (**Figure 2b-c**), plus, very often, connected shafts in the vicinity. However, more simple U, T and Y shaped burrows are also reported.

(a)

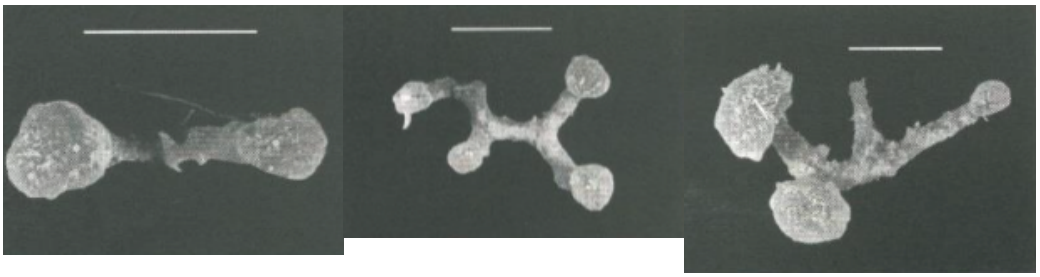
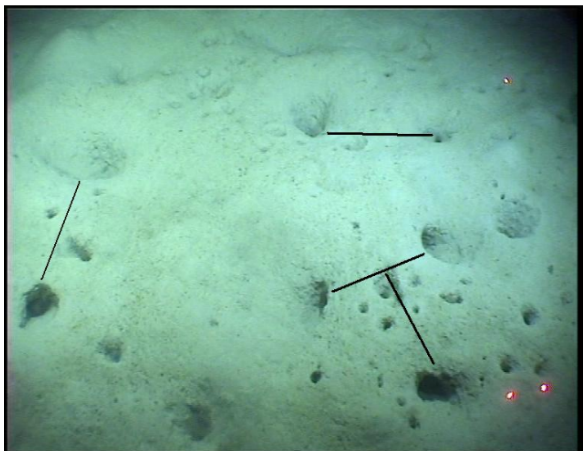


Figure 2a: Samples of resin casts of *Nephrops* burrows (Bell et al., 2018; scale bar lengths 20 cm)

(b)



(c)

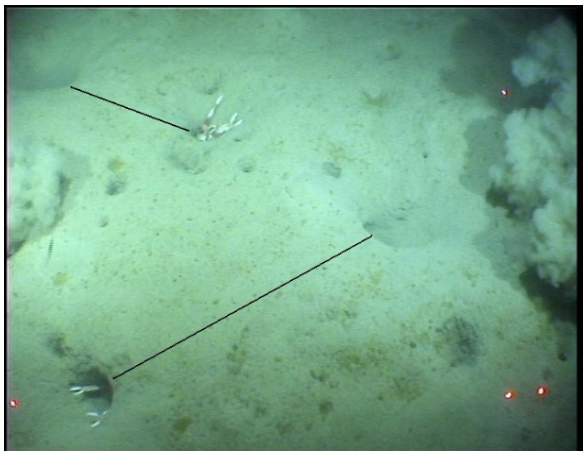


Figure 2b-c: Snapshots of *Nephrops norvegicus* burrows as taken by the under water TV apparatus in order to survey the population abundance in Aran grounds.
Black lines indicate connected burrow entry systems of the form «U» and «T». (**c**) Visible animals, very likely during door keeping activity (https://www.Marine.Ie/Home/sites/default/files/MIFiles/Docs/FisheriesEcosystems/Nephrops%20norvegicus%20Burrow%20Identification.pdf).

The animals spend most of the day in burrows and forage outside according to a diel rhythm (see sections below). While movement has not been explicitly studied on the Aran grounds, in study site close of it (Clew Bay) Merder et al. (2020) reported movement of recaptured individuals ranging between 21 m and 536 m from the point of release. The ability of the animals to select, built and maintain burrows may also be related to a dominance hierarchy.
Sbragaglia et al. (2017) showed that, higher ranked animals appeared more successful in getting burrows and in turn are less frequently evicted than lower ranked animals and

dominants spend a longer time inside the burrow and move over shorter distances reducing their susceptibility to predation. These results cast light into the group dynamics of this species and then the overall success of rank-related individual in winning territory, mating and food competition with an obvious influence on growth rate of the animal.

(I.2) "Misty blue[3]"

Throughout the evolution of the species, melatonin is often deemed as an important marker of an eventual internal clock (biological clock entrainment) and indicative of a circadian response.

Melatonin is present in the eyestalks of Norway lobsters and laboratory experiments showed that melatonin concentrations increase at higher light intensity. Structural eye analysis evidenced adaptation of ommatidia to the light intensity, leading to light-adapted and dark-adapted states. In the case of light-adapted ommatidium, pigment migrates from around the basement membrane to a position higher up the rhabdom layer.

Nephrops' eyes can therefore perceive the "blue" radiation between 470–480 nm and are proven to have a "blue" sensitive rhabdomere (Johnson et al., 2002). Within the range of 80–110 m depth, the blue light part of the sunlight spectrum (Mann and Lazier, 2006; Garrison, 2009) seems to be a good candidate for the biological clock entrainment (Johnson et al., 2002; Aguzzi et al, 2010; Chiesa et al., 2010).

While the compound eyes are deemed to be the main sensory organs involved in the biological rhythms, some rhythmic behaviours may be informed by information received from the caudal photoreceptor (Simon and Edwards, 1990; Chapman et al., 2000). Even though melatonin is a good candidate in the control of locomotory activity, a non photic stimuli (zeitgeber[4]) like the periodic hydrodynamic stimuli (as proxy of seabed tidal currents) has also been shown to influence the

3 "turns my whole world a misty blue" a homage to Ella Fitzgerald (1917–1996), and many other performers of the song written by Bob Montgomery (1937–2010).

4 First used by Ürgen Aschoff demonstrating that in addition to endogenous (internal) biological clocks, which synchronize biological rhythms, certain exogenous (external) cues, which he called zeitgeber, influence the timing of the internal clocks.

Nephrops burrow emergence behaviour with a strength that is dependent on the phase relationship with the light-darkness cycle (Sbragaglia, 2015). The mechanoreceptors distributed on body could also play a role in burrow emergence and movement patterns.

(I.2a) Marked variations in catches

At the scale of a year or a day, the level of the yields relies on the biological rhythms of the species. The animals behaviours determine catchability and in consequence a sustainable exploitation of the stock requires us to understand the behaviour, especially as it relates to burrow occupancy.

The distribution of catches when recorded at different hours of the day and at different depths reveal that on the upper shelf (< 30 m), peaks of captures are fully nocturnal, especially during full-moon phases while on the lower shelf (50–200 m) the active emergence is crepuscular (*i.e.* toward the sunset [dusk] and sunrise [dawn]) and is diurnal for upper slope area (> 200 m). In addition, by measuring the fluctuations in the percentage of empty stomachs, Aguzzi et al. (2004b, 2008) deduced that the feeding activity is strictly diurnal for upper slope (> 200 m) and lower shelf (50–200 m) inhabitants and hypothesised a similar behaviour for shallow shelf (< 30 m) populations. In contrast, the stomach contents of animals sampled in the Firth of Clyde (Scotland) by Parslow-Williams et al. (2002) indicated a feeding peak around dawn but not around dusk, even though animals were out of their burrows.

As depth increases, the locomotion pattern progressively dissociates into two components: the door-keeping behaviour, corresponding to a nocturnal activity at the burrow entrance likely related to territorial control (Aguzzi et al., 2008) and the emergence outside the burrow for foraging that appears to be crepuscular at lower shelf (50–200 m) or diurnal on the slope between 200–400 m (Chapman et al., 1972; Chiesa et al., 2010). Therefore, in Aran grounds, at depths ranging between 80 m to more than 110 m, *Nephrops* is expected to be active out of burrows (emergence) at dawn or dusk.

(I.2.b) Seasonal peaks: exposure and withdrawal of females

While there is some variability in catches associated with changes in the environment (natural stochasticity), the Aran grounds catches markedly increase and peak in spring, dominated by females. A similar but smaller increase is also recorded in autumn. Females leave their burrows in spring for hatching over several successive evenings, breaking off approximately 8 to 10 months of burrow living that commenced soon after egg laying (spawning) in autumn. Thus, in Aran grounds, the time series of landings seems to reflect this aspect of the behaviour of the animal.

The reproduction cycle is assumed to be annual, meaning that copulation takes place once a year when the female shell is still soft, soon after moulting, which happens after hatching between April and June approximately (Farmer, 1975; Bell et al., 2006; Smith et al., 2008). In Galway Bay, eastward of the Aran grounds, stage III larvae were sampled on 5th of April 2018 (McGeady et al., 2019) indicating eggs released during the February-March period.

Thus, under the "spell" of pheromones, the male initiates the courtship by stroking the female with his antennae for several minutes. Females are approached from behind, turned over and a spermatophore is transferred into the spermatheca. The inseminated females carry it through ovarian maturation until egg-laying on the pleopods for fertilization (spawning) occurring in late summer/autumn. Some differences in mating behaviour have been recorded (*e.g.* Katoh et al., 2013) and DNA analyses of fertilised eggs has shown that occasionally multiple matings/paternity have been detected (Streiff et al., 2004). Soon after fertilisation occurs, the females retreat into burrows for approximately 8 to 10 months, resulting in a higher percentage of males in the catches during this period (Farmer, 1975; Smith et al., 2008; Powell and Eriksson, 2013).

(I.3) Diet

Nephrops norvegicus is commonly considered to be an opportunistic predator and scavenger, feeding on a diverse range of prey: crustaceans, mollusc, polychaetes, echinoderms and fish (Cristo et al., 1998; Parslow-Williams et al., 2002; Bell et al., 2006; da Silva Santana et al., 2020). Fish appear to be an important item in the diet, with lower contributions from plankton and invertebrate sources. Suspended particulate organic matter has also been found to be important, ranging between 12% to

47% of the diet for both females and males (da Silva Santana et al., 2020). However, the contribution of the suspended organic matter in the diet is reported to be size related with higher proportions in smaller size classes compared to larger groups (for males in particular). Also, in spring and summer, suspension feeding is significantly higher for small-medium and small size males, respectively, rather than larger ones, whereas such differences are not seen in females (da Silva Santana et al., 2020).
Fishing intensity may also influence diet and/or prey availability. Isotopes analysis ($\delta^{13}C$, $\delta^{15}N$) of muscle tissue of specimens collected in the Irish Sea (Hinz et al., 2017) indicated changes in *Nephrops* diet shifting from benthic food towards a more planktonic based food target as a consequence of bottom trawling intensity.

(I.4) Pelagic life stage

As already seen, the fishing activity is intrinsically linked to the timing of emergence from the burrows and then the benthic lifetime. Yet, *Nephrops* life cycle comprises an additional distinctive phase encompassing different stages of growth of the animals: the pelagic lifespan.

(I.4.a) A critical period

Nephrops begins as a hatched pre-Zoe larvae swiftly followed by successive development stages called Zoe I–II–III and terminates with a near benthic stage animal that resemble the adult, namely, the Post-Larvae I (PL-I). “In fact, during the Zoea III, the larvae become increasingly negatively phototactic and reside at depth in a demersal (hyper-benthic) habitat” (Powell and Eriksson, 2013).
This pelagic life duration is variable (~40 days) and is influenced amongst other things by water temperature according to laboratory experiments (Dickey-Collas et al., 2000a; Briggs et al., 2002b).

(I.4.b) Advection and diel movement

In the Aran grounds most of the larvae stage I (94%) resides in the top 30m with the highest proportion (45%) observed between 10 and 20 m (McGeady et al., 2019) undertaking a diel vertical migration (twilight migration) of about 10 m made up of two accents (prior to sunset and sunrise) and two descents (Hillis, 1974; Hill, 1990a, 1991;

Hill et al., 1996, 1997; Powell and Eriksson, 2013; McGeady et al., 2019).
These "Zoea I larvae are active, swimming at around 10–30 mm per second increasing with stages" and have a "positive phototaxis towards 400–600 nm and high barokinesis" according to Powell and Eriksson (2013).
In Aran grounds the larval depth preferences usually coincides with a warmer water layer and the mean depth of *Nephrops* larvae was found to be essentially driven by variation in temperature (difference between surface and 60 m) and zooplankton biomass reflecting the compromise between growth rate, food availability and the risk of predation (McGeady et al., 2019).
During this pelagic stage the x-y components of the advection (that is, the lateral dispersal) is driven by the prevailing inertial current and is the determinant for the settlement upon a suitable substratum and hence the level of the recruitment and the density distribution of adults (Hillis 1974; Hill, 1990a, 1991; Hill et al., 1996, 1997; Emsley et al. 2005). It can be surmised that climate could exert its most influential action during this short pelagic period.
Oceanographic simulations of larval dispersal over the Aran grounds indicated larval retention levels between 14.4–15.8% (O'Sullivan et al., 2015) and 1% (McGeady et al, 2019). O'Sullivan et al. (2015) also highlighted larval interconnections between the Aran grounds, Slyne Head and Galway Bay during this pelagic stage on the basis of a "recipient-donor relationship", revealing the Aran grounds role as a larval supplier. Both approaches highlight the lack of a hydrological retention mechanism existing at time of hatching and during the larval cycle over Aran grounds, resulting in a high percentage of egg-larvae loss, which emphasises the importance of this environmental factor on the recruitment rate and hence the population abundance in FU17.

(II) Snapshots of a profitable fishery

In 2011, the *Nephrops* fishery in Ireland was estimated to be worth €32.1M (8,210 tonnes live weight) increasing to €75.2M in 2018 (10,893 tonnes live weight) and making it the second highest value landed demersal species (Stockbook, 2011, 2018). From 2011 to 2016 this mixed fishery yielded around €558M in total. Clearly, this species is a valuable source of revenue and has proven to be a good substitute for the depleted cod (*Gadus morhua*) stock. Nevertheless, the estimated FU17 (**Figure 3**)

landing values have been fluctuating over a number of years, for example between 2011–2016 the value fluctuated between €2.2M and €7M (see Anon., 2013–2016). Such inter-annual variations would certainly impact the dynamics of employment in the fishing sector and the number of vessel operating in the area (Meredith,1999; Foley et al., 2016). Within FU17, the Aran grounds account for ~88% of the total estimated burrow abundance, whereas, Galway Bay and Slyne Head account for ~8% and ~2%, respectively.

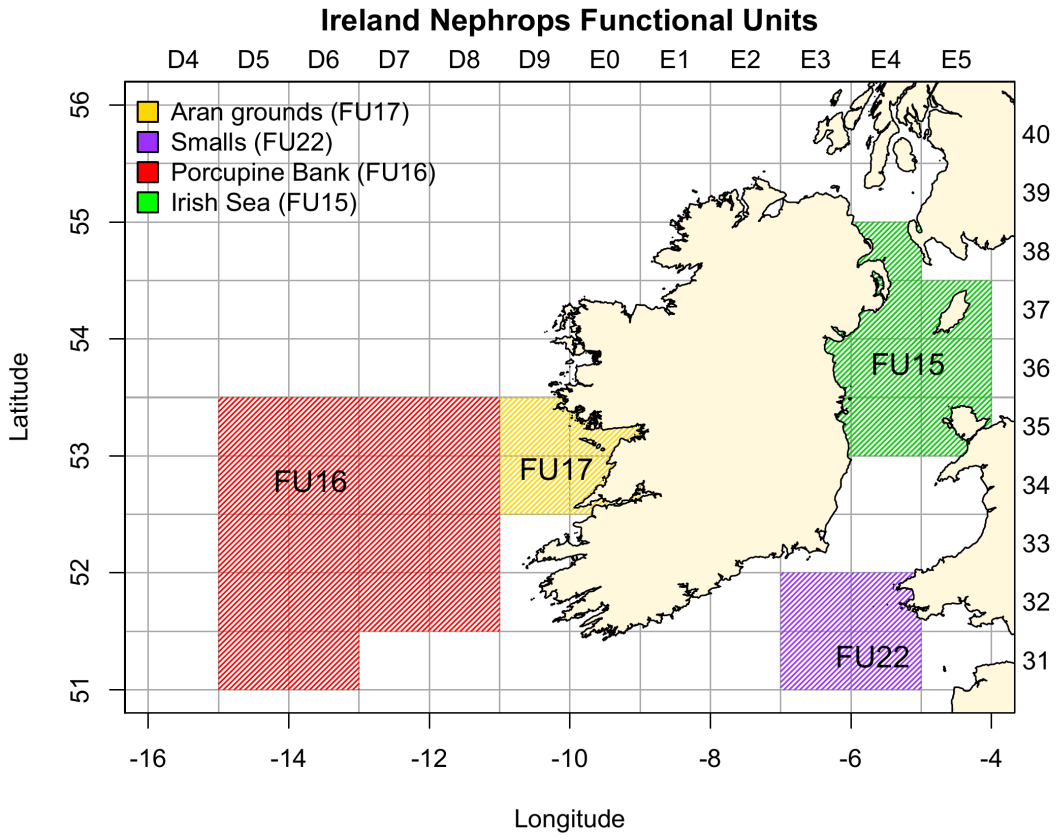


Figure 3: Geographical distribution of ICES functional units (FU) around Ireland and nearest areas subject to our landing time series analysis.

(II.1) "Horses" for crustaceans: fleets involved during 1995-2014

In the Aran grounds, during this period, *Nephrops* have been essentially harvested by bottom otter trawls. The bulk of the fleet is composed of vessels with under 500 horsepower (hp) with an obvious distribution around 250 hp in the late 90's (**Figure 4a-b**). Since 2000 the relative proportion of higher powered engine increased

until 2006 becoming the larger part of the fleet in years 2004–2006. Since 2002 and progressively, the 250–350 hp modal value of engine power distribution had leveled off to the benefit of lower and higher ones. This, coincided with the decline of the 20 m length vessels in the fleet during this period.

The striking trend is the constant increase of the 25 m vessel category since 2000 becoming the dominant category in 2009 and 2010 and contrasting with the dynamics of the 15m vessel category which is marked by a steady diminution and even almost a disappearance in 2003 and finally an upwards trend in the next following years. In 2007, the 20 m and 25 m size classes are equivalently the leading categories. Since 2008 there appears to be a move towards the smaller 15 m vessels again.

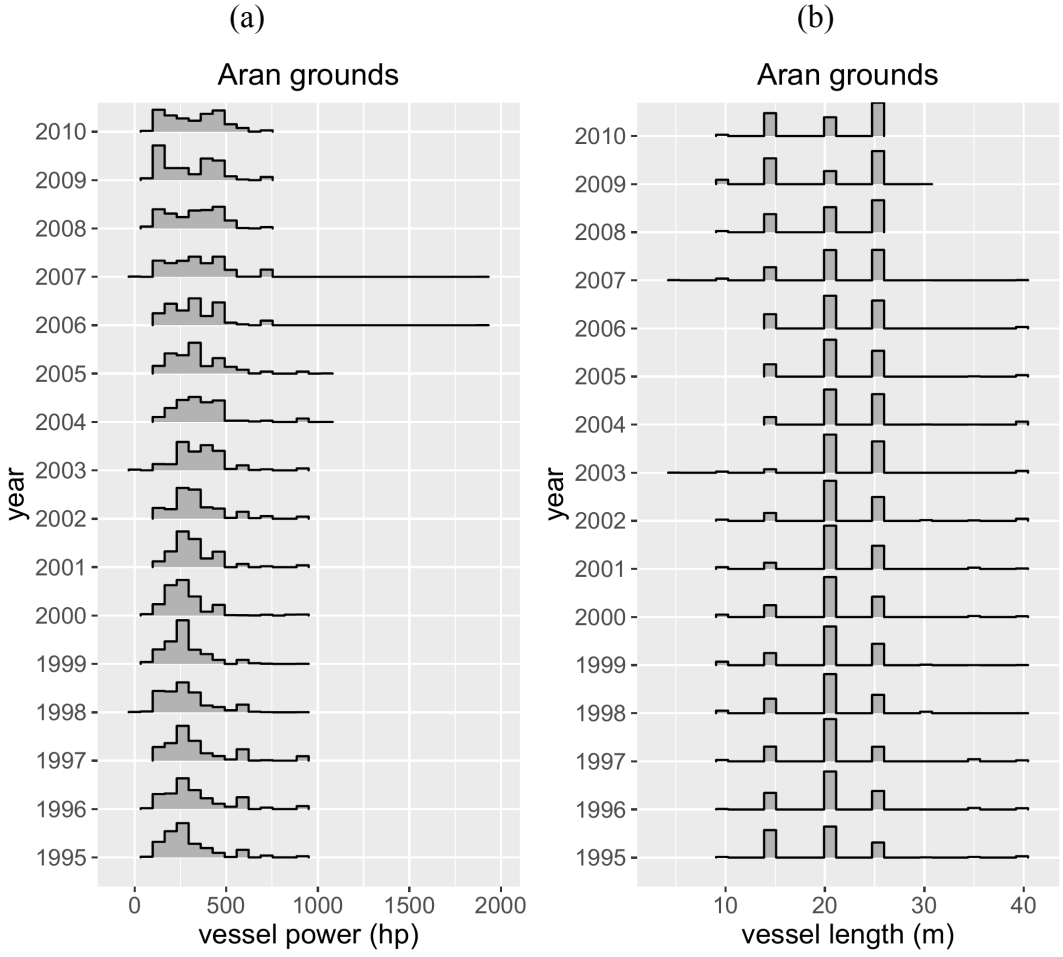


Figure 4 a-b: Evolution of vessel engine power (in horsepower, hp) and length (in metres, m) targeting *Nephrops norvegicus* in Aran grounds from 1995 to 2010 (source: Marine Institute, Ireland).

Are similar trends in changing fleet composition reflected in the landings?

Obviously, the proportion of the catches of the 15m vessels is decreasing dramatically since 2001, providing less than half of the yield for the period 1995–2000, while, the contribution of the 20 m and 25 m vessels remains the bulk of the landings (**Figure 5**). The 15 m vessels could appear to be the adjustment variable: have the 15 m vessels relocated out of area, withdrawn from the whole fishery, or more impacted than the 20–25 m by the decrease of *Nephrops* abundance? The answer requires a thorough analysis of much more detailed data and this supplementary knowledge is crucial for efficient management.

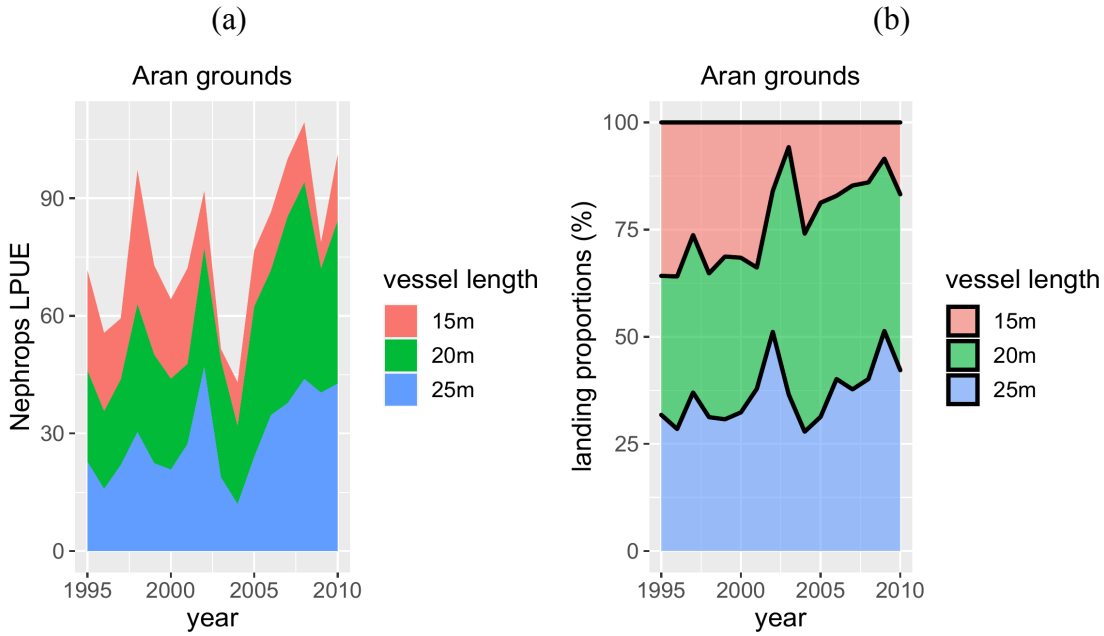


Figure 5: Evolution of Aran grounds *Nephrops norvegicus* fishery (**a**) landings per unit of effort (in kg/hours) and (**b**) proportions sorted by vessel length types from 1995 to 2010 (Source: Marine Institute, Ireland).

Are the Aran grounds fleets distinguishable from the remaining areas?

Similar to Aran grounds, the 20 m vessels are the principal size class operating in the Smalls (FU22) and the Western Irish Sea (FU15); although there is an increase of higher power engines during the last 16 years (**Figure 6c-d**, **Figure 6e-f**). We observe a heterogeneity in the distribution of the fleet composition in the last few years, in the case of the Aran grounds and the Smalls, possibly indicative of a dynamic induced by the collapse of the cod stock and the adaptive move towards the new fishing

opportunities. The Western Irish Sea fleet demonstrated a relative stability in boat sizes, illustrating that the historical yields have supported the fishing industry throughout this period.

In contrast, the Porcupine Bank (FU16) has a high proportion of engines of > 500 hp and vessel length of 25–35 m (**Figure 6a-b**). This composition reflects the distance of the fishing ground from the coast, the prevailing ocean conditions (*e.g*. depth of the continental slope) and the commonly targeted species on the Porcupine Bank. Thus, at any location, the available data bear witness to the fishing dynamics and the time scale (*e.g.* reconversion, adaptive behaviour of fishers…*etc*) ranging from an annual to an almost decadal time scale.

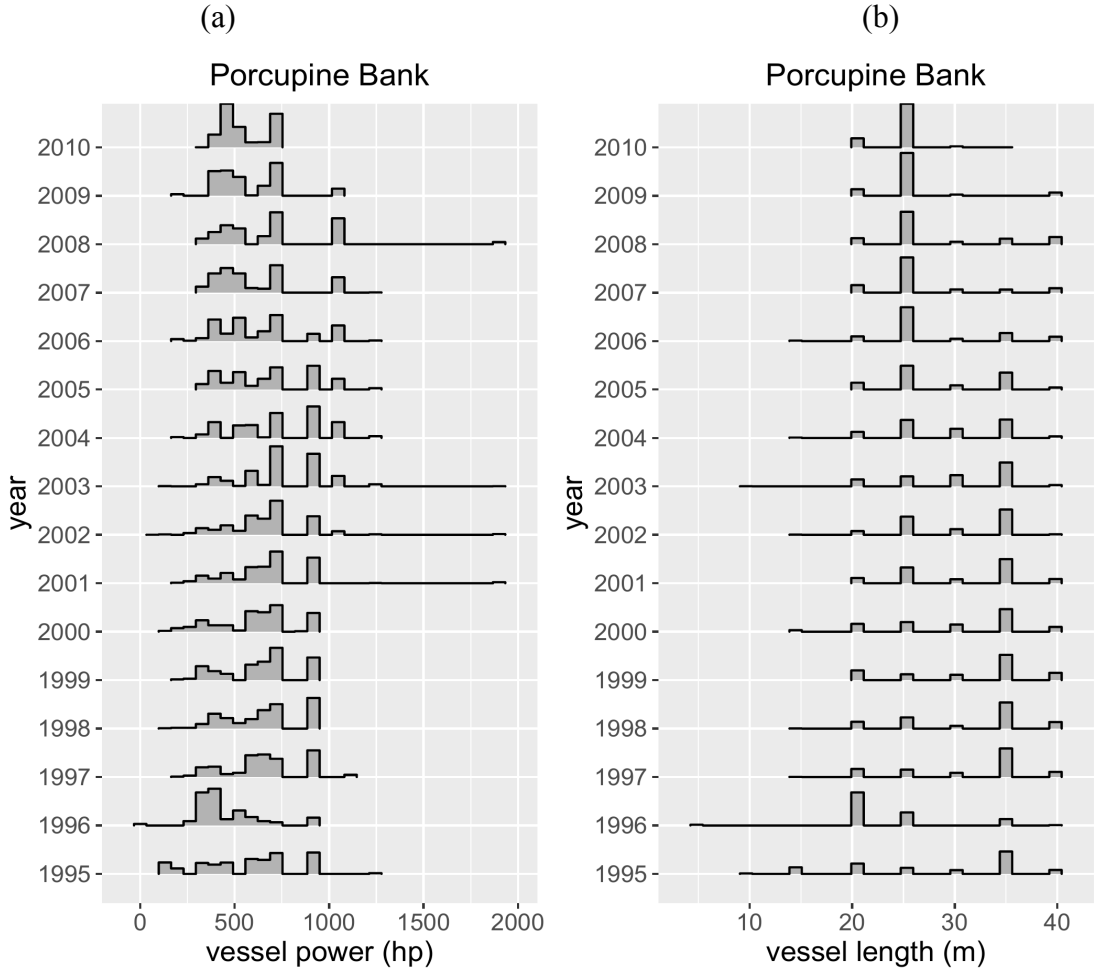


Figure 6a-b: Evolution of vessel engine power (in horsepower, *hp*) and length (in metre, *m*) categories harvesting *Nephrops norvegicus* over the period 1995–2010 in Porcupine Bank (Source: Marine Institute, Ireland).

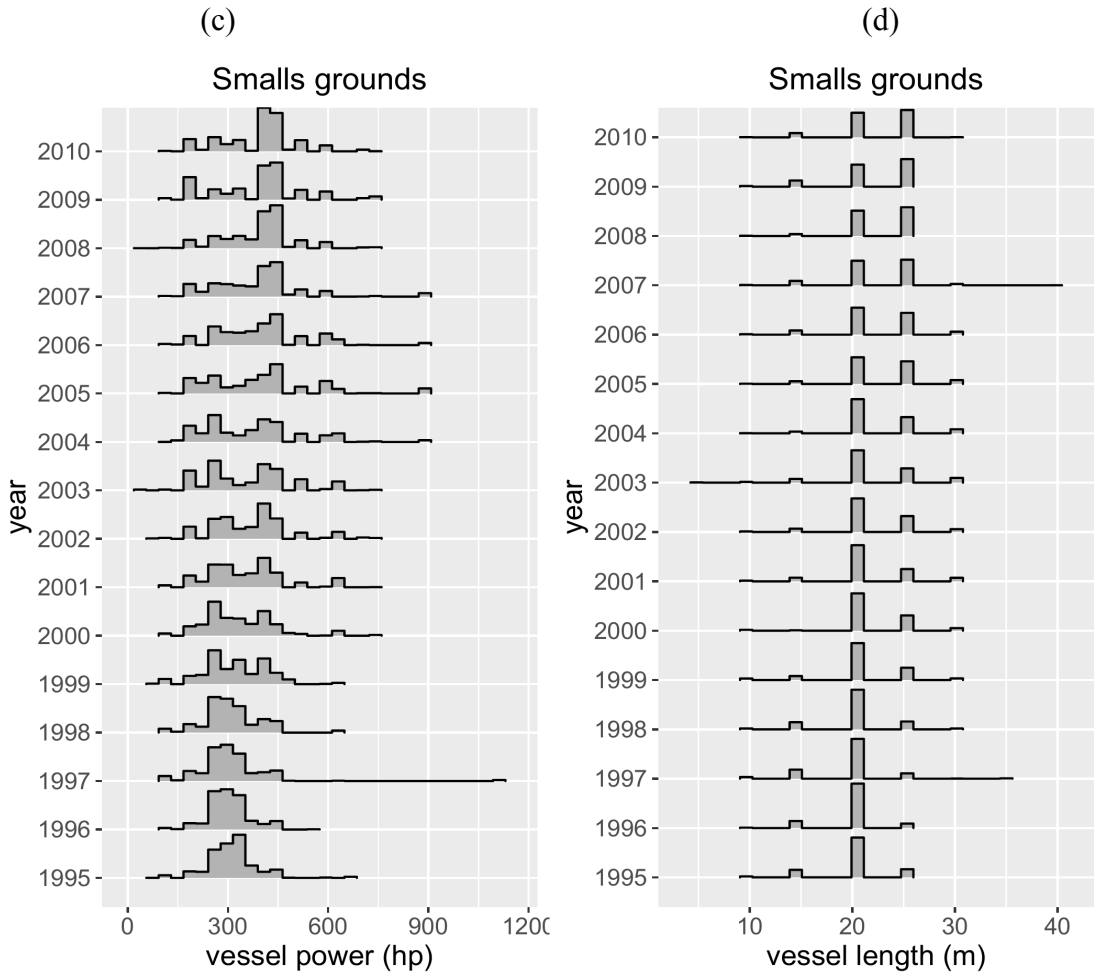


Figure 6c-d: Evolution of vessel engine power (in horsepower, *hp*) and length (in metre, *m*) categories harvesting *Nephrops norvegicus* over the period 1995–2010 in Smalls grounds (Source: Marine Institute, Ireland)

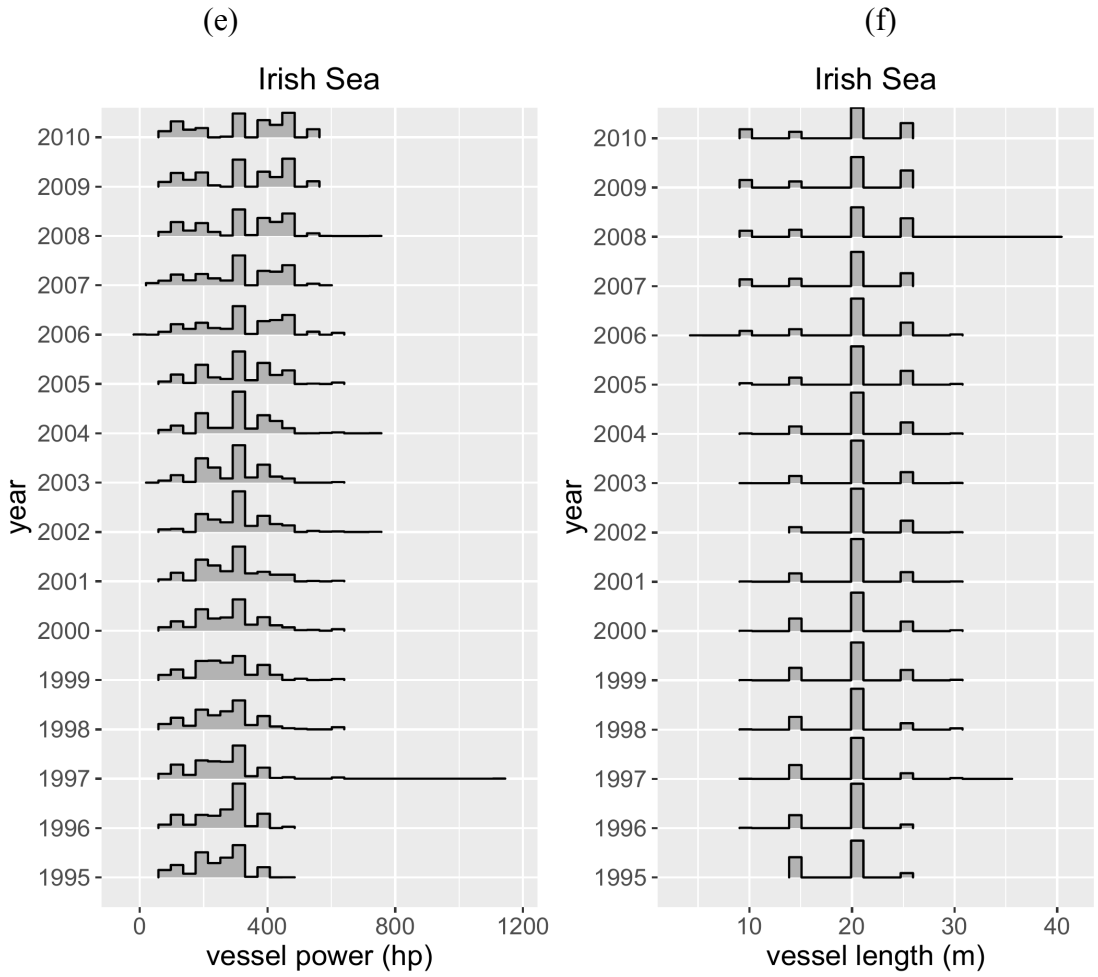


Figure 6e-f: Evolution of vessel engine power (in horsepower, *hp*) and length (in metre, *m*) categories harvesting *Nephrops norvegicus* over the period 1995–2010 in West Irish Sea (Source: Marine Institute, Ireland).

(II.2) Current management advice

(II.2.a) Under water TV (UWTV) basis for total allowable catch (TAC)

For the three geographical components of FU17 under current exploitation, namely Aran grounds, Slyne Head and Galway Bay, the under water TV (UWTV) surveys are central to calculating the catch options. It consists of a steel framed sledge, deployed from vessel, on which a forward facing camera is mounted and used to record a 10 minutes video footage of seabed to identify and count burrows provided optimal conditions are met (**Figure 7**)

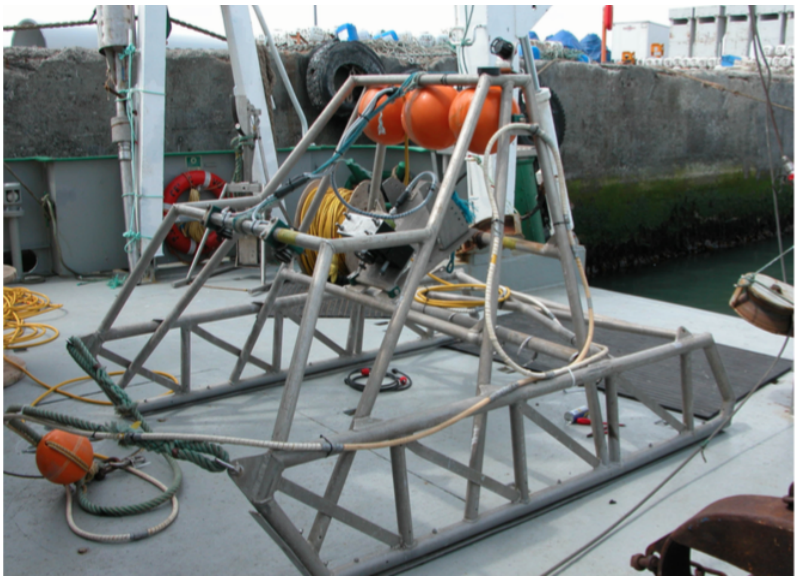


Figure 7: Picture of the Under water TV sledge used for *Nephrops norvegicus* burrow surveys with a camera fixed on.

The TV samples are translated into abundance of burrows through geostatistical approximation with an assumed occupancy ratio of 1 animal per burrow. The method is counting animals of a size not available to the fishery. Hence, a total allowable catch is produced annually from an estimated total removal (*i.e.* landings + dead discards in number) entailing a series of operations involving estimated proportions of discards (*e.g.* dead discards, survivors) as well as individual mean weight of landings and discards. Notice, since accounting for about 88% of the burrow abundance in this functional unit, the Aran grounds patch has been chiefly and regularly surveyed since 2002.

It is worth mentioning the 2 years lag between the observed data in use in the catch options and the effective time of this management advice. For instance, establishing a TAC for year (*t*) necessitates, at least, data recorded at (*t-1*) like the UWTV survey, and data at time (*t-2*) such as the mean weight of discards and landings, discard rate, discard survival rate, dead discard rate. This practical aspect of the management renders the tractability of the recruitment influence on the stock very difficult.

(II.2.b) Structural fragilities

(II.2.b.1) Ageing

The difficulty in ageing a species such as Escamarlà[5] renders an age-structured population analysis as a basis for formulating management advices untenable. Also, the high variability in the length-class structure of the Aran grounds stocks contribute to a level of difficulty regarding assessment procedures involving a snapshot of a length frequency distribution of the population/stock.

(II.2.b.2) Dubious data

Prior to 1988 landings data for this fishery are only available for "foreign" countries (mainly France) and the quality of landings data is dubious. Since 1988 reported landings data for the Irish fleet were obtained from EU logbooks. Only data from 1995 are deemed dependable.

(II.2.b.3) Tracking the effort

Over the years, vessels have become more efficient at catching *Nephrop*s. Recently, new behaviours have been observed: prawns are targeted on several other grounds within the same TAC area and periodicity in the occurrence of several vessels over zones is also accentuated. Finally, effort encompasses technical device capabilities (vessel engine performances, echo sounders abilities to detect shoal, net efficiency), as well as fishers skills and knowledge. Therefore, trying to quantify these subtleties into a single measure presents many challenges (a chimera).

(II.2.c) ICES assessment framework

In compliance with the ICES request towards a precautionary stock assessment, an advice F_{MSY} ranges [F_{lower}–F_{upper}] are derived to deliver, in theory, no more than a 5% reduction in the long-term yield compared with the maximum sustainable yield (*MSY*). Nonetheless, given the lack of analytical assessments, already mentioned, it is not possible to calculate F_{MSY} directly and therefore F_{MSY} proxies are used.
Scientists in charge of the stock have recourse to reference points $F_{0.1}$, F_{max} and $F_{35\%SPR}$

5 *Nephrops norvegicus* in Catalan.

derived from a length-based model (separable cohort analysis) fitted to the average length frequency distributions to give strength to the harvest rates table derived from the UWTV surveys (ICES WKNeph, 2009; ICES IBPNeph, 2015). The harvest ratio consistent with the combined sex $F_{0.1}$ is considered as the appropriate proxy for F_{MSY}. Yet, differences in growth and behaviour between males and females are observed. In consequence, should we reconsider this indiscriminate fishing mortality or harvest ratio and its effects on the Aran grounds? What is the impact of utilising this approach on the spawning stock biomass?

In order to fulfil the ICES management strategy evaluation, a population threshold of the number of individuals (noted $MSY\ B_{trigger}$) has been defined as the lowest stock size from which the abundance has increased to induce a reduction of the harvest rate.

Objectives of the study

This work is an opportunity to challenge all these concerns. In this work the salient aspects of the life history of *Nephrops norvegicus* are reviewed to help to inform a sustainable management strategy.

Concomitantly with the willingness of the Marine Institute to fund a project to probe into this valuable species off of Ireland, the growing size of the UWTV surveys time series (**Figure 8**) provides us with a glimpse to an acute situation of the population showing a decrease in burrow abundance against a backdrop of increasing landings.

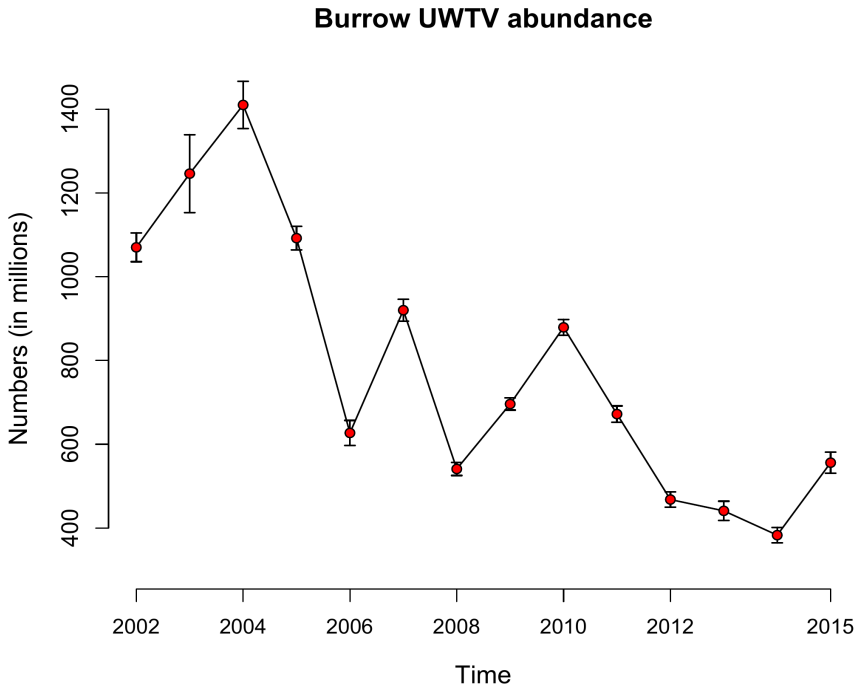


Figure 8: Estimated Aran grounds population abundance (in number) of *Nephrops norvegicus* from under water TV surveys (UWTV) from 2002 to 2015. Error bars indicate 95% confidence limits.

Thus, in this study the aims are to (1) examine the temporal fluctuations in landings (and lpues) of the Aran grounds to appraise the dynamics of the population abundance, (2) to investigate the spatial distribution of burrows and the factors contributing to the observed spatial patterns and finally (3) to inspect the stock status following decades of fishing in the Aran grounds. The thesis is presented as three data chapters, summarized below.

(1) Chapter Time Series Analysis

Time series analyses were carried out to examine the temporal fluctuations in landings of the Aran grounds *Nephrops* fishery and compared with the other main areas of harvest off the coast of Ireland: Smalls grounds (FU22), Porcupine Bank (FU16) and the west Irish Sea (FU15). The aim was to characterise variations in the population: are they transient, persistent, cyclical? and, to consider possible influences of climatic indices such as the North Atlantic Oscillation (NAO), the Arctic Oscillation (AO) and

the Atlantic Multi-Decadal Oscillation (AMDO).

However, explaining the trends seen in a time series are not without challenges, given the complexity of fisheries data, with environmental and anthropogenic influences, such as variations in stock size, environmental perturbations, changes in fishing and discarding patterns and fisheries management/restrictions. A number of modelling approaches were used to try to develop a predictive approach for modelling the stock dynamics.

The state space analysis of landing time series (Commandeur and Koopman, 2007; Durbin and Koopman, 2012) provided an estimate of the unobserved dynamics (*i.e.* the states) and the states modelling consisted of selecting stochastic intercept (or level) and seasonal cycle component, while the ordinary-least-square cumulative sum (ols-cusum) and ordinary-least-square moving cumulative sum (ols-mosum) allowed direct investigation of the dynamic trajectory of landings (Zeileis et al., 2002).

However, data collected sequentially in time, often, show serial dependence and require adapted modelling approaches. The outputs of the well known auto regressive-moving average modelling approach (arma) and its seasonal extension (sarima) were then engaged and compared to the state space fits of the time series (Box, Jenkins and Reinsel, 1994). Both approaches were implemented to monthly and annual data in the four main fishing areas over the time series from 1995 to 2010. Their predictive capabilities (forecastings) were used as a fisheries management tool. In fact, the forecastings provide information on future developments based on the past, making it possible to investigate whether data that become newly available in a series behave according to the expectation or not.

For each fishing ground, delayed density dependence, which traditionally describes a situation where population growth is controlled by negative feedback with a time lag, was informed. Two different time lags were assessed: month and year.

Finally, in order to inform the adequate spatial scale of *Nephrops* management, common trend dynamics in landings between fishing grounds and regional climate influence were examined through the dynamic factor analysis (Holmes et al., 2012, 2018b) and cross correlation function and provided provisional answers.

(2) Chapter Spatial Analysis

Throughout this work we have examined *Nephrops norvegicus* in relation to its environment.

Relative to its lifetime this crustacean is considered to be part of the macro-benthos community. The seabed type is crucial for this species and will induce the level of recruitment. Given that landings data have been seen to vary both seasonally and inter-annually, an independent assessment of burrow density is an essential key for the stock assessments. Hence, understanding the spatial distribution of burrows and the factors that affect distribution patterns is important for designing robust sampling programmes, which then inform management.

How is the population distributed on the Aran grounds? Could we recognise pattern(s)? What does the spatial dimension bring to management?

Using underwater TV census data covering the period 2002 to 2010, the spatio-temporal variability/stability of the burrow distribution and density was investigated by using geostatistical techniques and combining the resulting maps from ordinary kriging and the empirical orthogonal functions (Pebesma et al., 2012). Sub-areas were delineated using a density threshold (Indicator kriging), and either direct or crossed correlated relationship between years were indicated (cross correlation, regional variogram, co-kriging, Pebesma and Duin, 2005). In addition, the influence of fishing intensity (maximum covariance analysis, Taylor et al., 2013) and environmental factors like depth, seabed sediment content (linear and Loess regressions), and current surface (Ruiz-Cuetos et al., 2016) in shaping *Nephrops* burrow spread in Aran grounds were evaluated.

(3) Chapter Stock Assessment

The exploitation rate is the motif of the diagnosis of the actual status of the population. In general, three sources of information are needed for an appropriate starting point for a *Nephrops* stock assessment. First, the trawl survey provides information on size and weight composition (mean weight and sex ratio) while, secondly, the larval production values provide the effective fecundity of a mature female of mean size used in combination with, thirdly, the under water TV surveys to estimate the female spawning stock abundance or biomass via the mean weight of individuals derived from trawl

sampling.

In the Aran grounds, there is no measure of the reproductive potential of the mature population, that is to say, the spawning stock biomass (*SSB*) is unknown. The management advice is "exempted" from estimating the *SSB*. Moreover, without the capability to ascertain the fecundity, the tool kit of fisheries modellers for describing stock recruitment relationships becomes useless.

Then, what are the alternatives at our disposal to evaluate the rate of exploitation?

We deliberately set our sights on the production family models to avoid the well-known weaknesses of the analytical modelling for crustaceans. Subsequently the constant concern has been to select the method that can pass from a scenario with very little information to that allowing to integrate a greater number of data and information collected over years.

Thus, the bayesian framework appeared useful in data-poor scenarios since it allows the incorporation of prior knowledge and explicitly evaluates parameters and models uncertainty. Hence, a bayesian Schaefer production model (Myers and Millar, 1999; Froese et al., 2017) was implemented and the intrinsic growth rate (*r*) of the population, the carrying capacity (*k*) and the maximum sustainable yield (*MSY*) predicted using available landings data.

Although the data for this fishery were available from 1974 to 2014, given the catch history, there is more confidence in the data from 1995 onwards leading us to conduct the analysis for a shortened (1995 to 2014) and full (1974–2014) time series. In addition, fishing effort also changed during this period and as an alternative to the lpue index, a relative abundance index series, namely the stock size index, based on the under water TV surveys operated by the Marine Institute from 2002 to 2014 was used and inputted in a bayesian framework to compare the model outputs.

Developed for data poor stocks with uncertainty in stock productivity, fishing mortality rate, and stock status, CMSY (Froese et al., 2017) which is a refinement of the Catch-MSY approach (Martell and Froese, 2013) estimates biomass, exploitation rate, *MSY* from a credible set of (*r*-*k*) pairs. And, the probability ranges for *(r*) and (*k*) are fitted with a Monte Carlo approach to detect "viable" (*r*-*k*) pairs in compliance with the observed biomass trajectory. CMSY contributed to obtain qualitative stock information and provided indications of resilience which is a proxy for the capacity of a species to

withstand exploitation, ranging from very low to high (Froese et al., 2017; Froese and Pauly, 2015). In addition, surplus production and productivity were typified and linked to recruitment (Walters et al., 2008) while, the spawning potential ratio was informed using length based method LB-SPR (Hordyk et al., 2016; Hordyk, 2019).

Chapter 1 Time series analysis of *Nephrops norvegicus* landings off the coast of Ireland

Contents

Chapter 1 Time series analysis of *Nephrops norvegicus* landings off the coast of Ireland.....28

Abstract.....31

Introduction.....32

Aims of this Chapter.....35

Materials and Methods.....37

(I) Population abundance.....37

(I.1) State space approach.....37

(I.2) Ols-Cusum and Ols-Mosum.....40

(I.3) Forecasting.....41

(I.3.a) Forecasting with state space.....41

(I.3.b) Forecasting with Box-Jenkins.....41

(II) Climate influence.....42

(II.1) Regional climatic indices.....43

(II.1.a) North Atlantic Oscillations.....43

(II.1.b) Arctic Oscillation.....44

(II.1.c) Atlantic Multi-Decadal Oscillations.....45

(II.2) Detection of climate influence(s).....45

(II.2.a) Cross correlation function (ccf).....45

(II.2.b) Dynamic factor analysis (DFA).....46

Results.....48

(I) From observations to analysis.....48

(I.1) Dynamic structures.....55

(I.1.a) Trend levels.....62

(I.1.b) Seasonal components.....64

(I.1.c) Outliers and structural breaks.....68

(I.2) Long-term trends.....73

(I.3) Past values contribution to current landings.....76

(I.3.a) Sarima regressions.....76

(I.3.b) Delayed density dependence.....80

(II) Support to fishery management.....84

(II.1) Monitoring through forecasting.....84
(II.2) Common trends for connected waters.....87
(II.3) Climate influence.....89
Discussion.....94
Conclusion.....103

Abstract

Landings from 1995–2010 from commercial fishing vessels targeting *Nephrops norvegicus* constituted the basis of a time series analysis for estimating past and present biomass on the Aran grounds. This analysis was also undertaken for the main prawn fishing grounds around Ireland: the Smalls (FU22), the Porcupine Bank (FU16) and the west Irish Sea (FU15) for which a 12-month characteristic unit pattern was identified. For the Aran grounds, a random walk trend level made of successive cycles of 3-5 years with a stochastic seasonal component against a background of a steady decline in the abundance over two thirds of the time period was found. For Aran grounds (and Porcupine Bank) *Poisson* modelling of the data distribution was necessary to cope with the dynamic patterns of the landings in the case of state space method. The influence of the North-Atlantic and Arctic oscillations on the lpue series fluctuations ranging from months to years are highlighted and the presence of direct and delayed-density-dependent feedback mechanisms of regulation demonstrated. In addition, the time series modelling disclosed common trend pattern in landings for adjacent waters, which raises the question of how useful the ICES functional unit grid for the practical management of *Nephrops* in Ireland is and also provided an effective means to detect departure from fishing behaviours in the Aran grounds and Porcupine Bank.

Introduction

Effective fisheries management requires objectives to be established and appropriate actions selected that will, hopefully, result in the realisation of these objectives. A good management framework should incorporate regular monitoring and feedback of the implemented policy to help evaluate the degree of success in attaining the assigned targets. Information on the abundance of the fished population is needed to meet such management objectives, and landings or catches and fishing effort remain the basis for fisheries scientists to ascertain abundance. These data are also used in stock assessment models that are ultimately used in the regulation of the resource.

These data, collected over time, also enable scientists to use time series analysis as a monitoring tool. Time series analyses uses past events as the basis of projection into the future (forecasting) with the advantage of having learned from the time passed. The selected methods used here are oriented towards modelling and eventually explaining the changes in abundance of a *Nephrops norvegicus* population using information contained in the series to inform fisheries management decisions. In fisheries science the stock concept is traditionally preferred over a more biologically meaningful population "unit". Nonetheless, we should keep in mind that the stock constitutes, simply, a sub-population "with some definable attributes which are of interest to fishery managers" (Begg et al., 1999; Cadrin et al., 2005). However, the issues related to stock connectivity and meta-populations (Cadrin et al. 2005; O'Sullivan et al., 2015) as well as the growing acceptance of a move towards an integrated ecosystem fishing approach (FAO, 2003; Jennings, 2011, 2012; ICES WKIrish5, 2018) render the distinction in some cases thin, even obsolete. For some species, however, there is very limited genetic connectivity, and genetically distinct populations can result through isolation by distance or because of barriers to dispersal, prohibiting mixing: for instance, salmon return and spawn at a fixed site, known as natal homing, create such (reproductive) isolation (Quinn, 2005; Lin et al., 2008). These populations, or metapopulations, need special consideration in terms of management and conservation.

Fluctuations in Nephrops and factors that might influence inter-annual variation

A time-series based on fisheries data are the combined result of biotic and abiotic factors, often difficult to read and translate. *Nephrops* exhibit important fluctuations and distinct variations in landings over short spatial and temporal scales (Aguzzi et al., 2003a, 2004b, 2004c, 2008; see also the Marine Institute under water TV reports (UWTV) since 2002 for Aran grounds (FU17), 2003 for the west Irish Sea (FU15), 2006 for the Smalls grounds (FU22) and 2012 for Porcupine Bank (FU16)). This burrowing species has a preference for silt-clay (muddy) seabed sediments (Farmer et al., 1975; Campbell et al., 2009), and therefore the habitat may be patchy. Its behavioural and physiological rhythms affect its catchability at a diel and seasonal scale. In fact, the timing of emergence and duration vary according to water depth and light modulations (e.g. daylight phase, sun height, sun-moon angle, Agguzi et al., 2008, Agguzi et al., 2009a) and even inertial current (Agguzi et al., 2009b; Sbragaglia, 2015). In addition, periods of incubation in burrows of ovigerous females result in different exploitation patterns for males and females (see ***General Introduction***).

In addition to these endogenous patterns, various abiotic factors contribute to influence abundance and distribution. Since the larval settlement is a critical step and particularly because the post-larvae (or stage IV) need a suitable sediment to survive (Farmer et al., 1975; Powell et al., 2013 after Smith, 1987 and Santucci, 1926), the annual level of recruitment relies on the extent of the favourable vs unfavourable oceanographic circulation patterns to retain larval production over these specific sites, during the planktonic stage from hatching to larval stage (I-II-III-) IV. Thus, environmental conditions such as surface wind speed and direction can determine the success of the settlement (Hill, 1990a; 1991; Bailey et al., 1995; Hill et al. 1996, Hillis et al., 1996; Hill et al., 1997; Dickey-Collas et al., 1997; Dickey-Collas et al., 2000a; Horsburgh et al., 2000; Briggs et al., 2002).

Climate influence

Climatic impacts on marine resources have been seen in long-term records of fishing capture and in palaeoecological records (Cushing, 1982; Cushing, 1990; Finney et al., 2000, Fogarty et al., 2002; Stenseth et al., 2004; Hannesson et al., 2006; Gröger et al., 2011; Pitcher et al., 2001; Hare et al., 1999; IPCC 2013, 2014;

Merillet et al, 2020). For *Nephrops*, studies have stressed the important influence of sea temperature on the growth and success of the larvae during its water column life stage (Dickey-Collas et al., 2000a; Briggs et al., 2002b). Consequently, the prospect of a climate effect on abundance (Maynou and Sardà, 2001; González-Herraiz et al., 2009, Engelhard et al., 2010; González Herraiz et al., 2015) is relevant especially when trying to maintain a sustainable population while allowing exploitation; without including this potential effect may negatively impact the species and fisheries balance (Hare et al., 2010).

Moreover, *Nephrops* is also a valuable commercial species, subjected to fishing, which also influences recruitment. As a sedentary species, high-density areas may be targeted very effectively by fishers. This species is influenced by many fishing activities, including the impact of the gear (otter or beam trawl) on the habitat, the duration, timing and net selectivity (Drewery et al., 2010; Dimech et al., 2012) and of course the levels harvested. The decreasing landings recorded in European waters (Engelhard et al., 2010; Ungfors et al., 2013) indicate that there are clearly upper limits to fishing removal. Thus, we consider that highlighting, understanding and monitoring these temporal fluctuations in abundance are fundamental for reliable stock assessment. This leads us to answer questions such as: what are the patterns in stock fluctuations? Are they stable, temporary, aperiodic or periodic? Are the stocks subject to structural shifts? Is the abundance sensitive to external events like climate and to what extent? What type of intrinsic regulation could influence variations in abundance? Ultimately, can the dynamics of these systems be described in a reliable way which would allow us to model the fluctuations in a predictive system?

The question of whether catch/landings data are a useful proxy for abundance and the state of the stock is much debated (Hilborn et al., 2013; Pauly, 2013). In our case, we assume that the dynamical processes involved in stock fluctuations are reflected in the successive records of observed landing values and that variations in abundance reflect changes in growth of the population, regardless of environmental and fishery effects. In marine ecology, we rarely have perfect information and usually infer from some form of sub-sampling. In fisheries, scientific surveys are relatively scarce while landings data are more accessible.

Recent predictions of a looming disaster for world fisheries on the basis of catches or

landings time series (Worm et al., 2006; Pauly, 2009) prompted a cascade of reactions: "using catch (the weight of fish taken out of the sea) as a proxy for stock biomass (the weight of fish in the sea) is a major conceptual flaw" (*cit*. in Daan et al., 2011) and "catch trends overestimate the percentage of overexploited and collapsed stocks" (*cit*. in Branch et al., 2011); many fisheries scientists are sceptical of catch based methods to reflect stock status.

These reticences and reproaches (Wilberg et al., 2007; Daan et al., 2011; Branch et al., 2011; Hilborn et al., 2013) relating to the use of data to derive scientific conclusions and policy recommendations have been confronted and countered (*e.g.* Carruthers et al., 2011; Martell et al., 2013; Dick et al., 2011; Froese et al., 2012).

Throughout this thesis, the time series of "the weight of fish taken out of the sea" (*cit.* Daan et al., 2011) is considered to be a useful window providing a distorted image on "the weight of the fish in the sea". Other assumptions, as summarised by Froese et al. (2012) include that "catch cannot be taken from zero biomass, and in most commercial species the annual catch cannot be larger than the average annual biomass". Time series analysis of such data can give insights into the life cycle and behaviour of this species, in addition to the response to fishing. Even though catch data chiefly reflect records of the interaction of the fishery with the biomass, many other mechanisms including regulations (stringent fishery policy, closed areas), political and economic changes, shifts in environmental conditions, as well as endogenous behaviour (physiology and biology) contribute to shape the pattern(s) of the time series analysis.

In the case of *Nephrops norvegicus*, the use of this type of data is not without difficulties and for many reasons. In particular, there is a marked sex ratio bias in the catches related to biological features, early cohort stages are missing due to mesh size restrictions in the trawls and the degree of discarding overlays a tranche of uncertainty. Thus, from the start, the catches provide only a limited overview of the state of the exploited stocks.

Aims of this Chapter

A suite of statistical approaches was used to address a number of fundamental questions relating to abundance, the impact of fishing and climatic influence on *Nephrops* yields in Aran grounds.

A 16-year time series of annual harvests from the main fishing grounds around Ireland was used to explore the underlying dynamics of *Nephrops* population allowing to contextualise the current level of abundance for Aran grounds stock (state space, ols-cusum, ols-mosum). Fluctuations in the trends in terms of amplitude and duration, presence of structural breaks, frequency of outliers appear to be area specific, emphasising the ecosystem differences between fishing zone and sensitivity of *Nephrops* population to the fishing pressure.

Analysis of the relationships between the current observed value of lpue and its past ones suggested specific density dependence regulation (and potentially delay dependence form) for each stock and pinpointed the fishers behaviour adaptation to animal biology life time fluctuations (sarima).

By encompassing the landings time series of the main harvested areas (DFA) we examined the appropriateness of the functional unit of management used by ICES.

The potential influence of explanatory variables such as the North Atlantic Oscillation, Arctic Oscillation and Atlantic Multi-Decadal Oscillation indices on landings indicated contrasting leverage effect over areas (ccf, DFA).

Finally, the predictive capability of our time series analysis proved to be an effective mean for monitoring annual commercial landings by identifying departures from the average dynamical pattern of the captures (state space, sarima).

Materials and Methods

The landings and effort data are based on logbook data for the main fishing areas: FU15 (West Irish Sea), FU16 (Porcupine Bank), FU17 (Aran grounds), FU22 (Smalls) and are contingent on the accuracy of these data.

Since 1989, landings statistics for the Irish fleet were obtained from EU logbooks. Since 1995, vessels record daily retained catches and make a declaration of total landings (weight) on return to port. Irish fishing effort data are in hours of trawling for the Irish otter trawl *Nephrops* directed fleet and a threshold of 30% (in weight) of *Nephrops* in reported landings by trip is used to identify the landings and effort of this fleet (ICES WGCSE, 2010, 2017).

(I) Population abundance

A priori, we know very little about the underlying dynamics of the landings time series. The targeted population is continuously influenced at different temporal and spatial scales by various abiotic and biotic factors. As disentangling signals of increases or decreases in abundance is the primary task and the sample of successive observed fisheries data are regarded as representative of "true" abundance of the population, in addition to stochastic processes. Thus, the objective is to estimate the signal(s) of interest despite the presence of noise:

$$\text{Observation}_t = \text{Signal}_t + \text{Noise}_t$$

And because no phenomenon is fully deterministic, the noise is where different types of errors and uncertainty are amassed.

(I.1) State space approach

(Commandeur and Koopman, 2007; Durbin and Koopman, 2012)

The state space technique allows the operator to envisage putative underlying dynamics of the observed time series including season(s) (stochastic harmonics of varying frequencies) and/or trends (stochastic polynomials) that are indicative of the time scale response(s) of the stock.

Here, the signal(s) is explicitly assumed as a linear combination of a set of components called state variables which constitute the state vector (α_t) that describes the state of

the system at time *t*.

In this study, for each of the four areas (Aran grounds, Irish Sea, Smalls, and Porcupine Bank) the relevant state variables take the form of a stochastic intercept (or trend level) denoted μ_t augmented by a seasonal term γ_t. Note that the seasonal component is expressed in terms of harmonics, that is to say, a Fourier series that decomposes the periodic signal into the sum of a set of simple oscillating functions, namely sines and cosines ($j = 0,1\ldots,6$ accounting for the monthly data).

Then, the main purpose of the state space analysis is to infer $\alpha_t = \begin{pmatrix}\mu_t \\ \gamma_t\end{pmatrix}$ from a knowledge of the observations $y_1, \ldots, y_n$. In other words, we want to estimate the dynamics of the state α_t vectors which cannot be observed directly. Thus, this evolving system is determined by an unobserved series of state vectors (α_t) with which are associated a series of observations y_t.

This relationship is specified by the general linear gaussian state space system of equations:

(1) $y_t = Z_t\alpha_t + \varepsilon_t$ *observation equation*

(2) $\alpha_{t+1} = T_t\alpha_t + R_t\eta_t$ *state equation*

where Z_t relates linearly, the observations to the state variables. T_t the transition matrix, designs the linear combination of the "hidden" state components and R_t the selection matrix, allows stochasticity of any selected state variables by supplementing it with disturbance terms also called noise, denoted ε_t , η_t .

Note that $\varepsilon_t \sim N(0, H_t)$, $\eta_t \sim N(0, Q_t)$ and the initial state vector $\alpha_1 \sim N(a_1, P_1)$ are independent of each other.

The main goal of the state space modelling is to gain knowledge of the latent states α given the observations y . This is achieved by using two important recursive algorithms, the Kalman filter and smoothing.

From the Kalman filter algorithm we obtain the one-step-ahead predictions $a_{t+1} = E(\alpha_{t+1} / y_t, \ldots, y_1)$ the prediction errors $v_t = y_t - Z_t a_t$ and the related covariance matrices: $P_{t+1} = VAR(\alpha_{t+1} / y_t, \ldots, y_1)$ and $F_t = VAR(v_t) = Z_t P_t Z_t^T + H_t$.

Using the results of the Kalman filtering outputs above, the smoothing Kalman algorithm runs backwards in time providing the smoothed state estimation of

$\alpha_t, \ldots, \alpha_1$ given the entire sample of observations $y_t, \ldots, y_1$ noted $\hat{\alpha}_t = E(\alpha_t / y_n, \ldots, y_1)$ and its smoothed state variance $V_t = VAR(\alpha_t / y_n, \ldots, y_1)$.
Similar smoothed estimates can also be computed for the disturbance terms ε_t and η_t , and straightforwardly for the signal $\theta_t = Z_t \alpha_t$.
Collectively, this state space equations system allows us to estimate α_t when a new observation becomes available (via the observation equation) and to predict how it changes through time (via the state equation). The Kalman and Smooth filters are the empirical routines for doing this.

Poisson distributions for the landing time series

In this study, we also explore modelling the available landings per unit effort (lpues) lpues time series on the basis of the state space modelling with a *Poisson* distribution, in view of the 12 month period where the level of landings vary and are marked by the arrival and withdrawal of *Nephrops* females, associated with behavioural traits such as hatching, mating, spawning and burrowing of berried females.
In this case of non-Gaussian state space, the state equation is as in the Gaussian case, but the observation equation has the form $p(y_t / \theta_t) = p(y_t / Z_t \alpha_t)$ where $\theta_t = Z_t \alpha_t$ is the signal and $p(y_t / \theta_t)$ is the observational density. The signal θ_t is the linear predictor which is connected to the expected value $E(y_t) = \mu_t$ via a link function noted $l(\mu_t) = \theta_t$.
A *Poisson* distribution case with intensity λ_t and exposure u_t together lead to a log-link form $\theta_t = \log(\lambda_t)$ and hence $E(y_t / \theta_t) = VAR(y_t / \theta_t) = u_t e^{\theta_t}$.
The Gaussian distribution with mean μ_t and variance u_t results in $\theta_t = \mu_t$.

Outliers and structural breaks

Time series data often undergo sudden changes that affect the dynamics of the data either temporarily or permanently. New fishing regulations, exceptional natural phenomena or changes in fishing effort are some examples of events that may alter the overall dynamics of the population abundance. Therefore, the detection of outliers and structural breaks allows us to get closer to stock dynamics by illustrating how the stock behaves in response to known or unknown perturbation sources.

Thus, $\frac{\hat{\varepsilon}}{\sqrt{(Var(\hat{\varepsilon}))}}$ and $\frac{\hat{\eta}}{\sqrt{(Var(\hat{\eta}))}}$ the smoothed observation and state disturbance estimates of the disturbance terms (ε and η) given all the observations $y_1, \ldots, y_n$ are used to detect outliers and structural breaks.

Large decreases or increases are detected using both limits values of ±1.96 (~2) and ±3.65 corresponding to a two-tailed *t-test* and *Bonferroni test* at 5% and n=192 respectively.

(I.2) Ols-Cusum and Ols-Mosum

The ols-cusum and ols-mosum alternative methods to the state space approach allows to examine the trajectory of the landings series directly from landing values without the need, this time, to build a model. The charts derived from the both techniques can be considered to reflect the growth rate of the population, acknowledging the inherent issues of using landings data as a proxy for the *Nephrops* fluctuations.

We have used two approaches to identify structural changes in the data (following Zeileis et al., 2002; Zeileis et al., 2006; Zeileis et al., 2010; Zeileis et al., 2012).

First, the ols-cusum, involving the cumulative sum of the ordinary least square (ols) standardised residuals:

$W_n^0(t) = \frac{1}{\hat{\sigma}\sqrt{n}} \sum_{i=1}^{nt} \hat{u}_i \quad (0 \leqslant t \leqslant 1)$ (*i.e.* the empirical fluctuation process) with $\hat{u}_i = y_i - x_i^T \hat{\beta}^{(n)}$ where $\hat{\beta}^{(n)}$ is the ols estimate based on all observations and $\hat{\sigma}^2 = \frac{1}{n-k} \sum_{i=1}^{n} \hat{u}_i^2$.

Second, instead of the cumulative sum of all residuals, the ols-mosum requires a fixed number whose bandwidth is *a priori* determined via the parameter $h \in (0,1)$. This window is moved over the whole sample period. The resulting empirical fluctuation process (noted $\mathrm{efp}(t)$) is

$M_n^0(t|h) = \frac{1}{\hat{\sigma}\sqrt{n}} \sum_{i=\lfloor N_n t \rfloor^* + 1}^{\lfloor N_n t \rfloor^* + h} \hat{u}_i \quad (0 \leqslant t \leqslant 1-h)$ where $N_n = (n - \lfloor nh \rfloor^*)/(1-h)$ [6].

For these one-dimensional residual-based empirical processes $W_n^0(t)$ and $M_n^0(t|h)$ the limiting processes follow a brownian bridge distribution and therefore boundaries

6 $\lfloor \rfloor^*$ stands for the integer part of its content.

can be computed.

Thus, the explicit significance is that if $\mathrm{efp}(t)$ path crosses these boundaries ($\pm b(t)$) then the fluctuation is improbably large and hence the null hypothesis, Ho, of "no structural change" should be rejected at a significance level[7] $\alpha = 0.05$. . Note that, for the confidence band for the brownian bridge process, the percentiles of the least upper bound of the brownian bridge have been tabulated (Schumacher, 1984) yielding the value 1.3581 for $\alpha = 0.05$.

(I.3) Forecasting

Forecasting is what the whole procedure is designed to accomplish. Forecasts are useful not only because they provide information on future developments based on the past, but also because they make it possible to investigate whether data that becomes newly available in a series behaves according to expectations.

(I.3.a) Forecasting with state space

(Commandeur and Koopman, 2007)

In state space methods computing forecasts consists of continuing the Kalman filter after the end of the observed time series. The predictions are based on all available observations given by user.

(I.3.b) Forecasting with Box-Jenkins

(Cryer et al., 2008)

Although mainly relying on the state space modelling to identify patterns of population abundance from lpue data, the Box and Jenkins methodology provides a useful alternative for comparisons and as a tool to challenge results. In the Box-Jenkins modelling approach (Box and Jenkins, 1970; Box, Jenkins, and Reinsel, 1996), the current observed lpue time series is represented by a linear combination of the *p* most

7 Under this framework (Zeileis & al 2012), the natural boundaries $\pm b(t)$ could be proportional to the standard deviation function of the corresponding brownian bridge motion $b(t) = \lambda\sqrt{t(1-t)}$ where λ determines the confidence level. But the boundaries that are commonly used are linear, because a closed form solution for the crossing probability is known. So the standard boundary equals $b(t)=\lambda$ and it was chosen because it is tangential to $b(t) = \lambda\sqrt{t(1-t)}$ in *t=0.5* (recall that the Brownian Bridge starts in *0* at *t=0* and returns to *0* at *t=1*)

recent past values of itself, *AR(p)*, plus a weighted linear combination of (*q* finite) present and past "innovation" terms, *MA(q)*, that incorporate everything new in the series at time *t* that is not explained by the lpues past values.

The method requires a three-stage procedure (Hyndman, 2001). First, model identification and model selection, making sure that the variables are stationary, identifying seasonality in the dependent series (seasonally differencing it if necessary), and using plots of the autocorrelation and partial autocorrelation functions *(acf and pacf*) of the dependent time series to decide which (if any) autoregressive (*AR*) or moving average (*MA*) component should be used in the model.

Secondly, parameter estimation using computation algorithms available from R CRAN (R Core Team, 2018) to arrive at coefficients that best fit the selected seasonal auto-regressive integrating moving average model noted SARIMA.

And thirdly, statistical diagnostic tools were used to examine whether the estimated model conforms to the specifications of a stationary univariate process (testing serial correlation, homoscedasticity and normality of residuals). Deriving these parameter components of the sarima models is not straightforward and instead requires a try-and-leave procedure.

And, finally, under the procedures framework, the forecasting algebra simply reflects deviations from the mean process. The seasonal auto-regressive moving average model (sarima) does this by exploiting the autocorrelation pattern in the data (see ***Statistical Annexes A***).

(II) Climate influence

The climatic influence in the evolution of all life on Earth is unquestionable. However, the influence of climate is not always readily discernible at all trophic levels and for individual organisms. Here, we investigate the correlation between landings and selected climate indices such as the North Atlantic Oscillation (NAO), the Arctic Oscillation (AO) and the raw version of the Atlantic Multi-Decadal Oscillation. Notice that these time series data are updated regularly, but for the purposes of this study, we used the data updated in January 2015 from National Oceanographic and Atmospheric Administration (NOAA, https://www.noaa.gov).

(II.1) Regional climatic indices

(II.1.a) North Atlantic Oscillations[8]

The NAO refers to changes in atmospheric mass between the Arctic and the subtropical Atlantic, that swings from one phase to another (positive to negative) producing large changes in surface air temperature, winds, storminess and precipitation over the Atlantic as well as the adjacent continents. It affects the ocean through changes in heat content, gyre circulation, mixed layer depth, and salinity (Hurrel et al., 2009).

The Hurrel's NAO station based index is based on the difference of normalised sea level pressures (SLP) between Lisbon, Portugal and Stykkisholmur/Reykjavik, Iceland. Positive values of the NAO index are typically associated with a depression taking a more northerly route across the Atlantic. Stronger than average westerlies are observed over the middle latitudes, and wetter and milder weather occurs over western Europe (with more intense weather systems over the North Atlantic). Inversely, a negative index value corresponds to dryer and cooler weather.

The principal component based indices (PC based) of the NAO are the time series of the leading Empirical Orthogonal Function of SLP anomalies over the Atlantic sector, 20º–80ºN, 90ºW–40ºE. These indices are used to measure the NAO throughout the year, tracking the seasonal movements of the Icelandic low and Azores high. PC based indices are a more optimal representation of the full spatial patterns of the NAO and may be less noisy than the station-based indices. However, the PC based indices are not available as far back as station-based indices and are subject to any inherent weaknesses in the source data set and its gridding scheme. Station-based indices extend back to the mid-19th century or earlier. However, the stations are fixed in space and thus may not track the movement of the NAO centres of action through the annual cycle. In addition, individual station pressure readings can be “noisy” due to small-scale and transient meteorological phenomena unrelated to the NAO.

In case of the NAO data obtained from NOAA, the procedure used to calculate the Northern Hemisphere teleconnection indices is based on the Rotated Principal

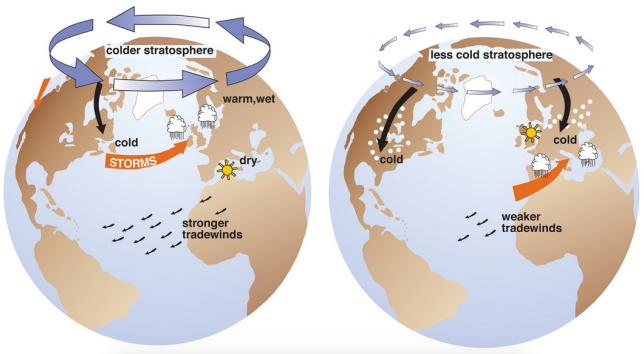
8 See Hurrell, James & National Center for Atmospheric Research Staff (Eds). Last modified 04 Aug 2018. “The Climate Data Guide: Hurrell North Atlantic Oscillation (NAO) Index (station-based).” Retrieved from https://climatedataguide.ucar.edu/climate-data/hurrell-north-atlantic-oscillation-nao-index-station-based.

Component Analysis used by Barnston and Livezey (1987). In addition, the indices are normalized using the 1981-2010 base period monthly means and standard deviations (see, https://www.cpc.ncep.noaa.gov/products/ precip/CWlink/pna/nao.shtml).

(II.1.b) Arctic Oscillation

The AO is a large-scale mode of climate variability, also referred to as the Northern (Hemisphere) annular mode (NAM). It is thought to explain on the order of about 20–30% of the total variance in the geopotential height and wind fields (Thompson, 2016), and in particular 23% of the extended winter mean (December-March) variance (Dec-Jan-Feb-Mar sea level pressure anomalies over the Atlantic sector; Hurrel, 2018). The AO index, according to Deser et al. (2000) describes the "relative intensity of a semi permanent, low-pressure centre over the North Pole. A band of upper-level winds circulates around this centre, forming a vortex.

As schematised (below) by Wallace (2000)[9] when the AO index is positive (left) and the vortex is intense, the winds tighten around the north pole, locking cold air in place (left).



A negative AO and weak vortex (right) allows intrusions of cold air to plunge southward into Europe. The NAO is considered a close relative of the AO and there are discussions about which index is more fundamentally representative of the atmosphere's dynamics (Deser et al., 2000; Wallace, 2000; Ambaum et al., 2001). Note that the indices are normalised by the standard deviation of the monthly index of the base period 1979-2000 (NOAA, http://www.Cpc.Ncep.Noaa.gov/products/precip/CWlink/daily_ao_index/ao.shtml).

9 Professor Emeritus, Department of Atmospheric sciences University of Washington, United state of America

(II.1.c) Atlantic Multi-Decadal Oscillations

The effect of sea temperature is important for the development and succession of larval stages of *Nephrops* and subsequently on recruitment (*e.g.* Briggs et al., 2002; Dickey-Collas et al., 2000a).

The Atlantic-Multi-Decadal-Oscillation is an index of long-term sea surface temperatures (SST) in the North Atlantic Ocean with cool and warm phases. The time series created are a smoothed version (noted AMDO in this study) and an unsmoothed version (noted unAMDO). Data were detrended from the Kaplan SST V2 (Kaplan SST V2 data are provided by the NOAA/OAR/ESRL PSD, Boulder, Colorado, USA, at https://www.esrl.noaa.gov/psd. See also NOAA's website for computational details and references at http://www.esrl.noaa.gov/psd/data/timeseries/AMO/ and http://ingrid.ldeo.columbia.edu/SOURCES/.KAPLAN/.EXTENDED/.v2/.ssta). Notice that the anomalies are based on the 1951–1980 time period.

(II.2) Detection of climate influence(s)

We examined the influence of NAO, AO, and AMDO on landings via the cross correlation function (ccf) method and dynamic factor analysis (DFA).

(II.2.a) Cross correlation function (ccf)

In order to avoid spurious cross correlation between the response variable Y_t (here lpues) and the covariates X_t (here, NAO, AO, AMDO) we computed ccf of the differenced lpues and climate indices denoted $\tilde{Y}_t = Y_t - Y_{t-1}$ and $\tilde{X}_t = X_t - X_{t-1}$ respectively.

The formula of the (sample) cross correlation function (ccf) is:

$$r_k(\tilde{Y}, \tilde{X}) = \frac{\sum (\tilde{X}_t - \bar{\tilde{X}})(\tilde{Y}_{t-k} - \bar{\tilde{Y}})}{\sqrt{\sum (\tilde{X}_t - \bar{\tilde{X}})^2}\sqrt{\sum (\tilde{Y}_t - \bar{\tilde{Y}})^2}} \quad \text{at all time lags} \quad k: 0, \pm 1, \pm 2, \pm 3, \ldots$$

although we are interested in the $k \leqslant 0$ ones reflecting the fact that $\tilde{X}$ is leading $\tilde{Y}$ by k units of time.

Sample cross-correlations peaks that are larger than $\pm 1.96/\sqrt{n = 192}$ in magnitude are then deemed significantly different from zero. However, possible false alarms[10] are

10 The number of false alarms is equal to *0.05* x number of cross correlation pairs (*=2.03*). Note, that the default maximum lags, at either left or right axis, as computed by the R software is *lag.max=10* x

also plausible (2.03, on average).

(II.2.b) Dynamic factor analysis (DFA)

DFA provides an opportunity to assess dynamic patterns in *Nephrops* landings around Ireland and to measure the climatic influence on the patterns. The spatial continuity of the waters of interest suggests that there is a high likelihood of intertwined fishing activity, which is fundamental to the question from the perspective of a "global" *Nephrops* fishery management.

Following the specific parameter constraints to ensure identifiability (Harvey, 1989; Zuur et al., 2003; Holmes et al., 2012 cited in Holmes et al., 2018a) the model is

$$(1)\quad \alpha_{t+1} = B\,\alpha_t + w_t \qquad w_t \sim MVN(0, I) \qquad state\ \ equation$$
$$(2)\quad y_t = Z\,\alpha_t + v_t \qquad v_t \sim MVN(0, R_t) \qquad observation\ \ equation$$

When needed, our selected environmental covariate(s) and effect(s) on the observations are all contained in d_t and D_t respectively, leading to slight modifications of the equation (2) of the model above:

$$(1)\quad \alpha_t = B\,\alpha_{t-1} + w_t \qquad w_t \sim MVN(0, Q_t)$$
$$(2)\quad y_t = Z\,\alpha_t + D_t\,d_t + v_t \qquad v_t \sim MVN(0, R_t)$$

Instead of the original lpues data series the already computed state levels for each zone noted L_A, L_S, L_P, L_I, are used and plugged into the DFA modelling framework to assess common trends.

Additionally, we substituted the atmospheric oscillation time series NAO and AO for their respective smoothed state space level while including the unsmoothed AMDO (from NOAA) directly.

The crucial difference with the univariate state space method is illustrated by the presence of the loading factors matrix (Z matrix) that counts for the underlying specified trends (α_1 and α_2):

$$\begin{bmatrix} L_A \\ L_S \\ L_P \\ L_I \end{bmatrix}_t = \begin{bmatrix} z_{A1} & 0 \\ z_{S1} & z_{S2} \\ z_{P1} & z_{P2} \\ z_{I1} & z_{I2} \end{bmatrix} \begin{bmatrix} \alpha_1 \\ \alpha_2 \end{bmatrix}_t + \begin{bmatrix} v_1 \\ v_2 \\ v_3 \\ v_4 \end{bmatrix}_t$$

with diagonal and equal covariance of observation error as the following

log10(N/m) with N the length of the observations and m the number of the series.

$$\begin{bmatrix} v_1 \\ v_2 \\ v_3 \\ v_4 \end{bmatrix}_t \sim MVN\left(\begin{bmatrix} 0 \\ 0 \\ 0 \\ 0 \end{bmatrix}, \begin{bmatrix} r & 0 & 0 & 0 \\ 0 & r & 0 & 0 \\ 0 & 0 & r & 0 \\ 0 & 0 & 0 & r \end{bmatrix}\right) .$$

Once again, the optimal (lowest mean square error) estimate of the unobserved states based on the observed data up to time (t) and the expected value of the hidden states conditioned on all the data are delivered by the Kalman-Filter-Smoother algorithm (Holmes et al., 2018a, 2018b).

Notice that a statistical addendum encompassing state space modelling and seasonal auto-regressive moving average algebra as well as list of additional tool definitions used for our time series analysis is provided in ***Statistical Annexes A***.

Throughout this study, the statistical analysis was performed using R (2018) software tools (Zeileis et al., 2002; Hyndman et al., 2008; Helske, 2010; Wickham et al., 2016; Helske, 2017; Chan, and Ripley, 2018; Holmes et al., 2018b; Hyndman et al., 2019; Stoffer, 2020).

Results

(I) From observations to analysis

Monthly observed Irish vessel landings per unit of effort (Kg/hours) from 1995 to 2010 were used in the time series analysis to determine patterns. For the four different fishing areas, the chronological sequence of annual lpue (Kg/hours) can be seen as a succession of peaks and troughs (**Figure 1.1**).

(a)

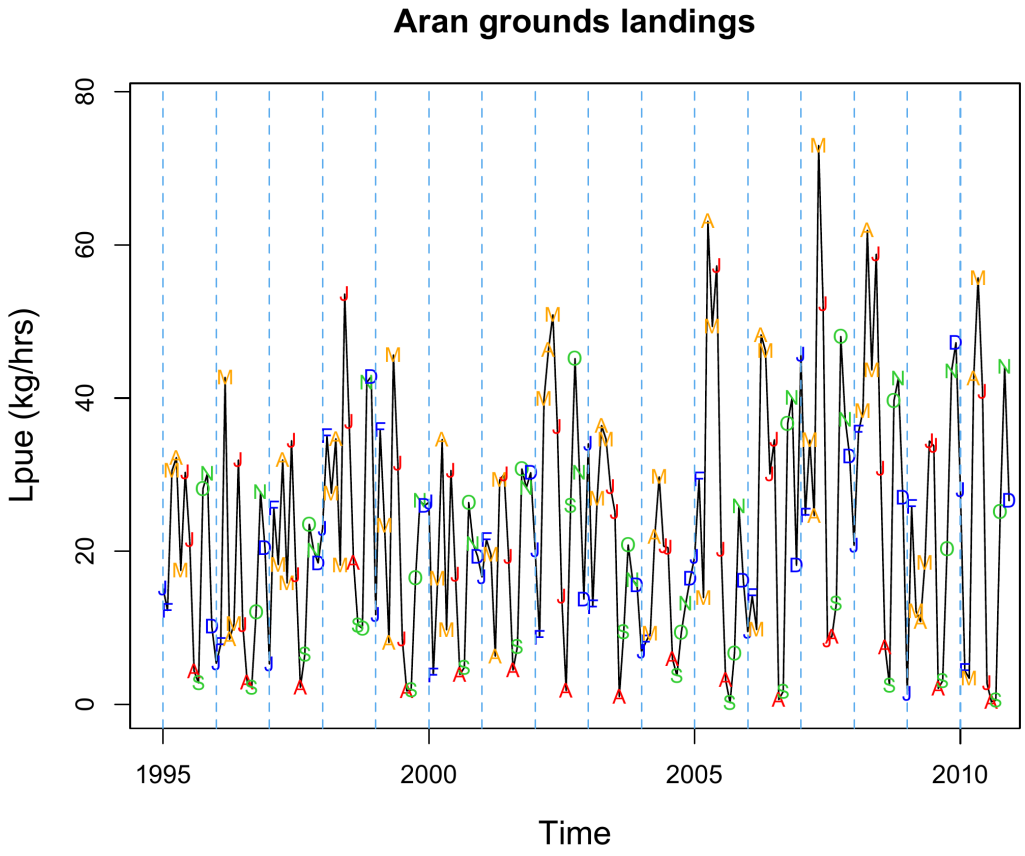


Figure 1.1a: Time series of monthly landings per unit of efforts (lpue, Kg/hours) from January 1995 to December 2010 for Aran grounds (FU17).

(b)

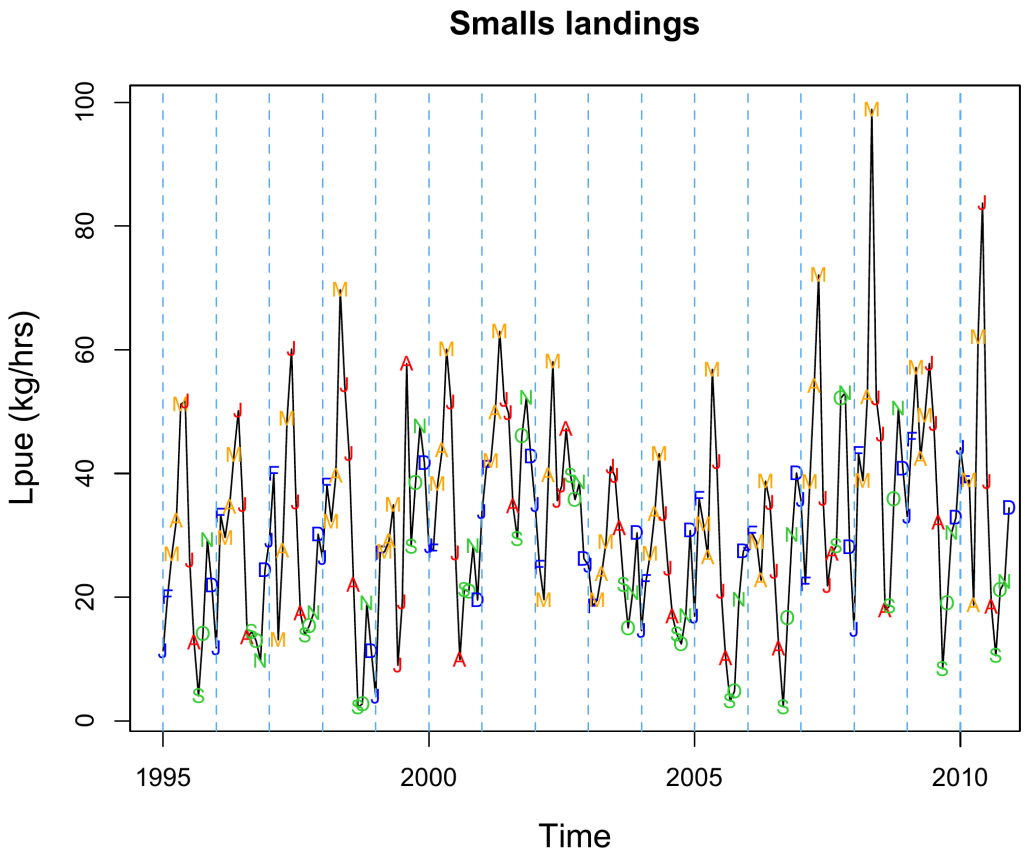


Figure 1.1b: Time series of monthly landings per unit of efforts (lpue, Kg/hours) from January 1995 to December 2010 for (**b**) Smalls (FU22).

(c)

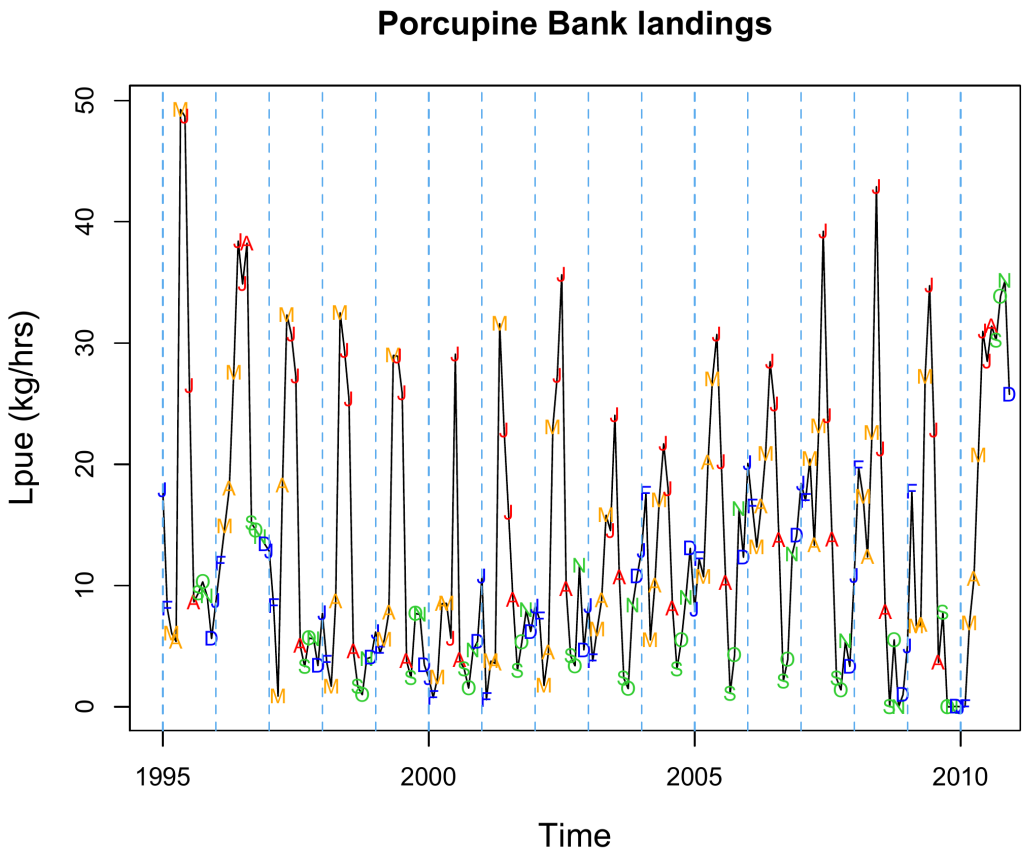


Figure 1.1c: Time series of monthly landings per unit of efforts (lpue, Kg/hours) from January 1995 to December 2010 for Porcupine Bank (FU 16).

(d)

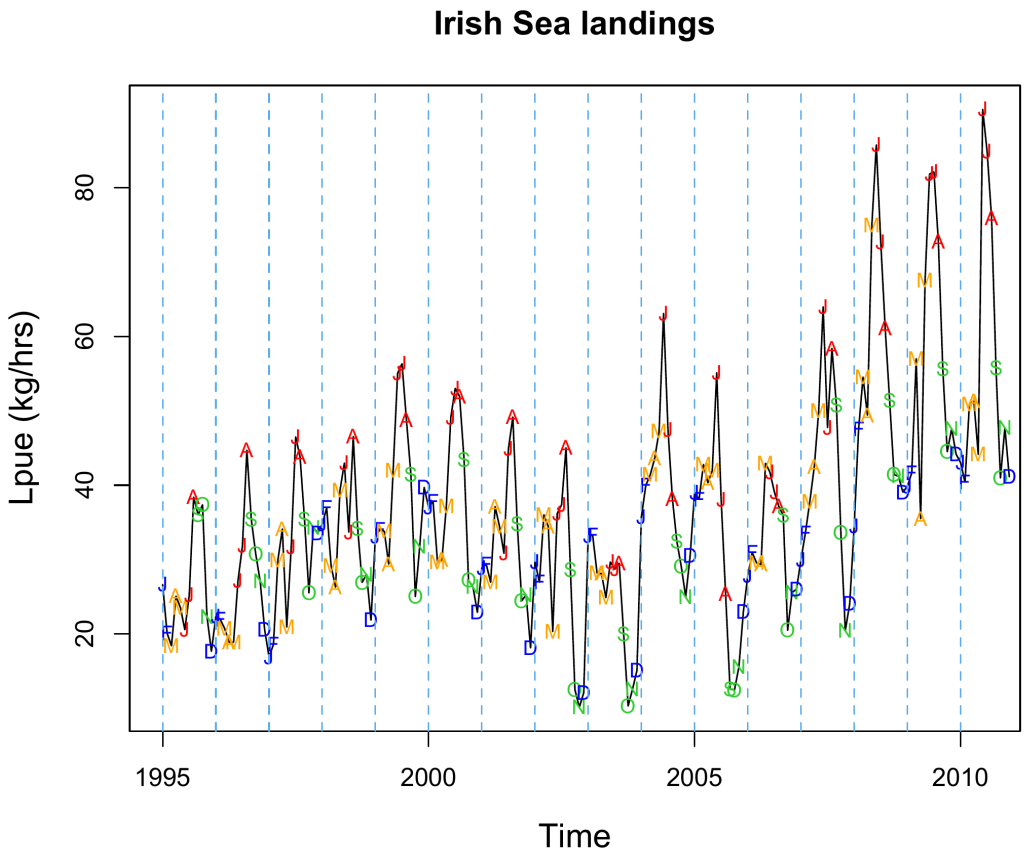


Figure 1.1d: Time series of monthly landings per unit of efforts (lpue, Kg/hours) from January 1995 to December 2010 for western Irish Sea (FU15).

Although the landing time series is an indication of the timing in fishing activity and the relative weight of the harvested quantity per zone, these data are somewhat limited. Monthly lpue values averaged over 16 years (16 x 12 calendar months) for each FU are displayed according to the recorded landings (**Figure 1.2**)

From 1995 to 2010, Aran grounds exhibits two obvious periods of high levels of capture in Spring (April-May-June) and Autumn (Oct-Nov-Dec), and is also marked by important inter-annual variability in the amounts caught (**Figure 1.2a**).

(a)

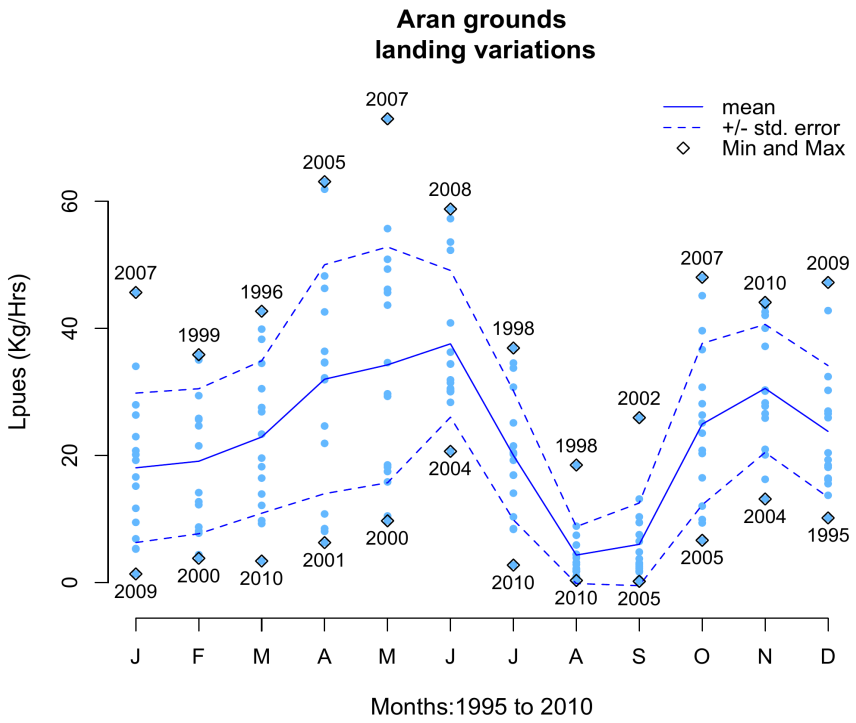


Figure 1.2a: Average Aran grounds (FU17) monthly lpue (Kg/hours) time series from January 1995 to December 2010. Monthly observed capture values are re-distributed vertically. Year occurrence of the minimum and maximum landings are indicated.

On average, for the Smalls**,** increased catches are recorded in Spring (Apr-May-June) and Autumn (Oct-Nov-Dec; **Figure 1.2b**). In contrast to Aran grounds, the vertical distribution of the monthly values (that is, inter-annual variability) is narrower and the standard error intervals to the mean catch encompass almost the whole variability of these 192 monthly values, underlying the very low number of outliers, particularly during the Spring and Autumn.

(b)

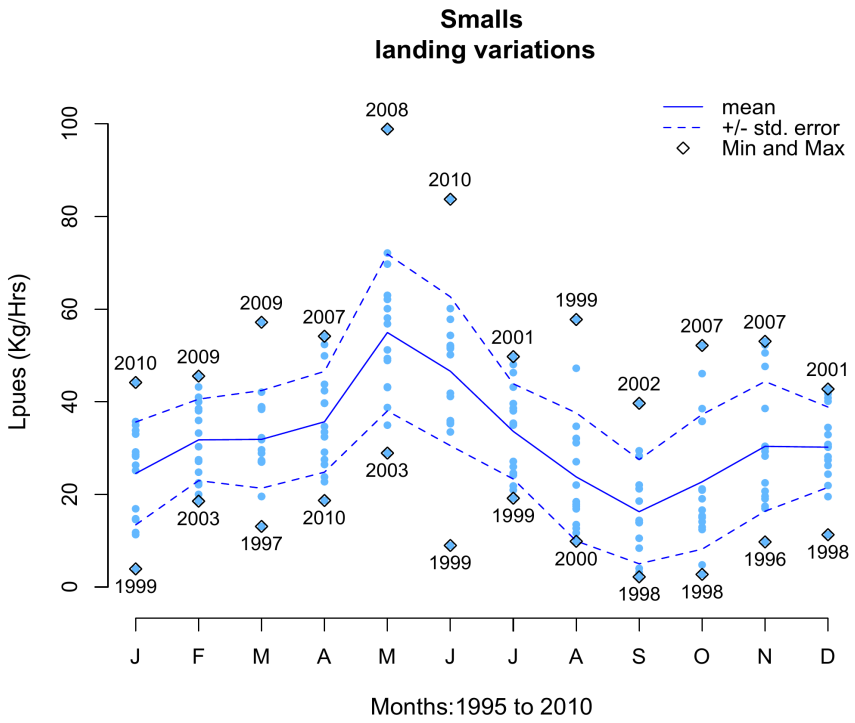


Figure 1.2b: Average Smalls (FU22) monthly lpue (Kg/hours) time series from January 1995 to December 2010. Monthly observed capture values are re-distributed vertically. Year occurrence of the minimum and maximum landings are indicated.

For the Porcupine Bank, over the same period, the yield pattern is dominated by a unique Gaussian bell shape in place in Summer, three times greater than the rest of the year (**Figure 1.2c**).

(c)

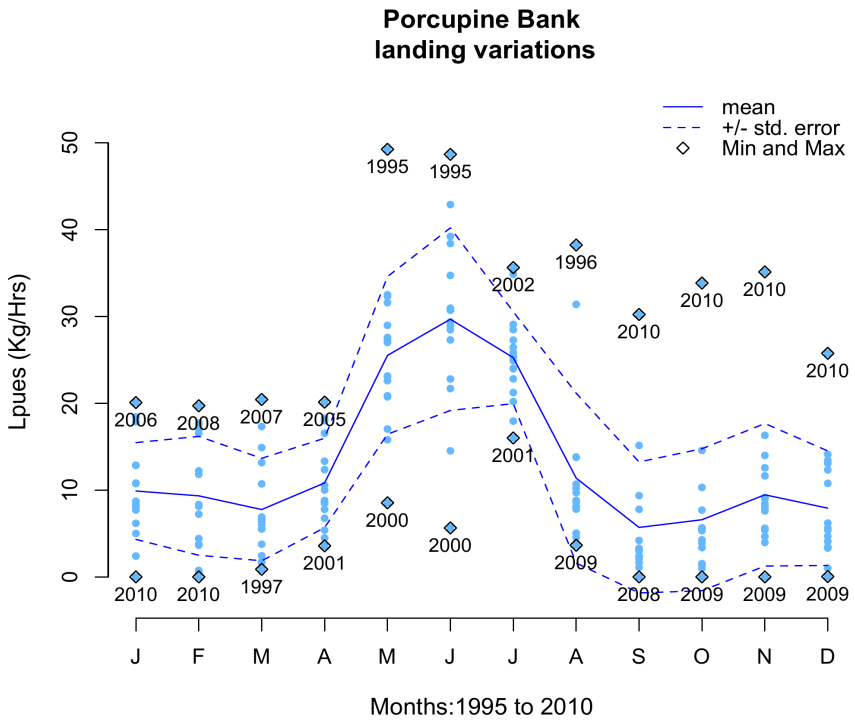


Figure 1.2c: Average Porcupine Bank (FU16) monthly lpue (Kg/hours) time series from January 1995 to December 2010. Monthly observed capture values are re-distributed vertically. Year occurrence of the minimum and maximum landings are indicated.

The Irish Sea pattern of the average captures is relatively constant and sustained throughout the years with a distinct Summer elevation (May-June-July; **Figure 1.2d**). It is noteworthy that only Aran grounds features an off-peak season (Aug-Sep).

(d)

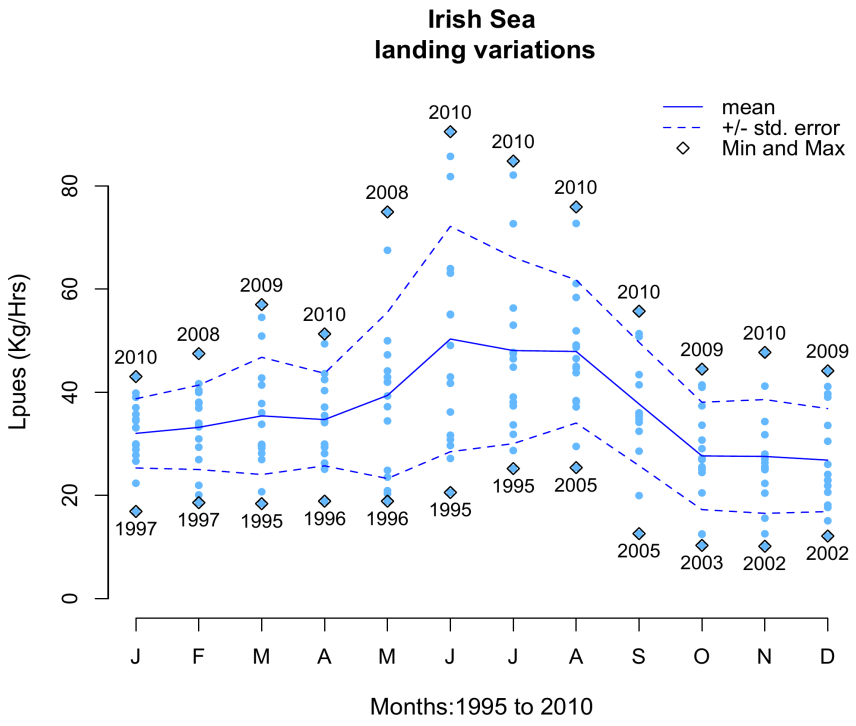


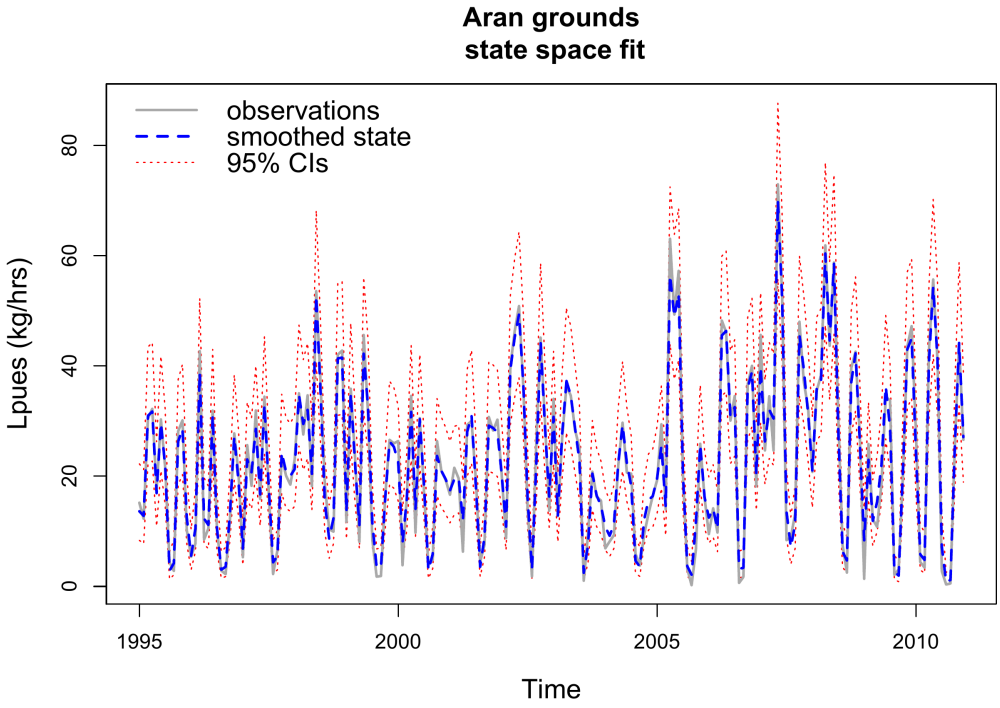
Figure 1.2d: Average Irish Sea (FU15) monthly lpue (Kg/hours) time series from January 1995 to December 2010. Monthly observed capture values are re-distributed vertically. Year occurrence of the minimum and maximum landings are indicated.

(I.1) Dynamic structures

Beyond these preliminary observations, additional analyses are required to examine the potential for underlying structures in the lpue dynamics over these 16 years.

The lpue time series were explicitly modelled by means of a stochastic intercept (also called trend level or level) plus a stochastic seasonal component on the basis of a Gaussian state space model for Smalls and Irish Sea and the non-Gaussian state space modelling using a Poisson distribution for the Aran grounds and Porcupine Bank (**Figure 1.3**).

(a)



(b)

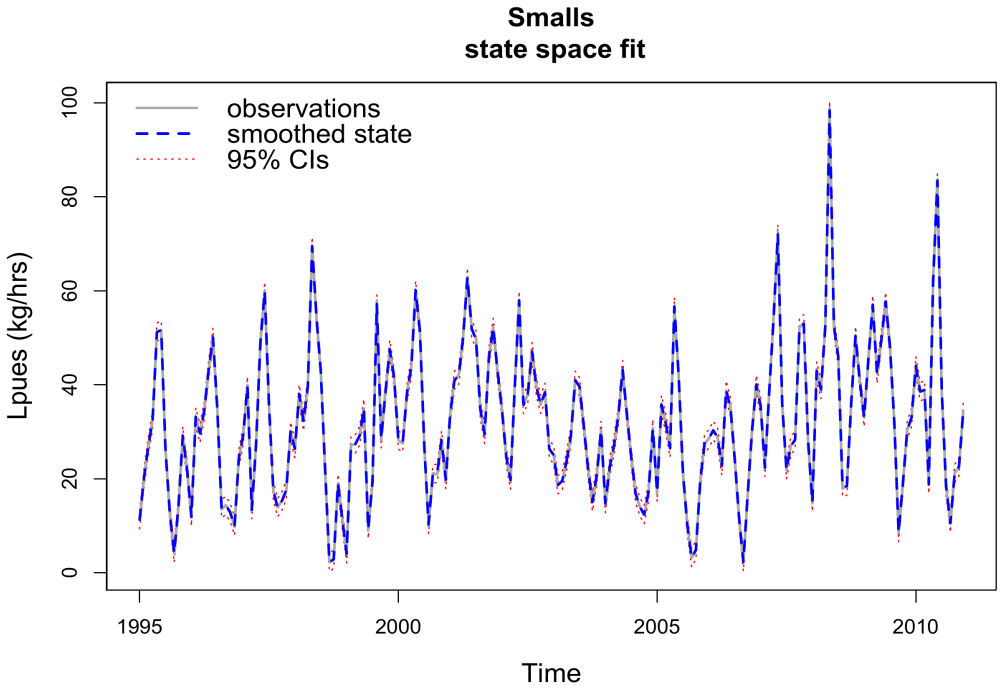
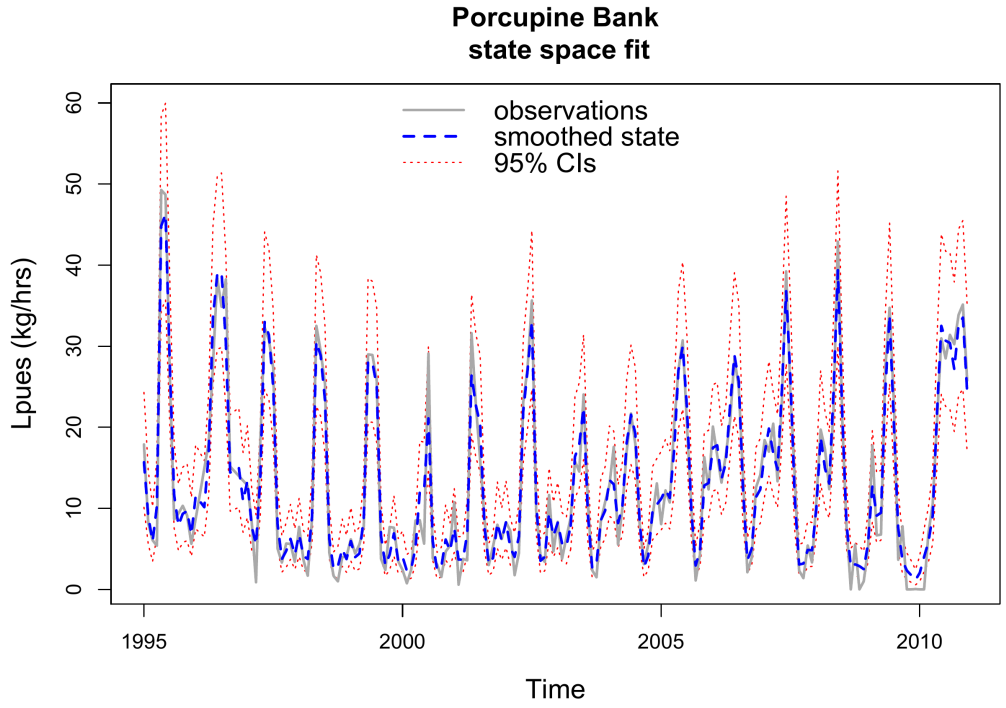


Figure 1.3 a-b: State space model fits of the observed lpue (Kg/hours) times series of (**a**) Aran grounds (FU17) and (**b**) Smalls (FU22) by mean of stochastic level and seasonal component. The 95% confidence interval limits (95% CI) are indicated.

(c)



(d)

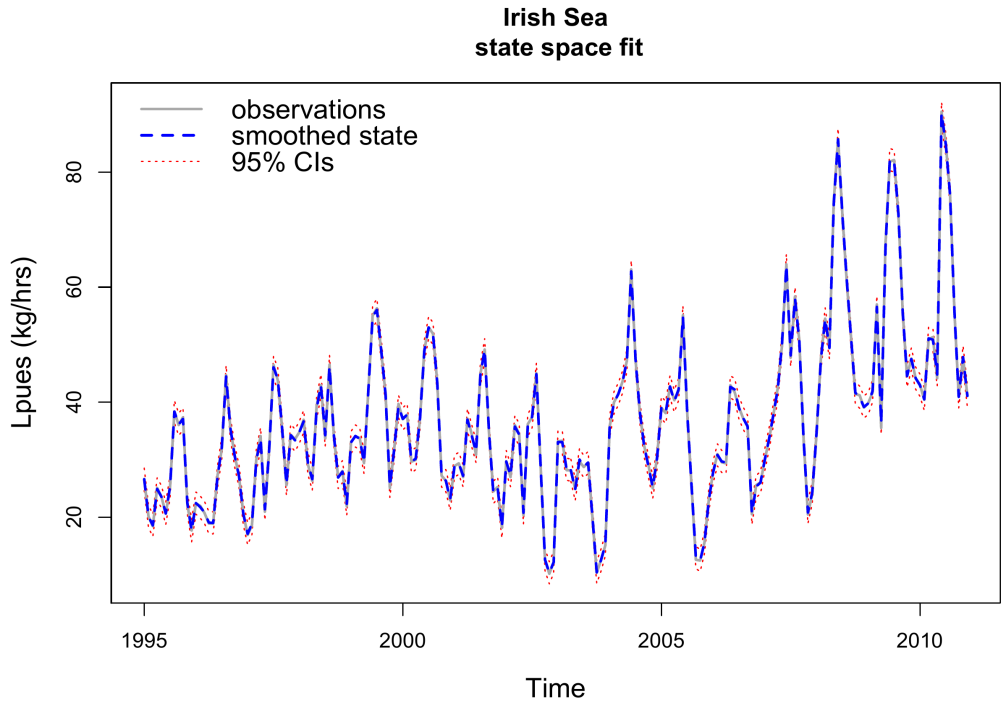


Figure 1.3 c-d: State space model fits of the observed lpue (Kg/hours) times series of (**c**) Porcupine Bank (FU16) and (**d**) western Irish Sea (FU15) by mean of stochastic level and seasonal component. The 95% confidence interval limits (95% CI) are indicated.

Fit diagnostics relied on tests applied to what are known as the standardized one-step-ahead prediction errors or standardised prediction errors. In addition, residuals from the selected models satisfied the important proprieties of independence (serial correlation) and homoscedasticity.

In fact, there is no reason to suspect serial correlation, and hence, the null hypothesis (*Ho*) of independence is not rejected for our models (**Figure 1.4**).

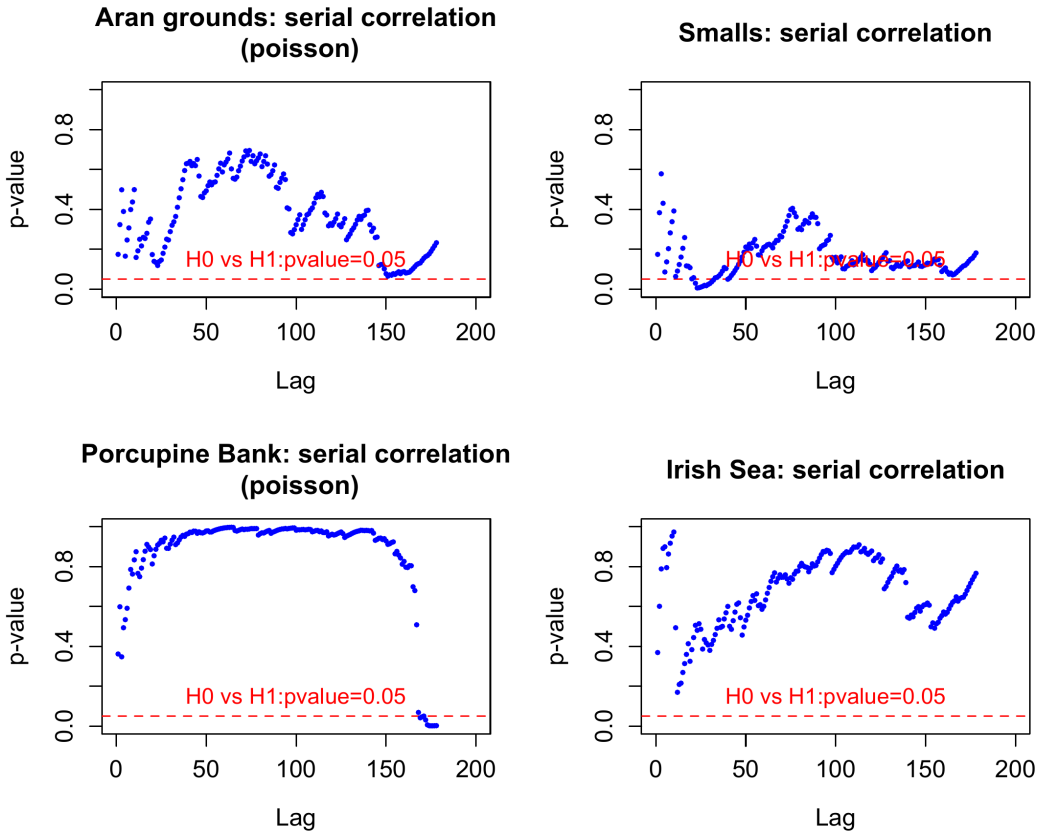


Figure 1.4: Serial correlation values (*Box-Ljung* statistic) of the standardised one-step prediction errors (irregulars) of the selected models corresponding to the Gaussian state space for Smalls and Irish Sea and the Poisson state space (with no importance sampling simulation) for Aran grounds and Porcupine Bank.

The assumption of homoscedasticity of the residuals, was a key factor for sorting between modelling fits (Table 1).

Although the upper ends of the Aran grounds and Porcupine Bank *q-q* plots of the residuals deviate from the *Normal* theoretical straight line (**Figure 1.5a**), observing right (that is, positive) skewness (**Figure 1.5b**), it does not raise undue concern for use

in the following model.

(a)

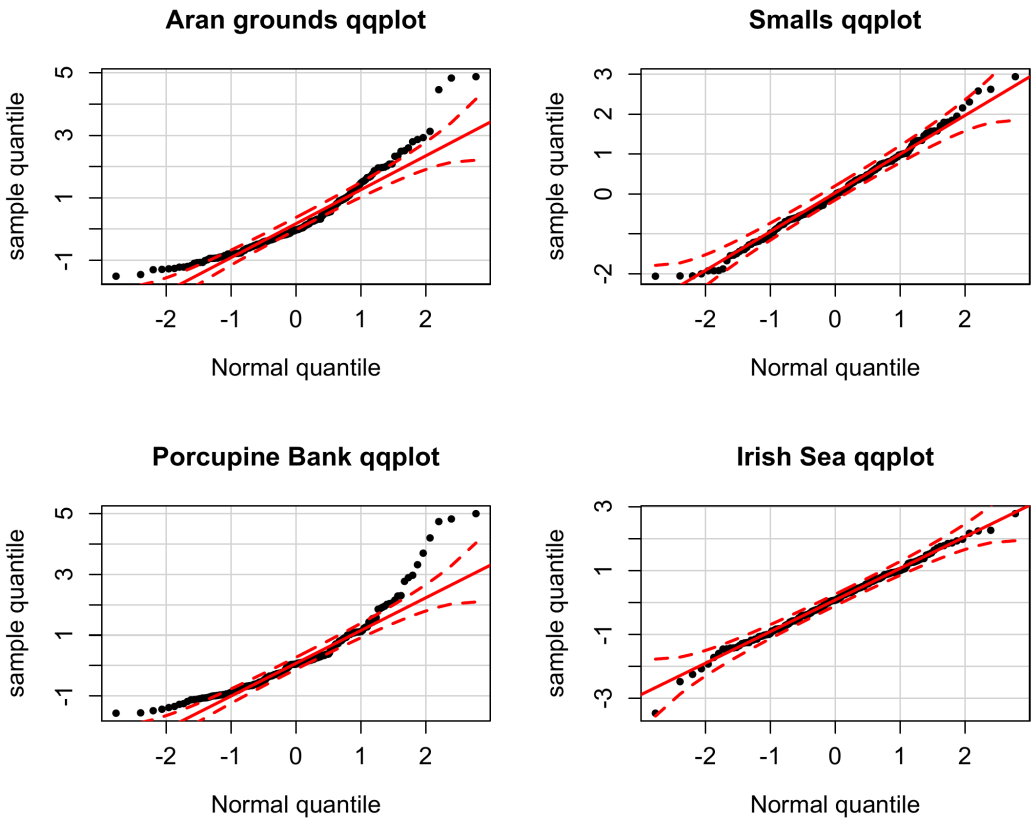


Figure 1.5a: Quantile-quantile plots of the standardised step-ahead prediction errors residuals of the state space modelling. Residuals of Aran grounds and Porcupine Bank are derived from *Poisson* state space modelling while Smalls and Irish Sea residuals stem from *Normal* state space modelling.

(b)

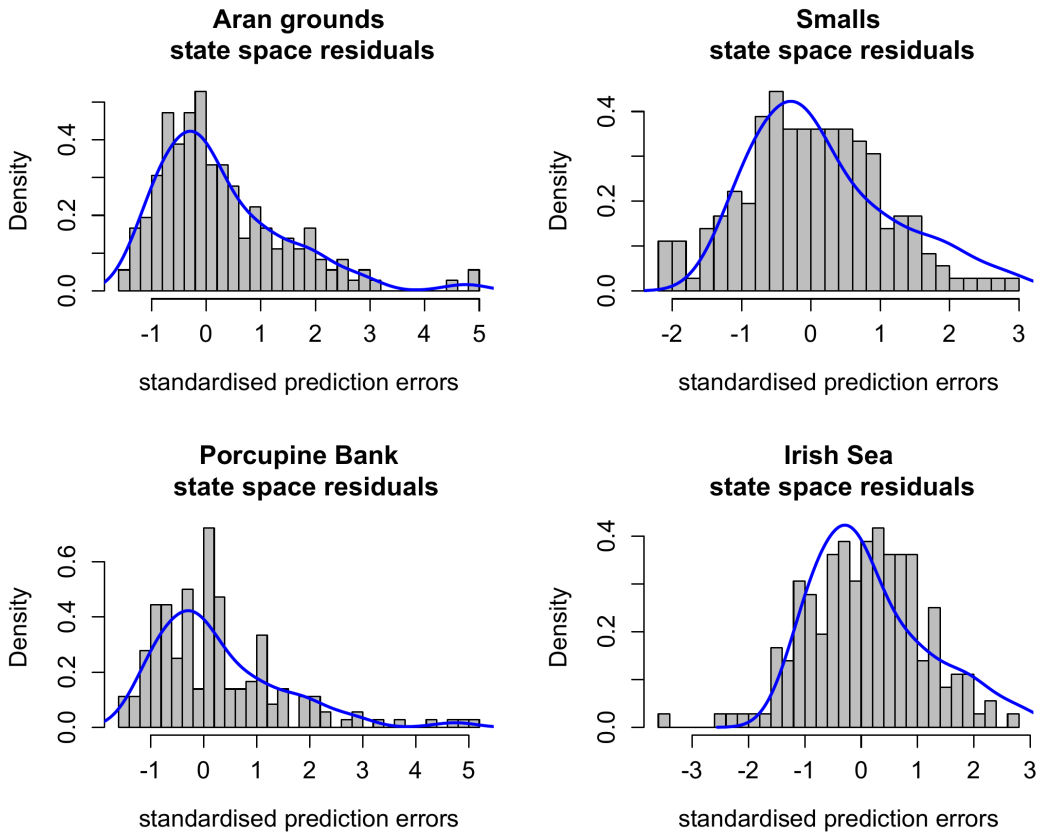


Figure 1.5 a-b: Histograms of the standardised step-ahead prediction errors residuals of the state space modelling. Residuals of Aran grounds and Porcupine Bank are derived from *Poisson* state space modelling while Smalls and Irish Sea residuals stem from *Normal* state space modelling.

Model selection was also made on the basis of other statistics and model outputs summarised in **Table 1.1**.

Table 1.1: Summary statistics used to compare the goodness-of-fit of the state space modelling with *Normal* and *Poisson* distributions for the lpues time series. (**1**) In case of *Poisson* models the smoothed estimates α computed from the conditional density $p(\alpha/y)$ (where y stand for observations) relate to the conditional mean of $p(\alpha/y)$ when using importance sampling simulation, and relate to the conditional mode of the $p(\alpha/y)$ otherwise (that is, no simulation). In the *Normal* case, the mode is also the mean. (**2**) The residuals corresponding to the first 12 values are not plotted in the figure, nor are they used in the diagnostic tests, because they correspond to the 12 diffuse initial state values which need to be estimated for the level and the seasonal (**3**) *MSE*, *MAD*, *MAPE* are for Mean Square Error, Mean Absolute Deviance and Mean Absolute Percentage Error respectively. *THEIL's U* compares the *MSE* of the model with the *MSE* of the trivial "no-change" model that predicts the next observation to be the same as the current one. (**4**) *ACF* and *PACF lags* stand for the number of lags in the *Auto-Correlation* and *Partial Auto-Correlation Functions* respectively, lying out of the boundaries (see **Figures A1** in ***Annexes A*** for retained models). A *two tailed t-test* at *5%* have been used to test the coefficient estimates.

	Aran grounds			**Smalls**		
	Poisson with sampling	Poisson	Normal	Poisson with sampling	Poisson	Normal
MSE	4.7	4.6	0.0	13.2	13.1	0.0
MAD	1.6	1.6	0.0	2.8	2.8	0.1
MAPE	0.2	0.2	0.0	0.1	0.1	0.0
U Theil	0.1	0.1	0.0	0.2	0.2	0.0
ACF lags	1	1	3	1	0	2
PACF lags	3	1	3	2	0	2
Homoscedasticity *(Bartlett test p-value)*	0.8	0.8	0.3	0	0.002	0.87
Significant coefficient	4	5	3	6	7	6
Log-Likelihood	-757	-757	-753	-759	-759	-730

Table 1.1 (continued)

	Porcupine Bank			**Irish Sea**		
	Poisson with sampling	Poisson	Normal	Poisson with sampling	Poisson	Normal
MSE	5.14	5.05	0.05	17.6	17.6	0.04
MAD	1.74	1.72	0.1	3.3	3.3	0.1
MAPE	0.29	0.29	0.1	0.1	0.1	0.0
U Theil	0.24	0.24	0.0	0.4	0.4	0.0
ACF lags	0	0	0	1	1	2
PACF lags	0	0	2	1	1	2
Homoscedasticity *(Bartlett test p-value)*	0.08	0.1	0.2	0.96	0.98	0.14
Significant coefficient	2	3	3	4	4	7
Log-Likelihood	-617	-617	-619	-675	-675	-639

For Smalls, the fundamental assumption of homescedasticity was only fulfilled with a *Gaussian* model while for Aran grounds the *Poisson* modelling increased the number of significant coefficients and led to deleting the *ACF* and *PACF* lag values, that were outlying significantly beyond the confidence limits suggesting possible dependence. For the Porcupine Bank the evaluation is more difficult. While the *Poisson* model performed slightly better in terms of serial correlation (**Figure A2** in ***Annexes A***) than the *Gaussian* one, the number of significant coefficient and *Log-likelihood* values are similar. However, the number of significant *partial correlation lags* are greater with the *Gaussian* model (**Table 1.1**). For the Irish Sea, the number of significant coefficients from *Gaussian* model is almost twice of the *Poisson* models (**Table 1.1**).

(I.1.a) Trend levels

The modelling approach brought to light a number of trends in the observed time series. At first glance, the striking results relates to the Porcupine Bank catches marked by a steep upward trend over 2010 contrasting with the past (**Figure 1.6c**). This “odd” pattern could be connected to the unusually high catch values of autumn-winter 2010 seen in **Figure 1.3c**.

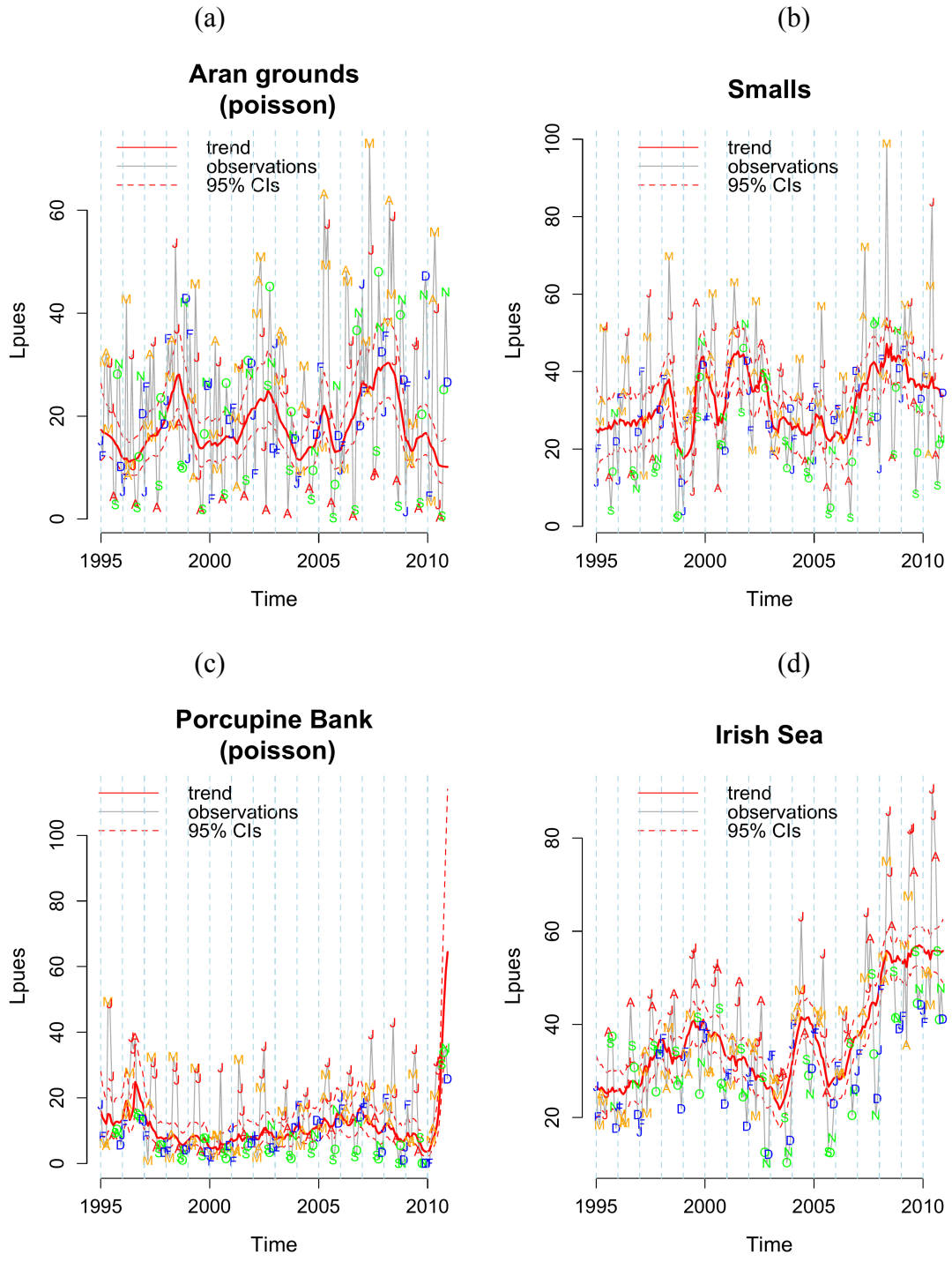


Figure 1.6: Stochastic levels and its 95% confidence interval superimposed to the landing per unit of effort (lpue in Kg/hours) time series. for Aran grounds (FU17), Smalls (FU22), Porcupine Bank (FU16) and Irish Sea (FU15).

The other salient point is the presence of fluctuations in the trends in terms of amplitude and duration. Undoubtedly, the fishing zones are subject to clear sequences of rise and

fall phases followed by flat sequences, suggesting the possibility of cycles at various time scales (**Figure 1.6**, **Table 1.2**).

Table 1.2: Duration of potential cycles for each area derived from the trend levels depicted in **Figure 1.6**. Notice that our trivial definition of a cycle contains an upward and downward branch. And between cycles we have flat sequences. (*) in the case of Smalls, the 2000-2003 cycle is made of successive sub-cycles of about 2 years.

	Aran grounds	**Smalls**(*)	**Porcupine Bank**	**Irish Sea**
Observed cycles	1997 to 2000 2001 to 2003 2004 to 2005 2006 to 2010	1998 to 2003 2007 to 2010 onward	2000 to 2009 2010 onward	1996 to 2003 2004 to 2005 2006 onward

In the context of this study where the time series analyses is a potential way to inform fisheries scientists about the dynamics of the *Nephrops* population, such trends and cycles allow us to contextualise management objectives that would not be the same, depending on whether yield was increasing, stable or declining.
From this perspective, we identified a steady downward trend in catches from 2008 to 2010 for Aran grounds, Smalls (**Figure 1.6a-b**) and earlier (2007) for the Porcupine Bank (**Figure 1.6c**) with the notable exception of 2010 which will be detailed later in the forecasting analysis. In contrast, the Irish Sea exhibited an increase of Lpues from 2006 to 2008 and stabilised at the highest level ever recorded in 16 years (**Figure 1.6d**). We consider the overall trend (**Figure 1.6**) as the longer-running dynamic of the coupled stock-fishing dynamic of the available time series, while, the seasonal element is a short time component
(**Figure 1.7**).

(I.1.b) Seasonal components

The second structure disclosed is the seasonal component that sometimes takes the form of ephemeral switches among neighbouring months or reveals longer time changes in peak occurrence of monthly lpues (**Figure 1.7**). Also of note, for the Porcupine Bank, the 2010's monthly patterns of the seasonal component do not depart from the previous course (**Figure 1.7c**), despite the sudden and singular increase in the catches previously

identified on the trend level component (**Figure 1.6c**).

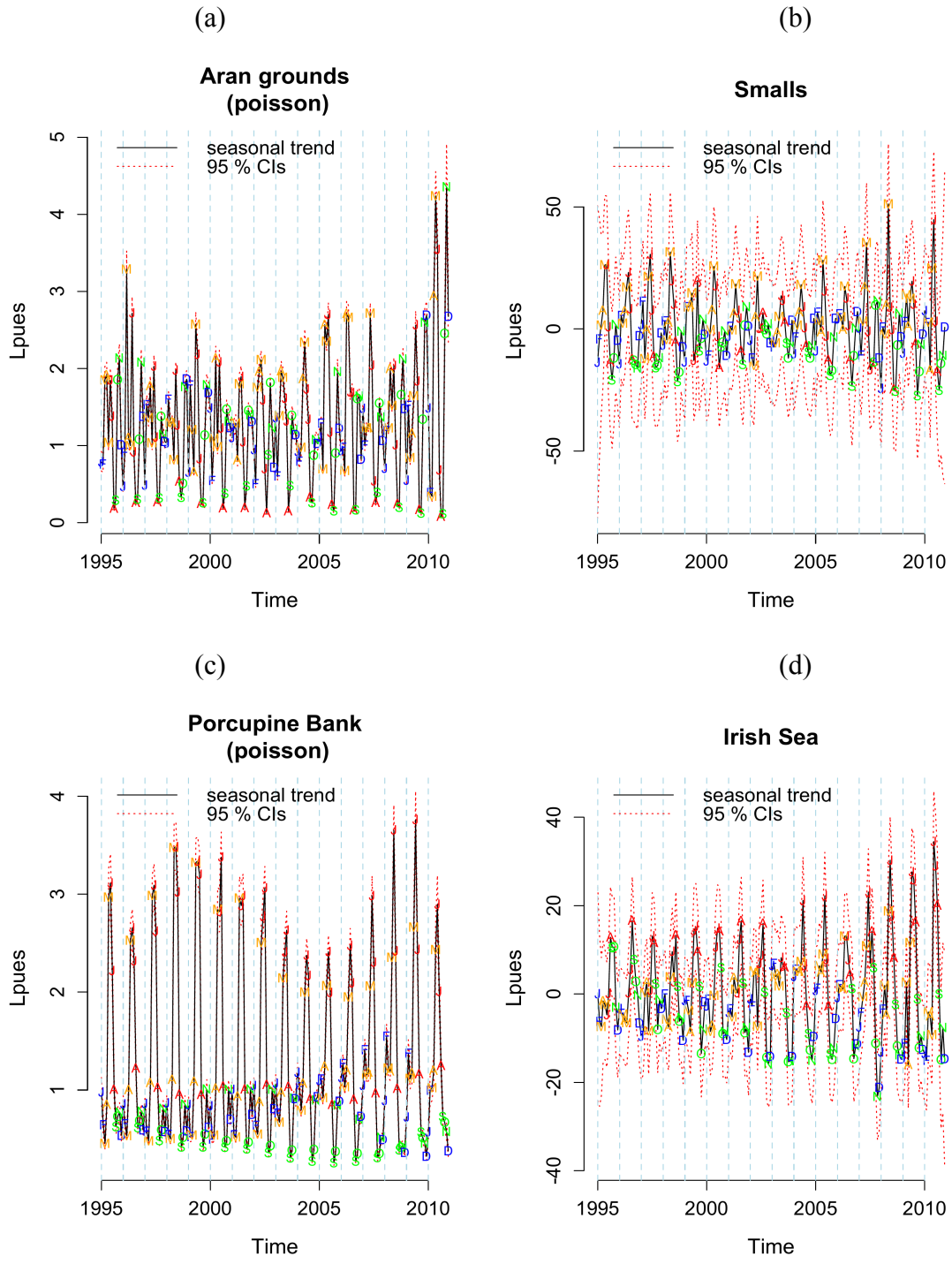


Figure 1.7: Stochastic seasonal component (harmonics) outputs of the state space modelling for (**a**) Aran grounds, (**b**) Small, (**c**) Porcupine Bank and (**d**) Irish Sea.

For the Smalls, maximum yields are annually recorded between May-June (**Figure 1.7b**

and **Figure 1.8e**). It is noteworthy, that since 1999 catch breakthroughs of months like oct-nov, ordinarily lower, compete with summer yields, underlining the importance of the autumn fishing activity (**Figure 1.1**, **Figure 1.7b**, **Figure 1.8e-f**).

In Aran grounds the maximum catchability of female *Nephrops* features in spring (mainly, April-May, **Figure 1.7a** and **Figure 1.8a**) and like the Smalls shows a second period of fishing activity in autumn (**Figure 1.8b**).

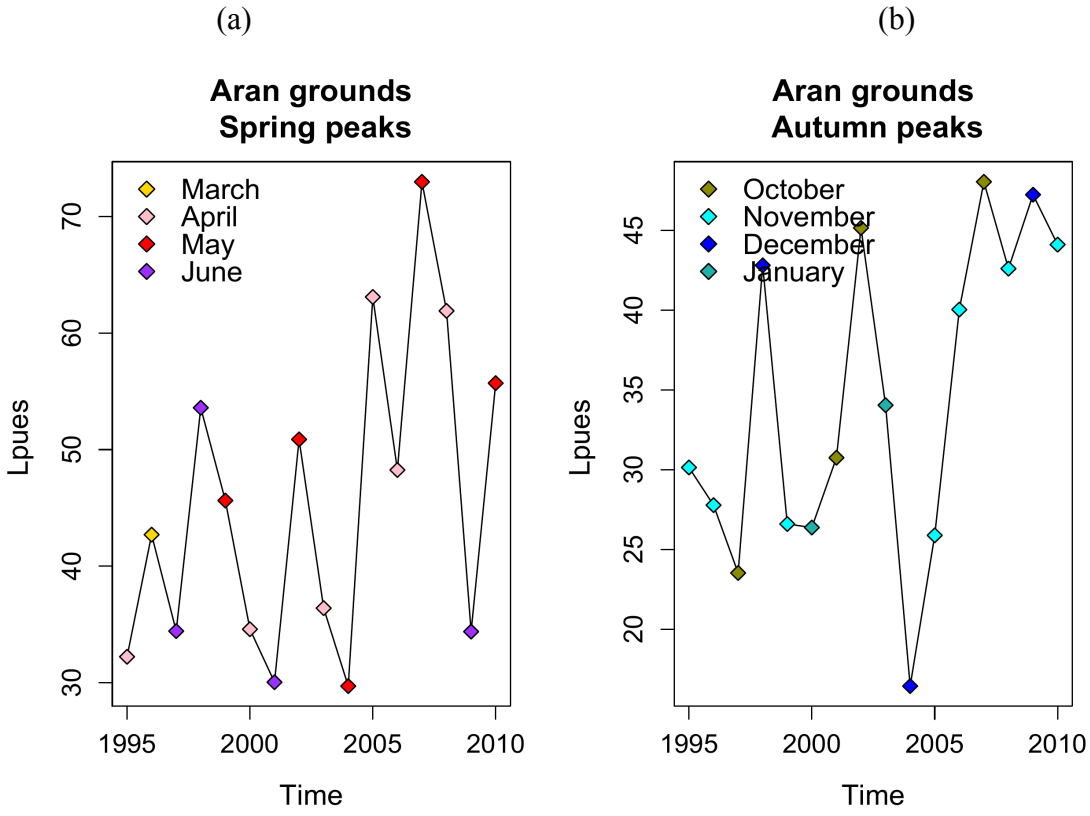


Figure 1.8 a-b: Time series of highest (peaks) lpues (kg/hours) within the raising level periods of *Nephrops* harvest from January 1995 to December 2010 for Aran grounds.

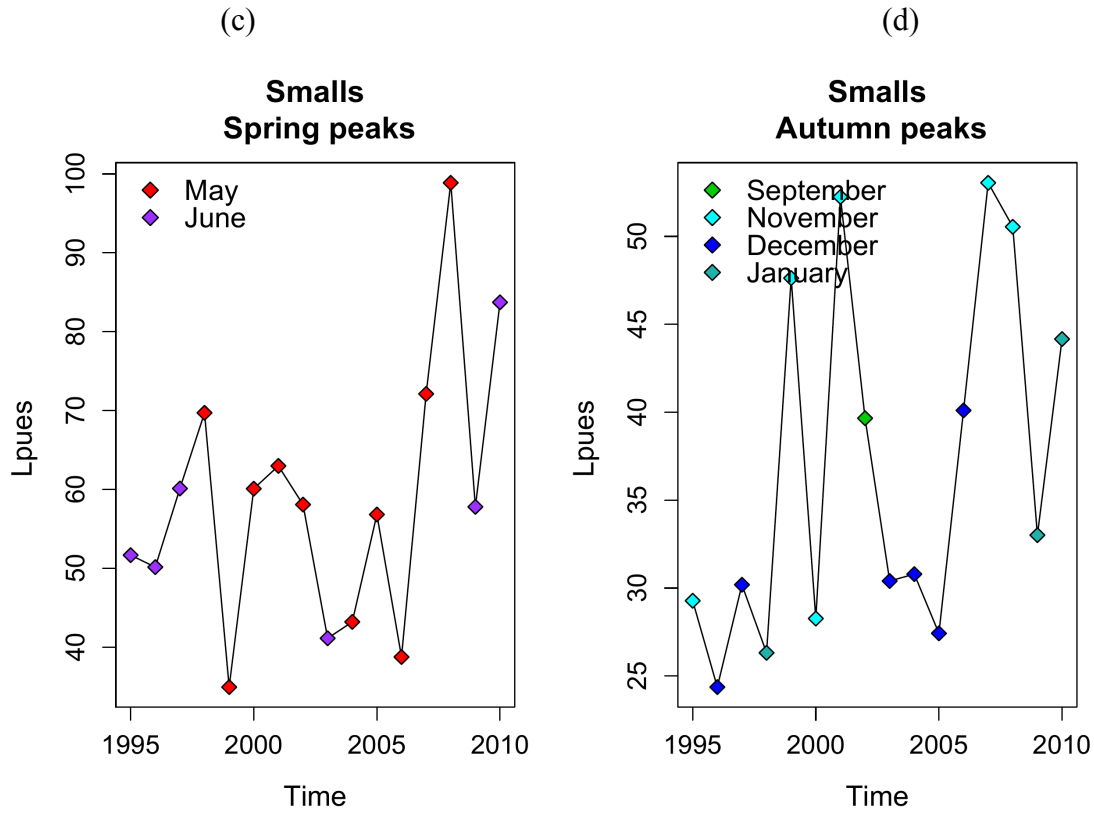


Figure 1.8 c-d: Time series of highest (peaks) lpues (kg/hours) within the raising level periods of *Nephrops* harvest from January 1995 to December 2010 for Smalls

In the case of the Irish Sea, since 2003, June substitutes for August as the most frequent month with highest landings. Such a shift took place in 1 year (**Figure 1.7d**, **Figure 1.8f**). For the Porcupine Bank highest landings are regularly distributed between May-June-July. Monthly patterns over these 16 years are easily tractable and we notice the growing interest in February fishing (**Figure 1.8e**).

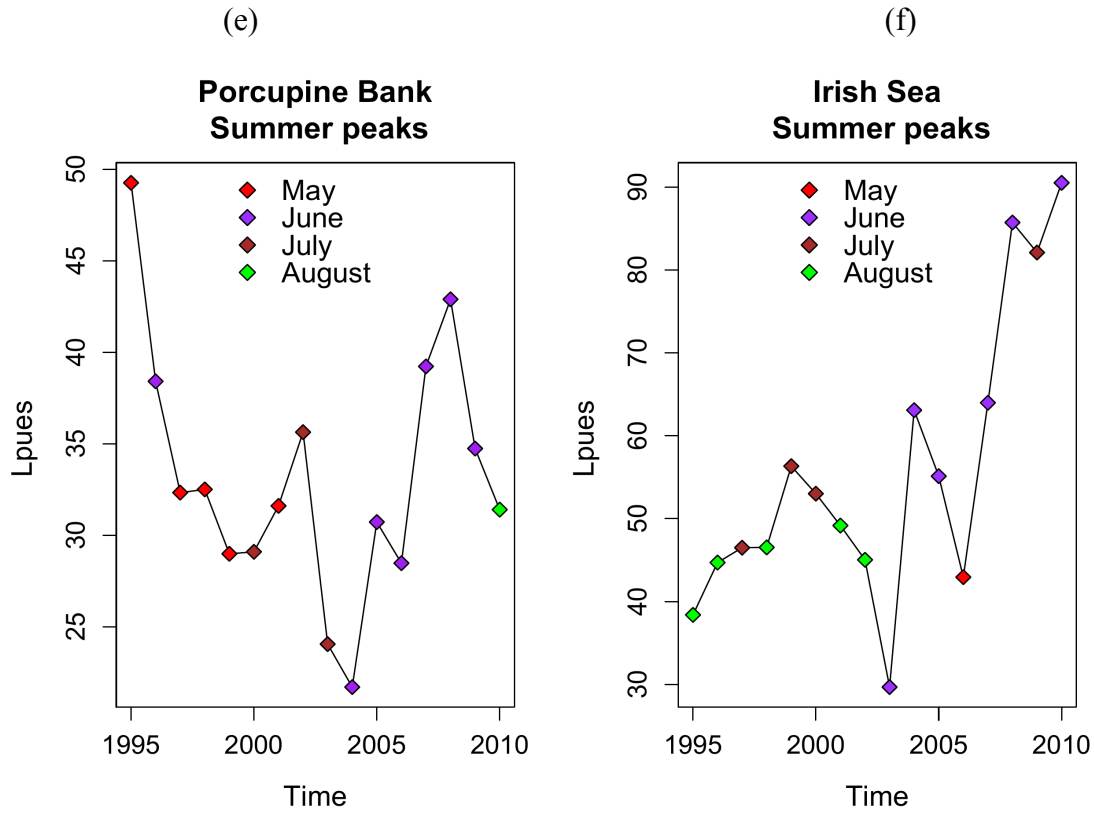


Figure 1.8 e-f: Time series of highest (peaks) lpues (in kg/hours) within the raising level periods of *Nephrops* harvest from January 1995 to December 2010 for (**e**) Porcupine Bank, and (**f**) Irish Sea.

(I.1.c) Outliers and structural breaks

Analysis of residuals from the modelling approaches can further help illuminate *Nephrops* population dynamics.

Inspection of the standardised smoothed observation "disturbances" allows the detection of possible outlier observations in a time series, while the inspection of the standardised smoothed state disturbances makes it possible to detect structural breaks in the trend level of our times series.

In **Figure 1.9** both versions of these smoothed disturbances are displayed for the stochastic local level and seasonal models applied to the time series of *Nephrops* lpues around Ireland.

Applying the usual 95% confidence limits of ±1.96 corresponding to a *two-tailed t-test* at the 5% level, shown in **Figures 1.9 a-h** as two red straight horizontal lines, we see that ~10 time points (9.6=192/(1/0.05) are expected to exceed the 95% confidence limits, purely based on chance. Even though Aran grounds, Smalls,

Porcupine Bank and Irish Sea state disturbances suggest that the series do not contain state breaks, we deliberately chose to examine the extreme values, lying outside of the conservative *Bonferonni test* (purple horizontal lines).
For the *Bonferonni* threshold, most of the outliers are recorded in the 2000's (**Figure 1.9a-d**) while level breaks are only identified for the Smalls (1999 Jul., **Figure 1.9e-f**) and the Porcupine Bank (2010 Jul., **Figure 1.9g**).

Table 1.3: Summary of the outliers (from smoothed observation disturbances) and structural breaks (from smoothed state disturbances) retained after the *Bonferroni test* at 5% with a threshold of ±3.65.

	Aran grounds	**Smalls**	**Porcupine bank**	**Irish sea**
Outliers	2005 Sep 2009 Jan 2010 Aug	1999 Aug	2009 Sep	2009 Apr
Structural breaks	No	1999 Jul (55)	2010 Jul (187)	No

For the Porcupine Bank, the identification of level breaks in the dynamic of the lpues series occurs in Aug 2010 (**Figure 1.9g**), coincident with records of unusually high landing values during the Autumn 2010.
In the case of Smalls, observation disturbance pinpoints the high level of catch recorded in August 1999 (outlier) which is at odds with the habitual timing of high values of lpues over these 16 years (that is, May and June).
Preceding by one month the aforementioned outlier, the state break of Jul-1999, also marks the start of a period of rises and falls in captures lasting 5 years (1999–2004, **Figure 1.6b**). We note that during this period a significant break in the trajectory of the lpues is detected according to the less conservative *t-test* (±2). Nevertheless, these changes in the trajectory are temporary and do not take the form of a shift in the trend.
In the case of the Irish Sea, the April 2009 outlier (**Figure 1.9d**) corresponds to a drop in lpues (**Figure 1.6d**).
In conclusion, the significant breaks in the trajectory of the population as detected by the smoothed level disturbance signals are only temporary changes and do not take the form of a level shift.

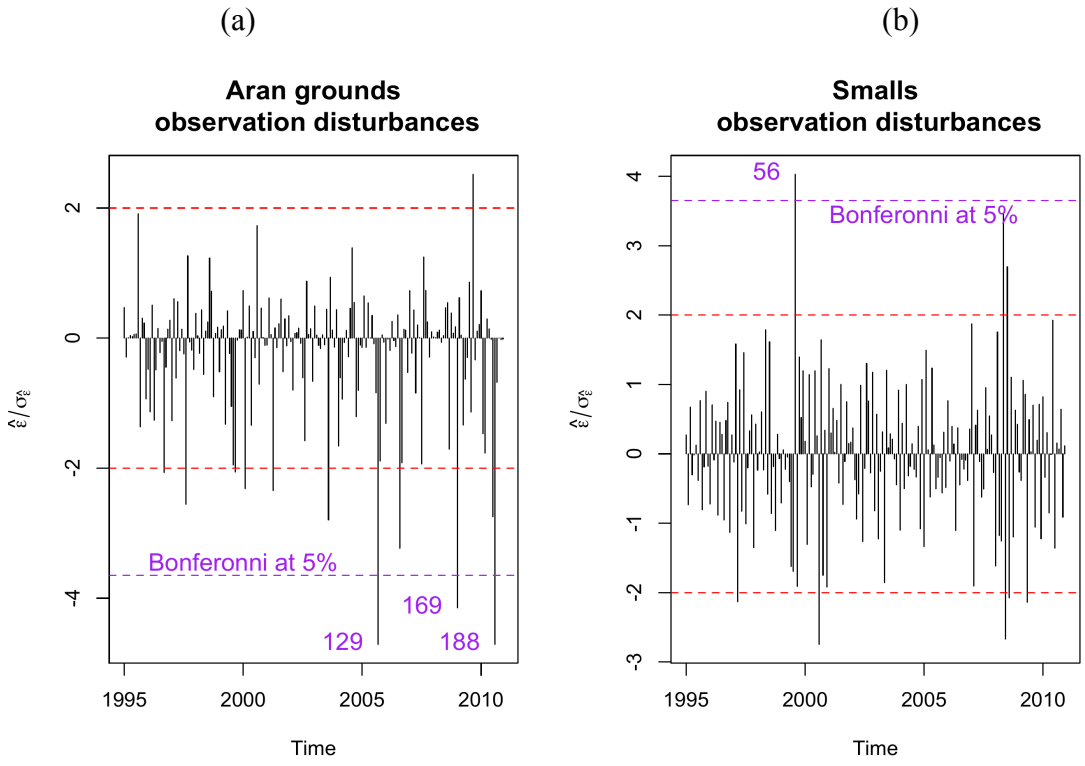


Figure 1.9 a-b: Standardised smoothed observation disturbances for outliers detection for (**a**) Aran grounds (FU17), (**b**) Smalls (FU22). The *Bonferonni test* at 5% (purple dashed line) with a threshold of ±3.65 along with a *two-tailed t-test* at 5% (dashed red line) with a threshold of ±2 are indicated.

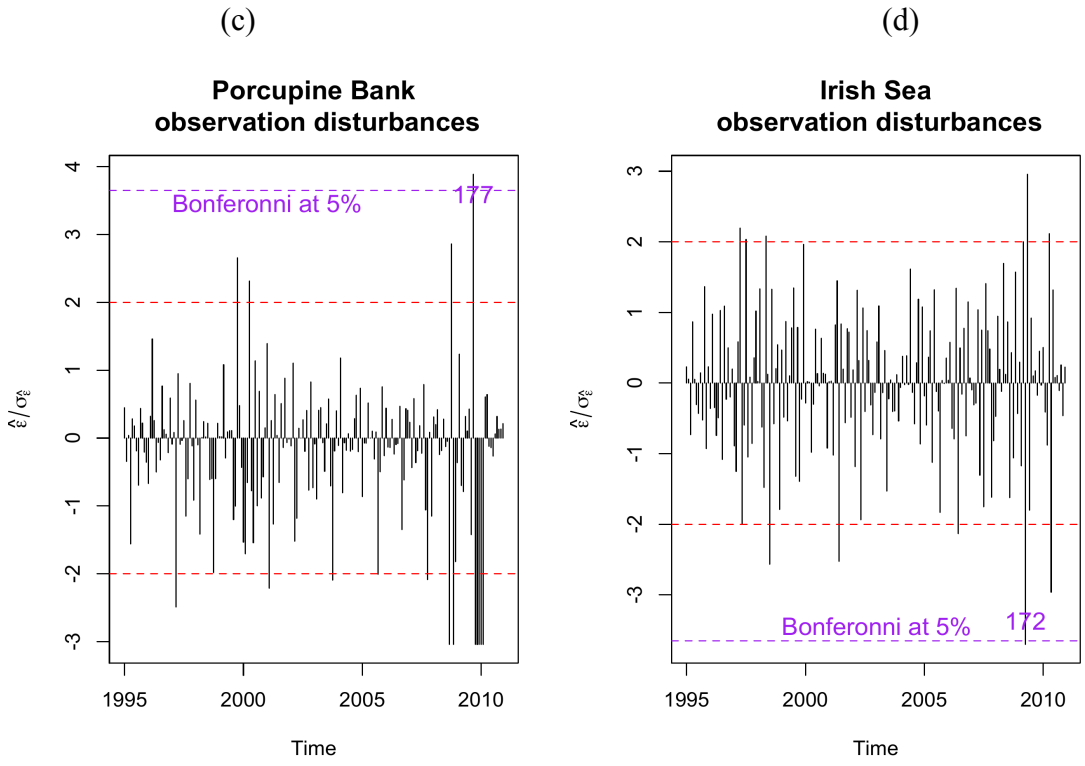


Figure 1.9 c-d: Standardised smoothed observation disturbances for outliers detection for (**c**) Porcupine Bank (FU16) and (**d**) Irish Sea (FU15). The *Bonferonni test* at 5% (purple dashed line) with a threshold of ±3.65 along with a *two-tailed t-test* at 5% (dashed red line) with a threshold of ±2 are indicated.

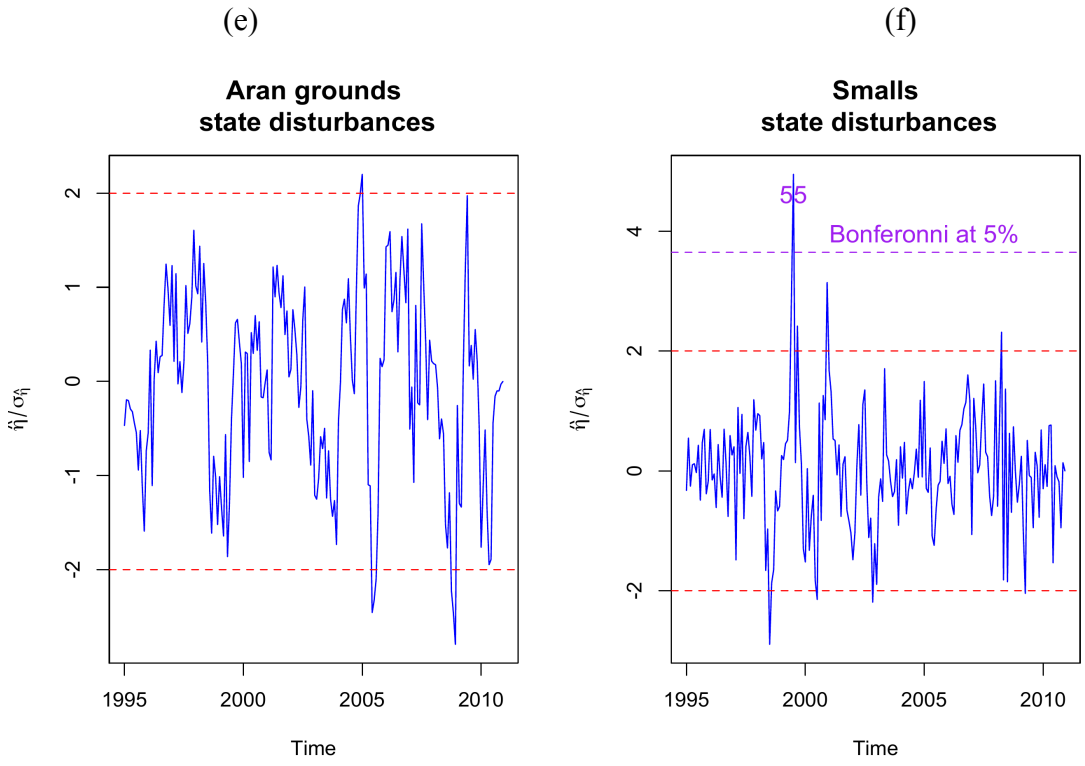


Figure 1.9 e-f: standardised smoothed level disturbances for structural breaks identification are shown for (**e**) Aran grounds (FU17), (**f**) Smalls (FU22). The *Bonferonni test* at 5% (purple dashed line) with a threshold of ±3.65 along with a *two-tailed t-test* at 5% (dashed red line) with a threshold of ±2 are indicated.

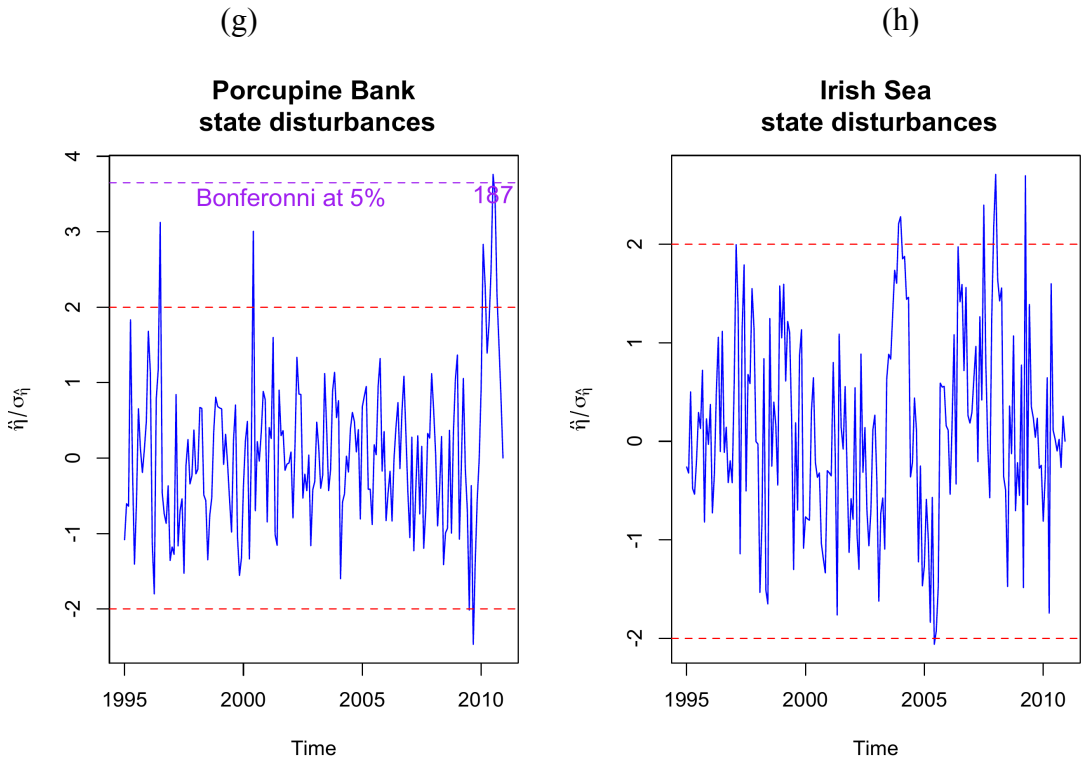


Figure 1.9g-h: standardised smoothed level disturbances for structural breaks identification are shown for (**g**) Porcupine Bank (FU16) and (**h**) Irish Sea (FU15). The *Bonferonni test* at 5% (purple dashed line) with a threshold of ±3.65 along with a *two-tailed t-test* at 5% (dashed red line) with a threshold of ±2 are indicated.

(I.2) Long-term trends

So far, the identification of temporal changes in the stocks have been estimated from the modelling procedure (state space) assuming and testing presence of trend (here, stochastic intercept or level) and seasonal cycle. In contrast, using cumulative or moving sum of standardised residuals (ols-cusum and ols-mosum respectively), in other words, examining the landings data, provide the opportunity to test the presence of structural changes directly from the data without prior assumptions (**Figures 1.10**). From a general point of view, the ols-cusum fluctuations of the growth rate of the stocks (the departure from the reference line of 0 in the case of the standardised residuals) exhibit a steady decline from 1995 to 2005 at least. But distinctive features are also detected in each fishing zone.

In fact, since 1997 and over the next 12 years (until mid-2009) the Irish Sea fluctuations are considered improbably large indicating that the null hypothesis H_0 of "*no structural*

change" is rejected at a significance level $\alpha=0.05$ (boundaries test line in **Figure 1.10a**). In Aran grounds and Smalls, the global decreasing trends are altered by a sequence of positive and negative rates (recovery and drop) that could underline the existence of shorter cycles.

In spite of being below the reference line since 2001, Porcupine Bank is never recorded outside the "boundaries".

(a)

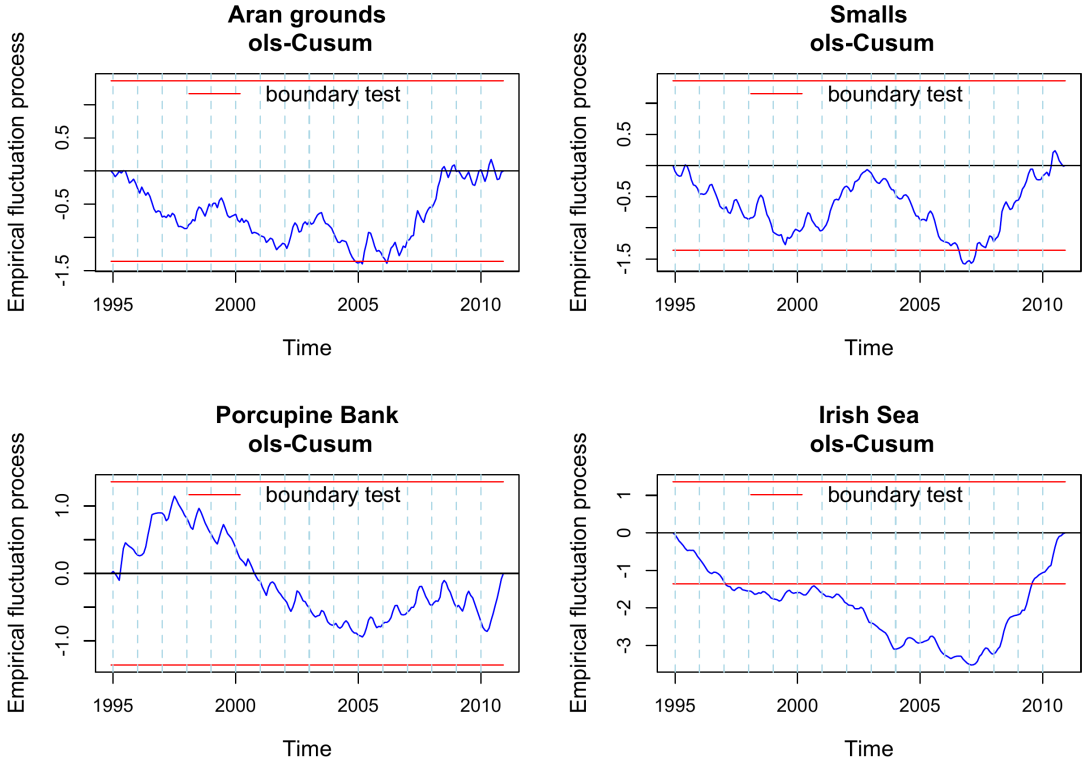


Figure 1.10a: ols-cusum estimates of structural changes from the landings data (lpues).

The ols-cusum structural change test is based on cumulative sums of the common ordinary least square (ols) residuals. The red lines (±3.3581) indicates the boundaries test of the brownian bridge at $\alpha=0.05$ (Schumacher 1984).

(b)

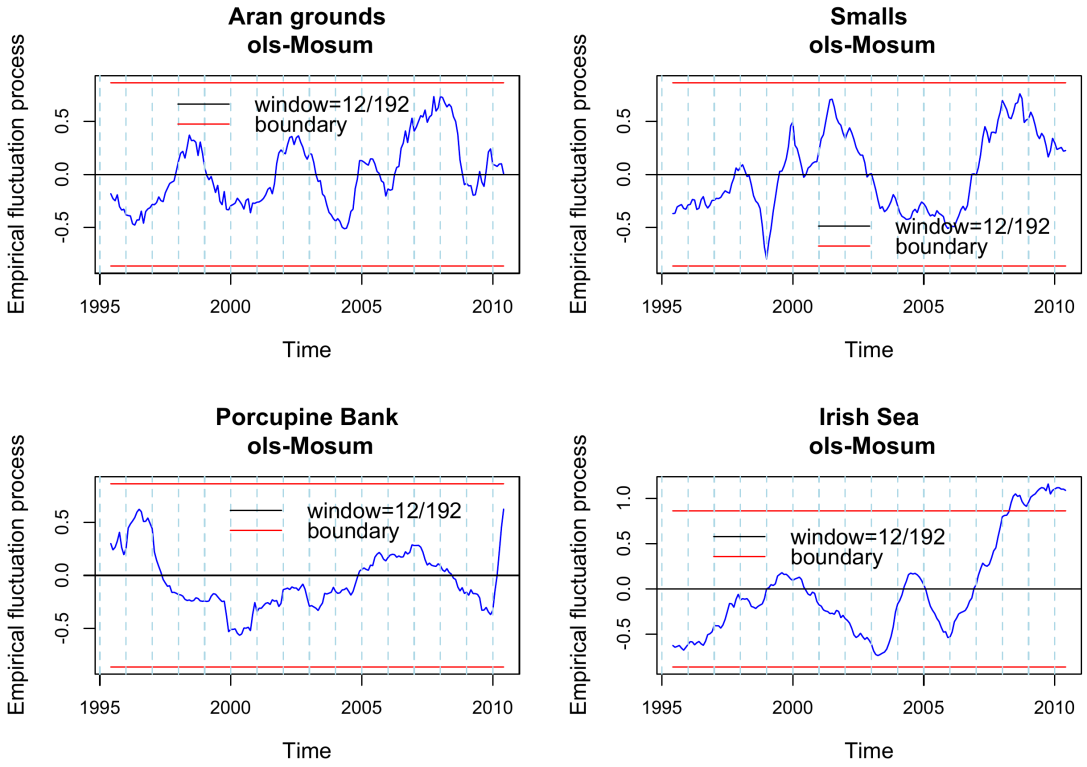


Figure 1.10b: Ols-mosum estimates of structural changes from the landings data (lpue).

The ols-mosum relies on the analysis of the moving sum of residuals where detection of structural change is based on the sum of a fixed number of residuals in a data window whose size is determined and which is moved over the whole sample period. The red lines (±1.3581) indicates the boundaries test of the brownian bridge at $\alpha=0.05$ (Schumacher 1984).

By considering the moving sum of the residuals (ols-mosum) with a data window of 12 months, we again find the trend levels already identified by the state space approach (**Figure 1.6**) confirming these components of the landings.

Finally, the ols-cumsum and ols-mosum derived patterns of the lpues are considered to be the long and medium responses of the *Nephrops* abundance to the abiotic and exploitation conditions at each harvested area.

(I.3) Past values contribution to current landings

(I.3.a) Sarima regressions

From the previous state space approach, two main dynamical components (level and season) have been portrayed for each landings series. The Sarima(p,d,q)(P,D,Q)$_{12}$ Box-Jenkins modelling (**Table 1.4**), suggests a relationship between the current observed value of lpue and its past ones (AR) as well as the moving average (MA) components encompassing the external (random) events or shocks that produce immediate effects for short periods of time.

By rewriting the sarima models into the regression-like form, the contribution of each lagged value to the current landing (Y_t) is now easily accessible.

The annual periodicity ($s=12$) is expressed by the variable Y_{t-12}, nonetheless, its weight is reduced and even considerably diminished by the neighbouring lagged values as in the case of the Smalls and the Irish Sea, the latter being negative. Also, note that the multiplicative nature of the sarima model implies that the coefficients of W_{t-13}, W_{t-14}, and W_{t-16} (respectively Y_{t-13}, Y_{t-14}, Y_{t-16}, Y_{t-17}) are the product of the coefficients of W_{t-1} and W_{t-12}, W_{t-2} and W_{t-12}, W_{t-4} and W_{t-12} (respectively Y_{t-1} and Y_{t-12}, Y_{t-2} and Y_{t-12}, Y_{t-4} and Y_{t-12}, Y_{t-5} and Y_{t-12}) rather than free parameters. Following this seasonal correction, the prominent influence of Y_{t-1} is highlighted.

Note that the distant past value (Y_{t-5}) in the Aran grounds data was included to address the significant *lag 5* of the partial-autocorrelation function.

Table 1.4: Outputs of the sarima modelling fits retained for the time series analysis.
Notice the formula of the general intercept $\alpha_{intercept} = \mu(1 - \phi_1 - \phi_2 - \ldots - \phi_p)$ were μ stands for the mean estimate. *p-value* for *t-test* less than *0.05*, *0.01* and *0.001* are flagged *, ** and *** respectively.

Aran grounds: Sarima (5,0,0)(1,0,1)$_{12}$ $Y_t = \alpha_{intercept} + 0.2073Y_{t-1} + 0.1935Y_{t-5} + 0.9761Y_{t-12} - 0.2023Y_{t-13} - 0.1888Y_{t-17} + W_t - 0.8324W_{t-12}$								
Coefficients	ar1	ar2	ar3	ar4	ar5	sar1	sma1	mean
Estimates	0.2073**	0	0	0	0.1935**	0.9761**	-0.8324***	22.7053***
s.e.	0.0711	0	0	0	0.0692	0.0215	0.0757	4.2961
σ^2 estimated as *145*; *log likelihood= -753.12*; *AIC=1518.23*; *AICc=1518.68*; *BIC=1537.78*								

Smalls: Sarima (1,0,1)(1,0,1)$_{12}$ $Y_t = \alpha_{intercept} + 0.3102Y_{t-1} + 0.9967Y_{t-12} - 0.3091763Y_{t-13} + W_t + 0.3279W_{t-1} - 0.9455W_{t-12} - 0.3100295W_{t-13}$								
Coefficients	ar1	ma1	sar1	sma1	mean			
Estimates	0.3102*	0.3279*	0.9967***	-0.9455***	31.8419***			
s.e.	0.1271	0.1311	0.0149	0.1239	4.1939			
σ^2 estimated as *117.7*; *log likelihood=-736.28*; *AIC=1484.56*; *AICc=1485.01*; *BIC=1504*								

Porcupine Bank: Sarima (1,0,4)(1,0,1)$_{12}$ $Y_t = \alpha_{intercept} + 0.5699Y_{t-1} + 0.9635Y_{t-12} - 0.5490Y_{t-13} + W_t + 0.2003W_{t-4} - 0.7073W_{t-12} - 0.1416722W_{t-16}$								
Coefficients	ar1	ma1	ma2	ma3	ma4	sar1	sma1	mean
Estimates	0.5699***	0	0	0	0.2005**	0.9635***	-0.7075***	15.1246**
s.e.	0.0609	0	0	0	0.0743	0.0252	0.0942	5.1256
σ^2 estimated as *41.05*; *log likelihood = -633.08*; *AIC=1278.17*; *AICc=1278.62*; *BIC=1297.71*								

Irish Sea Sarima (1,1,1)(1,0,1)$_{12}$ $Y_t = \alpha_{intercept} + 1.5806Y_{t-1} - 0.5806Y_{t-2} + 0.8803Y_{t-12} - 1.3914Y_{t-13} + 0.5111Y_{t-14} + W_t - 0.9438W_{t-1} - 0.5020W_{t-12} + 0.4737W_{t-13}$								
Coefficients	ar1	ma1	sar1	sma1				
Estimates	0.5806***	-0.9438***	0.8803***	-0.5020**				
s.e.	0.0827	0.0382	0.0708	0.1511				
σ^2 estimated as *56.98*; *log likelihood = -658.99*; *AIC=1327.98*; *AICc=1328.3*; *BIC=1344.24*								

By plotting Y_t against the lagged landings Y_{t-1} and Y_{t-12} (**Figure 1.11**), the large

scattering of the distributions in the case of Aran grounds could explain both the relative weakness of the coefficient of Y_{t-1} (*0.20*) for the model *(5,0,0)(1,0,1)*$_{12}$ (**Table 1.4**), and the considerable underestimate of the fit (**Figure 1.12a**). The simple inspection of lagged relationships for the 4 areas (**Figure 1.11**) also confirms the correlation between the current yield values with the Y_{t-1} and Y_{t-12} past ones, which is consistent with our simple and seasonal parameters choice of the sarima modelling (*p* and *P*, **Table 1.4**).

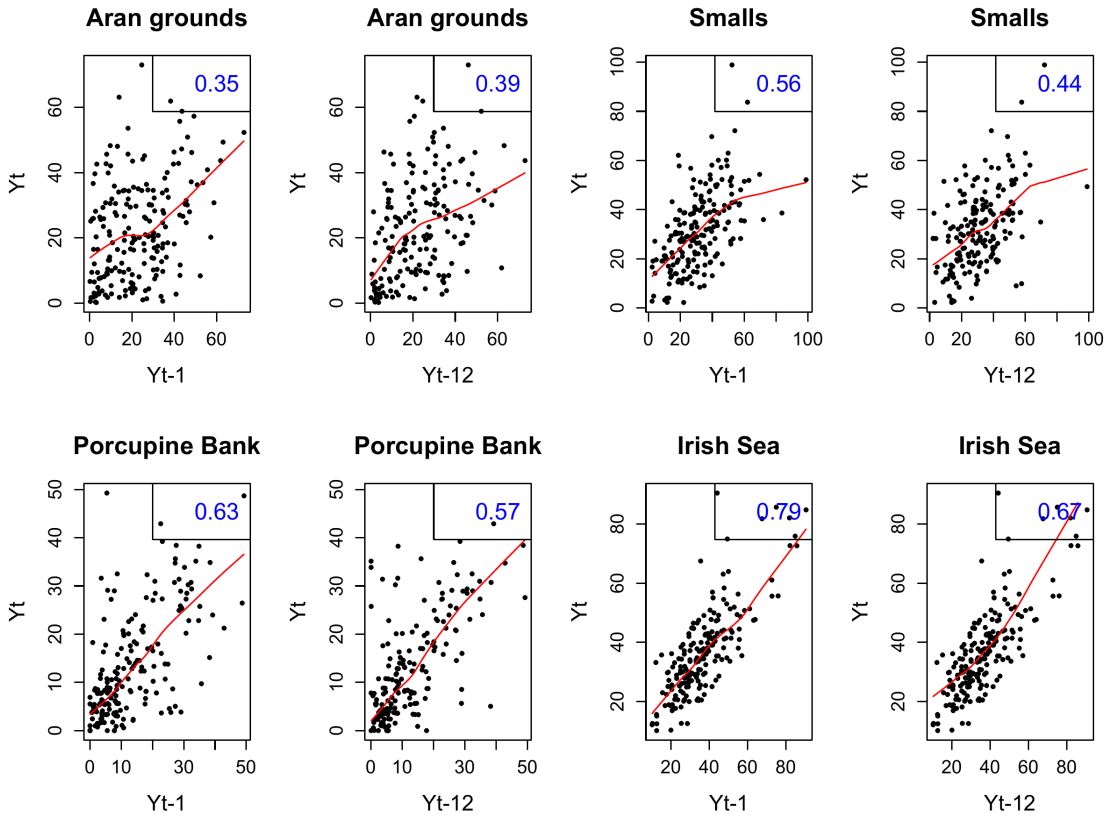


Figure 1.11: Scatter plots of the current landings (Y_t) versus the *lag1* (Y_{t-1}) and *lag12* (Y_{t-12}) landings. Data are l995–2010 lpues time series. In order to help with the visual examination of the relationship, a weighted scatterplot smoothing regression (*lowess*) is added (red line). The *Pearson correlation coefficient* estimates of the relationship are displayed. Notice that the *lag1* and *lag12* display the highest *Pearson correlation coefficient* values for all areas.

In general, the observed patterns are quite well captured by the models (**Figure 1.12**) and satisfy the assumptions of independence, homoscedasticity and normality (**Figure A1** in ***Annexes A***). It is noteworthy that for the Porcupine Bank, the unexpected autumn-winter 2010 lpues are identified since a large segment of the fit deviates from

the observations but not from the prior sequence of the series (**Figure 1.12c**).

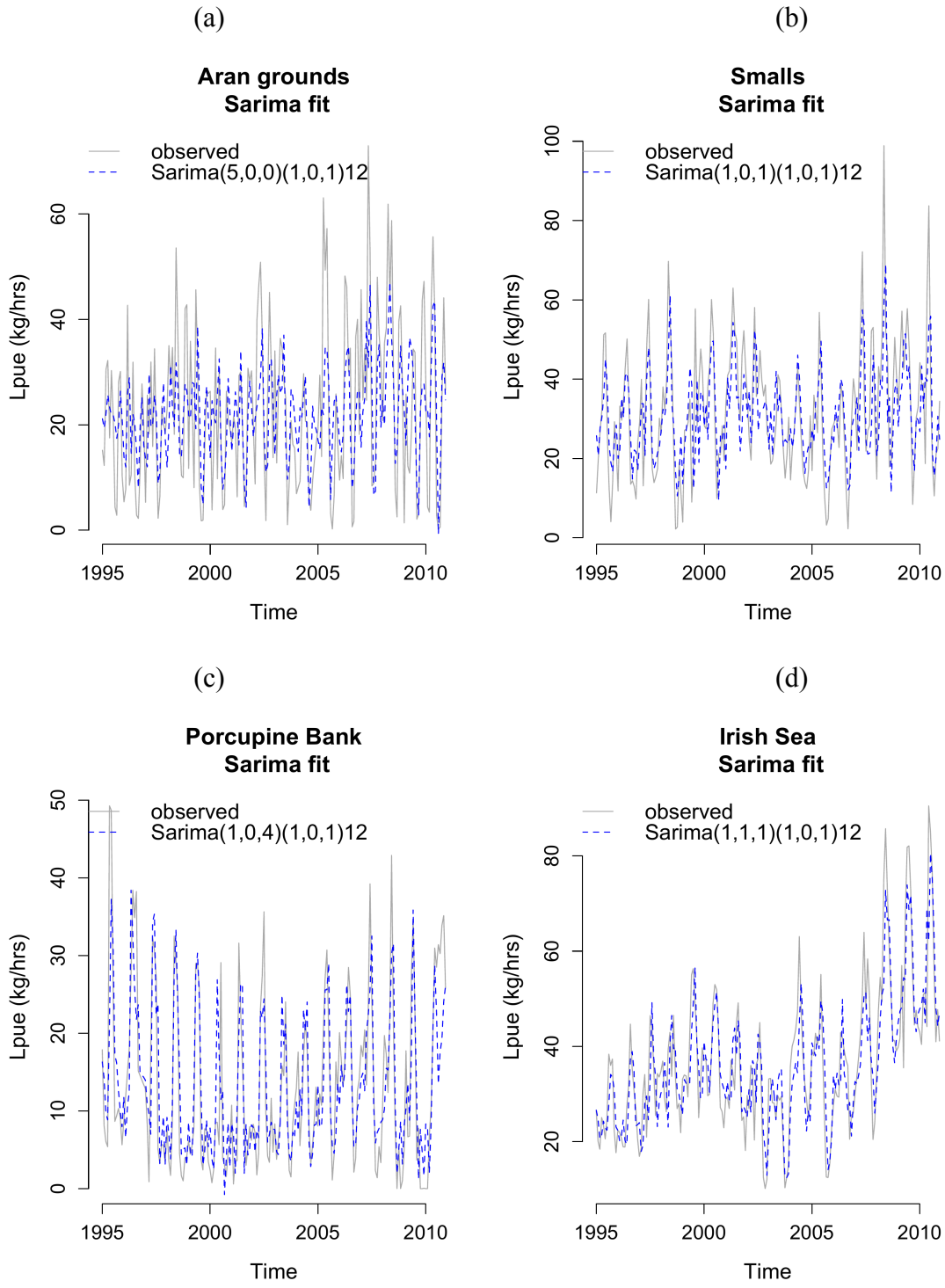


Figure 1.12 a-b-c-d: Sarima modelling fits for the 1995–2010 lpue (Kg/hours) times series of (**a**) Aran grounds (FU17), (**b**) Smalls (FU22), (**c**) Porcupine Bank (FU16) and (**d**) Irish Sea (FU15).

Furthermore, to comply with the required stationarity of the Box-Jenkins modelling (*i.e.* sarima), we have recourse to an integration of order 1 ($d=1$) for the Irish Sea data (see ***Statistical Annexes A***). The component Y_{t-2} in the regression-like form of the Irish Sea sarima model $(1,1,1)(1,0,1)_{12}$ (**Table 1.4**) reflects this technique, also called difference of order $d=1$, and should not be otherwise interpreted.

(I.3.b) Delayed density dependence

So far, with almost two decades of data, some patterns of population changes have been described (**Figure 1.6** and **Figure 1.10**). At this stage the mechanisms that generate these fluctuations are not defined, but rather, we examine the way that changes in the "growth rate" of the populations are affected by the current (and/or lags in) density.
In plotting the per capita replacement rates (Y_t/Y_{t-1} against Y_{t-1}) we notice the density-dependent relationship form of each stock (**Figure 1.13a**).

(a)

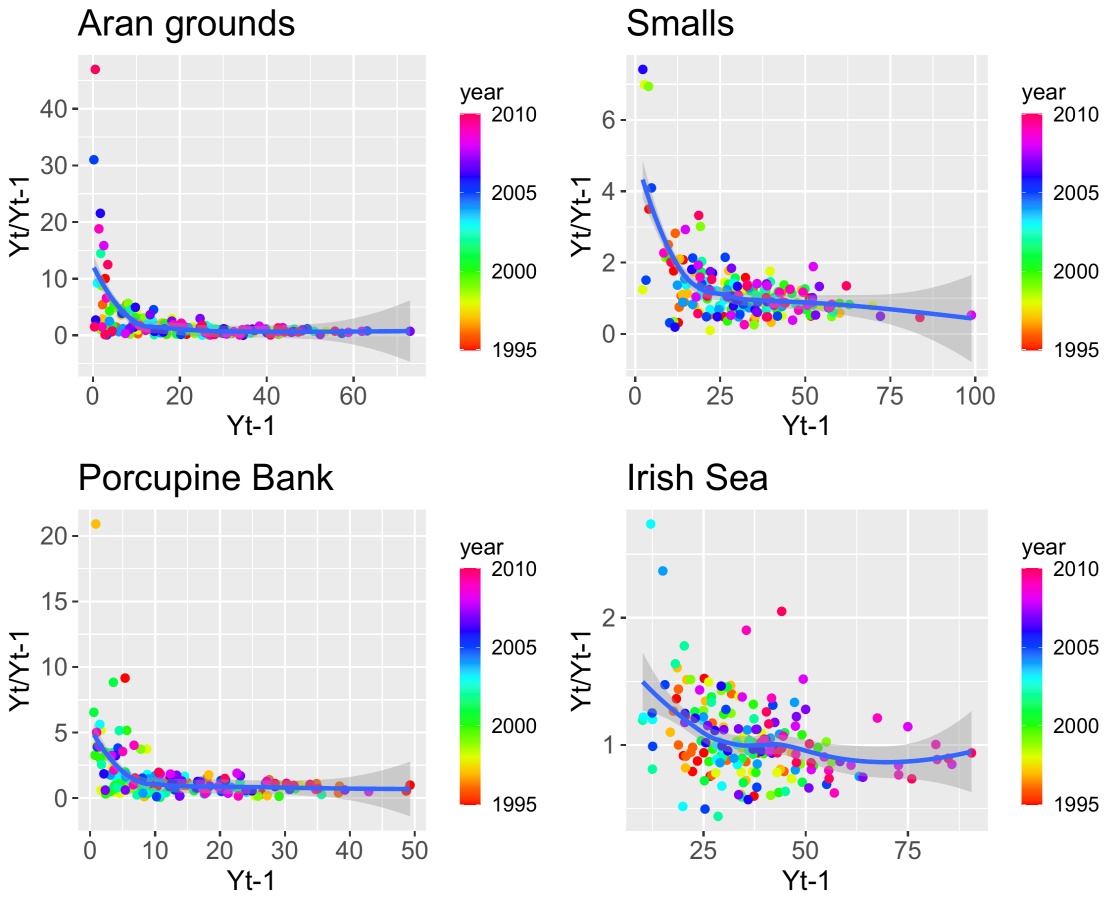


Figure 1.13a: View of the density structures of the per capita replacement rate (Y_t/Y_{t-1}) against lagged density (Y_{t-1}) where the logarithm transformation takes care of the presence of the heteroscedasticity and a loess fit is added to evaluate the relationship. Y_t stands for the observed lpue series from 1995 to 2010.

(b)

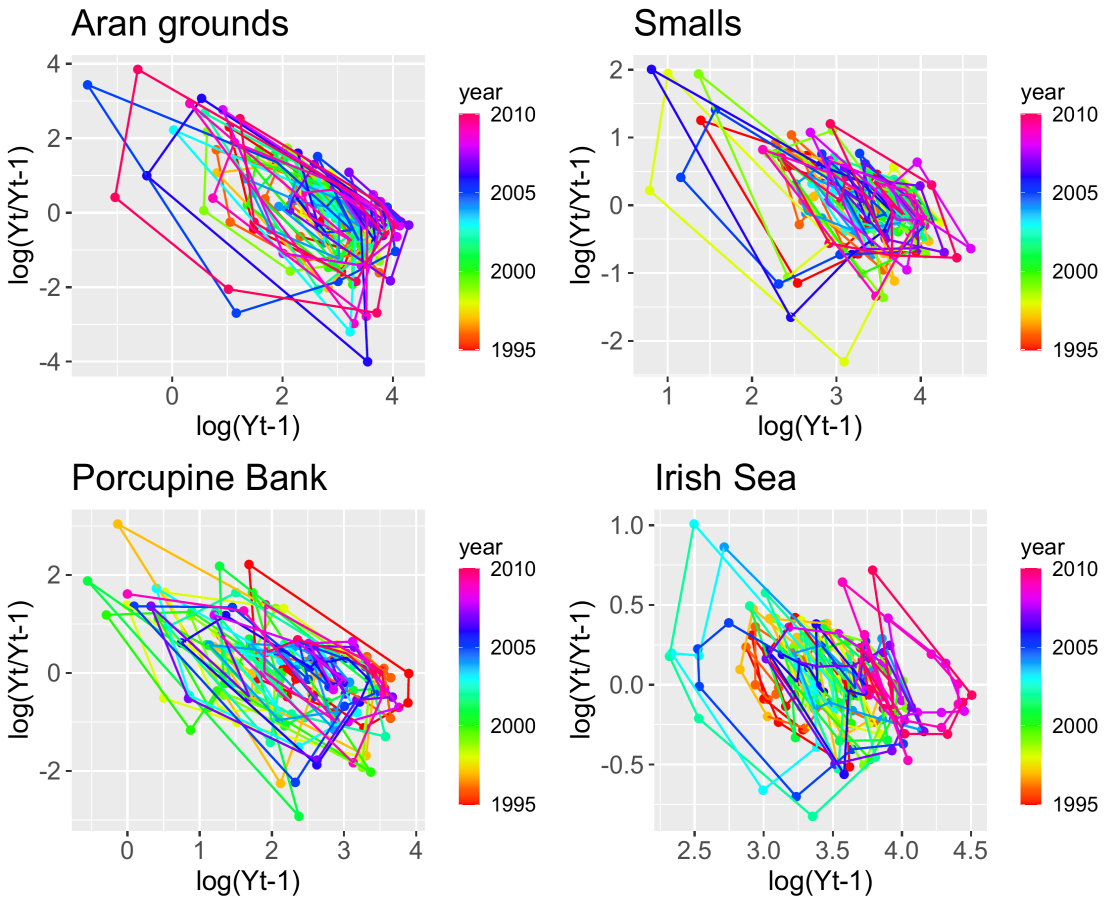


Figure 1.13b: View of the realised per capita rate of change $r_t=\ln(N_t/N_{t-1})$ against $\ln(N_{t-1})$.

A variation of this approach using the realised per capita rate of change $\ln(Y_t/Y_{t-1})$ against $\ln(Y_{t-1})$ reveals the dynamic trajectory of the current population density against the lagged one (**Figure 1.13b**). A back-and-forth fluctuations suggests a direct density-dependent regulation while a circular clockwise orbits acknowledge a delayed-density-dependent feedback. Examination of the successive phase plots over the 16 years shows dominant clockwise (convergent) patterns (**Figure A11** in ***Annexes A***) and we note the irregular amplitudes of the clockwise patterns displayed from year to year. In addition, in light of the sarima results (**Table 1.4**), the functional form of this density dependence relationship was also examined on the basis of the significant sarima correlation found between the current yield Y_t and the Y_{t-1}, Y_{t-12} past values (noted *lag1* and *lag12* in **Figure 1.14**)

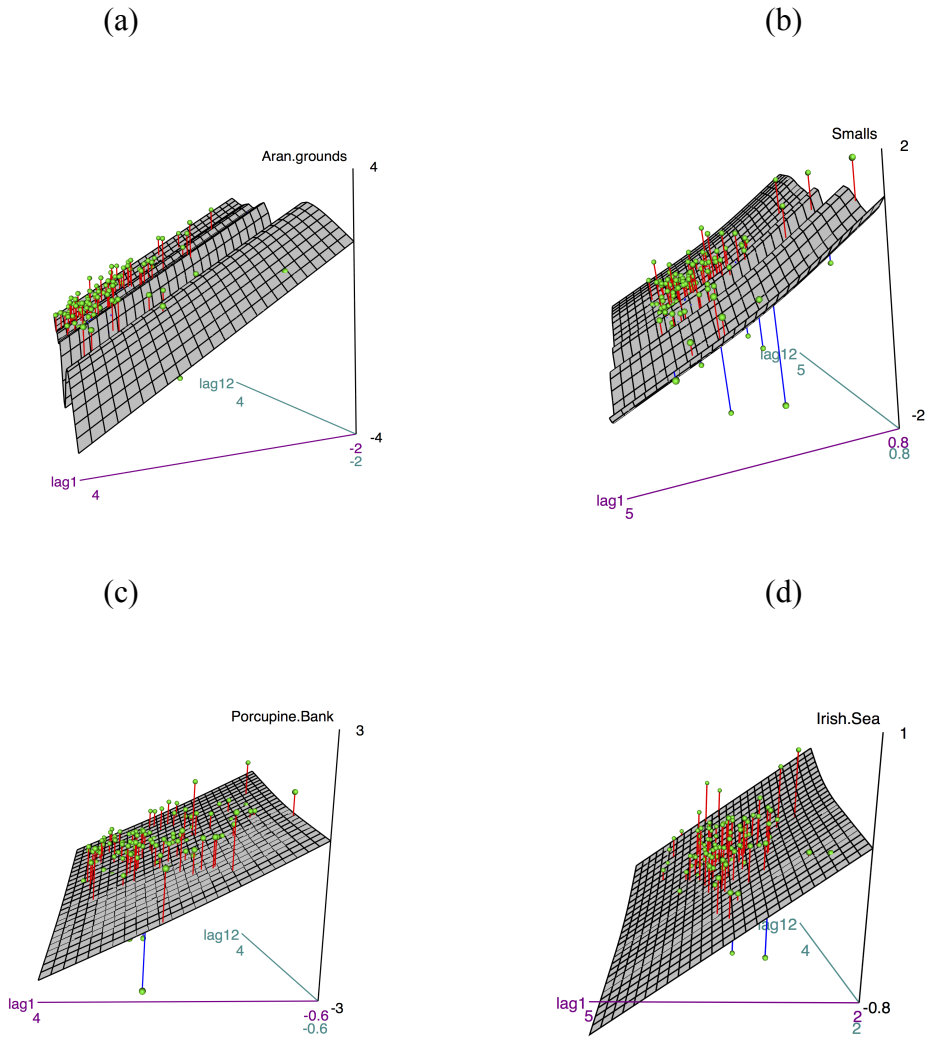


Figure 1.14 a-b-c-d: Regression response surface fits between the rate of change per capita in density ($log(Y_t/Y_{t-1})$ and the lagged yields ($log(Y_{t-1})$ and $log(Y_{t-12})$ noted *lag1* and *lag12*, respectively). It is implemented for Aran grounds (A), Smalls (S), Porcupine Bank (P) and Irish Sea (I) on the basis of a generalised additive modelling with a cubic spline smoother. The orthogonal projections on the surface of the resulted residuals are indicated for visual inspection of the quality of the fits. Y_t stands for the observed lpue series from 1995 to 2010.

Overall, regarding the shapes of response surfaces fits, Aran grounds, Smalls, Porcupine Bank and Irish Sea show regular decreasing slopes towards the higher lag1 value, indicating a direct density dependence negative feedback over the rate of change in density.

Aran grounds and Smalls feature more “wiggling forms” (nonlinearity), suggesting that the density change is subject to more variability (oscillation) in direction of increasing

lag12 values that quantify delayed density dependence regulation (**Figure 1.14a-b**). In contrast, for Porcupine Bank and Irish Sea the surface is flat along the *lag12* (**Figure 1.14c-d**).

(II) Support to fishery management

(II.1) Monitoring through forecasting

Forecasting is an essential tool for managing a stock. Forecasting in time series analysis requires a model and, on the basis of the state space and sarima results, we are now able to envisage building such a model which encompasses the already identified dynamic components. Such forecasting models summarise the main dynamic points of these past 16 years of fishing activity conveyed by the lpues and hence, any significant departure of the predicted pattern from the observed landings should draw our attention and be further examined.

Thus, although handling the predictions on different bases (see **Materials and Methods**) the state space and sarima forecasting patterns of Aran grounds, Smalls and Irish Sea broadly resemble each other (**Figure 1.15**).

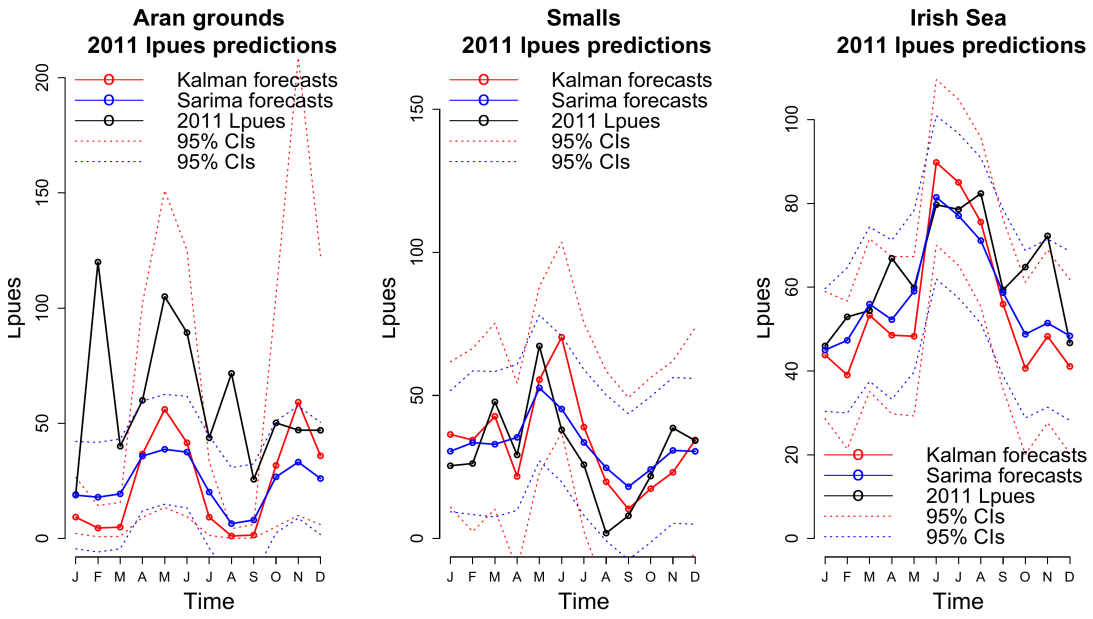
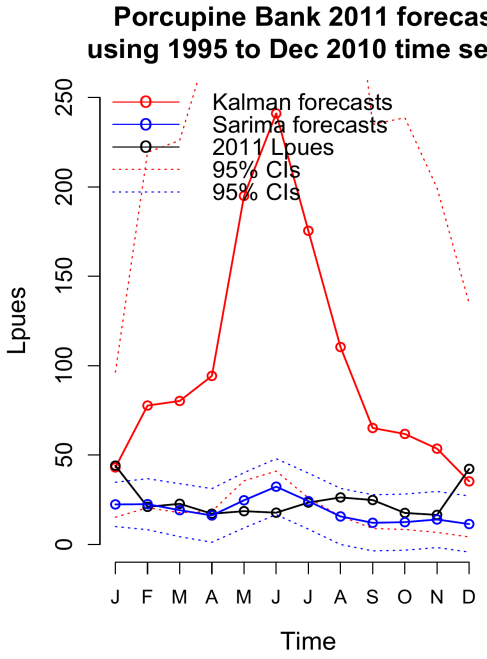
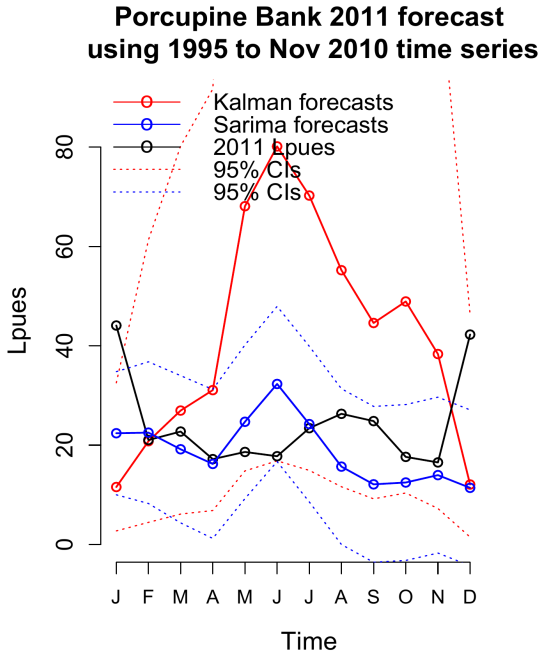


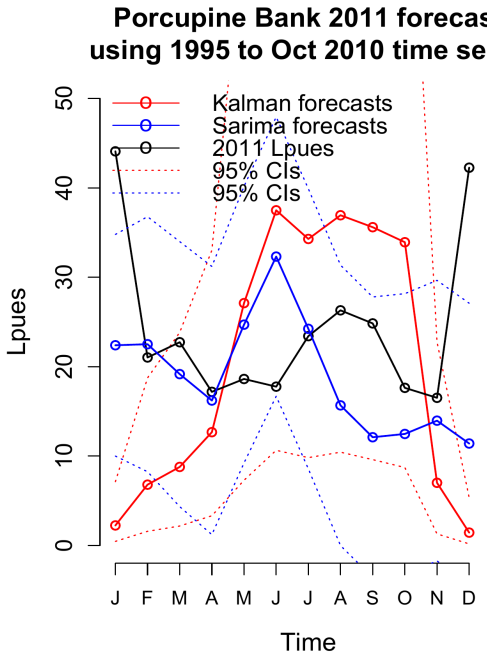
Figure 1.15: 12 month lpue (Kg/hours) forecasting obtained from state space and sarima models for the year 2011 on the basis of the 1995-2010 data. Observed 2011 lpues values (black) enable comparison of model performances.

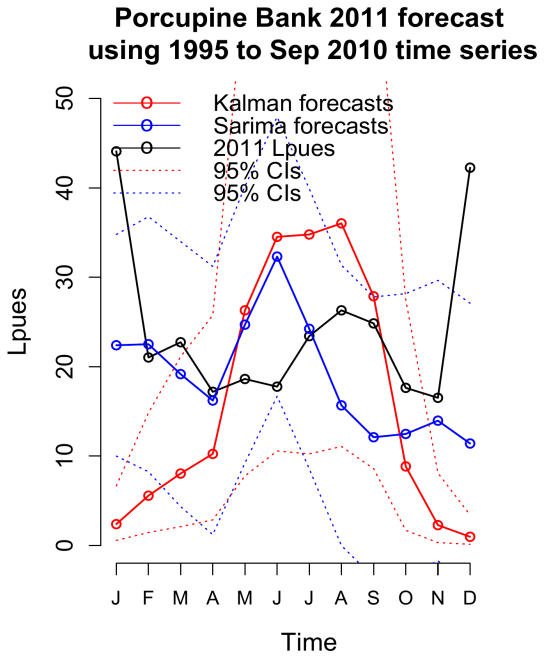
On average, both approaches show important similarities between the predictions and observations for the Smalls and the Irish Sea. While in the case of Aran grounds, the forecasting technique reveals a high degree of divergence for Feb-Aug. with the observed lpues lying far beyond the state space and sarima confidence intervals. Recall, that over 16 years, Aug. has the lowest monthly fishing activity in this FU (**Figure 1.2a**).

Forecasting the 2011 Porcupine Bank landings was not straightforward and gave rise to more detailed consideration. In fact, this time, the sarima and state space predictions are unexpectedly distant (**Figure 1.16**). The state space overestimates the level of the actual catches. In addition, conspicuously, the typical Gaussian bell pattern that marked the dynamic lpues during the 16 years (**Figure 1.2c**) vanished from the observed 2011 lpues.


Porcupine Bank 2011 forecast
using 1995 to Dec 2010 time series
Kalman forecasts
Sarima forecasts
2011 Lpues
95% CIs
95% CIs
Lpues
0
50
100
150
200
250
J F M A M J J A S O N D
Time


Porcupine Bank 2011 forecast
using 1995 to Nov 2010 time series
Kalman forecasts
Sarima forecasts
2011 Lpues
95% CIs
95% CIs
Lpues
0
20
40
60
80
J F M A M J J A S O N D
Time


Porcupine Bank 2011 forecast
using 1995 to Oct 2010 time series
Kalman forecasts
Sarima forecasts
2011 Lpues
95% CIs
95% CIs
Lpues
0
10
20
30
40
50
J F M A M J J A S O N D
Time


Porcupine Bank 2011 forecast
using 1995 to Sep 2010 time series
Kalman forecasts
Sarima forecasts
2011 Lpues
95% CIs
95% CIs
Lpues
0
10
20
30
40
50
J F M A M J J A S O N D
Time

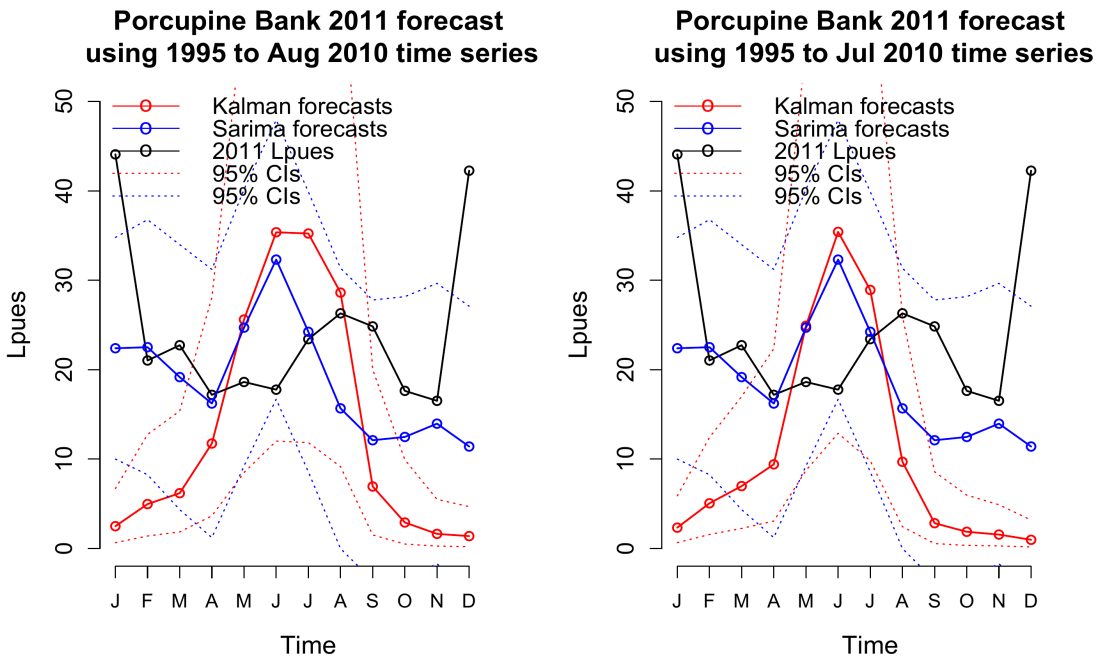


Figure 16: State space and sarima forecastings of the 2011 lpues (Kg/hours) for Porcupine Bank. The plots show the sensitivity of the state space predictions caused by the sequential withdrawal of the months August, September, October, November and December from the forecasting computation.

The state space method appears to be sensitive to the unusually high landing values of Aug-Sep-Oct-Nov-Dec (**Figure 1.2c**), and removing it sequentially enabled visual evaluation of the leverage effect on the discrepancy between sarima and state space predictions (**Figure 1.16**). In contrast, we note the lack of responsiveness of the sarima to this recent change in the level of capture.

(II.2) Common trends for connected waters

Dynamic Factor Analysis (DFA) was used to examine common trends in the 4 fishing zones or functional units (FUs) around Ireland (**Figure 1.17**).

The model with 2 common trends highlights the co-variations among the four time series of catches and turns out to be the optimal fitted model with an *AICc=1521* (**Figure 1.17a**, **Figure A2** in ***Annexes A*** for 1 common trend case).

According to the factor loadings (**Figure 1.17b**) the 1st trend seems to track the dynamics of the Aran grounds, Smalls and Porcupine Bank while the 2nd trend clearly groups the Irish Sea and Smalls together. It is worth pointing out the “hinge” position of

the Smalls with respect to its sensitivity to both trends, perhaps, reflecting its geographical location (**Figure 1.17b**).

(a)

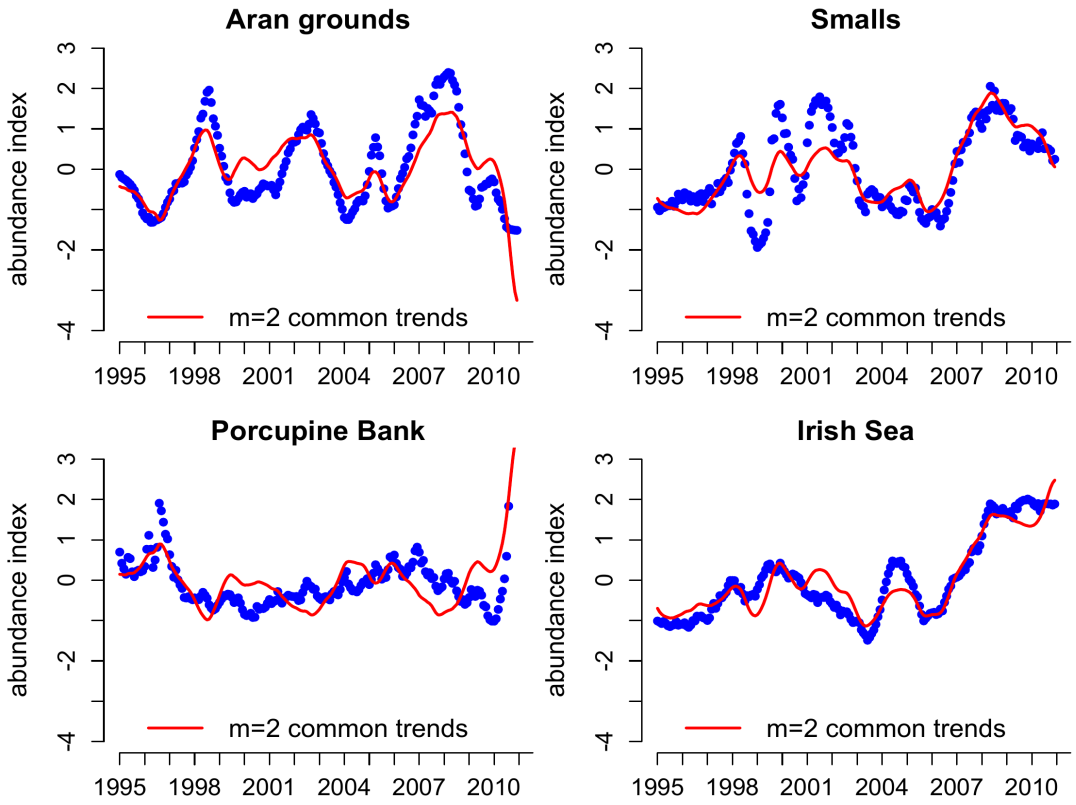


Figure 17a: Dynamic Factor Analysis modelling fit with 2 underlying common trends (*AICc=1521*). In comparison, the 1 common trend model gives an *AICc=1879* (see **Figure A2** in ***Annexes A***).

(b)

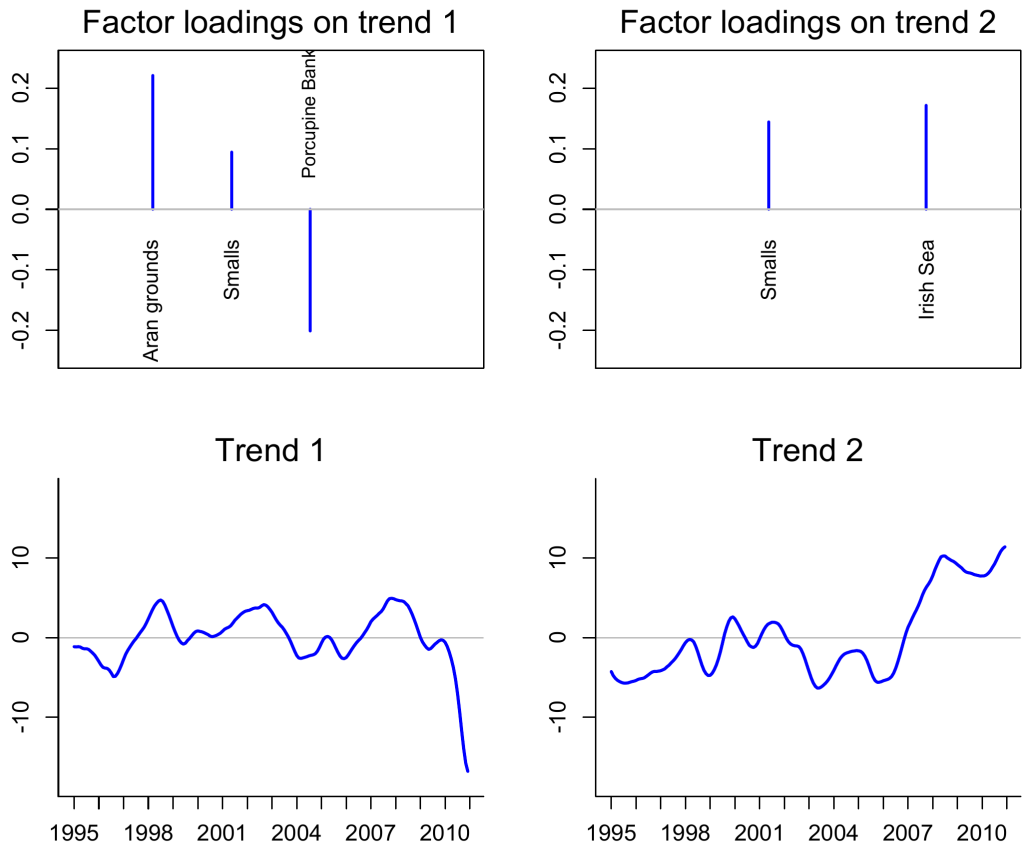


Figure 1.17b: Factor loadings associated to DFA modelling fit with 2 underlying common trends after varimax rotation.

(II.3) Climate influence

In the context of fisheries management, the time series analyses provides the opportunity to cast light on climate factors that may have influenced the landings data. By highlighting either covariations or contrasts in the dynamics of the *Nephrops* yield between the main fishing grounds of Ireland, the DFA also enabled us to examine the potential influence of regional climate indices (NAO, AO and AMDO).

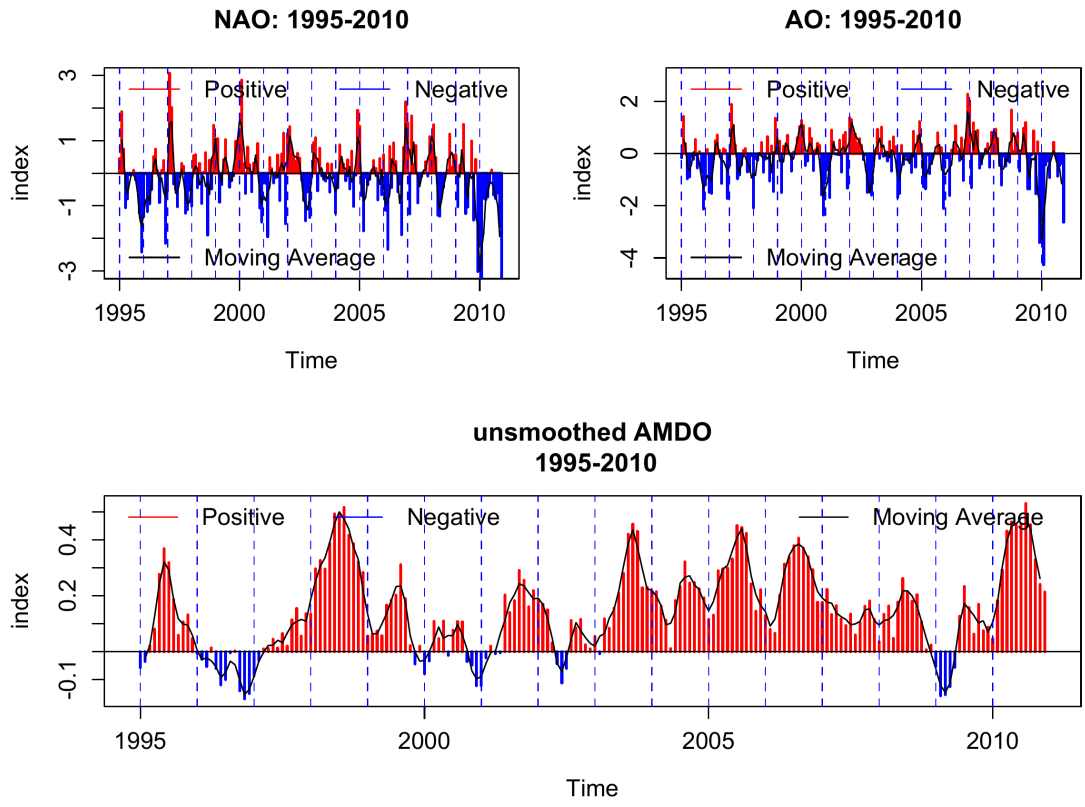


Figure 1.18: North Atlantic Oscillation time series (top left), Arctic oscillation time series (top right) and Atlantic-Multi Decadal oscillation time series (bottom).

Different combinations of NAO, AO and AMDO versions of these regressors were included in the optimal model of 2 common trends and the resulting improvement compared using AICc (**Table 1.5**).

Table 1.5: Reported *AICc* values of the Dynamic Factor Analysis (DFA) models combining available climate indices. The fits listed below correspond to combinations of our optimal model of 2 common trends with climate index (or combinations of it). Recall, NAOpc and NAOsb stand for principal component and station based indices of NAO respectively (see ***Materials and Methods***).

	no covariates	**NAOpc**	**AO**	**unAMDO**	**NAOpc unAMDO**	**AO unAMDO**	**NAOpc AO**	**NAOsb**	**AMDO**
AICc	1521	1506	1509	1507	1444	1453	1437	1517	1524

Beforehand, each climate index was subject to a state space analysis (through Kalman

smooth-filter means) to determine trends (called level in the terminology of the state space analysis) which then served as covariates. For the Atlantic-Multi-Decadal Oscillation, the smoothed and unsmoothed versions available from the NOAA were used (**Figure 1.19**).

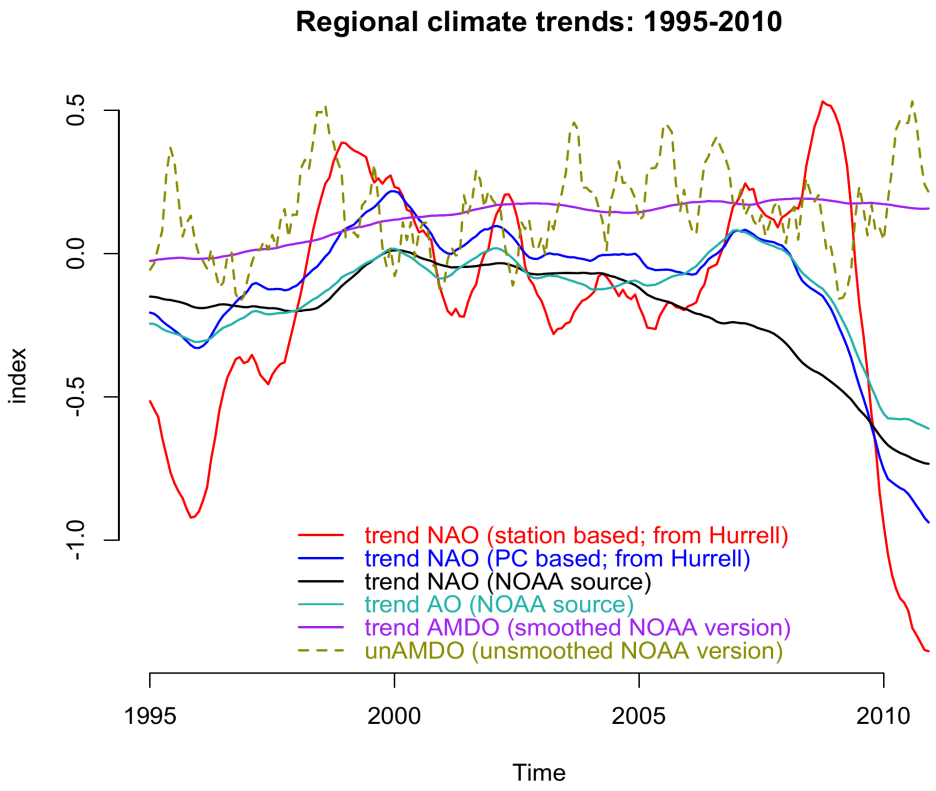


Figure 1.19: Trend level of regional climate indices derived from the state space analysis implemented on 3 different North Atlantic Oscillation data (NAO) time series (PC based, station based from Hurrell university corporation for atmospheric research and NOAA, see ***Materials and Methods***), Arctic Oscillation (AO) time series (NOAA). Note that the smoothed version of Atlantic Multi-Decadal Oscillations (AMDO) time series is already available at NOAA.

The inclusion of the NAO (PC based) and (unsmoothed) AMDO coupled covariates provides the best improvement in our reference model of 2 common trends (*AICc=1444*, **Table 1.5**, **Figure 1.20**).

The juxtaposition of the fit involving climate covariates versus the reference model makes it possible to locate the portions of it accountable for the climate influence (**Figure 1.20**). For the AMDO, the gain in the fit mostly related to the Porcupine Bank

and marginally the Aran grounds for the period 2006-2009, the Irish Sea for the period 2009-2010 and the Smalls for the period 2003-2006 (**Figure 1.20**). In contrast, the (PC based) NAO is solely influential for large sequences of the Porcupine Bank lpues series (**Figure A4** in ***Annexes A***).

Note, that even though the duet NAO (PC based) and AO led to the lowest *AICc* value (*1437*, **Table 1.5**) there was a high degree of (*Pearson*) correlation (*0.95*) between the two derived trends and a coefficient of *0.85* between both indices (**Figure 1.19**), resulting in this scenario being discounted.

(a)

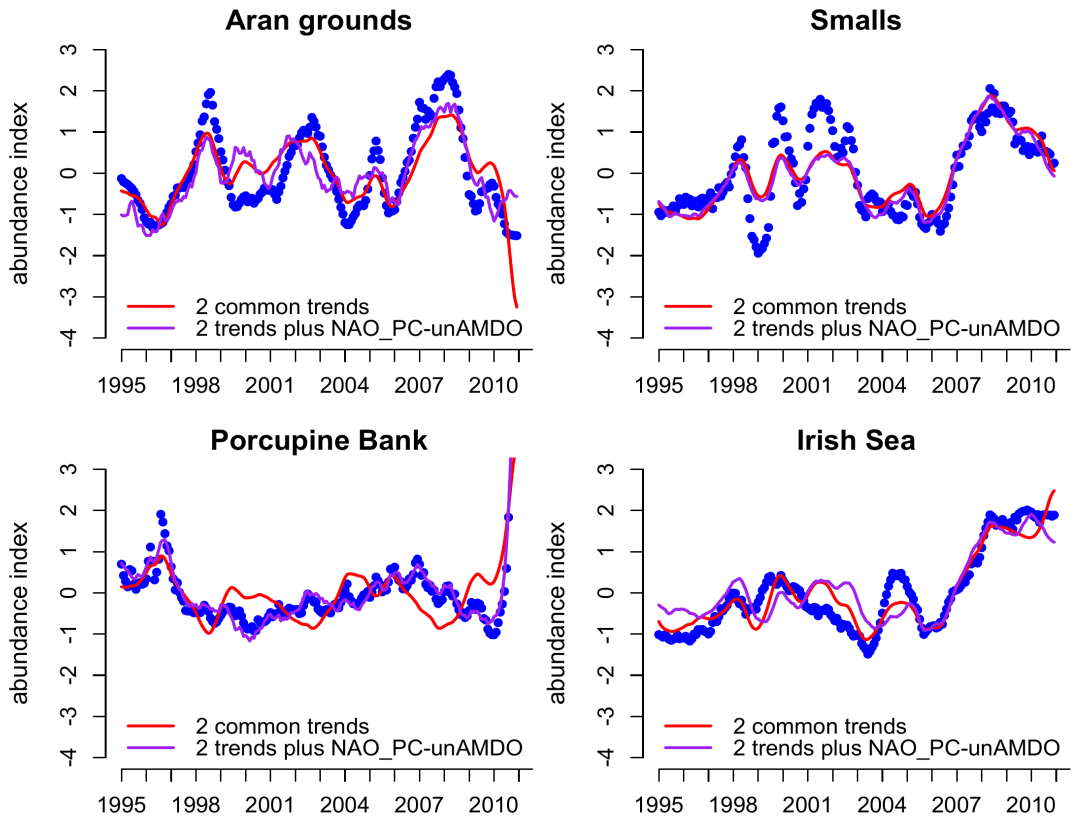


Figure 1.20: Dynamic Factor Analysis fit with 2 common trends and regional climate trend level NAO (PC based North Atlantic Oscillation index) and AMDO (unsmoothed Atlantic Multi Decadal Oscillations index) for period 1995-2010 (*AICc=1444*).

On the other hand, cross correlation function (ccf) estimates between lpues and potential regional climate indices reveal that landings are either positively or negatively

correlated to the NAO and AO indices and that their lingering effects ranged from 3 months to more than 7 years (**Table 1.6**). The whole auto-regressive models were sensitive to NAO (significant *p-values*, **Table 1.6**) and the influence of the Arctic Oscillation with the notable exception of Smalls. Notice, in order to avoid spurious effect due to the potential correlation between climate indices, testing their significant influence necessitated to run our models (**Table 1.6**) by considering them separately.

Table 1.6: Summary of the significant sensitivity of the auto-regressives models (sarima) to the climate influence (NOA, AO and AMDO) identified by the cross correlation function (ccf) approach. Significant lags are tested following the bottom-up [(1)] method. [+] and [-] signs indicate respectively the positive and negative correlation between lpue and the climate index. Notice, that under the Box-Jenkins framework, statistical criteria are not enough for a selective procedure, additional commitment of the practitioners through insights and intuitions are needed and even recommended which is adversary appreciated. When lags are closed we choose the highest **ccf** coefficient otherwise we compared their significance separately according to the sarima models. Since the potential relationship involve current lpue values and past indices we use the term lag. Notice that *p-value* for *t-test* less than *0.05*, *0.01* and *0.001* are flagged *, ** and *** respectively.

Sarima models	NAO index	AO index	AMDO index
Aran grounds: **$(5,0,0)(1,0,1)_{12}$**	Lag3*[-] (3 months)	Lag3**[-] (3 months) Lag10*[-] (10 months)	No
Smalls: **$(1,0,1)(1,0,1)_{12}$**	Lag27***[+] (2.25 years) Lag26**[-] (2.16 years)	No	No
Porcupine bank: **$(1,0,4)(1,0,1)_{12}$**	Lag41*[+] (3.41 years)	lag21**[+] (1.75 years)	No
Irish sea: **$(1,1,1)(1,0,1)_{12}$**	Lag88*[+] (7.33 years) lag5***[+] (5 months))	Lag4**[-] (4 months)	No

Discussion

By examining 16 years of monthly *Nephrops* landings from the West (FU17, FU16), South (F22) and East (FU15) fishing areas off the coast of Ireland using time series analyses, we highlighted distinctive components in the landings in each of these areas. The direct influence of the animal's biology and behaviour on the fishing activity is underlined.

A fundamental unit of 12 months, characterised by a steep rise in catches taking place in late winter-early spring, culminating in Summer, reflects the hatching, moulting and mating behaviours of this benthic species. This followed by a decline in landings and finally, a lower Autumn peak, with some area specific variations, co-incident with the spawning period of the reproductive cycle. The retreat of berried females into their burrows, where they remain until the next hatching period induces a proportional decrease in the landings during this period (**Figure 1.2**).

The time series analyses also casts light on additional features in the landing fluctuations.

General decrease of the yield

For each fishing area, an overall long term decrease in the landings occurred, with some variation in the duration and timing of the decline: 10 years (1995–2005) for the Aran grounds, 11 years (1995–2000 and 2003–2007) for the Smalls, 8 years (1997–2005) for the Porcupine Bank and 12 years (1995–2007) for the Irish Sea. Such consecutive negative trajectories for almost 2/3rds of the 16 years in the time series is a worrying signal (**Figure 1.10a**).

Short term variability

On a relatively shorter time scale, the sequences of rise and fall phases, similarly identified by using different approaches (**Figure 1.6**, **Figure 1.10b**) are likely to be the short term response of the population to the fishing activity. In particular, the Smalls and Aran grounds give examples of the amplitude in the variability (**Figure 1.2a-b**, **Table 1.2**) of the *Nephrops* availability knowing that during these 16 years the fishing effort of the fleet has grown (See ***General Introduction***).

Density dependence

The results suggest a (delay) density-dependent type of regulation (phase plots and fitted response surfaces of **Figures 1.13 & 1.14**) in line with the time scale of the trend and levels of fluctuation in the abundance. Theoretically, competition for food and habitat (Campbell et al., 2009) might affect the variability of the population abundance. In addition, hydrological conditions may also act to retain (or not) the larval production over suitable habitat patches and cause fluctuations in density (Hill, 1990a; Hill et al., 1997).

Monthly variability within the "rising" periods like Summer and Autumn has been also detected (**Figure 1.8a-f**) and illustrates the natural stochastic component of the stock dynamics.

Hence, the aforementioned structures of the population dynamics contribute to lessen the tacit belief that the *Nephrops norvegicus* stock is resilient to high fishing pressure, giving rise to the idea of an abundant and even unlimited resource.

Contextualising management

Thus, in terms of a management decision, the identification of these various components raises concern about the appropriate timing of management measures.

For instance, a biomass threshold ($B_{trigger}$) reference was introduced into the assessment (2015) and is defined as the lowest stock size from which the (UWTV) abundance has increased (*i.e.* the 2008 UWTV estimate). Then, when the burrow abundance decreased significantly below the *MSY* $B_{trigger}$, the ICES *MSY* approach states that under such conditions, the F_{MSY} harvest rate (calculated as the landings + dead discards over the UWTV abundance estimate) should be reduced by multiplying it by the ratio of current abundance to *MSY* $B_{trigger}$ (ICES IBPNeph, 2015). However, in light of the patterns and trends disclosed in this study (**Figure 1.6** and **Figure 1.10a-b**), such a mitigation approach should have been considered earlier when successive years of a decreasing tendency in lpues (**Table 1.2**) and/ or decline in abundance (**Figure A9** in ***Annexes A***) were identified. It is likely more opportune and appropriate to trigger a decrease in the harvest rate in light of this information rather than waiting to hit an absolute threshold value. This time series approach should thus be considered along with other fishing regulation tools.

Limitation

After outlining the trajectories of each of the time series presented here, it should be noted that given the relatively short data window (that is, 16 years of data records) we cannot overlook the possibility of a broader cycle encompassing the observed successive phases of (-) and (+) ols-cusum and ols-mosum slopes (**Figure 1.10a-b**) or the cycles and sub-cycles of the trends (**Figure 1.6**) that could at best validate our conclusions or disqualify them. This is an inherent difficulty in time series analyses but it is also the exciting aspect of this approach, to deal with pieces of the process of interest (here time series of landings) and better inform the outcome.

Climate variability: related climate effect

Investigating the regional climate influence on the stocks around Ireland indicated significant sensitivity to NAO and AO (**Tables 1.5, 1.6**, **Figure 1.20**).

According to dynamic factor analysis, the NAO explanatory variable effect is recognised for a large sequence of the Porcupine Bank landings (**Figure 1.20** and **Figure A4**) and marginally for the remaining areas. The cross correlation approach brought to the fore the delayed effect ranging from 3 months to 7 years of NAO and/or AO indices on the lpues (**Table 1.6**).

These results illustrate either a direct or indirect response of the species to climate variability (Ottersen et al., 2004). Post et al. (2004) state that "lagged population responses to large scale climatic variability may arise when the proximal abiotic factors influencing the population dynamics is itself correlated with regional atmospheric processes at some time in the past". In other words, the influences of the NAO and AO are translated locally into a series of physical events acting in various ways on the species life history.

For example, larval development has been shown to be temperature dependent and the relationship between the incubation duration (period between egg laying and hatching) and temperature was experimentally proven (Farmer, 1975; Dickey-Collas et al., 2000a; Briggs et al., 2002b). Atmospheric and oceanic inter-actions (wind, internal wave, heat exchange, upwelling...*etc*) influence the depth of the euphotic zone, and subsequently the concentration of nutrients available to phytoplankton for photosynthesis and hence the growth of *Nephrops* in the planktonic phase (Pochelon et al., 2009).

Thus, we have potential serious stress factor candidates of physical forcing by the climate. However, co-occurrence does not necessarily prove causality, it requires more data and details to validate this relationship. It is not clear which attribute(s) of the regional climate(s) are acting on the *Nephrops* and their response to these changes.

Aggregate data/ Effort issues

Catch and fishing effort data refer to aggregate data from different kinds of vessels. There have been considerable changes to vessel length and power over these 16 years (see ***General Introduction***). What appears to be a recent decrease (of about 5 years) in fishing days-effort (**Figure A6** in ***Annexes A***) is more likely not an overall decrease in effort since most of the fleet are now characterised by higher engine power (see **Figure 10** in ***General Introduction***). This strongly suggests that the effort index should be re-evaluated. Moreover, the amount of fishing effort allocated to *Nephrops* is deduced from the relative proportion (in weight) of a mixed fishery. In consequence, this crude calculation augments the difficulty in accurately evaluating the fishing pressure on the stocks.

Fishers behaviours

The sarima regression-like forms (**Table 1.4**) emphasized the short (1 month, Y_{t-1}) and seasonal (12 months, Y_{t-12}) lagged effects of the past landing values on the current ones. It is likely that this reflects the average seasonal (Y_{t-12}) adjusting behaviour of the harvesting by fishers and also throughout the year (Y_{t-1}). In fact, every year and for all the functional units (FU17, FU16, FU22, FU15), the major upward trend in captures corresponds to the regress from the burrows of the females after hatching (**Figures 1.2**; Bell et al., 2006) to reach a peak, which is memorised by fishers and translated into the significant Y_{t-12} auto-regression lag. Since the collapse of the cod stock, the growing interest in *Nephrops* along with other demersal species that are fished throughout the year gives support to the significant auto-regression of lag Y_{t-1}.

Box-Jenkins and state space issues

We mostly relied on state space modelling outputs to depict the evolution of the lpue time series of *Nephrops norvegicu*s. However, throughout this study, the data were

explored to identify the components of the dynamics of these series and to make them relevant for stock management. This often required comparing outputs from tools with relatively similar objectives but based on different assumptions, for instance sarima and ols-cusum, ols-mosum. These multiple approaches facilitated the interpretation of the outputs.

The key advantage of the state space modelling relied on its capacity to allow the user to explicitly attempt different structural components that make up the series, such as trend, seasonal cycle etc...

We also resorted to non-Gaussian state space models for the Aran grounds and Porcupine Bank lpues time series by assuming a Poisson distribution which is commonly used and described in population and community ecology as "it gives the distribution of the number of individuals, arrivals, events, counts, in a given time (or space) unit of counting effort if each event is independent of all the others" (Bolker, 2007). It enabled us to provide adequate models to describe the cyclical arrival and disappearance of the females that impact catchability considerably, as we have seen throughout this study. Nevertheless, it appears that substituting for a Poisson state space model was not necessary for the Smalls and the Irish Sea (**Table 1.1**) indicating much less expected impact of the female behaviour on the dynamic pattern of these data. Essentially, the sarima was helpful in providing a prediction on the basis of the past 16 years of data records in order to compare with the state space forecastings and it showed limitations in the case of Porcupine Bank forecasting of the 2011 landings (**Figures 1.15 & 1.16**). Notice that the sarima outputs and its parameter specifications (p, q, P, Q) depend directly, and excessively, on the form of the predominant signal that generates non stationarity. Although a linear trend (either positive or negative slope) is somehow easy to withdraw to obtain stationarity, other mixed and more complex patterns would have necessitated higher differencing *($d>1$)* leading to an increase in the risk of altering the data as for instance, spurious signals identified due to over-differenced data (Cowpertwait et al., 2009). Moreover, despite the availability of numerous unit root tests, we constantly had to face the question: how close to stationarity are we? And this is a hard question to answer in contrast to the state space method, for which such a prerequisite is unnecessary. In addition, as regression-like method, the Box-Jenkins modelling approach involves risk of over-parameterisation.

Forecastings

The lpue prediction estimates of the sarima and state space are close in the case of the Smalls, Irish Sea and Aran grounds (**Figure 1.15**) but diverge in the case of the Porcupine Bank (**Figure 1.16**). In addition, despite similar patterns in output for the Aran grounds, we observe a striking contrast between expected and observed lpues in 2011 for both techniques.

In the Aran grounds, the months concerned (Feb-Mar-Apr-May-June and Aug 2011) exceeded by far any previous harvested level (**Figure 1.2a**) and the upper confidence limits of the forecasting fit (**Figure 1.15a**). For the Porcupine Bank, Jan. and Dec. 2011 are clearly out of kilter with the level of the past catches of the same months (**Figure 1.2c**, **Figure 1.16**).

Nevertheless, the salient difference between these two areas resides in the fact that the unusual catches take place before 2011 in Porcupine Bank, that is to say, in Summer 2010 (**Figure 1.16**) enabling the state space method to detect it as illustrated by the steep rise of the trend level in 2010 (**Figure 1.6c**). While, for Aran grounds, the abnormal values are only restricted to the year 2011, and, in consequence, are clearly "invisible" for both procedures as they relied on data from 1995 to 2010 only.

Thus, the capacity of the state space modelling to update as new data are sequentially embedded in the process, render it more sensitive to unusual values. The state space process used this new information to adjust the forecasting accordingly and this led to an overestimate in the predicted landings (**Figure 1.16**). Sarima does not present such adaptive capability and, paradoxically, the poor prediction points out the advantage of the state space method over the sarima. The state space model was able to detect the unusual values recorded in 2010 that caused the discrepancy in the predicted values for the year 2011.

Forecasting for management

Hence the state space forecasting models have proven their ability to detect outstanding values and sort between two types of unexpected values that brought about modification of the trends or those that were exceptional and temporary, as for Porcupine Bank and Aran grounds, respectively. For example, the smoothed state disturbance result highlighted July 2010 as a state break point (187 in **Figure 1.9g**) for the Porcupine

Bank.

In this sense our models provide reliable quantitative and qualitative benchmarks for management purposes within a one year horizon. In fact, new regulations for the Porcupine Bank, by prohibiting fishing over a sub-area, had ramifications on (mostly) the Aran grounds. The new rules "altered" the "usual behaviour" of the fishermen and took the form of an odd swap between the Aran grounds and Porcupine Bank. The possibility of mis-reporting, or under-reporting of catches or re-distribution of catches to other areas, may also explain some of the peculiar lpues observed.

Common water

We depicted tendencies and fluctuations for each stock illustrating the fact that each population evolves within its own physical and biological environment and different fishing pressure leading to distinctive regulation mechanisms (**Figure 1.14**) and sensitivity to abiotic factors such as the large scale NAO, AO and AMDO climatic indices (**Figure 1.20**, **Table 1.5**, **Table 1.6**). Nevertheless, by pinpointing common trends in the lpue time series (**Figure 1.18**) and suggesting a "connection" between adjacent waters, it may be possible to envisage an implementation of a regional fishery policy encompassing, at the very least, sets of "connected" waters instead of ICES functional unit only. The spatial dimension conveyed by VMS data could play a part in this construction (Gerritsen et al., 2011). For Aran grounds, in the last few years the fishery has become significantly more concentrated in time (see ***Chapter 2 Spatial Analysis***). Vessels only fish the ground for short periods and record higher daily landings. In FU 22, the Irish vessels >18 m target *Nephrops* in several other FUs to optimize catch rates depending on tides and weather. These larger vessels freeze the catches at sea and have become increasingly prevalent since 2006 (ICES WGSCE, 2010, 2017). This change in behaviour reflects a generally more mobile behaviour by *Nephrops* targeting vessels which switch between grounds (ICES IBPNeph, 2015) and, clearly, underscores the benefit of using vessel monitoring system for a spatial track of the actual harvested ground.

Discards

Discarding refers to the portion of the catches that are returned at sea, either dead or

alive, for diverse reasons including management (e.g. net design, size regulation, catch composition) and/or economic motives (*e.g.* market selection: the first-hand sale is higher for the larger animals) along with fishing behaviour (Catchpole et al., 2008; Cosgrove et al., 2018).

When the Common Fisheries Policy was reformed in 2012, one of the main changes was to eliminate the practice of throwing unwanted commercial catches overboard (discarding) leading to an objective that by 2019, the general rule is that no commercial fishing vessel can return any quota species of fish, of any size, to the sea once caught (EU, 2013; EU, 2016).

The survival rate values of *Nephrops* in European seas as reviewed in Méhault et al. (2011) are variable: for example, it is estimated that 45 to 65% of *Nephrops* survive being discarded in the Bay of Biscay, 31% in North West of Scotland (*cit.* Ulmestrand et al., 1998), 23 to 60% in the South of Portugal (*cit.* Castro et al., 2003) and 31% on the West coast of Scotland (*cit.* Harris et al., 2005). The assumed discard survival rates of *Nephrops* for Aran grounds (FU17), Smalls (FU22) and Irish Sea (FU15) are 10%, 25%, and 10%, respectively (Anon., 2014abc) which are well below those recorded from elsewhere. Discards in the Porcupine fishery are considered negligible (Anon., 2014d). As a targeted species of a mixed fishery the new EU landing obligations compels the fishing industry to hold discards on board and integrate it systematically into fisheries data. There has been a recent recognition of the importance of the inclusion of discard data into reliable single stock assessments and the ecosystem implications in the European Union. Would these changes have changed our findings if the landings time series were augmented with discards?

We believe not, since, the conclusive results of our study are related to patterns in relative abundance rather than an estimate of absolute abundance or a population estimate. Nevertheless, it is inconceivable to attempt to manage a stock rigorously without including this portion of the catches (Pauly et al., 2016; Zeller et al., 2018). The work undertaken by Pauly et al. (2016) to reconstruct catches taking into account the different types of unreported captures as “discards” have led them to state that from 1950 to 2010 "the global marine fisheries captures are overall 53% higher than the reported data as recorded by the FAO”. Despite the notable exceptions of the Arctic Sea, and Indian -Antarctic-Southern Ocean, the results, sorted by FAO areas, confirm

this inflation as the major contrast with the patterns derived from missing discard data. Hence, inflation of the catches may signal or amplify an underlying trend (Zeller et al., 2005).

Nevertheless, two important outcomes in Pauly et al. (2016) and Zeller et al. (2005) are of great concern in our case. The study stresses the fact that by including "discards" a global decline from 1996 to 2010 was observed, rather than a "stability" phase and moreover the gradual shrinkage is stronger ("over three times that of the reported data as presented by FAO on behalf of countries").

The extent and level of discarding (now and into the future) is crucial since we purposively advocate for the use of time series analyses of the landings as a support for fishery management decisions.

Of course, these patterns may vary between fishing species, area, sub-area and functional unit as in our case, however, instead of hampering any progress in the use of lpues, including discards may help to move towards more accuracy in deciphering the dynamic components of abundance, and the implementation of the fishing regulation in order to keep track of the state of fisheries. We believe that such reconstruction of catches including discards (Zeller et al., 2005, Pauly et al., 2016) and potential misreporting (Watson et al., 2001) could be fruitful to ascertain stock status for the ones still deemed "sustainable" and endured 30 years (at least) of industrial fishing.

Conclusion

We examined *Nephrops* population dynamics from fishery dependent landings and effort data as a proxy for the relative abundance over a 16 year period. While these data undoubtedly have limitations (Pauly, 2013; Hilborn et al., 2013), we attempted, against a background of changes in oceanographic processes (using climatic indices) and in fishery activity to detect signals in the data that would be plausible and useful for management. We have pinpointed that the four main areas show important variability in abundance at different time scales that emphasises the amount of uncertainty that perhaps needs to be considered when implementing allowable catch advice.
Abiotic causes of the fluctuations are also very likely in relation to recruitment and density dependence regulation. We were however, unable to ascertain clear and unambiguous explanations for many of the dominant patterns seen in this study, in other words, we lack the information on the generating mechanisms.....for the moment.

Chapter 2 Spatial Analysis of the Aran grounds stock of *Nephrops norvegicus*

Contents

Chapter 2 Spatial Analysis of the Aran grounds stock of *Nephrops norvegicus*….104

Abstract....106

Introduction....107

Aims of this chapter....109

Materials and Methods....111

(I) Burrow counts....111

(I.1) Sampling area....111

(I.2) Burrow density....111

(II) Environmental and anthropogenic factors....112

(II.1) Mud and bathymetry....112

(II.2) Wind and currents....113

(II.3) Fishing pressure....114

(III) Geostatistical based approaches....115

(IV) Spatio-temporal analysis....117

(IV.1) Empirical orthogonal function....118

(IV.2) Contrast method....118

(IV.3) Spatial indicators....119

Results....121

(I) Lessons from data exploration....121

(I.1) Stability of spatial indicators....123

(I.2) Habitat dependence....128

(II) Geostatistical features....134

(II.1) Skewness and normality....134

(II.2) Edges versus midfield occupation....136

(II.3) Predictions with mud....144

(III) Factors of influence....152

(III.1) Surface currents advection....152

(III.2) Fishing pressure....163

Discussion....171

Conclusion....177

Abstract

Using geo-referenced information from underwater TV surveys, the spatio temporal patterns of the Aran grounds *Nephrops norvegicus* population distribution from 2002 to 2010 was investigated in relation to its habitat and fishing exploitation. A linear geostatistics based approach revealed a patchy distribution, varying in size and intensity over the years meanwhile sub-areas with density threshold constantly < 20% were delineated. Analysis of this variability showed an overall depletion of burrow abundance over the central area of the study contrasting with its margins and this led to an increase of vessel search activity with effort >10 hours towards the periphery. Though the mud content of the seabed contributed to enhance the quality of this spatio-temporal trend, it was not sufficient alone to explain the spatial variability in burrow distribution. In addition, this spatial framework was used to evaluate the influence of the surface current prevailing during the larval life stage over the area of study on recruitment and our method highlighted the potential of the remote sensing data.

Introduction

Landing statistics of *Nephrops norvegicus* from all countries show that 66,544 tonnes were landed in 2010. Most of this came from the North-East Atlantic where Ireland with its 7,800 tonnes (11.7%) is the second highest country in terms of tonnage (FAO, 2010). The *Nephrops* fishery in ICES area VII is extremely valuable with landings in recent years worth around 100 million euros at first sale, supporting an important indigenous processing industry (Meredith, 1999; Lordan et al., 2011; Foley et al., 2016). Thus, for the Republic of Ireland, sustaining this fishery is crucial.

For an optimal management strategy, demographic information for the exploited species is necessary. However, for *Nephrops*, effective stock assessment is hampered because of the difficulty in age determination, coupled with important diel and seasonal landing variations associated with the species behaviour and biology. For instance, *Nephrops* emerge daily from their burrows under optimum environmental illumination to feed and females disappear for almost six months leading to a sex ratio bias in the catches/landings over the whole year (Rice et al., 1971; Chapman et al., 1975; Aguzzi et al., 2008). Additionally, confidence in the commercial landings data are undermined by a lack of knowledge of the proportion of discards and survival rates and, to some extent, by misreporting. Under controlled circumstances, trawl surveys provide useful indices of local abundance (Tuck et al., 1997ab). However, because they are influenced by many factors such as weather conditions, sea state, neap tides and the strong diurnal pattern, this independent source of information is not deemed a satisfying method for measuring stock trends (*e.g.* Bailey et al., 1993, Briggs et al., 2000). In Aran grounds, trawl surveys exhibit a high degree of variability in biological parameters between sampled sites of the same stock unit (ICES IBPNeph, 2015) also reported from elsewhere (Tuck et al., 1994; Briggs et al., 1995; Tully et al., 1995). These limits have led to alternative assessment approaches and the rapid conversion to the underwater TV (UWTV) survey method for stock assessment.

UWTV survey

Implemented since 2002, the survey targets three geographically isolated *Nephrops* grounds (Galway Bay, Slyne Head and the Aran grounds) of which the Aran grounds is

by far the largest and most important in terms of the fishery. The Aran grounds stock (FU17) covers ICES rectangles 34–35 D9–E0 within VIIb. This stock is included as part of the total allowable catch for Area VII.

Habitat

This main *Nephrops* stock inhabits an extensive area of muddy sediment which lies to the West and Southwest of the Aran Islands. Muddy sediment is important for *Nephrops* to excavate its burrows (Campbell et al., 2009), and this means that the distribution of suitable sediment defines the species distribution.

The Eastern flank of the ground shallows up quickly but the majority of the ground is gradually deepening from around 100–110 metres with the deepest parts to the Southwest.

Other salient traits of this ecosystem are the weak currents that occur throughout the water column over the ground, although, there is a well-documented bottom density front on the Eastern flank of the ground (Nolan and Lyons, 2006). This is a seasonal feature, which establishes in May and persists until Autumn. The front causes a persistent jet like flow from South to North close to the seabed and its mean position varies from year to year by up to 30 kilometres (ICES WKNephTV, 2007). The timing and position of the jet may influence the recruitment and settlement success of post-larval *Nephrops* because it could potentially advect larvae from the area (ICES WKNeph, 2007).

Stock

In this instance, the stock definition (Begg et al., 1999) coincides with the spatial extent of the suitable sediment patch of about 1,000 km^2 on average.

Thus, for determining its abundance we used video footage (10 minutes) of the seabed collected at each station derived from a grid design. Following a standard survey protocol (ICES WKNeph, 2007, 2009), these videos result in a census of *Nephrops norvegicus* burrows.

On average, the Aran grounds account for ~88% of the total estimated burrow abundance from FU17 while Galway Bay and Slyne Head account for ~8% and ~2%, respectively. This selected survey approach allows abundance estimates and estimation

uncertainties to be determined using geostatistical approaches, increasing our capacity to relate biomass and patterns of distribution.

Catchability/ Impact of fishing

The fishery on the Aran grounds operates throughout the year, with distinctive seasonal patterns in Spring-Summer and Autumn (see ***Chapter 1 Time series Analysis***). The trawling method of fishing dominates the landings in the Aran grounds; currently 90% of the fishery employs twin-rigged vessels, all of which are from otter trawls. The catchability is strongly influenced by the behaviour of the animal, through their availability on the seabed (see ***General Introduction*** and ***Chapter 1 Time Series Analysis***). The burrows extend between 20–30 cm below the mud surface, and animals within burrows are unlikely to be caught by a passing trawl. Daily, they are caught when they emerge from their burrows to forage (Aguzzi et al., 2003b, 2004ab, 2008, 2009). Adults probably only undertake very small-scale movements (a few 100 m). Merder et al. (2020) reported between 21 m and 500 m distance travelled by recaptured individuals, supposedly for seeking shelter. Nevertheless, *Nephrops* habitat is readily accessible to trawling and the fishing impact is obvious.

Aims of this chapter

In the Aran grounds, the UWTV method is now treated as an absolute measure of *Nephrops* abundance by the International Council for the Exploration of the Sea (ICES WKNeph, 2009). Hence, cartography of the burrow distribution is of interest because it could reflect regional differentiation in productivity and sensitivity to fishing removal. It has been reported that density limits growth, and smaller sizes are recorded on grounds with higher density, even within an area that is considered to be inhabited by the same population (Johnson et al., 2013). Thus, a stock may be divided into a number of smaller "stocklets", with different population densities, size, growth rate and size at first maturity (Briggs et al., 1995; Tully & Hillis, 1995; Maynou et al., 1996; Maynou and Sardà, 1997; Afonso-Dias et al., 1998; Campbell et al., 2009; Haynes et al., 2016).

The aim in this chapter is to characterise the spatial distribution of *Nephrops* settlement on the Aran grounds.

Spending most of its entire life as an epibenthic dweller animal, we tested the leverage effect of seabed sediment components (the sand-silt-clay), along with the water depth, on the spatial variability of the density observed. We also investigated the potential impact of the ocean surface current patterns on the population abundance.
Nine years of geo-localised burrow counting were utilised to map the density distribution and detect (variable vs constant) spatial structure(s) while spatio-temporal analysis of annual burrow distribution was used to identify spatial trends in abundance and evaluate the fishing activity role accordingly.

Materials and Methods

(I) Burrow counts

(I.1) Sampling area

Either during the phase of settlement following its water column life cycle or as burrow dwellers, *Nephrops* appears to be very sensitive to seabed sediment composition. Mud patches of mainly silt and clay with a variable proportion of sand is considered preferential sea bottom habitat. Located at the mouth of Galway Bay on the west coast of Ireland, the Aran grounds, named after the group of islands of the same name, is the second most important fishing mud patch in terms of size and yield for the Republic of Ireland.

For the Aran grounds, the initial design, in 2002, was based on a grid of 3*3 nautical miles (nm) with two random stations selected within each square. Since 2003, a randomized fixed grid design was used, where a point (or a station) is picked at random and the subsequent stations are sampled at a fixed distance of 2.5 nm north-south and east-west. Note that from 2003 to 2010 the survey distance between stations was 2.25 nm and every 3.5 nm or 6.5 km since 2012 (Anon., 2017). Note also that the grid has been extended in an adaptive way until the boundaries (the perimeter of the ground) are established (that is, until the burrow densities are at, or close to, zero).

(I.2) Burrow density

At each station, an underwater camera mounted on a sledge is deployed. Once stable on the seabed, a 10 minute tow records footage of an area of the seabed corresponding with a field of view of 75 cm (72 cm between 2002–2006) over which burrow complexes are identified, counted and finally converted into density per m^2 after selecting the appropriate distance over ground from various positional signals.

Surveys generally take place in early June. However, in 2003, due to poor weather and technical problems the coverage was poor compared with the other years. In 2004, meteorological conditions delayed the completion of the survey, and consequently, approximately 50% of the remaining stations were carried out one month later, in July (ICES WKNephTV, 2007).

(II) Environmental and anthropogenic factors

To examine some of the possible causes of changes in distribution and the density of burrows we evaluated the effects of three environmental covariates (mud, bathymetry, wind) and assessed the impact of fishing pressure.

(II.1) Mud and bathymetry

The relationship of the *Nephrops* stock to its direct habitat was investigated. Purposively, we have selected the silt-clay (*i.e* mud) proportion of the seabed sediment and the bathymetry (*i.e.* depth) to gauge the influence on animal density distribution. Sediment samples from several years: 2002 (*n=60*), 2003 (*n=29*), 2004 (n=30) and 2006 (*n=74*) were compiled for mapping based on particle size analysis results from samples collected from 2002–2006 under water TV surveys. A Duncan and Associates day-grab was used for sediment sampling and the particle size analysis of the sediment samples was carried out using a Low Angle Lazer Light Scattering (LALLS) method using a Malvern Instrument (ICES WKNephTV, 2007).

In addition, the principal system employed for the recording of bathymetric data throughout the surveys was an echo sounder (single or multibeam) installed on the Irish marine institute research vessel *Celtic Voyager*.

Mud and bathymetry covariates were interpolated over the area of interest with the *B-cubic splines* using R (2018) computing language (Finley et al., 2017).

Analysis of this relationship led us to explore the following linear regression equations for mud:

$$\boldsymbol{M1}: density_t = \beta_t * rateMud + residuals_t$$
$$\boldsymbol{M2}: density = \beta * rateMud + residuals$$

and depth covariates:

$$\boldsymbol{D1}: density_t = intercept_t + \beta_t * depth + residuals_t$$
$$\boldsymbol{D2}: density_t = factor_{year} + \beta * depth + residuals_t$$
$$\boldsymbol{D3}: density = \beta * depth + residuals$$
$$\boldsymbol{D4}: density = intercept + \beta * depth + residuals$$

In addition, the smooth Loess regression is used for visual inspection. It is a non-parametric method where least squares regression is performed in localised subsets, which makes it a suitable candidate for smoothing. Ranging between 0 to 1, the span argument controls the degree of smoothing: the greater the value of span, the more

smooth is the fitted curve (R Core Team, 2018).

(II.2) Wind and currents

We also undertook to explain the burrow distribution by considering the planktonic stage of the animal's life cycle. The time window during which the winds induce surface currents is likely the time that exerts influence through advection of larval dispersal and to some extent burrow distribution. In order to identify such hydrological traits, we used remote sensing data. We choose 5 days period average (noted *D1*, *D2*,..*etc.*) of ocean surface wind and current over the months of March, April and May for the period 2002 to 2010, which are assumed to cover the main hatching sequences. The ocean circulation dataset used is the product of the Ocean Surface Current Analysis (OSCAR[11]) obtained from the Jet Propulsion Laboratory (JPL) and Physical Oceanography Distributed Active Archive Center (podaac) developed by Earth and Space Research (ESR).

The wind dataset is derived under the Cross-Calibrated Multi-Platform (CCMP) project. The CCMP datasets combine cross-calibrated satellite winds obtained from Remote Sensing Systems (REMSS) using a Variational Analysis Method (VAM) to produce a high-resolution (0.25 degree) gridded analysis. The CCMP data set includes cross-calibrated satellite winds derived from SSM/I, SSMIS, AMSR-E, TRMM TMI, QuikSCAT, SeaWinds, WindSat and other satellite instruments as they become available from REMSS (Atlas et al., 2011).

Azimuth and magnitude

The zonal and meridional components of both ocean surface currents and winds are expressed in terms of speed (magnitude) and direction (azimuth).

The current (or wind) vector components (u_i, v_i) are respectively the zonal and meridional velocity and are expressed in current (or wind) speed $|v_{H_i}| = \sqrt{u_i^2 + v_i^2}$ and direction $d_{H_i} = atan2(u_i, v_i)$.

11 The OSCAR product was developed by Gary Lagerloef, Fabrice Bonjean and Kathleen Dohan from ESR. The data have been created by NASA Goddard Space Flight Center (GSFC) within the NASA framework Cross-Calibrated, Multi-Platform Ocean Surface Wind Velocity Product for Meteorological and Oceanographic Applications.

Mean Azimuth

We assumed that vectors are of unit length (*i.e.*, module) $r=1$ and the azimuths are analysed based on that premise. Hence, the circular mean direction $\bar{d}_{H_0}$ is obtained by transforming the set of input azimuth $d_{H_1}, d_{H_2}, \ldots, d_{H_n}$, given in term of angles, to rectangular ones $r\cos d_{H_i}, r\sin d_{H_i}$ and using the direction of their resultant vector $\boldsymbol{R}=\left(\sum_i^n \cos d_{H_i}, \sum_i^n \sin d_{H_i}\right)=(C,S)$ and its length $R=\|\boldsymbol{R}\|=\sqrt{C^2+S^2}$:

$\cos \bar{d}_{H_0}=\frac{C}{R}$, $\sin \bar{d}_{H_0}=\frac{S}{R}$ or

$$\bar{d}_{H_0}=\arctan(S/C)=\begin{bmatrix}\arctan(S/C), & \text{if} \quad C>0, \quad S\geqslant 0\\ \pi/2, & \text{if} \quad C=0, \quad S>0\\ \arctan(S/C)+\pi, & \text{if} \quad C<0,\\ \arctan(S/C)+2\pi, & \text{if} \quad C\geqslant 0, \quad S<0,\\ \textit{undefined}, & \text{if} \quad C=0, \quad S=0.\end{bmatrix}$$

(Jammalamadaka et al., 2001).

Notice, that the near surface velocity is directly derived from sea surface height, wind stress and sea surface temperature. It is the sum of the geostrophic, Ekman-Stommel and thermal wind currents. The total velocity is the vertical average over a surface layer thickness of 30 metres, *i.e.* 15 metres mean depth (Atlas et al., 2011).

In addition, the wind datasets combine cross-calibrated satellite winds to produce a spatial resolution of 0.25 degrees Latitude x 0.25 degrees Longitude over a temporal scale of 5 days. The data consists of 6 hour sets that are time averaged over 5-day periods (*D1*, *D2*,...etc).

All wind observations and analysis fields are referenced to a height of 10 metres above the sea level (Bonjean et al., 2002). These are then converted to obtain the cartesian coordinates, where different conventions are used to describe direction, and degrees/radians were converted when necessary.

The statistical analysis of these ocean and wind vector components of the Aran grounds zone and peripheries was performed using R (2018) software tools (Ruiz-Cuetos et al., 2016; Agostinelli and Lund, 2017; Lamigueiro and Hijmans, 2018).

(II.3) Fishing pressure

The spatial distribution of *Nephrops* was also investigated by examining the relationship between density and fishing effort, using data from the on board vessel monitoring

system (VMS). The data available for this study covered the period November 2005 to August 2010. In the case of the Aran grounds, *Nephrops* directed activity was defined for VMS pings where >30% of daily operational landings was reported to be *Nephrops*. Gerritsen et al. (2011) provide details of how these positional data from fishing vessels are linked to logbooks.

Maximum Covariance Analysis (MCA)

The maximum covariance analysis (MCA) approach examines the covariance of the two combined data fields of interest, namely, the burrow density ordinary kriging predictions maps and the rasterised vessel monitoring system data, utilising a singular value decomposition (SVD) algebra of the coupled fields. To perform the SVD we constructed a temporal cross-covariance matrix between the two space and time dependent data fields. The MCA method then identifies pairs of coupled spatial patterns, with each pair explaining a fraction of the covariance matrix between the two fields, called squared covariance fraction: only modes with strongly coupled variations are identified (Björnsson et al., 1997, Taylor et al., 2013).

(III) Geostatistical based approaches

In geostatistics, spatial correlation, if present, is measured from observational data and modelled through a variogram.

The data provide informations (values) about a regional variable (burrow density) $z(s)$ at a given region (Aran grounds) which is a realisation of a parent random function $Z(s)$ that is the (inaccessible) true settlement of *Nephrops norvegicus*.

In theory, the detection of the variation in space of this random function $Z(s)$ is possible by taking its increment $Z(s) - Z(s + h)$ and calculating the theoretical variogram or the semi-variance at lag (h) $\gamma(h) = \frac{1}{2} E\left[\left|Z(s) - Z(s + h)\right|^2\right]$ under the "hypothesis of intrinsic stationarity of order two" (Matheron, 1965).

This theoretical variogram is approximated by the experimental or sample variogram computed from the data z(s): $\gamma(\boldsymbol{h}) = \frac{1}{2N_h}\sum_{i=1}^{N_h}(z(s_i) - z(s_i + h))^2, \quad \forall h \in \boldsymbol{h}$ that measures the variability of the burrow density for a set of data *i=1,2,...* separated by a lag (h) (Webster and Oliver, 2007; Bivand et al., 2013).

Under this assumption, the spatial correlation depends only on the distance (h) between sites and not the site locations. (N_h) is the number of pairs of data points separated by a lag (h) within the chosen sequence of distance intervals and the orientation of the vector ($\boldsymbol{h}$).

Finally, $Z(s)$ noted $Z(s) = m + e(s)$ could be seen as a signal composed of a deterministic drift m plus a residual part $e(s)$ representing the spatial signal of the regionalised variable in the midst of noise.

In the case of ordinary kriging m will be an unknown constant mean and in the case of universal kriging m will take, in this study, the form of the equation ***M1*** above.

The variogram is a fundamental step in recognising the spatial structure(s) in the regionalised variable. The behaviour near the origin reflects the continuity and the spatial regularity of the burrow density (the regionalised variable).

By visual examination of the 10 minutes camera sweeps of the seabed, burrow complex successions appear to be heterogenous at some sites and very smooth in progression in others. At this scale, microstructure in the distribution of *Nephrops norvegicus* density could easily be conceived taking into account the very sedentary (with very short-range foraging excursions) and territorial nature of this species. However, this microstructure is "a structure with a range shorter than the smallest inter-point distance" (*cit* in Chiles and Delfiner, 2012) and hence we consider this potential microstructure not perceptible at the scale of the study.

In addition, including a nugget term related to the amount of short range variability (microstructure) and/or the sampling error (measurement and/or positioning errors) in the data will be transferred to any estimates produced (Clark, 2001, 2010). Recall, our aim is to display patterns in *Nephrops* burrow distribution rather than estimating abundance values.

Mapping burrow density with indicator kriging is a simple (and crude) way to envisage spatial structure. It is obtained by transforming the response variable and converts a continuous variable (burrow sample density) to a binary variable (presence/absence or 0/1). From the samples, we have chosen the first 20th quantile and the median values as thresholds to coerce to 0 (respectively to 1) the density values under and above it. Hence, for each year and threshold, a resulting variogram model is fitted leading to a presence/absence annual map with its associated probabilities.

The cross-variogram is the natural generalisation of the variogram for lag (h) and describe the way in which two regionalised variables $Z_i(s)$ and $Z_j(s)$ are spatially related:

$$\gamma_{ij}(h) = \tfrac{1}{2} E\left[\left\{Z_i(s) - Z_i(s+h)\right\}\left\{Z_j(s) - Z_j(s+h)\right\}\right]$$ (Matheron, 1965)

Co-kriging prediction with mud

With the kriging method we estimate unknown values of burrow density from observed values of the same variable. With co-kriging a secondary variable may provide useful information. Here, the additional variable is the information conveyed in each variogram fit that precedes one in time.

Following the finding of a strong relationship between density and the mud content of the seabed over these 9 years, the annual residuals derived from the regression equation (that is, **M1**) have been pooled leading to the choice of an exponential model

$$\gamma_{fit}^{\text{Exp}}(h) = \begin{bmatrix} c_0 & \text{if } |h|=0 \\ c_0 + c_1\left(1-\exp\left(-\frac{h}{a}\right)\right) & \text{if } |h|>0 \end{bmatrix}$$ with nugget effect c_0, partial sill c_1,

and practical range $3a$.

Hence, the key of the co-kriging resides in fitting models to both the direct and the cross variograms that are "proportional" to the global variogram above. The pooled variogram $\gamma_{fit}^{Exp}(h)$ and the cross variograms are "proportional" $r_{ij} * \gamma_{fit}^{\text{Exp}}(h)$ where r_{ij} is the point-wise correlation between years (i) and (j). For each observation point in year (i) the spatial nearest neighbour observation in year (j) is obtained, and a correlation is calculated (Pebesma and Duin, 2005). So, the fitted variograms have the same range but different sills and nuggets. The sill is the total variance where the empirical variogram appears to level off, and is the sum of the nugget (if any) plus the partial sills. Then, each of the partial sills is adjusted by least squares to the closest value that will result in positive definite matrices in order to obtain a linear model of co-regionalisation (**Figure B6**; Pebesma, 2004; Rossister et al., 2012).

(IV) Spatio-temporal analysis

Our objective here is to describe the evolution (trend) of the spatial structure(s) of the burrow distribution in time and outline the main features.

(IV.1) Empirical orthogonal function

Empirical orthogonal function (EOF), also known as principal component analysis or factor analysis, is a technique that aims at finding a relatively small number of independent variables (factors) that capture most of the observed variance (information) and convey as much of the original information as possible without redundancy (orthogonality property). In other words, the method finds the spatial patterns of the variability in the data.

We have one gridded density field per year $D(x, y, t)$ resulting from the ordinary kriging predictions, relying on the corresponding variogram fit and we performed an EOF analysis over these 9 consecutive years leading tow

$D(x, y, t) = PC_1(t)\,EOF_1 + PC_2(t)\,EOF_2$ here the $EOF_{1\&2}$ represents the spatial features retained, and $PC_{1\&2}$ the principal components or factor loadings indicating the weight of these spatial patterns over these years (Pebesma, 2012).

(IV.2) Contrast method

Like the EOF**,** and despite a different theoretical basis, the Contrast method (Pebesma et al., 2005) sketches the spatial trends in the scattering of the animals over the nine year period, enabling a useful comparison of the results of both approaches.

If we note $\hat{Z}(s) = [\hat{Z}(s, t_1), \ldots, \hat{Z}(s, t_9)]^T$ the 9 Co-kriging predictions and $\sum(s)$ the corresponding [9 x 9] var-covariance matrix (diagonal and off-diagonal, respectively), then the contrasts between these annual maps are

$C(s) = \lambda \hat{Z}(s) = \lambda_i \sum_{t=1}^{t=9} \hat{Z}(s, t_i)$.

Thus, a simple approach for estimating the gradual change over time is to calculate the contrast that would estimate the regression slope for 9 years by ordinary least squares

$\hat{Z}(s, t) = \beta_0(s) + \beta_1(s)t + e(s, t)$ with $t \in [2002, 2003, \ldots 2010]$.

These contrast coefficients are obtained by the usual ordinary least square equations applied to the regression model $Y = \beta X + e$ with (Y) the response vector and (X) the design matrix with the predictor variables in its columns. The vector of contrast coefficients (λ) is estimated by $(X^TX)^{-1} X^TY$, and the second row of $(X^TX)^{-1} X^T$ contains the contrast coefficients (**Table M1**).

Table M1: the contrast coefficients (λ) used to determine burrow density change trend from 2002 to 2010.

Year	2002	2003	2004	2005	2006	2007	2008	2009	2010
λ	-0.067	-0.050	-0.033	-0.017	0.000	0.017	0.033	0.050	0.067

(IV.3) Spatial indicators

Several spatial indicators have been used to characterise the spatial distributions of *Nephrops* population over the mud patch including the *centre of gravity* (*cg*) corresponding to the mean geographic location of the population weighted by its density, the *standard deviation ellipse* (*sde*)
that helps to characterise the dispersion of point observations along two orthogonal axes the semi-major [σ_y] and semi-minor [σ_x] and to capture the directional bias in the spatial point pattern. In fact, the ellipse will be oriented in the direction of maximum dispersion by accounting for the skewed feature of the density distribution; also, the *eccentricity* (*E*) that is a measure of how "out of round" an ellipse is. It is given by the formula

$E = \frac{a}{c}$ where [*c*] is the distance from the centre to a focus and [a] is the distance to that focus to a vertex. The formula produces a number in the range [0,1]. If the eccentricity is zero, the ellipse is not squashed at all and so remains a circle. If it is equal to 1, it is completely squashed and looks like a line. Then, *E* evaluates the elongation of the population, in other words its anisotropy (or isotropy). Finally, since our population may be distributed into several spatial clusters (coined "stocklets" in the case of *Nephrops*), Woillez et al. (2007) proposed an algorithm to identify the *number of patches* by attributing each sample to the nearest patch, with respect to a maximal threshold distance to its *cg* (here, set to the variogram practical ranges listed below in **Table M2**). "The algorithm starts from the sample value displaying the maximum density, and considers every other sample in decreasing order of density. The maximum value initiates the first patch, then, the current sample value is attributed to the nearest patch, if the distance to its *cg* is smaller than the given threshold distance" (range parameter of the variogram). Otherwise, the current sample value defines a new patch. Spatial patches whose abundance is greater than 10% of the overall abundance are retained. The result is then the number of spatial patches".

Table M2: Parameter values of the spherical variogram models fitted to the sample variograms for years 2002-2010.

Year	**2002**	**2003**	**2004**	**2005**	**2006**	**2007**	**2008**	**2009**	**2010**
Range (km)	20	14.99	13.16	16.02	11.16	19.15	15	16	16.37
Sill	0.1946	0.1607	0.2960	0.1817	0.0736	0.1517	0.0656	0.1396	0.1385

The geostatistical and spatio-temporal analysis were carried out using R (2018) software tools (Pebesma, 2004; Pebesma, 2012; Gräler et al., 2016; Becker et al., 2018; Bivand and Lewin-Koh, 2018; Renard et al., 2018; Ribeiro et al, 2018).

Results

(I) Lessons from data exploration

The contours of the area of study reflect the amount of ground covered by the sampling scheme of the available data, chiefly corresponding to the UWTV surveyed area. In Aran grounds, *Nephrops norvegicus* occupy a slope that goes from –80 to –100 metres, excavating burrows on the seabed with a variable range of silt and clay sediments (**Figure 2.1a-b-c**).

(a)

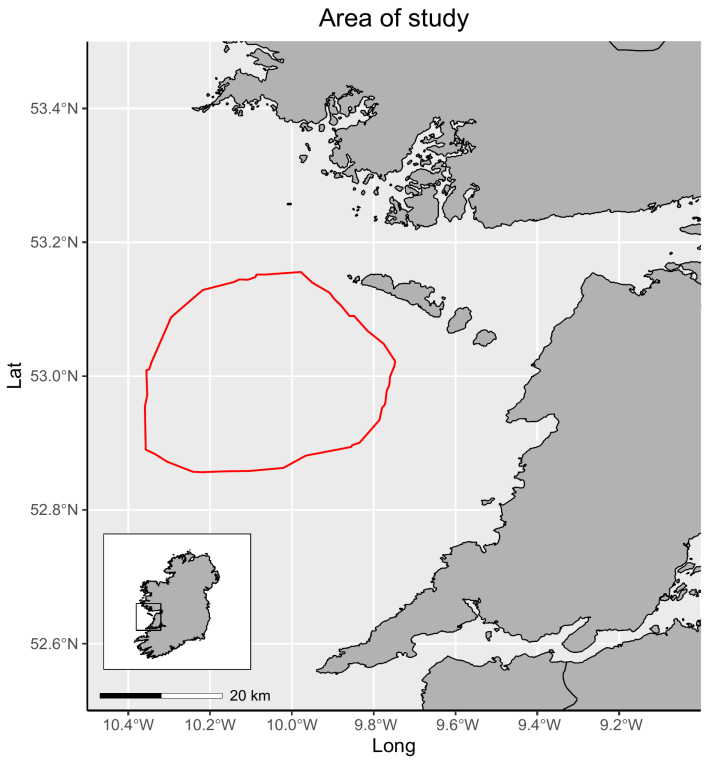


Figure 2.1a: Location of the Aran grounds mud patch (red line).

(b)

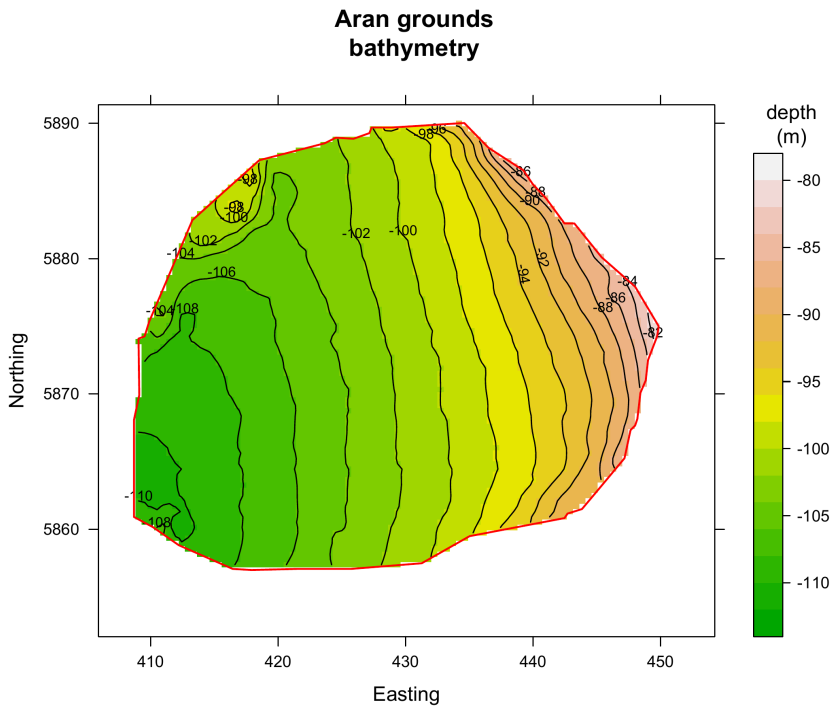


Figure 2.1b: Bathymetry over the area of study approximated with multilevel *B-splines* using R (2018) software (Easting/northing coordinates in UTM zone 29, WGS84).

(c)

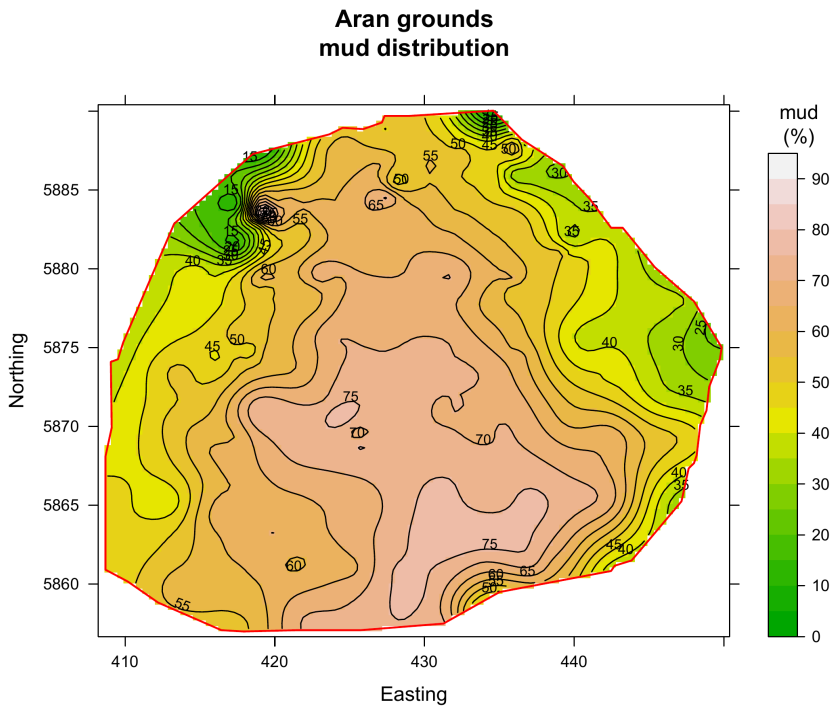


Figure 2.1c: Cartography of mud proportion over the area of the study generated by *B-splines* interpolation of year surveys 2002, 2003, 2004 and 2006. The mud fraction in the sediment is composed of silt and clay according to Folk classification. Easting/northing coordinates in UTM zone 29, WGS84.

(I.1) Stability of spatial indicators

Applied directly to the observed samples, the spatial indicators (**Figure 2.2**) feature a relatively stable spatial pattern over the period of study, with the notable exception of 2003, which is characterised by an incomplete sampling of the area due to poor weather conditions.

The dispersion of the weighted centre of gravity (*cg*) extends over a North-South axis mainly (**Figure 2.2a**). Examining the variability in scale and order of the maximum dispersion direction (σ_y the major axis of the ellipse of deviation) and the eccentricity values (*E,* the flatness of the ellipse) suggest annual differences in the shape and elongation of the population but within a limited range (**Figure 2.2c-d**).

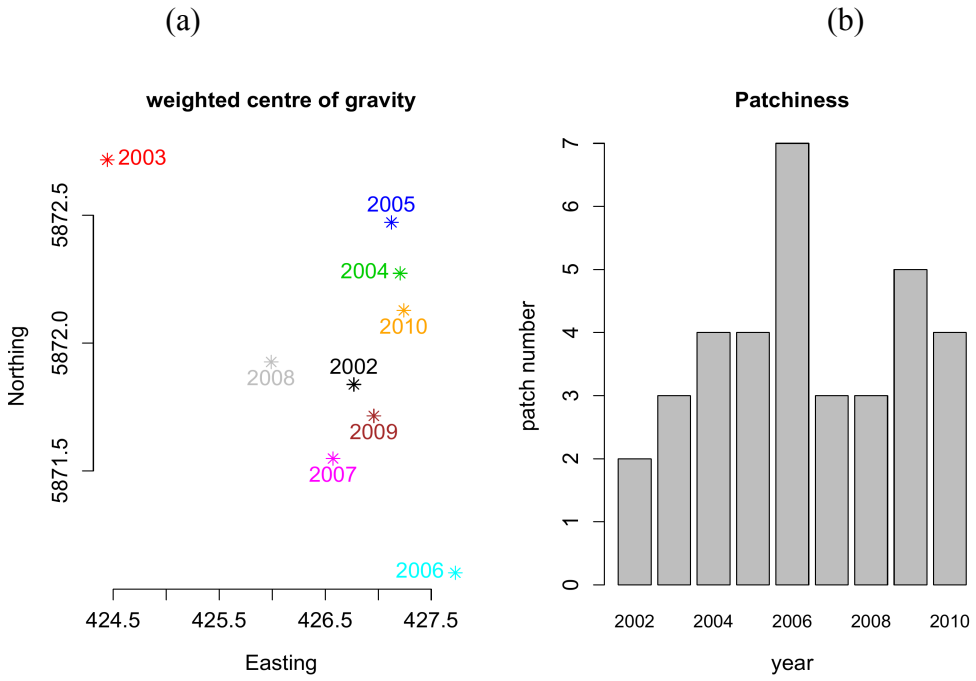


Figure 2.2 a-b: Spatial indicator measures of the burrow dispersion **(a)** Dispersion of the weighted *center of gravity* (*cg*), (**b**) Estimated annual number of patches following Woillez et al. (2017). Easting/northing coordinates in UTM zone 29, WGS84.

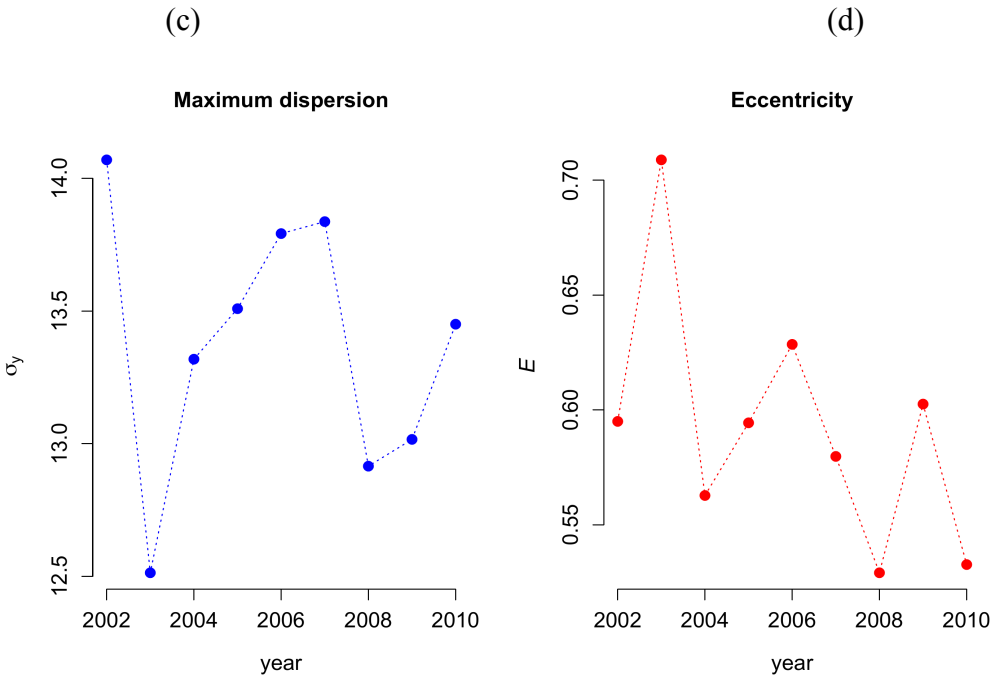


Figure 2.2 c-d: Spatial indicator measures of the burrow dispersion: (**c**) Variability of the *maximum dispersion* (σ_y) (**d**) *Eccentricity* (*E*) or measures of the flatness of the ellipse. Recall, if an ellipse is close to circular it has an *eccentricity* close to zero while, if an ellipse has an *eccentricity* close to one it has a high degree of ovalness. Easting/northing coordinates in UTM zone 29, WGS84.

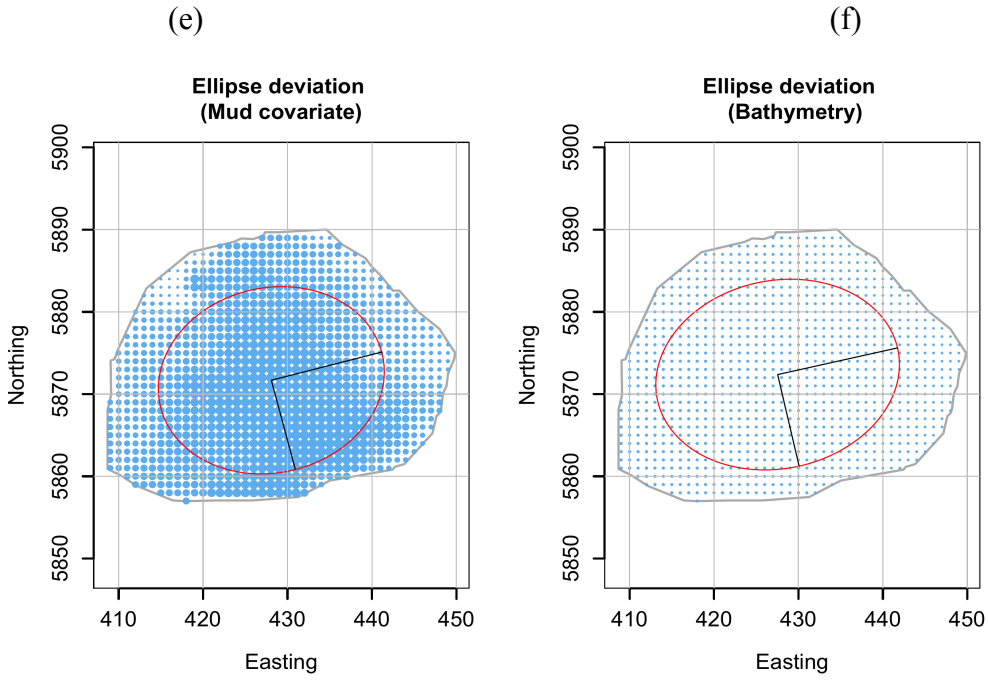


Figure 2.2 e-f: *Standard deviation ellipse* technique applied to (**e**) the mud seabed content and (**f**) the depth covariates. Easting/northing coordinates in UTM zone 29, WGS84.

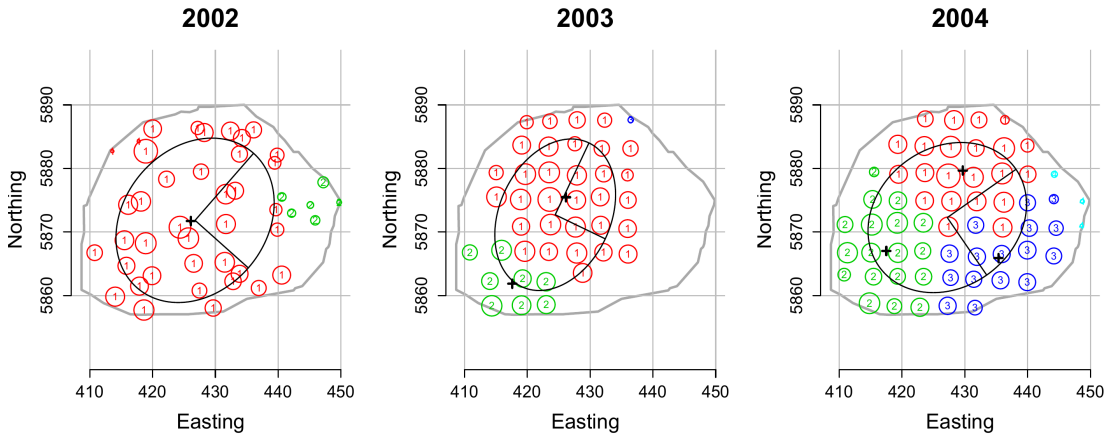
Performing the standard deviation ellipse technique on both bathymetry and mud reveals the north-east dominant direction for both covariates (**Figure 2.2e-f**) and underlines the importance of the seabed substratum, often *a priori* deemed as a determinant factor affecting the burrow distribution.

It is not surprising to see a similar north-east dispersion for the depth since these two explanatory variables are linked from a geological point of view (and date back to the last glacial period).

In fact, winds, rain and tides continuously remove particles from the land and the interplay between hydrology, the depth and the slope of the continental shelf act as a sieve separating coarser from finer particles (that is, mud). This could explain the 0.35 Pearson correlation coefficient between mud and depth (*p-value=4.139e-16*).

By relating the weighted *centre of gravity* (***cg***) and the range parameters of the spherical models (**Table M2**) we obtain disparate numbers of patches for each year in accordance with the varying pattern of the predictions maps (**Figure 2.3**). The north-east direction is predominant over these years despite annual fluctuations.

(a)



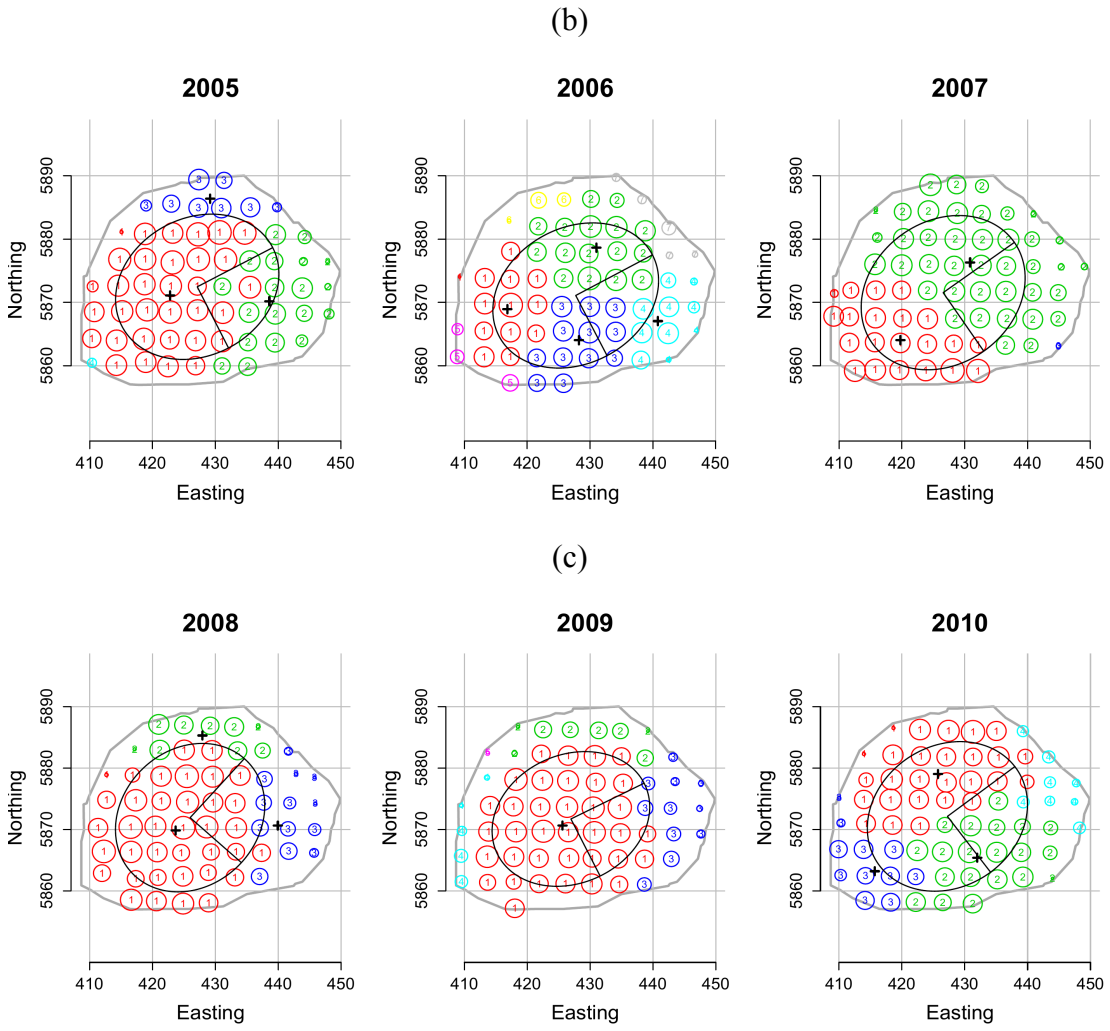


Figure 2.3 a-b-c: Patchiness distribution of the Aran grounds *Nephrops* population.

The identification of spatial patches is dependent on the choice of the distance limit corresponding to the practical range of the variogram models fitted in the geostatistics analysis (see **Table M2** in ***Materials and Methods***). Note that the sampled locations and their relative density values are represented by the size of the circle while the colours are used to ease the visual identification between different patches. The *barycentre* of each patch is indicated by a (black) cross. The borders of the area of study are also shown (grey line). The easting/northing coordinates correspond to UTM zone 29, WGS84.

However, the major issue resides in the smallest number of patches in 2002 (**Figure 2.2b**) that could be related to the sensitivity of the method to the type of sampling design (**Figure 2.3**). Recall that during this year a stratified random grid was applied as opposed to a fixed one for the subsequent years.

(I.2) Habitat dependence

Sediments that contained less than 40% mud are located at the borders of the patches and mostly in the Northern half of the area (beyond 5875 Northing). As noted previously (**Figure 2.1c**), there is also a relatively homogeneous central zone of sediment with more than 60% of mud.

There is an increase in the density of burrows with the proportion of mud in the sediment (loess fit) which is not surprising given the linear modelling results (**Figure 2.4a**). However, the flat segment of the curve suggests that beyond a certain threshold (about 50-60%) this positive relationship ceases and a visual examination reveals a minimum of about 20% mud is typical to maintain a burrow, even though we record a unique and very unusual value of 7.55% over the 516 coordinates selected for this spatial approach analysis. Nonetheless, comparing all the values below 20% seems to confirm the outlier status of this value (**Table 2.1**). Thus, in Aran, the burrow densities range with a minimum of 14.46% of mud and a maximum of 82.85% and it is difficult to infer an optimal percentage.

Table 2.1: Easting/northing coordinates of sites with less than 20% mud content in the seabed.

Coordinates	417.797E–5884.266N	419.91E–5887.279N	434.171E–5889.743N	415.866E–5884.522N	418.555E–5886.69N	418.665E–5886.51N
% Mud	19.05	18.03	7.55	16.22	14.46	19.35

In the case of water depth, despite a quite similar behaviour of the loess curves around 95 meters, a sufficient number of very low densities are recorded beyond this value making interpreting difficult (**Figure 2.4b**).

(a)

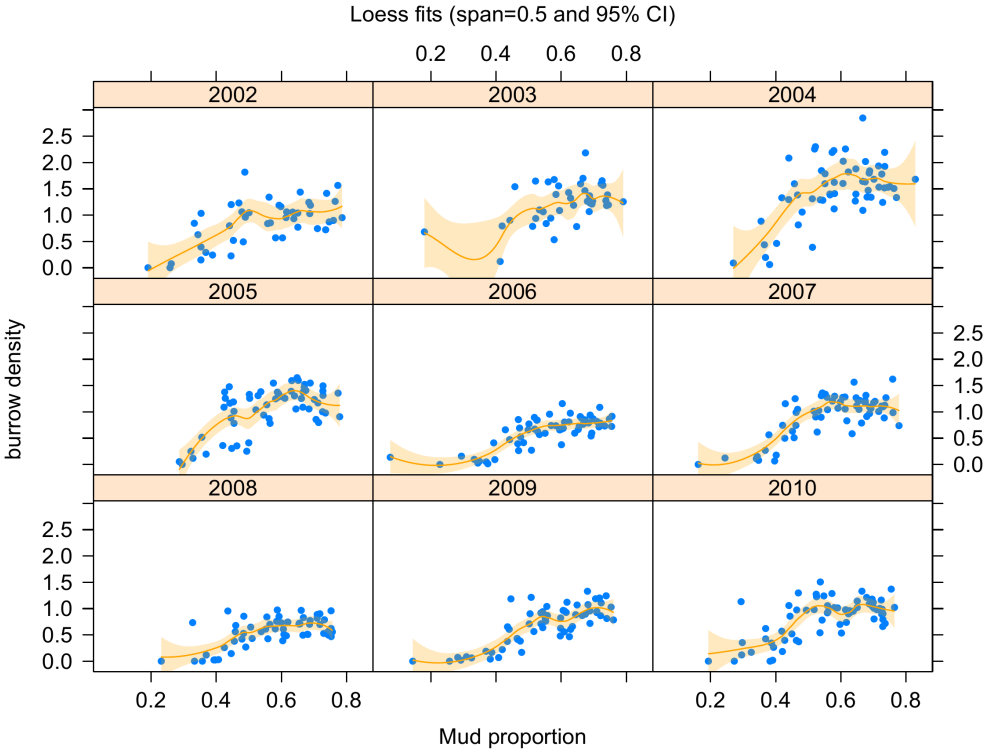


Figure 2.4a: Burrow density relationship with mud seabed content covariates using *Loess* regression.

(b)

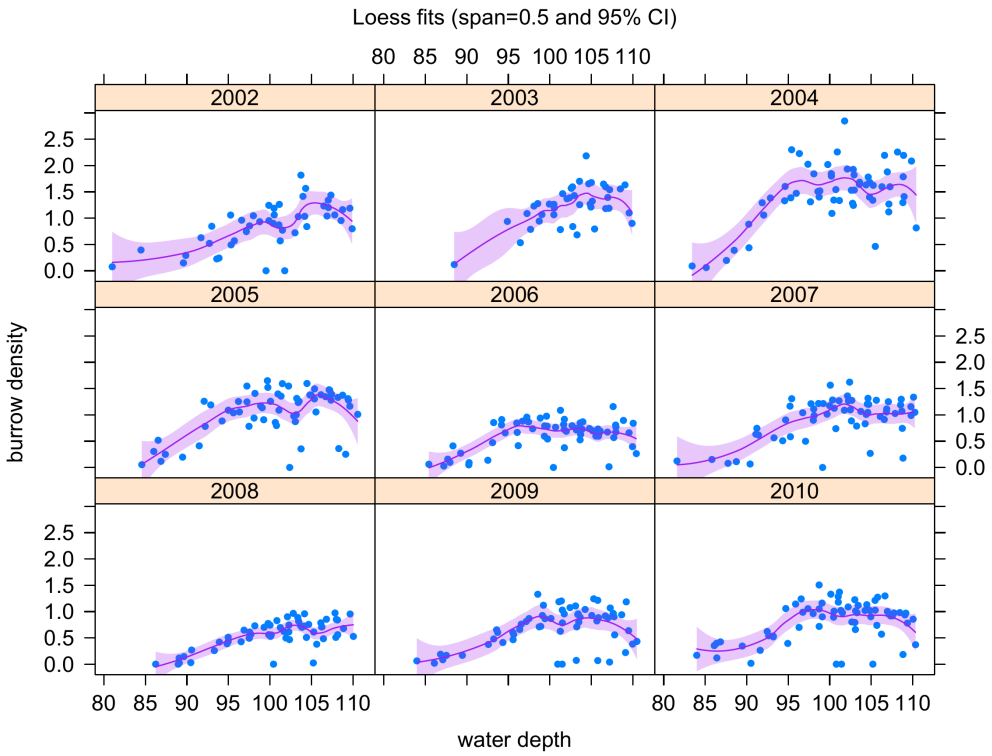


Figure 2.4b: Burrow density relationship with bathymetry (metres) covariates using *Loess* regression. Easting/northing coordinates in UTM zone 29, WGS84.

Regression analysis

After statistical investigation, two linear regression models were used for each covariate:

M1: $density_t = \beta_t * rateMud + residuals_t$ with an *adjusted r-squared* (r^2) ranging within [0.879–0.934] and

D1: $density_t = Intercept_t + \beta_t * depth + residuals_t$ with an (r^2) between [0.15–0.45].

With a significant (*p-value=4.139e-16*) *Pearson correlation* coefficient of *0.35* between the depth and the mud proportion, caution is required in the interpretation of the results with any combination of these 2 variables.

For mud, we intentionally omitted models including intercepts (not shown here) since only two years 2006 (*p-value < 0.05*) and 2009 (*p-value < 0.005*) are statistically significant while substituting it with year as a factor leads to only 5 significant coefficients: 2004, 2006, 2008, 2009, and 2010 (with *p-value <0.005)* respectively.

In addition, yearly fitting ***M1*** (**Table 2.2**, **Figure 2.5a**) is preferred over the pooled one ***M2*** (**Figure 2.5a**).

Table 2.2: Slope coefficients of equation ***M1*** $density_t = \beta_t * rateMud + residuals_t$ (* stands for *p-value <0.005)*.

β_{2002}	β_{2003}	β_{2004}	β_{2005}	β_{2006}	β_{2007}	β_{2008}	β_{2009}	β_{2010}
$1.585^{(*)}$	$2^{(*)}$	$2.507^{(*)}$	$1.875^{(*)}$	$1.142^{(*)}$	$1.66^{(*)}$	$0.987^{(*)}$	$1.306^{(*)}$	$1.487^{(*)}$

(a)

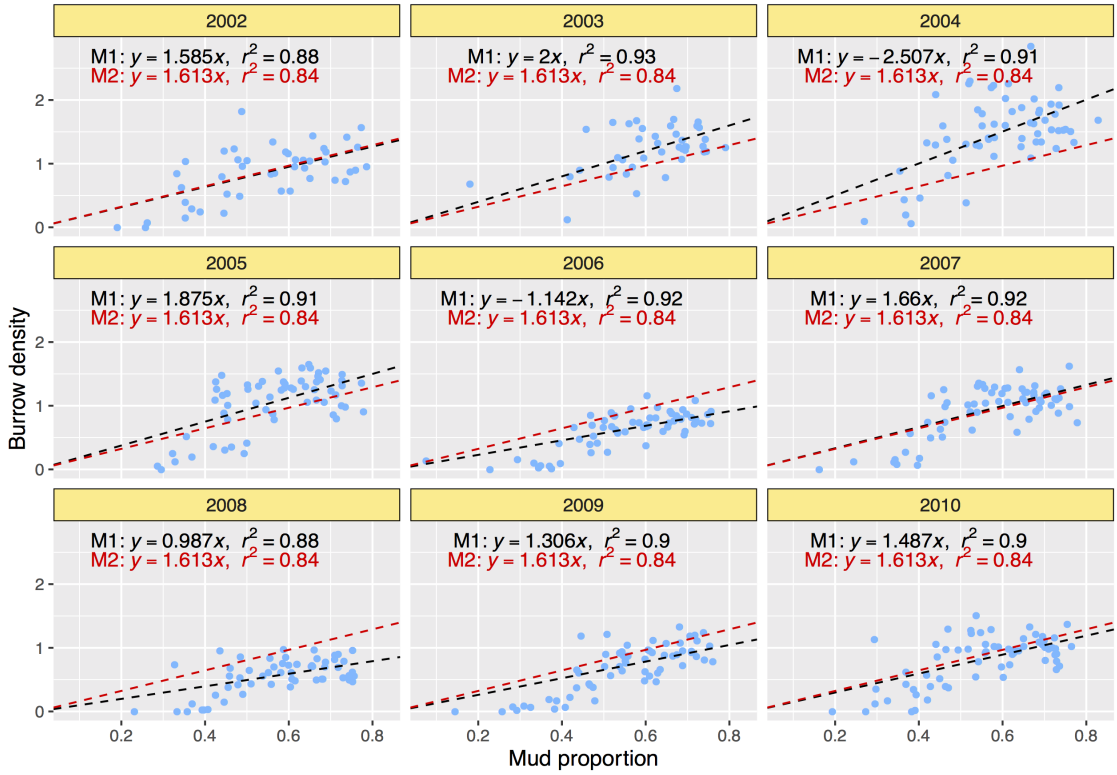


Figure 2.5a: Linear regression models for evaluating the burrow density relationship with seabed content covariate.

M1: $density_t = \beta_t * rateMud + residuals_t$ (black) and ***M2***: $density = \beta * rateMud + residuals$ (red) correspond to the use of the mud variable (silt, clay and sand). Notice that r^2 stands for the adjusted square of the correlation between the response and the fitted values and it is interpretable as the proportion of variation of the response variable around its mean accounted for by the regression.

(b)

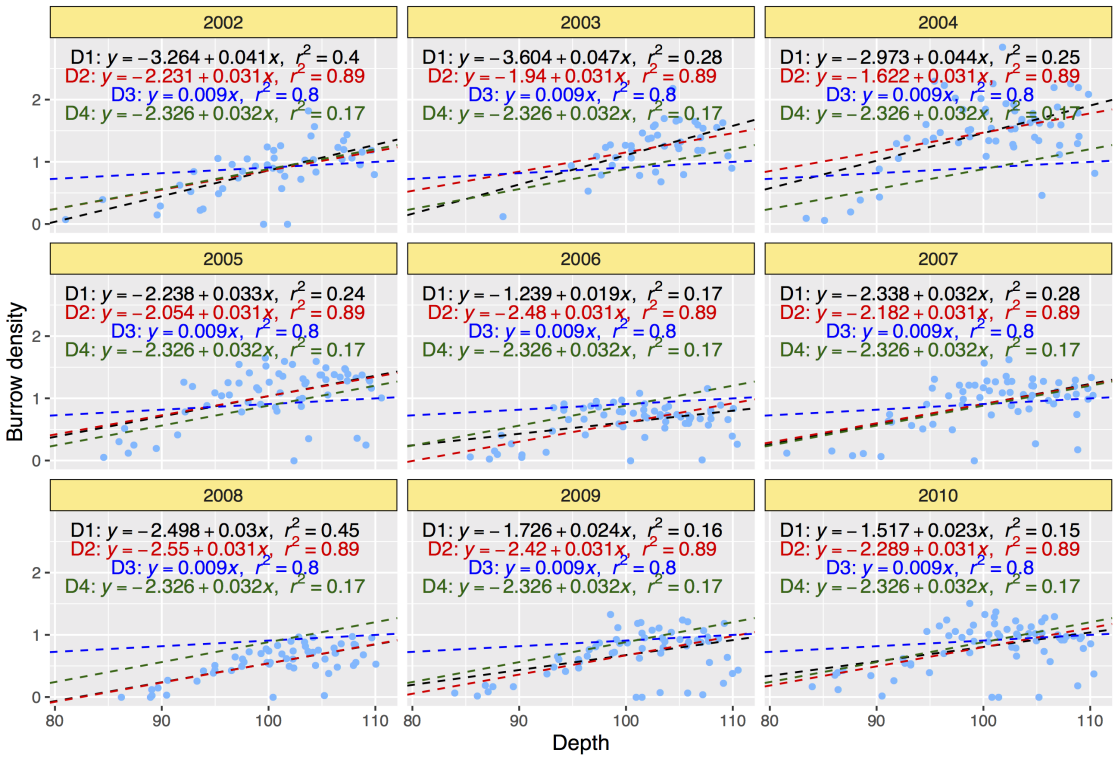


Figure 2.5b: Linear regression models for evaluating the burrow density in relation with depth (bathymetry in metres).

D1: $density_t = intercept_t + \beta_t * depth + residuals_t$ (black),

D2: $density_t = factor_{year} + \beta * depth + residuals_t$ (red), ***D3***: $density = \beta * depth + residuals$ (blue), ***D4***: $density = intercept + \beta * depth + residuals$ (green). Notice that r^2 stands for the adjusted square of the correlation between the response and the fitted values and it is interpretable as the proportion of variation of the response variable around its mean accounted for by the regression.

For the depth covariate, the intercepts are always highly significant and fitting with a time varying intercept (***D1***) or years as factors (***D2***) gives, by far, the best (r^2) values when compared with ***D4*** and ***D3*** respectively (**Figure 2.5b**), suggesting an annual variability in the relationship between density and depth.

Nevertheless, for each covariate when components in equations ***M1*** and ***D1*** are imposed to be independent of time, as equations ***M2***, ***D3***, ***D4*** and compared to the yearly linear equations **M1** and ***D1*** we observe that the obvious mismatches between them appear in 2004 and 2008 and more or less in 2006. This emphasises that the residual variability does not vary considerably and underlines the limitations of using mud and depth as parameters to explain the distribution and level of the burrow densities as described in

Table B1 in ***Annexes B*** and the violin plots (see later **Figure 2.7b**).

Scatterplots of the response variable against each of the spatial coordinates can sometimes reveal spatial trends (**Figure 2.6**). Again, to aid the visual detection we added the loess smooth curve. No particular trend in the Northern direction was observed, however, as we approach the coastline, a decrease in the density values (Eastern direction) was detected. This may be linked to the features of the covariates discussed previously, in particular, the lowest proportion of mud localised at the Eastern sides of the area.

(a)

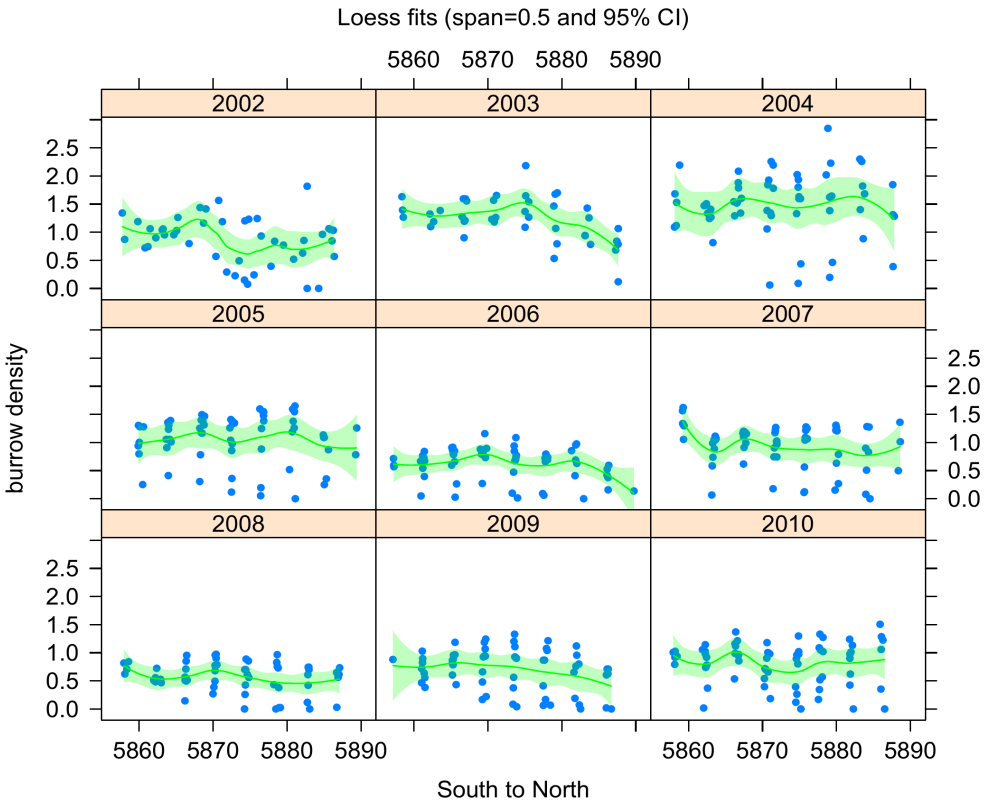


Figure 2.6a: Burrow density distribution in relation to **s**outh-north direction using *Loess* regression. Easting/northing coordinates in UTM zone 29, WGS84.

(b)

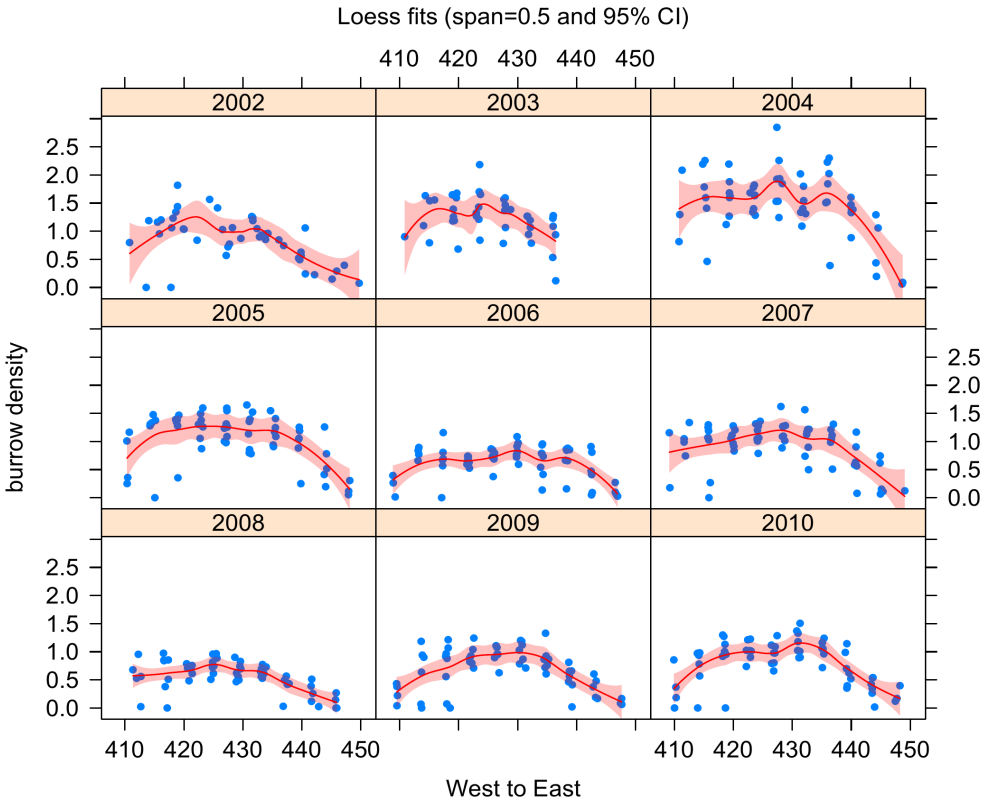


Figure 2.6b: Burrow density distribution in relation to west-east direction using *Loess* regression. Easting/northing coordinates in UTM zone 29, WGS84.

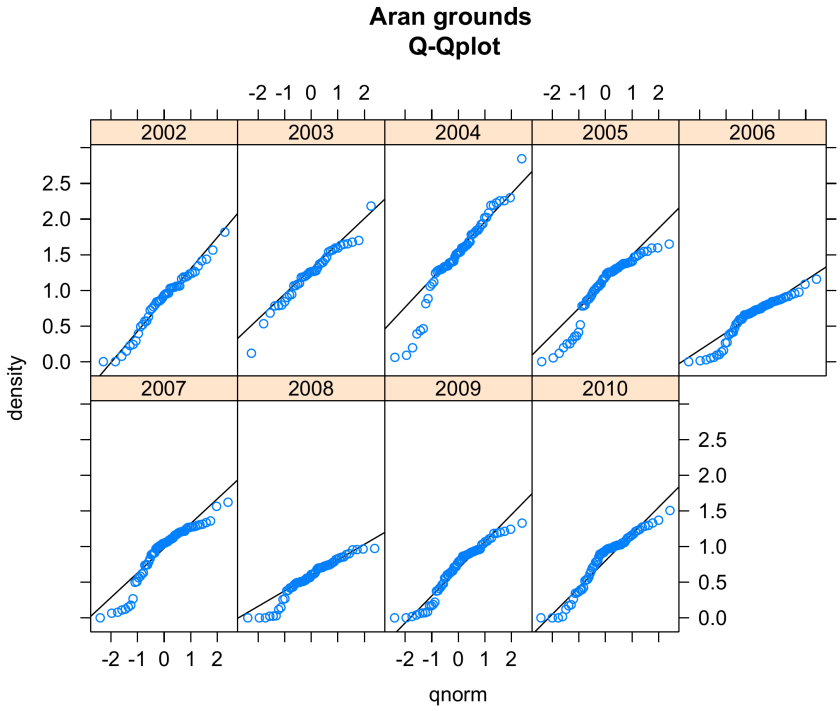
(II) Geostatistical features

(II.1) Skewness and normality

The normality (or gaussian) assumption of the data is very sensitive in the field of geostatistics. Using the quantile-quantile plot (**Figure 2.7a**), we assumed the data were normally distributed (here illustrated by the straight line).

The so-called violin plot (**Figure 2.7b**) retains the compact structure of a box-and-whisker plot as well as the details of a density plot. It shows the asymmetric distributions in burrow density towards the low density values which is also confirmed by the skewness values ranging from –0.94 to –0.29. The years 2006 and 2008 present the lowest means, median and max values of burrow density (**Table B1** in ***Annexes B***).

(a)



(b)

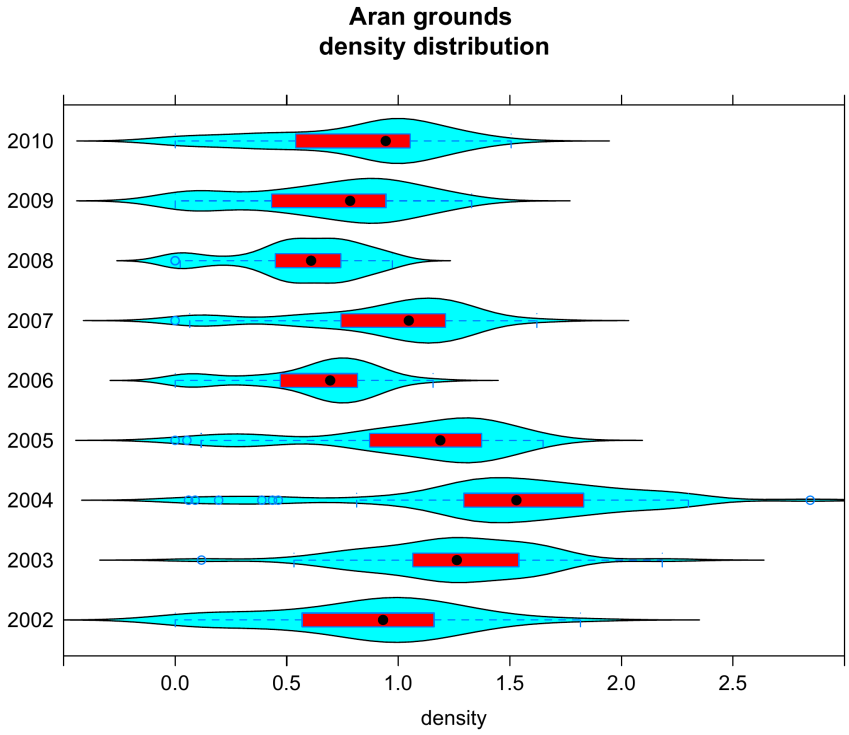


Figure 2.7: **(a)** *Normal quantile-quantile plot* to evaluate normality of the data. (**b**) *Violin plot* and *Box-plot* of burrow density distribution as surveyed by UWTV from 2002 to 2010. Thickness of the violin form makes it possible to assess cluster density around values.

(II.2) Edges versus midfield occupation

Ordinary kriging produces spatial interpolations based on the variogram models derived from the samples of the annual under water TV surveys. The lattice key colour legend allows a straightforward comparison over the 2002-2010 period (**Figure 2.8**). Thus, even though fluctuating in their forms and colour intensity, these spatial patterns display lower patches of density at some edges in contrast with a central zone recording higher density. This is in line with our previous description of the mud distribution in relation to burrow abundance (**Figure 2.4a**). Indicator kriging maps (**Figures B2 & B3** in ***Annexes B***) with the probability of burrow density >20th as well as median quantiles thresholds confirm this spatial regional split. Notice that the higher variance values of 2003 and 2004 illustrate the poor weather conditions faced during the surveys (ICES WKNeph TV, 2007). For 2002, the high level of variance is explained by the stratified random survey design used at that time, which arises with gaps in the spatial cover leading to an increase in the kriging predicted variances.

(a)

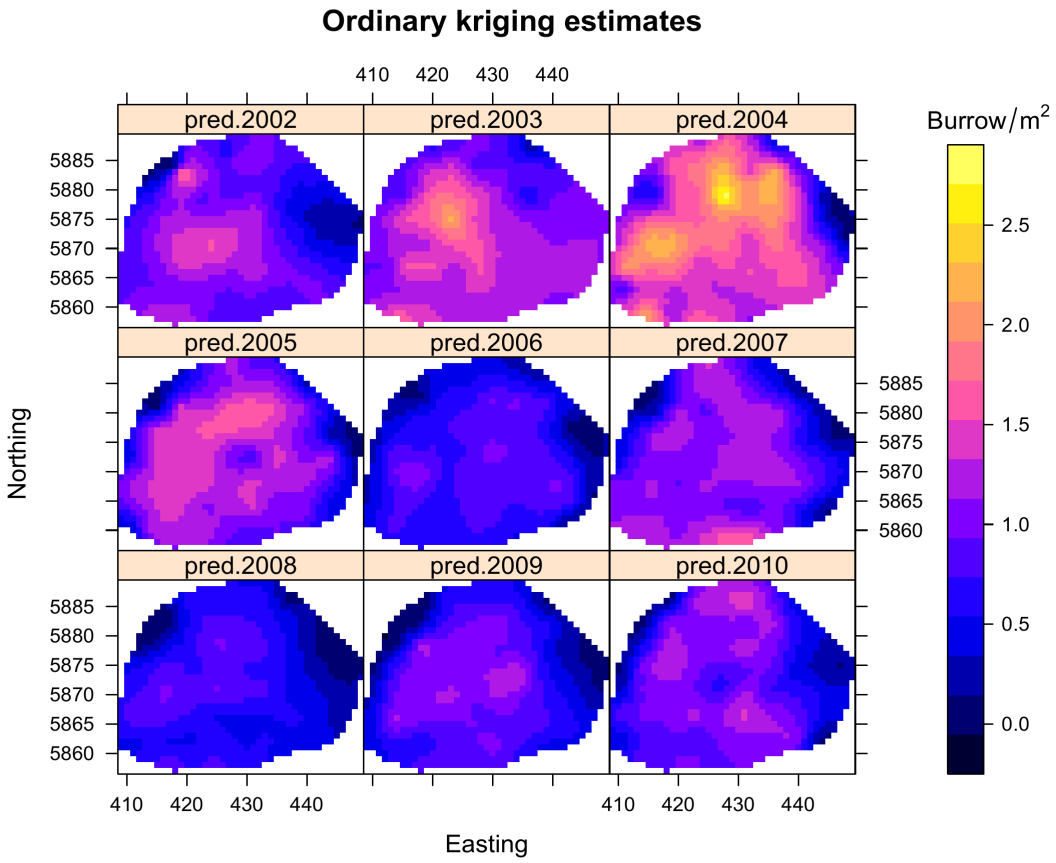


Figure 2.8a: Ordinary kriging estimates of burrow density from 2002–2010 using under water TV survey counts of burrow density over the Aran grounds patch. Easting/northing coordinates in UTM zone 29, WGS84. Lattice key colour legend gradient indicates low (dark blue) to high burrow density values per m^2 (yellow)

(b)

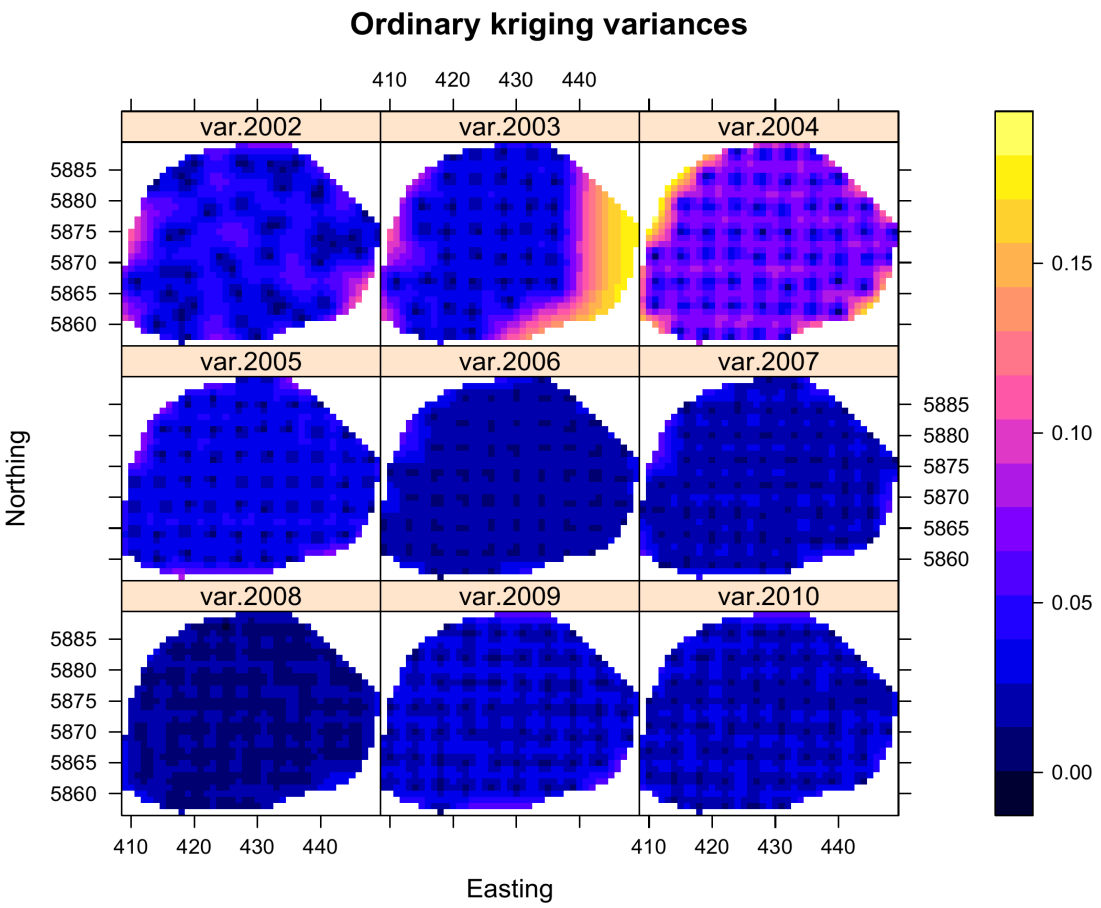


Figure 2.8b: Covariance estimates of the ordinary kriging estimates of burrow density.

EOF was used to quantify the temporal dynamics of these spatial patterns (**Figure 9**). EOF_1 is the pattern on which the data projects most strongly, in other words, the pattern most frequently realised. The EOF_2 is the most commonly realised but under the constraint of orthogonality to the first one. Note that EOF_3 is the most frequently realised pattern that is orthogonal to both EOF_1 and EOF_2 and so on. We have considered that EOF_1 and EOF_2 explain most of the behaviour of the data since the cumulative proportion of variance explained is 80.5% with 71.19% for EOF_1 and 9.40% for EOF_2. Hence, we also have assumed that the remaining EOFs are noise.

Table 2.4: Proportion of variance explained by each EOF.

EOF_1	EOF_2	EOF_3	EOF_4	EOF_5	EOF_6	EOF_7	EOF_8	EOF_9
0.719	0.0941	0.0564	0.0416	0.0345	0.0281	0.0140	0.0134	0.0061

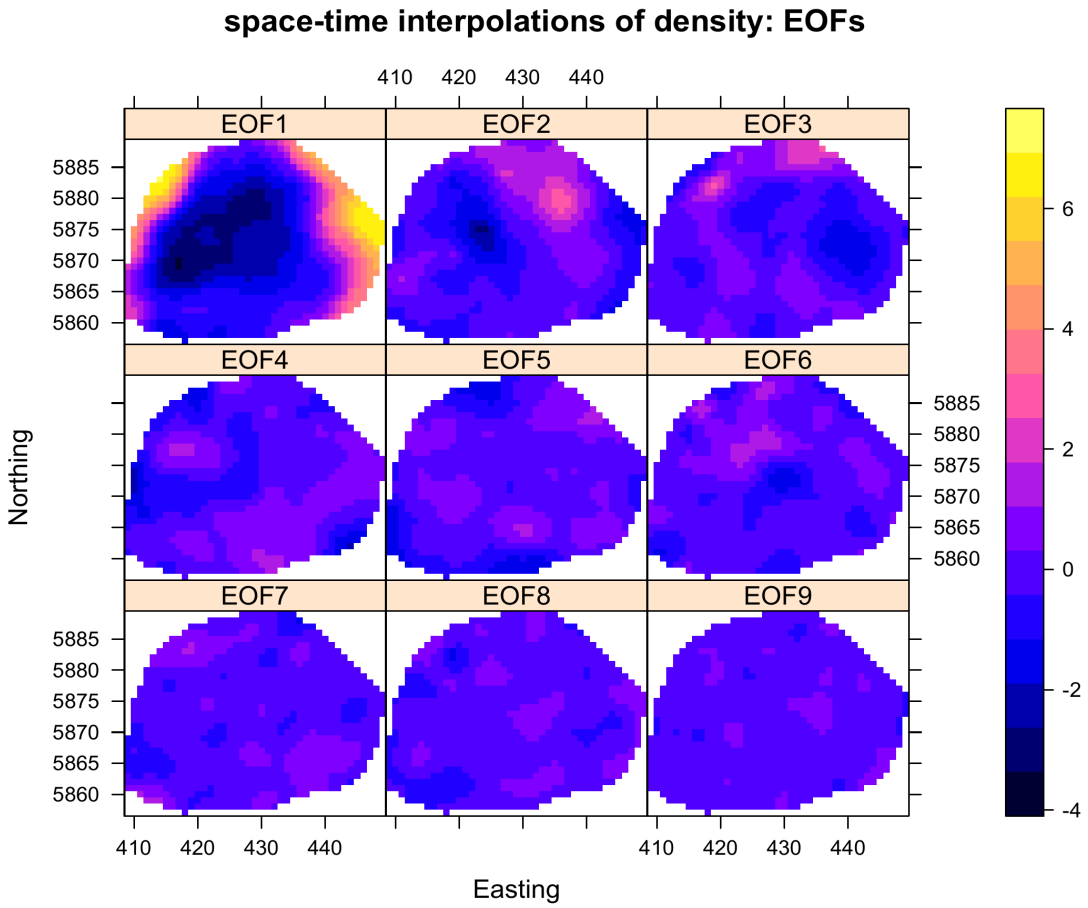


Figure 2.9: Empirical Orthogonal Function technique applied to the 2002–2010 years of ordinary kriging predictions maps of burrow density. Easting/northing coordinates in UTM zone 29, WGS84.

In addition, the amplitude of principal components, standardised to have zero mean and 1 unit variance, estimates the importance of each spatial pattern (EOF_1, EOF_2) through time (**Figure 2.10**). Comparative analysis of the variability in the changed sign (positive vs negative) shows a clear cut-off at 2006 for PC_1 with relatively high values of the loading coefficients underlining the weight of EOF_1 in explaining the variance of the data cloud.

The crucial step is to name what each selected map (EOF_1 and EOF_2) means qualitatively. EOF_1 illustrates the general trend of density over these 9 years: the map

shows a negative trend for the central zone of our area of interest and conversely, an increase in the Eastern and Western margin sides.

(a)

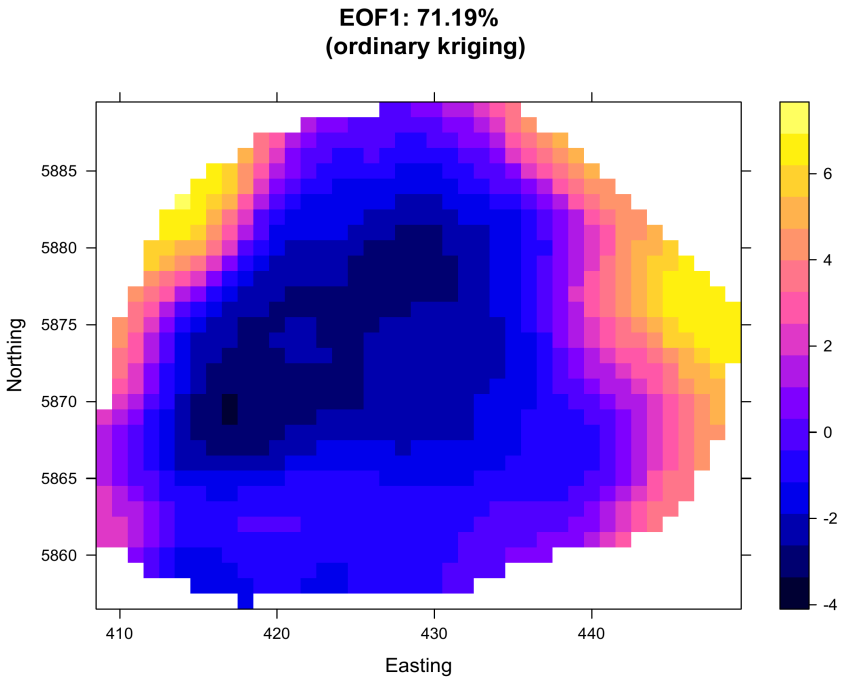


Figure 2.10a: The first empirical orthogonal factor (EOF_1) of the 2002–2010 annual kriging predictions. Accordingly, 71.19% of the variance of the cloud is explained by EOF_1. Easting/northing coordinates in UTM zone 29, WGS84.

(b)

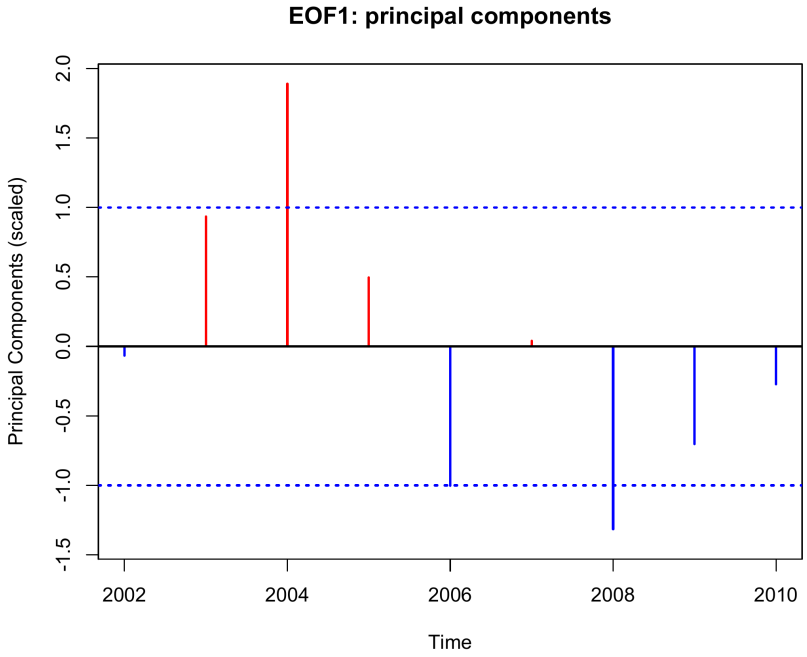


Figure 2.10b: Principal components (PC_1) associated to the first empirical orthogonal factor (EOF_1).

With respect to the PC_2 set, EOF_2 is mainly explained by the years 2003 and 2004 (**Figure 2.11**). This field pattern seems to illustrate a strong antagonism or shift between 2003 and 2004.

(a)

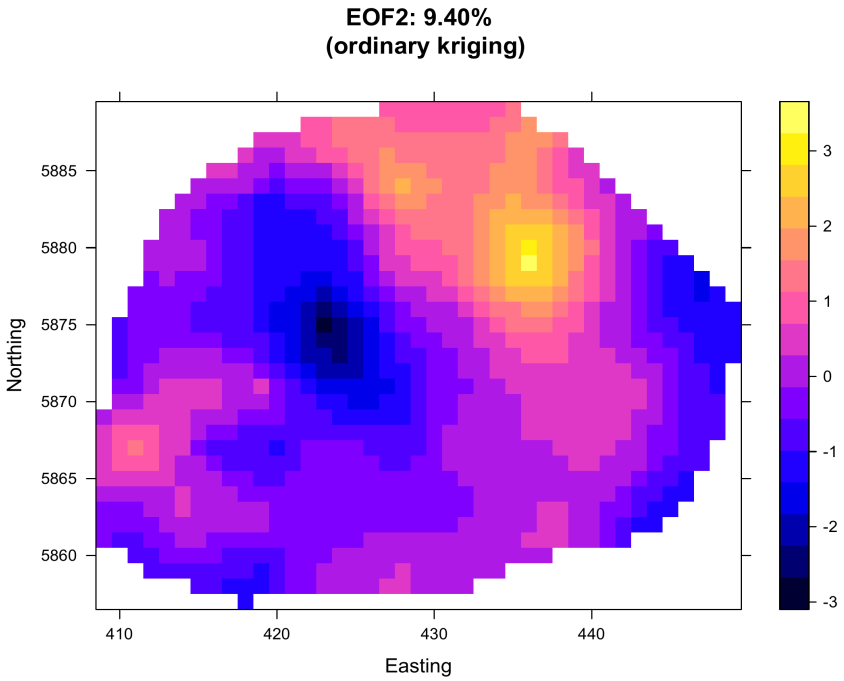


Figure 2.11a: Second empirical orthogonal factor (EOF_2) of the annual kriging predictions. Easting/northing coordinates in UTM zone 29, WGS84.

(b)

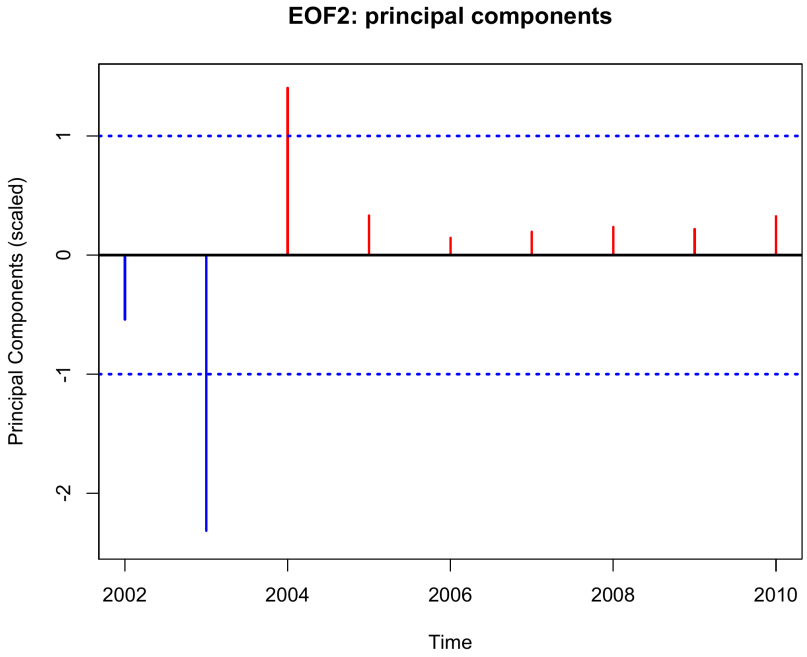


Figure 2.11b: principal components (PC_2) associated to the second empirical orthogonal factor (EOF_2) of the 2002–2010 annual kriging predictions.

(c)

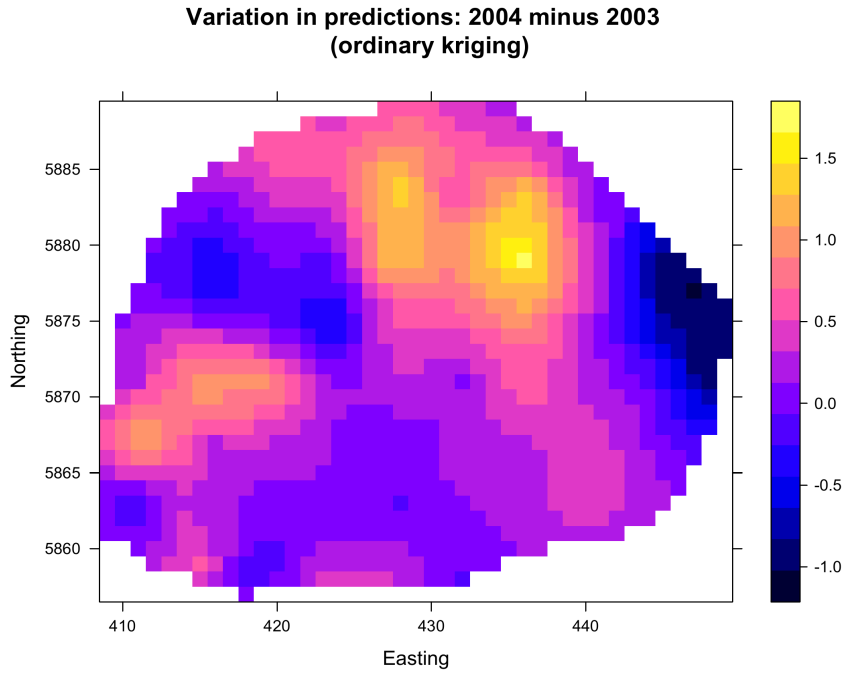


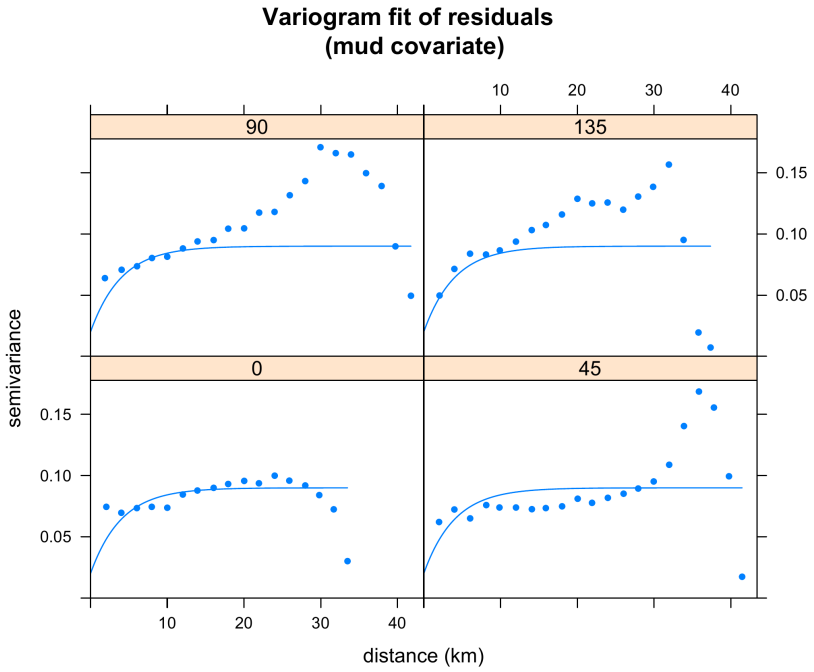
Figure 2.11c: Spatial pattern resulting of the difference between EOF_1 and EOF_2 maps.

EOF_2 expresses only 9% of the variance of the data and secondly, $EOF_{1\&2}$ are orthogonal to each other ensuring independence of the resulting maps.
Mapping the variations in the predictions between 2004 and 2003 (**Figure 2.11c**) exhibits notable regional similarities with the EOF_2 map. Hence, we consider that EOF_2 could depict a departure from the general trend represented by EOF_1. Although EOF_2 has been examined in detail, it is more judicious to ignore it due to the very narrow information contained in it (recall, only 9% of the variance).

(II.3) Predictions with mud

The contribution of mud was investigated further by looking at the spatial and temporal variability of the burrow density including it by fitting a variogram of the pooled residuals obtained from all available years (**Figure 2.12a**). The computed cross correlation coefficients (**Figure 2.12b**) and cross variography (**Figure 2.13**) makes it possible to relate each of the 9 years of observed burrow densities.
Apart from the year 2003 (due to conditions of survey, see ***Materials and Methods***), the correlation matrix values are high (>0.50) suggesting a strong relationship between the current level of burrow density and the previous years (**Figure 2.12b**).

(a)



(b)

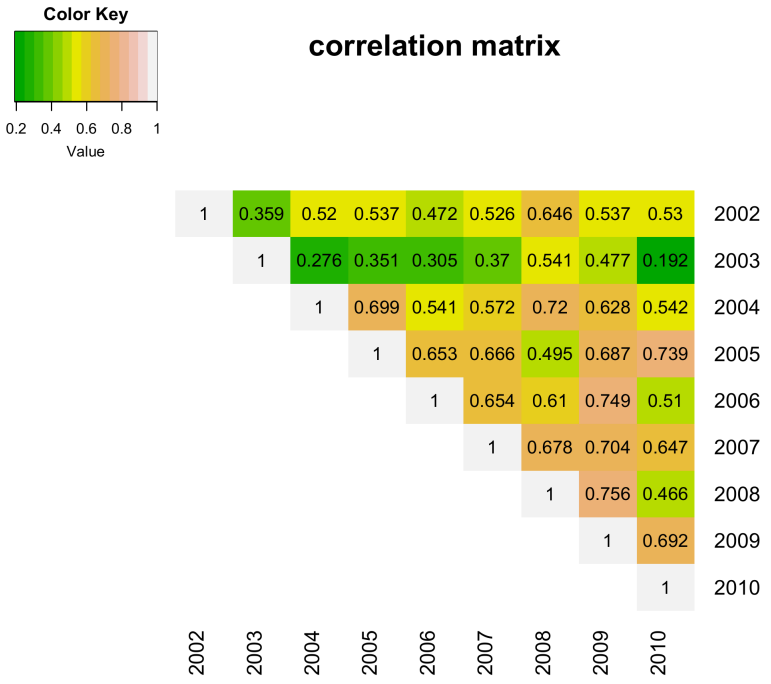


Figure 2.12: **(a)** Exponential variogram model (with nugget c_0=*0.02,* partial sill c_1=*0.07* and practical range (3a)=*12km*) fitted to the directional (0º, 45º, 90º, 135º) experimental variograms of the pooled residuals derived from $density_t = \beta_t * rateMud + residuals_t$ **(b)** Correlation matrix entries (r_{ij}) obtained by inverse distance weight.

Between two under water surveys carried out regularly in June, the new dwellers are counted, even though the coexistence of juveniles and adults in the same burrow is frequent. Meanwhile, such high (r_{ij}) coefficients for adjacent years echoes the time series analysis results concerning the strong influence of lagged landings values on the current ones (see ***Chapter 1 Times Series Analysis***).

In certain cases, the scaled cross variograms fits appear to underestimate the true temporal correlation (blue line, in **Figure 2.13a**)

(a)

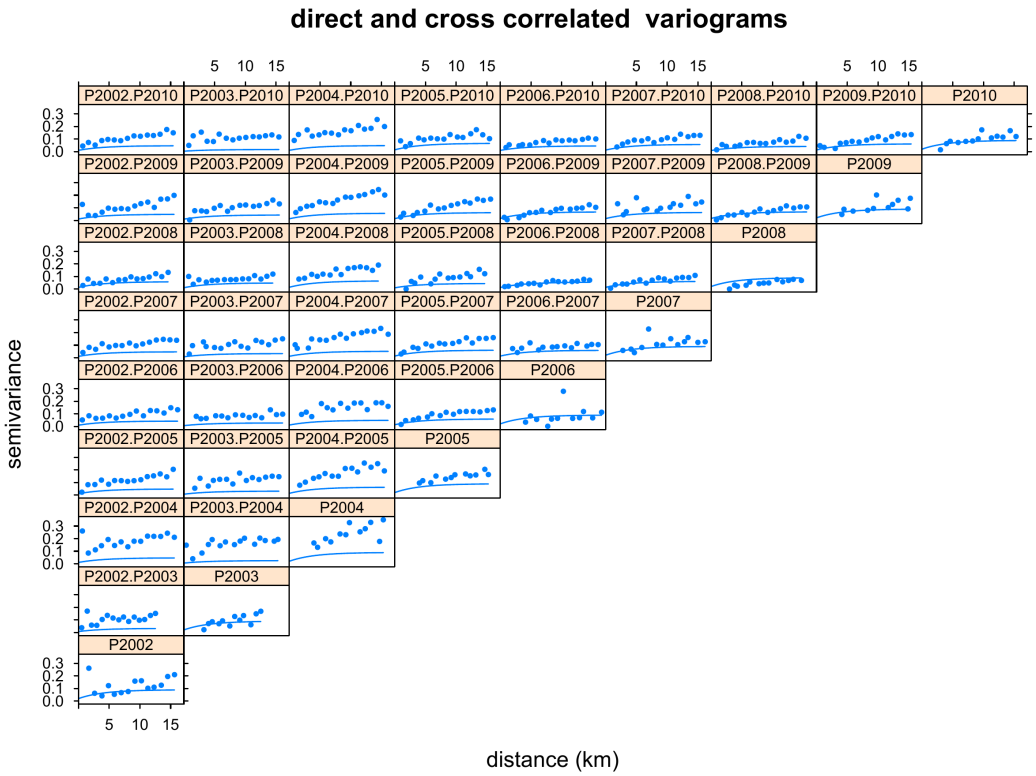


Figure 2.13a: Direct variograms (bottom diagonal) and cross variograms (off diagonals). The fitted models for all direct variograms were set to the model fitted to the pooled variogram (**Figure 2.12a**) and the cross variograms are scaled version of it using matrix of correlations coefficient (r_{ij}, see **Materials and Method**).

(b)

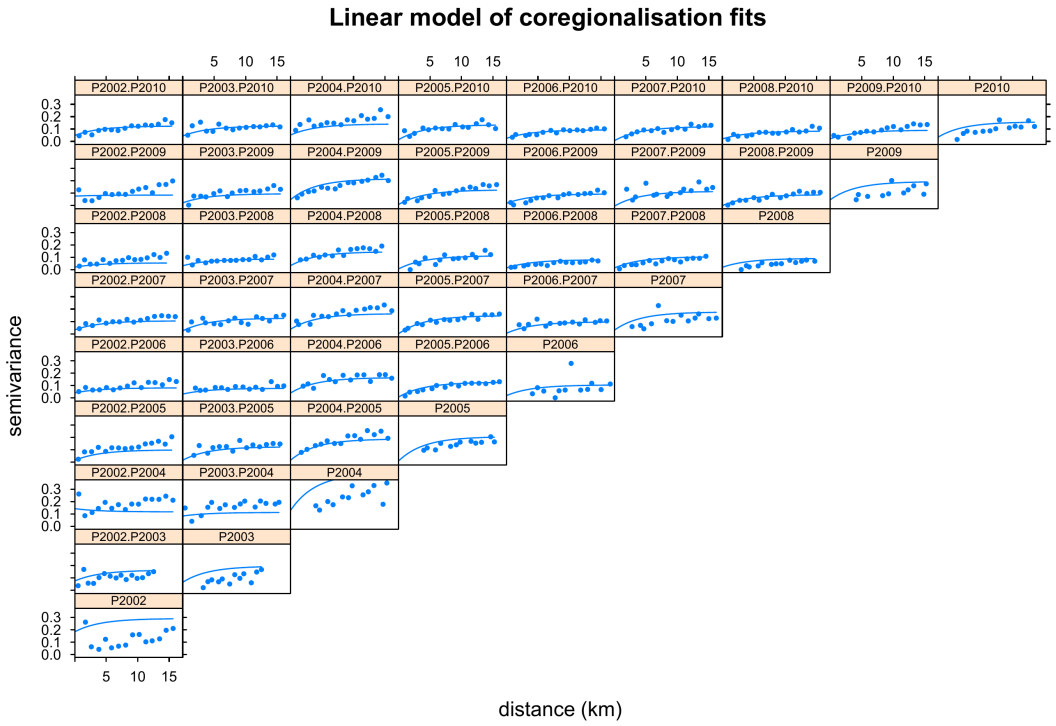


Figure 2.13b: Direct variograms (bottom diagonal) and cross variograms (off diagonals) along with fitted linear model of co-regionalisation (blue) ensuring non-negative prediction variances when used for spatial prediction (cokriging).

Now the resulting universal co-kriging predictions of the spatial variations of the burrow distribution share the informations brought by the regional variogram adjusted by the coefficient of correlation and the mud as a predictor (**Figure 2.14**).

(a)

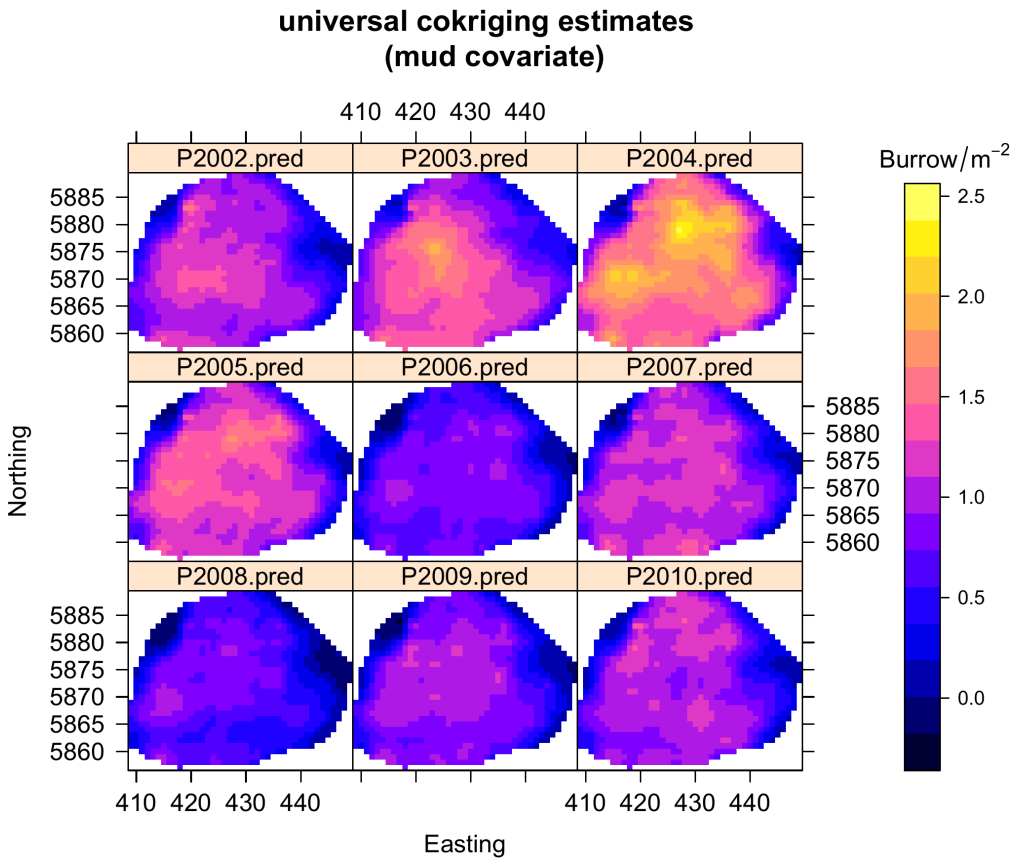


Figure 2.14a: Universal co-kriging burrow density estimates of years 2002 to 2010. Easting/northing coordinates in UTM zone 29, WGS84.

(b)

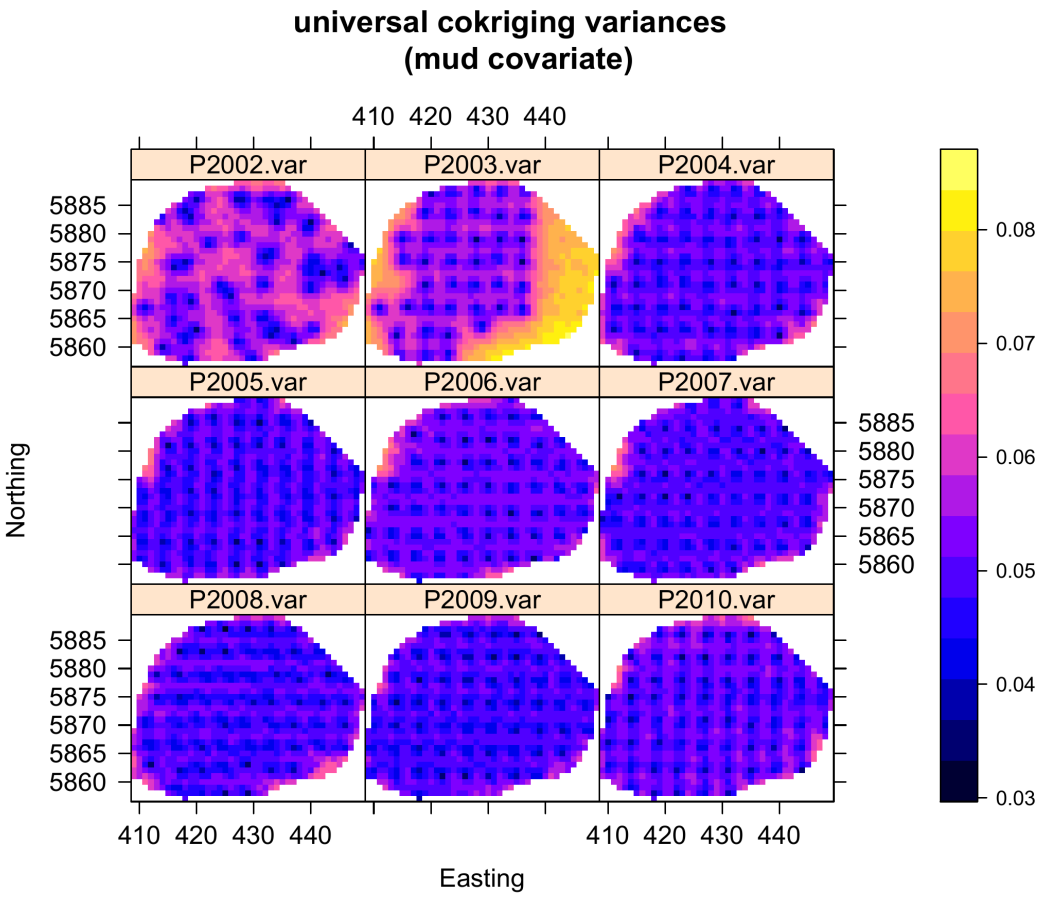


Figure 2.14b: Variances of the universal co-kriging predictions. Easting/northing coordinates in UTM zone 29, WGS84.

Temporal changes

The resulting predictions are now "contrasted" over these nine years to display a trend estimates in the change in density (**Figure 2.15**). The contrast method points to a clear overall decrease in the density over these nine years and provides us with the opportunity to differentiate between the sub-areas regarding the sign and amplitude of the changes. The west half of Aran grounds has shown a drastic reduction in density, with less of a reduction seen towards the east border sides. The method also reveals the presence of patches with increasing burrow density at the vicinity of 5885N–430E and 5860N–435E.

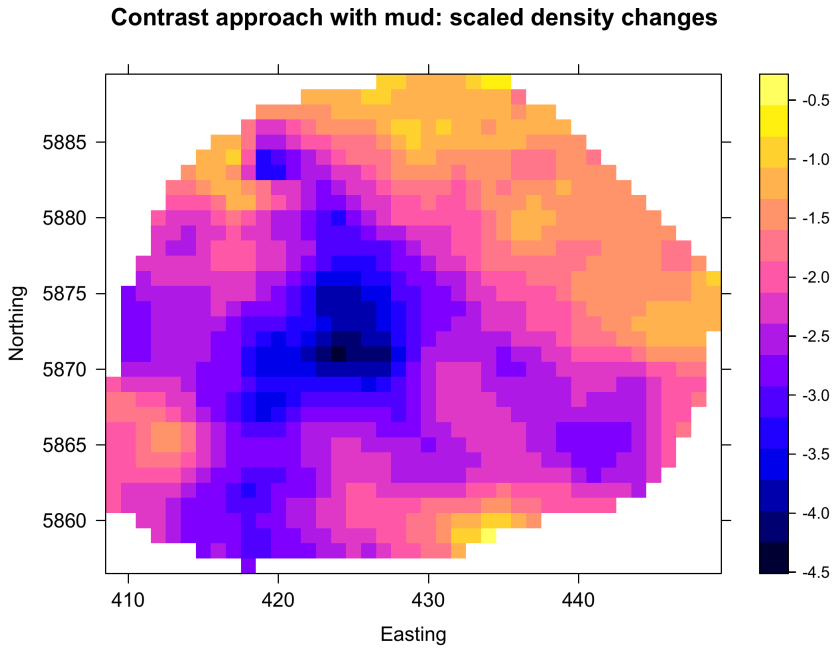


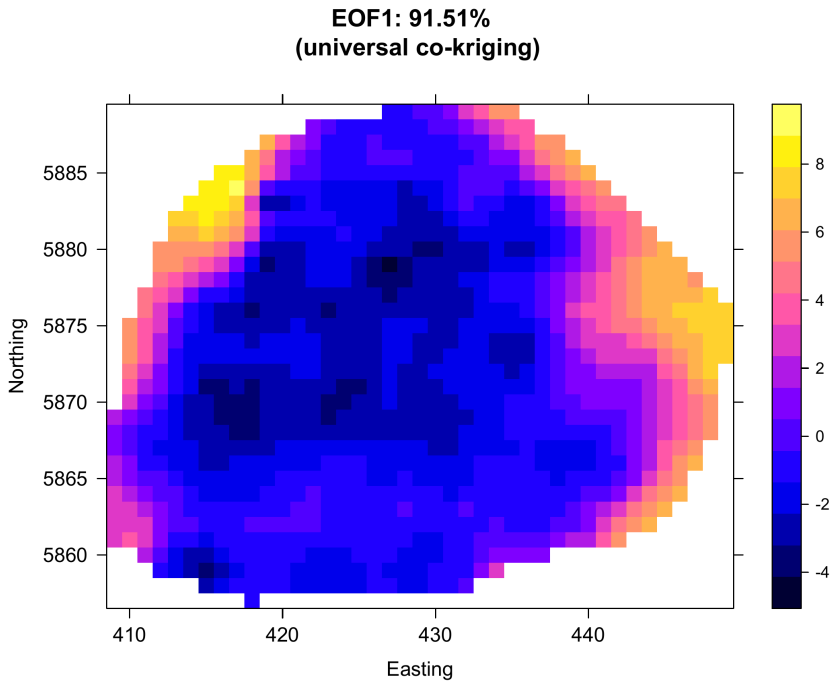
Figure 2.15: Trend estimates from the contrast approach as yearly change in burrow density for the period 2002 to 2010. The changes are scaled (*i.e.* divided by their standard errors). Easting/northing coordinates in UTM zone 29, WGS84.

The EOF applied to density predictions derived from the universal co-kriging approach using mud as a variable confirms the depletion of the central zone over these 9 years (**Figure 2.16a-b**) and improves (+20%) the power of attraction of the first orthogonal factor (EOF_1) with its 91.51% of variance explained.

By performing a universal co-kriging with mud as predictor covariate we exhausted the variability explained by the sea floor sediment, and unveiled the temporal spatial variability that is still persistent (principal components, PCs, in **Figure 2.16c**).

By examining the year to year predictions of density abundance (**Figure 2.14a**), we observe an increase until 2004 followed by a steady decrease that is in agreement with the UWTV records (**Figure B5** in ***Annexes B***).

(a)



(b)

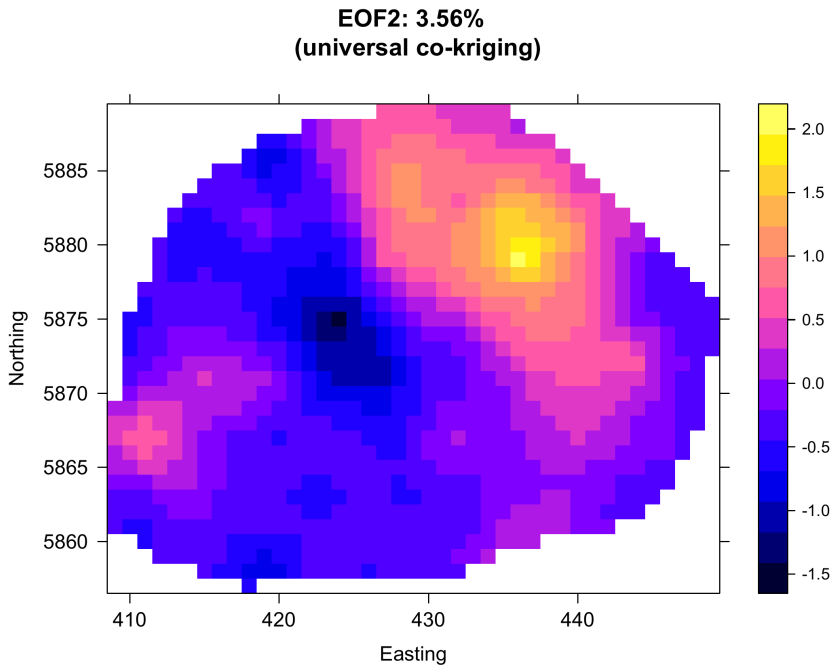


Figure 2.16 a-b: First and second empirical orthogonal factors ($EOF_{1\&2}$) of the 2002–2010 universal co-kriging maps.

(c)

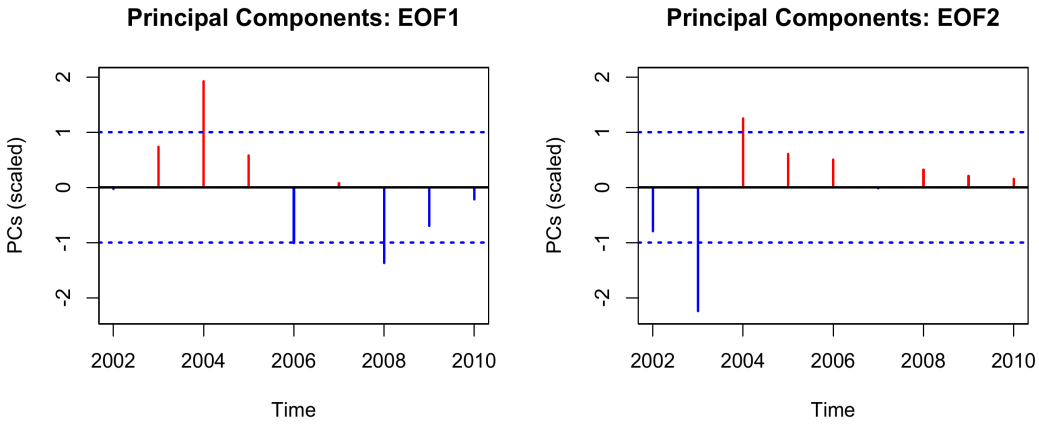


Figure 2.16c: Scaled principal components ($PC_{1\&2}$) of the corresponding $EOF_{1\&2}$.
In comparison to the variance explained value of 71.19% of the EOF_1 computed from the 2002–2010 ordinary kriging predictions maps (**Figures 2.9** & **2.10**), here, the variance explained by EOF_1 (here, 91.51%) is improved by 20%. Easting/northing coordinates in UTM zone 29, WGS84.

In addition, the EOF approach points out the year 2004 and 2008 (highest loading coefficients, **Figure 2.16c**) in compliance with their respective level of abundance, *i.e.* the highest and the lowest recordings of *Nephrops* burrows between 2002 and 2010. Thus, including such explanatory variables brought a refinement over EOF outputs derived from ordinary kriging prediction cloud points.

(III) Factors of influence

(III.1) Surface currents advection

The larval stage duration is temperature dependent and larval mobility seems to increase after 10 days of passive drift. The swimming speed varies from 0.0001 to 0.00015 m/s and consequently, we believe that the larval dispersal in Aran grounds is mainly driven by regional hydrological traits.

Wind vectors, particularly near the coast, may be questionable and potentially spurious due to factors like rain contaminated data and/or residual land reflections that are of importance in processing satellite backscatter data (**Figure 2.17**). There is also a lack of information in the vicinity of the Aran grounds inshore edge for both types of data.

For illustrative purposes we provide cartographies of currents and winds for the year

2002. For ease of visual examination we scaled (and not centred) the slope with an arbitrary value instead of the standard deviation.

(a)

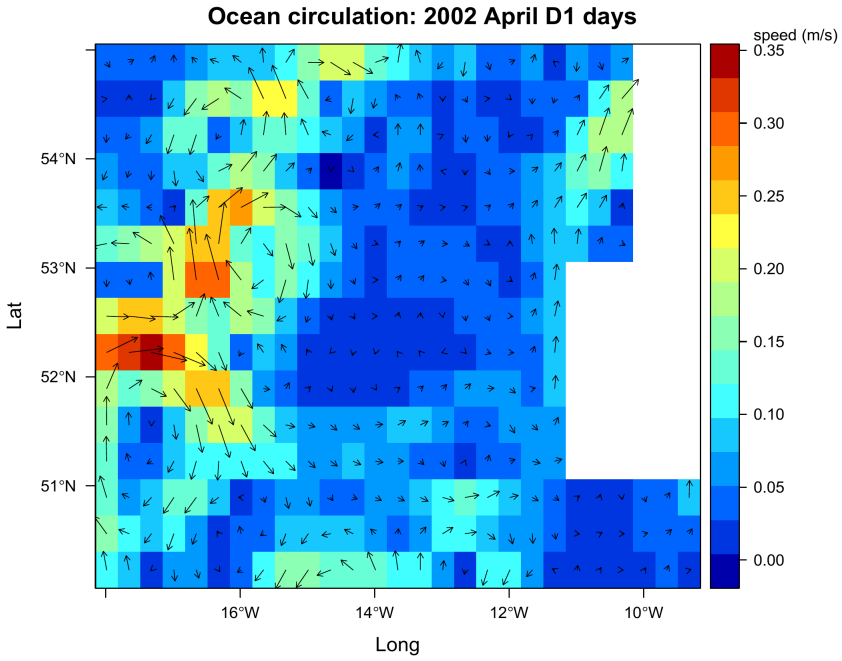


Figure 2.17a: Averaged surface ocean circulation over a 5-day period.

The total current velocity (m/s) is the vertical average over a surface layer thickness of 30 metres (thus, 15 metres mean depth). 5-days means starting on the first day of each year. In leap years, the pentad starting on 2/26 will include 6-days such that the starting date for each pentad remains the same across all years.

(b)

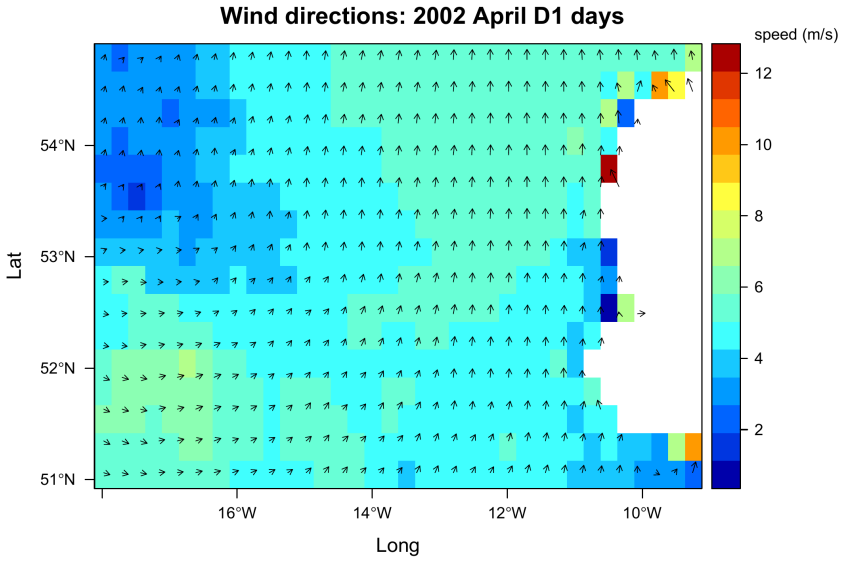


Figure 2.17b: Averaged wind circulation direction over a 5-day period.

The wind datasets combine cross-calibrated satellite winds to produce a spatial resolution of 0.25 degrees latitude x 0.25 degrees longitude over a temporal scale of 5 days noted. *D1*, *D2*, etc... It consists of 6 hour sets that are time averaged over 5-days periods. 5-days means starting on the first day of each year. In leap years, the pentad starting on 2/26 will include 6-days such that the starting date for each pentad remains the same across all years. For the wind, all observations and analysis fields are referenced to a height of 10 meters above the sea level.

These snapshots yield static views of a dynamical phenomenon. Examining a long period of maps from 2002 to 2010 outlines regionally constant features, mainly gyres, bordering northern, southern and western sides of a relatively "calm" zone roughly lying between 51.5°N to 54°N of latitude and –15°W to –10°W of longitude and marked by both a notable diminution of the magnitude of the velocity and the difficulty to discern by eye the pattern of the water mass circulation (**Figure 2.17a**).

It is worth noting that Aran grounds is situated in the central east half of this delimited area. For this reason, we have reduced the geographical extent of our study window to focus on this area and carried out a cartesian projection of the current (and wind) vectors to obtain a synthesis plot retaining directional drifts and speed over the period of interest from March-April-May (**Figures 2.18a-b-c-d-e-f-g-h-i-j**).

Thus, for 2002, over the 18 periods (*D1* to *D18*) corresponding to March April and May, the resulting synthesis plot of the wind changes depicts a quite circular drift of the mean wind vectors in particular since April *D11* suggesting a potential clockwise gyre acting as a retention zone for larvae. A look at the ocean circulation drift confirms this (**Figure 2.18b**).

(a)

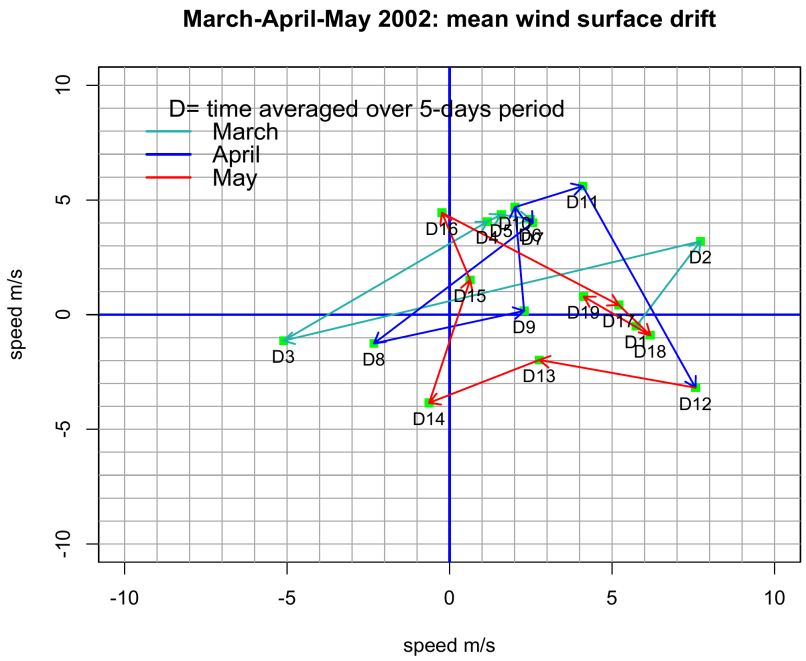


Figure 2.18a: Cartesian projections of mean wind surface drift vectors during the period of March-April-May for the year 2002 over the area –18°W, –9°W and 51°N, 55°N.
Note that for illustrative purposes similar projections of the mean directional wind patterns are computed for the years 2002 to 2010 (see **Figures B7** in ***Annexes B***).

(b)

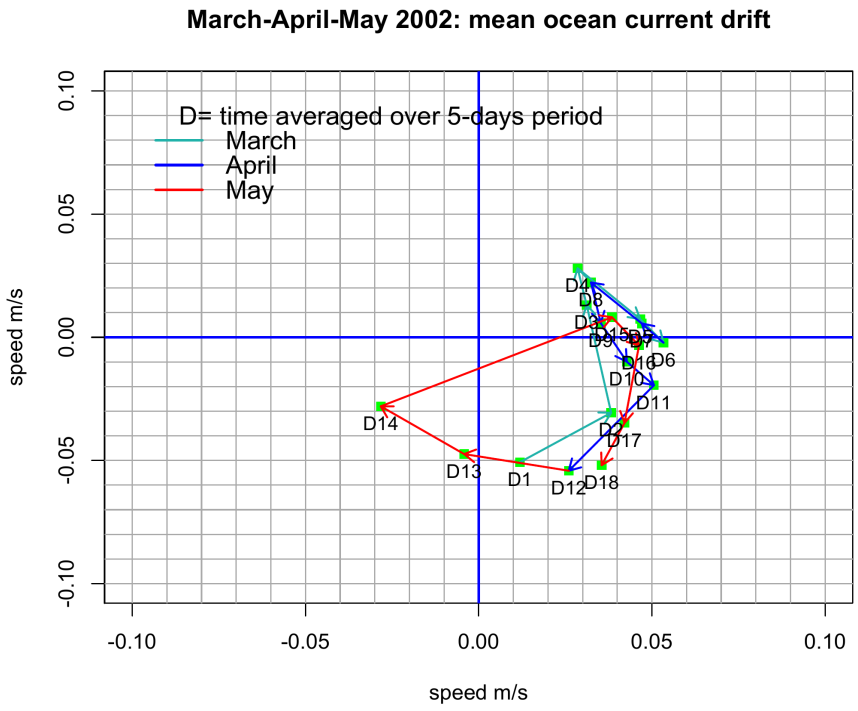


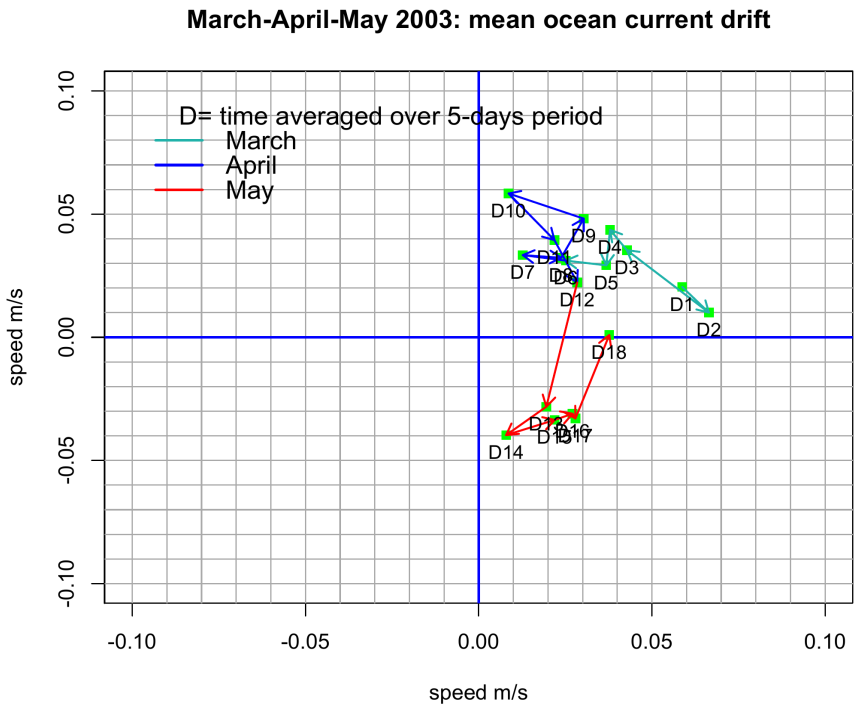
Figure 2.18b: Synthesis of prevailing mean surface ocean circulation patterns during the period of March-April-May for year 2002 over the zone of interest enclosed within a rectangle of –15°W to –9°W and 51°N to 54°N.

Examining the April-May winds, we note that 2002 is unique in exhibiting a somehow clockwise pattern in comparison to the very variable profiles of the remaining years for the same periods (**Figure B7** in ***Annexes B***).

In 2003, the ocean current drift over April-May describes a North to South circulation turning back in the last week of May and ending at mid-way (**Figure 18c**), while in 2008, since March, the waters flow from South to North with a striking (and temporary) monthly time inversion

(**Figure 2.18d**).

(c)



(d)

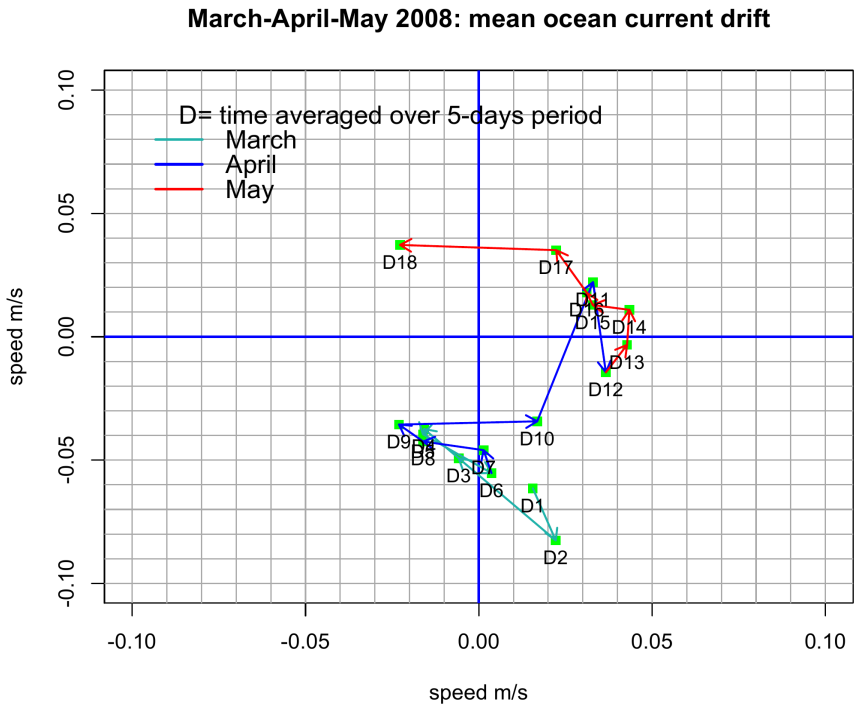


Figure 2.18 c-d: Cartesian projection of mean current drift vectors prevailing during the period of March-April-May for years 2003 and 2008 within a rectangle of –15°W to –9°W and 51°N to 54°N.

In 2005 and 2010 the circulation features a large range in directions and subsets corresponding to the monthly patterns of March, April and May can easily be distinguished (**Figure 2.18e-f**).

(e)

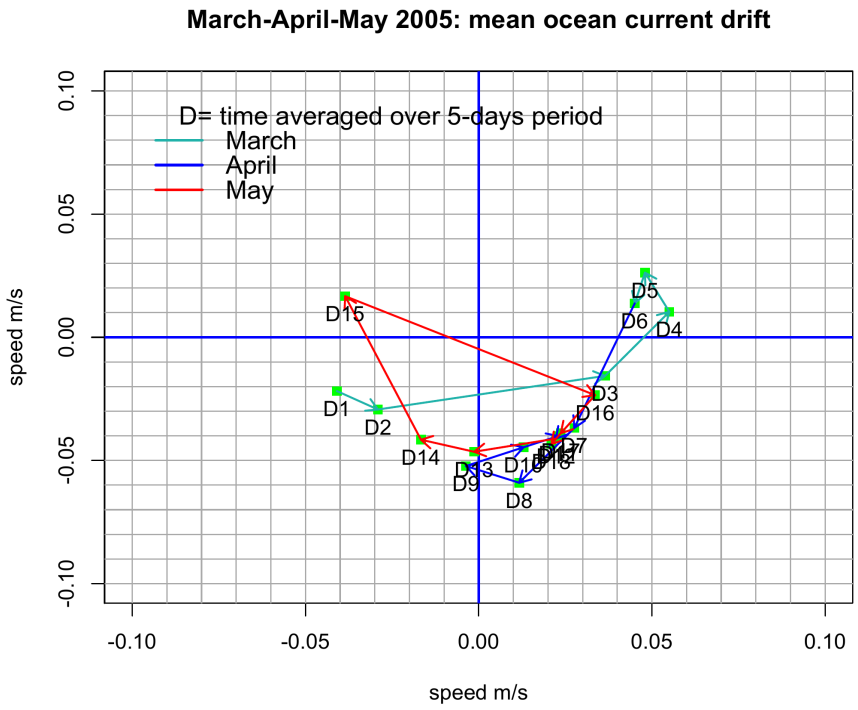


Figure 2.18e: Cartesian projection of mean current drifts prevailing during the period of March-April-May for years 2005 within a rectangle of –15°W to –9°W and 51°N to 54°N.

(f)

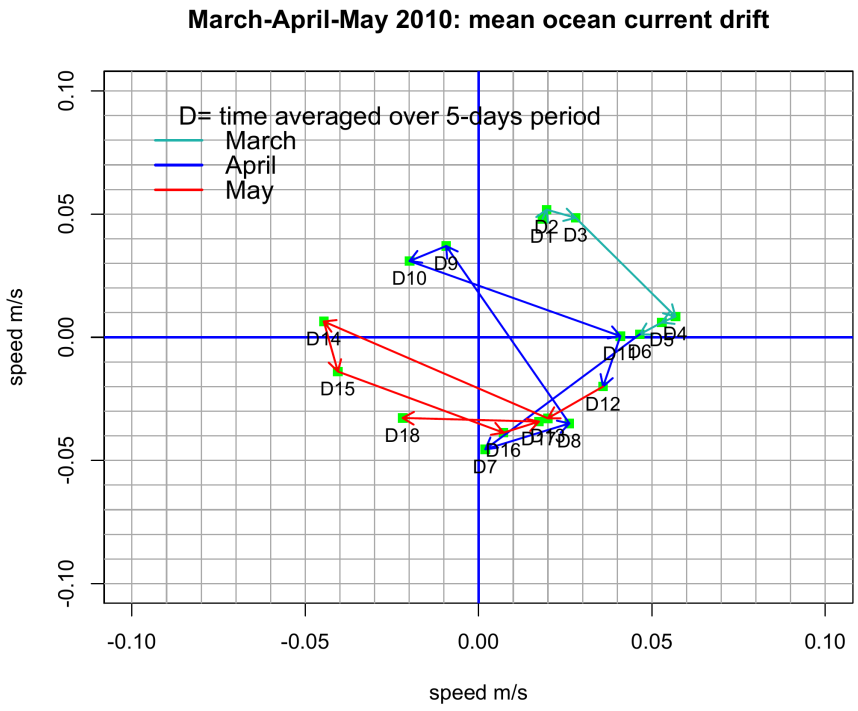
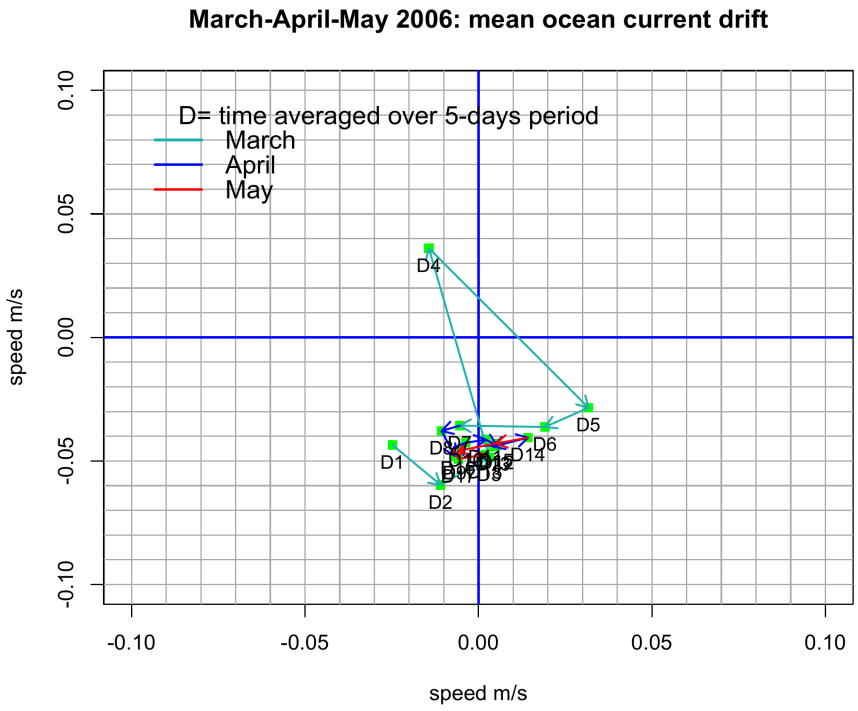


Figure 2.18f: Cartesian projection of mean current drifts prevailing during the period of March-April-May for year 2010 within a rectangle of –15°W to –9°W and 51°N to 54°N.

In contrast, 2006 and 2009 are marked by an obvious low inertia of the currents (**Figure 2.18g-h**).

(g)



(h)

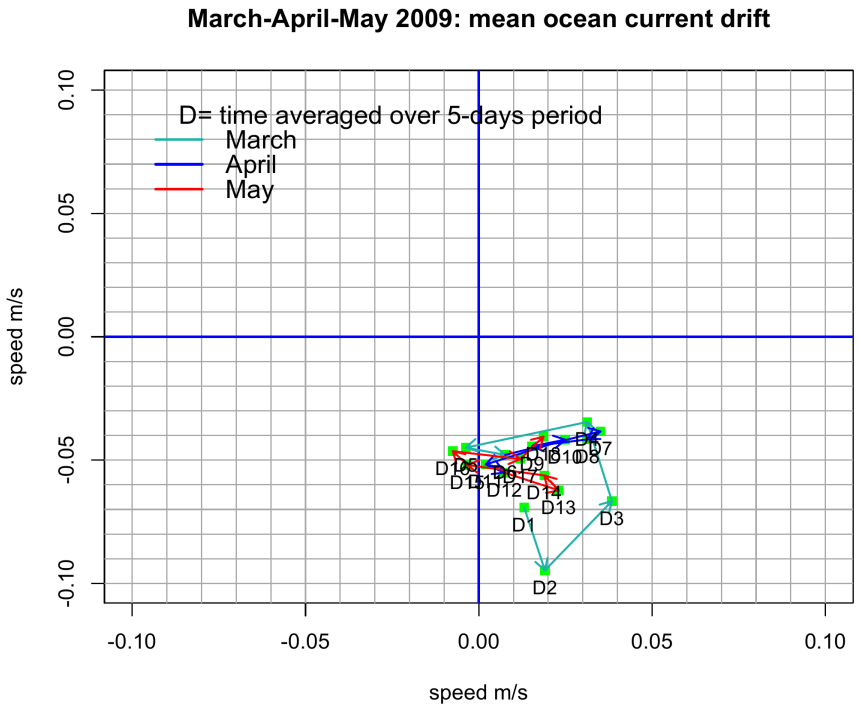


Figure 2.18 g-h: Cartesian projection of mean current drift vectors prevailing during the period of March-April-May for years 2006 and 2009 within a rectangle of –15°W to –9°W and 51°N to 54°N.

While, in comparison, the patterns of current movement in 2004 and 2007 spatially extend a little further (**Figure 2.18i-j**).

(i)

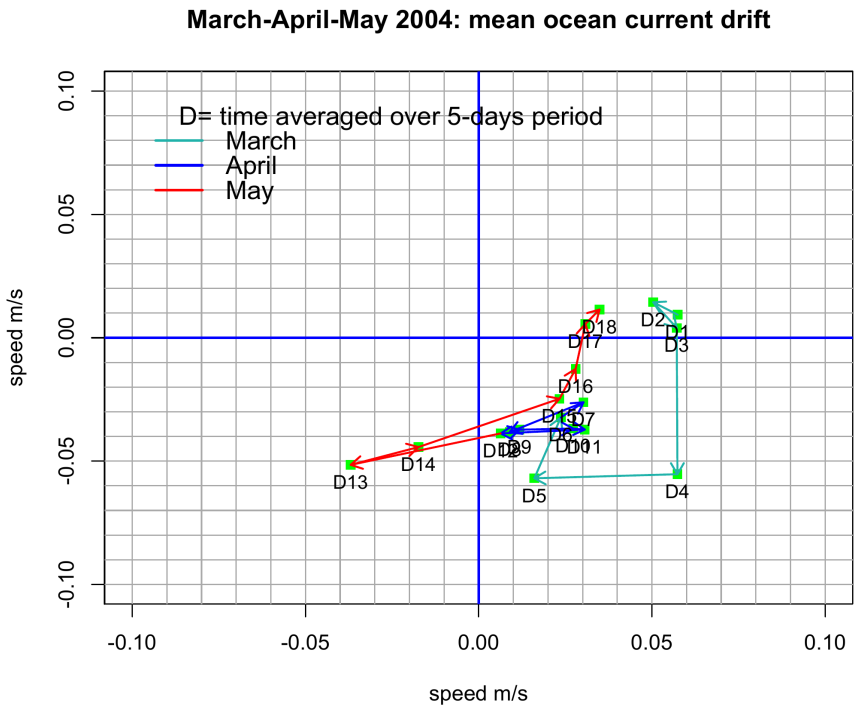


Figure 2.18i: Cartesian projection of mean current drift vectors prevailing during the period of March-April-May for years 2004 within a rectangle of –15°W to –9°W and 51°N to 54°N.

(j)

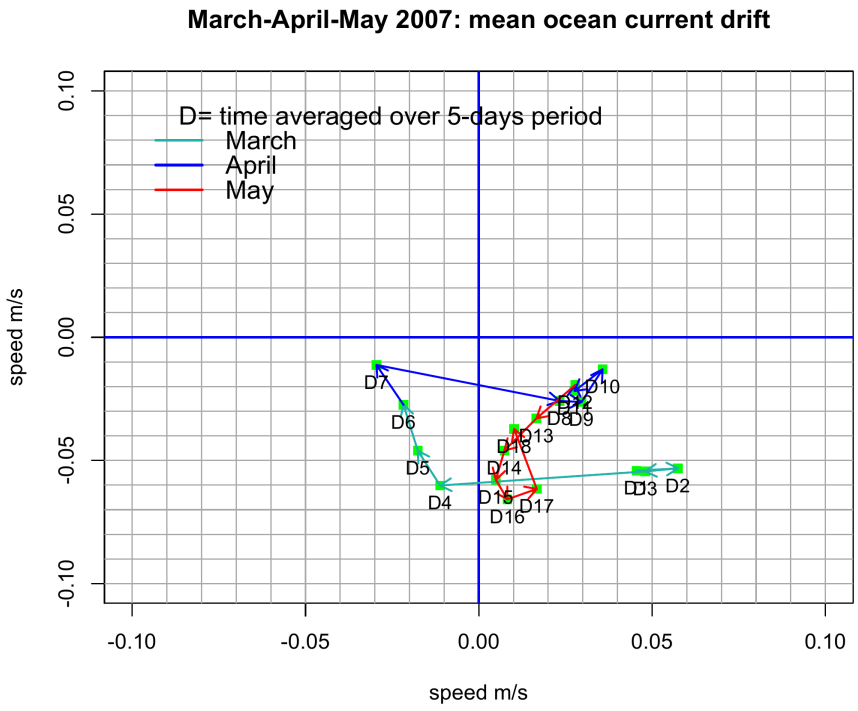


Figure 2.18j: Cartesian projection of mean current drift vectors prevailing during the period of March-April-May for years 2007 within a rectangle of –15ºW to –9ºW and 51ºN to 54ºN.

From a general point of view, we observe that in most of the cases the beguining of April (*D7*) and end of May (*D18*) positions are quite close together allowing us to assume that any particle carried in this circulation will return more or less to its initial position. Only 2003 and 2008 diverge from this general pattern with its South-North direction, although attenuated in the case of 2003, regarding the March extension of the current and then the resulting distance between May (that is, *D18*) and March (that is, *D1*).

For 2007, even though April *D7* is far away from May *D18*, 2007 falls into the category of current characteristics mentioned earlier, that is to say, confined pathway (low speed) and proximity of the "tail" and the "head" (*D8* and *D18*, **Figure 2.18j**). Also, by including the March branch of the flow, 2004 pattern ends in a position (*D18*) close to *D1* (**Figure 2.18i**).

(III.2) Fishing pressure

Using Maximum Covariance Analysis (MCA) with vessel monitoring system data (VMS) and burrow density, three modes are revealed. The first pair of patterns (Mode 1, **Figure 2.19a**) describes the largest fraction of the square covariance ($SCF_1=69\%$) and each succeeding pair pattern (Mode 2 and 3 in **Figure 2.19b-c**) describes a maximum fraction of square covariance ($SCF_2=18\%$, $SCF_3=14\%$ respectively) that is unexplained by the previous pairs. Although deemed significant with the North's rule of thumb test, care should be taken in interpreting mode 3 as it lies close to mode 2.

The *Pearson correlation* values (*0.96, 0.99, 0.96*) of the pair of the expansion coefficients indicate how strongly related the coupled patterns are. Nevertheless, the very short time sequence (only 4 years, 2006-2009) limits the interpretation of the information conveyed by the coupled dynamic time series of each pair. Note that VMS data have been rasterised to fit with the spatial resolution of the ordinary kriging predictions.

In Aran grounds, 69% of the square covariance (mode 1) is explained by a spatial heterogeneity in the distribution of positive (+) and negative (–) correlations in the VMS data, contrasting with a global homogeneous and smooth spread of (+) correlations over the burrow density field (**Figure 2.19a**). Whereas, the mode 2 is characterised by the emergence of two zones, showing a peripheral and a central zone displaying (–) and (+) correlations, respectively, combined with a wide central area of (–) correlation values in the fishery activity map (**Figure 2.19b**).

The last mode 3 shows an inversion of the previous polarity accompanied by a patchy map of fishing effort with (+) correlations mainly localised along the meridian 430E and the East edge of the field (**Figure 2.19c**).

(a)

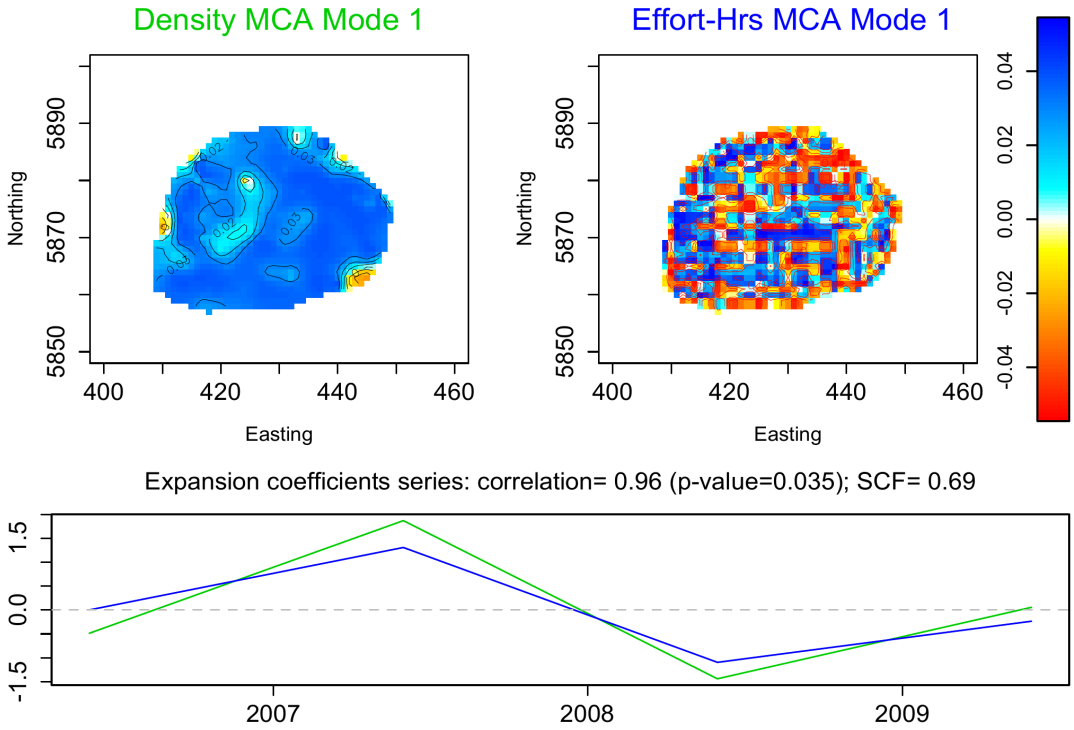


Figure 2.19a: Mode 1 of maximum covariance analysis (MCA) of burrow density and fishing effort in Aran grounds.

(b)

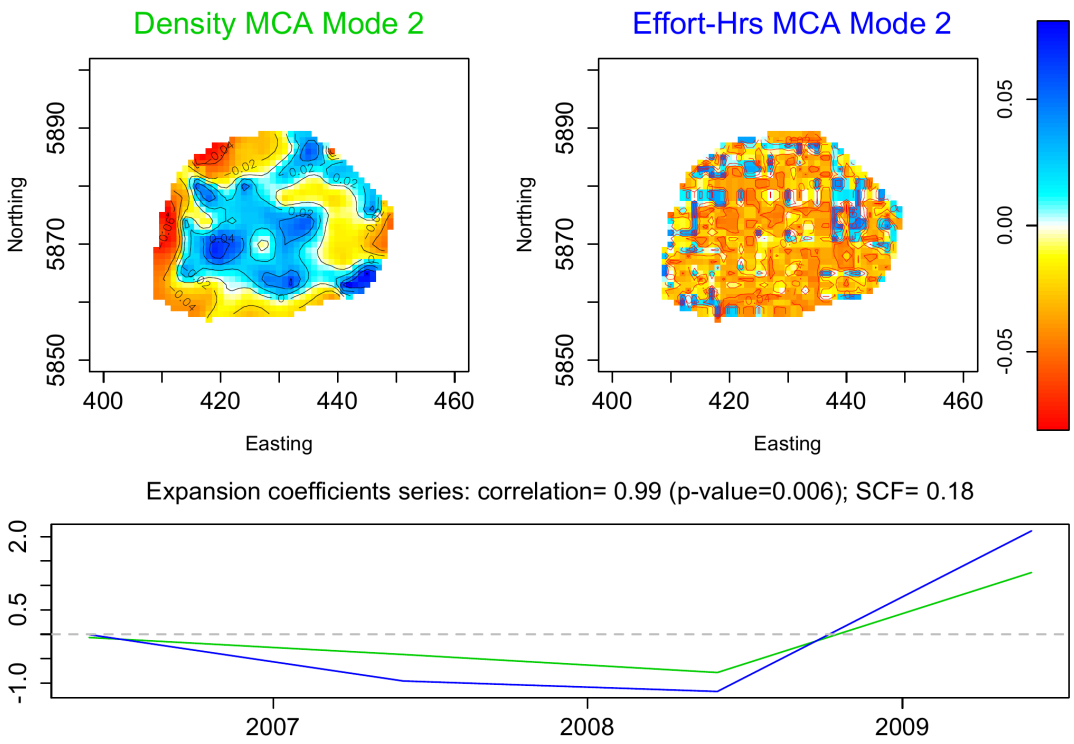


Figure 2.19b: Mode 2 of maximum covariance analysis (MCA) of burrow density and fishing effort in Aran grounds.

(c)

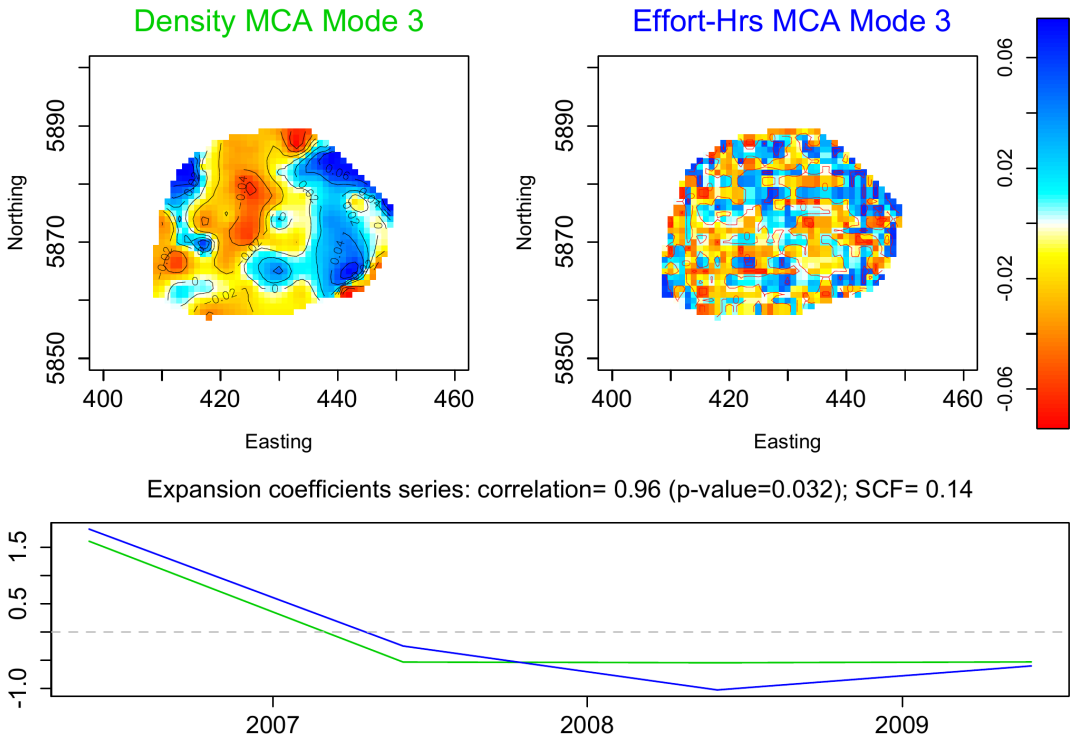


Figure 2.19c: Mode 3 of maximum covariance analysis of burrow density and fishing effort in Aran grounds.

MCA identifies structures in pairs of coupled spatial (structure) patterns. The two combined data fields are fishing pressure (derived from vessel monitoring system data) and geostatistical cartography of burrow density (derived from ordinary kriging). A set of singular values is associated with each pair of vectors (analogous to the eigenvalues). Each pair of spatial patterns (Mode) describes a fraction of the square covariance (SCF) between the two variables. Thus, MCA picks out structures that "explain" the maximum amount of covariance between two data sets. The scale colour bar represents the correlation value, indicating how strongly related are the couple pattern. For this study, the VMS data only covers the period of 2006 to 2009. Easting/northing coordinates in UTM zone 29, WGS84.

By examining the rasterised VMS data (**Figure 2.19d**), we report similar patterns as depicted from mode 1 and mode 3. Years 2008 and 2009 feature a decreasing number of hours spent over the central zone. In contrast, in 2006 and 2007 fishing effort was more regularly spread over the whole area, illustrating a shift in the fishing behaviour over the

time period. Thus, the singular value decomposition, leading to mode 2, highlights the intensity of effort over the central zone that has been blurred by the stand alone display of VMS data.

Overall, as expected, there is an opposite relationship between burrow density and fishing effort.

(d)

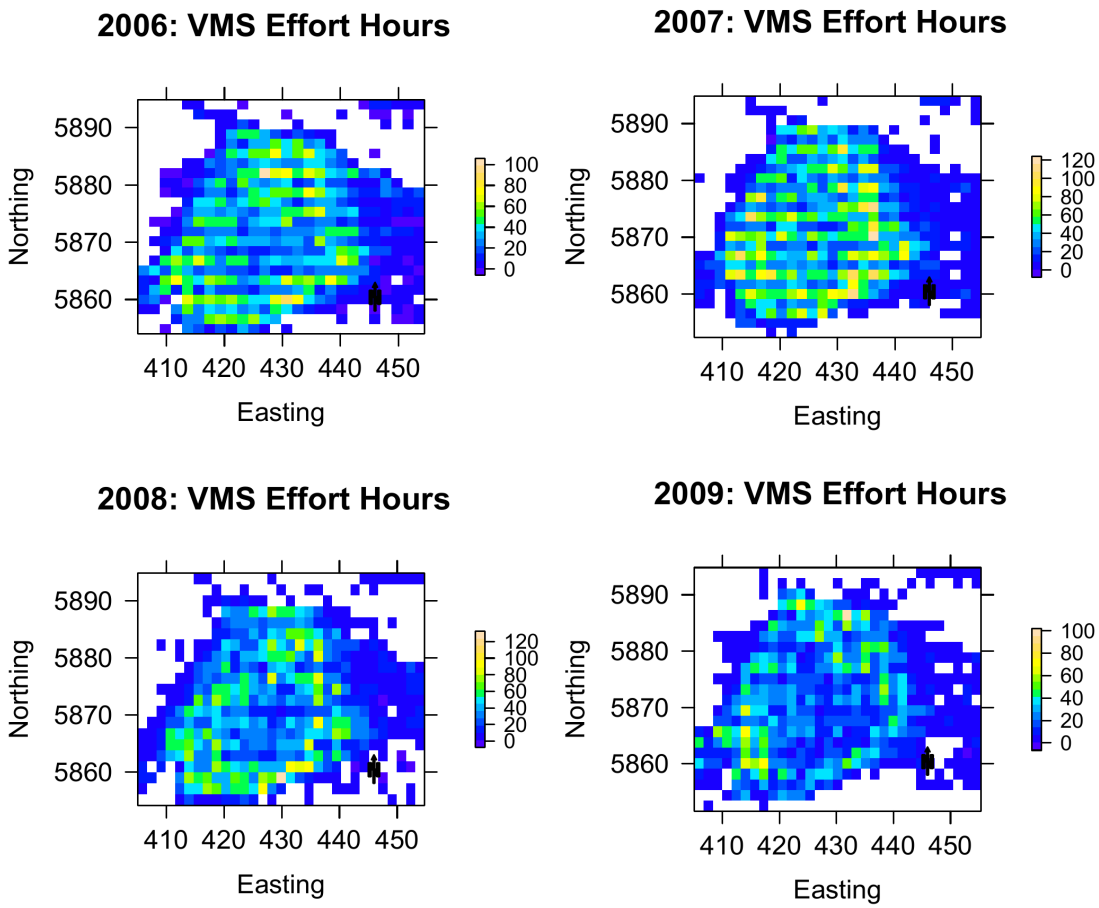


Figure 2.19d: rasterised 2006, 2007, 2008, 2009 vessel monitoring data used in the MCA approach. Easting/northing coordinates in UTM zone 29, WGS84.

Towards a peripheral redeployment of vessels

The general fishing effort pattern changed in 2009. In fact, beyond 10 hours of fishing effort a clear abandonment of the central zone (**Figure 2.20a**) in favour of the peripheral area is highlighted and this is accentuated by a higher fishing effort (**Figure B4** in ***Annexes B***).

In 2009, 50% of the (experimental) cumulative distribution function of the effort is about 7.41 hours (**Figure 2.20d**) and the shrinking of the density distribution of the fishing effort curve around this value in 2009 is obvious, contrasting with the flattened-bimodal form of the previous years. In addition, note that, whatever the intensity of the activity (5, 10, 15 or 20 hours), there is a decreasing trend in fishing effort versus the area fished (**Figure 2.20b**). These statistical traits could suggest a possible new fishing strategy over the Aran grounds patch.

(a)

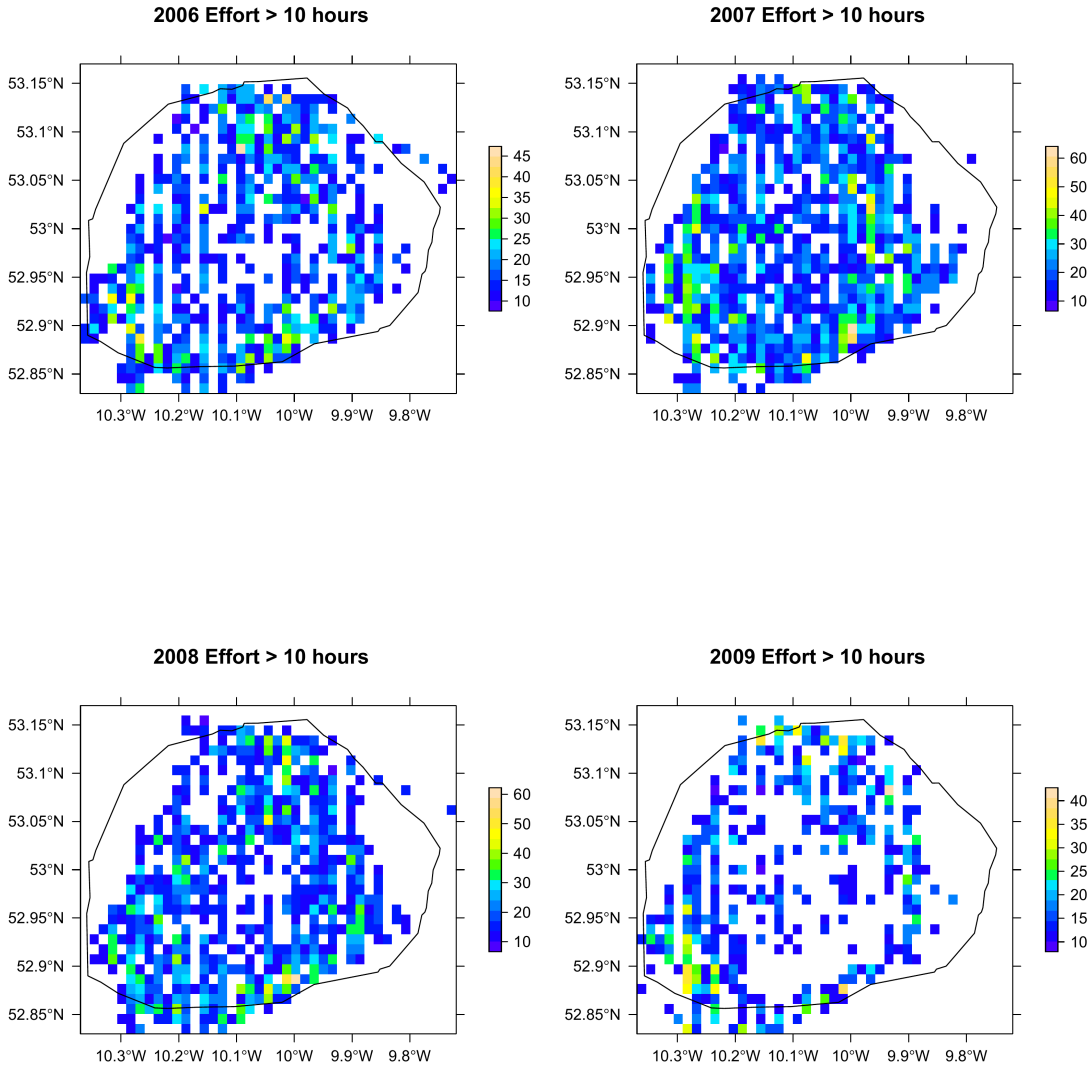


Figure 2.20a: Rasterised maps of the fishing effort distribution higher than 10 hours in Aran grounds using vessel monitoring system data for the period 2006–2009.

(b)

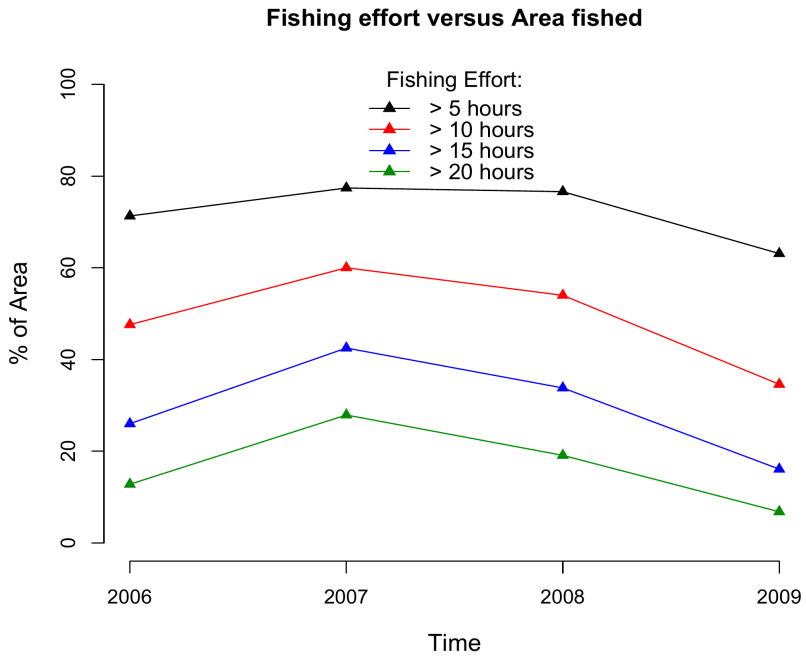


Figure 2.20b: Relative area covered by *Nephrops* fishing actvity in relation to effort for period 2006–2009 in Aran grounds using vessel monitoring system data.

(c) (d)

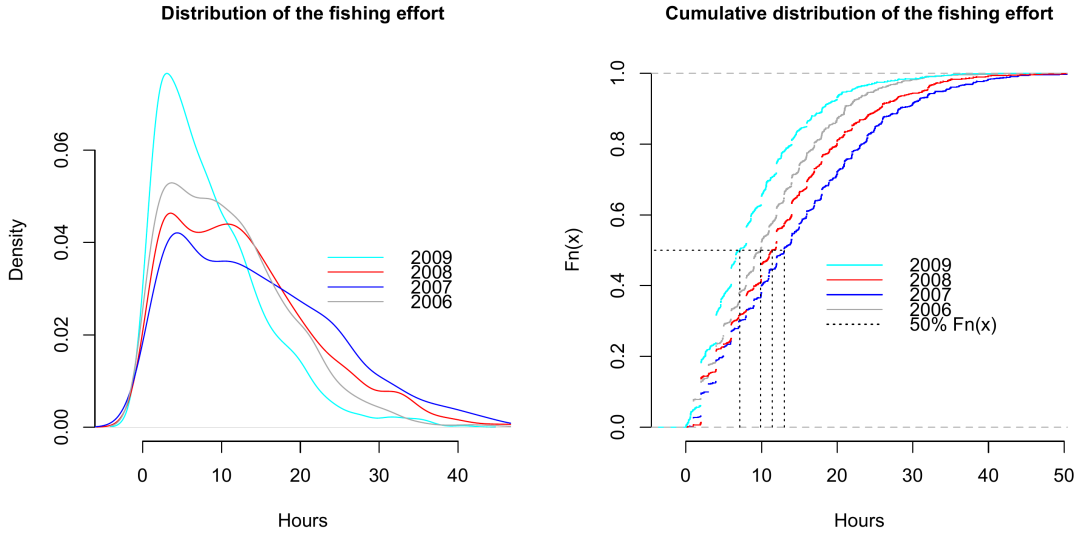


Figure 2.20 c-d: (**c**) Density distribution of effort and (**d**) cumulative distribution of the effort in Aran grounds during the period 2006–2009 using vessel monitoring data.

The 50% cumulative distribution function of the fishing effort is reached at values of 9.8 hours, 13 hours, 11.4 hours and 7.1 hours for years 2006, 2007, 2008 and 2009, respectively.

Discussion

This study aimed at describing the spatial distribution of the *Nephrops norvegicus* population in the Aran grounds over the years 2002-2010 and relating this to the status of the stock.

We used kriging to generate annual maps of burrow densities to evaluate spatial patterns in abundance and used variograms to quantitatively summarise the spatial distribution. We selected the spherical model because its shape matches well with what was observed: an almost linear growth in burrow density up to a certain distance then a stabilization. In fact, the theoretical model has a linear behaviour at small separation distances near the origin and maintains a quasi linear behaviour up to the sill (Isaaks and Srivastava, 1989; Chiles and Delfiner, 2012). The experimental semi-variograms showed linear trends at particular directions and this appears after the range is passed indicating that within this range (radius) density distribution patterns are safely modelled (Clark, 2001; **Figure B1** in ***Annexe B***).

Spatial structural traits

From many perspectives, the spatial distribution of this benthic species has remained stable. Burrows were rarely recorded in substrates with less than 20% mud (**Table 2.1**). After the **indicator kriging** analysis, we note that the lower densities (< 20%) are always located at the edges of the Aran grounds (**Figure B2** for a thorough overview). This steady state is also confirmed by the short distances separating the (weighted) centre of gravity of the observed samples (**Figure 2.2a**, top left).

In addition, during the 9 years, the semi-major axes of the standard deviation ellipses have been regularly pointing in the East-North direction (**Figure 2.3**) disclosing a constant orientation in the pattern of the density distribution at large scale, very likely in line with the seabed habitat influence on recruitment and growth (Campbell et al., 2009; Merder et al., 2020). Thus, as previously described for Mediterranean areas (Fariña et al., 1994; Maynou et al., 1998ab; Morfin et al., 2012), the presence of spatial structure for *Nephrops* in the North East Atlantic water is also identified.

However, some variability within this framework was also observed. Between years, surface extent and forms of kriging predictions have fluctuated. Indicator kriging maps

with median density thresholds showed important successive shrinks of the South-West quarter of the Aran grounds in 2003, 2004, 2005, 2007 and 2010 (**Figure B3** in ***Annexes B***). In addition, a decrease in the global abundance of burrows over the area of study was observed (**Figure B5** in ***Annexes B***).

Although the time dimension is not explicit, the spatio-temporal approaches used in this study provides an insight into the spatial density changes. The amplitudes of change are now spatially illustrated. Both the EOF and the contrast methods highlighted the global decrease in density (**Figures 2.10 & 2.15**) highlighting an acute depletion in abundance in the central zone.

Covariate contributions

The mud content of the seabed contributed to enhance the quality of the spatio-temporal approaches to model population density. In fact, variances of universal co-kriging predictions were substantially reduced in comparison to ordinary kriging (**Figure 2.14** vs **Figure 2.8**). This also resulted in a higher percentage of variance explained by the first **EOF** increasing from 71.19 to 91.51 %.

As a consequence, the spatial sub-area differences in abundance were more easily discernible (**Figure 2.10** vs **Figure 2.16**). Nevertheless, despite this important influence on the spatial distribution of density, it does not help to explain variability in Aran grounds yield of these sub-regions (**Figure 2.14**). We then investigated the potential impact of additional environmental and anthropogenic factors.

Current patterns

Many studies have linked the presence of gyre circulation to the larval retention phenomena maintaining larval drift in the vicinity of the zone of hatching or suitable bottom sediment (e.g. Hillis, 1988, White et al., 1988; Hill, 1990a; Hill et al., 1990b; Hill, 1991; Hill et al., 1996, Hillis, 1996; Hill et al., 1997). In Aran grounds, hatching is supposed to start in April approximately (Farmer, 1975; Bell et al., 2006; Smith et al., 2008). On Galway Bay grounds, eastward of Aran grounds, stage III larvae were sampled on 5th of April 2018 (McGeady et al., 2019) indicating eggs released during the period of February-March, supporting our choice to include the March branch of the average surface flow.

Thus, current circulation patterns from the prevailing flows in the ocean surface layer during March April and May could help to explain, the recruitment rate and hence the level of abundance recorded by UWTV surveys **(Figure B5** in ***Annexes B***). From the analysis of the variability of the patterns exhibited from 2002 to 2010, we suggest that the regular proximity of the "tail" and "head" segments of the current drifts could serve as an indication of a retention circulation mechanism over the Aran grounds (**Figure 2.18a-b-c-d-e-f-g-h-i-j**) which necessitates further investigation and, in addition, we surmise that such favourable head-tail conditions, whether involving April-May subset or March-May, could influence positively the success rate of settlement and hence contributing to the variability of the abundance. Last, but by no means least, results of our approach have undeniably suffered from the low resolution of the satellite data available for this study.

Fishing pressure

The spatial heterogeneity displayed in the VMS data and highlighted by MCA mode 1 (69%, **Figure 2.19a**) could result from the movements between fishing areas to maintain a high catch rate (Hilborn, 1985; Hilborn et al., 1987) and unsurprisingly, we observe a quite homogeneous response of the stock in terms of its directional variability to the fishing effort. This phenomenon could illustrate the effective targeting of the fishing effort (Bell et al., 2005).

This study also shows that 32% (18% + 14%, respectively SCF_2 and SCF_3 of mode 2 and mode 3, **Figure 2.19b** and **Figure 2.19c**) of the covariance between burrow density and fishing effort corresponds to a shift in the areas targeted by fishers (**Figure 2.19d**). The middle site is no longer preferred, reflected by a decrease in trawling intensity (**Figure 2.20a**). Without doubt, this move in the fishery strategy is attributable to a decrease in *Nephrops* abundance. Finally, by coupling the density of burrows with fishing effort, it is possible to differentiate spatially the relative strengths and weaknesses of this link and, potentially, to understand the variability in *Nephrops* biological parameters between survey samples within the same stock. Lagging the pair expansion coefficients (or principal components) would have been useful in order to pinpoint the exact turning point, but the very short number of years involved prevents us pursuing this further.

Historically, the higher fishing effort in the central zone of Aran grounds is likely related to the larger body size of *Nephrops* in this area. A marked increase of the fishing effort at the periphery is clearly observed in 2008 (**Figure 2.19d**) which is also the lowest abundance ever recorded for the 2002-2010 period (**Figure B5** in ***Annexes B***). In other words, the decrease in the stock over the central zone compelled fishers to alter their spatial fishing strategy by considering other patches to balance the effect of the diminishing resource of their preferred area. However, it should be noted that the change in fishing strategy does not mean, in any way, a lack of activity, and as a result, the fishing pressure continued on the central sub-population.

Other causes of spatial variability

Although each of the methods used have inherent uncertainty, as illustrated by the underestimates observed in applying the cross correlated variance technique (**Figure 2.13**), and the year to year variation of the experimental variograms for kriging (**Figure B1** in ***Annexes B***), each method illustrated similar trends (**Figures 2.10, Figure 2.15 & 2.16**). This variability has been recognised in other areas (*e.g.* Morfin et al., 2012) but from our point of view, it accentuates the difficulty in distinguishing between resilience and overexploitation of a fish stock by only using geostatistical approaches.

Perspectives

This study has shown the ability for the UWTV to track the evolution of the stock. It illustrates that spatial management on the Aran grounds is possible and should be implemented as part of the management of the stock. One option is to implement a closed area by removing a part of the ground from the adverse effects of fishing, which would likely also lead to increased abundance in adjacent areas. Results of larval trajectory modelling (Marta-Almeida et al., 2008; O'Sullivan et al., 2015; McGeady et al., 2019) provide a valuable contribution to the management and conservation of the species. In the case of Aran grounds, the connectivity between adjacent fishing *Nephrops* patches has been highlighted and is believed to be fundamental for the renewal of the Galway Bay and Slydes stocks (O'Sullivan et al., 2015). However, the adoption of spatial management requires much more information on the species

including density dependence effect. In this regards, in Clew Bay, localised further North of Aran grounds, Merder et al. (2020) observed a density-dependent suppression of growth (in body size) for males with a disproportionate effect on slower growing males. Meanwhile, the spatial distributions of smoothed growth did appear to differ between sexes where male growth was higher in peripheral areas compared to the central area where catches were higher and females with higher growth tending to be in the central fished area.

We see that translating the current management of the Aran grounds *Nephrops* fishery into a more spatially explicit management regime (*e.g.* Kraak et al., 2012) would require not only a real time track of each vessel (*i.e.* fishing effort) along with targeted catches (*e.g.* Dodler et al., 2018) at high resolution, but also, a better understanding of the *Nephrops* habitat biotope interaction within its dynamic ecosystem and the mechanisms involved in the density dependence effects that reflect a piece of such comprehension. From this perspective vessel monitoring system data implemented in Aran grounds since 2005 for vessels >15 metres (Gerritsen et al., 2011) and more recently for vessels > 12 metres, provides an explicit spatial overview of the fishery activity.

It broadens the opportunity to implement indicator tools for integrated fishery management for instance by measuring the occurrence of suitable *Nephrops norvegicus* habitat (Eastwood et al., 2007; Stelzenmüller et al., 2008), as well as the frequency of trawling, the trawled versus untrawled areas...etc, allowing to measure the status of impacted seabed biota on fishing grounds for instance (*e.g.* community biomass removal, time of recovery, Hiddink et al., 2017). Bottom trawling intensity have been reported to influence the diet of *Nephrops norvegicus* shifting from benthic food towards a more planktonic based food target (Hinz et al., 2017). For Aran grounds, already available VMS data should be translated into bottom trawling intensity index and such cartography examined in pair with *Nephrops* diet analysis from areas subject to different fishing intensity and evaluate its effect on fishery (*e.g.* weight).

Under the European Union fisheries management framework, the fundamental scale for implementing the total allowable catch or quota for any fish stock is the area of management divided in functional units. In the Aran grounds case, the results presented here confirm that the size of the functional unit is appropriate, due to the fact that the fishery ground matches the corresponding mud patch habitat. Such a clear geographical

delimitation of the population, coupled with sedentary behaviour of the species, facilitates monitoring of the *Nephrops* stock, in contrast to highly mobile species, characterised by various migration sites along their life cycle (*e.g.* herring, *Clupea harengus*). However, this positive aspect is counterbalanced by the advection phenomenon impacting considerably the level of the recruitment (White et al., 1988; Hill, 1990a; Hill et al., 1990b), which is not yet understood in the case of *Nephrops* stock in Aran grounds despite recent results (Nolan and Lyons, 2006).

Conclusion

This spatial analysis provides evidence of a dynamic reduction in the abundance of *Nephrops* over the whole Aran ground patch.
Widening the scope of our exploration of the status of *Nephrops* by including the spatial dimension of the data pleads for an ecosystem approach to management. In fact, the spatial dimensions allows us to map yield onto the gridded habitat and provides a suitable framework to built a bridge between habitat requirements and the management of a stock.

Chapter 3 Evaluation of the Aran grounds *Nephrops norvegicus* stock status

Contents

Chapter 3 Evaluation of the Aran grounds *Nephrops norvegicus* stock status.....178

Abstract.....180

Introduction.....181

Aims of this chapter.....185

Methods and Materials.....187

(I) Methods.....187

(I.1) Bayesian biomass production model (BM).....187

(I.2) Catch Maximum Sustainable yield (CMSY).....190

(I.3) Length-based spawning potential ratio (LB-SPR).....191

(II) Materials.....193

(II.1) Under water TV counts.....193

(II.2) Landings.....194

(II.3) Effort.....194

Results.....195

(I) Bayesian production modelling.....195

(I.1) Convergences and fits.....195

(I.2) Biomass, fishing mortality and MSY.....200

(I.3) Stock status: overfishing and depletion.....207

(II) Stock response.....210

(II.1) Resilience (r) and abundance (k).....210

(II.2) r-k pairs and exploitation rate (F/F_{MSY}).....218

(III) Yield and recruitment.....224

(III.1) Production and productivity.....224

(III.2) Spawning potential ratio (GTG-LBSPR).....227

Discussion.....233

Conclusion.....245

Abstract

In the Aran grounds, independent under-water TV surveys carried out from 2002 to 2021 indicate a large and steady decrease in *Nephrops norvegicus* burrow number, from 1070 to 331 million. On the basis of landings data covering the period 1974–2014, a number of different approaches were used to determine the stock status. Under a Bayesian state space framework, a Biomass Model (BM) with Schaefer surplus and Catch MSY method (CMSY) were chosen to address the lack of age data and predict parameters of interest (e.g. *r, K, MSY,* F_{MSY}, B_{MSY}). Both approaches highlighted a decline in biomass with the notable exception of the Biomass Modelling using a lpue index of abundance. The landing levels exceeded the estimated *MSY* since 1995 and reduced exploitation rates between 1995 and 2006 did not improve the stock level. Meanwhile, a length-based assessment of the spawning potential ratio (LB-SPR) relied on Beverton-Holt life history ratios and length frequency distribution surveys, indicated worrying stock levels. This study reveals indicators of an unsustainable trajectory for the *Nephrops* fishery in the Aran grounds.

Introduction

Fishery

Nephrops norvegicus is a commercially important species distributed throughout the North East Atlantic and Mediterranean Sea. Recent landing statistics from all countries show that 66544 tonnes were landed in 2010. Most of this came from the North-East Atlantic where 38600 tonnes (58.1%) were taken by the United Kingdom, and 7800 tonnes (11.7%) by Irish vessels (Ungfors et al., 2013). For the Republic of Ireland the fishery is extremely valuable: for example, in 2011, *Nephrops* was estimated to be worth €32.1 million, equivalent to 8210 tonnes live weight, and ranked next after the leading mackerel (*Scomber scombrus*) fishery worth 56.6 million € and 68978 tonnes (Stockbook, 2011). In 2018, this increased to 10893 tonnes worth €75.2 million, making it the second highest value demersal fisheries species in Ireland (Stockbook, 2018). This fishery is also crucial in terms of socio-economic factors: for instance, vessels from localities such as Ros a Mhíl, Dingle, Union Hall, Dunmore East, Clogherhead and Kinsale mainly exploit the *Nephrops* fishery and, without it, the majority of vessels in the fleet would cease being economically viable (Meredith, 1999; Foley et al., 2016). Ros an Mhíl in Connemara is the main base for the Galway and Aran co-operative fishing fleet. In 2013, the total landed value of fish at this port was €15.5 million, all landed by Irish vessels and *Nephrops* was the most valuable species landed accounting for 71 % of the landings value and increasing from 11.8% by volume in 2004 to 24.57% in 2013 (Foley et al., 2016).

According to Foley et al. (2016) the impact of the fishing and fish processing industries of Ros an Mhíl spreads far beyond the immediate locality: at the regional level, an estimated 213 jobs and €50m of output in the economy of Co. Clare and Co. Galway depend directly and indirectly as a result of the 119 jobs and €15.5 million output directly associated with the fishing sector.

In addition, in the context of an 8% reduction in the overall value of seafood landed in Irish ports in 2018, the fall in volume was offset somewhat by the rise in price of some species like *Nephrops* (+13%), Mackerel (*Scomber scombrus*, +19%) and Brown crab (*Cancer pagurus*, +58%) according to the Ireland's Seafood Development Agency (BIM, 2018).

Landings data

Available landings data from the Aran grounds goes back to 1974. The quality of historic landings data are not well known. Prior to 1988, landings data for this fishery were only available to the ICES Working Group for France. There were no landings reported from Ireland, although there was probably some catch. Since 1989, landings statistics for the Irish fleet were obtained from EU logbooks. Since 1995, vessels record daily retained catches in operations and make a declaration of total landings on return to port. Since 2012, most vessels in the fleet have been using electronic logbooks (EC Regulation 1224, 2009 and EC Regulation 404, 2011). Vessels are required to electronically report catches on board in each 24 hour period.

From 1995 to 2010, the number of Irish vessels reporting landings of *Nephrops* from FU17 (Aran grounds) has oscillated between 40–50 tonnes and those with annual landings >10 tonnes per year can be considered the main participants in the fishery, accounting for about 85% of the total landings with 20–30 vessels (ICES WGCSE, 2018).

During this period, the stock was exploited exclusively by vessels using otter trawls, with the majority using twin-rigs nets with 80mm mesh. The number of boats has remained quite stable but there has been an increase in fishing power (see ***General Introduction***, ICES WKNeph, 2009).

Effort

More than 90% of the Irish landings of Aran grounds *Nephrops* come from trips where *Nephrops* was the target species, and by-catch species included anglerfishes (*Lophius* spp.), whiting (*Merlangius merlangus*), haddock (*Melanogrammus aeglefinus*) and megrim (*Lepidorhombus whiffiagonis*) (Stockbook, 2018).

This fishery can be characterised by a typical average pattern of catches over the annual period marked by two high levels of capture in early-Summer, and in early Autumn associated with the end of the incubation period and the spawning time (see ***General Introduction***).

In the past, individual vessel behaviour exhibited long periods of time spent in the area. Some vessels appeared to be fishing on a continuous basis throughout the year. In the last few years, the fishery has become significantly more concentrated in time. Vessels

only fish the ground for short periods but record higher daily landings. This change in behaviour reflects a generally more mobile behaviour by *Nephrops* targeting vessels, which switch between grounds as the prawns become available (ICES IBNeph, 2015). Effort data for FU17 are available from 1995 for the Irish otter trawl *Nephrops* directed fleet. The efficiency of vessels has improved significantly since 1995 with increased twin rigs initially being used and since 2012 quad rigs are deployed. On-board technology has also improved considerably. However, these factors are not well documented in a way that can be readily standardised in a lpue time-series (likely to be a negatively biased/underestimated because it is not adjusted for efficiency or behavioural changes; ICES WKNeph, 2007; ICES WKNeph, 2009; ICES IBNeph, 2015). Either expressed in Kw-days or in hours fished-days, the measures of fishing effort show fluctuations of relatively high amplitude (see **Figure 10** in ***General Introduction*** and **Figure A11** in ***Annexes A***, respectively) over this time series. However, as noted previously, in the case of Aran, the *Nephrops norvegicus* fishing effort is calculated from the total effort of the mixed fishery in proportion to the prawns caught.

Current management

Over the period of interest 1974-2014 the quality of historic commercial landings data is not well known. There are a few observations of both under and over reporting for certain years (2003-2005 and 2008) but it is not possible to correct landings using this information as it is not known how representative it is (ICES WKNeph, 2009 page 139). The trend in the landings data from 1974 to 2014 (**Figure 3.2a**) describes a steady period of decline until 1988, an increase throughout the 1990's with some fluctuations, peaking in 1999 at more than 1,400 tonnes, followed by a "yo-yo" pattern of values superimposed on an average phase of rise and fall.

The Irish landings have been reported to have been close to quota for the total allowable catch in this area since around 1997.

Currently, the catch advice in time (*t*) is determined from the product of the estimated *MSY* harvest rate[12] and the estimated abundance from the UWTV survey in time (*t-1*)

12 actually, a *MSY* harvest ratio selected from (combined male and female) $F_{0.1}$ proxy estimates derived from separable cohort analysis implemented for different average length frequency distribution (ICES IBNeph, 2018).

that gives the total number of removals under the *MSY* approach. This total is then partitioned into landings and discards based on recent discard rates and translated into landed and discarded weights by applying mean weights derived from recent data (Bell et al., 2018 page 37).

A biomass threshold noted $B_{trigger}$ was recently included in the assessment and is defined as the lowest stock size from which the abundance has increased and is used to "trigger" a reduction of the maximum sustainable yield (*MSY*) harvest rate.

Stock Status

From 0.79 individuals per m^2 (ind/m^2) in 2002 to 0.28 ind/m^2 in 2014, the decrease in density of *Nephrops norvegicus* in the Aran grounds is approximately 65% in only 12 years of exploitation. While the number of burrows has decreased dramatically, from 1070 to 383 million, at the same time, on average, the fishery reported an increasing trend in landings. Thus, the abundance of burrows in Aran grounds more than halved between 2004 and 2006 and since then, the stock continued to decline and fluctuate at a lower level.

According to Garstang (1900) and Graham's law of fishing (1943), the fundamental question remains the same in fishery science: "are we in a situation where an increasing effort reaches a maximum catch before falling when the numbers removed from the stock cannot be replaced by recruitment"? Even though it is simplistic and prone to missing the characteristic features associated with individual species and ecosystems that are impacted by fishing activity, this statement is still valid and will be the main thread throughout this analysis of the status of the stock.

However, the difficulty in determining appropriate reference points due to *Nephrops* life history characteristics, including specific physiological and behavioural changes, such as moulting and the seasonal female ingress and emergence from burrows contribute to the difficulties in carrying out stock assessments. Age based stock assessments cannot be used, necessitating a cohort analysis approach, which raises concerns about fishing selectivity patterns. The long term impact on the population induced by the strong sex ratio bias recorded during the period of the highest fishing activity is a risky oversight. Thus, the use of alternative methods, designed to operate with these limited insights into the targeted stock is required.

Aims of this chapter

We selected two approaches, the bayesian production or biomass modelling (noted BM, Meyers and Millar, 1999) and the catch-maximum-sustainable-yield (CMSY, Martell et al., 2013; Froese et al., 2017) to outline the status of the Aran ground *Nephrops norvegicus* stock.

By pooling all the biological aspects involved in the biomass dynamics, the Schaefer surplus production model type within the BM provides the means to infer a number of parameters and reference points (*e.g. r, k, MSY,* F/F_{MSY} and B/k) despite the lack of age composition data.

While, the CMSY relies on the "viable" pairs of intrinsic growth rate (r) and carrying capacity (k) to inform the biomass trajectories (calculated with a Schaefer production model) compatible with the observed landings. The methods allow the biomass depletion levels prevailing during the period of the landings to be quantified. Additional analysis of the modelling outputs were used to evaluate the compensatory capacity of the population and its production and productivity from 1974 to 2014. Since, life history traits (Beverton and Holt, 1959; Beverton, 1992; Jennings and Dulvy 2008) of a population or species determine its ability to cope with natural environmental variability, as well as to compensate for increased death rates due to anthropogenic perturbations (Bjørkvoll et al., 2012; Juan-Jorda et al., 2015), we relied on biological traits based on expert judgement and available length frequency distributions to examine the spawning stock status in response to the fishing pressure (LB-SPR, Hordyk et al., 2014, 2015abc; Prince et al., 2015; Hordyk et al., 2016). This ratio of the production of a depleted population relative to its unfished one (Goodyear, 1980; O'Farrell et al., 2005; Brooks, 2007) has gained popularity for data-limited fisheries (Brooks et al., 2010; Mangel et al., 2013; Hordyk et al., 2014; Hordyk et al., 2015abc; Nadon et al., 2015; Prince et al., 2015; Hordyk et al., 2016; Then et al., 2018; Hommik et al., 2020).

By implementing these different tools we have created a framework in an attempt to overcome some of the difficulties inherent in *Nephrops norvegicus* biology and behaviour. We were able to estimate the status of the stock consistent with the observed trend decline of the population abundance and casting light over an unsustainable exploitation of the stock with implications for subsequent management. For instance,

from 2000, Aran grounds stock featured high fishing rate and low biomass records. The relative biomass B/k ranges within [0.5 to 0.3] with a tendency towards its lower B/k limit. We recorded a drop of the productivity combined with an estimated low resilience for the species that potentially weakens the stock response to the fishing pressure. In addition, under bayesian state space approach, index of abundance based on the effort measured in Kw-days appeared to be far less sensitive to the actual decline trajectory of the biomass rising serious concern about its use as proxy of abundance in management. Thus by settling the current situation of the stock, this study contribute to facilitate the path towards a stock recovery.

Methods and Materials

(I) Methods

(I.1) Bayesian biomass production model (BM)

Using a Bayesian framework approach can be helpful in this scenario as *Nephrops norvegicus* population dynamics have important pieces of missing information that need to be inferred (biological reference points) and often, fisheries data are highly variable and sporadic in nature, which are characteristics easily tackled under the state space bayesian framework.

Although based on a somewhat crude simplification of fish population dynamics, biomass production model remain a tool of choice for providing fisheries management advice in situations in which there is a lack of age composition data enabling the use of age based assessment methods. BM uses time series of cach and abundance to estimate productivity and this analysis uses the bayesian state-space modelling framework with a Schaefer yield component also termed surplus production. Here, we use the approach of Froese et al. (2017) initially developed by Meyer et al. (1999).

State-space modelling explicitly relates the state variable (the unobserved "true" biomass) to the data at hand (catches/landings,...*etc.*). Catches/landings and effort data are used here without the assumption that the population is in equilibrium.

Thus, a first equation is generated to mimic the dynamic of the hidden biomass including fishery removals:

$B_{t+1}=\left(B_t+r\,B_t\left(1-\frac{B_t}{k}\right)-C_t\right)\cdot e^{\varepsilon_t}$ (the state or process equation)

and a second equation:

$I_t=q\,B_t e^{\omega_t}$ (the observation equation) relating the data to the hidden process. In other words, the index of abundance (I_t) is linked to the biomass (B_t) through the catchability coefficient (q). The available information on the unknown real biomass consists, ideally, of independent proxies.

To account for different sources of uncertainty in the dynamics of the population, the state and the observation equations are augmented with error terms ε_t and ω_t respectively. In addition, the process variance, σ_p^2, as well as the sampling and

measurement errors made on observations, namely the observation variance σ_o^2 are included and defined as inverse gamma priors.

The Schaefer form of the surplus or yield is $r\,B_t\left(1-\frac{B_t}{k}\right)$.

In order to improve the effectiveness of the Gibbs sampling and mixing when using the MCMC technique, the latent variable B_t is re-parameterised in $P_t=\frac{B_t}{k}$ leading to the biomass production equation $P_{t+1}=P_t+rP_t\left(1-P_t\right)-\frac{C_t}{k}$ (Meyer et al., 1999).

It is important to note that under this bayesian framework, we have considered two types of indices as proxy of abundance. First, the fishing effort measured in Kilo-watt-Days is used to estimate catch per unit effort and linked to abundance through $CPUE_t=q\cdot B_t$. More appropriately, this should be $LPUE_t=q\cdot B_t$ since landings are a more realistic measure of the prawn harvest on the Aran grounds

The second index, namely, the stock size index (SSI_t, **Table M1**) relates to the number of surveyed burrows and here we set to 1 the absolute value of surveyed burrows of the year 2002 and calculated the relative rate of abundance for the subsequent years of the survey and incorporated this into the model through $SSI_t=q\,B_t$.

Table M1: Stock size index from 2002 to 2014 noted SSI_t and relies on the abundance, in number, of the burrow as surveyed by the Under Water TV.

Year	2002	2003	2004	2005	2006	2007	2008	2009	2010	2011	2012	2013	2014
SSI$_t$	1.00	1.164	1.317	1.02	0.585	0.859	0.505	0.650	0.821	0.628	0.437	0.412	0.357

Thus, in the bayesian approach the prior range distributions of the key parameters of interest (r), (k) and (q) are fundamental to define the statistical space from which to sample.

The prior range of the maximum intrinsic growth rate of the population (r) is directly translated from the resilience classification of the species as provided in FishBase (**Table M2**; Froese et al., 2000; Froese and Pauly, 2015). Also, stock depletion levels are assumed for the initial, intermediate and final years of the landing time series in relation to the following classification of the relative biomass (B/k): low [0.01–0.4], medium [0.2–0.6] and high [0.5–0.9] (**Table M2**).

However, setting the carrying capacity (k) prior range necessitates to make a number of assumptions following Froese et al. (2002, 2017): first, "unexploited stock size (k) is larger than the largest catch in the time series, because it is highly unlikely that a fishery finds and catches, in a single year, all individuals of a previously unexploited stock. Thus, maximum catch in the time series was used to inform the lower bound of (k)" (Froese et al., 2017). Second, "the maximum sustainable catch expressed as a fraction of the available biomass (F_{MSY}) depends on the productivity of the stock. This relationship was accounted for by dividing maximum catch by the upper and lower bound of (r) and using these values as the benchmarks for the lower and upper bounds of (k)" (*ibid*). And third, "maximum catch will constitute a larger fraction of (k) in substantially depleted rather than lightly depleted stocks" (*ibid*).

Hence, with an assumed low prior relative biomass *(i.e. $B/k \leq 0.5$)* for the recent year period (2014), the lower (k_{low}) and upper (k_{high}) limits of the carrying capacity (k) estimates are:

$k_{low} = \frac{max(C)}{r_{high}}$ and $k_{high} = \frac{4 \cdot max(C)}{r_{low}}$ (Froese et al., 2017).

Concerning the coefficient of catchability (q) for stocks with low recent prior relative biomass (*i.e.* B/k ≤ 0.5), Froese et al. (2017) determined the lower (q_{low}) and upper (q_{high}) prior range boundaries as follow:

$$q_{low} = \frac{0.5 \cdot r_{gm} \cdot LPUE_{mean}}{L_{mean}} \text{ and } q_{high} = \frac{1 \cdot r_{high} \cdot LPUE_{mean}}{L_{mean}}$$

where L_{mean} and $LPUE_{mean}$ stand for the mean values of landings and landing per unit of effort taken over the indicated years of available index data: 2002 to 2014 for UWTV index (SSI_t) and 1995 to 2014 when using Kw-days based index, Notice that (r_{gm}) is for the geometric mean of the prior-r range.

For the bayesian state space implementation, (q),(k) and (r) prior ranges are then translated into prior density functions by assuming they are log-normally distributed (Froese et al., 2016, 2017) and the expert skill is all embedded in the estimated prior ranges of these key parameters (r, k, q).

Then, we assumed prior (r) range between [0.05–0.5]. For the 1974–2014 landing time series period we assumed prior ranges for relative biomass (B/k) at initial (1974), intermediate (2006) and final (2014) years within [0.2–0.6], [0.01–0.4] and [0.01–0.4]

respectively. Hence, prior range estimates for (k) (10^3 tons) and (q) are [2.29–91.5] and [6.72e-05–4.25e-04] respectively.

While, for 1995–2014 landings series, we assumed relative biomass level of [0.2–0.6] for initial year (1995) and [0.01–0.4] for intermediate (2006) and final (2014) years, resulting in (k) (10^3 tons) and q prior range limits of [2.1–84.1] and [2.09e-04–1.32e-03] respectively.

In this bayesian modelling, the joint distribution embraces these priors on the parameters, the process and the observation equations of the model to derive the full conditional distribution that is to say:

$$[Parameters,\ Process,\ Observables / Covariate] = [Parameters] \times [Process / Parameters\,;\, Covariate] \times [Observables / Process,\ Parameters]$$

equivalent to

$$[(q, \sigma_o, r, k, \sigma_p),\ B_{1:n},\ I_{1:n} / L_{1:n}] = [(q, \sigma_o, r, k, \sigma_p)] \times [B_{t+1} / B_t, (r, k, \sigma_p); L_t] \times [I_t / B_t, (q, \sigma_o)]$$

Just Another Gibbs Sampler (JAGS, Plummer, 2003) was used to generate the Monte Carlo Markov Chains (MCMC) by sampling from this full conditional distribution. We used 280000 iterations, a burn-in of 180000 and a thin value of 100 in the case of BM applied to the 1974–2014 (1995–2014) time series to address the MCMC sampling autocorrelation issues (if present). Convergence assessments (Brooks-Gelman-Rubin test, auto-correlation, trace plots, running-mean and kernel density) were also carried out on the retained 1000 draws per chain (x3) (see ***Results*** and ***Annexes C***).

(I.2) Catch Maximum Sustainable yield (CMSY)

LPUE and SSI_t indexes of abundance are only used for the biomass modelling (BM) implemented on the basis of the Schaefer surplus production model (Schaefer, 1954) while CMSY method (Martell et al., 2013; Froese et al., 2017) relates to catch/landing data and resilience of the species (that is, the capacity of a species to withstand exploitation) to estimate quantities of interest like *MSY* ($rk/4$), F_{MSY} ($r/2$), exploitation rate (F/F_{MSY}) and B_{MSY} ($k/2$).

In fact, the pillars of the CMSY approach are the (r-k) relationship and the observed catches/landings time series data used to feed the procedure to determine (r) and (k). Therefore, the information required is the assumed prior ranges of the intrinsic rate of population growth (r), and the carrying capacity (k) along with the assumed initial,

intermediate and current range of the depletion levels of the (relative) biomass (*B/k*) (**Table M2**). Thus, (*r*) and (*k*) candidates are randomly drawn from within the prior range of (*r*) and (*k*) and sorted as viable (*r-k*) pairs, that is to say, corresponding to the biomass trajectories (computed using a BM with Schaefer production model) compatible with the observed catches/landings and the prior ranges of the assumed level of (*B/k*) (**Table M2**).

Notice that the cloud of the viable (*r-k*) pairs is subject to a routine implemented by Froese et al. (2017) to determine the most probable (*r*), (*k*), *MSY* and related fisheries reference points. In addition, a linear decline of the Schaefer surplus production was considered if the biomass falls below $0.25 \cdot k$.

Table M2: Prior range for *r* parameter based on FishBase categories of species resilience (Froese and Pauly, 2015) and prior biomass classes in relation to ratio range *B/k*.

Prior r range	Resilience
[0.6–1.5]	High
[0.2–0.8]	Medium
[0.05–0.5]	Low
[0.015–0.1]	Very low

Biomass	Prior B/k range
Low	[0.01–0.4]
Medium	[0.2–0.6]
High	[0.5–0.9]

(I.3) Length-based spawning potential ratio (LB-SPR)

In order to maintain yield, the reproductive dynamics of the fish population and the impact of harvesting must be understood.

Recent works (Bjørkvoll et al., 2012; Juan-Jorda et al., 2015) have shown that trait such as the spawning potential ratio of a population determines its ability to cope with natural environmental variability, as well as compensating for increased death rates due to anthropogenic perturbations.

To estimate the ratio of fished and un-fished spawning per recruit and circumvent the lack of reliable age data for *Nephrops norvegicus,* we had recourse to a length-based

model as developed by Hordyk et al. (2015abc; Hordyk et al., 2016; Hordyk, 2019) relying on the size composition data of the exploited stock and the life history ratio (M/K) of the natural mortality to the growth coefficient[13], considered to be influential in determining productivity, resilience and overfishing limits (Beverton and Holt, 1957; Beverton, 1992; Prince, 2015)

Thus, on the basis of the von Bertalanffy growth equation and assuming a per recruit model, Hordyk et al. (2016) demonstrate that the number per recruit that are alive at each length (L) can be determined by using the life history ratio (M/K) and the asymptotic length (L_∞). For the prediction of the size composition, they included size-dependent mortality by considering vulnerability to fishing (logistic selectivity curve), variability of natural mortality rate at length (allometric relationship) and the individual variation of the growth by assuming that there are (g) sub-cohorts and each of these growth-type-group (GTG) has a different L_∞ but a shared growth parameter (K).

Then, assuming reasonable estimates of M/K, L_∞, coefficient of variation ($CV_{L\infty}$) and size-at-maturity ($L_{50\%}$, $L_{95\%}$), the (GTG) LBSPR model uses the maximum likelihood method to estimate the relative fishing mortality (F/M) and size selectivity (L_{S50} and L_{S95}) from representative sample of the length structure of the catch by minimising the difference between the observed and the expected length composition, and then, calculates the spawning potential ratio (SPR) by comparing the proportion of reproduction of the fished stock relative to the unfished state.

Data and input parameters for (GTG) LBSPR

We restricted our study to the female *Nephrops* as SPR refers to relative egg production. Length frequency distribution were obtained from beam trawl surveys with 80 mm standard diamond mesh and a 20 mm codend line, available for years 2006, 2007, and 2009–2014. In order to "mimic" length catch data we only considered length data above the minimum landing length of 25 mm (L_c). Notice that estimations are independent year-on-year.

In relation to natural mortality rates $M=0.2$, $M=0.3$ and the coefficient of variation $CV_{L\infty}=0.1$, we assumed 4 scenarios encompassing, all other things being equal, the range of values available as potential proxies for the von Bertalanffy growth equation

13 Here, the capital letter (K) stands for the growth coefficient, in contrast with the carrying capacity (k)

coefficients (K and L_∞) for female *Nephrops norvegicus* in Aran grounds (FU17). The usual proxies are $K=0.08\ yr^{-1}$ and $L_\infty=57\ mm$ (ICES IBNeph, 2015) based on estimates of Scottish stocks by Pope and Thomas (1955). In addition, we included Haynes et al. (2016) evaluations of K and L_∞ due to the proximity of the Clew Bay (county Mayo) further north to Aran grounds. In this latter study, K and L_∞ female parameters were calculated by releasing 1177 tagged individuals in western Ireland in summer 2013 and recaptured 207 (100 males and 107 females) in 2014 (an average of 344 days later) and 38 (12 males and 26 females) in 2015 (654–665 days later). Notice that L_∞ was estimated using the individuals captured in 2013, which is then used to derive K values from the tagged *Nephrops norvegicus* recaptured in 2014 ($K=0.067\ yr^{-1}$), in 2015 ($K=0.117\ yr^{-1}$) and by pooling both years ($K=0.077\ yr^{-1}$).
The female logistic (carapace) length-maturity at 50%, ($L_{50\%}$) is estimated at 22 mm from 2008–2014 sampling data (ICES IBNeph, 2015) and assumed $L_{95\%}=24.5\ mm$ at 95%. The coefficients alpha ($\alpha=0.000684$) and beta ($\beta=2.963$) of the carapace length-weight relationship ($W=\alpha CL^{\beta}$) are derived from Scottish stock estimates (ICES IBNeph, 2015) and the coefficient $b=2.566$ of the power curve relationship between the realised fecundity (*i.e.* the number of eggs extruded) and the carapace length of female (aCL^{b}) is estimated from the western Irish Sea *Nephrops* stock (Briggs et al., 2002b).
(GTG) LBSPR also assumes the typical per-recruit model assumption that the stock is in a steady state, and the differences between observed and expected length distributions are not due to variability of recruitment or fishing mortality (*i.e.* constant recruitment and fishing pressure, Hordyk et al., 2015abc).

(II) Materials

(II.1) Under water TV counts

Since 2002, early in June, annual underwater television surveys (UWTV) take place on the Aran grounds covering three geographically discrete mud patches namely, Aran grounds, Galway Bay and Slyne Head corresponding to the ICES area FU17.
The number of *Nephrops* burrows in the seabed are counted using a video camera mounted on a metal frame sledge towed over the seabed for approximately 10 minutes. For each area, the burrow density is estimated using geo-statistical extrapolation.

(II.2) Landings

Available landings data for Aran grounds date back to 1974, with data relating to fishing activity from France, Ireland and to a lesser extent the United Kingdom. In an attempt to quantify the quality of the landings data subjectively, the periods 1974–1994 and 1998–2007 have been deemed potentially to be of poor quality (**Table C1** in ***Annexes C***). The confidence in the quality of the records is higher for the 1995–1997 and 2008–2014 parts of the time series.

(II.3) Effort

Over time, the efficiency of the vessels has increased in many aspects, for example, the net designs improved significantly (from twin rigs to quad rigs) since 2012, on-board technology has seen dramatic upgrades and boats with engine power of 250 Kilo-Watts and more, constitute now the larger part of the fleet. While fishing effort in Kilo-Watt-days (recorded since 1995) has been chosen to be the proxy of the fishing intensity, it should be noted that the ICES Inter-Benchmark Protocol of *Nephrops* in FU17 (ICES IBNeph, 2015) acknowledges that it is not adjusted for efficiency or behavioural changes. Throughout this chapter all statistical analyses were carried out using R[14] (R Core Team, 2018)

14 R core Team 2018 packages used in this chapter are indicated in References.

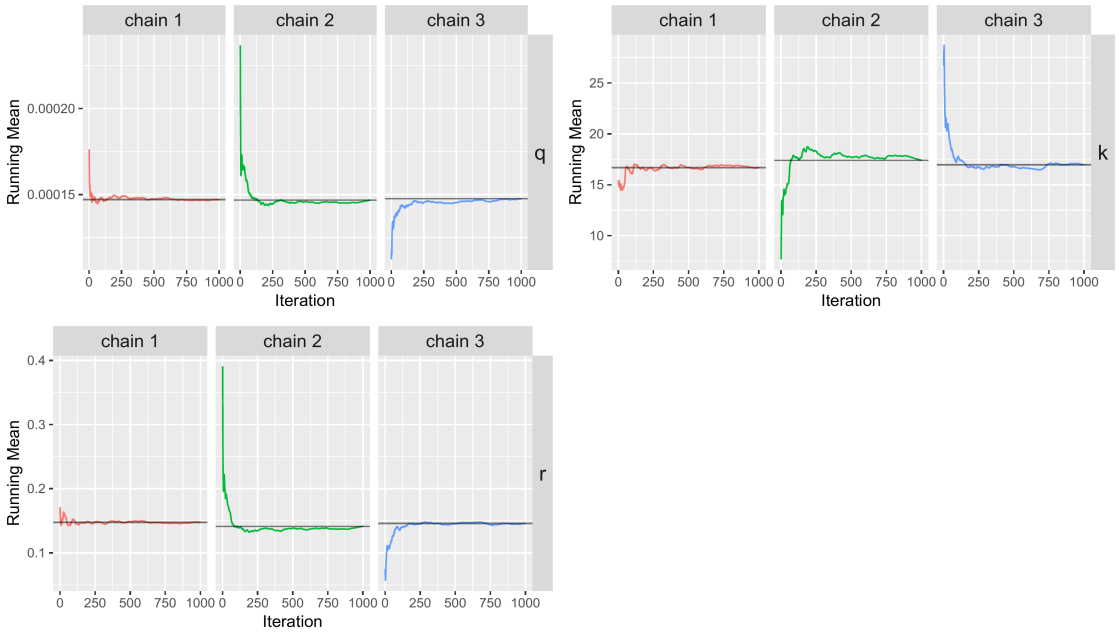
Results

(I) Bayesian production modelling

(I.1) Convergences and fits

Bayesian posterior sampling using MCMC shows that the simultaneous chains wiggle and overlap well. The autocorrelation coefficients are either very small or quickly vanishing, indicating that the chain moves randomly from one iteration to the next. In addition, the potential scale reduction factor for the parameters of interest *r*, *k* and *q* decrease to 1 (**Figures C1** and **C2** in ***Annexes C***). These results confirm that convergence is reached and the posterior model space is well explored and we moved to the targeted distribution, even though, we note that the shrinking factors (**Figure C1** panel 4 in ***Annexes C***) for the model involving the period 1974–2014 needed more iterations before dropping to 1 (suggesting possible structural heterogeneity in the mean and variance between sub-periods).

panel (a)



panel (b)

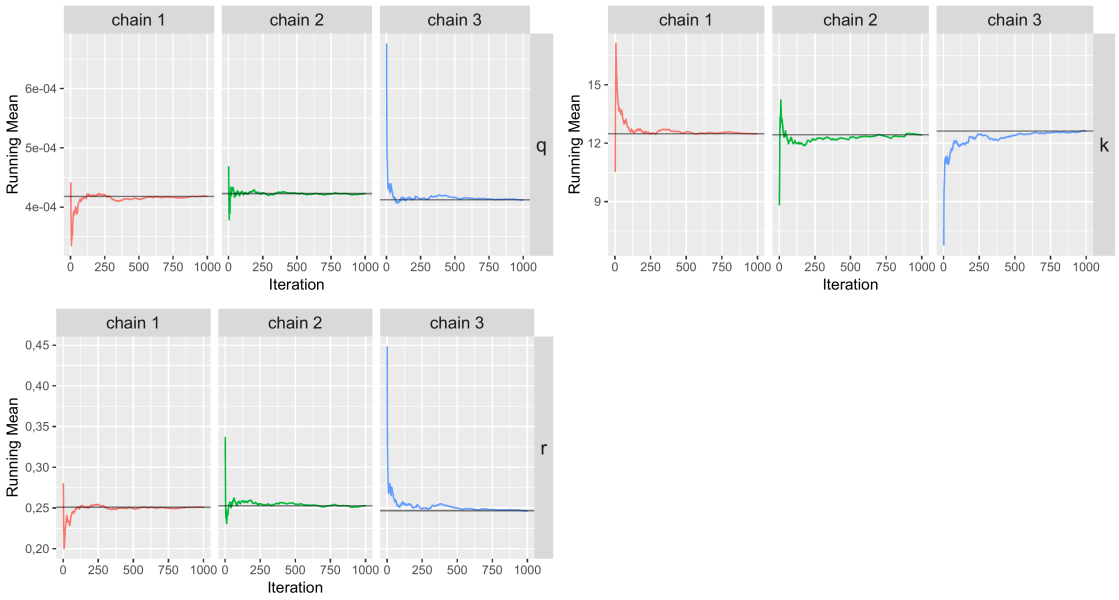


Figure 3.1: Running mean patterns (*i.e.* the iterations against the mean of the draws up to each iteration) for the catchability coefficient *q,* carrying capacity *k*, and the intrinsic growth rate *r*, for the 1974–2014 (**panel a**) and 1995–2014 (**panel b**) data sets.

Ultimately, the fluctuations of the observed landings per unit effort (lpue) are mostly around the mean of the posterior predictive lpue index (**Figure 3.2b**) allowing us to consider that our state-space modelling is a reasonable fit for the data. Despite a relatively high level of fishing effort (355673 KiloWatts-days) we observe a decrease in the lpue in 2004 with a marked discrepancy between the predicted and the observed data (**Figure 3.2d**). Moreover, the highest UWTV abundance estimate is recorded in the same year (**Figure 3.2c**). This sudden plunge might be attributable to environmental factors, such as a long period of poor weather preventing the deployment of fishing vessels, rather than an endogenous process.

Thus, as regards these overall performances (convergence and fits), the posterior distributions of the biological reference points derived from our bayesian modellings (**Figure 3.2a-b**) can be used to portray the status of the Aran grounds stock.

(a)

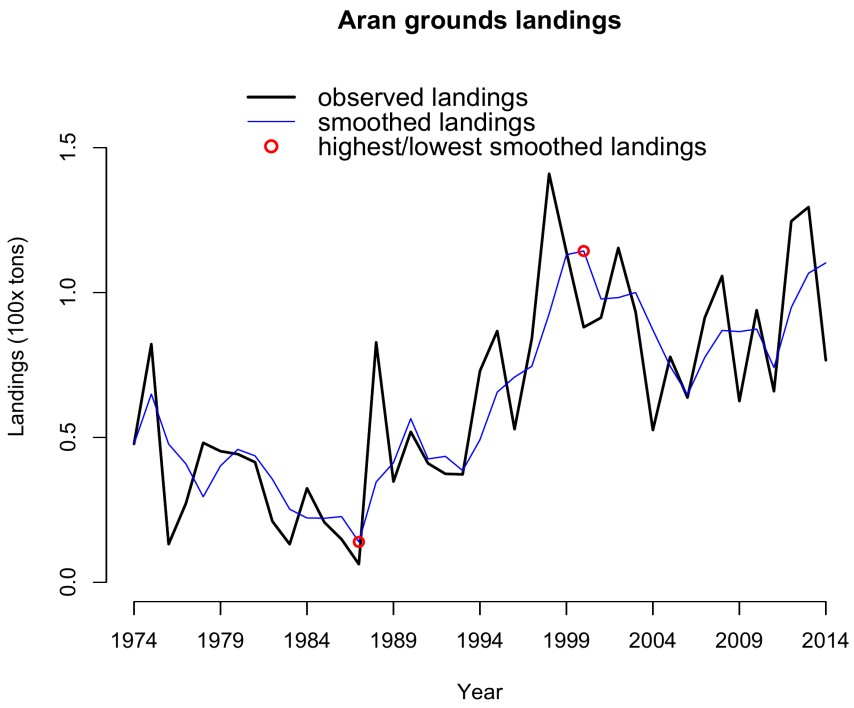


Figure 3.2a: Observed *Nephrops norvegicus* landings time series from 1974 to 2014. To avoid exceptional values of landings in the estimation of the prior biomass, the 3 years moving average with an indication of highest/lowest of the landing time series (red circles) are used (Froese et al., 2016).

(b)

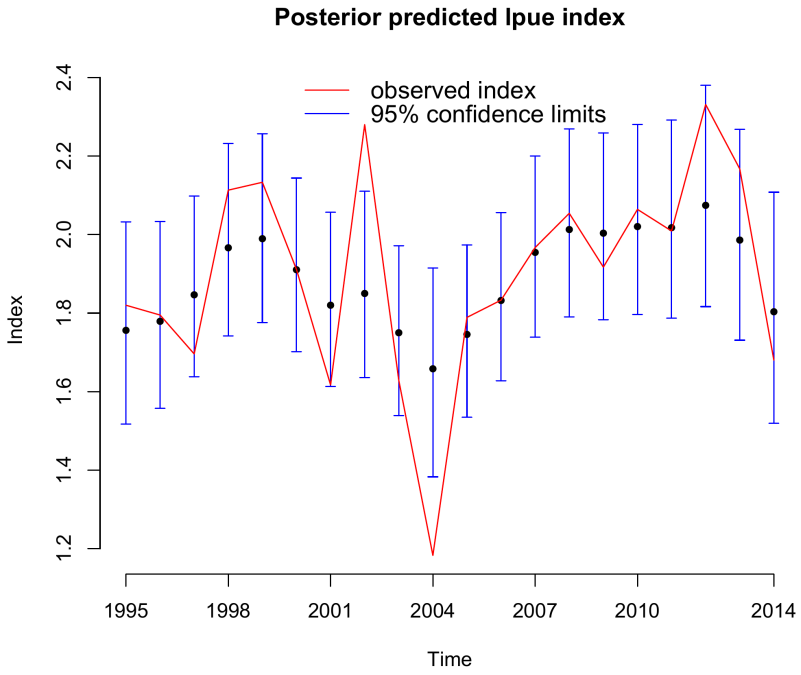


Figure 3.2b: Estimates of the posterior predictive distributions of the lpues index together with its 95% bayesian credible interval (blue error bar).

(c)

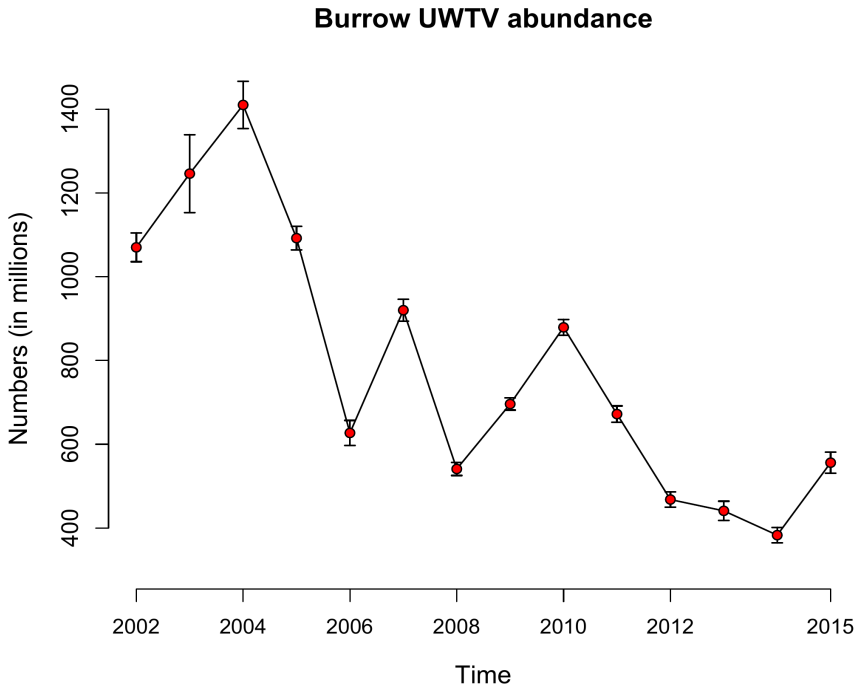


Figure 3.2c: 2002–2015 under water TV abundance estimates (in numbers) of Aran grounds *Nephrops* population (Source: Marine Institute, Ireland). Error bars indicate 95% confidence limits.

(d)

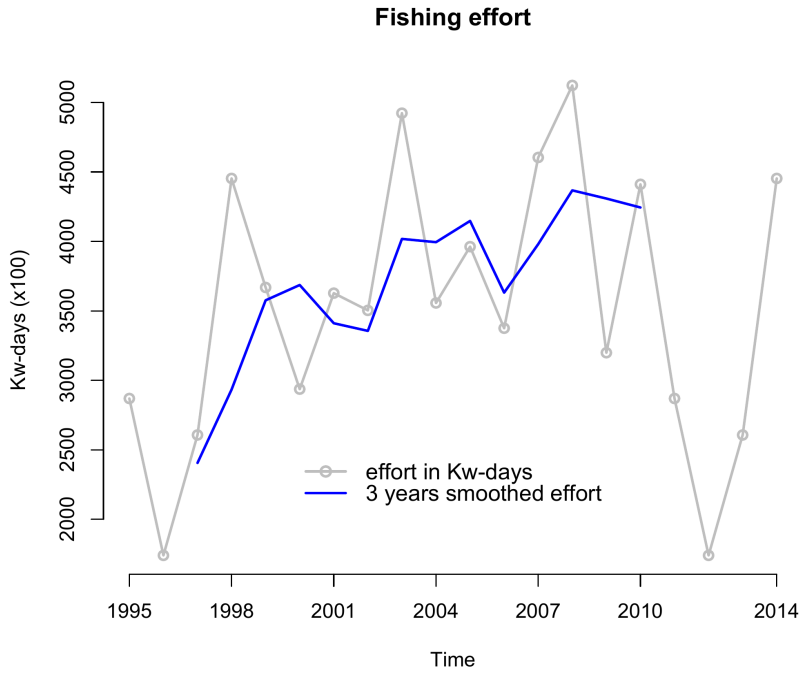


Figure 3.2d: Observed and smoothed total fishing effort of vessels > 30% landing threshold from 1995 to 2014 in Kilo-Watts-days (Kw-days).

(I.2) Biomass, fishing mortality and MSY

Biomass

Under the bayesian biomass modelling framework (BM), using either the stock size index (SSI_t) or the KiloWatts-days effort as a proxy for the abundance of *Nephrops norvegicus* in the Aran grounds, two very dissimilar patterns of the biomass trajectory were revealed.

In the case of the stock size index, the biomass appears to have decreased steadily since 2000 and passed under the 0.5 threshold ratio B/B_{MSY} in 2010, highlighting the strong depletion of the population (**Figure 3.3a**). In contrast, in the case of the lpue index, the stock alternates between a smooth rise and fall lying within a B/B_{MSY} range of [0.5–1] (**Figure 3.3b**).

(a)

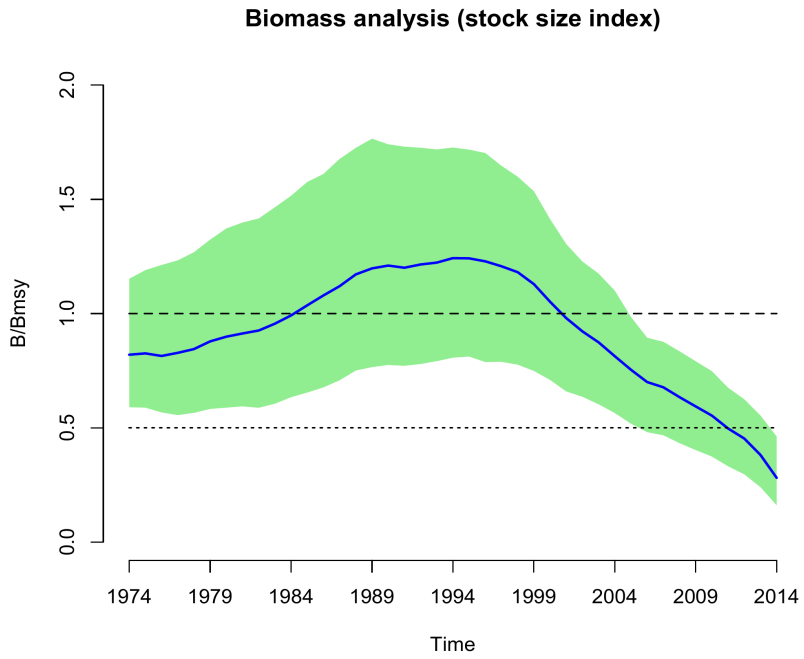


Figure 3.3a: Posterior distribution of the relative biomass (B/B_{MSY}) with its 95% bayesian credible interval bandwidth (green ribbon) using the 1974–2014 time series of landing.

(b)

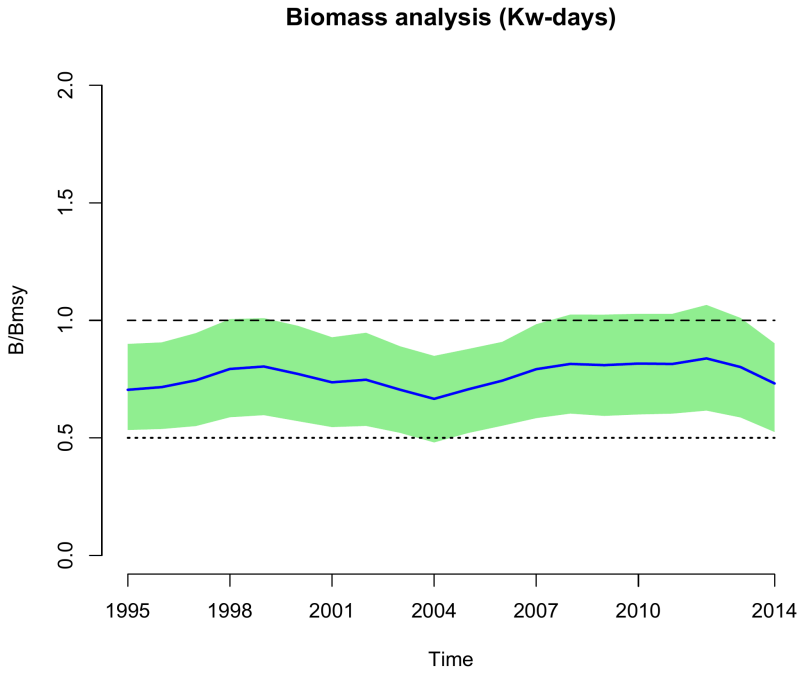


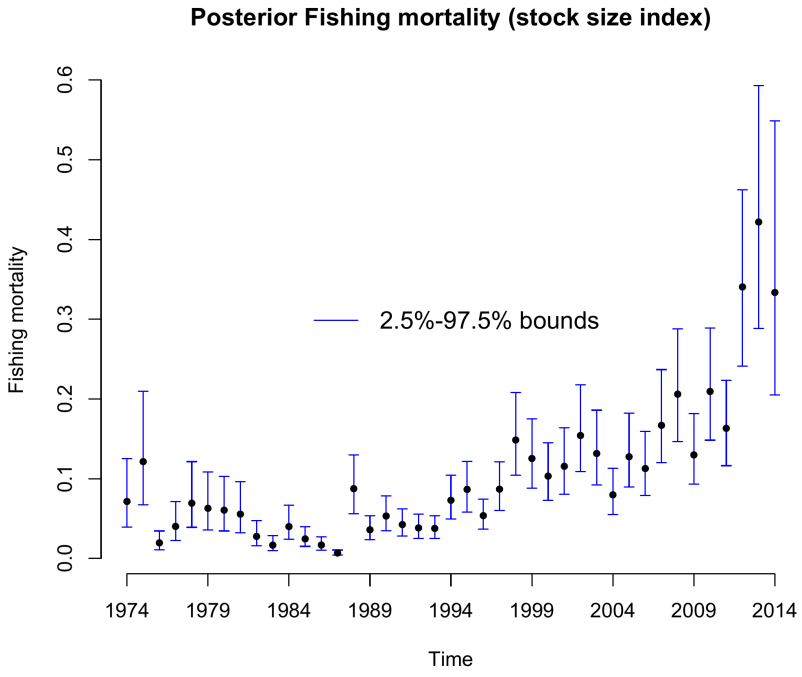
Figure 3.3b: Posterior distribution of the relative biomass (B/B_{MSY}) and its 95% bayesian credible interval bandwidth (green ribbon) using the 1995–2014 set of landings.

Fishing mortality

Despite differences in the length of the time series data (1974–2014 vs 1995–2014) and the type of abundance index used, the fishing mortality of both approaches describes, globally, a pattern of up and down fluctuations (**Figure 3.4a-b**). During the period 1995 to 2014 the fishing mortality is marked by successive up and down phases.

The striking discrepancy relates to the level of exploitation for the years 2012, 2013 and 2014 (**Figure 3.4c-d**).

(a)



(b)

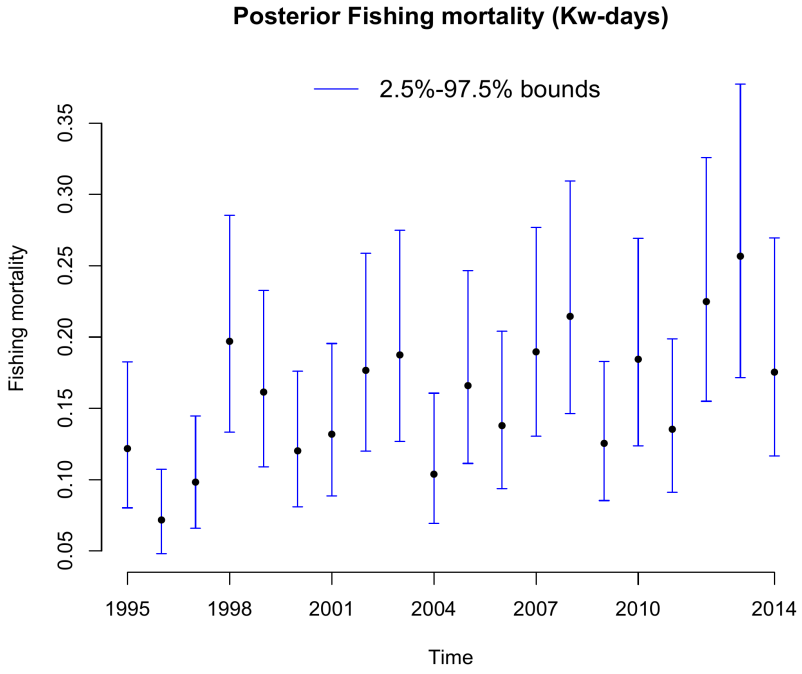
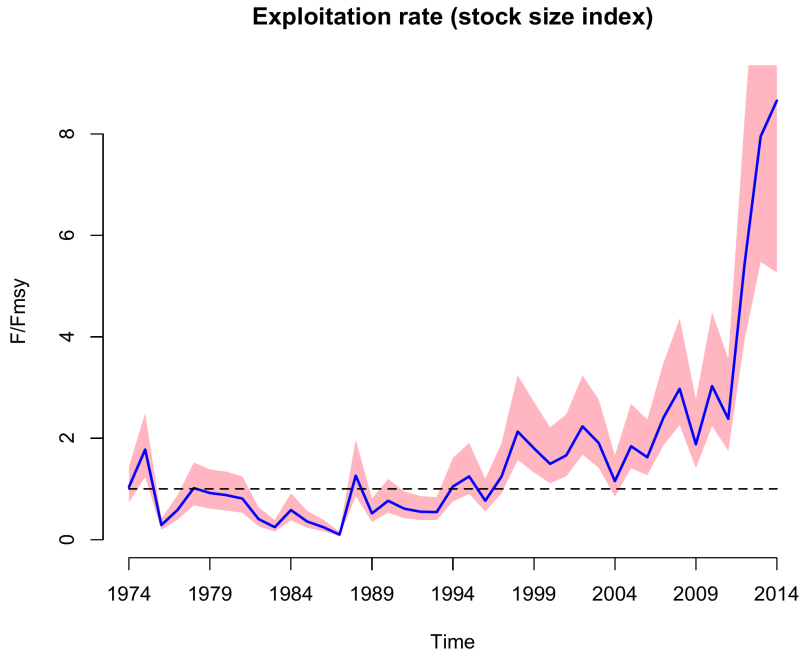


Figure 3.4 a-b: Posterior fishing mortality results of the bayesian surplus production modelling approach (BM) using 2002–2014 stock size index (**a)** and 1995–2014 Kw-days fishing effort (**b**). Error bars correspond to the 95% bayesian credible interval.

(c)



(d)

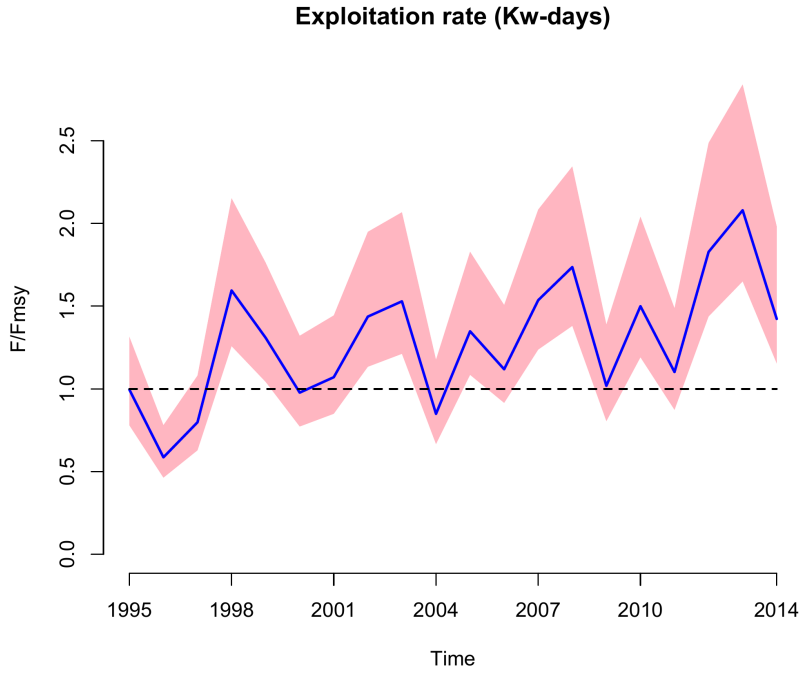


Figure 3.4 c-d: Posterior exploitation rate results of BM modelling based on (**c**) 2002–2014 stock size index and (**d**) 1995–2014 Kw-days fishing effort. The shaded (pink) areas correspond to the 95% credible bayesian interval.

The results stemming from the 1974–2014 model depict an exploitation rate moving closely around the level of 1 until the mid-90's and continuously increasing thereafter, escalating to a rate of 8 in only 3 years (2011 to 2014). Likewise, the analysis from the 1995–2014 KiloWatts effort series reports an F/F_{MSY} ratio beyond 1, underlining the concern over the Aran grounds stock status.

Thus, the downward course in the biomass from the late 90's to 2014, as shown by the 1974–2014 model (**Figure 3.3a**), as well as the saw-like motion of the exploitation rate beyond the ratio value of 1, in the case of the 1995–2014 modelling, suggest that the stock was subjected to a high exploitation rate (**Figure 3.4d**).

In examining the raw fishing effort values, we note alternating short phases of peaks and troughs, where even quite stable in-between periods are obvious (**Figure 3.2d**). The available fishing effort data (in Kw-days) from 1995 to 2014 (**Figure 3.2d**) indicates a clear upward trend over this period as disclosed by the 3 years moving average smoothing. Meanwhile, from 1995 to 2014 the number of vessels involved in the fishery has been relatively stable, however, the vessel power increased from a mean of 175 KiloWatts at the start of the time series to most vessels having a larger power of 250 KiloWatts at the end of the time series (see ***General Introduction***).

MSY

Finally, according to the bayesian posterior mean *MSY* and its 2.5%–97.5% inter quantile range, the stock appears to be very often harvested at levels higher than *MSY* in the case of the 1995–2014 model (**Figure 3.5**, **Table 3.1**) and clearly overexploited regarding the 1974–2014 *MSY* reference, with values even beyond the upper bounds of maximum sustainable yield. In addition, discarding likely aggravates the situation. Recall, that over the 1995–2014 period, the fishing effort increased (**Figure 3.2d**) and it was very likely the case in 1974–1995 despite our lack of data to measure this potential trend.

Table 3.1: Posterior mean estimates of the maximum sustainable yield (*MSY*) from the BM modelling. Results are arranged according to the length of data time series (1974–2014 versus 1995–2014) and their corresponding indices (Stock Size Index vs Lpue, respectively). The 2.5% and 97.5% percentiles are indicated.

Model	MSY	Lower 2.5%	Upper 97.5%
1974–2014	560	408	768
1995–2014	744	584	947

(a)

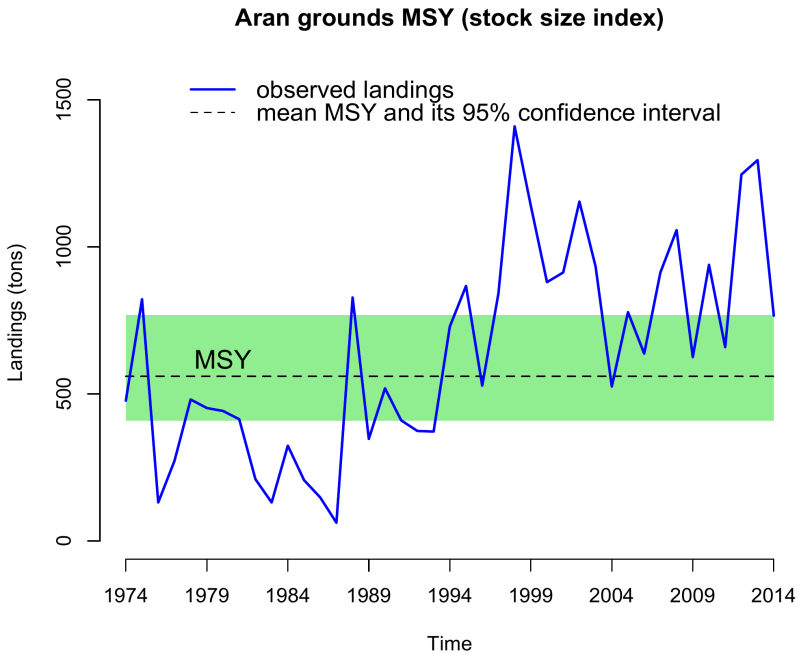


Figure 3.5a: Maximum sustainable yield (*MSY*) estimated by the BM modelling together with its 2.5th and 97.5th percentiles (green ribbon) in the case of 1974–2014 landing time series and Stock Size Index.

(b)

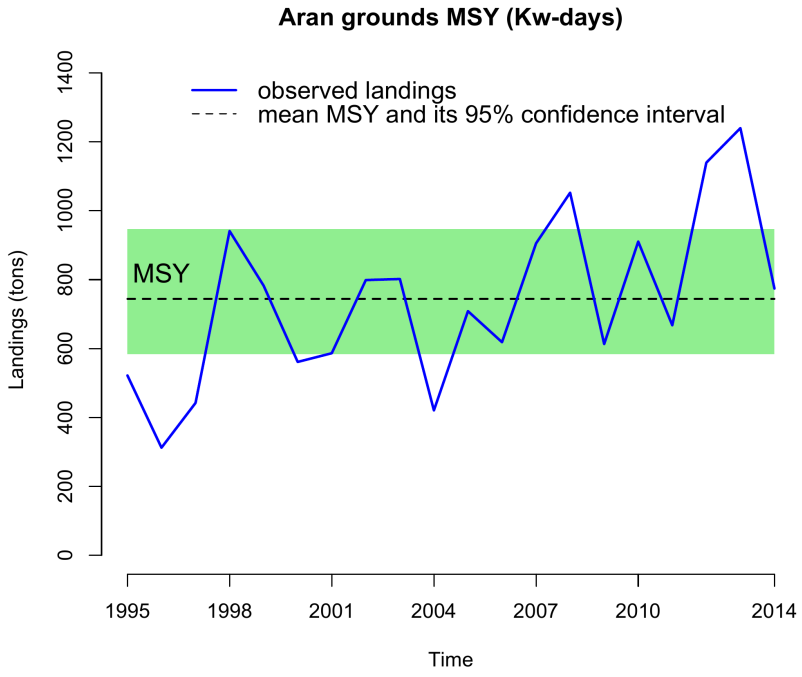


Figure 3.5b: Maximum sustainable yield (*MSY*) estimated by the BM modelling together with its 2.5th and 97.5th percentiles (green ribbon) in the case of the 1995–2014 landing data set and the Lpue index using Kw-days as a proxy for the fishing effort.

(I.3) Stock status: overfishing and depletion

Finally, we used the "equilibrium" curve, which is a Schaefer parabola modified to its right side to account for the assumed reduced recruitment at relative biomass $B/k < 0.25$ (**Figure 3.6**) and the Kobe plots (**Figure 3.7**) to determine the status of the stock from these reference points.

The results from the bayesian production modelling indicate that the landings from 1974 to 2014 fall beyond the parabola signalling the occurrence of overfishing. In particular, of concern is that in recent years the stock underwent successive years of severe stock depletion passing under the level of B/k=0.3 from 2011 to 2014.

Even though the outputs from the 1995–2014 landings and the lpue index are less worrying concerning the range of the B/k values [0.4–0.3], the decrease in biomass is confirmed ($B/k < 0.5$).

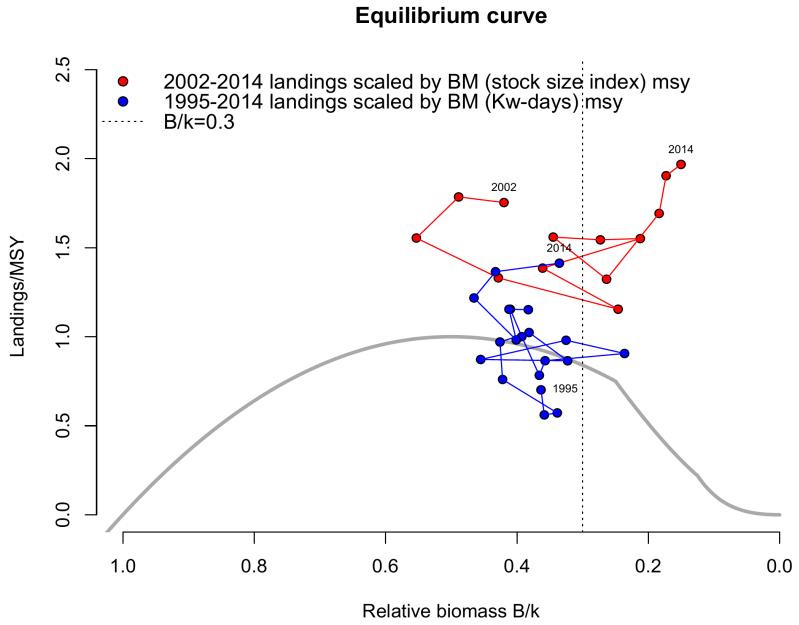
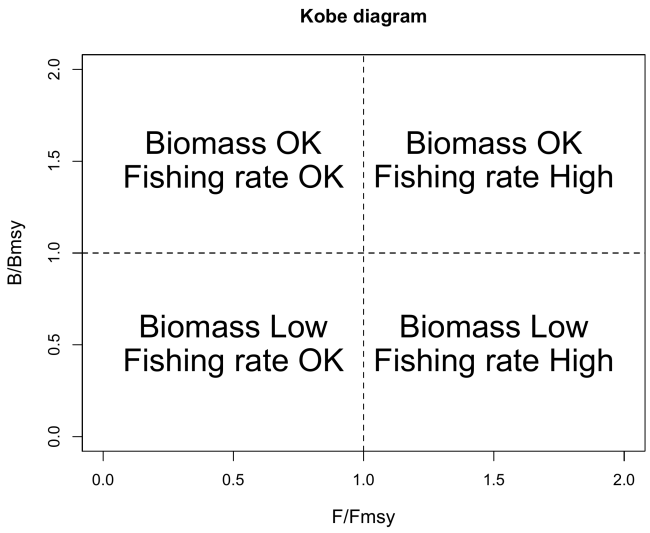


Figure 3.6: The "Equilibrium curve" plot shows the theoretical Schaefer parabola with landings expressed relative to *MSY* on the Y-axis and decreasing biomass relative to *k* on the X-axis. The right side of the parabola is indented because below 0.25*k*, a linear decline of surplus production due to reduced recruitment is assumed (following Froese et al., 2016). 1974–2014 and 1995–2014 observed scaled landings series are displayed indicating the relative stock depletion level over the period.

By typifying the trajectory of the relative stock size B/B_{MSY} and exploitation rate F/F_{MSY} in one of the following four categories



the Kobe plot enables us to also evaluate the status of the fishing stock over time.

According to BM with the 1995–2014 landings, *Nephrops* are subject to overfishing and draws attention to the level biomass depletion. However, we note a (very) short sequence of incursions into the bottom left quadrant characterised by a "safe" fishing rate (1995-1996-1997, 2000 and 2004, **Figure 3.7b**) while the B/B_{MSY} level is still low with no amelioration.

Biomass modelling (BM) coupling the stock size index with the information provided by a longer time series of landings (1974–2014) highlighted important changes in the *Nephrops* status during this period. In summary, following a clockwise pattern, the fishery starts from a relatively "sustainable fishing pressure and low biomass" position (bottom left quadrant) and ends up with a severe depletion and very high exploitation rate (**Figure 3.7a**).

(a)

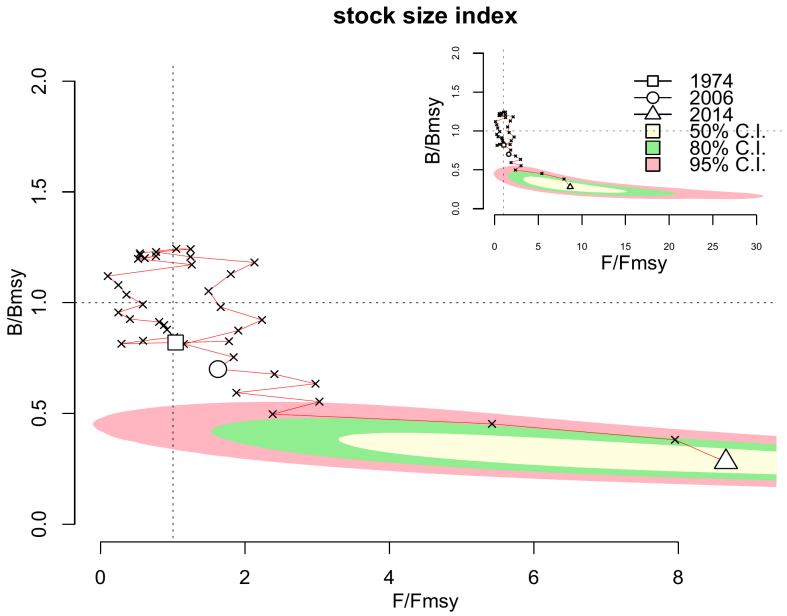


Figure 3.7a: Kobe plot of *Nephrops norvegicus* Aran grounds stock in the case of the 1974–2014 landing data set and Stock Size Index under the BM framework

(b)

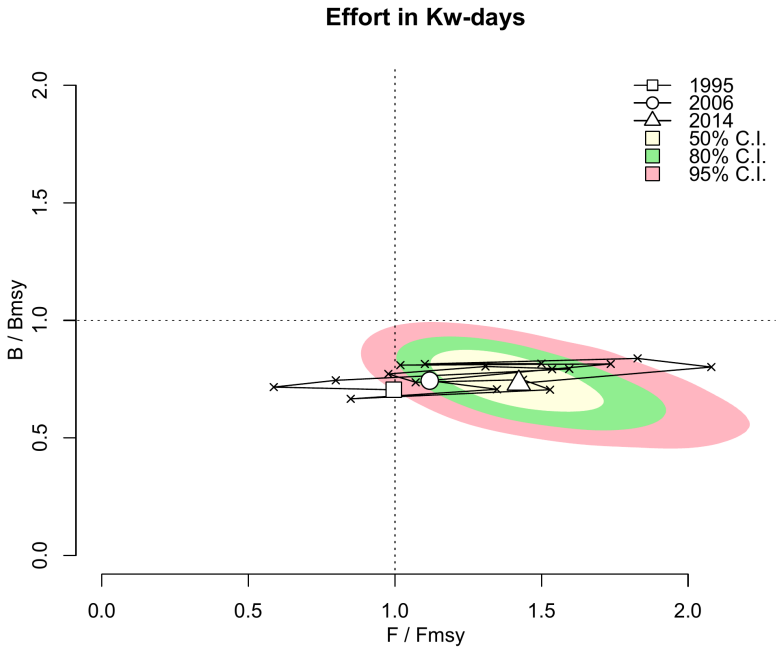


Figure 3.7b: Kobe plot of *Nephrops norvegicus* Aran grounds stock in the case of the 1995–2014 landing data set using Kw-days as proxy of the fishing effort under the BM framework.

(II) Stock response

(II.1) Resilience (*r*) and abundance (*k*)

Several biological parameters have been used to classify a fish population or species into categories of high, medium, low and very low resilience and the intrinsic rate of population growth (*r*), which is the maximum rate of population increase for a given stock in a given ecosystem, is a useful facet of the capacity of a species to withstand exploitation. Note that the classification of resilience is often a matter of author objectivity (**Table 3.2a-b-c**).

Table 3.2: Main resilience classifications often refered to in literature on marine environmental science.

Table 3.2a: Martell et al. (2013) classification				
resilience	High	Medium	Low	Very low
r (year^{-1})	1.5–0.6	1–0.2	0.5–0.05	0.1–0.015
Table 3.2b: Musik (1999) classification				
resilience	High	Medium	Low	Very low
r (year^{-1})	>0.5	0.5–0.16	0.15–0.05	<0.015
Table 3.2c: Froese et al. (2015) classification (fishbase.org)				
resilience	High	Medium	Low	Very low
r (year^{-1})	1.5–0.6	0.8–0.2	0.5–0.05	0.1–0.015

At first glance, the posterior annual intrinsic growth rate (*r*) values of the Schaefer surplus in the BM models (**Table 3.3**) indicate that the population might be classified either as a population with Low to Medium resilience according to all "classification" scales (**Table 3.2**). Note that with a value of *0.243*, the maximum intrinsic growth rate (*r*) derived from the 1995–2014 data is almost twice that resulting for the entire data set 1974–2014 (*0.136, s.e. 0.05*).

By examining the mean (*r-k*) points found for each biomass modelling (**Table 3.3**) and its stretch towards the lower-upper range limits of the (*r*) values of each (*r-k*) cloud (**Figure 3.8**) we consider that the most appropriate grouping value is provided by the class [0.05–0.5] which is identified as low (**Table 3.2 a-c**). As noted previously, this classification is based on a measure of the sensitivity of a species population to changes relative to other fished species and it is an evaluation of its capacity to respond to altered living conditions attributable to environmental factors and/or fishing (Pauly and McClean, 2003; Pauly, 2010).

Table 3.3: Posterior *r*, *k*, and *q* parameters estimates from the Bayesian state space Schaefer biomass modelling (BM). Results are arranged according to the length of the time series and their corresponding indices: 1974 to 2014 with stock size index versus 1995–2014 with lpue index. The 2.5% and 97.5% confidence limits are in brackets.

Posterior parameters	Mean 1974-2014	St. Dev.	Median	Mean 1995-2014	St. Dev.	Median
r	0.136 (0.068–0.271)	0.05	0.138	0.243 (0.155–0.381)	0.06	0.24
K	16415 (9784–27540)	4790	16100	12207 (7891–18883)	2860	12230
q	1.47e-04 (1e-04–2e-04)	2.46e-05	1.45e-04	4.10e-04 (2.8e-04–5.9e-04)	7.995e-05	4.09e-04

The modelling outputs highlight the well known functional form of the (*r-k*) relationship where an increase in (*k*) leads to a decrease of (*r*) (**Figure 3.8 c-d**). And, in order to gauge the relevance of the (*k*) estimates we used a very coarse methodology consisting of the product of the under water TV abundance in (million) numbers by the annual individual mean weight (in gramme) or its overall mean weight and then used it as a proxy for the upper limits of the population in tons (**Table 3.4**). Although simplistic, we consider the carrying capacity (*k*) values derived from our modelling reliable.

Table 3.4: Coarse estimate of Aran grounds *Nephrops* abundance in tonnes.
Method 1 is the product of UWTV burrow counts (in million number) x annual individual mean weight (in gramme). Method 2 is the product of UWTV burrow abundance (in million numbers) x overall mean of individual weight (in gramme).

	2002	2003	2004	2005	2006	2007	2008	2009	2010	2011	2012	2013	2014
Method 1	22684	26415	25521	20092	NA	NA	11847	17469	22150	13843	9547	9525	8655
Method 2	22985	26766	30289	23458	13469	19763	11621	14951	18882	14435	10053	9473	8227

Differences in the (*Pearson*) correlation values of the pairs *MSY-q* and *MSY-k* between data sets (1974–2014 vs 1995–2014 sets) as well as absolute (*q*) estimates are seen (**Figure 3.8a-b**). In comparison, a positive correlation coefficient (*+0.25*) for *MSY-k* (**Figure 3.8b**) and a quite identical but negative coefficient value of (*–0.29*) between *MSY* and *k* is detected by the 1974–2014 model (**Figure 3.8a**).

The catchability estimated in the 1995–2014 model ($q_{1995\text{-}2014}$ = *4.10e-04*) is about 3 times higher than the one deduced from the 1974–2014 model ($q_{1974\text{-}2014}$ = *1.47e-04*). However, BM modelling with 1995–2014 set reports a lack of connection (*–0.0047*) between *MSY* and the catchability (*q*), likely reflecting the limited sensitivity of our model to the information brought by the Kilo-Watts as a measure of the fishing effort and contrasting with the stronger relationship (*+0.35*) detected in the case of the 1974–2014 landings data set (**Figure 3.8a-b**).

(a)

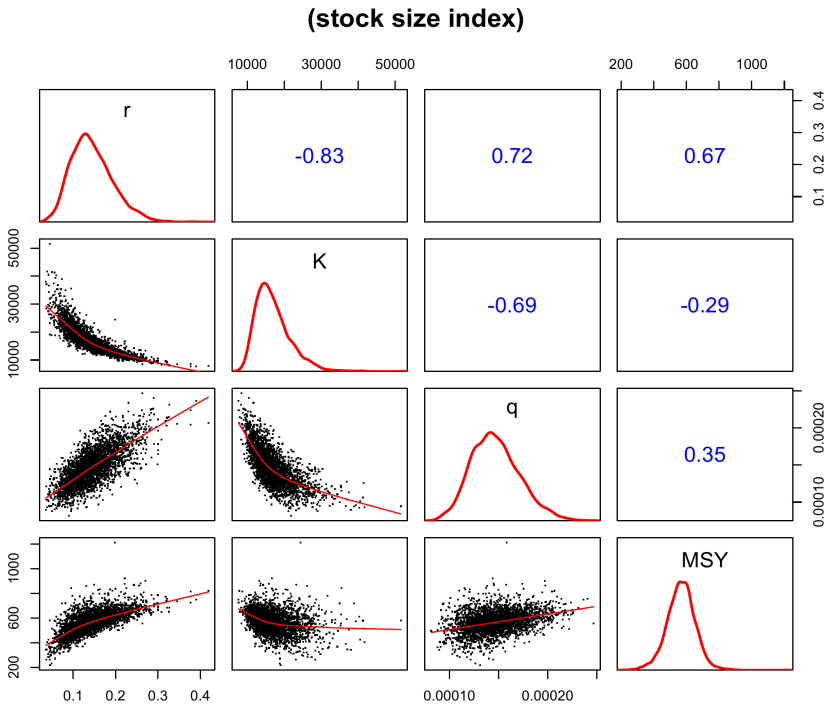


Figure 3.8a: Join and marginal posterior distributions estimates of parameters *r*, *k*, *q* and *MSY* under BM framework using 1974–2014 landing data set and Stock Size Index. *Pearson* correlation values (blue) and l*owess* fits are indicated (lower off-diagonal).

(b)

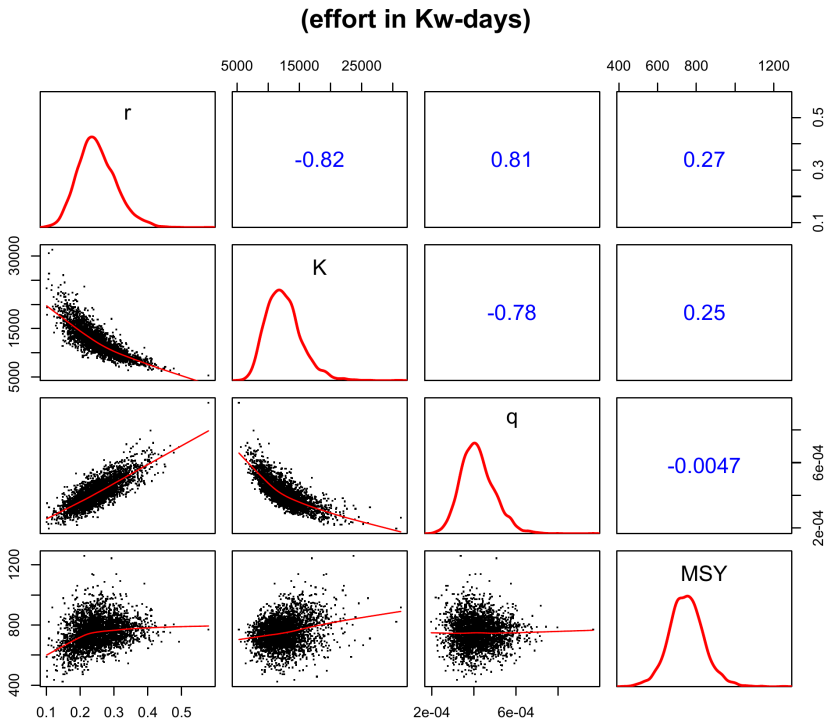


Figure 3.8b: Join and marginal posterior distributions of parameters *r*, *k*, *q* and *MSY* under BM framework using 1995–2014 landing data set and Kilo-Watts-days effort index as proxy for fishing effort. *Pearson* correlation values (blue) and *lowess* fits are indicated (lower off-diagonal).

(c)

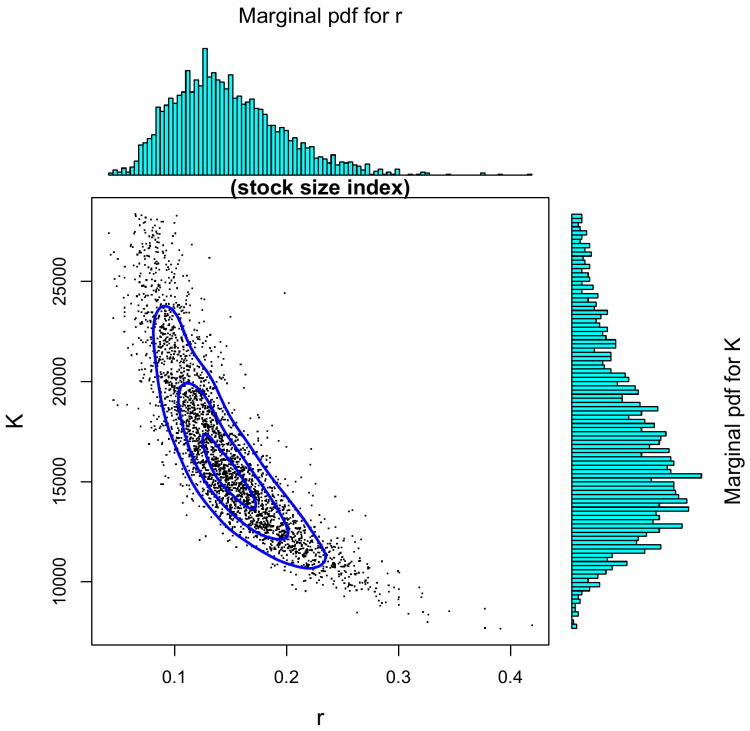


Figure 3.8c: Relationship of the posterior distribution of *r-k* Schaefer parameters obtained under BM framework using 1974–2014 data set and Stock Size Index. The marginal distributions are shown in the top and right panels. The smoothed iso-density contours over the joint mcmc draws represent 95% bayesian credible interval.

(d)

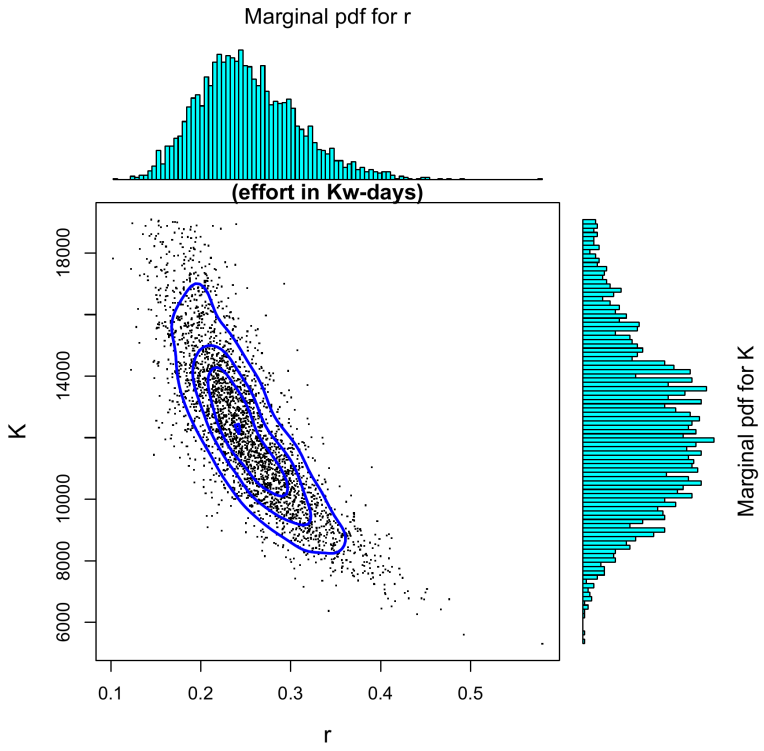
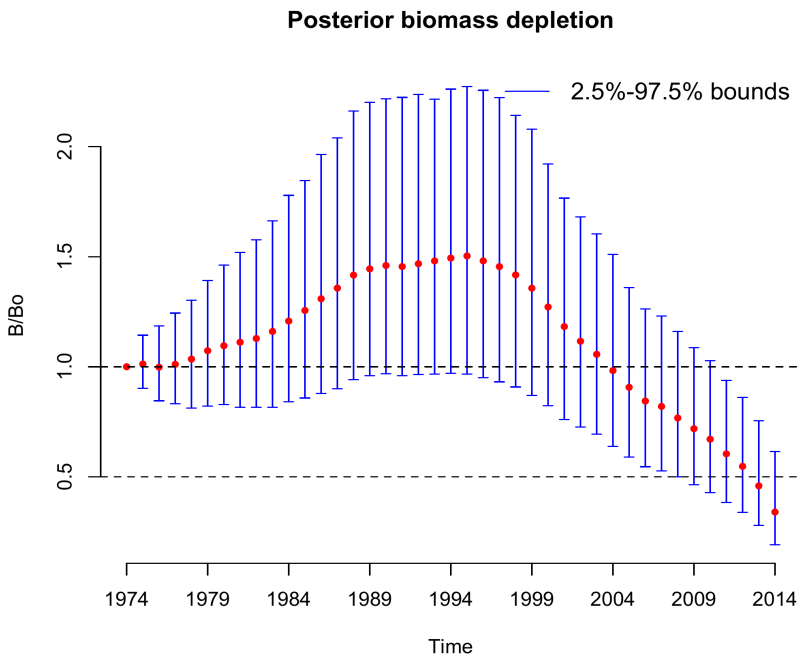


Figure 3.8d: Relationship of the posterior distribution of *r-k* Schaefer parameters obtained under BM framework using 1995–2014 landing data set and Kw-days effort index as proxy for fishing effort. The marginal distributions are shown in the top and right panels. The smoothed iso-density contours over the joint mcmc draws represent 95% bayesian credible interval.

As noted previously, the two types of proxy of the abundance used are qualitatively very dissimilar (see ***Materials and Methods***). One is directly linked to the fishing effort as Kilo-Watts per days, whereas, the stock size index (SSI_t) is related to the abundance of *Nephrops* as estimated by UWTV mean. In fact, the 1974–2014 model using the SSI_t index, identified an acute biomass depletion contrasting with the 1995–2014 model using the Kw-days (**Figure 3.9**).

(a)



(b)

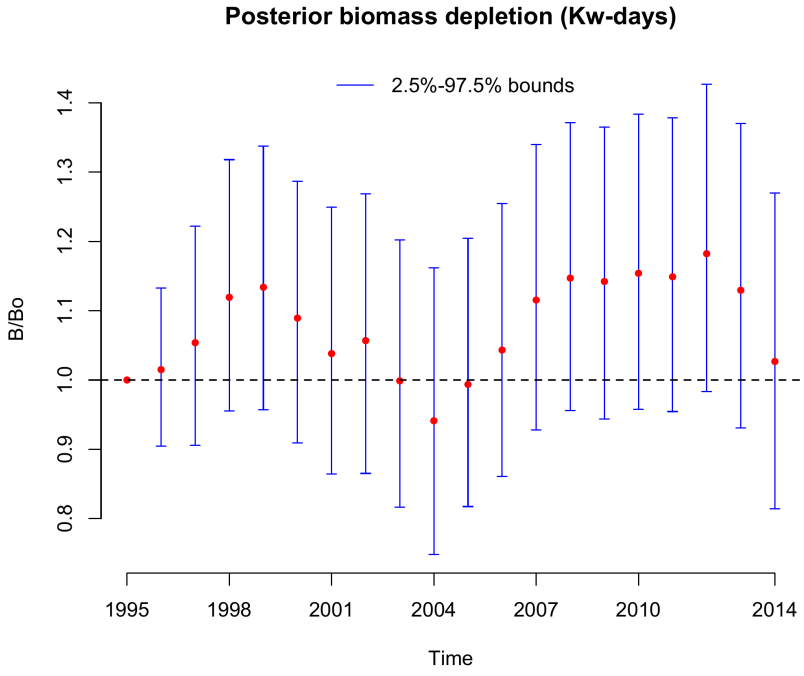


Figure 3.9: Posterior biomass depletion estimate and its 95% credible interval from BM modelling in the case of (**a**) 1974–2014 landing dataset using Stock Size Index and (**b**) in the case of the 1995–2014 data set using Lpue index derived from the Kilo-Watts-days as measure of the fishing effort.

(II.2) *r-k* pairs and exploitation rate (F/F_{MSY})

Note that because the bayesian implementation of a biomass Schaefer model comes with a quantifiable amount of uncertainty it is used as a benchmark for the CMSY (Froese et al., 2017). Also, according to Knezevic (2008) and Hedderich et al. (2015) non-overlapping confidence limits between CMSY and the biomass state space model indicates significantly different estimates at the 95% level. In this regard, the well mixed confidences limits of the CMSY and BM estimated biomass trajectories reinforce our previous diagnosis (**Figure 3.10**).

(a)

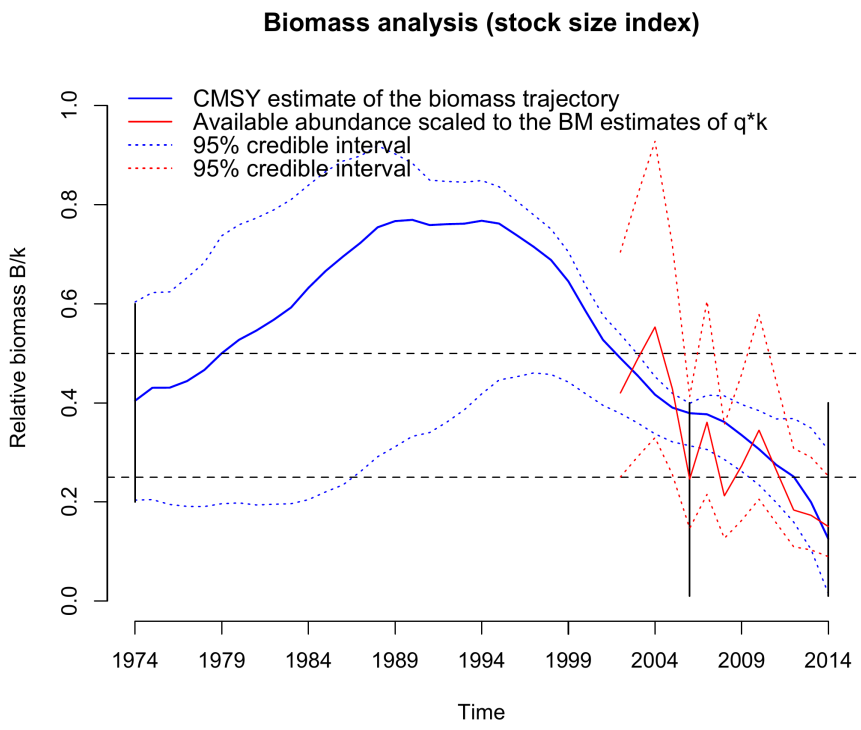


Figure 3.10a: Biomass trajectory predicted by the CMSY method in the case of 1974–2014 data set and Stock Size Index. Prior ranges of the relative biomass (B/k) are indicated by vertical (black) lines corresponding to "Medium", "Low" and "Low" choices for the years 1974, 2006 and 2014 respectively. *B/k=0.3* and *B/k=0.5* values are indicated in black horizontal dashed lines.

(b)

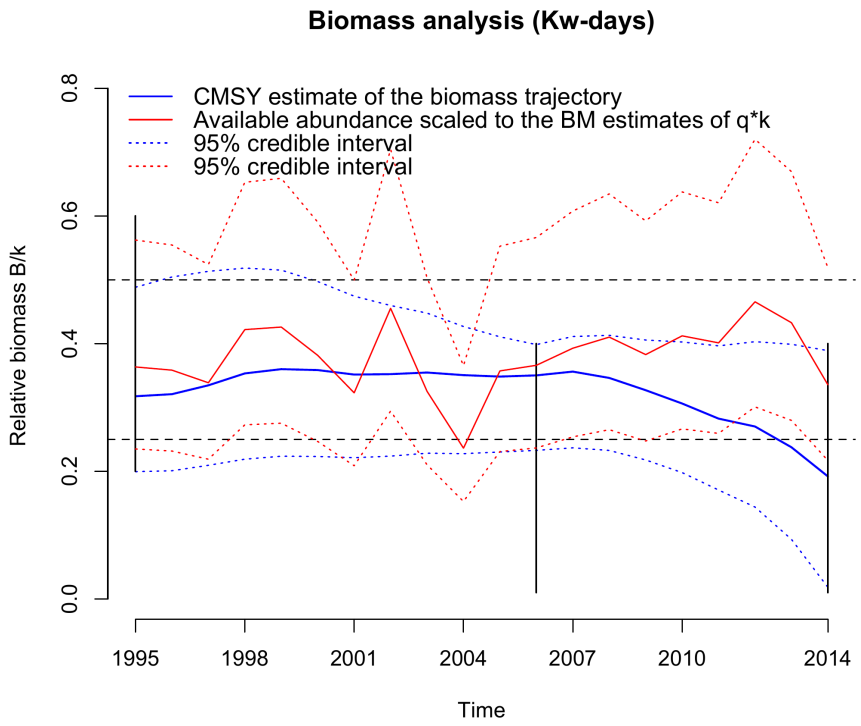
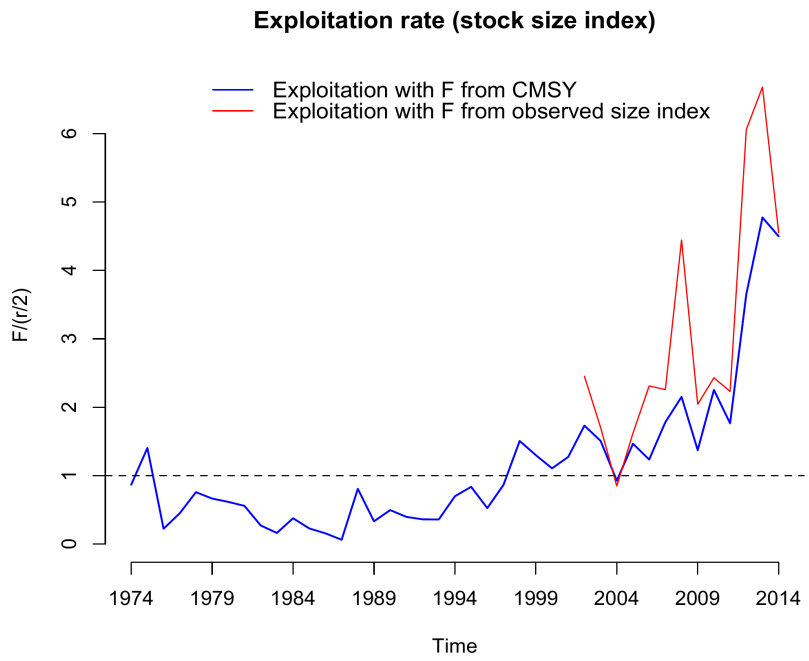


Figure 3.10b: Biomass trajectory predicted by the CMSY method in the case of 1995–2014 data set and Lpue index derived from the Kilo-Watts-days as measure of the fishing effort.
Prior ranges of the relative biomass (*B*/*k*) are indicated by vertical (black) lines corresponding to "Medium", "Low" and "Low" choices for the years 1995, 2006 and 2014 respectively. *B/k=0.3* and *B/k=0.5* values are indicated in black horizontal dashed lines.

Similar to the BM approach, CMSY reported an intensive rise in the rate of the exploitation (F/F_{MSY} or *F/(r/2)*) since 2005, (**Figure 3.11**, **Figure 3.4**) corresponding to the record of a biomass decrease in the case of the BM 1974–2014 model (**Figure 3.9a**) and later (after 2005) in the case of the 1995–2014 BM model (**Figure 3.9b**).

(a)



(b)

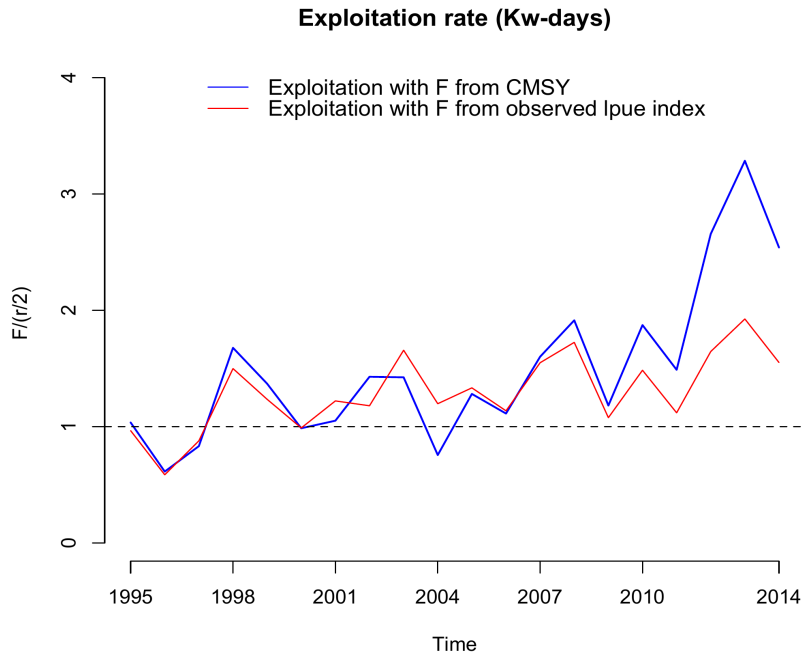


Figure 3.11: Aran grounds relative exploitation rate F/F_{MSY} as estimated by CMSY and BM methods for *Nephrops norvegicus* stock in the case of (**a**) the 1974–2014 landing data set with Stock Size Index and (**b**) the 1995–2014 data set with Lpue index derived from the Kilo-Watts-days as measure of the fishing effort.

The CMSY management reference points (r, k, MSY) fall within the limits of the equivalent BM outputs (**Tables 3.6**, **Table 3.1**, **Table 3.3**). In the case of the 1995–2014 landings, the proximity of the BM and the CMSY estimates of r (with $r^{BM}_{1995-2014}=0.243$ and $r^{CMSY}_{1995-2014}=0.282$, **Figure 3.12b**) reinforces our confidence in the BM approach.

(a)

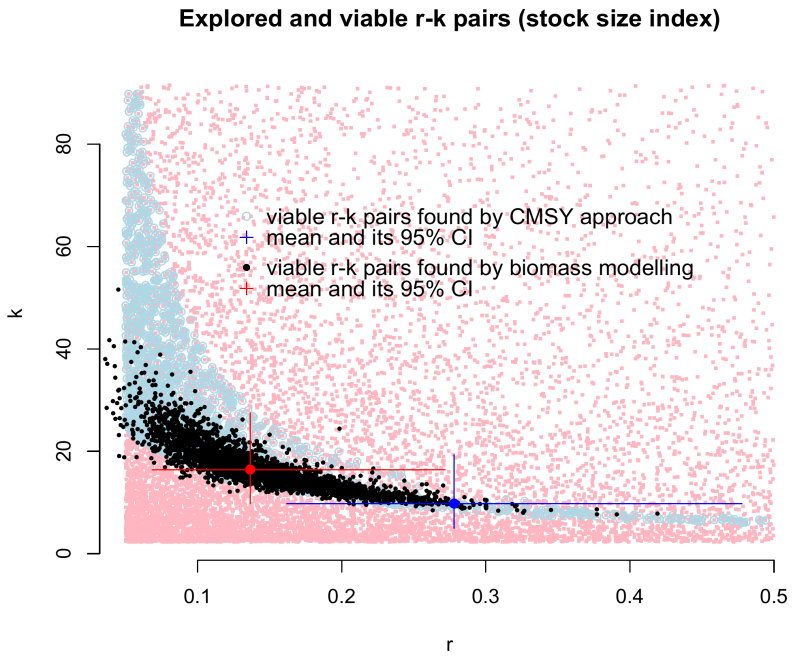


Figure 3.12a: Explored *r-k* Schaefer parameters space (pink dots) and viable (*r-k*) pairs spaces for *Nephrops* Aran grounds stock found by Biomass and CMSY modelling using 1974–2014 landing data set. The mean most probable (*r-k*) are shown with indications of the 95% confidence limits (red and blue crosses). The black dots show the estimates of the bayesian Schaefer biomass modelling (BM) while the light blue ones the CMSY method.

(b)

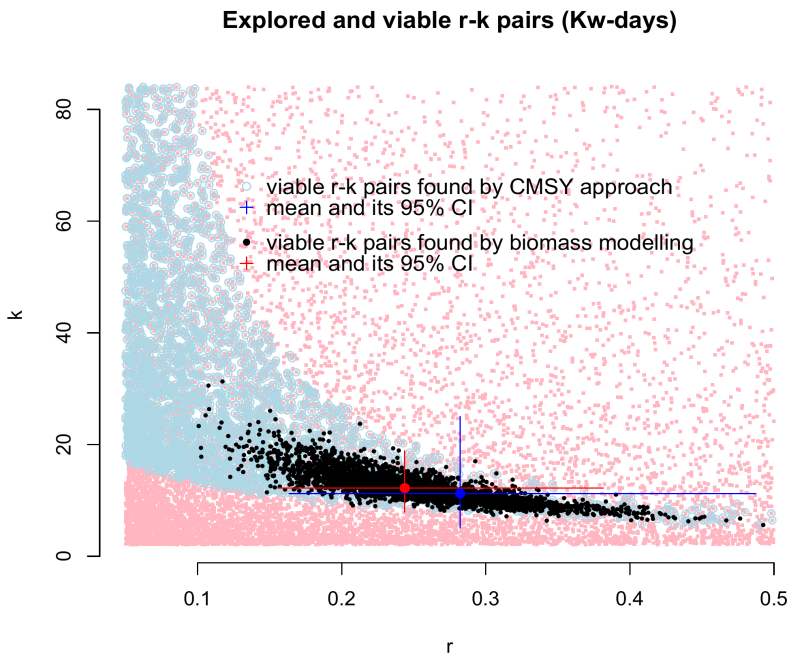


Figure 3.12b: Explored *r-k* Schaefer parameters space (pink dots) and viable (*r-k*) pairs spaces for *Nephrops* Aran grounds stock found by Biomass and CMSY modelling using the 1995–2014 data set. The mean most probable (*r-k*) are shown with indications of the 95% confidence limits (red and blue crosses). The black dots show the estimates of the bayesian Schaefer biomass modelling (BM) while the light blue ones the CMSY method.

While $r^{BM}_{1974-2014}=0.136$ is clearly lower than $r^{CMSY}_{1974-2014}=0.278$ in general, the (*r*) estimates of the CMSY and BM are in line with the grouping class [0.05–0.5] corresponding to a low resilience category retained in this study (Froese et al., 2015; **Table M2**; **Table 3.2c**).

Table 3.6: CMSY mean estimates of *r*, *k*, *MSY* and relative biomass in the case of 1974–2014 landing series leading to altogether 4226 viable trajectories for 1638 *r*-*k* pairs and in the case of 1995–2014 leading to 7839 viable trajectories for 2944 *r*-*k* pairs.
The 95% confidence limits (2.5th and 97.5th percentiles) are indicated in brackets.

	1974-2014 CMSY estimates	**1995-2014 CMSY estimates**
r	0.278 (0.162–0.48)	0.282 (0.163–0.487)
***k* (*tons*)**	9780 (4952–19310)	11250 (5057–25027)
***MSY* (*tons*)**	680 (518–892)	794 (483–1304)
Last year relative biomass	0.125 k	0.19 k

Recall that although the equilibrium condition is not assumed in this study, nevertheless, the "equilibrium" curve in the background is useful for comparing the CMSY and BM evolving status of the stock (**Figure 3.13**). From the 2000's, BM and CMSY relative biomass *B*/*k* ranges within [0.5 to 0.3] with a trend towards its lower *B/k* limit and beyond.
Note that dots falling on the parabola indicate catches that will maintain the respective biomass. While those above the parabola will shrink future biomass; and below the parabola allow future biomass to increase.
With landings data from 1974 to 2014, the CMSY trajectory portrays obvious distinctive periods in the status of the stock. From 1974 to early 90's CMSY estimates are far below the equilibrium curve suggesting that catches were consistently less than surplus production, allowing the stock to increase. For the remaining period, CMSY identifies over-exploitation (dots above the curve) and show an inexorable decline of the *Nephrop*s stock (**Figure 3.13**).
Moreover, the CMSY and the 1974–2014 BM report successive years of alarming levels of stock size with B/k < 0.3.

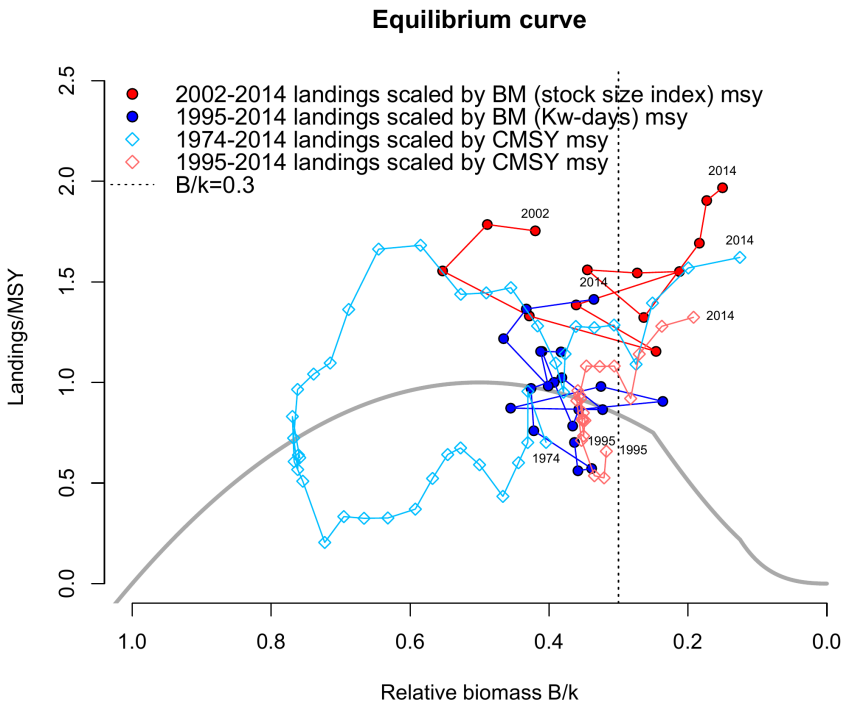


Figure 3.13: Theoretical equilibrium curve with theoretical Schaefer type parabola. Observed landings are expressed relative to the MSY estimates methods on the Y-axis and the decreasing biomass relative to *k* on the X-axis. Recall, that the right side of the parabola is indented because we assumed a linear decline of surplus production below 0.25 *k* due to reduced recruitment (Froese et al., 2016, 2017).

(III) Yield and recruitment

(III.1) Production and productivity

In theory, the surplus production model is based on the assumption that a fish stock produces an excess or surplus abundance (or biomass) that can be harvested. These surplus yield models are used to search for the largest fishing mortality rates that can be offset by increased population growth, normally measured as changes in population biomass (B_t) per unit time (Jennings et al., 2003; King, 2007). The annual surplus production SP_t, equals $B_{t+1} - B_t$ plus the catches C_t.

The plot *SP vs B* provides a signature of whether and how production has depended on stock size; that is, on whether stock size has been an important limiting factor for *SP*. By examining the relationships between the surplus production (*SP*) and the stock size

(*B*) over these 41 years we clearly distinguish two stock periods: from 1974 to 2003 and from 2004 to 2014 (**Figure 3.14a-b**)

(a)

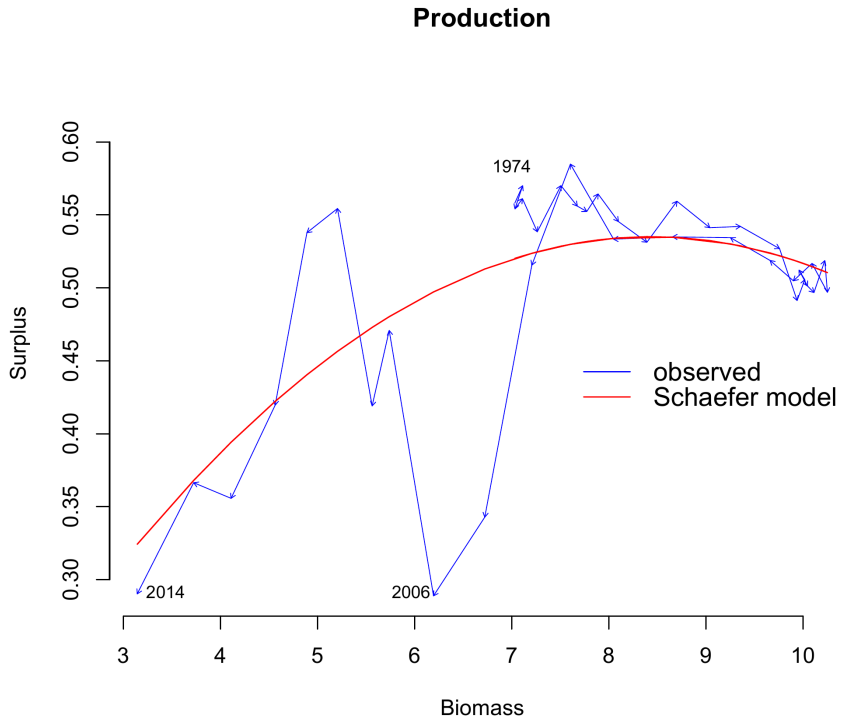


Figure 3.14a: Surplus production of the Aran grounds stock from 1974 to 2014.

By mean of a quadratic linear regression ($r_0B–r_1B^2$) forced to pass through the origin, a Schaefer surplus model (red line) is fitted to the biomass estimates (*B*) derived from BM modelling using 1974–2014 data set. r_0=*0.1268* is the intrinsic rate of population increase and the ratio r_0/r_1 (=*16.87e+03*) is an estimate of the average unfished biomass B_0.

(b)

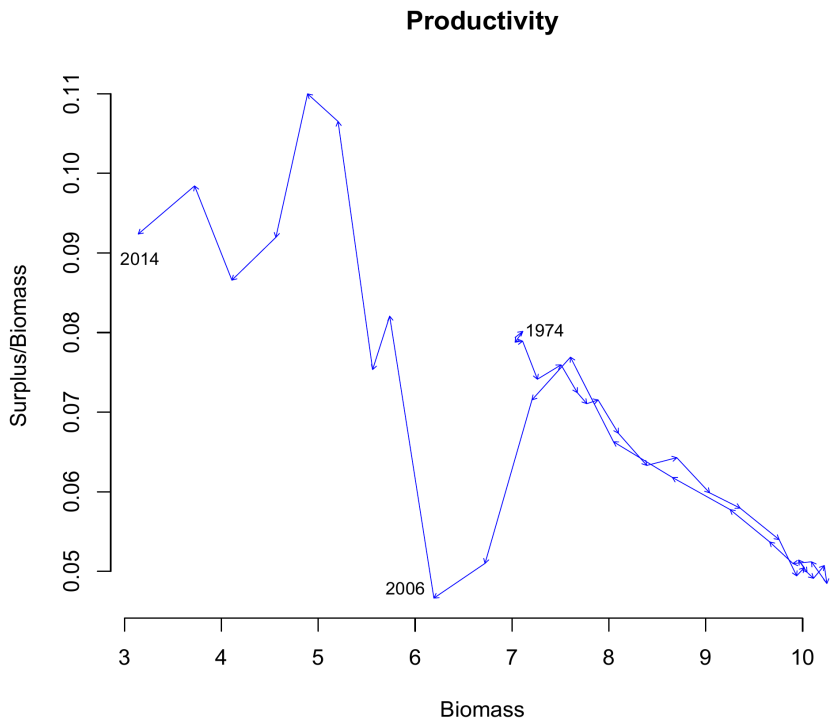


Figure 3.14b: productivity of the Aran grounds stock from 1974 to 2014. The year 2006 correspond to the lowest reported estimate of the burrow abundance by means of UWTV survey

In the case of *Nephrops norvegicus* we surmise that the length of time from hatching (water column) to identified burrow by UWTV could reasonably be about 2 years and very few survey observations reveal burrow dwellers of 1.5 years old. While, we estimate an average of 3–4 years for recruitment in fishing from settlement on the seabed.

Thus, the effect on the abundance of positive recruitment is long-term and such effect of recruitment causes a clockwise loop in successive *SP vs B*; high *SP* then causes *B* to increase for 1 or more years and then to later fall. According to Walters et al. (2008), clockwise hook-cycles in the data suggest that *SP* variations can be explained by stock recruitment anomalies.

From 1974 to 1994, we observe a succession of clockwise hook cycles of 3–4 years until 1994. This period is also characterised by an increase of *B* (**Figure 3.14a**) and a decrease in the productivity *SP/B* (**Figure 3.14b**). Since then, a clear stationary declining is shown through *SP vs B*. The UWTV surveys also point out to the general

depletion of the stock (**Figure 3.2b**).

From the plot of productivity (**Figure 3.14b**) stocks have exhibited a strong compensatory response, that is, increases in *SP/B* at low stock sizes (as suggested by Walters et al., 2008). Note that the recruitment decline precedes stock decline, *i.e*. is involved (along with fishing) in causing the decline of the biomass.

(III.2) Spawning potential ratio (GTG-LBSPR)

In fisheries, the compensatory capacity of a population is seen as the process of adapting to exploitation. When depletion of biomass is observed, fisheries managers begin to look for evidence of changes in traits such as size, individual growth, natural mortality and reproductive capacity. For Aran grounds, the average weighted mean of female carapace length (26.45 mm) is very close to the minimum conservation size (25 m) meanwhile the occurrence of the highest peaks of catch in spring coincides with the emergence of females for hatching/mating, the presence of the heaviest females and importantly, the lowest proportion of males (30%) in the relatively high volume fished (ICES IBPNeph, 2015) during this period. Thus, fishing impact on female stock rises concern and (GTG) LBSPR method provides a valuable insight into the potential level of sustainability of the stock.

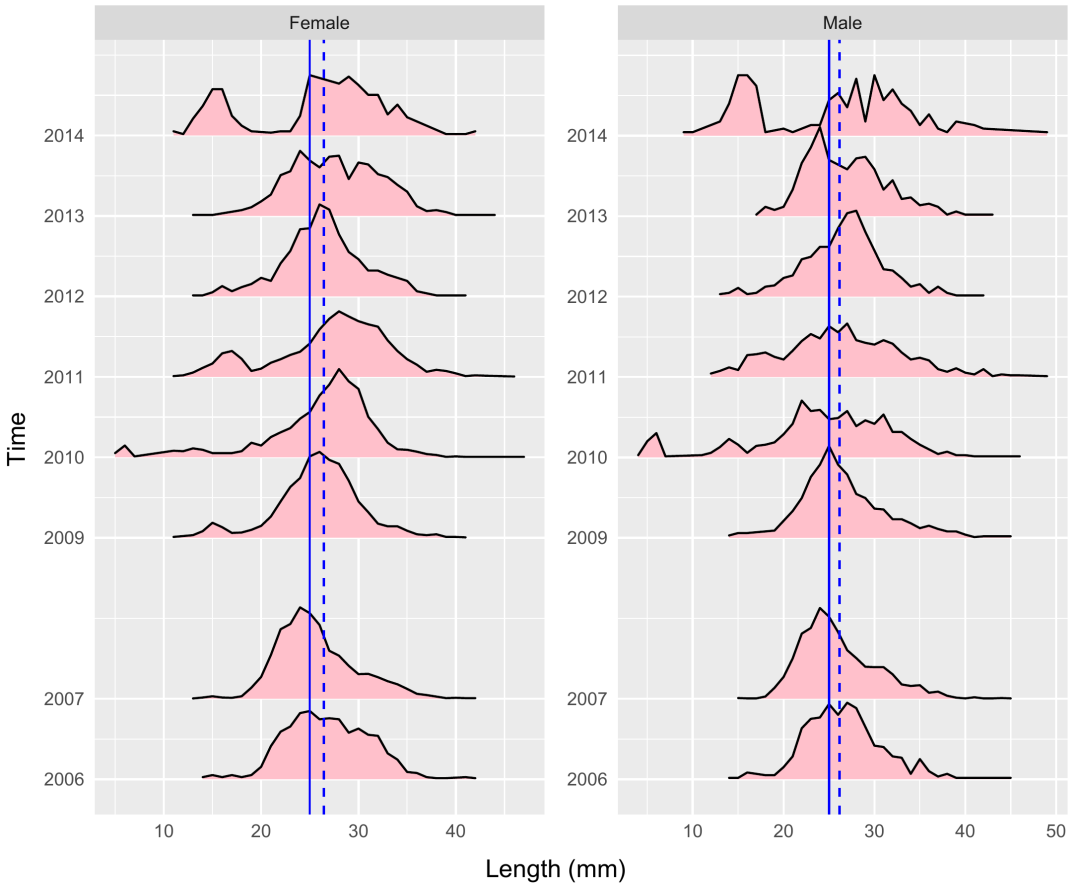


Figure 3.15: Length carapace frequency distributions of *Nephrops norvegicus* in Aran grounds. Data are from Marine Institute beam trawl surveys for years 2006, 2007, and 2009 to 2014. Averaged weighted means (dashed line) for female (26.45 mm) and male (26.15 mm) with the minimum carapace size landing of 25 mm (solid line) are indicated.

Over these years, when natural mortality rate of $M=0.2$ is applied for mature female, according to the spawning potential ratio (*SPR*) values, the status of the *Nephrops* stock ranges from fully to heavily exploited, and overfishing is suggested in the cases of assumed growth rates K=$0.117\ yr^{-1}$ and $K=0.08\ yr^{-1}$ (**Table 3.7**, **Figure 3.16a**)

We also notice the sensitivity of the outputs to the assumed asymptotic length (Hordyk et al., 2015c) since the estimated *SPR* increases as the L_∞ decreases (from $L_\infty=56\ mm$ to $L_\infty=55.2\ mm$) despite the proximity of the life history traits ($M/K=2.5$ and $M/K=2.59$ respectively; **Table 3.7**, **Figure 3.16a**).

Also, for $M=0.2$, the SPR value in 2010 (**Figure 3.16a**) has an outstanding large confidence interval disclosing a poor fit to the length data for this year (**Figure 3.16c**

left), while, by increasing the natural mortality rate to *M=0.3*, the (GTG) LBSPR size fit is improved (**Figure 3.16c** right).

Assuming a natural mortality level of *M=0.3*, usually assigned to males and immature females, led to a potential improvement concerning the recruitment for all scenarios, nonetheless, for 1 scenario (*M/K=2.56, K=0.117*), the *SPR* level is still fluctuating at unsafe settings for most of the years (**Figure 3.16b**, **Table C2** in ***Annexes C***).

Though the LBSPR method indicates a substantial mitigation of the exploitation rate (*F/M*) since 2010, with both assumed *M=0.2* and *M=0.3* natural mortality rates, SPR ratios exhibit slower recover, and particularly in the case of *M=0.2*.

Table 3.7

LBSPR model outputs for *SPR* and *F/M* for Aran grounds (FU17) using 2006, 2007, 2009–2014 beam trawl surveys according to variable proxy for the VBGF coefficients *K* and L_∞.

Common input parameters of these runs are $M=0.2$, $L_{50\%}=22$ *mm* and $L_{95\%}=24.5$ *mm* length-maturity(at 50% and 95%, respectively), the coefficients $\alpha=0.000684$ and $\beta=2.963$ of the carapace length-weight relationship $W=\alpha CL^{\beta}$ (ICES IBNeph, 2015) and the coefficient b=*2.566* of the power curve relationship between the realised fecundity (i.e. the number of eggs extruded) and the carapace length of female aCL^{b} estimated for the western Irish Sea *Nephrops* stock (Briggs et al., 2002b). The brackets stand for the 95% confidence interval of the estimated *SPR* and *F/M*.

Input parameters: K=0.077 yr^{-1}, M/K=2.59, L_∞=55.2 mm, $L_{50\%}$=22 mm, $CV_{L\infty}$=0.1								
	2006	**2007**	**2009**	**2010**	**2011**	**2012**	**2013**	**2014**
SPR	0.347 (0.31–0.37)	0.312 (0.29–0.32)	0.279 (0.26–0.29)	0.295 (0.27–0.31)	0.387 (0.36–0.41)	0.303 (0.27–0.32)	0.415 (0.37–0.45)	0.407 (0.36–0.45)
F/M	1.54 (1.28–1.79)	1.78 (1.61–1.94)	2.32 (2.09–2.54)	2.82 (2.44–3.19)	1.57 (1.35–1.78)	2.03 (1.72–2.33)	1.12 (0.92–1.31)	1.15 (0.90–1.39)
Input parameters: K=0.117 yr^{-1}, M/K=1.7, L_∞=55.2 mm, $L_{50\%}$=22 mm, $CV_{L\infty}$=0.1								
SPR	0.196 (0.17–0.21)	0.175 (0.16–0.18)	0.157 (0.14–0.16)	0.175 (-0.21–0.56)	0.225 (0.21–0.23)	0.171 (0.15–0.18)	0.235 (0.21–0.25)	0.230 (0.20–0.25)
F/M	2.82 (2.43–3.20)	3.19 (2.94–3.43)	3.99 (3.65–4.32)	2.78 (2.55–3)	2.87 (2.54–3.19)	3.55 (3.09–4)	2.19 (1.89–2.48)	2.24 (1.87–2.6)
Input parameters: K=0.067 yr^{-1}, M/K=2.98, L_∞=55.2 mm, $L_{50\%}$=22 mm, $CV_{L\infty}$=0.1								
SPR	0.416 (0.37–0.45)	0.375 (0.35–0.39)	0.335 (0.31–0.35)	0.351 (0.33–0.37)	0.459 (0.43–0.48)	0.363 (0.33–0.39)	0.496 (0.45–0.54)	0.486 (0.43–0.54)
F/M	1.22 (1–1.44)	1.43 (1.28–1.57)	1.90 (1.70–2.09)	2.33 (2–2.66)	1.25 (1.06–1.43)	1.64 (1.37–1.90)	0.85 (0.67–1.02)	0.88 (0.66–1.09)
Input parameters: K=0.08 yr^{-1}, M/K=2.5, L_∞=56 mm, $L_{50\%}$=22 mm, $CV_{L\infty}$=0.1								
SPR	0.318 (0.28–0.34)	0.285 (0.27–0.30)	0.255 (0.24–0.26)	0.270 (0.25–0.28)	0.356 (0.33–0.37)	0.278 (0.25–0.30)	0.380 (0.34–0.41)	0.372 (0.33–0.41)
F/M	1.71 (1.44–1.97)	2.96 (1.78–2.13)	2.54 (2.30–2.77)	3.07 (2.66–3.47)	1.75 (1.51–1.98)	2.22 (1.89–2.54)	1.26 (1.04–1.47)	1.30 (1.04–1.55)

(a)

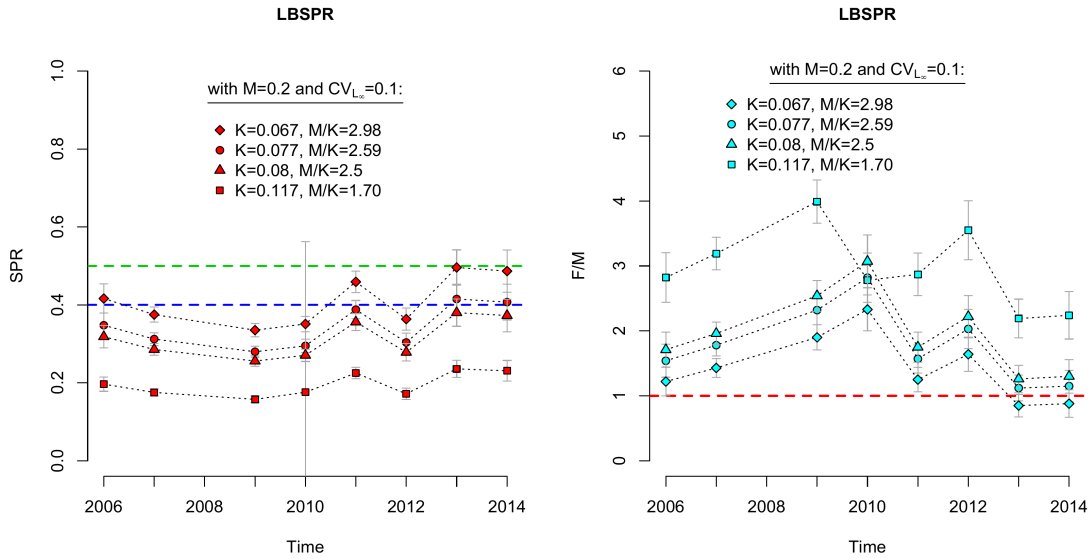


Figure 3.16a: LBSPR model estimates of spawning potential ratio (*SPR*) and exploitation rate (*F/M*) for Aran grounds *Nephrops* stock (FU17).

We assumed $CV_{L\infty}=0.1$, $L_{50\%}=22\ mm$ and $L_{95\%}=24.5\ mm$ in relation to natural mortality rates $M=0.2$ and $M=0.3$ and varying estimates of female Bertalanffy growth coefficients: $K=0.067\ yr^{-1}$, $K=0.077\ yr^{-1}$, $K=0.117\ yr^{-1}$ with asymptotic length $L_{\infty}=55.2\ mm$ (Haynes et al, 2016). Horizontal dashed lines indicate *SPR* ratios of 0.4 (blue), 0.5 (green) and exploitation rate $F/M=1$ (red).

(b)

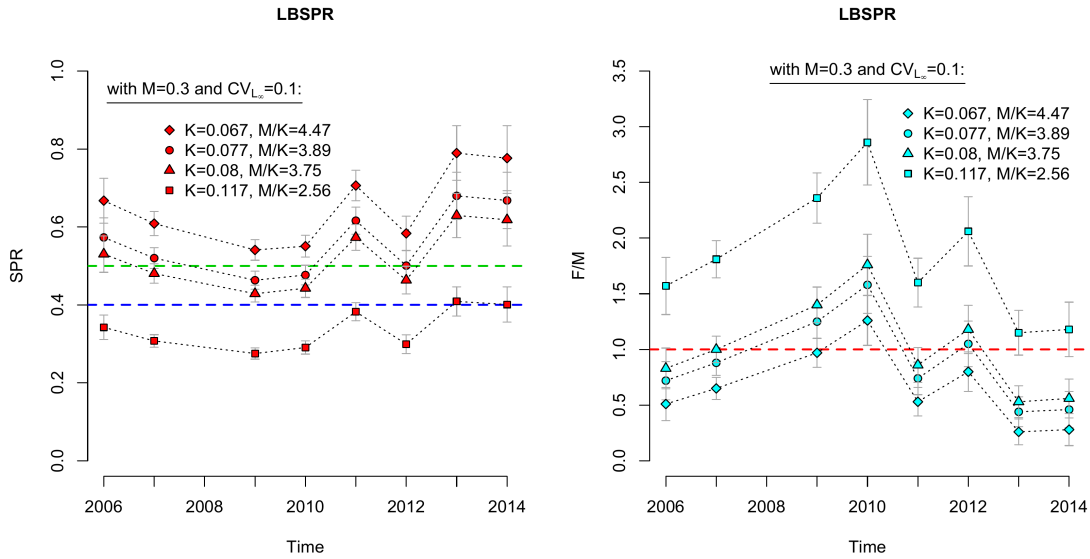


Figure 3.16b: LBSPR model estimates of spawning potential ratio (*SPR*) and exploitation rate (*F/M*) for Aran grounds *Nephrops* stock (FU17) assuming $CV_{L\infty}=0.1$, $L_{50\%}=22$ *mm* and $L_{95\%}=24.4$ *mm* in relation to natural mortality rates *M=0.2* and *M=0.3*.

Estimate of female Bertalanffy growth coefficients $K=0.08\ yr^{-1}$ with $L_{\infty}=56$ *mm* (ICES IBNeph, 2015) was used. Horizontal dashed lines indicate *SPR* ratios of 0.4 (blue), 0.5 (green) and exploitation rate *F/M=1* (red).

(c)

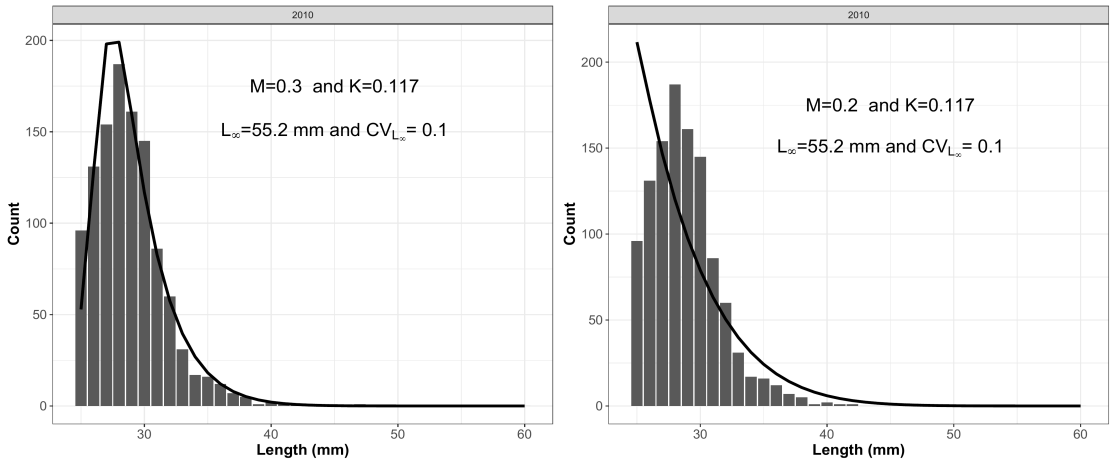


Figure 3.16c: LBSPR example size fits for 2010 assuming *M=0.2* (left) and *M=0.3* (right).

In the *F/M* ratio reported in the (GTG) LB-SPR model, the value for fishing mortality refers to the highest level of *F* experienced by any single size class.

Discussion

Despite contrasting approaches, BM and CMSY derived reference points indicated that the *Nephrops norvegicus* stock on the Aran grounds endured unsustainable fishing pressure. BM uses landings and abundance to estimate productivity and CMSY relies on landings and productivity to estimate biomass, while, both approaches deliver standard fisheries reference points such as *MSY* (*r k/4*), F_{MSY} (*r/2*) and B_{MSY} (k/*2*).

CMSY outputs should be compared to corresponding parameters and abundance estimates derived from fully or partly assessed stocks, where biomass or catch/landing-per-unit- effort data are available in addition to catch data (Froese et al., 2017). Purposively, BM (with Schaefer yield) has proven to be a suitable framework for stock assessment of *Nephrops norvegicus* and in this context, the BM estimates were used for evaluating reference points derived from the CMSY. We observed that the 95% confidence limits of the CMSY predictions for *r*, *k* and *MSY* included the BM estimates, suggesting good agreement between the two methods (**Table 3.1**, **Table 3.3**, **Table 3.6**; Smith, 1995; Knezevic, 2008; Hedderich et al., 2015).

F/F_{MSY}

Indication of over-exploitation also took the form of the F/F_{MSY} ratio surpassing 1 for almost two decades (**Figures 3.11**), although the results differ in terms of intensity with respect to the data set used in the analysis. Both BM and CMSY estimates disclosed a discrepancy between exploitation and F_{MSY} (**Figure 3.4 c-d**, **Figure 3.11**). Interestingly, the CMSY identified lower rates when it is tuned with lpues based on Kilo-Watts per days (**Figure 3.11**).

Biomass

Over the last 16 years of the reported time series of landings, the stock was characterised by a low biomass level and high fishing rate (**Figure 3.7**). Going back to 1974 highlighted the historical variation of the stock status going through diverse states as depicted by the Kobe plot (**Figure 3.7**).

In addition, even though, the equilibrium curve is not suitable for parameter estimation, it is useful for "understanding" the status of the stock from both the CMSY and BM

estimates and comparing them. Thus, the stock has been subjected to recurrent episodes of over-exploitation (values beyond the equilibrium curves, **Figure 3.13**).

For CMSY relative biomass B/B_{MSY} estimates were located under the threshold of *0.5k*, with the level of the depletion, ranging from substantial to severe, depending on the time series of landings used in the modelling approaches (**Figure 3.10**). In contrast, BM only pinpointed alarming decreasing trends when using the stock size index SSI_t (**Figure 3.3**).

The CMSY approach allowed the inputting of assumptions about the biomass depletion level (from low, medium, to high) over the start, intermediate and final sequences of the observed landing time series, opening the possibility to evaluate all the derived quantities (reference points) in the context of the estimated abundance reported by the UWTV surveys. By implementing $\boldsymbol{CMSY}_{Kw-days}^{1974-2014}$ with different levels of the relative biomass (*B/k*) assigned to the start, intermediate and final time of the times series, led to a B/B_{MSY} ratio between (*0.5–1*) for the 1995–2014 period in all cases (**Figure C5** in ***Annexes C***). The sensitivity of CMSY to the depletion priors is mainly reflected in the years before 1995 that are identified with high fishing rate and low biomass (**Figures C5** *in* ***Annexes C***).

Among all the reference points enumerated here, the maximum sustainable yield (*MSY*) is likely the one that draws our attention first. In general, the reported landings values mostly exceed the estimated *MSY* determined by both the BM and CMSY approaches (**Figure 3.5**).

The concept of *MSY* has long been discussed (Larkin, 1977; Punt et al., 2001) and some have strongly advised against using it as a target (Hilborn, 2002; Holt, 2011). In this study, *MSY* as well as all other reference points, are used as indicators of the current status of the stock and are not used as objective management points. In fact, the natural temporal fluctuations in yield (see ***Chapter 1 Time Series Analysis***), combined with the difficulty in knowing the level of fishing effort at which this maximum occurs, and how it varies from year to year, in addition to the lack of knowledge concerning the potential impact on recruitment and ultimately on resilience (*r*) due to the existence of a strong sex ratio bias reported in the period of highest fishing activity, render the *MSY* target realistically not achievable. In addition, the relevance of applying a proportion (harvest rate) to the absolute abundance of the population (derived from under water TV survey)

as the baseline to determine total allowable catch levels, without knowledge of the proportion of mature individuals in the population is questionable. In fact, there is no reference for the effective stock. Thus, perturbation of the female population abundance, that is to say, spawning stock biomass is not considered explicitly but rather alluded to by monitoring the sex ratio, mean length by sex and maturity for female.

r-k relationship

In the Schaefer surplus (or yield) model, (*r*) expresses the theoretical rate of increase of a population per individual after aggregating all important individual life traits such as birth, death, fecundity, age structure and others. Thus, although, the surplus production model pools various processes that determine population fluctuations, its (*r*-*k*) outputs have been useful in illustrating that the Aran grounds stock is of low resilience and paves the way to address interesting questions.

On the other hand, the carrying capacity (*k*) in the Schaefer surplus production model refers to the hypothetical maximum biomass (or number) that the habitat can support and is also used to represent the population upper limit. However, it is less evident that (*k*) in the logistic family models depends on birth and death as well as the mechanisms determining how these rates change with density (Kindsvater et al., 2016). Thus, life history traits (*r* = birth-death) and physiology interact with the environment to determine population abundance (that is, fluctuations) and in consequence, the maximum abundance (*k*) is not fixed.

Nevertheless, using the CMSY method where the strategy consisted fundamentally of searching for the (*r*-*k*) pair(s) that give rise to an estimated biomass trajectory compatible with the catch/landing series data provides a very useful indication of the order of magnitude of (*r*) and (*k*) (**Table 3.3**, **Table 3.6**, and **Table 3.7**).

BM and CMSY identified the negative correlation between (*r*) and (*k*) (**Figure 3.8b-d** and **Figure 3.12**) which illustrates a form of negative feedback or density dependence mechanism involving biological, physiological and environmental parameters acting solely or in tandem, to explain the rises and falls of the biomass (*e.g.* competition, growth, fecundity, energy allocated to reproduction, starvation, cannibalism, or predator aggregation). All other things being equal, we notice that such (*r*-*k*) relationships indicate that the data alone do not allow us to clearly disentangle a very abundant

population (large *k*) with rather low growth rates (*r*) from one with a lower (*k*) but a higher (*r*) (**Figure 3.8**).

In this study, CMSY *r* estimates appear higher than BM estimates. In fact, using the Monte-Carlo filtering of the (*r*-*k*) space the CMSY method is selecting the (*r*-*k*) ones within the tip region of the ellipsoid cloud of (*r*-*k*). While, the mean *r* estimate of the BM approach is derived from the full range space of (*r*-*k*) pairs. For CMSY, this is based on the underlying principle that defines *r* as the maximum rate of increase for the examined population, which should be found among the highest viable *r* values (Froese et al., 2017). Interestingly, when considering the same data length (1974–2014 and 1995–2014), estimates for the period 1995–2014 are very close ($r^{CMSY}_{1995-2014}=0.282$, $r^{BM}_{1995-2014}=0.243$) contrasting with the striking case of the 1974–2014 series ($r^{BM}_{1974-2014}=0.136$, $r^{CMSY}_{1974-2014}=0.278$). In both cases, CMSY is still selecting the productivity *r* within the tip of the ellipsoid, while, for BM method, including 1974–1994 data stretches the space range of the (*r*-*k*) pairs in particular towards the lower (*r*-*k*) values and hence explains the lower mean *r* value obtained. Such results illustrate the discrepancy between the periods 1974–1994 and 1995–2014 in terms of the potential trajectory of the biomass and associated reference points (*e.g. r*, MSY...). Is it worth achieving regarding the question of the reliability of the data for the 1974–1994 period? We are still convinced of the interest to include the information brought by such data despite the amount of uncertainty, provided that our analysis does not ignore it.

Compensatory capacity

Kindsvater et al. (2016) proposed four strategies: precocial, opportunistic, survivor, and episodic to categorise species based on their life-history traits and compensatory capacity. In brief, a vertical dimension (adult mortality rate) goes from species with low adult mortality, large body size and low abundance called the slow life histories, to those with fast life histories characterised by high mortality, small body size and high abundance, and a horizontal extension is inserted to account for juvenile mortality rate representing the variation in compensatory capacity.

In the Western Irish Sea, *Nephrops* accounted for 94% of the biomass at its trophic level (Hill, 2007) and footage from the Aran grounds seabed surveyed by under water

cameras confirm the large amount of prawn relative to the other observed macro benthic invertebrates.

Thus, in an attempt to broadly categorise life-history traits to inform the compensatory capacity of the Aran grounds stock, we observe that the reproductive strategy (high fecundity), the abundance (high number of individuals), the relatively early time of maturity ($L_{50\%}$=*22 mm* carapace length or approximately 3 years), the precocial female care of eggs (enhancing fecundity-berried phase), the sensitivity to environmental factors as illustrated by the match-mismatch hypothesis (involving ocean current pattern set up), the water temperature influence on egg-larval stages, all converge to suggest an "opportunistic" categorisation. However, given the continuum facet of this classification there is a need to temper this assertion regarding species such as anchovies (*Engraulis ringens*) and herring (*Clupea harengus*) which are typically the extreme representatives of this category. In fact, in comparison to the usually high juvenile mortality reported for these species, the presumably high *Nephrops* recruitment loss is related to the settlement phase on the seabed and oceanic current drift, that is to say, the early stages of its life cycle and not the juvenile time. In addition, the large numbers of anchovies/herring are subject to high predation mortality and act as a direct feeding source for many predators, which underlines the concept of key species. In contrast, although *Nephrops* are important in the diet of cod (Chapman, 1980; Du Buit, 1995) and other benthic predators such as cephalopods and anglerfish (Coll et al., 2006), they do not appear to have a similar "key forage species" role in the food-web in Aran grounds at this stage of our knowledge.

In Aran grounds, even after a positive recruitment, the population recovery is delayed by the time it takes to reach maturity (3 years on average), during which time the stock continues to endure depletion and increasing fishing mortality that threatens the expected bounce back (Rothschild, 2015). Thus, high fecundity is not sufficient to guarantee sustainability.

Recruitment

In order for fish stocks to persist, successive generations must replace each other on average. This means that fishing should not reduce the egg production or amount of spawning per recruit (*SPR*) below a threshold level that is necessary for replacement.

For a given level of exploitation, *SPR* is a quantitative measure of the compensatory capacity of the species to sustain the harvest with its reproductive strategy.
LB-SPR outputs for Aran grounds indicate worrying level of *SPR* for many scenarios on the basis of growth rate and natural mortality hypotheses (**Figure 3.16a-b**).
In the most favourable case of assumed lower natural mortality, *M=0.2*, for mature female in relation to a long time period of fishing avoidance due to burrow retrieve of female after spawning, *SPR* is still mainly under the level of *SPR=0.4* and fluctuate up and down around *SPR=0.3*
Notice that values of *SPR* replacement (% *SPR*) in the range of 20–35% are frequently used to characterised recruitment overfishing (Clark, 2002; Mace, 1994; Gabriel and Mace 1999) however some species with low resilience have % *SPR* as high as 40–60% (Mace and Sissenwine, 1993).
While, assuming *M=0.3* (**Figure 3.16b**) appears critical as illustrated by the highly variable *SPR* status of the Aran grounds stock ranging from overfished to good, *i.e* suggesting no concern about the capacity of the stock to sustain the current fishery, and this despite the general trend pattern of *Nephrops* population abundance passing from 1.09 burrows/m^2 in 2004 to 0.28 burrows/m^2 in 2014 (Anon., 2018) and the severe depletion of the stock as highlighted by the BM and CMSY approaches. In this regard, within the LB-SPR framework, the combination of slower growth ($K=0.0.077–0.067\ yr^{-1}$ leading to $M/K=2.56–4.47$ ratios respectively) and higher natural mortality ($M=0.2$ to $M=0.3$) reduces the number of large individuals in the population and smaller individuals contribute more to the total unfished biomass. And because of the assumption of the knife-edge selectivity in LB-SPR (*i.e.* not all length classes of a stock are vulnerable to fishing) fish smaller than L_c are not vulnerable to fishing mortality and only experience natural mortality while all fish larger than L_c are fully vulnerable to fishing mortality (Recall that LBSPR is tuned with $L_c=25\ mm$ and $L_{50\%}=22\ mm$ and $L_{95\%}=24.5\ mm$). Thus, the effect of the larger class of smaller individuals on the SPR level is positive. Hence, it appears more realistic to assume *M=0.2* in this situation.
LBSPR estimation is also considered to be sensitive to the asymptotic length mis-specification (Hordyk et al., 2015c) and in fact, in situations where proxies are close in terms of growth rate parameters, for instance $K=0.077\ yr^{-1}$ and $K=0.08\ yr^{-1}$ but vary in

L_∞ (L_∞=*55.2 mm* vs L_∞=*60 mm* respectively) estimates of *SPR* differ accordingly (**Figure 3.16a**). However, Haynes et al. (2016) believed that the L_∞=*55.2 mm* is underestimated, since the largest female captured in the field at Clew Bay was *57 mm* carapace length which is close to the Pope and Thomas (1956) estimates of mature and immature females (L_∞=*56 mm* and L_∞=*60 mm*, respectively) determined for Scottish stocks and used as proxy for Aran grounds stock (ICES IBNeph, 2015). Thus, the samples from which L_∞ and *K* parameters are derived are likely to come from population impacted by fishing and where size structure of the stock is already potentially affected leading to bias estimates

In fact, the removal of lager individuals and the selective removal of faster-growing individuals (Lee Phenomenon; Lee, 1912; Kraak et al., 2020) might leave behind a stock with a depressed observed mean length becoming cumulatively dominated by slower-growing individuals that could affect the estimates of the von Bertalanffy parameters like L_∞ and *K*.

Moreover, for *Nephrops norvegicus* in Aran grounds $L_{50\%}$ (maturity length at 50%) is highly variable from year to year, ranging from *19 mm* to almost *23 mm* in years 2006, 2007, 2009–2014 (ICES IBNeph, 2015) and assuming $L_{50\%}$=*19 mm* resulted in an expected increase of *SPR* (Hordyk et al., 2015c) that, however, do not affect the general status of the spawning potential of the stock we already identified with *M=0.2* and $L_{50\%}$=*22* mm (**Figure C6a-b** in ***Annexes C***)

We see the uncertainties are important, and as recalled by Prince et al. (2015) “there is considerable natural variation in these ratios and the relationships between size, age, and reproductive potential that they determine it”. And, assuredly, the reported variability of the sampled size of *Nephrops norvegicus* due to its “stocklet” spatial structures in relation to the seabed (Tully et al., 1995; Haynes et al., 2016) will contribute to increase the uncertainty over the *SPR* values. As well, the LBSPR method is feeded with biological indicators (*K*, L_∞, length of maturity $L_{50\%}$ and $L_{95\%}$) that are known to be very variable regarding sex and spatial area (Tully et al., 1995; Haynes et al., 2016; Merder et al., 2020) within the same functional unit for *Nephrops norvegicus*.

Thus, at this stage, regarding the constant depletion of the reported number of burrows by the UWTV surveys from 2002 to 2014 (**Figure 3.2c**) we plead for a more conservative approach to determine the average status of the *SPR* of the Aran grounds

stock (**Figure 3.16a**).

Besides, our concern about the female ratio bias in catches (reaching up to 70%) during the period of female emergence that constitute on average, for the period 1995-2010, more than 40% of the entire landings (in weight) of Aran grounds still exists. Such targeted withdrawal of active females could influence the recruitment and contribute to weaken the capacity to sustain the fishing mortality and then the resilience of the population. In fact, in line with the observed increase in *SP/B* at low stock sizes (strong compensatory response, **Figure 3.14**), the important weight of females at time of highest harvesting volume and also the proximity of the average landings carapace length of female (26.45 mm) with the minimum conservation reference size (25 mm) we could conjecture that this higher prevalence in the catch of females could have affected female resilience and the ability of the population to sustain the growing fishing pressure encountered and that the fishing pressure may have induced structural change in age (or size) of the population towards the younger and smaller specimens causing reduced mean fecundity, that is to say, there is a proportional paucity of older more fecund individuals. However, there is no evidence of reduction in size reported for *Nephrops norvegicus* within European waters (Johnson et al., 2013).

Regulation through density-dependent mechanisms is underlined in the case of *Nephrops* (**Figures 3.8b-d** and see ***Chapter 1 Time Series Analysis***). The supposedly main factors acting to reduce the size (or growth) of animals are limitations of food (Bailey, 1986; Parslow-Williams et al., 2001), space, and positive recruitment bias which reintroduces competition for food and space. In fact, we observe that size-density effects do occur at the scale of many functional units where we observe an inverse relationship between mean burrow density (derived from UWTV surveys) and mean weight (calculated from landings data) as well as between the modal carapace length derived from catches (and corresponding to the overall modal length extracted across all years) versus the mean density (Johnson et al., 2013). Moreover, as burrow dwellers with a limited foraging range, patches of high density are easily targeted by fisheries, and hence, the impact on the stock of an increasing effort, as observed in Aran grounds (**Figure 3.2d**), is likely to have a significant negative effect. Nevertheless, *Nephrops* spend the vast majority of their time in burrows where they are less vulnerable to predation and inaccessible to trawl fisheries contributing to the resilience of the

population.

Production and Productivity

Displaying the surplus production (*SP*) and productivity (*SP/B*) against biomass (*B*) gave a conspicuous demonstration of the non stationarity of the population in the 2000's (**Figure 3.14**) occurring in tandem with the biomass decline also reported by the under-water TV surveys undertaken since 2002 (**Figure 3.2c**). While our results highlight the potential impact of the fishing activity on the current stock status of *Nephrops*, we cannot ignore the possibility that the decline in abundance might be caused by reduced recruitment induced by environmental factors acting in congruence with fishing. Furthermore, we may assume, that the 2002–2014 stock size index (SSI_t) relies on a too short time series of UWTV survey and in consequence, to the influence of an unusually high recruitment recorded at the start of the series. In addition, from an ecosystem standpoint, fishing alters predator-prey and competition relationships as shown in Walters et al. (2008), Pauly and McLean (2003) and Pauly (2010).

Walters et al. (2008) also affirm that ["stocks that have not exhibited an increase in *SP/B* at low stock sizes"] (*i.e.* a strong compensatory response) ["have very likely been over-fished over the whole period of historical record"]. Besides observing such a response for the Aran grounds stock, we put forward evidence of over-exploitation and the critical situation of the stock.

The question is whether the severe depletion has been due to overfishing in the most recent time (*i.e.* 90's onward) or earlier.

At this stage, and in line with previous results, many arguments are in favour of the recent years, but we cannot overlook the information brought by the two peaks of "declared" landings in 1975 and 1988 for which 828 and 822 metric tons were fished respectively; a volume commonly superseded in the 2000's but illustrating the capacity to harvest at this level at that time. It would be very naïve to think that the fishing industry would have refrained from fishing and particularly during the 70's and 80's a period marked by incentives (*e.g.* subsidies policy, financial aid programme) to expand the markets for fish product, and to facilitate fishing by increasing the number of vessels and their modernisation that ended in over-investment (COM Green paper, 2001; Lutchman et al., 2009).

Against this background, it is likely that misreporting of catches and discards occurred and that landings were totally underestimated (Driscoll et al., 1979; Jensen, 1999), opening up the possibility that over-exploitation originated over a longer time frame[15]. Obviously, over these decades not every decrease in yield originated from fishing, but evidence of an environmental effect is not easily discernible. Nonetheless, in previous work, we highlighted the leverage effect of the North Atlantic Oscillation on landings trends (see ***Chapter 1 Time series Analysis***) and highlighted the atypical oceanic circulation pattern prevailing in 2003 over the Aran grounds: in fact, the April-May hydrological setting featured a north-south drift (see ***Chapter 2 Spatial Analysis***). Moreover, since the length at 50% maturity (22 mm) is approximately reached at the age of 3 (years), the 2006 decrease in biomass (**Figure 3.2c**), also identified by the productivity track path technique (**Figure 3.14b**), could reflect this important loss of larvae for recruitment. This time, the 2006 stock fall might be attributable to factors not linked to the stock size.

Data

This study necessitated using the time series of landings associated with either the fishing effort in Kilo-watts-days or the UWTV estimates of burrow abundance.
As previously mentioned (see ***Introduction***) the historical quality of the available landing data led us to distinguish two time series. On the one hand, the use of the 1974–2014 allowed us to exploit potential long-term patterns, despite the poor confidence in the reported landings prior to1988. On the other hand, we clearly rely on the data period from 1995–2014 marked by a rise in the quality of the data collected, in particular, the fishing effort data for FU17 available from 1995 for the Irish otter trawl *Nephrops* directed fleet.
BM with *Lpue* index of abundance did not indicate a cause of concern about the level of

15 According to Driscoll, D. J. and N. McKellar (1979) in [The Changing Regime of North Sea Fisheries]: “The most extreme example of lack of enthusiasm to prosecute, once a violation had been detected, was provided by Ireland. Over the ten-year period 1964–1973 Ireland discovered 288 apparent violations by Irish vessel of NEAFC rules with regards to mesh size and taking undersized fish, yet prosecuted on only seven occasions” (page 136). “Note also that the percentage of fishery inspection visits resulting in report of apparent violations of NEAFC mesh-size regulations by its member is unequivocal!”(table 6.1 page 137).

the stock. B/B_{MSY} quantities were found bounded between 0.5 and 1 over almost two decades (1995-2014) (**Figure 3.3b**) and the B/B_0 ratios manifested no cause for concern (**Figure 3.9b**). However, during the same period the fishing effort, either measured in Kilo-watts-per days or in hours-days (from 1995), was continuously growing and the independent surveys (UWTV) unveiled a rapid decline of the population from 2004 to 2014 with a burrow abundance in 2014 estimated at only 35% and 25% of the levels of the years 2002 and 2004, respectively, highlighting the severe drop that occurred. In the Aran grounds, the lpue index relying on Kilo-watts-per day did not highlight the ongoing decline of the stock size and the side effect of using such an index has already been recognised (Hilborn, 1985). This led us to derive an index from the UWTV (SSI_t) which succeeded in capturing the decrease in the biomass and the increase in the exploitation rate (F/F_{MSY}) of the last 3 years (**Figure 3.14**).

Fishing Effort

During the period 1995 to 2014 the fishing effort time series (**Figure 3.2d**) is marked by repeated relative short phases of up and down trends and the striking contrast in the magnitude of the peaks and troughs.

A plausible explanation could be that fishers sequentially adapt their fishing behaviour (effort spent over the Aran grounds zone) in relation to their perception of the abundance and adjust their behaviour. Since regularly, the *Nephrops* level of harvest clearly peaks in Spring and Autumn, such information is easily accessible and included by professionals and used to evaluate the yield of their routinely targeted areas. Hence, the variability of effort could be the result of such "gauged" abundance and serve as a motive to target *Nephrops* elsewhere (other FUs) in order to maintain a valuable activity.

Against a backdrop of a global growing interest in this valuable species particularly since the collapse of the Cod stock (*Gadus morhua*), it seems reasonable to consider these successive sequences as the result of the interplay between components acting at different time scales; for instance, policy regulations (*e.g.* total allowable catch) and technical improvements.

Note also, that the fishing effort time series retained by the Marine Institute corresponds to a percentage of the global fishing effort over the Aran grounds. This is to screen out

non *Nephrops* directed effort. The fishing effort is deduced from the proportion of landed *Nephrops* over the entire harvested species by weight. It is obvious that using this approach is limited in term of insight, and particularly for a mixed fishery where all species are equivalently targeted. The increase in the spatial and temporal resolution of vessel monitoring system could greatly enhance the accuracy of the fishing effort when connected to the spatio-temporal distribution of *Nephrops* density (*i.e.* patchiness). For example, in their attempt to support the implementation of the EU's landing obligation (that is, counting all fish caught against quota) in highly mixed fisheries like in the Celtic Sea, Dolder et al. (2018) illustrated the potential of using spatial data. Using catch data from seven fisheries-independent surveys (over 1990–2015), the analysis of nine species counting for more than 60% of landings (by towed gears) indicated a spatial and temporal pattern in the assemblage of these fish over the surveyed area. Such species distribution maps opens the possibility to target species while mitigating unwanted ones. Such spatial information could be adapted to the *Nephrops* fishery and help to decouple the targeted and bycatch *Nephrops* grounds and in consequence enhancing accuracy in the measurement of the associated effort.

Conclusion

Using a combination of disparate approaches and statistical techniques, the results are consistent in relation to the general status of the Aran grounds stock: the *Nephrops norvegicus* fishery faces serious challenges to maintain this valuable activity and the launch of the independent surveys in 2002 has demonstrated its importance to the management of the stock into the future.

General Discussion

Contents

General Discussion.....246
Introduction.....248
(A) Resilience of the Aran grounds population.....249
(A.1) Estimated resilience.....250
(A.2) Spatial entry for resilience.....250
(B) Towards an ecosystem approach of fisheries management.....253
(B.1) Widening the field of view.....253
(B.2) Sorting between vessels.....254
(B.3) Indicators for what?.....255
(C) The spatial dimensions of *Nephrops*.....256
(C.1) Adapted growth and patches.....256
(C.2) The geographical range keys.....257
(D) Climate strands: recruitment in jeopardy?.....259
(D.1) A warming ocean.....260
(D.1.a) Depressed pycnocline.....260
(D.1.b) Diminution of oxygen.....260
(D.1.c) Shifting distribution.....261
(D.2) A North-South response of *Nephrops norvegicus* to climate change?.....262
(E) Fishery induced selection.....264
(E.1) Investigating fishery induced selection for the Aran grounds stock.....265
(E.2) An exhausted female stock as a witness mark of a fishing induced evolution?
.....266
Conclusion.....269

Introduction

Throughout this work I strove to determine the state of the *Nephrops norvegicus* population on the Aran grounds.

Overall, several alternative statistical and modelling approaches were applied to assess this highly valuable commercial species, with a complex life-history. This necessitated the examination of different types of data featuring various attributes: spatial information (under-water TV surveys, vessel monitoring system...), biological indices (length of maturity, Bertalanffy growth parameters, fecundity...), and temporal changes (landings time series, estimated average discards). Analysis of the outputs derived from these sources enabled me to tackle entirely or partially many questions in relation to the major theme running through this study, that is, the status of the exploited stock of *Nephrops norvegicus* on the Aran grounds. Clearly, the key word of "status" can also be interpreted as the "health" of the stock and can be approached from a fishing exploitation perspective. However, fishing is one of the multiple facets illustrating the interaction of humankind with a piece of its surrounding ocean and it is important that an ecosystem framework is established to embrace the full scale of these facets in accordance with one of the pioneers of the ecosystem approach, namely, Margalef (1998) and its definition: "La ecología[16] es la rama de la biología que estudia las relaciones de los diferentes seres vivos entre sí y con su entorno[17]". Thus, information on stock status and exploitation rates is the first step to implement a sustainable management system for this resource, for the people that rely on this fishery and to move simultaneously towards an integrated fishery management system in compliance with recent European Union fishery objectives (called an ecosystem approach of fishery management). This study contributes to our understanding of the population dynamics of *Nephrops* on the Aran grounds including its response to fishing and the natural environment.

Nevertheless, it must be acknowledged that further analyses are needed to evaluate the utility of the methods before they can be operationalised to produce management advice

16 from the ancient Greek oïkos=house or environment, and logos=discourse or study of.

17 my own translation: "the ecology is the branch of the biology studying the relationships between livings and surroundings".

in the case of the Aran grounds stock. The estimated status of the stock as shown here could be used as complementary or additional information to be integrated into the iterative mechanisms to comply with the objectives of a harvest strategy or harvest control rules depending on the conclusions.

Harvest control rules are essential for quota-managed fisheries and are used to determine the annual total allowable catch (TAC) while, harvest strategies link changes in management to the estimated status of the stock (Smith et al., 2014).

In this final chapter, the salient features and results of this study are highlighted in order to contextualise them and incorporate them into a wider ecological/environmental perspective. A practical series of actions to strengthen management of *Nephrops norvegicus* in Aran grounds are also suggested.

(A) Resilience of the Aran grounds population

During this study, the term "resilience" was used as a way of characterising *Nephrops norvegicus*. It appeared as an auxiliary term rather than an objective ascribed to this study. However, when trying to understand and to explain the patterns of change of an ecological system, this concept is very useful (Baho et al., 2017). From an ecologist perspective, the most consensual definition is that it means "the capacity of a system to maintain key ecological functions, processes and feedbacks in the face of perturbations and disruptions" (*cit.* Klinger et al., 2017; Hodgson et al., 2015). We can interpret this in a practical way by considering the answers to a series of fundamental questions such as: is the system of interest returning to a prior state or reconfiguring into something very different? How are human and/or natural sources of disturbance absorbed within the dynamic system? Thus, indicators are chosen to quantify attributes of resilience purposively targeted and that, interestingly, inform their users (ecologists, engineers, resource managers, stakeholders...etc). In fact, these descriptors are specific and attributes of resilience subject to choice (Gunderson, 2000; Gunderson et al., 2002; Gunderson, Allen and Holling, 2010; Standish et al., 2014; Baho et al., 2017; Timpane-Padghamet et al., 2017).

(A.1) Estimated resilience

Over the 1995–2010 time period, the high variability in the occurrence of the minimum and maximum values of landings (see ***Chapter 1 Time Series Analysis***), the considerable non stationarity of the surplus-production model and productivity, accompanied with the decreasing trend in biomass (**Figure 3.10** in ***Chapter 3 Stock Assessment***), but also the (lag) influence of regional climate indices such as the North Atlantic Oscillation and the Arctic Oscillation on harvests, and the presence of a (delay) density dependence regulation (see ***Chapter 1 Time Series Analysis***) all contribute to the interpretation of "resilience" for *Nephrops* population off the coast of Galway, especially to fisheries managers. In parallel with this qualitative stand, quantitative measures of resilience were derived either from the analysis of the health status of the stock through a bayesian biomass modelling (BM) with a Schaefer yield or data limited method (CMSY) that led us to classify the Aran grounds population in the category of low resilient species enduring overexploitation (see ***Chapter 3 Stock Assessment***). There are, however, overlapping values at the lower edge of the medium category according to Musik (1999) and Froese et al. (2015) classification that could suggest Low to Medium resilience for this stocks.

Although fragmented, all these elements combined provide the first attempt at appraising the capacity of the stock to withstand the current fishing pattern and to delineate the putative responses of the population to the abiotic stressors in the context of a dramatic decrease in abundance where the major factor of influence is very likely fishing.

However, there are some remaining questions such as are these results the signals of an ongoing reorganisation (transition), the evidences of an already new state (*i.e.* tipping point) or simply perturbations near the initial equilibrium? What is clear is that fisheries managers need to recover the population and, despite focusing on climate change, Timpane-Padgham et al. (2017) provides a useful summary of a range of resilience attributes that are suitable for use by managers at different scales (e.g. species, populations, sites, habitat) in restoration programmes.

(A.2) Spatial entry for resilience

According to Holling (1992) "ecosystems are structured and maintained by a relatively

small set of dominating processes that operate at different spatial and temporal scales which generate discontinuous distributions of features in the ecosystem". Recall, that *Nephrops norvegicus* is habitat specific and the seafloor is a determinant factor for recruitment success (Smith et al; 2008; Campbell et al., 2009). Thus, the observed patchiness or "stocklet" spatial structures inform and illustrate a facet of this, resulting in the dynamic organisation of the ecosystem. *Nephrops* density is "entrained by the discontinuous structure and texture" of the seafloor (mud-sand distribution). Its spatial arrangement reflects the differences in, and interactions among internal and external elements of their environment. And the geometry of its distributions over time reflects in part the (morphological) attributes of *Nephrops norvegicus* that are influenced by interaction with ecological structures and patterns at different scales (Holling, 1992; Gunderson L. H. and Holling C. S, 2002; Allen and Holling, 2002; Gunderson, L. H., Allen, C. R., Holling, C. S., 2010).

For instance, the current topography and edaphic structure of the Aran grounds is as a result of geomorphological and hydrological processes lasting centuries to millennium and encompassing hundreds to thousands of kilometres. Meanwhile, the surface currents pattern prevailing over the Aran grounds area (about 1000 km^2) between March-April-May is crucial in determining the spatial patterns of *Nephrops* burrows (see ***Chapter 2 Spatial Analysis***). Besides, 16 years of *Nephrops* targeting resulted in variations in the density distribution between sub-area in FU17 (see ***Chapter 2 Spatial Analysis***)

We see factors of influence are of diverse scales of order and type and encompassing it is needed for developing simple representations of this complex system (Allen and Holling, 2002) in order to detect and assess disturbances and/or changes in this ecosystem.

Thus, monitoring resilience (*i.e*. perturbations of the system) requires records of key variables presumed to reflect the underlying dynamic(s) that shape the current state of the studied system.

Examples of key variables include the trophic relationships and position of *Nephrops* with the wider ecosystem, making necessary to acquire information about the functional trait(s) of *Nephrops* within the ecosystem and the food web in order to analyse the potential consequences (*e.g.* response diversity, redundancy) of the dramatic decreased of burrow number passing from 947 million burrows in 2002 to 383 in 2014 (Anon.,

2018).

Functional properties of species have been suggested as an important determinant in how biodiversity interacts with ecosystem processes and resilience. And, based on these properties, species can be organized into different ‘‘functional groups’’ representing a collection of species that share some common attributes (defined by the investigator): for example, species trophic position, morphology, size, physiology, mobility, taxonomic background, or a combination of these (McGill et al., 2006; Nyström et al., 2008; Angler et al., 2015).

Thus, this notion of resilience clearly reactivates the need of a broader view of the *Nephrops* fishery, that is to say, an ecosystem approach (Vasilakopoulos et al., 2015, 2017). However, determining the operational limits (that is, the framework) is not straightforward (Link et al., 2014; Allen et al., 2015; Allen et al., 2016) but we could (*i*) explicitly utilise the geographical boundary of the quite homogenous seabed habitat of *Nephrop*s of the Aran grounds mud patch, to inform the prevailing geo-chemical, organic matter component and flux and primary production over this area), (*ii*) evaluate the fishing pressure endured (for each targeted species) in relation to the context and historical background of the fishery industry over the area including the potential side impact on life in the seabed within this period and (*iii*) link the main targeted fishes (among them *Nephrops norvegicus*) and bycatches from a food-web and functional group perspective in order to delineate the initial level of an integrating approach of the fishery in Aran grounds.

Within this framework, identification of ecological functions is facilitated and potential perturbations of species distribution more perceptible. The workability of this methodology requires cross scale variability in the use of biotic and abiotic signals that is the definition of panarchy[18] (Gunderson and Holling, 2002; Allen and Holling, 2002; Allen et al., 2015). Thus, spatial resilience is just a means to identify the “of what” and

18 panarchy: “derived from the Greek god of nature, Pan, combined with archy, from the Greek for “rules” and hence “rules of nature” is a term used to describe how variables at different scales interact to control the dynamics and trajectories of change in ecological and social-ecological systems (Gunderson et al. 1995; Holling 2001; Gunderson and Holling, 2002). Panarchy is a theory suggesting that in ecological and other complex systems, abrupt changes occur as a result of the interaction of slow, broad variables with smaller, faster variables” (page 431 in Foundation of Ecological Resilience edited by Gunderson L. H., Allen C. R., Holling C. S., 2010).

the "to what" of resilience (Carpenter et al., 2001) in a more manageable roadmap, or in other words, an endeavour to operationalise it in a real-ocean-world in order to avoid being lost in the maze of its many facets (Standish et al., 2014; Brown and Williams, 2015).

Interest in quantifying resilience has led to the development of a statistical toolbox adapted to temporal and spatial data types, within a chart flow scheme (Dakos et al., 2012; Kéfi et al., 2014; Dakos et al., 2015; Scheffer et al., 2015; Dakos et al., 2017) to detect and interpret underlying dynamics. For instance, Spanbauer et al. (2014), using the Fisher Information indicator with palaeoecological records of diatom species abundance of Foy lake, pinpointed early signals of an "impending regime shift" that took the form of a prolonged instability augmenting a decrease in resilience. But more importantly, these authors underscored the likelihood of not detecting an ongoing ecological transition or regime shift as suggested by Hastings et al. (2010), which would have helped managers to adapt quickly. In fact, from the resilience perspective, the inadequacy of various fisheries regulatory regimes (open access, limited entry, individual transferable quotas, or territorial use rights) to respond to latent environmental changes affecting either the distribution or abundance of targeted species could produce deleterious effects as suggested by Ojea et al. (2017).

Nonetheless, we can easily measure the advantages of questioning the resilience of *Nephrops* from the Aran grounds.

(B) Towards an ecosystem approach of fisheries management

(B.1) Widening the field of view

An integrated approach of fisheries management implies a broader view of fishing activity in relation to the marine system and requires examination of various natural and anthropogenic factors of influence at multiple levels at which an "ecosystem approach" can be adopted in practice (Link and Browman, 2014).

For instance in Celtic Sea, Merillet et al. (2020), using the species assemblages from 2000 to 2016 from a dataset of 1,175 hauls from bottom trawl surveys (EVHOE), found that "fishing was an important factor structuring species assemblages at the beginning of the time series (2000's) but decreased in importance after 2009, likely caused by a

change in spatial distribution of fishing effort, following a change in targeted taxa". In addition, the commercial species are a very small part of marine biodiversity but the quantity extracted is far from being negligible in the context of a food-web (Pauly et al., 1998, 2003, 2010; Branch et al., 2010) and habitat impact (Jennings et al., 2001a; Kaiser et al., 2006; Hiddink et al., 2007; Hiddink et al., 2017).

In the Aran grounds, the *Nephrops* population has endured many years of low abundance (under water TV surveys, see ***General Introduction***) and its effects on the local marine community structure should be investigated and so in connexion with the perturbations already experienced by the ecosystem (*e.g. Gadus morhua* stock collapse). Management of the population on the Aran grounds should be linked to the concept of community functioning (biotope). Then, by reporting the biodiversity observed at each surveyed station, the UWTV footage can help in our understanding of the dynamics of the benthic communities. These collected ancillary sources of information cover zones of shallow and deep water (Galway Bay, Slyne head grounds and Aran grounds and Porcupine Bank for example) reflecting the variability of its habitat.

Unfortunately, most of the time, the ecosystem approach is a management option rising when the targeted stocks are already threatened and then, this integrated system is identified and associated with stringent regulation policies that are required for stock recovery and, indeed, logically perceived as severely restrictive for fishers. Such a scenario does not serve the purpose of obtaining buy-in from stakeholders.

(B.2) Sorting between vessels

The path towards an integrated management system requires of researchers to evaluate the performances and ecological impact of the operating fleets.

In Aran grounds, although a number of specialised vessels were recently observed, the bulk of the fleets off the coast of Ireland involved in the *Nephrops* fishery still target multiple commercial species and areas. Thus, sorting among "virtuous/sinful" fleets appear indispensable regarding the decreasing abundance of the FU17 population (see ***Chapters 1 Time Series Analysis and Chapter 3 Stock Assessment***).

Gascuel et al. (2012, 2014) provided a practical attempt to map the performance versus the impacts of fishery activity on specific areas despite the lack of vessel monitoring system data. For the North Sea and Celtic Sea (referring to VII-e-f-g-h-j-k, IIIa, VI-a-b-

c, and VII-d ICES subdivisions) the authors were able to identify some fleet segments that exhibited poor-to-important economic performances with low-to-high ecological impacts

By translating fishing activity into geographical dimension, VMS data made such analysis easier to implement in Aran grounds and, potentially higher resolution increasingly accurate. It is of note that Hinz et al. (2012) warned about the subterfuge of the "confidentiality rights of fishers" evoked by European officials in charge of fishery questions to restrain VMS data accessibility and acquisition of higher spatial resolution data. A situation that will forcefully lessen the number of studies and analysis from the research community that is, yet, fundamental for progressing the field.

(B.3) Indicators for what?

For an integrated fisheries management, the indicators should reflect features related to diversity, biomass, size structure, trophic levels, nutrients cycling and the flows of energy (such as respiration-consumption-production, initially modelled by Odum in the 50's) and assessing the environmental and socio-economic descriptors in achieving the prescribed goals for which it was implemented in the first instance is needed.

Fulton et al. (2005) have evaluated the "robustness" of a list of indicators using a biogeochemical ecosystem modelling approach representing the dynamics of populations, communities, habitats and the food chain including fishing effects. Their simulations underscored that there is no unique indicator capable of delivering a thorough picture of the state of the ecosystem. Rather, a suite of tools, each focusing on different attributes and based on different data types are needed (**Table 3.4** in Fulton et al., 2005 for guideline details). Appropriate indicators should (*i*) first, target the species with a "fast turnover rate", such as primary producers like phytoplankton, zooplankton and bacteria, that are considered to be very sensitive to any alteration in the system; (*ii*) secondly, consider the species fished, including by-catch, as a useful tool to assess the current status of that part of the food-web and then evaluate this by looking at trophic structure, using "fishing down the food-web" (Pauly et al., 1998) and "fishing through the food-web" (Essington et al., 2006) impacts; (*iii*) and thirdly, because of its fundamental role in carbon and nitrogen cycling and recycling (Hill, 2007) enhance the integration of the benthic community into the ecosystem qualitative-quantitative

appraisal of the fishing activity and so in link with the potential macrobenthic community perturbations of the fishing activity (Jennings et al., 2001a; Hiddink et al., 2007; Hiddink et al., 2017). Finally, managers should (***iv***) select animals at the top of the food web that convey information on how heavily the food chain has been impacted by human activity. Usually it is species featuring relatively slow life history dynamics (*e.g.* pinnipeds, toothed whales…etc.).

Fulton et al. (2014) assessed the complex trade-offs that exist when trying to satisfy the various ecological, economic and social objectives at the heart of this ecosystem approach. Each of the management strategies explored was proven to have their own set of strengths and weaknesses. Fulton et al. (2004, 2007, 2014) highlighted the key role of the spatial dimension in the relative success of any management policy. Although, such ecosystem based fisheries management system requires a huge amount of information we should start by implementing simple models that take advantage of already available information and case studies that can feed into an ecosystem approach for the Aran grounds and then becoming the framework for an integrated fisheries approach of *Nephrops norvegicus.*

(C) The spatial dimensions of *Nephrops*

(C.1) Adapted growth and patches

The relatively high geographical variability in the size structure inside a functional unit stock is one of the salient feature of this species (Tully and Hillis, 1995; Tuck et al., 1997a; Eiríksson et al., 1999; Haynes et al., 2016; Merder et al., 2020). This illustrates admirably its sensitivity to the environment at different scales and in relation to interaction between individuals (Sbragaglia et al., 2017; Merder et al., 2020) taking the form of a patch organisation (see ***Chapter 2 Spatial Analysis***). Rather than evoking an inherent difficulty to establish demographic parameters, routinely required for a classical stock assessment, we should instead underline the animals capacity to exist at different geographical scales, likely, in relation to local food availability, water temperature, hydrodynamic conditions and sediment type. This reflects the resilience of the stock underpinned by phenotypic plasticity.

Also, latitudinal variations in L50/minimum berried size of female *Nephrops* in the

North-East Atlantic and Mediterranean waters, tended to indicate relatively higher values in the more southerly areas, lower values in the intermediate latitudes (55º–43º North) and more transitional values at the most northerly latitudes (figure 2.22 in Eiríksson, 2014). This geographical gradient illustrates the species response (*i.e.* fitness) to variability of the prevailing biological and physical factors (*e.g*. density, water temperature…etc) exerting influence on growth rate and hence size at maturity.
Within Clew Bay situated at the northernmost end of the Aran grounds, Merder et al. (2020) detected density dependent effects on growth and survival over a study area of approximately 500x500 m^2. The spatial distribution of the (smoothed) growth was found to be higher in peripheral areas for males while female growth tended to be higher in the central (more) fished area. In addition, highest variance in growth was recorded at between 10 and 15 m for males and the presence of growth rate heterogeneity within sampling circles below 20 m was identified for females.
Thus, the next challenge is to evaluate the appropriate spatial scale for assessment in terms of population organisation (*i.e.* number of patches and their dimensions; see ***Chapter 2 Spatial Analysis***) and the bio-physical components prevailing at this geographical level. In this regard, the geostatistical analysis (see ***Chapter 2 Spatial Analysis and Annexes B***) could contribute to the selection of sub-areas and the design of a finer sampling grid to investigate this aspect of *Nephrops* monitoring, without excessive cost implications.

(C.2) The geographical range keys

In the case of *Nephrops,* total allowable catches within the European Union are agreed internationally at ministerial level, with a proportional allocation used to determine the quotas for individual nations. In the Republic of Ireland "a pool system with monthly allocations which are the same for each vessel within a certain group" is utilised (Ungfors et al., 2013). In practice, the Aran grounds catch options are decided using information derived from a fishery independent survey (see ***Chapter 3 Stock Assessment***).
Nevertheless, the issue of the appropriate spatial scale for monitoring is recurrent and for good reasons. In several parts of this study I simultaneously had recourse to the functional unit (FU) and beyond in order to provide a better understanding of the

dynamic of landings and then an efficient management strategy (see ***Chapter 2 Spatial Analysis & Chapter 1 Time Series Analysis***). For instance, the ripple effects on Aran grounds landing levels in response to a new regulation implemented in the Porcupine Bank (FU16) was evident, suggesting that managers can digress from the current functional unit spatial template (*i.e.* FU) and adapt. The implementation of an ecosystem approach will undoubtedly require a new spatial scheme.

Defining fishing grounds informs the space allocation of the marine resource among all users and spatial tracking records of fleets is fundamental for this purpose.

In the Aran grounds, where *Nephrops* fisheries are dominated by otter trawlers, vessel monitoring system (VMS) positional data (Gerritsen and Lordan, 2011) coupled to kriging analysis revealed that fluctuations in burrow density between 2002-2014 resulted in a redeployment of fishing effort to the periphery as a result of a depletion of the stock in the historically targeted central zone (see ***Chapter 2 Spatial Analysis***). A map of the spatial distribution of fishing effort and activity including fishing over all zones and types of gear is required, particularly since there has been an expansion in the use of marine protected areas and/or seasonal closures as tools for implementing a sustainable fishing scheme. In the case of England, Jennings and Lee (2012) underlined the importance of the relationship between landing weight and value, which was deemed to convey more information regarding the geographical distribution of fishery activity.

Exploring and improving this approach in terms of space and time will provide a better understanding and analysis of the "sea users" and will undeniably ease the management and the monitoring of fishing activities in the overlapping zones of interest, and help to quantify by-catches and allocated quotas, including information from vessels that originate from multiple countries.

Rijnsdorp et al. (2011), Kraak et al. (2012) and Dolder et al. (2018) gave a glimpse of the extent of possibilities for management purposes offered by these spatio-temporal data provided that the spatial and temporal scales are adequate.

Nephrops norvegicus is a benthic species mainly captured by bottom trawling gear which is by far the most wide spread cause of disturbance of the seabed in Eropean Union (Jennings et al., 2001a; Hiddink et al., 2007; Hinz et al., 2009; Reiss et al., 2009; Lambert et al., 2012; Hiddink et al. 2017). In such circumstances, VMS information

(although limited to vessels > 12 m) provides much more precise measures of fishing in space and time. As pointed out by Hinz et al. (2012) the fishing effort distribution pattern in general has been found to be markedly sensitive to grid resolution (Mills et al., 2007) and patchily distributed on larger scales (> 1 nautical miles), whilst it tends to be randomly distributed below 1 nautical mile (Rijnsdorp et al., 1998). Then the design of any indicators quantifying the spatial distribution of fishing and more specifically the benthic response to it, must consider spatial scale otherwise the reliability of the measures would be undermined.

(D) Climate strands: recruitment in jeopardy?

By highlighting the impact of both the North Atlantic Oscillation and the Arctic Oscillation on the Aran grounds and Porcupine Bank landing dynamics and pointing out the (positive and lagged) significant correlations between NAO and the Irish Sea harvest of *Nephrops* (see ***Chapter 1 Time Series Analysis***) evidence is provided that major yields off the coast of Ireland are subject to climatic influence, and, implicitly, underscores the necessity to include it in any assessments that provide management advice, even though catches from other areas, such as the Smalls did not appear to be influenced by either of these large scale indices.

In the results contained in the reports of the inter-governmental panel on climate change (IPCC, 2013, 2014, 2019) we have now an appropriate framework to investigate and evaluate environmental forcing on marine populations around Ireland in general and *Nephrops norvegicus* in particular. In fact, observed shifts in chemical, physical and biological processes of the ocean system have been examined and discussed by scientific working groups of the IPPC and ultimately modelled to assess the consequences on either the planet or at a regional level. Of course, the reliability of these projections relies on the degree of uncertainty in our knowledge, as seen in this study. However, the train has gained momentum and we should take advantage of the progress made through the IPPC's rounds in order to explore the projected impacts on *Nephrops* (and other species) along the coasts of Ireland.

(D.1) A warming ocean

Thus, what are these key findings that entail risks upon the *Nephrops* stocks in short or long terms?

According to the IPCC (2019) terminology, it is virtually certain (*i.e* > 99% probability) that the upper ocean (0–700 m) has warmed by 0.33 W m^{-2} (±0.03) from 2005 to 2017 (fluxes in W m^2 are averaged over the Earth's entire surface area, Table 5.1 in IPCC, 2019) and very likely (*i.e* > 90% probability) to have been stratifying since 1970. The upper 200 m stratification increase is in the very likely (*i.e* > 90% probability) range of between 2.18–2.42% from 1970 to 2017 (section 5.2.2 in IPCC, 2019). In addition, in response to ongoing ocean carbon uptake, the ocean is continuing to acidify and evidence is increasing that ocean's oxygen content is declining (section 5.2.2.3 Box 5.1; Table 5.2 in IPCC, 2019).

Of note, the depth range of the Aran grounds population distribution is within the upper 75 m of the water column, and it is expected that this changing ocean features will be more prominent in the near future (Table CB1.1 in IPCC, 2019).

(D.1.a) Depressed pycnocline

This stratification of water will undoubtedly act during the resident time of Zoe larvae within the top 40 metres where they experience a vertical migration between dusk and dawn, rising to within 20 m depth (Hillis, 1974; Hill, 1990a; Hill et al., 1990b, 1997). In fact, higher water temperatures will likely deepen the pycnocline and consequently the zone of trapped nutrients. In addition, the successive stages of larvae (I-II-III-VI) preceding the settlement phase on the seabed are temperature dependent and their resilience (fitness) to the predicted warming trend is clearly unknown.

(D.1.b) Diminution of oxygen

Hypoxic conditions have already been reported in the Kattegat and the Adriatic (Bell et al., 2006) and this phenomenon can cause severe disruption to the natural behaviour of emergence patterns, locomotory activity as well as mass mortality if dissolved oxygen [O2] drops below ~25%. Juveniles appear to be more sensitive to hypoxia than adults (Eriksson et al., 1997). In addition, in the long term, even a moderate hypoxia would alter the rate of growth due to the direct impact on the

metabolism.

(D.1.c) Shifting distribution

Shifts in spatial distribution of marine species in the North-East Atlantic have already been documented (Engelhard et al., 2014). Beaugrand et al. (2014) investigated the expected spatial distribution of abundance of *Calanus finmarchicus* as a function of sea surface temperature, photosynthetically active radiation, and chlorophyll-a concentration data. Their results showed that an increase in temperature is expected to generate a poleward shift in the species spatial distribution. Then, we can presume multiple and complex side effects for local food-webs: like a concomitant movement of species feeding on relocated copepods, dramatic falls and increase of others etc…
The planktonic community structure would then likely be deeply altered, engendering a cascade of reactions diffusing the food-web.
Since for *Nephrops* the success of the settlement phase and recruitment relies on the hydrological mechanisms allowing the retention of the eggs and larvae over the suitable type of seabed substratum (Hill et al., 1997) it is very likely that any shift, even temporary, in the weather conditions (e.g. wind, storms) that could disrupt this short favourable environmental window would seriously impair the sustainability of the Aran stock. In particular, as underlined previously, wind duration-direction-intensity has an impact on the variability of *Nephrops* abundance (see ***Chapter 2 Spatial Analysis***). In addition, in the case of *Nephrops* such a profound disorganisation could also affect the host parasite dynamics, by augmenting the prevalence of the infection by *Hematodium* sp. (Stentiford et al., 2001; Briggs et al., 2002a) and ultimately, threaten abundance.
Styf (2014) carried out the first ever analysis of the effect of multiple stressor changes caused by altered climate conditions, for instance, ocean acidification, hypoxia, manganese [Ma2+] exposure, temperature and salinity on the early developments of *Nephrops* such as embryonic development (yolk amount), larval stage (Zoe I-III), juveniles and finally egg-bearing females with fanning activity. She showed the importance of the synergistic effects of these water compounds contrasting with the lack of impact when dealing with a single one. Interestingly, the author also suggested that genetic variation may explain the range of tolerance observed among individuals of the

same life stage which could be related to the (maternal) genotype tolerance ("similar to the urchin *Heliocidaris erythrogramma* example of maternal transmission"; *cit.* Schlegel et al., 2012 in Styf, 2014) giving weight to the argument for fishery induced evolution.

More recent work continues to quantify the geographical and phenological shifts seen as a result of the global warming (Howes et al., 2015; IPCC SM, 2019). It would therefore be advantageous to formally include the potential climate forcing into the fishery regulation process for *Nephrops*.

(D.2) A North-South response of *Nephrops norvegicus* to climate change?

It is also relevant to highlight here, the pitfall of systematically referring to a climate connection when an undecipherable dynamic trajectory is encountered (Votier et al., 2008).

For instance, according to FAO statistics of captures as also reported by Ungfors et al. (2013), the yield of *Nephrops* from the main Southern waters of Europe have decreased (**Figure 1**) while in northerly coastal areas like the Celtic Sea, Irish Sea, and North Sea, landings are considered more or less stable following a 20–30 years period of increase (see **Figure 1** in ***General Introduction***).

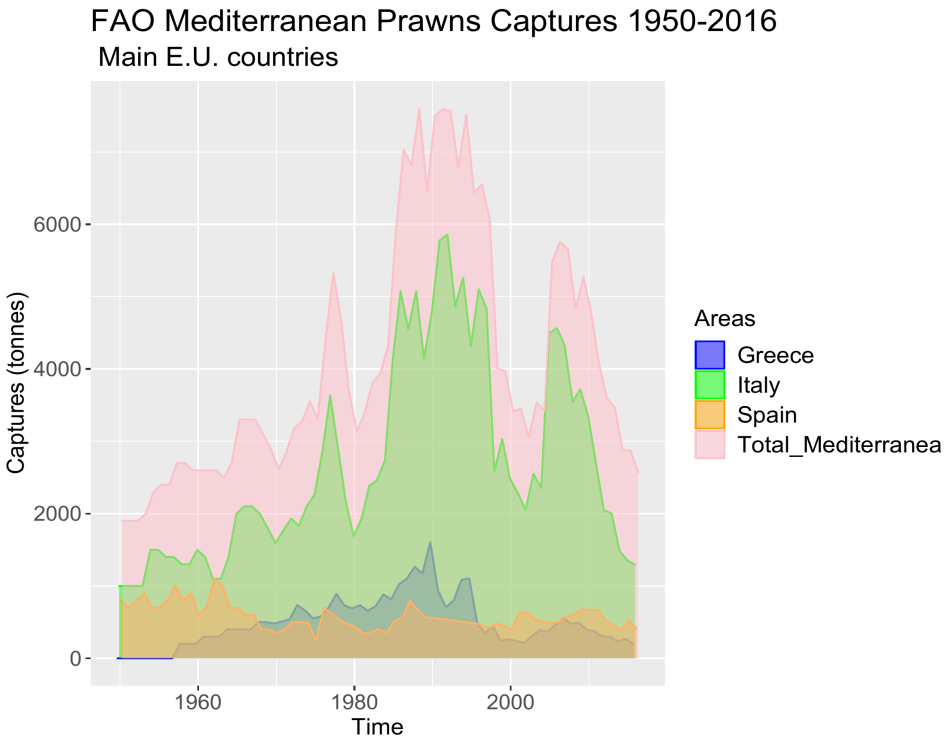


Figure 1: Evolution of *Nephrops norvegicus* Mediterranean captures from 1950 to 2016 (Source FAO, 2018 StatFishJ v2018.1).

Such regional difference in the capture trends promptly caused a south vs north approach of these fisheries in favour of an environmental influence of this putative regional shift.

However, the present study shows that the Aran grounds stock (FU17) should not be categorised as "secure": in fact, the under water TV surveys highlighted the decline of the population in the last decade (2002–2014) and this study pinpointed the likelihood of a longtime overexploitation (see ***Chapter 3 Stock Assessment***). In addition, by undertaking a comparative time series analysis of landings originating from different locations off the coast of Ireland (see ***Chapter 1 Time Series Analysis***) discrepancies between the underlying dynamics in each of the grounds were identified, as well as their different sensitivity to climatic indices like the NAO and the AO, illustrating the fitness of *Nephrops norvegicus* in a delimited geographical range yet inside the northern part of western Europe.

This variability in the adaptive capacity of *Nephrops* populations to fit in with its habitat

is well illustrated by the disparity in the timing of activities such as emergence, retraction, and door-keeping in response to a range of depths, light and hydrodynamic modulation prevalent in the sites (Aguzzi and Sardà, 2008; Aguzzi and Company, 2010). In addition, intra-regional differences in relation to biological attributes such as growth, size at maturity, fecundity potential of females, spawning and hatching periods were observed that underline the importance of examining populations at the appropriate spatial scale. Examining specifically each stock in relation to the fishing pressure exerted on the settlement process does not prevent us from exploring in parallel environmental factors. Nonetheless, while climate change likely has an influence it should not be used to negate the impact of overfishing and cast a shadow over the co-responsibility of many actors/sides involved in fisheries in Europe.

(E) Fishery induced selection

During the second half of the 20th century fishing pressure and its corollaries, namely, discards, by-catch and habitat damage have led to a worldwide decline in the fish resource with few exceptions (Pauly, 2010). And, in 2017, when it comes to evaluate the progress made to achieve MSY objectives in line with the directive 2008/56/EC of the European Parliament and of the Council establishing a framework for community action in the field of marine environmental policy (STECF, 2019), the numbers speak themselves: in North-East Atlantic, for the 64 to 70 stocks which are fully assessed, the proportion of overexploited stocks (*i.e.* $F>F_{MSY}$) is about 40%, and for the 46 stocks for which both reference points are available the proportion of stocks outside the safe biological limits (*i.e.* $F>F_{pa}$ or $B<B_{pa}$) lies around 35%. While in the Mediterranean Sea and the Black Sea, the situation is worse, with 87% of the assessed stocks overfished and a significant lack of knowledge about fishing pressure and reproductive capacity (COM, 2020). And this in a context where the prospects of meeting policy objectives and targets in terms of state of marine ecosystems and biodiversity and pressure and impacts on marine ecosystems are “largely not on track” according to the European Environmental Agency (EEA, 2019 page 134). In fact, the abundance of more than 25% of marine bird species assessed in the North-East Atlantic has dropped considerably, around 40% of Mediterranean elasmobranchs are declining and many are data deficient,

and 33% of the reports on marine turtles under the Habitats Directive[19] were in unfavourable conservation status and 67% unknown (COM, 2020) for instance.
Our inability to learn from such declines and to prevent their aggravation (Froese et al., 2010, 2013, 2018) have revealed our lack of knowledge about the behaviour and ecology of exploited species and more generally the sea. It is therefore reasonable to question whether decades of heavy and selective fishing have induced an evolutionary response (Law, 2000) that could explain the low abundance of *Nephrops*.

(E.1) Investigating fishery induced selection for the Aran grounds stock

Allendorf et al. (2009) highlighted traits likely to be affected by unnatural selection in harvested population: sexual maturation at an earlier age and size/ reduced fertility/ reduced growth rate/ attenuated phenotypes/ reduced weapon size or body size/ altered distribution of reproduction (truncated or altered seasonality)/ Reduced boldness in foraging or courtship behaviour/ potentially reduced productivity/ altered migration routes...*etc*.
Are we in a situation of such induced selection differentials caused by the fishing activity for *Nephrops*?
Along the European coasts of the Mediterranean Sea from Straits of Gibraltar to the Aegean Sea using 6336 hauls from 1994 to 1999 (MEDITS project) Abello et al. (2002) suggested that demographic structure among geographical sectors as well as in total mortality appear to be highly related to different exploitation level. In western mediterranean sea off Barcelona (Spain), Sarda (1998) reported a mean size decrease of carapace length of 4 mm for males and 3.6 mm for females over the past 20 years and considered it as symptomatic of overexploitation of the resource. While, Dimech et al. (2012) showed a non-significant reduction in mean size of *Nephrops* between trawled and non-trawled areas within the Maltese 25 nautical miles fisheries management zone. Closer to Aran grounds, when examining fishing pressure influence on size in Irish Sea

19 Habitats Directive: adopted in 1992, the Council Directive 92/43EEC of 21 May 1992 on the conservation of natural habitats and of wild fauna and flora aims to promote the maintenance of biodiversity, taking account of economic, social, cultural and regional requirements. It forms the cornerstone of Europe's nature conservation policy with the Bird Directive and establishes the EU wide Natura 2000 ecological network of protected areas, safeguarded against potentially damaging developments.

West, Johnson et al. (2013) reported that the length frequency data from catches during recent years (2002–2008) have not dramatically changed from historical levels observed in 1960–1962 (Cole, 1965 in Johnson et al., 2013).

Thus, referring to trait, supposedly impacted by the prevailing fishing regime, is not straightforward, and in the case of Aran grounds such analysis requires historical records of data not at hand in time of this PhD. Also, size at which 50% of female were mature ($L_{50\%}$) recorded from 2002 to 2014 (for selected months June to August) appear highly variable from year to year, showing no evidence of trend (Figure 10.4.2 page 65 in ICES IBPNeph, 2015).

Notice, that similar great variations in carapace length estimates $L_{50\%}$ are seen in certain areas, such as 24–34 mm CL on Icelandic grounds (Eiríksson, 2014), 21–35 mm CL in the Firth of Clyde (Tuck et al., 2000), 21–28 mm CL in the Irish Sea (McQuaid et al., 2006) and 23–31 mm CL off south Portugal (Figueiredo, 1982).

Noteworthy, Johnson et al. (2013) identified significant (spearman) correlation coefficient (ρ) between mean burrow density vs modal carapace length in the catches (ρ=*–0.91, p-value=0.000*), mean weight landings (ρ=*–0.69, p-value=0.001*) and male asymptotic length (ρ=*–0.49, p-value=0.02*) for a number of FUs stock around Ireland and United Kingdom among them Aran grounds. In our spatio-temporal analysis of *Nephrops* distribution from 2002 to 2010, we disclosed a drastic reduction in density of the central zone of our area of interest with less of a reduction seen towards the margins (see **Figures 2.10** & **2.15** in ***Chapter 2 Spatial Analysis***) and reveal an increasing fishing effort towards the periphery (**Figure 2.20a** in ***Chapter 2 Spatial Analysis***). Hence, we surmise potential density-dependent control effect on size and weight accordingly (Merder et al., 2020).

(E.2) An exhausted female stock as a witness mark of a fishing induced evolution?

In Aran grounds, over these 16 years (1995–2010), the April-May-June-July period of harvest corresponded to 46.46% of the whole yield, and April-May-June constituting 40.95% of the landings in weight, with a tendency to lump the fishing activity around this period in the recent years (see ***Chapter 1 Time Series Analysis***). But, it is important to note that this massive removal concurs with the growing rate of females in the catches reaching up to 70% according to the sampling analysis conducted by the Marine

Institute since 2002 (figure 10.3 page 64 in ICES IBPNeph, 2015). The sex ratio is an important biological parameter to inform the sustainability of a commercial stock since it is a crucial component estimate of the spawning stock biomass which in turn is directly involved in the recruitment level and ultimately the yield (Hilborn and Walters, 1992; Jennings et al., 2001b; King, 2007; Haddon, 2011).

In addition, on the basis of a length frequency data, the GTG-LBSPR (Hordyk et al., 2016) estimates of the potential recruit of the Aran grounds stock showed worrying levels of the female spawning potential ratio from 2006 to 2014 (**Figure 3.16** in ***Chapter 3 Stock Assessment***). Does it affect the reproductive success of *Nephrops* in the Aran grounds and influence its resilience?

Obviously, in the case of the Aran grounds stock, there is a pressing need to incorporate this removal into stock assessments. When removing larger and more active females we might expect negative feedback on reproduction success through the viability of offspring in particular. As the reproductive strategy of *Nephrops* is characterised by active female care of extruded fertilised eggs mainly consisting of oxygenation by pleopod ventilation (fanning activity). In addition, the embryonic development stage that varies from 6 to 10 months depending on latitude and corresponding to the burrow retreat of females (Farmer, 1975, Sardà, 1995; Mori et al., 1998) is sustained throughout that time by the relatively large amount of yolk. Therefore, a weakening of the female population by fierce fishing selection could alter the quality of this nourishing substance and further affect the recruitment rate. For instance, according to Eiríksson (2014), in South West, South and South East waters of Iceland, variations in sex ratio of prawns were observed and relationships were found between female sex ratio and carapace length, catch per unit of effort and stock biomass during 1961–2010, displaying apparent fishery-induced effects on sex ratio.

Is this key role of females already threatened in the Aran grounds?

It is important to consider this matter by examining the potential side effects caused by a departure from the steady sex ratio. The absence of *in situ* measurements should not prevent us from considering, in conjunction with the overexploitation underlined in this study, this hypothesis for explaining the decrease in abundance.

We see, “Fisheries induced selection affects any trait that determines how individual fish are exposed to fishing. And to the extent that the affected traits possess any genetic

variability, the resultant selection differentials become incorporated into a fish population's gene pool" (*cit.* Heino et al., 2015).

After decades of intensive exploitation of the Aran stock coupled with a dramatic decline in abundance, the likelihood of a fishery induced evolution is high and it would be useful to evaluate it. In fact, such effect will determine the appropriate time scale of the stock recovery scheme necessary to potentially undo/reverse the directional selection caused by fishing, acknowledged to be very long (Law, 2000, 2007).

Conclusion

From an assemblage of assessed stocks to an ecosystem mindset?

There are very contrasting dynamic patterns of *Nephrops* populations off coast of Ireland (see ***Chapter 1 Time Series Analysis***) illustrating the fingerprints left by the local history of the harvesting strategies and the ecosystem characteristics of the area of interest. By conducting an evaluation involving data collected at different spatial and temporal scales the assessment of the status of the *Nephrops* stock in the Aran grounds has been enhanced.

However, the results should be regarded as a "quantitative" approach of the assessment rather than an ecosystem approach. The amount harvested (in weight and/or numbers) was used to portray the state of the abundance, ignoring the broader aquatic context of fishing like modification of habitats, restructuring of trophic linkages, change in the demographic structure of prey and predators, change in ecosystem productivity, modification of energetic pathways, change in genetic diversity or frequencies and species invasions, among others potential effects (Fulton 2004).

Already in 1900, Walter Garstang[20] (1900) made it explicit in his essay investigating the alleged depletion of the benthic fisheries of England and Wales: "*We have, accordingly, so far as I can see, to face the established fact that the bottom fisheries are not only exhaustible, but in rapid and continuous process of exhaustion; that the rate at which sea fishes multiply and grow, even in favourable seasons, is exceeded by the rate of capture. The rate of exhaustion is shown to be different for different species of fish. The more valuable flat fishes, plaice and prime fish, show the most marked signs of diminished and diminishing abundance. These differences should obviously be noted, and if possible still further elucidated, in order that the difficulties in the way of remedial measures may be intelligently anticipated and met.*"

Since then, the Food and Agriculture Organization (FAO) of the United Nations reported that, worldwide, the fraction of fish stocks that are within biologically sustainable levels have decreased from 90% in 1974 to 65.8% percent in 2017, meanwhile, the percentage of stocks fished at biologically unsustainable levels

20 (1868–1949) Professor of Zoology in charge of Fishery Investigations under the Marine Biological Association; late Fellow of Lincoln College, Oxford.

increased from 10% in 1974 to 34.2% in 2017 (page 47 in FAO, 2020). And in this regard, in 2020, Europe is not outdone exposing the clear failure to meet the "maximum sustainable yield" goal (EEA, 2020).

Thus, the ecosystem approach to fisheries explicitly reinstates fishing activity within the limits of ecosystem functioning, and, this ecological integration, augmented with economic and social objectives into the management of the fishing activity in specific geographical areas, will result undoubtedly in the mitigation of the current yield and hence the derived incomes. Hence, finding a socially viable pathway will require from the whole society a clear will to communalise this cost.

Without undermining the existing concepts to evaluate the stocks status (Murawski, 2000), it is undeniable that moving further towards such integrative management approach will require us to modify thoroughly the management guidance and goals (Pitcher and Pauly, 1998; Pitcher, 2001, 2005; Link et al., 2014; Link et al., 2019).

To depart from the ancient world

For instance, in their attempt to accommodate the complexities inherent in combining single and multispecies fisheries management Kraak et al. (2012) and Dolder et al. (2018) still illustrate the ancient "world[21]" despite referring to an ecosystem approach of management. How?

Both approaches are spatial in the sense that the fishing area is discriminated in terms of assemblages of fish caught (Dolder et al., 2018) and tariffs that could be applied to fishing in particular locations and time following Kraak et al. (2012).

The results from Dolder et al. (2018) use the spatial dimension of the marine ecosystem in fisheries management, recalling the spatial arrangement of the ecosystems components and its role over the spatial distribution of species but also in the dynamics of ecosystems as explicitly stressed in Holling (1992) and how relevant to the human use of the natural resources it is (Cumming, 2011).

Similarly, recognising the spatial variability of the fishing pressure in agreement with the species density distribution and its habitat impact, Kraak et al. (2012) use the direct, precise and accurate measure of fishing effort as determined from satellite VMS to

21 Antonio Francesco Gramsci (1891–1937) "The crisis consists precisely in the fact that the old is dying and the new cannot be born; in this interregnum a great variety of morbid symptoms appear". Prison notebooks 1971.

optimise the management. Both illustrate the utility of the spatial approach of the effort for controlling mortality of particular target species or assemblages. However, the aforementioned cases only provide new implementation of the same management that led us where we stand now.

Kraak et al. (2012) advised to assign increasing involvement of industry although they have always been in the heart of political/economic decision at national and European level through surrogates (or proxies), then, why should it be workable this time?

In contrast, the ecosystem approach to fisheries management requires introducing a selection of state variable(s) in the management of stock(s) and where the ecological attributes as well as the socio-economic aspects of the exploitation of the marine resources should explicitly lead the management process (Jennings et al., 2005; Jennings, 2011, 2012; Fulton et al., 2004, 2005). However, from my point of view, the willingness to depart from the ancient "world" relies essentially on the ability of the selected state variable(s) to produce a vivid account of the health of the sea in order to favour a move towards a high resilience of the ecosystem and not a repeated path to *MSY*.

However, those currently concerned with fishing activity and its environmental consequences cannot agree how to solve the problem. More stringent guidelines are claimed, others argue that attempting to regulate more and more will be counterproductive and worsen the situation; and arguments for privatisation, public regulation, or regulation emanating from those directly involved (fishers) are recurrent once a new depleted stock is reported or "*MSY* objectives not reached (EEA, 2020)

Could the "commons" pave the way to a new approach of the sea?

In Europe, reference to "commons", from sea users, coined centuries ago as reported by Dyson (1977) and quoted in Pauly and Maclean (2003): [by 1376, only some six years after the introduction of the trawl, trap fishers petitioned the king (Edward III) about the decline of fish the trawl was causing by "destroying the flowers of the land beneath the water, and also the spat of oysters, mussels and other fish upon which the great fish are accustomed to be fed and nourished." And "by which instrument in many places the fishers take such quantity of small fish that they know not what to do with them; and

they feed and fat their pigs with them, to the great damage of the Commons of the Realm and the destruction of the fisheries."].

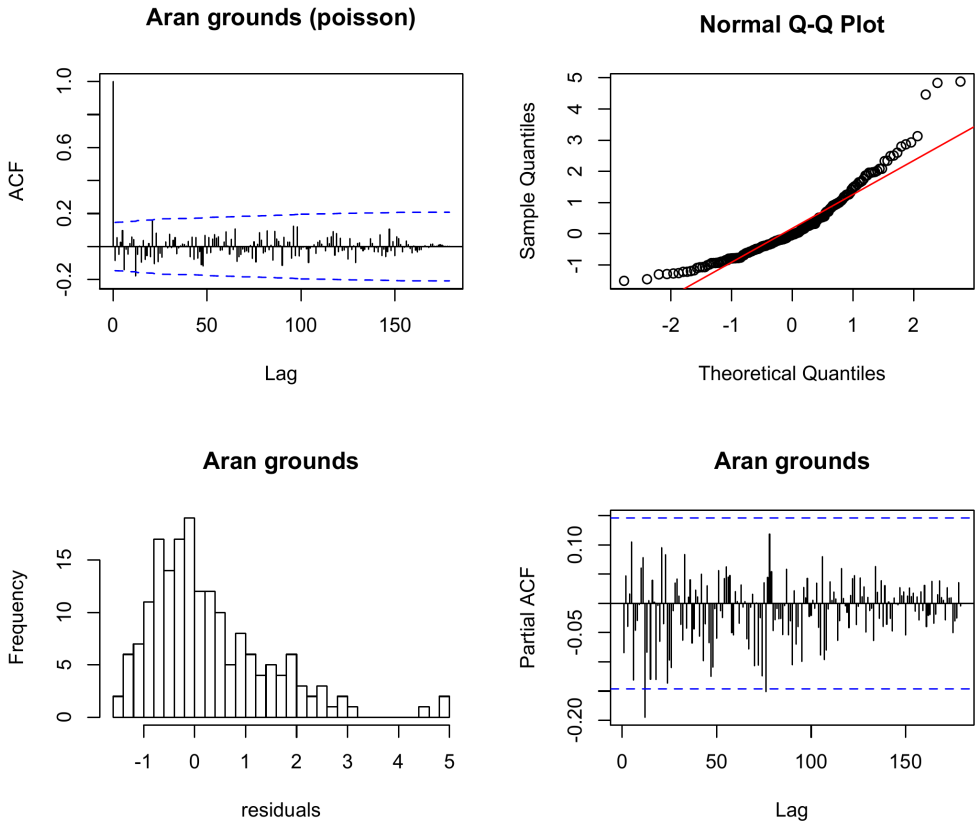
Thus, we see that "commons" combine resources (common pool resources), citizens (or a community), rules, and standards negotiated in a cooperative framework to manage a shared resource (Ostrom, 1990). And of course we observe diversity of behavioural and institutional determinants that are at the source of the use of common resources and "illustrate the capacity of individuals sharing a commons to extricate themselves from various types of dilemma situations and to escape tragic outcomes" (Ostrom, 1990). Thus the "commons" is a political thought which has run through many societies for many generations and resurfaces now in a situation of disruption of the ecosystems, challenging our capacity to drop failed rules of management and consider other motivations.

From my point of view, we should extend the community sense beyond the fishery Industry and national representatives and encompass a broader view involving the ecosystem (itself) as a rightful member, and, be able to change our stand point in order to perceive our human shaped world from an ecosystem side. In fact, the past abundance and size of the current depleted species either 50, 100, or 1000 years ago, are in many cases well informed (Finney et al., 2000; Pitcher, 2001) witnessing a not so distant past that created the circumstances enabling our current way of life and that, in the same way, could help selecting desirable and realistic objectives for an ecosystem approach and from a marine ecosystem standpoint (Pitcher, 2005).

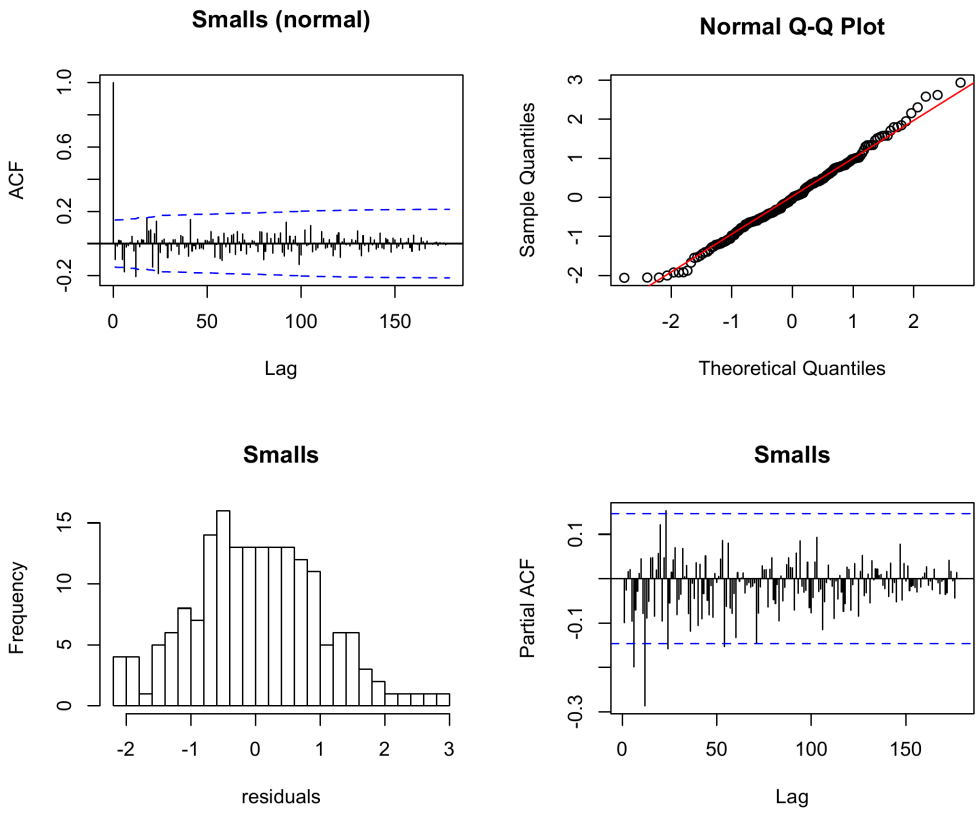
Thus, in my opinion the willingness to depart from the ancient "world" resides mainly in the choice of the ecosystem state variable(s) introduced in the management and its power to shape the whole ecosystem approach to fisheries management and be the pivotal of its implementation.

Annexes A

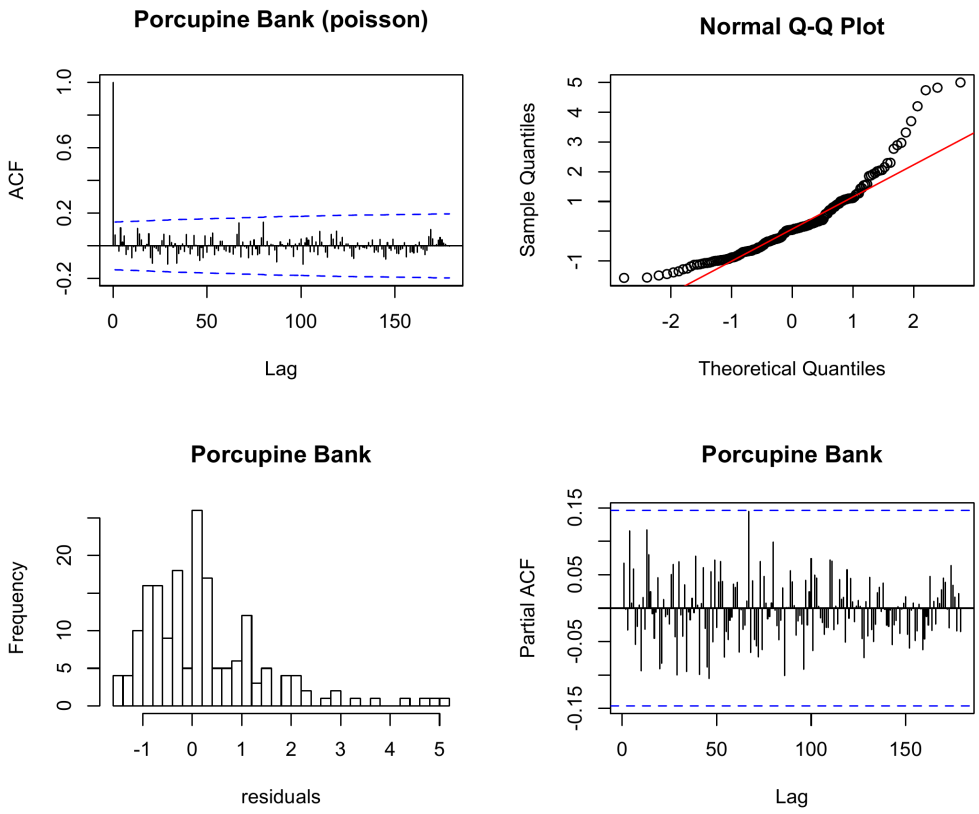
(a)


Aran grounds (poisson)
ACF
Lag
Normal Q-Q Plot
Sample Quantiles
Theoretical Quantiles
Aran grounds
Frequency
residuals
Aran grounds
Partial ACF
Lag

(b)


Smalls (normal)
ACF
1.0
0.6
0.2
-0.2
0
50
100
150
Lag
Normal Q-Q Plot
Sample Quantiles
3
2
1
0
-1
-2
-2
-1
0
1
2
Theoretical Quantiles
Smalls
Frequency
15
10
5
0
-2
-1
0
1
2
3
residuals
Smalls
Partial ACF
0.1
-0.1
-0.3
0
50
100
150
Lag

(c)


Porcupine Bank (poisson)
ACF
Lag
Normal Q-Q Plot
Sample Quantiles
Theoretical Quantiles
Porcupine Bank
Frequency
residuals
Porcupine Bank
Partial ACF
Lag

(d)

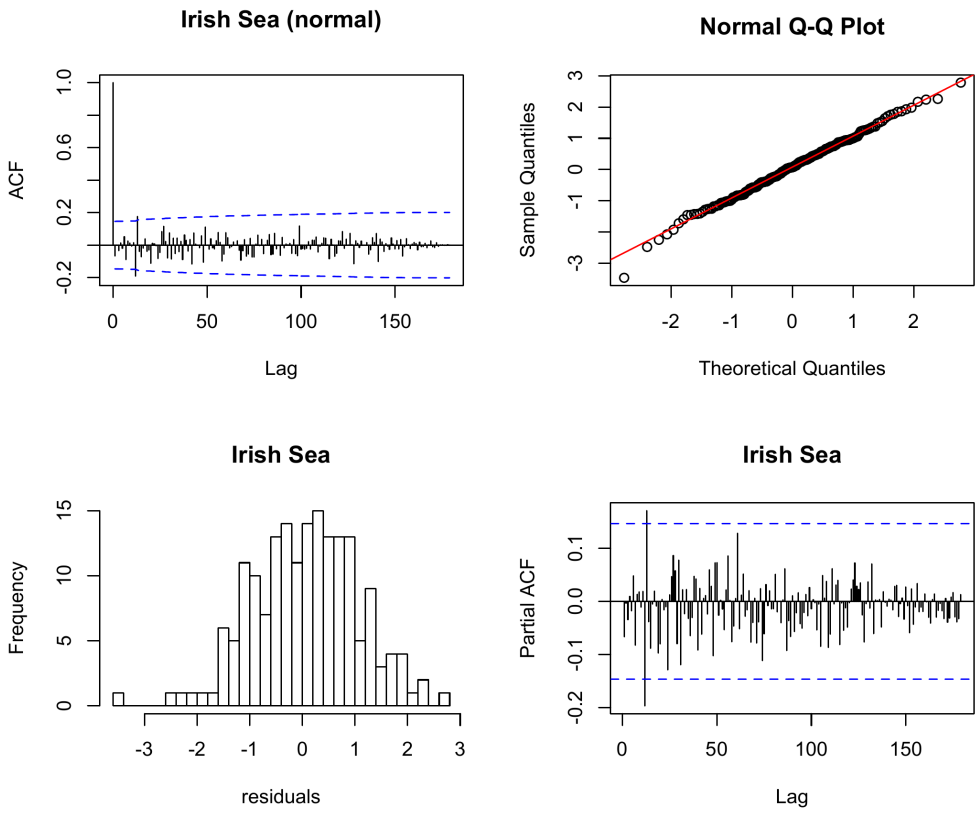


Figure A1a-b-c-d: Diagnostic tools of the standard prediction error residuals of the state space model fits using A*uto-correlation function* (*ACF*, **top left**), *Normal quantile-quantile plot* (**top right**), histograms (**bottom left**) and *Partial auto-correlation function* (*PACF*, **bottom right**). Residuals of Aran grounds and Porcupine Bank are derived from state space modelling with *Poisson* distribution while Smalls and Irish Sea residuals stem from state space modelling using *Normal* distribution

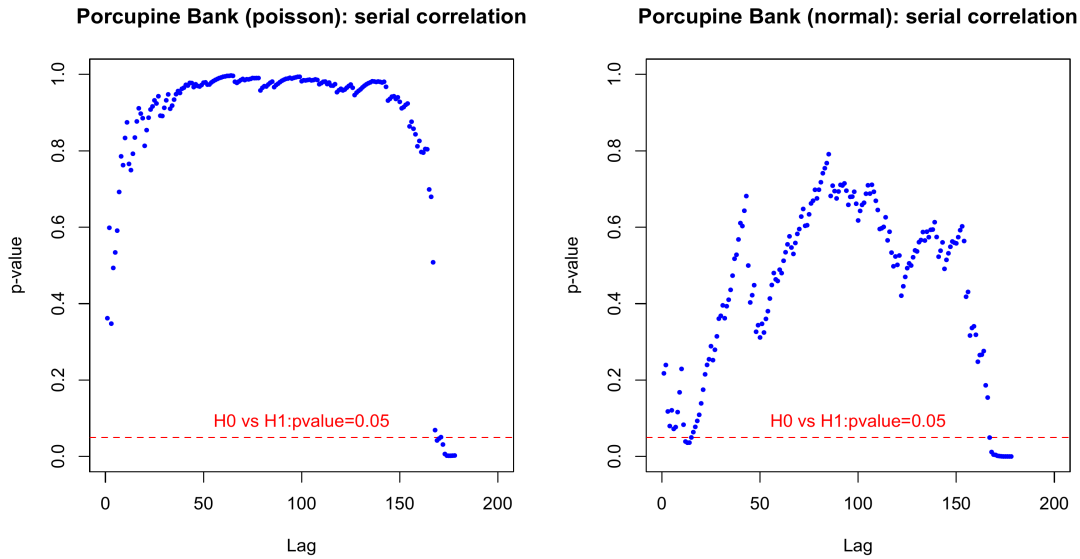


Figure A2: Porcupine Bank *Ljung-Box test* of serial correlation of the *Poisson* (**a**) versus *Normal* (**b**) state space modelling fits of the 1995–2010 lpues time series.

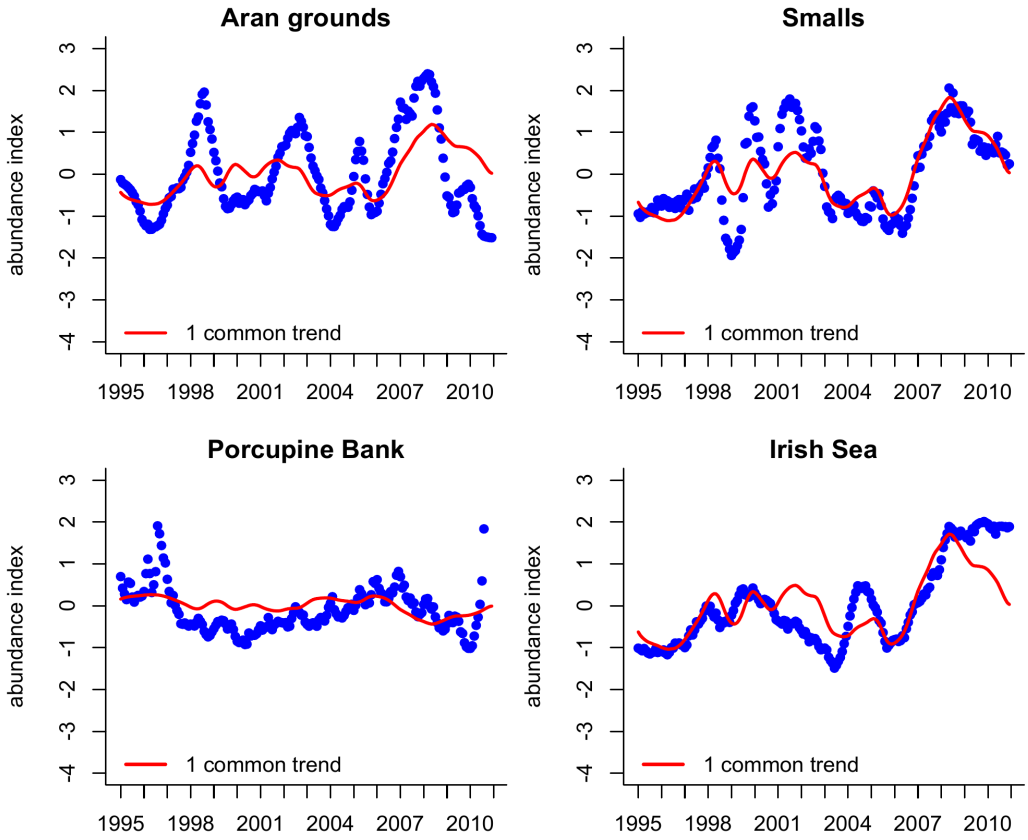


Figure A3: Dynamic Factor Analysis fit of the observed 1995-2010 standardised lpues times series of Aran grounds, Smalls, Porcupine Bank and Irish Sea with a model involving 1 common trend (red line, *AICc=1879*). Recall, that our retained model correspond to a 2 common trends (*AICc=1521*).

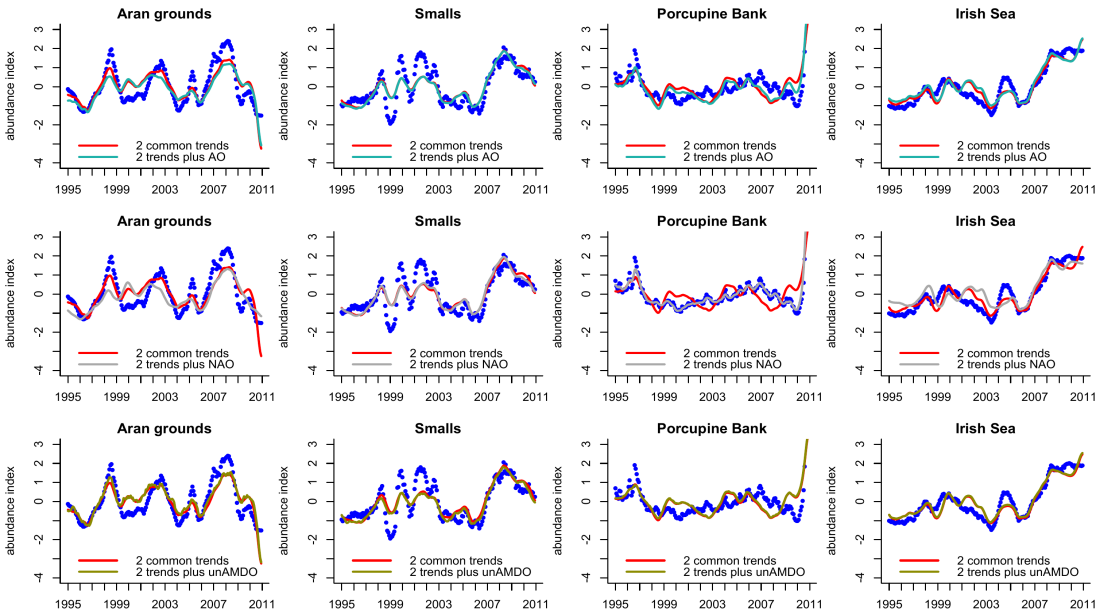
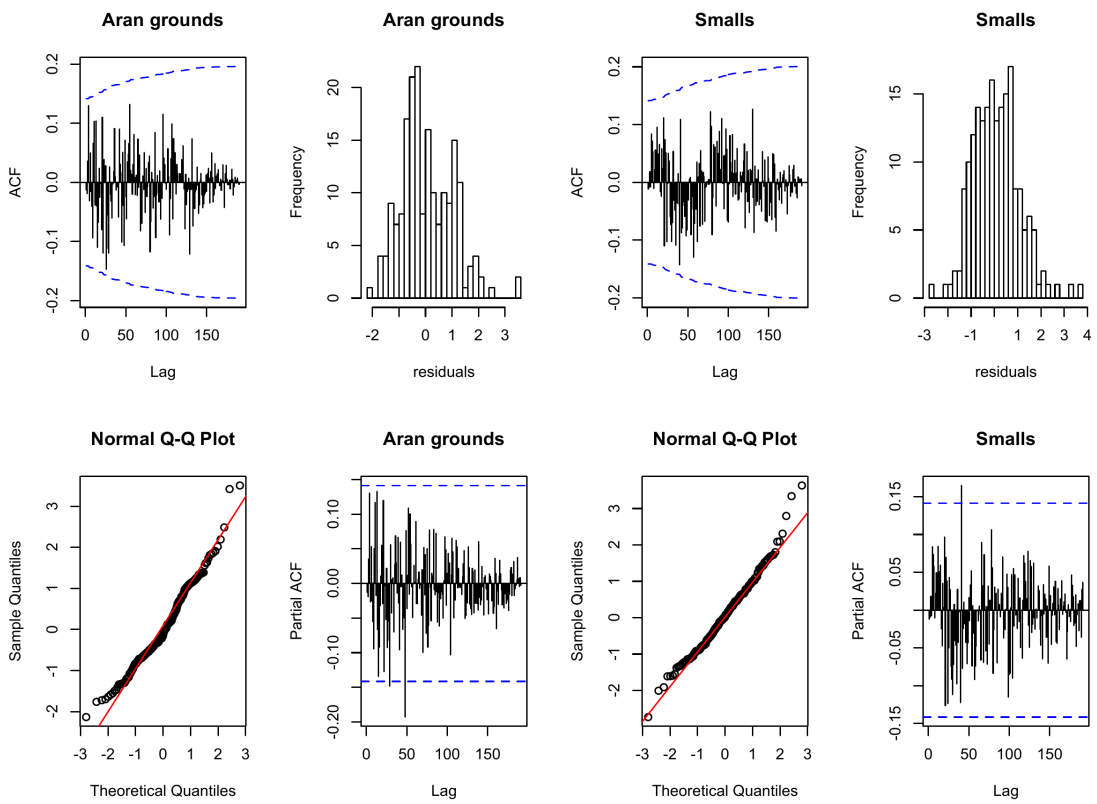


Figure A4: Dynamic Factor Analysis modelling fits of the observed 1995–2010 standardised lpues times series involving regional climate covariates (AO, NAO, unAMDO) plus 2 common trends. The 2 common trends model with no-covariate leads to an *AICc=1521*, when 2 common trends model with Arctic Oscillation covariate (AO) provides an *AICc=1509* (**top row**). The 2 common trends plus the PC based North Atlantic Oscillation covariate (abreviated NAO) provide an *AICc=1506* (**medium row**). While, the 2 common trends model with unsmoothed Atlantic Multi-Decadal Oscillations covariate (unAMDO) levels at *AICc=1507* (**bottom row**). More details on covariates in ***Materials and Methods*** *in* ***Chapter 1 Times Series Analysis***.

(a)


Aran grounds
ACF
Lag
Aran grounds
Frequency
residuals
Smalls
ACF
Lag
Smalls
Frequency
residuals
Normal Q-Q Plot
Sample Quantiles
Theoretical Quantiles
Aran grounds
Partial ACF
Lag
Normal Q-Q Plot
Sample Quantiles
Theoretical Quantiles
Smalls
Partial ACF
Lag

(b)

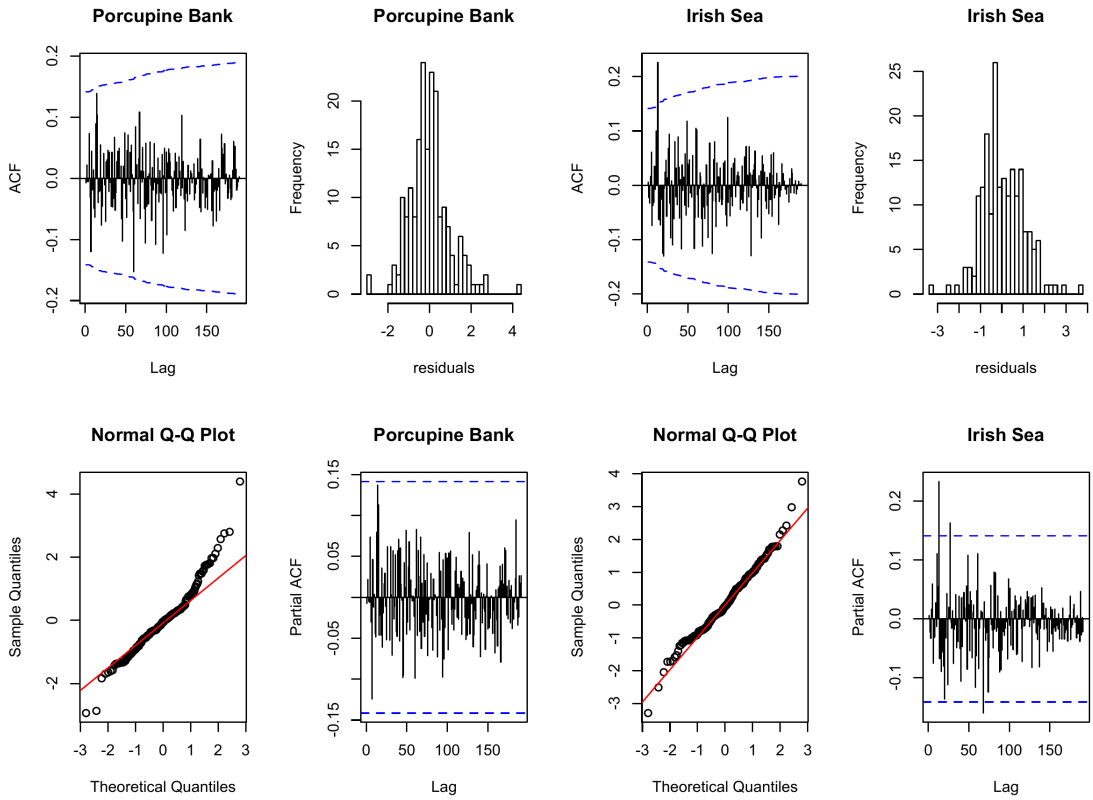


Figure A5a-b: Diagnostic tools of the standardised residuals of the Sarima modelling fit *(5,0,0)* $(1,0,1)_{12}$ for Aran grounds, *(1,0,1)*$(1,0,1)_{12}$ for Smalls, *(1,0,4)*$(1,0,1)_{12}$ for Porcupine Bank and *(1,1,1)* $(1,0,1)_{12}$ for Irish Sea using *partial and auto-correlation function* (*PACF, ACF* respectively), histogram and Normal *quantile-quantile plot*.

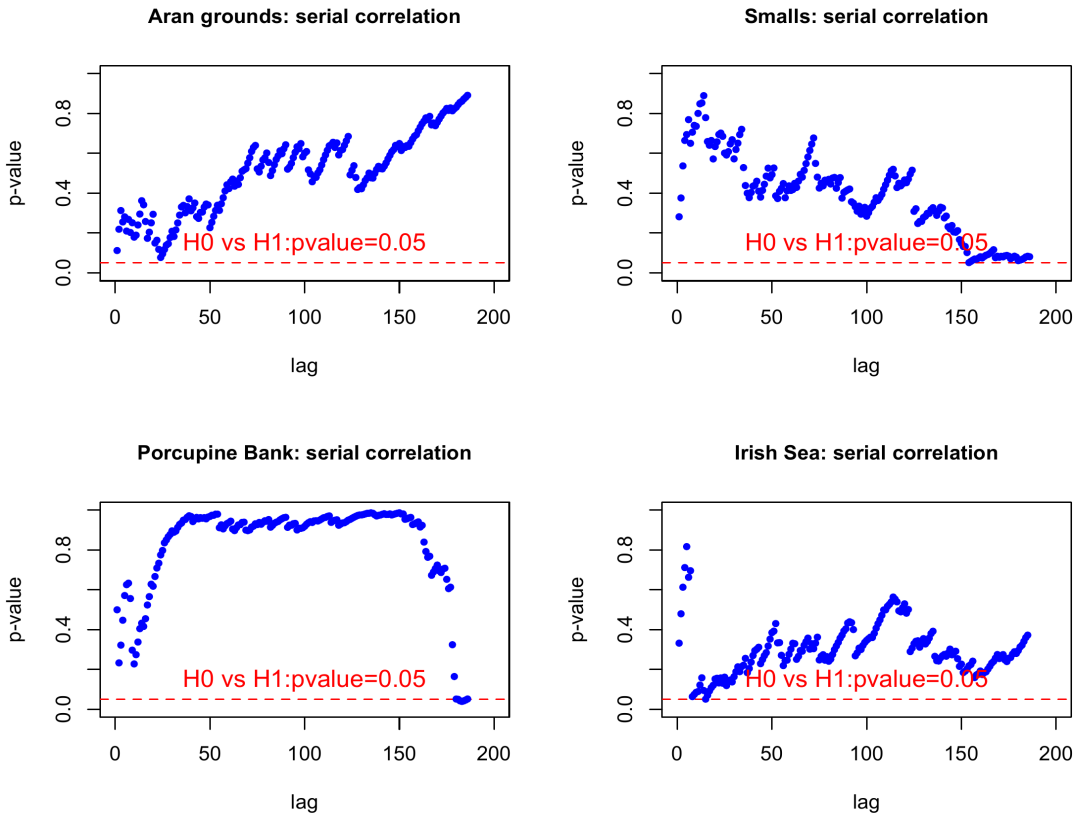


Figure A6: *Ljun-Box test* of the serial correlation of the standardised residuals of the Sarima modelling fit $(5,0,0)(1,0,1)_{12}$ for Aran grounds, $(1,0,1)(1,0,1)_{12}$ for Smalls, $(1,0,4)(1,0,1)_{12}$ for Porcupine Bank and $(1,1,1)(1,0,1)_{12}$ for Irish Sea.

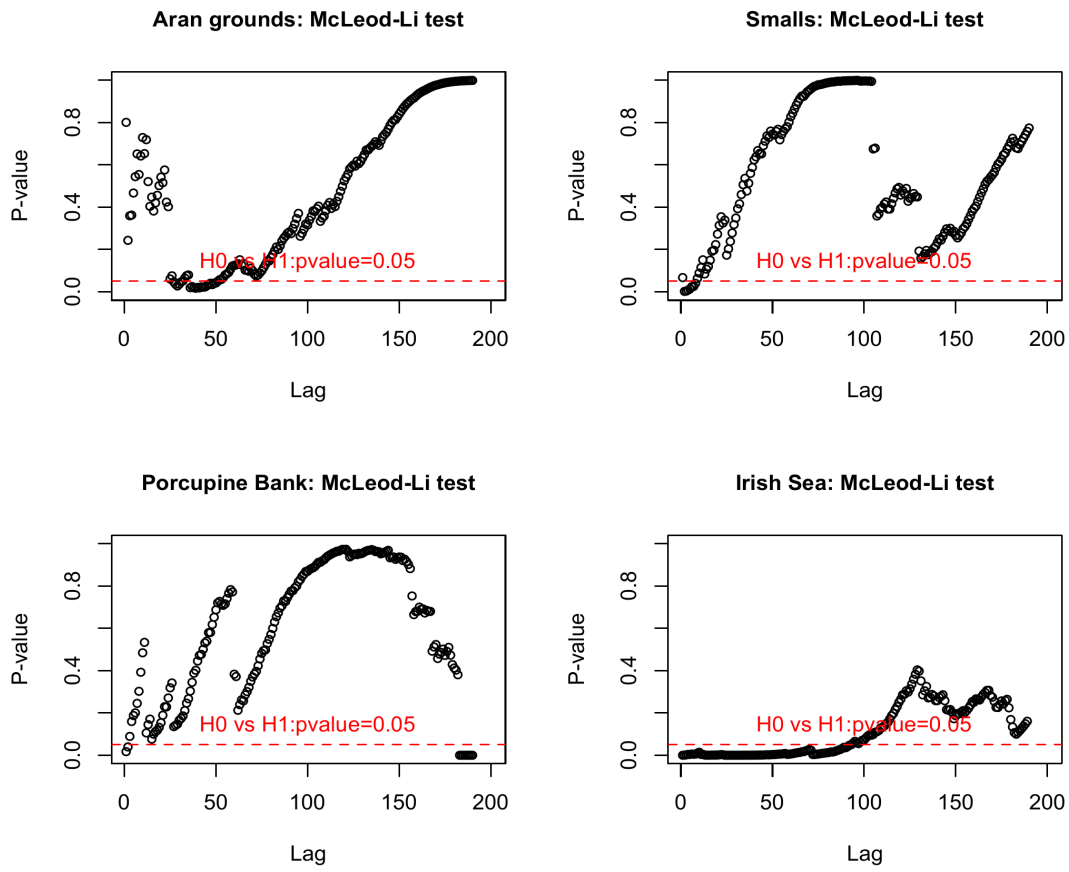


Figure A7: *McLeod-Li test* (homoscedasticity test) of standardised residuals of the Sarima modelling fit $(5,0,0)(1,0,1)_{12}$ for Aran grounds, $(1,0,1)(1,0,1)_{12}$ for Smalls, $(1,0,4)(1,0,1)_{12}$ for Porcupine Bank and $(1,1,1)(1,0,1)_{12}$ for Irish Sea.

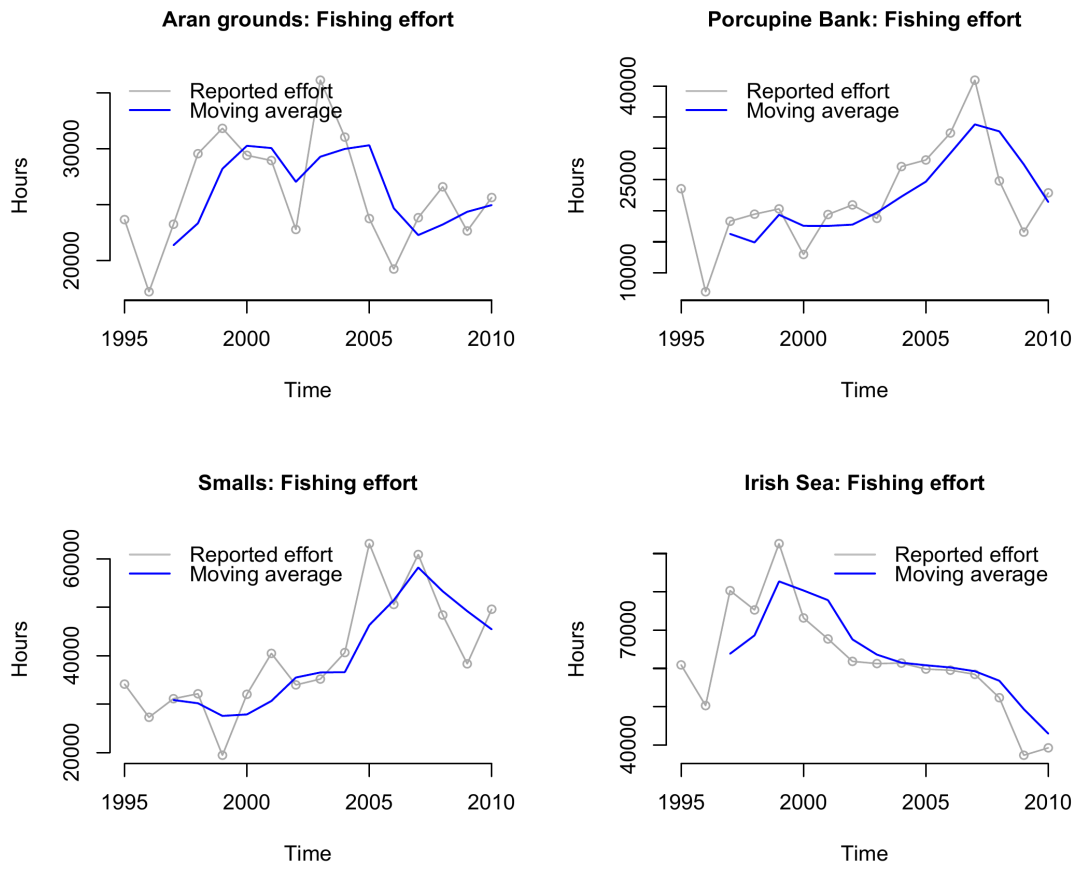


Figure A8: Reported effort in hours from 1995 to 2010 for the four main *Nephrops norvegicus* fishery areas corresponding to Aran grounds (FU17), Porcupine Bank (FU16), Smalls (FU22) and west Irish Sea (FU15). We use the smooth capability of the moving average technique to highlight the trends in the fishing effort.

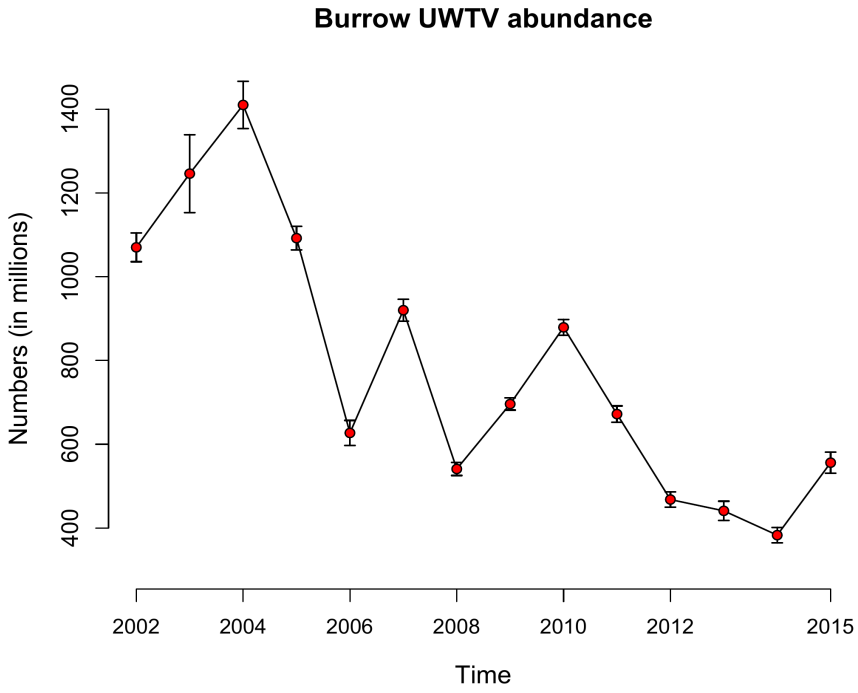


Figure 9: Under water TV abundance estimates (in numbers) of Aran grounds *Nephrops* population from 2002 to 2015 (Source: Marine Institute, Ireland). Error bars indicate 95% confidence limits.

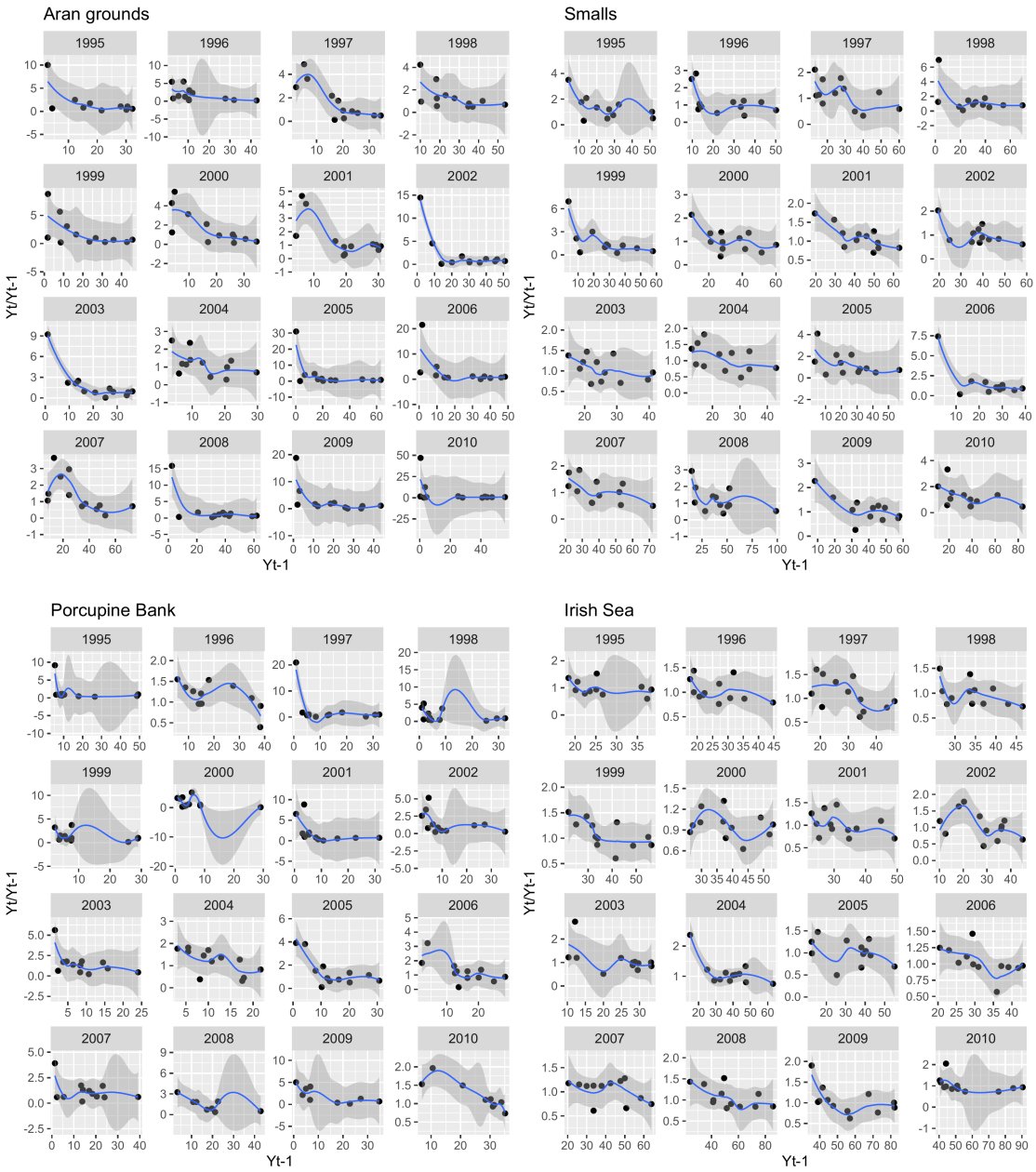


Figure A10: Annual density dependence relationship from 1995 to 2010 using *Nephrops* monthly landing per unit of effort (Y_t) for each area of study. In order to ease eye examination, a smooth l*oess regression* with its 95% confidence limits have been added.



Figure A11: Phase plots from 1995 to 2010 using monthly *Nephrops* landing per unit of effort data (Y_t) for each area of study.

Statistical Annexe A

Part A

Throughout the study, we conducted our model selection by examining the outputs derived from the fits using mainly residuals diagnostics (*acf*, *pacf*, *ccf*, *Ljung Box test*, *McLeod-Li test*) and model performance (*AIC*, *MSE*, *MAD*, *MAPE*, *U-Theils*).

(A.1) Analysis of residuals

Independence

Independence (or dependence) of residuals is examined by means of (sample) *auto-correlation function* (*acf*), the *Ljung-Box test* and the (sample) *Partial Autocorrelation Function* (*pacf*).

Sample auto correlation function (acf)

$$\hat{r}_k = \frac{\sum_{t=k+1}^{n} (Y_t - \bar{Y})(Y_{t-k} - \bar{Y})}{\sum_{t=1}^{n} (Y_t - \bar{Y})^2} \quad \text{for} \quad k = 1, 2, \ldots \ .$$

The plot of the coefficients $\hat{r}_k$ versus lag *k* is the correlogram and "significant" ones are lying over $\pm 1.96 \times 1/\sqrt{192} = \pm 0.1414$ limits.

Ljung Box test (or portmanteau test)

Described as $Q^* = n(n+2)\left(\frac{\hat{r}_1^2}{n-1} + \frac{\hat{r}_2^2}{n-2} + \ldots + \frac{\hat{r}_K^2}{n-K}\right)$ where $\hat{r}_k$ are the coefficients of the sample *acf*. Note that fitting an erroneous model would tend to inflate Q^*. It has an approximate *Chi-square* distribution with $K - p - q$ degrees of freedom. So, for *p-value >0.05* there is no evidence to reject the Ho hypothesis of "error terms are uncorrelated". Note that the maximum lag *K* selected is somewhat arbitrarily.

Partial auto-correlation function (pacf)

Computing the correlations between Y_t and Y_{t-k} after removing the effect of the

intervening variables $Y_{t-1}, Y_{t-2}, Y_{t-3}, \ldots, Y_{t-k+1}$ produces the partial autocorrelation coefficients ρ_{ii} . By replacing ρ_i by $\hat{r}_i$ coefficients we obtain the sample partial auto-correlations function, according to the Yule-Walker equations.

$$\rho_{ii} = \begin{cases} \rho_1 & for\ i = 1 \\ \dfrac{\rho_i - \sum_{j=1}^{i-1} \rho_{i-1,j}\rho_{i-j}}{1 - \sum_{j=1}^{i-1} \rho_{i-1,j}\rho_j} & for\ i = 2,\ldots,k \end{cases}$$

where $\rho_{ij} = \rho_{i-1,j} - \rho_{ii}\rho_{i-1,i-j}$ with (*j=1, 2,...,i–1*)

Homoscedasticity

Since both arima and sarima modelling approaches assume weak stationarity of order 2 (that is to say, ergodicity) then, the *McLeod-Li test* checks for the presence of conditional heteroscedasticity by computing the *Ljung-Box test* with the squared data.

Normality

Normality was checked by the visual inspection of the *Normal quantile-quantile plots* and the histograms.

(A.2) Model performances

The commonly used criteria to estimate performances of fitted model candidates are the mean absolute deviation (*MAD*), *mean square error* (*MSE*), *mean absolute percentage error* (*MAPE*), *Akaike Information Criterion* (*AIC*) and *U-Theil's*:

$MAD = \frac{1}{n}\sum_{t=1}^{n}|e_t|$, $MSE = \frac{1}{n}\sum_{t=1}^{n}e_t^2$, $MAPE = \frac{1}{n}\sum_{t=1}^{n}\frac{|e_t|}{Y_t}$ where e_t is either standardised innovation or observed residuals.

Akaike information criterion

Statistically, the goodness of the fit is estimated through the Akaike information criterion (*AIC*): $AIC = 2 \times K - 2\log L(\Theta|\boldsymbol{Y})$ where K is the number of estimated parameters and $L(\Theta|\boldsymbol{Y})$ the maximum value of the likelihood function.

We also used AICc which adds an extra penalty term for the number of parameters:

$AICc = -2\log L(\Theta|\boldsymbol{Y}) - K \times n(n-K-1)$ with (n) the length of the data.

For time series analysis the *AICc* tends to select complex models when the time series is short, a bootstrapped *AIC* variant, noted *AICb*, is also used as small-sample corrector for autoregressive state space models:

$\text{AICb} = -2\log L(\Theta|\boldsymbol{Y}) - 2\left(\frac{1}{N_b}\sum_{i=1}^{N_b} - \log\frac{L(\hat{\Theta}^*(i)|\boldsymbol{Y})}{L(\hat{\Theta}|\boldsymbol{Y})}\right)$ where $\hat{\Theta}$ is a maximum likelihood parameter set under the original data y and $\hat{\Theta}^*(i)$ is the maximum likelihood parameter estimated from the i^{th} bootstrapped data set $y^*(i)$ and N_b is the number of bootstrap data sets (Cavanaugh and Shumway, 1997 after Stoffer and Wall, 1991 cited in Holmes et al, 2018a).

The performances can also be assessed by the *Theil' U* statistic which compares the *MSE* of the model with the *MSE* of the trivial "no change" model. In other words, a value of *Theil'U* less than one means that the model produces a better fit, on average, than the no change model (Theil, 1966; Petris et al., 2009).

$U = \sqrt{\frac{\sum_{t=2}^{n}(Y_t - f_t)^2}{\sum_{t=2}^{n}(Y_t - Y_{t-1})}}$, f_t is either the forecast one-step-ahead forecast result of the Kalman Filter or the fitted sarima values.

Part B

(B.1) Modelling with Sarima: Box-Jenkins approach (Box and jenkins, 1970; Box, Jenkins, and Reinsel, 1996):

The discrete-time sequence of observations representing the stochastic process can be decomposed into a pair of uncorrelated processes (the Wold decomposition): on the one hand, the linear function of past observations Y_t called the auto-regressive part (*AR*), and on the other hand, a linear combination of lags of a white noise process w_t named the moving average (*MA*) representing the previous random shock events that might have affected the dynamic of the observed sequence.

Both parts constitute the $ARMA(p,q)$ model and provide a parsimonious

description of the signal embedded in the time series in terms of two series of polynomials that is

$Y_t = \phi_1 Y_{t-1} + \phi_2 Y_{t-2} + \ldots + \phi_p Y_{t-p} + w_t - \theta_1 w_{t-1} - \theta_2 w_{t-2} - \ldots - \theta_q w_{t-q}$ with (p) and (q) parameters of order indicating the last time influence affected by the previous observations and the random noise, respectively.

However, very often, as already mentioned, data collected show non stationarity. Hence, the general arma class of models have been broadened to cope with the presence of trends and periodicity (seasonality) giving rise to arima and sarima means.

Trend

The presence of trends in the data induces non-stationarity and the integrated arima model has the capacity to deal with it through difference. In fact, a time series (Y_t) is said to follow an *ARIMA*(*p, d, q*) model if a stationary *ARMA*(*p, q*) process is attained after one or two lag differences of the data (*i.e. d=1 or d=2*). It should be noted that the higher orders are questionable and should be avoided. To detect departure from the stationarity, we had recourse to the *Kwiatkowski-Schmidt-Shin-Phillips* (*KPSS*), *Philip-Perron* and *Augmented Dickey-Fuller tests*.

Thus, the general *ARIMA*(*p, d, q*) can be expressed concisely as a combination of $\phi_p(B)(1-B)^d(Y_t-\mu)=\theta_q(B)w_t$ polynomials: where the (*AR*) characteristic polynomial corresponds to $\phi_p(B)=(1-\phi_1 B-\phi_2 B^2-\ldots\phi_p B^p)$, the (*MA*) to $\theta_q(B) = (1 - \theta_1 B - \theta_2 B^2 - \ldots\theta_q B^q)$ and $(1 - B)^d$ serving to address the non-stationarity component through the first or second difference if needed. Here $\mu_t = E(Y_t)$ is accounted for the mean of the process.

Technically, a backshift operator B , also called a lag operator, that operates on the time index of a series and shifts time back one time unit or more to form a new series, is often used to render the resulted general equation more readable visually. As example of which is as follow:

$B^1 Y_t = Y_{t-1}$, $B^{12} Y_t = Y_{t-12}$, $(1-B)Y_t = Y_t - Y_{t-1}$ and $\nabla^d = (1 - B)^d$.

Season

Embodying the seasonal effect requires joining polynomials at the (*AR)* and (*MA)* sides

of the $ARIMA(p,d,q)$ that is to say $\Phi(B)=(1-\Phi_1 B^{12}-\Phi_2 B^{2\times 12}-\ldots\Phi_P B^{P\times 12})$ and $\Theta(B)=(1-\Theta_1 B^{12}-\Theta_2 B^{2\times 12}-\ldots\Theta_Q B^{Q\times 12})$ respectively, leading to $\phi(B)\Phi(B)(1-B)^d(1-B^S)^D(Y_t-\mu)=\theta(B)\Theta(B)w_t$. Summarised as follow $SARIMA(p,d,q)\times(P,D,Q)_S$ it can be seen that the chosen (P,D,Q) parameters work similarly to (p,d,q) by informing the general polynomial characteristics of the periodicity and that $(1-B^S)^D$ counts for the difference of order D to cope with the seasonal non-stationarity if needed.

Recall that seeking these parameters components of the Sarima models is not straightforward and instead requires a try-and-leave procedure.

(B.2) Forecasting (algebra) with Box-Jenkins (Cryer et al., 2008)

Under the Box-Jenkins framework, the objective is to produce an optimum prediction, that is to say, with the minimum error in terms of the *mean square error* (*MSE*) criterion. The *MSE* forecast, l time unit ahead, is given by the conditional expectation $\hat{Y}(l)=E(Y_{t+l}|Y_1,Y_2,\ldots,Y_t)$.

By noting l the forecasting horizon and t the forecasting origin, the general *ARMA* difference equation form for computing forecasts is given by:

$$\hat{Y}(l)=\phi_1\hat{Y}_t(l-1)+\phi_2\hat{Y}_t(l-2)+\ldots+\phi_p\hat{Y}_t(l-p)+\theta_0$$
$$-\theta_1 E(e_{t+l-1}|Y_1,Y_2,\ldots,Y_t)-\theta_2 E(e_{t+l-2}|Y_1,Y_2,\ldots,Y_t) \quad \text{where}$$
$$-\ldots-\theta_q E(e_{t+l-q}|Y_1,Y_2,\ldots,Y_t)$$

$$E(e_{t+j}|Y_1,Y_2,\ldots,Y_t)=\begin{cases}0 & for\ \ j>0\\ e_{t+j} & for\ \ j\leq 0\end{cases} .$$

Note that $\theta_0=\mu[1-\phi_1-\phi_2-\ldots-\phi_p]$ and that $e_t(l)$ is the forecast error given by $e_t(l)=Y_{t+l}-\hat{Y}_t(l)$. The noise terms $e_{t-(q-l)},\ldots,e_{t-l},e_t$ appear directly in the computation of the forecasts for leads $l=1,2,\ldots,q$.

However, when $l>q$ the autoregressive portion of the difference equation takes over, and we have $\hat{Y}_t(l)=\phi_1\hat{Y}_t(l-1)+\phi_2\hat{Y}_t(l-2)+\ldots+\phi_p\hat{Y}_p(l-p)+\theta_0$ for $l>q$.

Thus, the general nature of the forecast for long lead times will be determined by the autoregressive parameters $\phi_1,\phi_2,\ldots,\phi_p$ (and the constant term θ_0 which is related to the mean of the process).

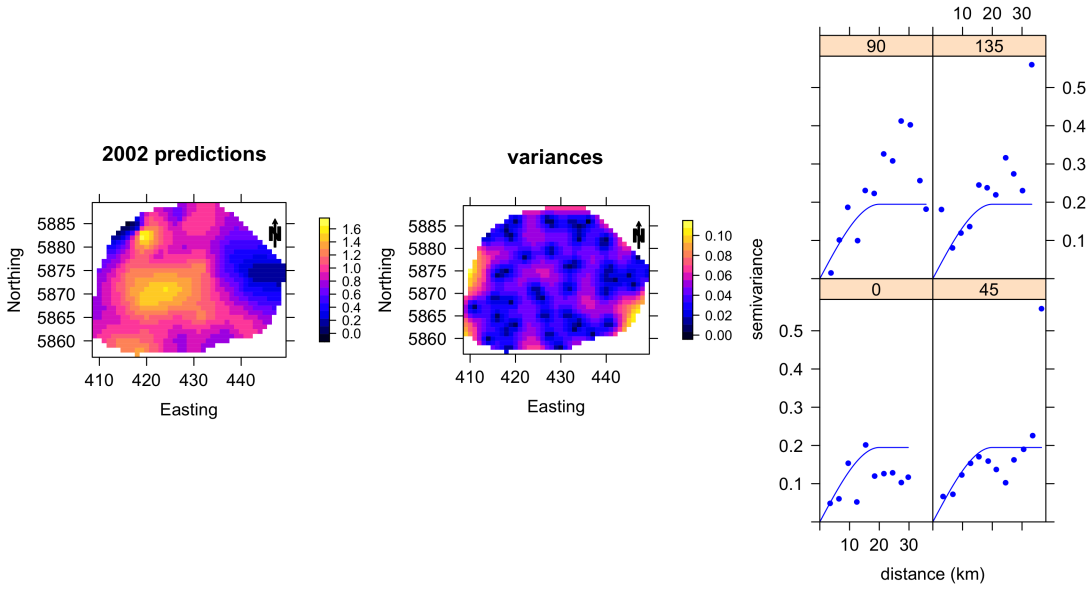
Finally, the forecasting algebra above is all nested in the relation $\hat{Y}_t(l) - \mu$ that simply reflects deviation from the mean process and for which the roots of the characteristic equation will determine its general behaviour. It is important to note that for large lead times this deviation from the mean decays to zero as the forecasting horizon l increases and that the long-term forecast is simply the process mean μ .

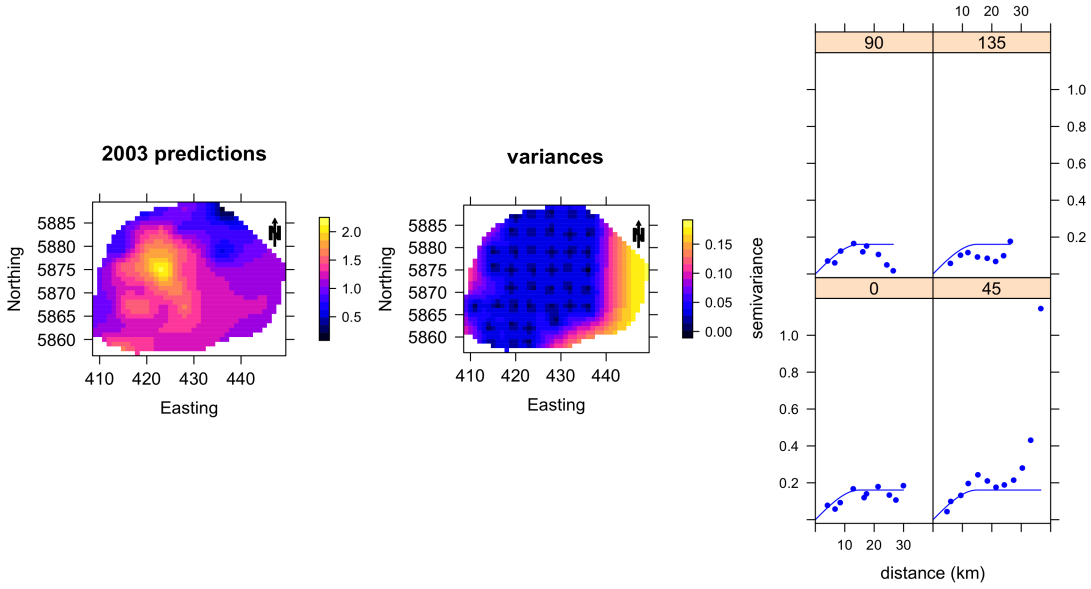
(B.3) Forecasting (algebra) with state space (Commandeur et al., 2007)

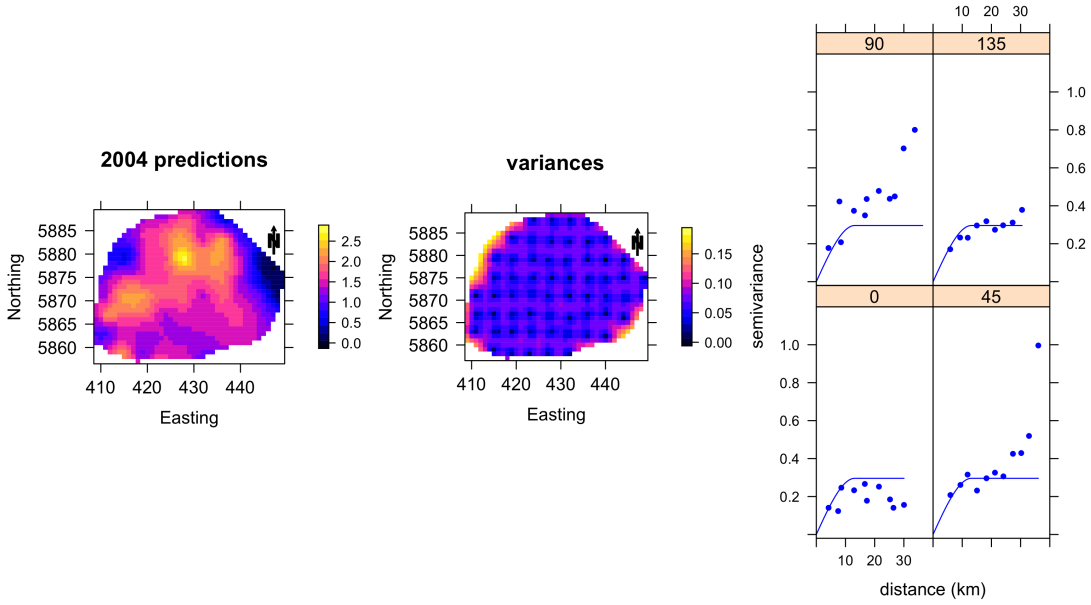
In state space method computing forecasts consists of continuing the Kalman filter after the end of the observed time series. In the absence of new observations the best option is to move the filtered state forward as is. When we arrive at the end of a series, that is to say $t=n$, the update of the filtered state equals $a_{n-1} + K_{n-1}(y_{n-1} - Z_{n-1}^T a_{n-1})$. At this stage there is still one observation left which has not yet been used in the Kalman filter updating process. This is the last observation y_n of the series. This last observation can be used to update the filtered state at time point $t = n + 1$ as follows $a_{n+1} = a_n + K_n(y_n - Z_n^T a_n)$.

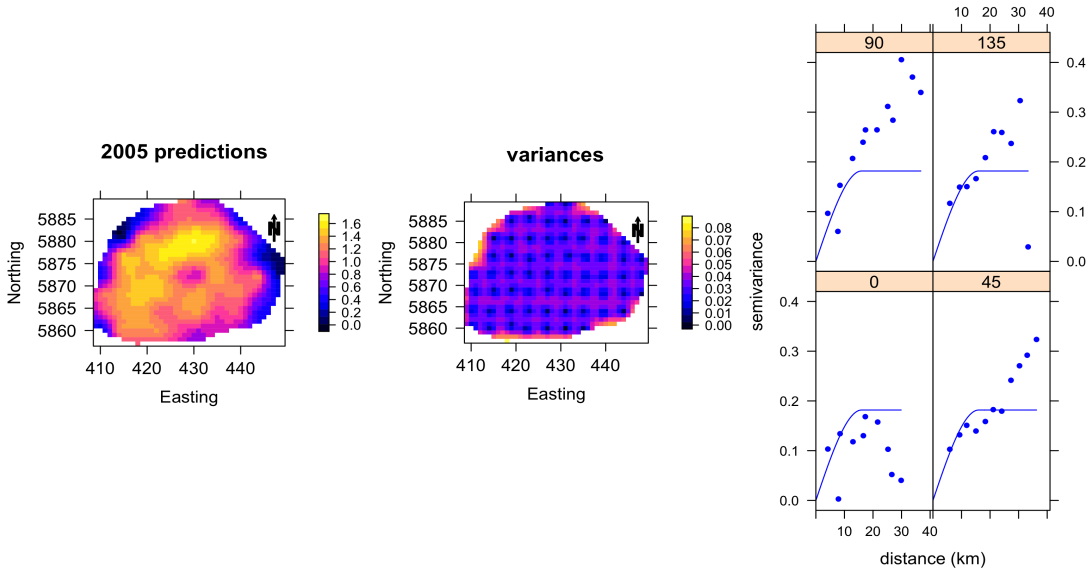
Now, all the available information in the series have been used, and from $n+1$ onwards the filtered state no longer changes. Letting $\bar{a}_{n+1} = a_{n+j}$, the forecasts are simply obtained from $\bar{a}_{n+1+j} = T_{n+j}\bar{a}_{n+j}$ for $j = 1, \ldots, J-1$ where J is the lead time (that is, the number of time points for which the forecasts are calculated). It may be noted that the same values are obtained by continuing the Kalman filter recursion provided that we set $v_{n+j} = 0$ and $K_{n+j} = 0$ for $j = 1, \ldots, J-1$.

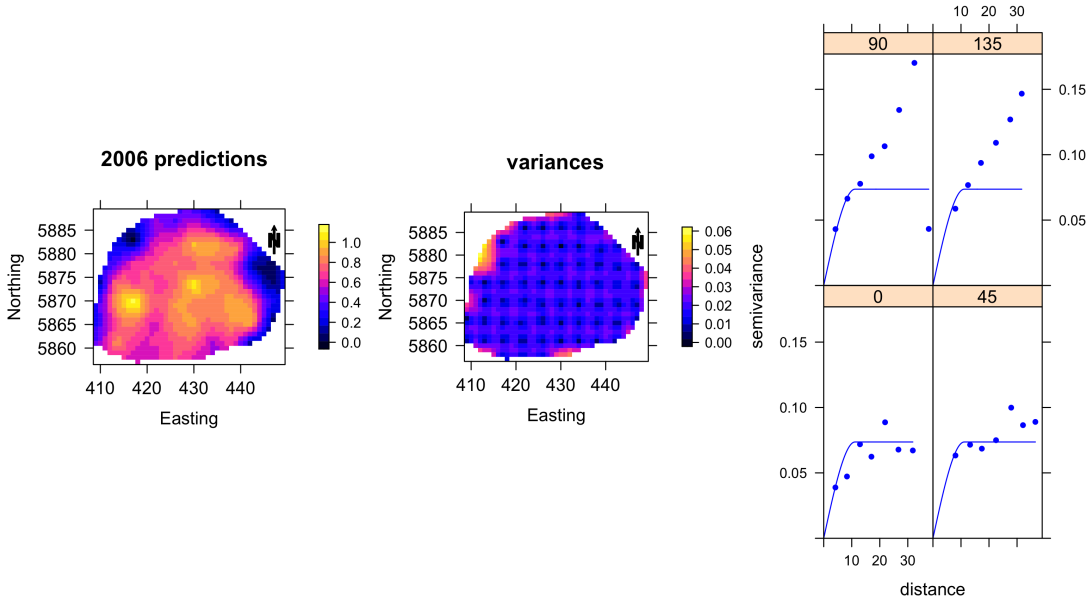
Annexes B

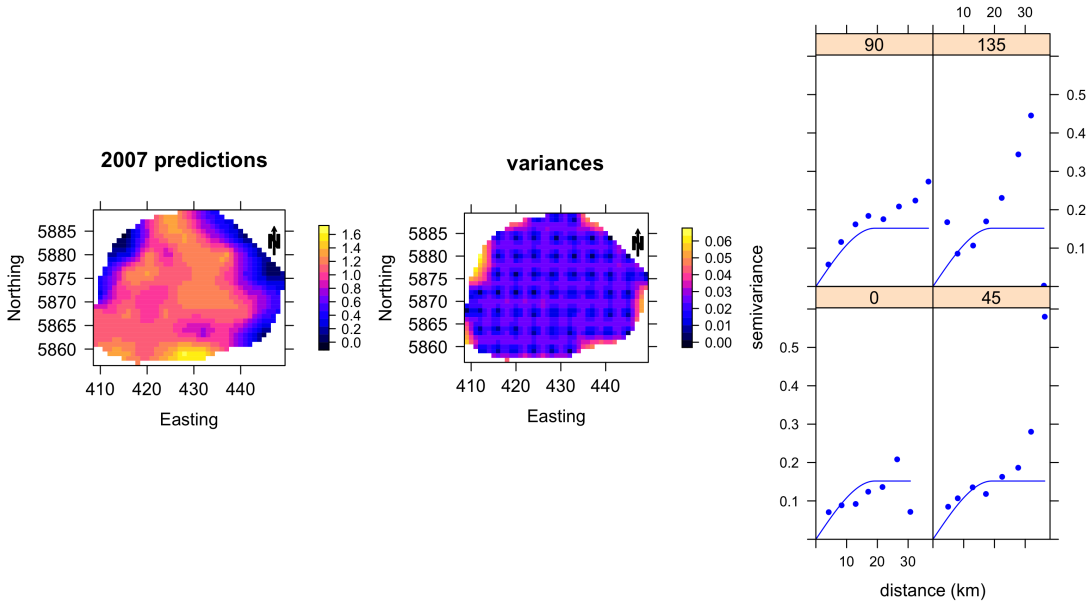

2002 predictions
variances
Northing
Easting
semivariance
distance (km)
90
135
0
45

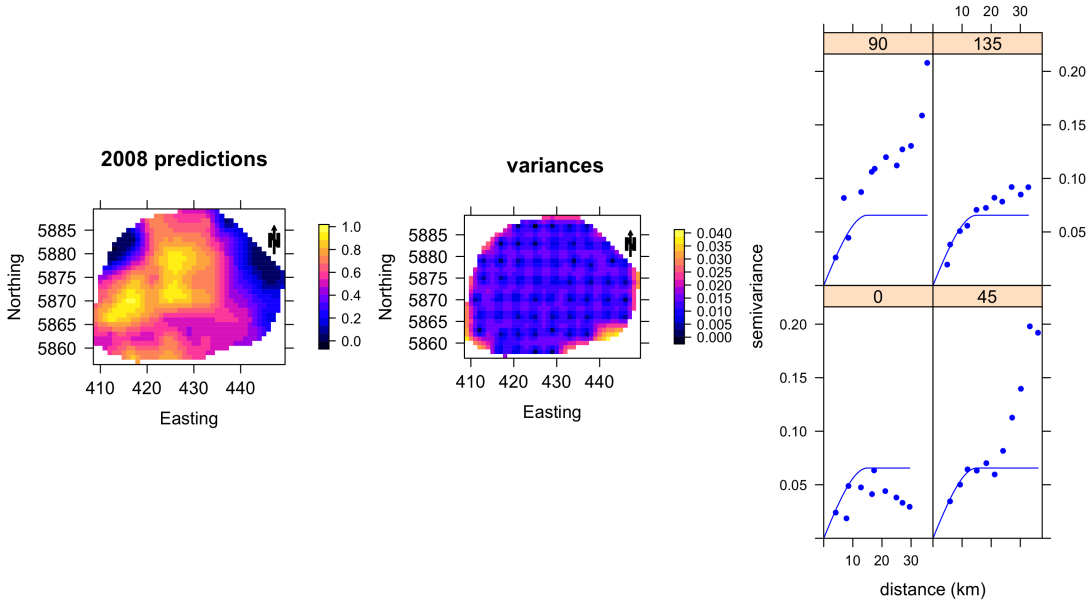

2003 predictions
variances
Northing
Easting
semivariance
distance (km)
90
135
0
45

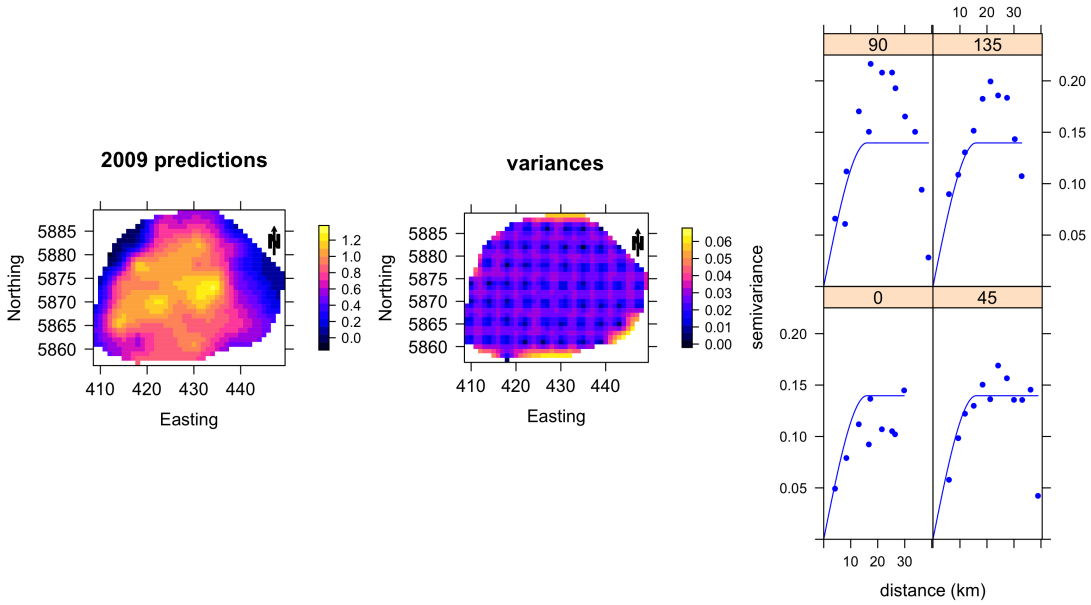

2004 predictions
variances
Northing
Easting
semivariance
distance (km)
90
135
0
45


2005 predictions
variances
Northing
Easting
semivariance
distance (km)
90
135
0
45


2006 predictions
variances
Northing
Easting
semivariance
distance
90
135
0
45


2007 predictions
variances
Northing
Easting
semivariance
distance (km)
90
135
0
45


2008 predictions
variances
Northing
Easting
semivariance
distance (km)
90
135
0
45


2009 predictions
variances
Northing
Easting
semivariance
distance (km)
90
135
0
45

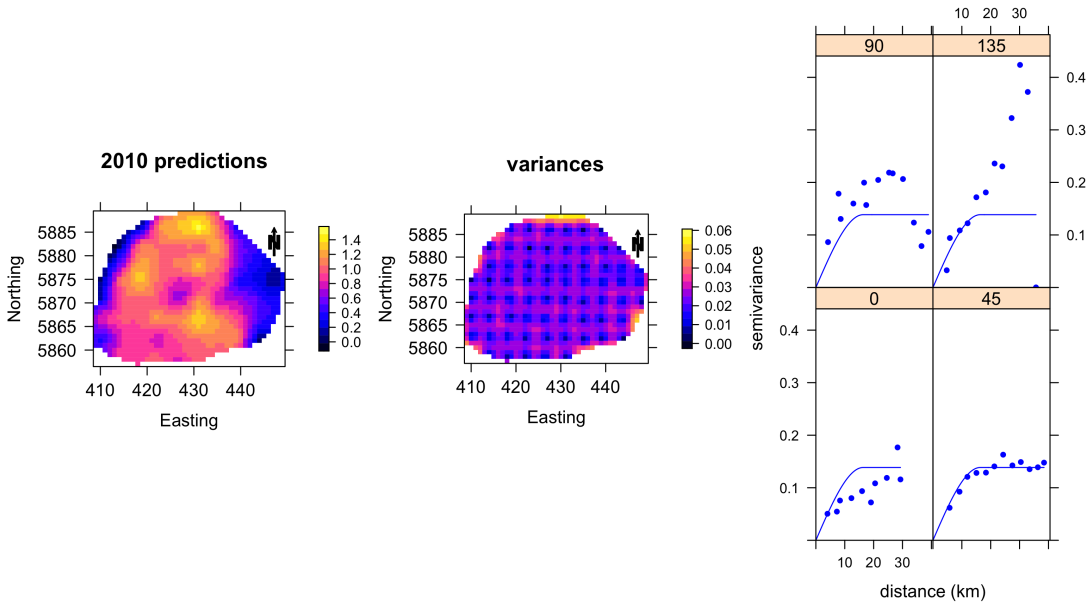


Figure B1: Maps of ordinary kriging burrow density predictions, variances and fitted variogram models. Note that we assumed spherical modelling in all cases with no nugget effect (see ***Materials and Methods*** *in* ***Chapter 2 Spatial Analysis***). Easting/northing coordinates in UTM zone 29, WGS84.

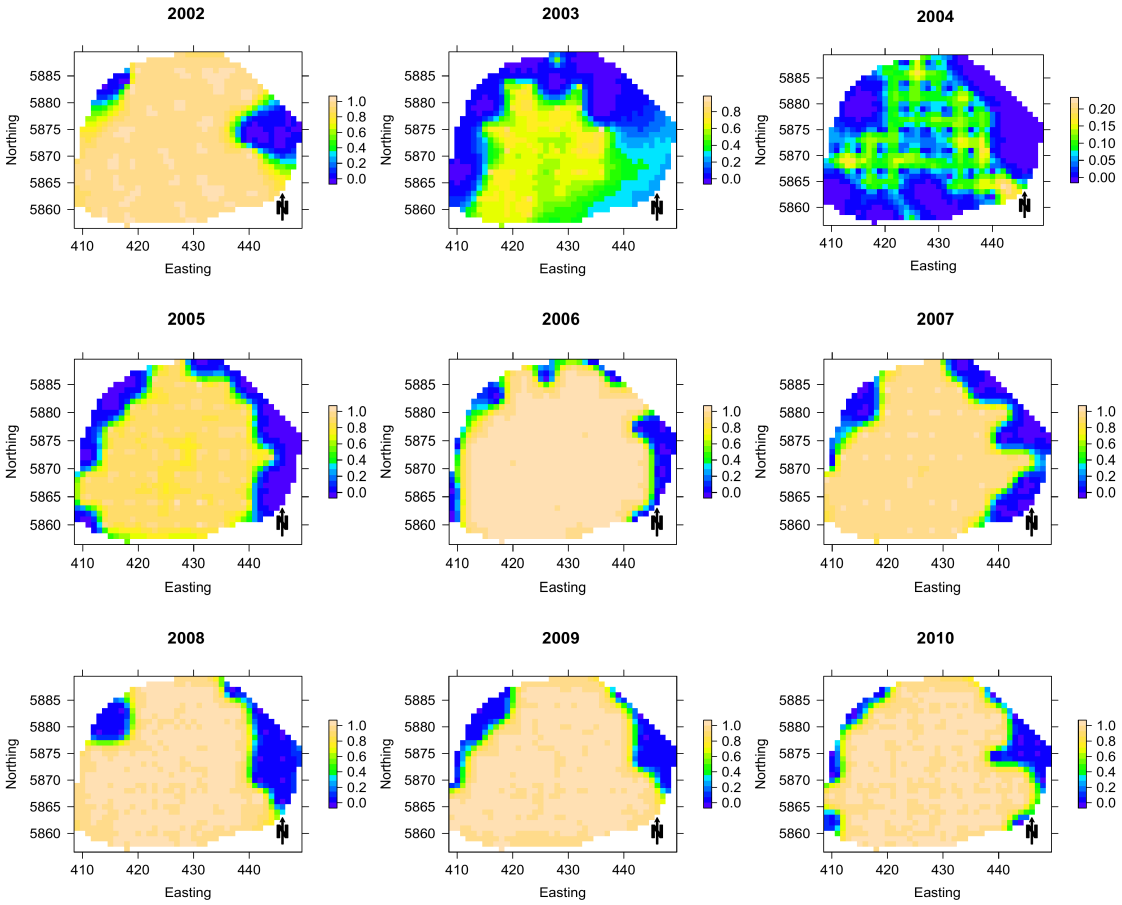


Figure B2: Annual indicator kriging maps with the probability of density >20% (or < 20%) census. Easting/northing coordinates in UTM zone 29, WGS84.

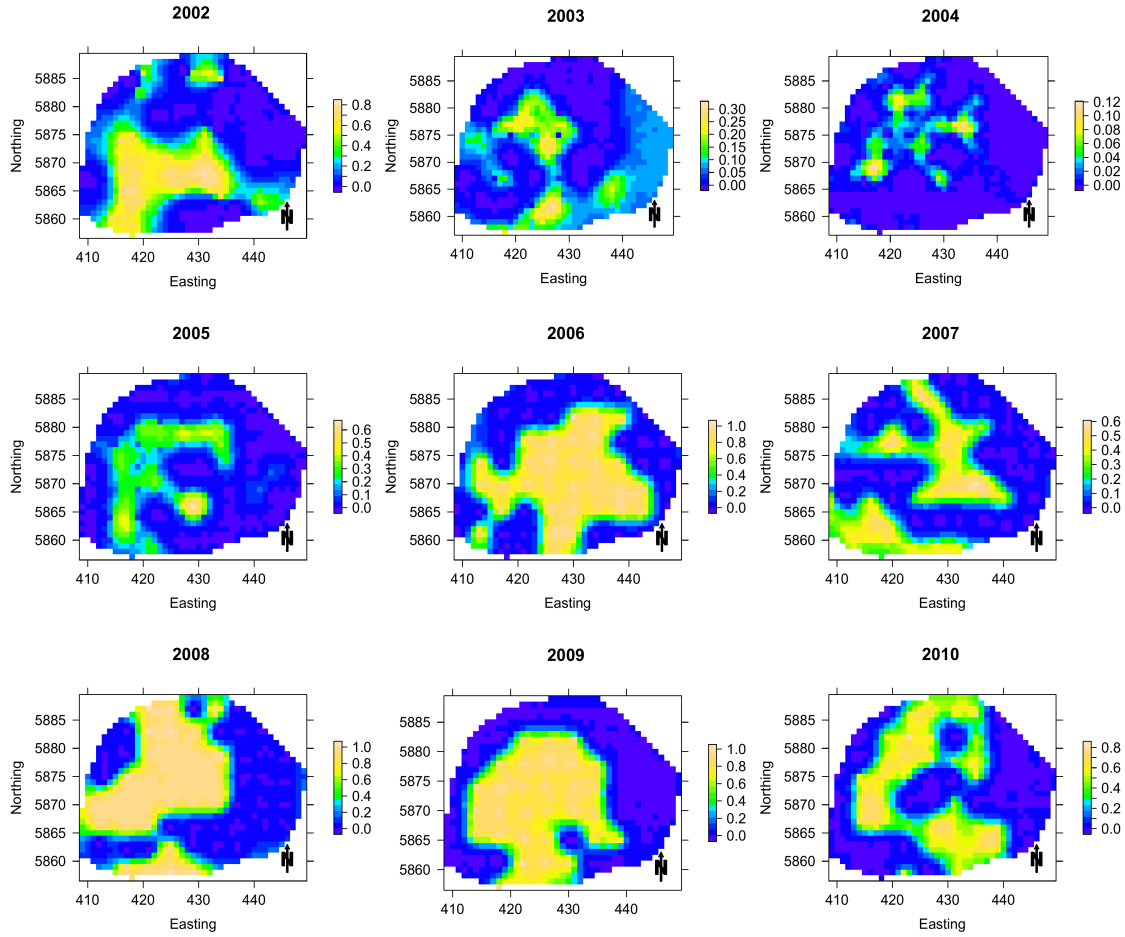
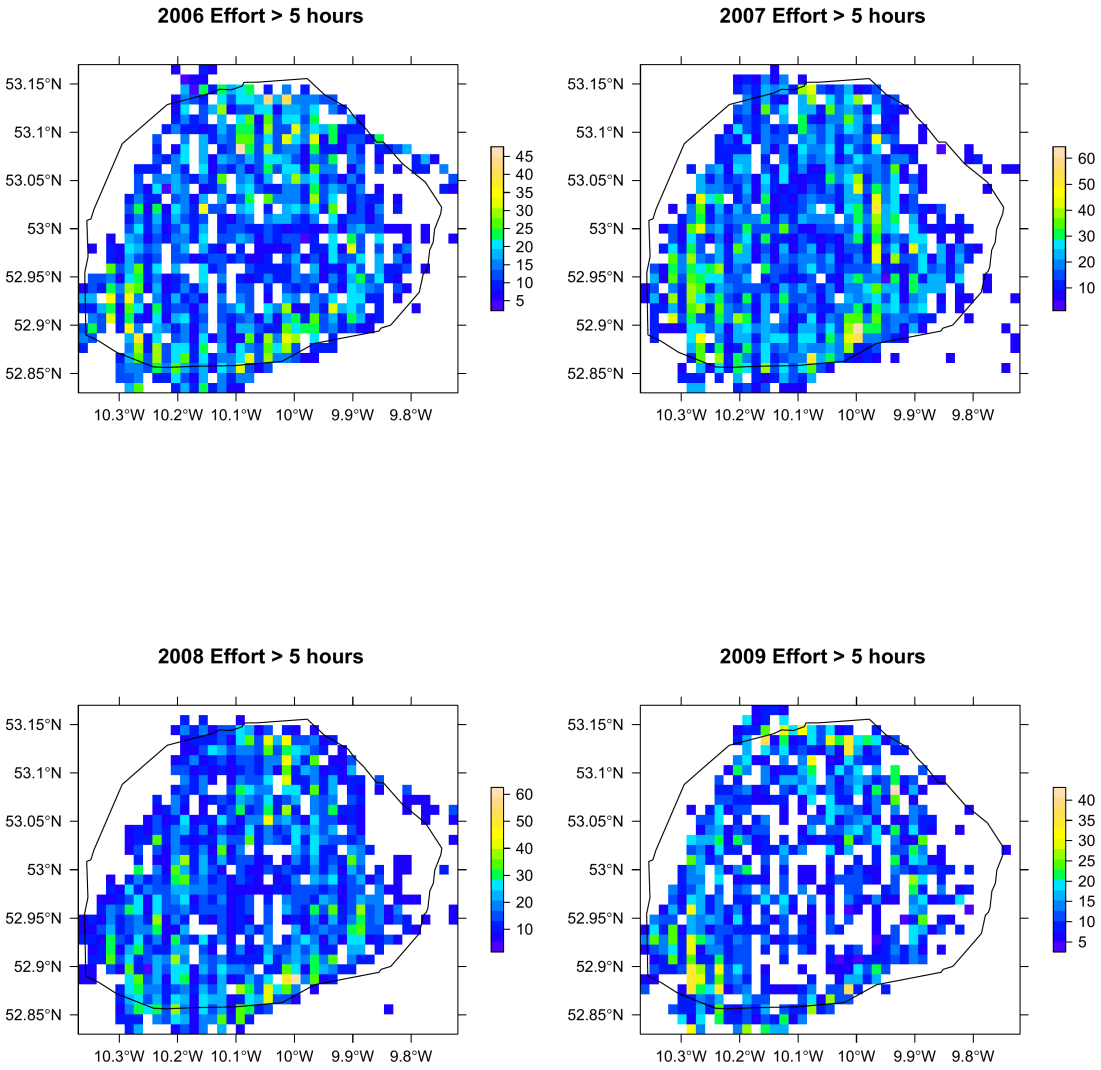
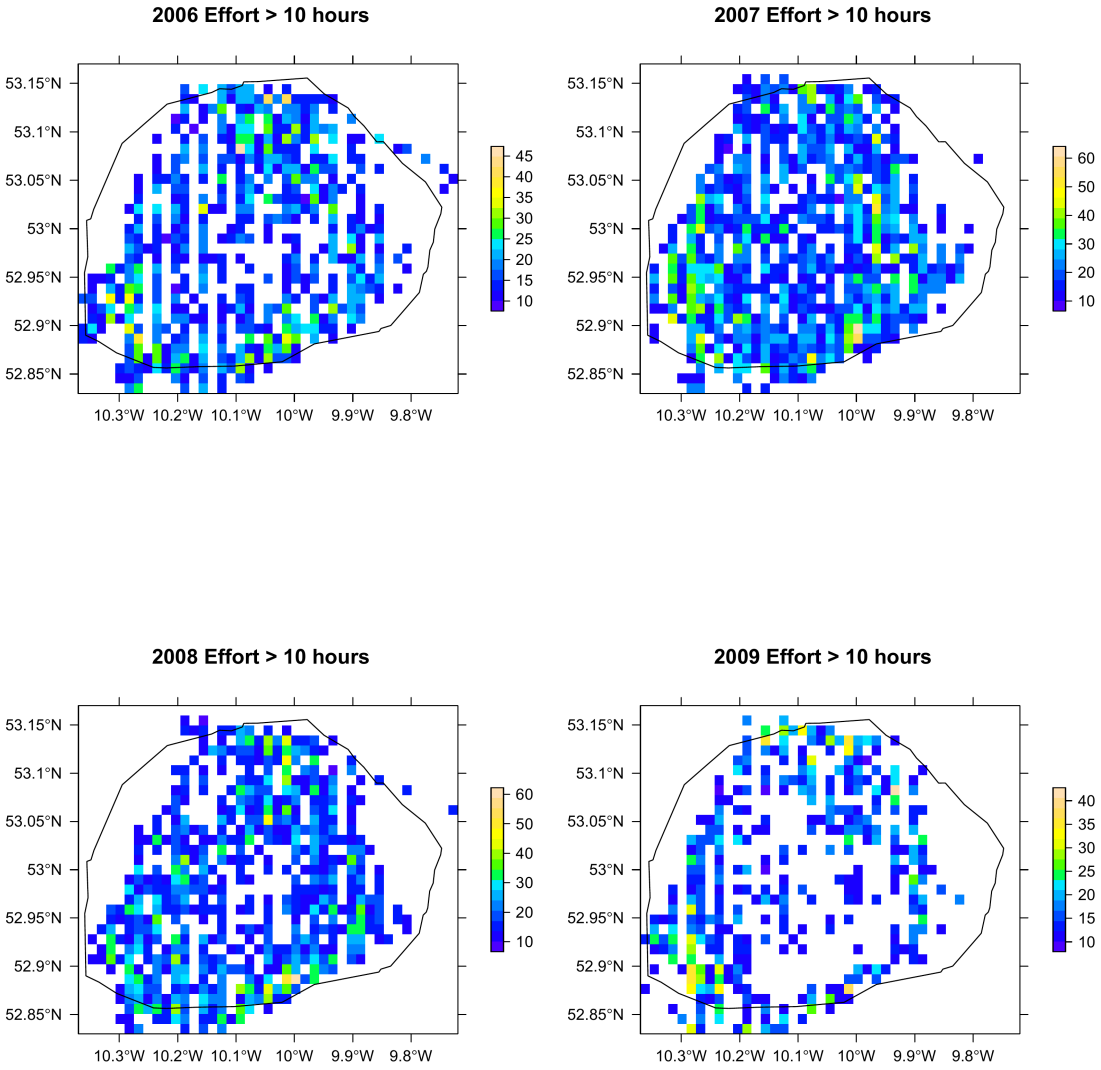


Figure B3: Annual indicator kriging maps with probability of density > 50% (or < 50%) census. Easting/northing coordinates in UTM zone 29, WGS84.

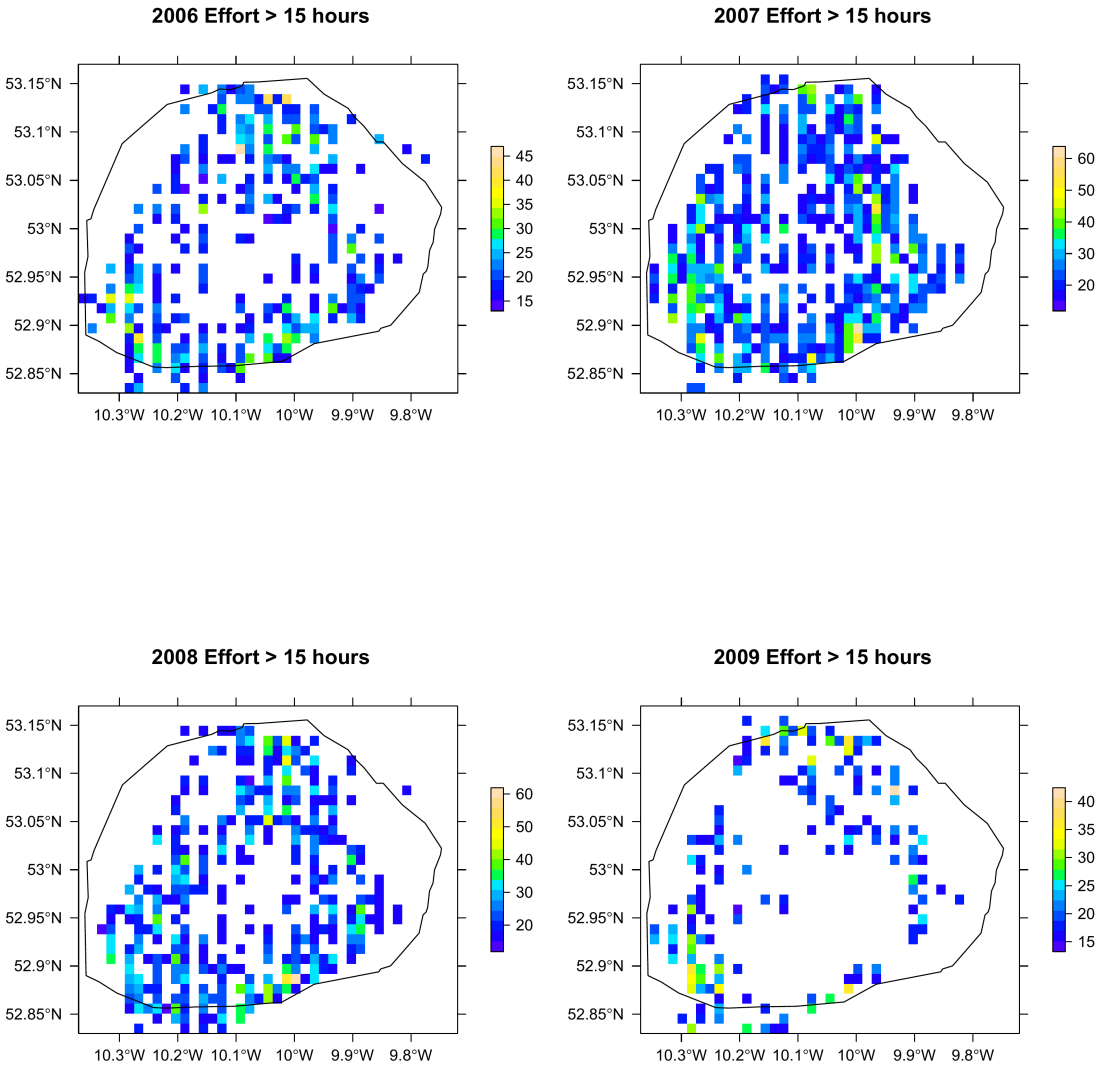
(a)


2006 Effort > 5 hours
2007 Effort > 5 hours
2008 Effort > 5 hours
2009 Effort > 5 hours
53.15°N
53.1°N
53.05°N
53°N
52.95°N
52.9°N
52.85°N
10.3°W
10.2°W
10.1°W
10°W
9.9°W
9.8°W
45
40
35
30
25
20
15
10
5
60
50
40
30
20
10
60
50
40
30
20
10
40
35
30
25
20
15
10
5

(b)


2006 Effort > 10 hours
2007 Effort > 10 hours
2008 Effort > 10 hours
2009 Effort > 10 hours
53.15°N
53.1°N
53.05°N
53°N
52.95°N
52.9°N
52.85°N
10.3°W 10.2°W 10.1°W 10°W 9.9°W 9.8°W
45 40 35 30 25 20 15 10
60 50 40 30 20 10
60 50 40 30 20 10
40 35 30 25 20 15 10

(c)


2006 Effort > 15 hours
2007 Effort > 15 hours
2008 Effort > 15 hours
2009 Effort > 15 hours
53.15°N
53.1°N
53.05°N
53°N
52.95°N
52.9°N
52.85°N
10.3°W 10.2°W 10.1°W 10°W 9.9°W 9.8°W
45 40 35 30 25 20 15
60 50 40 30 20
60 50 40 30 20
40 35 30 25 20 15

(d)

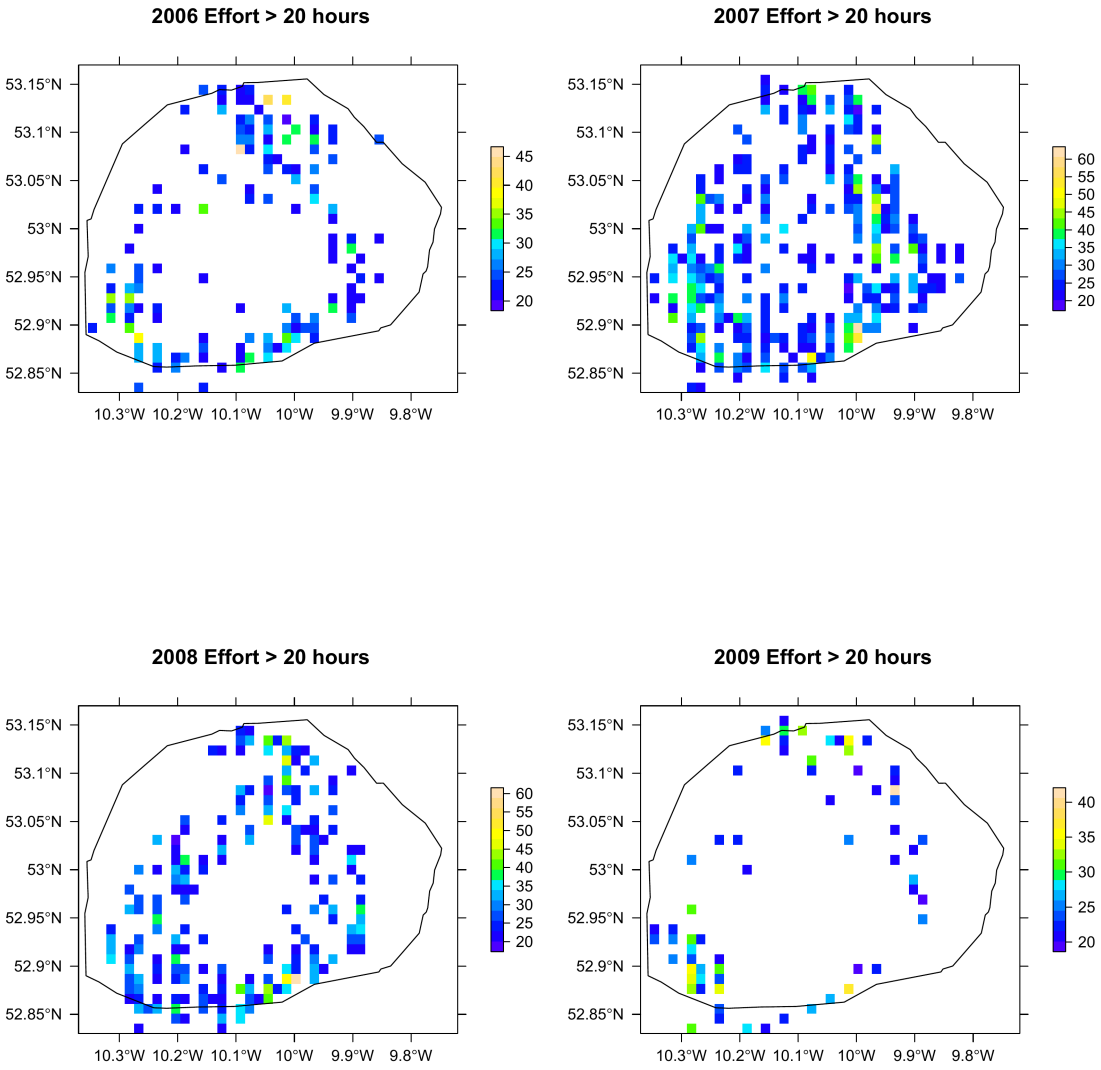


Figure B4a-b-c-d: Rasters of fishing activity over the Aran grounds site arranged by hours. The area of study (grey border) is divided into spatial geographic units (rectangles called "cells" or "pixels") that can store the fishing effort in hours during the period 2006 to 2009 as derived from the vessel monitoring system data.

(e)

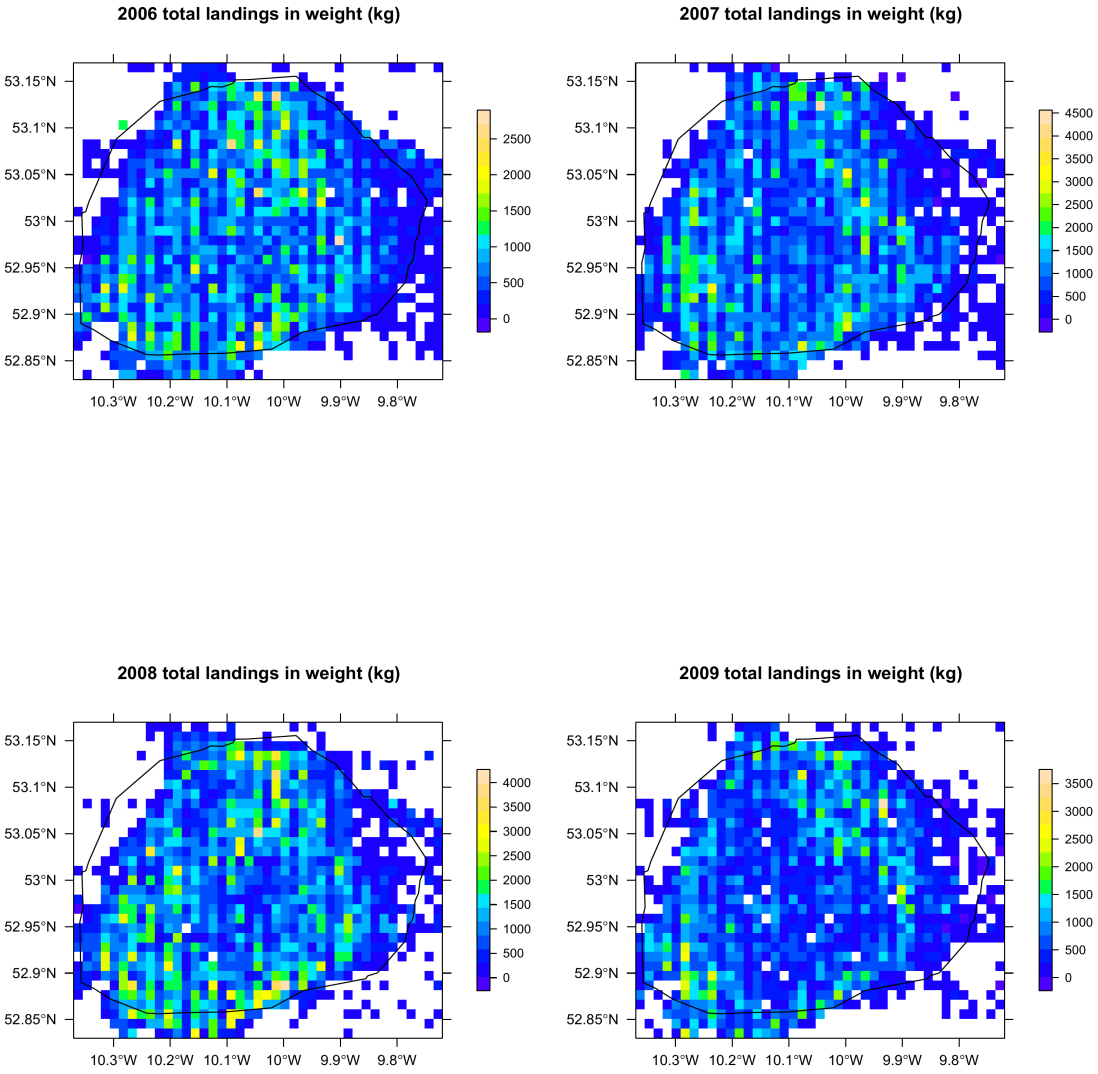


Figure B4e: Geo-localization of the *Nephrops norvegicus* yields using rasterisation of the vessel monitoring system data available for years 2006-2007-2008 and 2009 (data source: Marine Institute, Oranmore, Ireland).

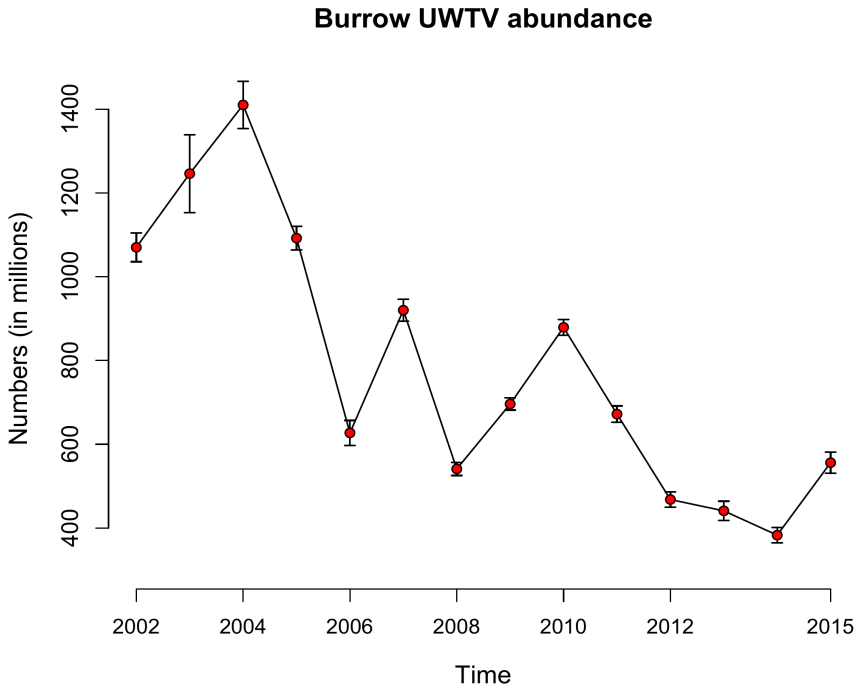
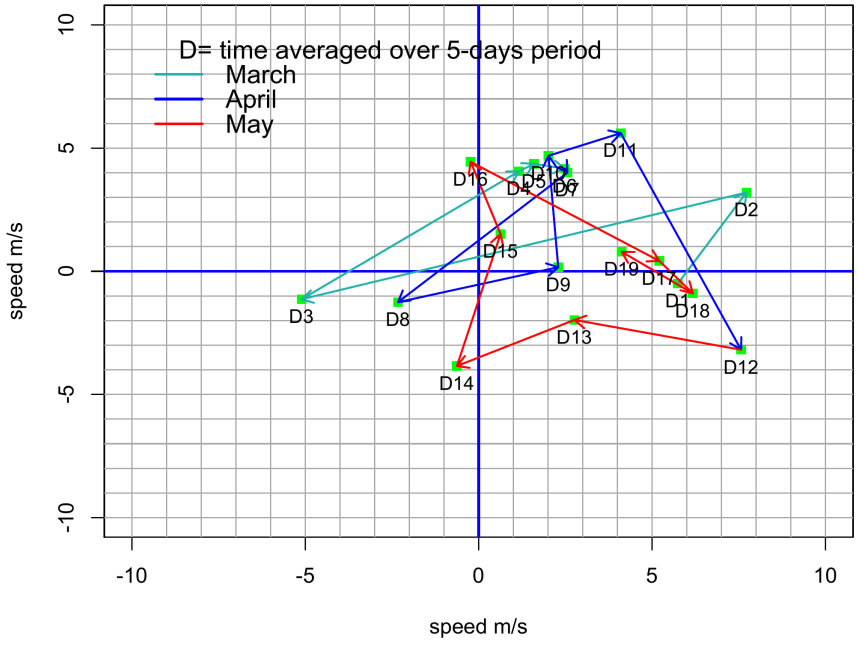
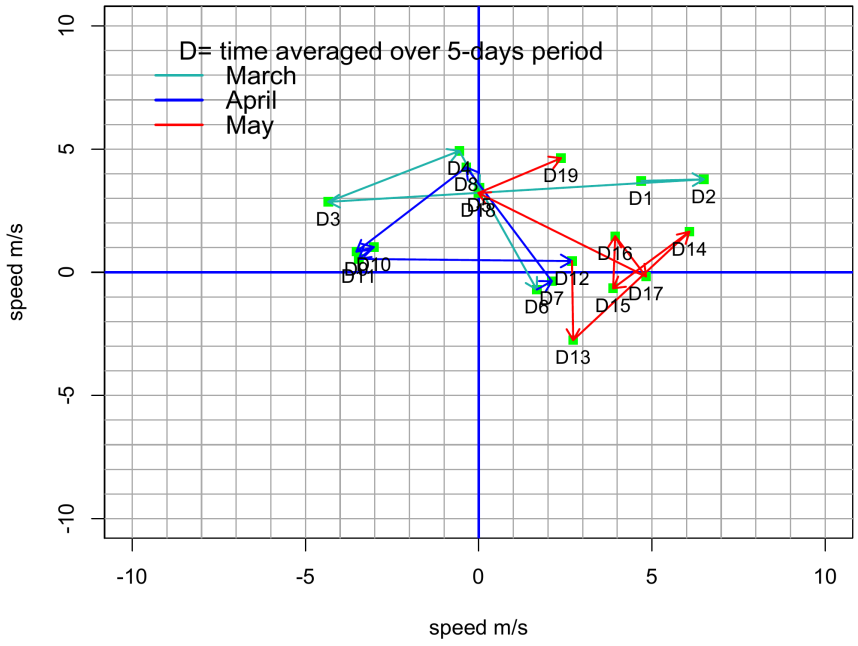


Figure B5: Under water TV burrow abundance (in numbers) from 2002 to 2015 (Source: Marine Institute, Ireland).

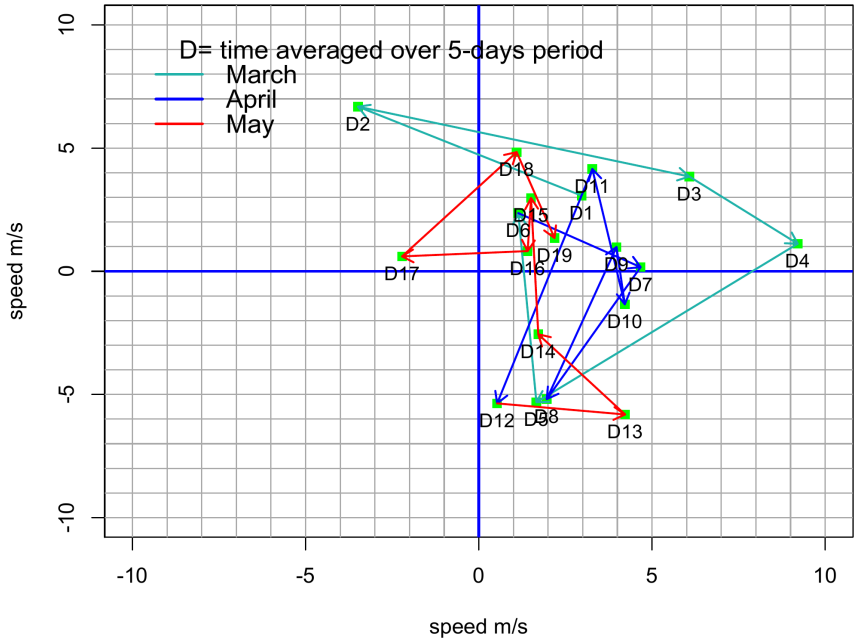
March-April-May 2002: mean wind surface drift



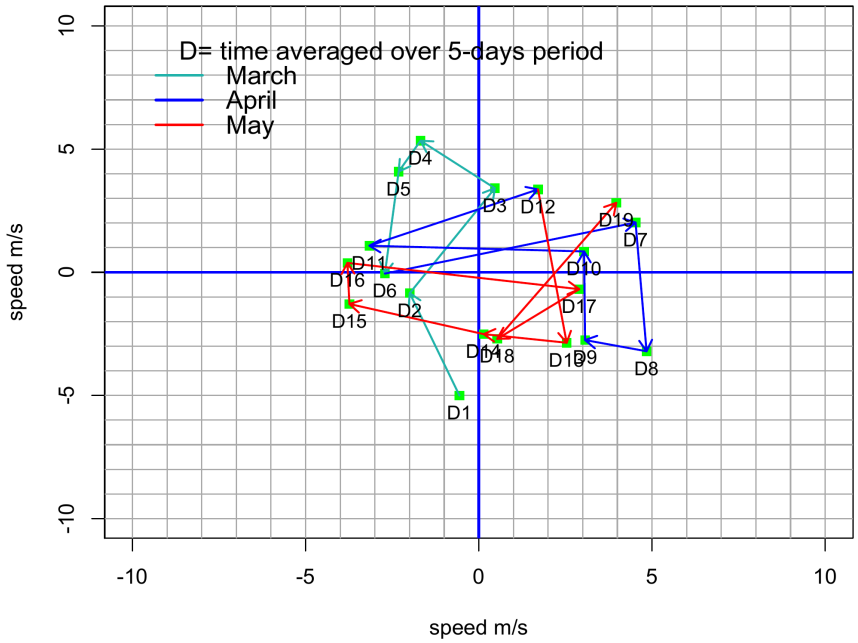
March-April-May 2003: mean wind surface drift



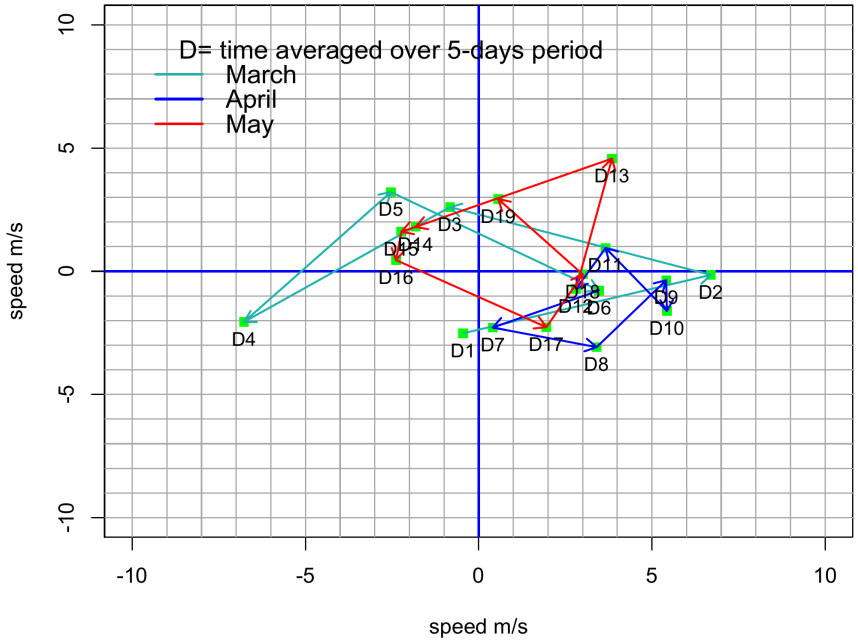
March-April-May 2004: mean wind surface drift



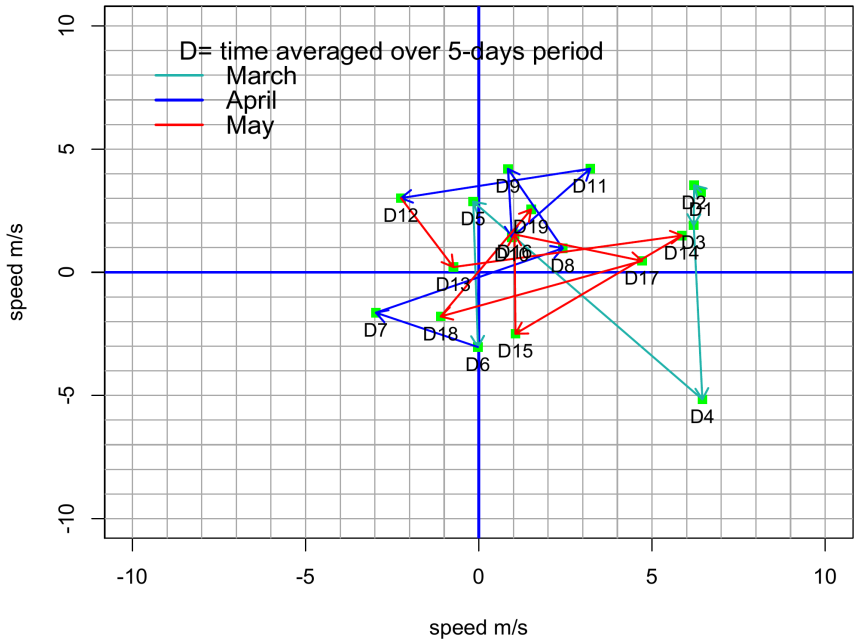
March-April-May 2005: mean wind surface drift



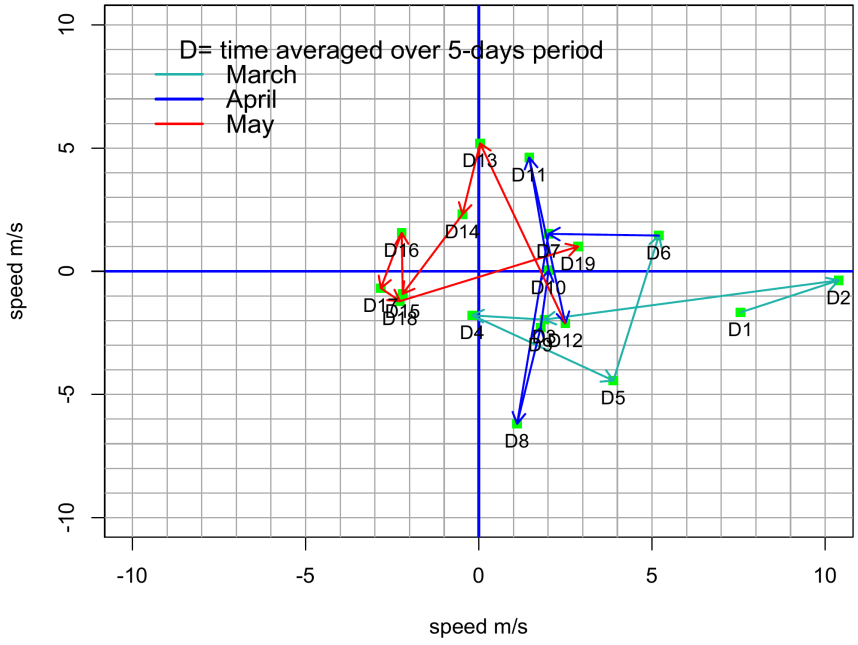
March-April-May 2006: mean wind surface drift



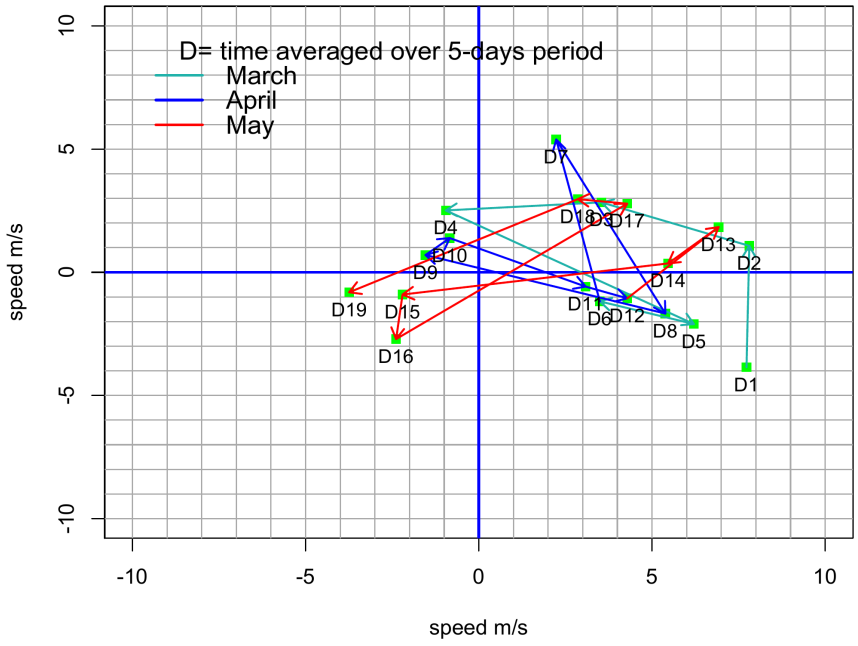
March-April-May 2007: mean wind surface drift



March-April-May 2008: mean wind surface drift



March-April-May 2009: mean wind surface drift



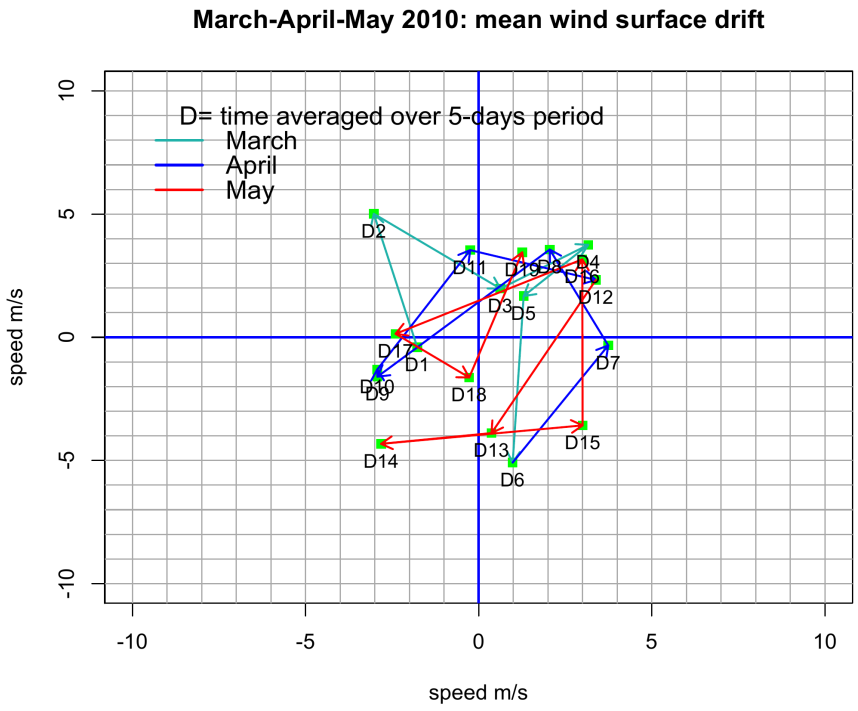


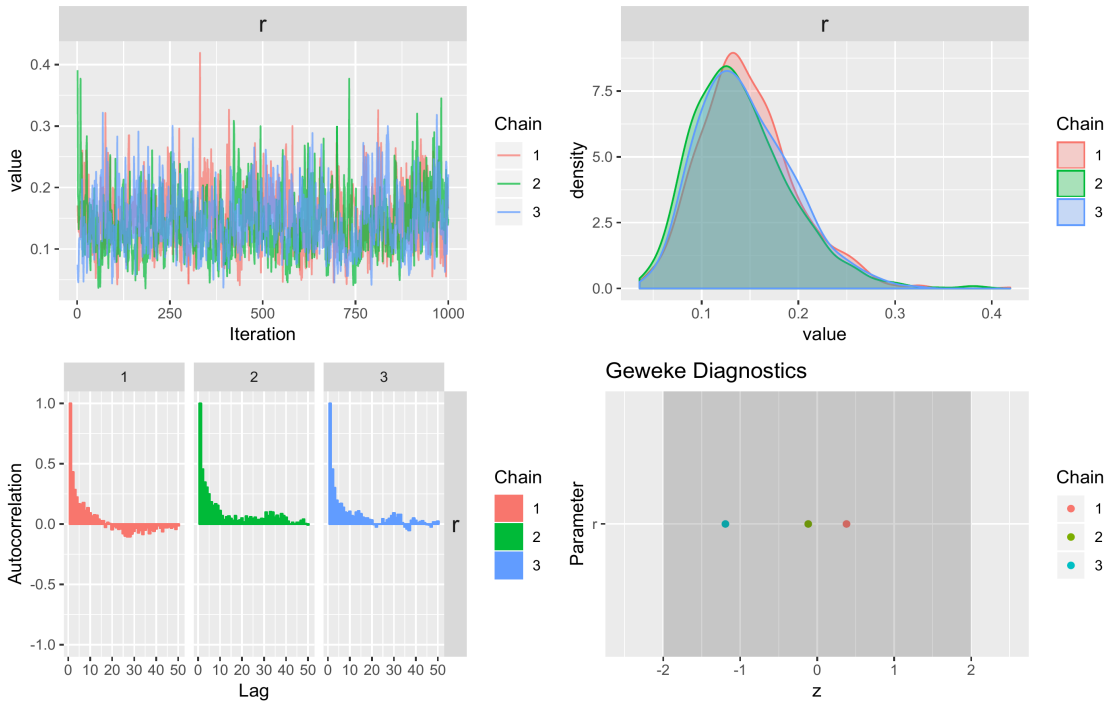
Figure B7: Plots of wind circulation synthesis of the March-April-May period for years 2002 to 2010 over the area delimited by (–18ºW, –9ºW) and (51ºN, 55ºN) using *Atlas FLK v1.1* derived surface winds (level 3.5). Data description: time average of level3.0 products for the periods of interest, created by *NASA Goddard Space Flight Center under the NASA REASON CAN: a Cross-Calibrated, Multi-Platform Ocean Surface Wind Velocity Product for Meteorological and Oceanographic Applications*.

Table B1: Statistics of burrow density distribution from UWTV surveys from 2002 to 2010: *mean*, *median*, *skewness,* m*aximum density, coefficient of variation (CV) and standard deviation (sd).*

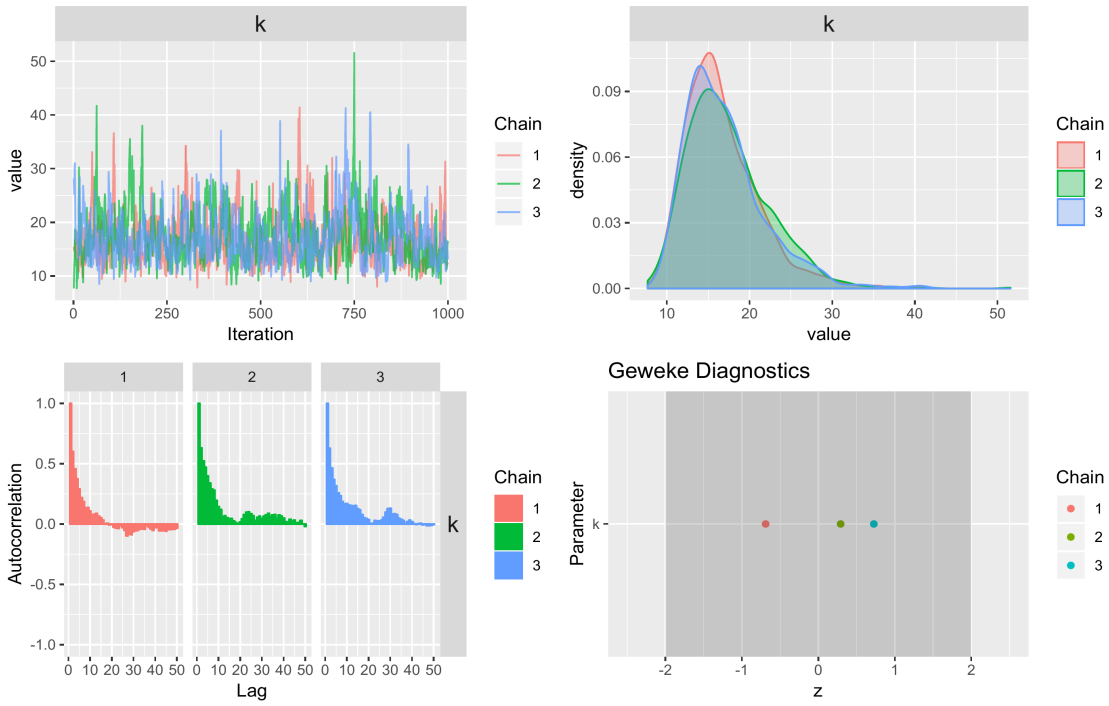
Years	***Median***	***Mean***	***Skewness***	***Maximum density***	***CV***	***sd***
2002	0.93	0.86	-0.29	1.82	0.49	0.42
2003	1.26	1.24	-0.41	2.18	0.31	0.38
2004	1.53	1.49	-0.60	2.85	0.38	0.56
2005	1.19	1.05	-0.94	1.65	0.41	0.44
2006	0.69	0.62	-0.77	1.16	0.46	0.29
2007	1.05	0.93	-0.91	1.62	0.42	0.39
2008	0.61	0.56	-0.67	0.97	0.48	0.27
2009	0.78	0.69	-0.44	1.33	0.54	0.37
2010	0.94	0.82	-0.66	1.51	0.46	0.38

Annexes C

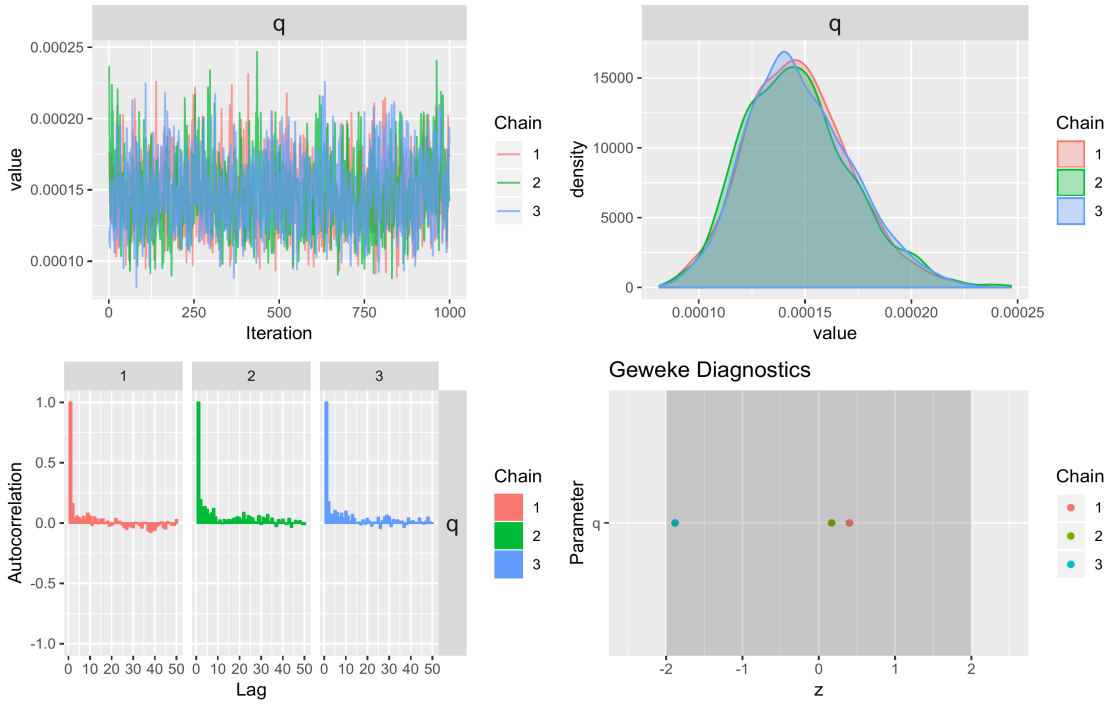
panel (1)



panel (2)



panel (3)


q
value
Iteration
Chain
1
2
3
density
Autocorrelation
Lag
Geweke Diagnostics
Parameter
z

panel (4)

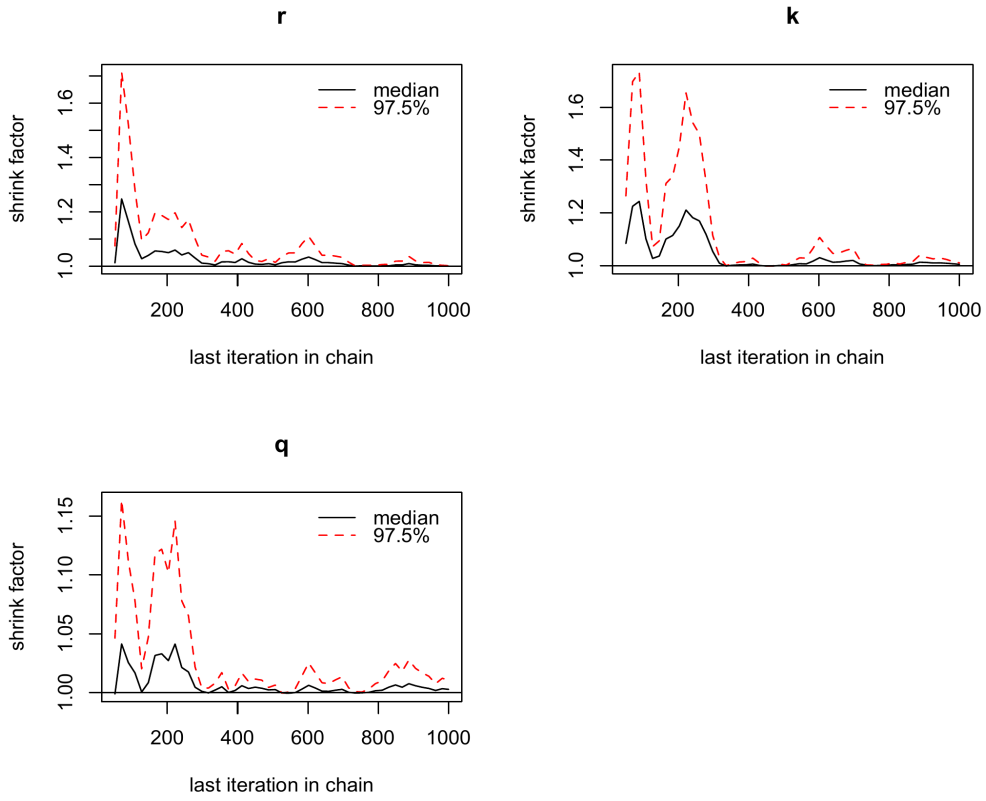
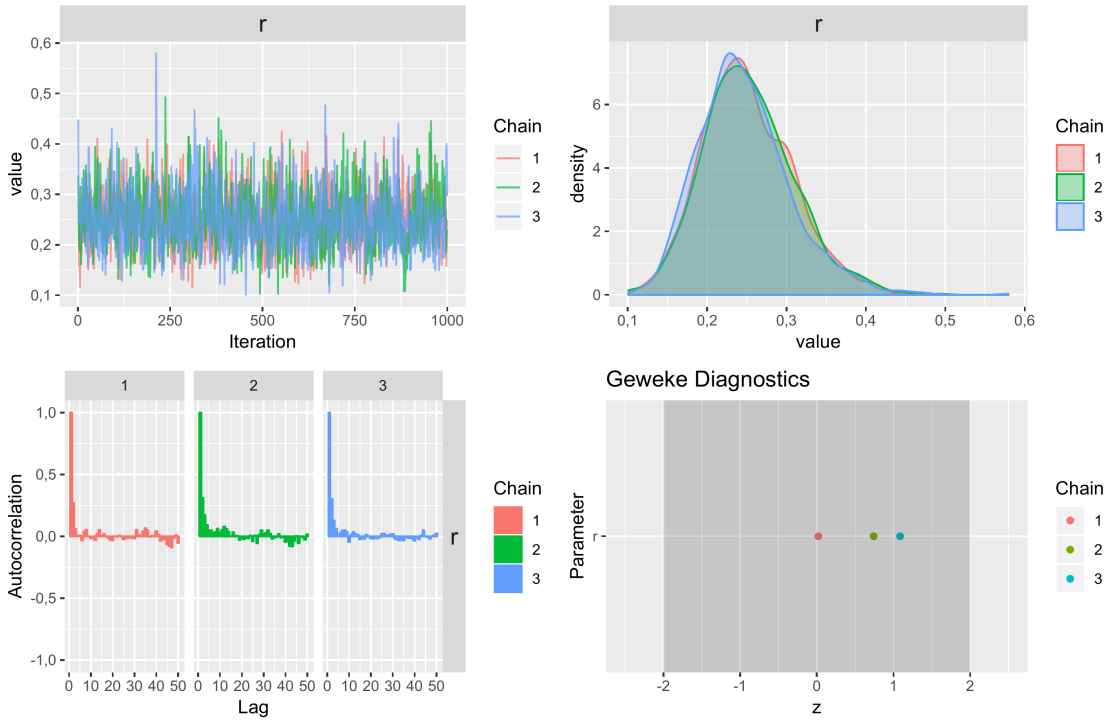


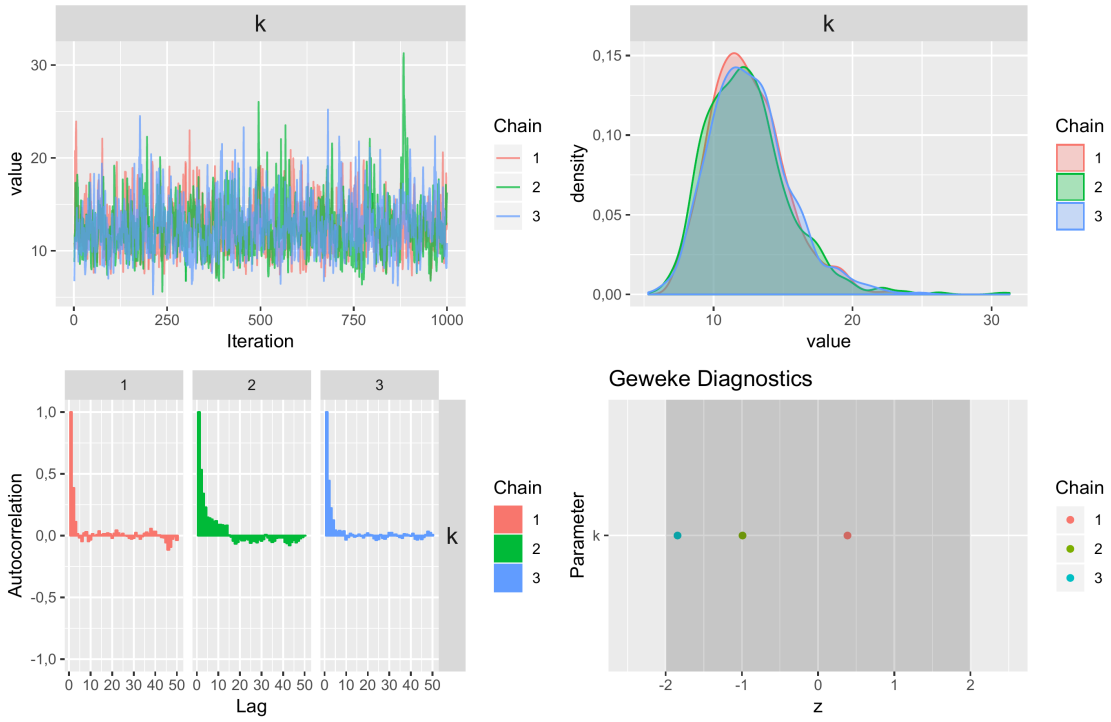
Figure C1: Visual and statistics diagnostic of MCMC convergence for each parameter resulted of the Bayesian Modelling using 1974–2014 landings.

Sample traces (**top left in panel 1-2-3**) appear reasonably well mixed. Autocorrelation functions (**bottom left in panel 1-2-3**) decrease dramatically as k lags increase indicating that the chains move randomly from one iteration to the next. The posterior densities (**Top right in panel 1-2-3**) or MCMC estimates of the parameters are well seize. The Geweke (1992) diagnostic (**bottom right in panel 1-2-3**) is appropriate for analysis of individual chain when convergence of the mean of some function of sampled parameters is of interest. It is based on test for equality of the means of the first 10% and the last 50% part of a Markov chain. If the samples are drawn from the stationary distribution of the chain, the two means are equals and *Geweke's statistic* has an asymptotically standard normal distribution. The test statistic is a standard *Z-score*. *Shrink factors* (or *Potential scale reduction factors*) of parameters *r*, *k* and *q* makes a comparison of within-chain and between-chain variances. According to Brooks and Gelman (1998), if it is close to 1, we can conclude that each of the *m* (=*3*) sets of *n* (=*1000*) simulated observations is close to the target distribution. Otherwise, the simulated sequences have not yet made a full tour of the target distribution.

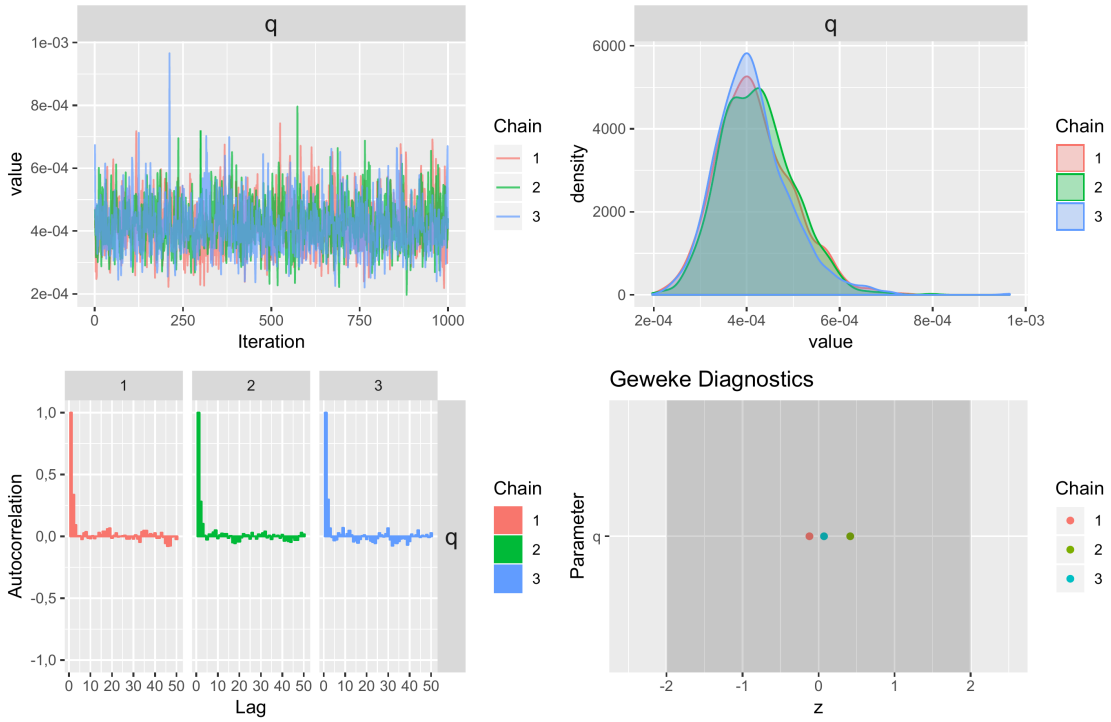
panel (1)



panel (2)



panel (3)


q
value
Iteration
Chain
density
Autocorrelation
Lag
Geweke Diagnostics
Parameter
z

panel (4)

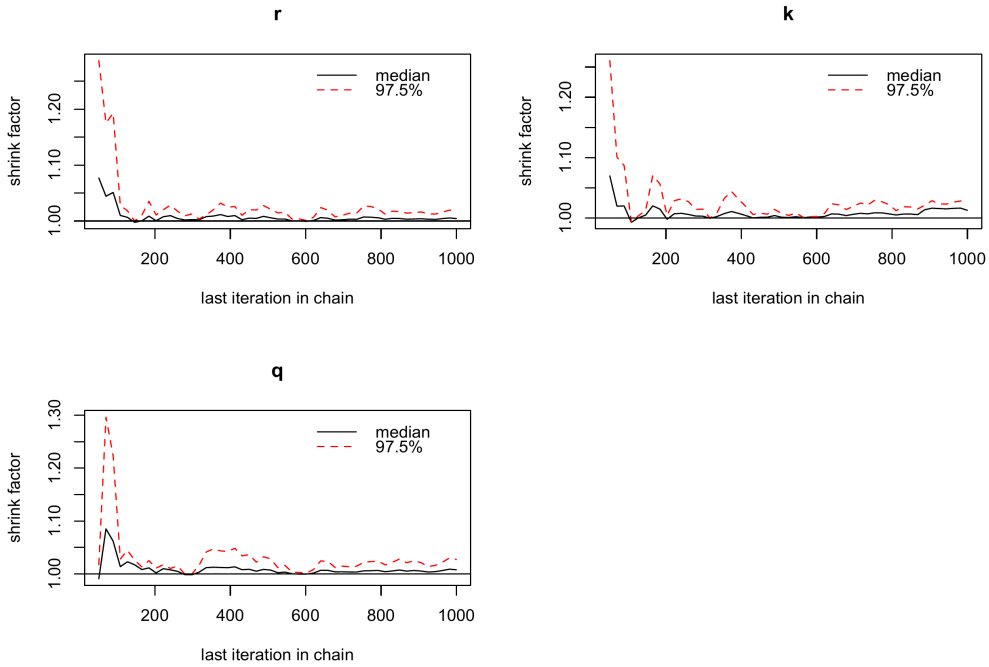
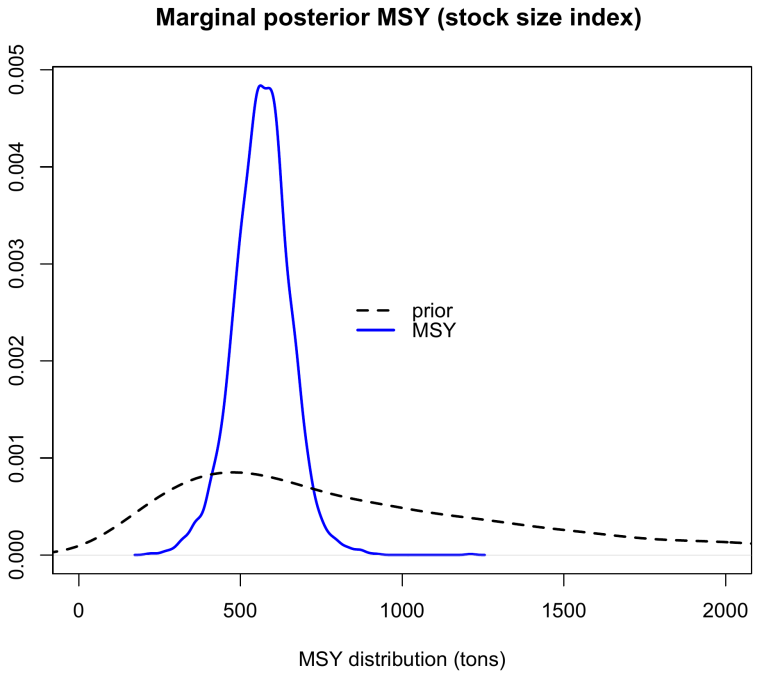


Figure C2: Following suite of the visual and statistics diagnostic of mcmc convergence for each parameter in the case of Bayesian model of a Schaeffer biomass model fitted to 1995–2014 landings series with an lpue index relied on Kw-days measure of the fishing effort.

Trace plots show good mixing (**top left in panel 1-2-3**). *Autocorrelation* values reduce quickly (**bottom left in panel 1-2-3**). *Geweke's statistics* (**bottom right in panel 1-2-3**) lie between [–2, +2]. In less then 50 iterations, *shrink factors* (or *potential scale reduction factors*) of parameters *r*, *k* and *q* drop at 1 (**panel 4**) indicating good convergence.

(a)



(b)

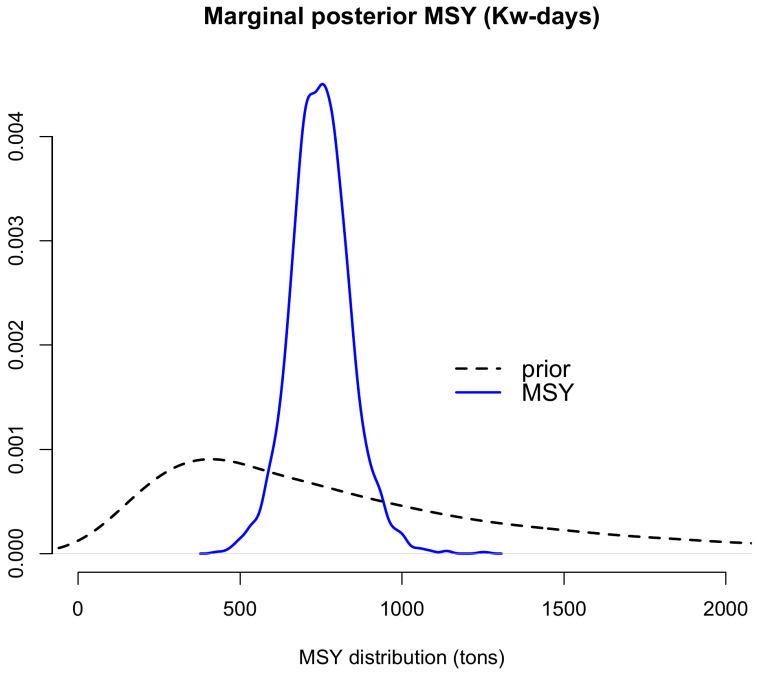
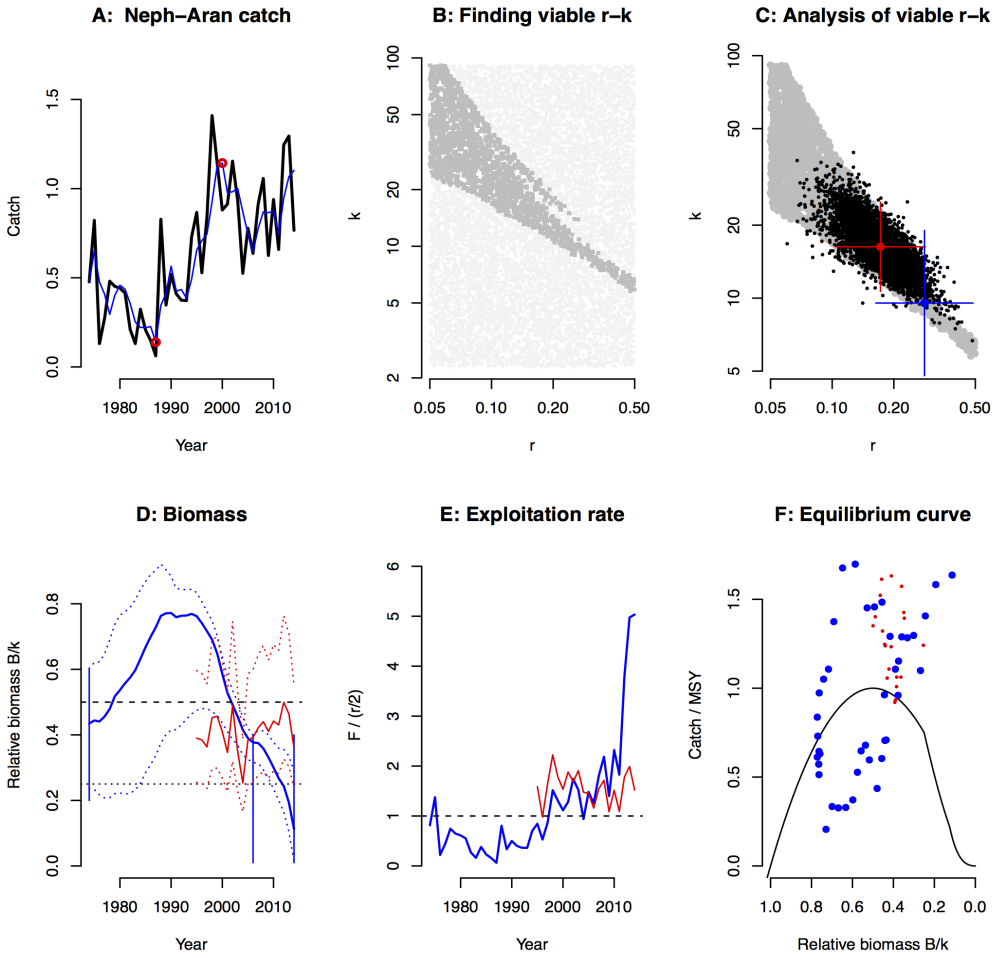
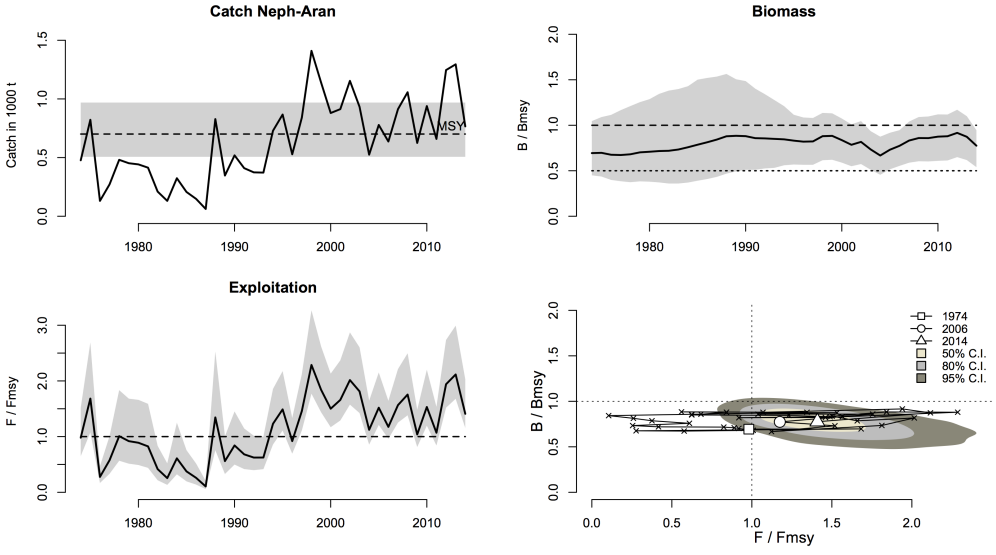


Figure C3a-b: Prior and posterior distributions of the maximum sustainable yield of the state space bayesian surplus production model. The case of the stock size index is more conservative.

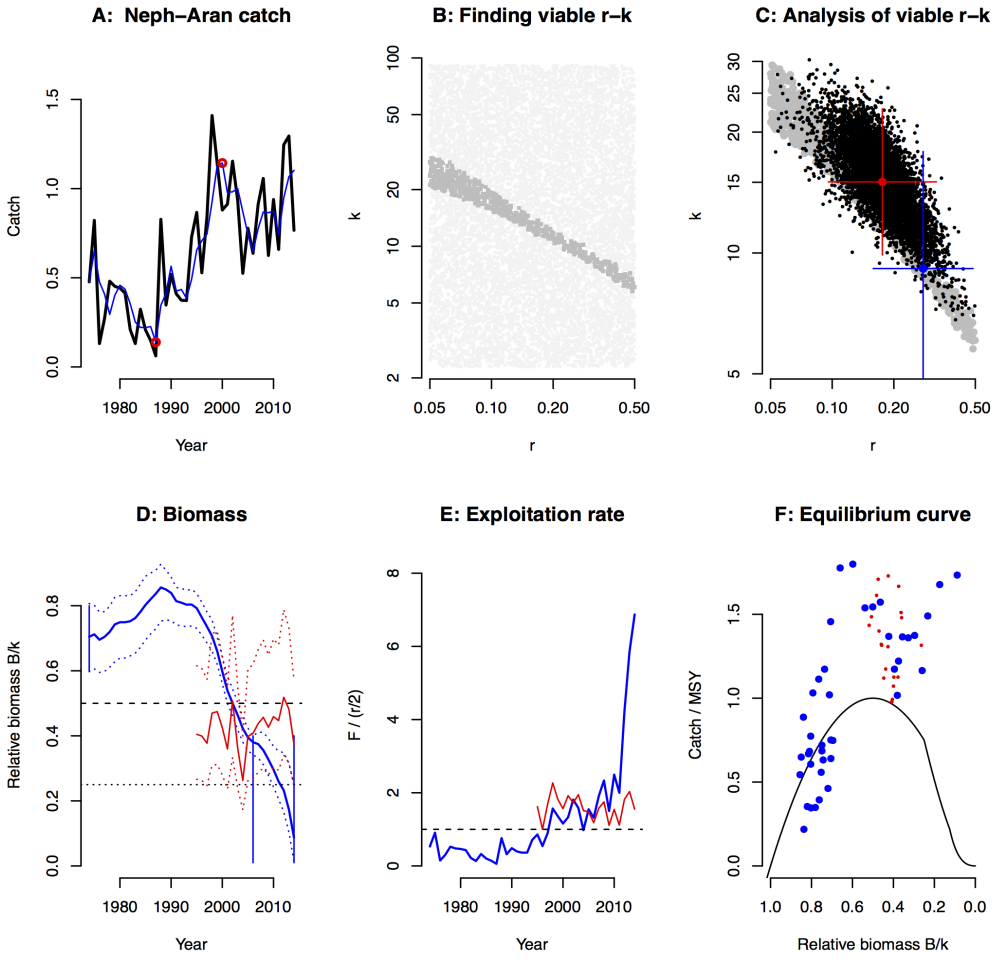
panel (1)



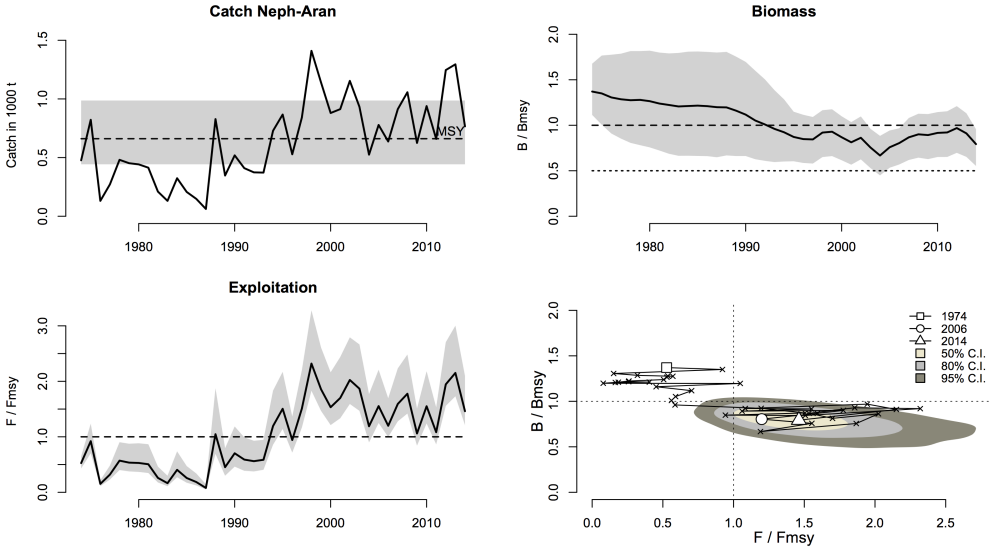
panel (2)



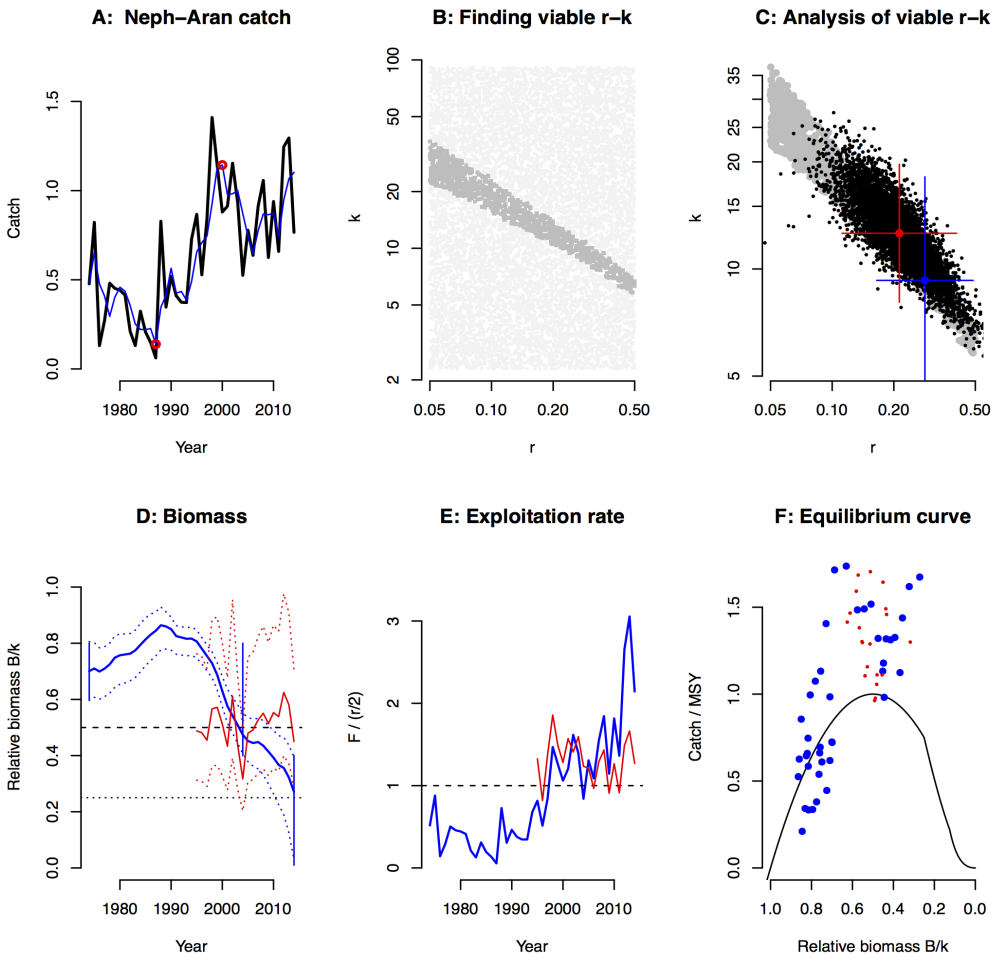
panel (3)



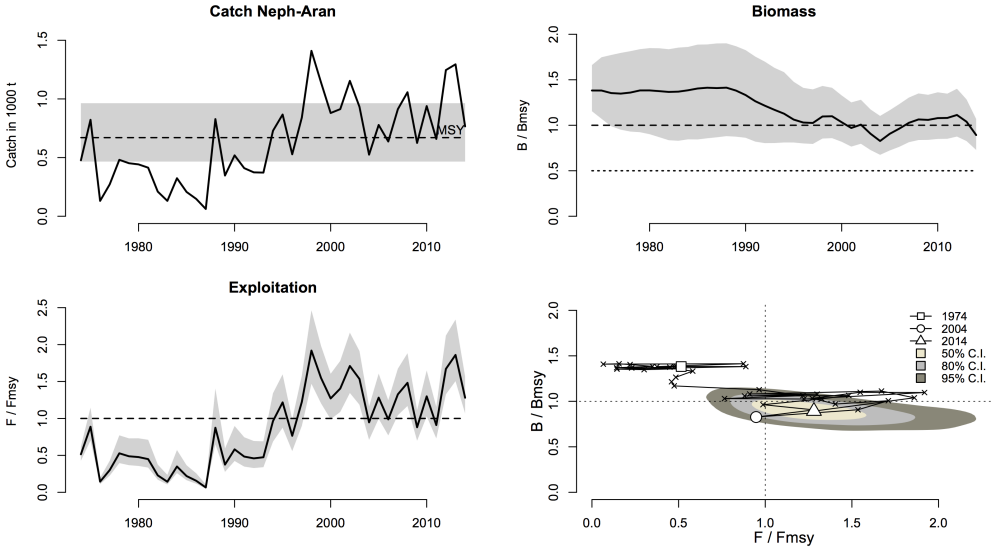
panel (4)



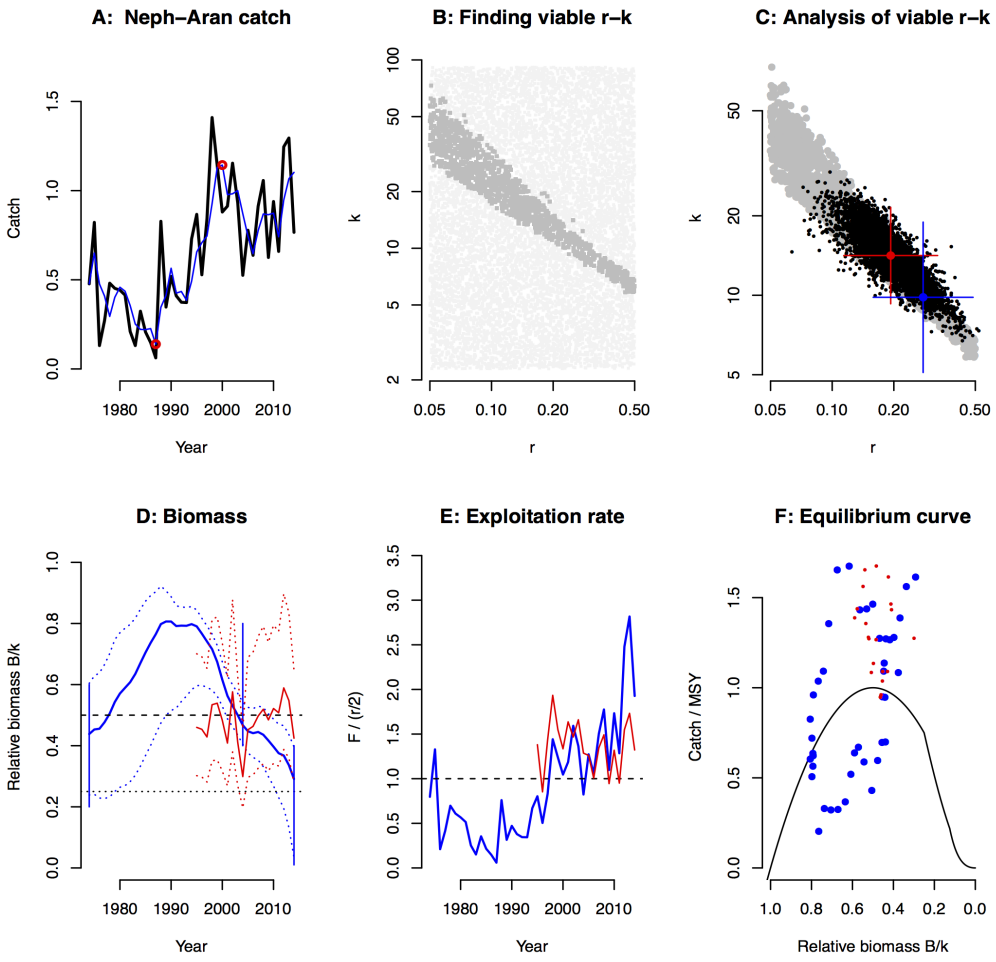
panel (5)



panel (6)



panel (7)


A: Neph–Aran catch
Catch
Year
B: Finding viable r–k
k
r
C: Analysis of viable r–k
k
r
D: Biomass
Relative biomass B/k
Year
E: Exploitation rate
F / (r/2)
Year
F: Equilibrium curve
Catch / MSY
Relative biomass B/k

panel (8)

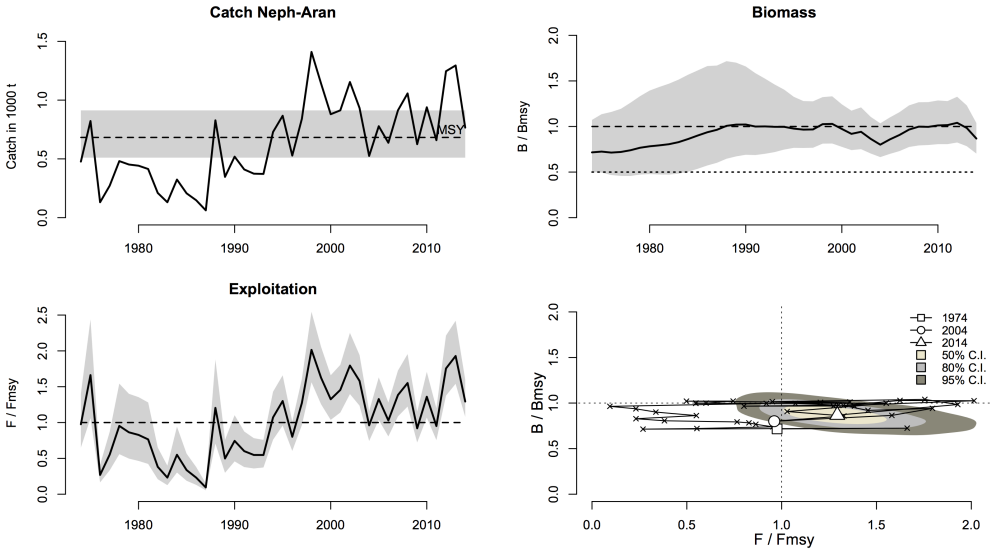
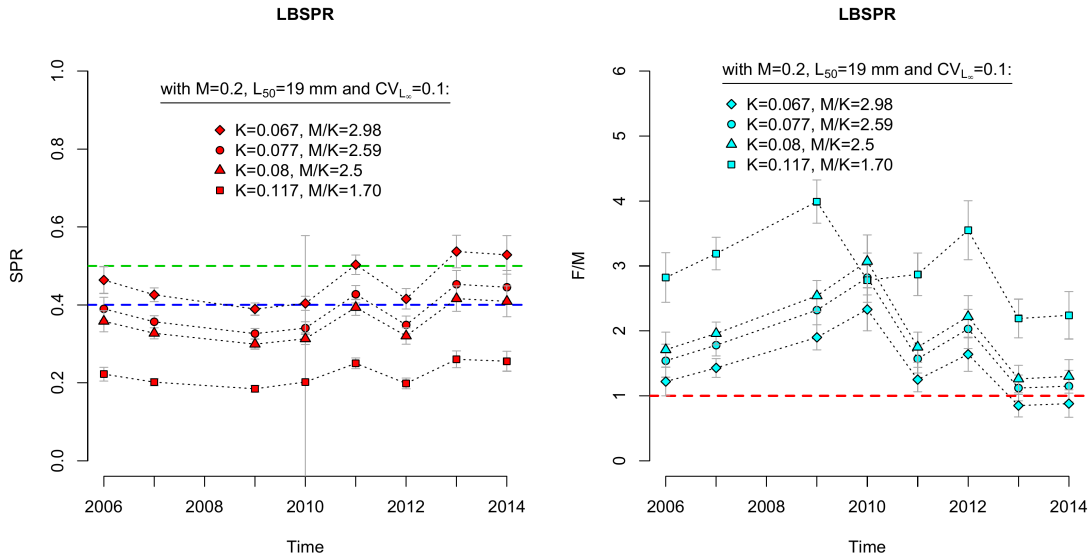


Figure C5: Results of different implementations of the CMSY method by assuming various hypothesis regarding the level of depletion of the stock at the initial and intermediate time of the 1974–2014 period. Here, we use the 1974–2014 landings time series as well as the Kilo-watt-days measures of the fishing effort obtained from EU logbooks of the 1995–2014 period. The sensitivity of the biomass trajectory to the prior ranges (blue vertical line) of the stock depletion is evidenced (**bottom left in panels 1-3-5-7**). Notice, that throughout this procedure we imposed a high level of depletion [0.2–0.4] for the end time of the 1974–2014 series and ignored other possibilities and so in compliance with the reported UWTV abundance.

(a)



(b)

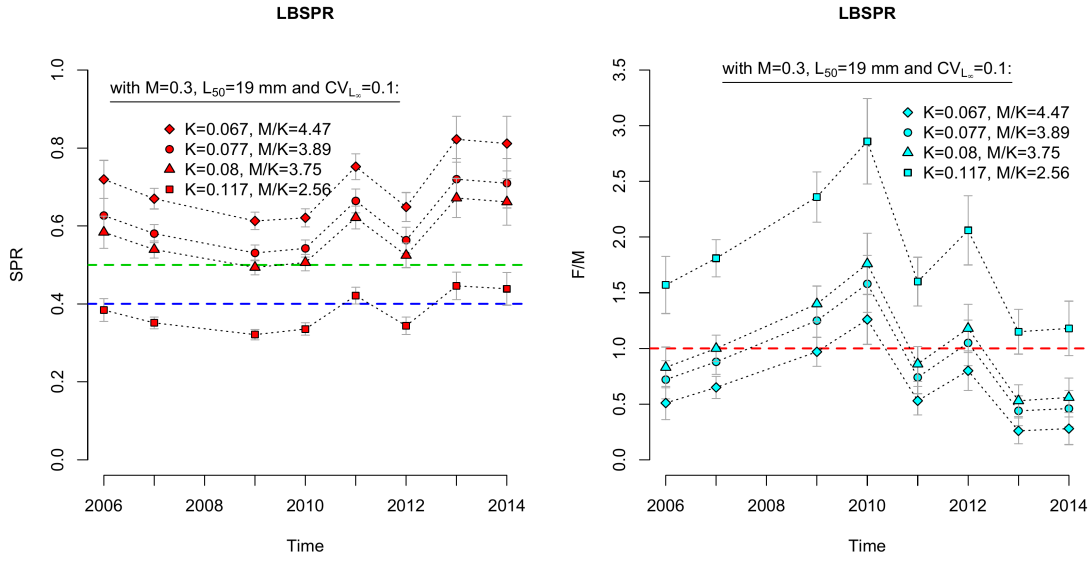
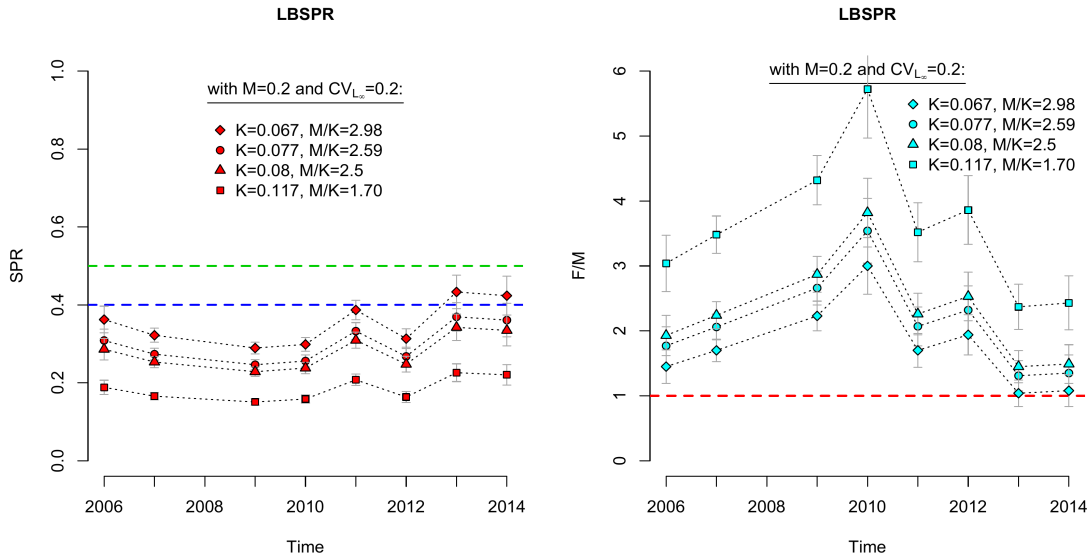


Figure C6a-b: LBSPR model estimates of spawning potential ratio (*SPR*) and exploitation rate (*F/M*) for Aran grounds *Nephrops* stock. Estimates assumed $CV_{L\infty}=0.1$, $L_{50\%}=19$ *mm* and $L_{95\%}=24.5$ *mm* maturity-lengths (at 50% and 95%, respectively) in relation to natural mortality rates $M=0.2$ and $M=0.3$ with varying estimates of female Von Bertalanffy Growth Function (VBGF) coefficients: $K=0.067\ yr^{-1}$, $K=0.077\ yr^{-1}$, $K=0.117\ yr^{-1}$ with asymptotic length $L_{\infty}=55.2$ *mm* (Haynes et al, 2016) and $K=0.08\ yr^{-1}$ with $L_{\infty}=56$ *mm* (ICES IBNeph, 2015).

(c)



(d)

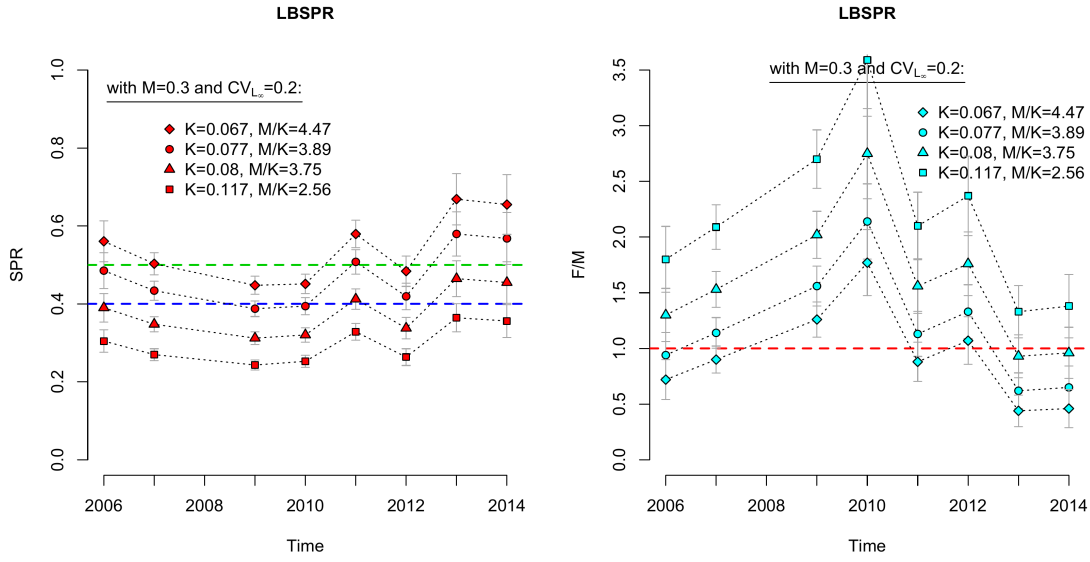


Figure C6c-d: LBSPR estimates of *SPR* and *F/M* for Aran grounds *Nephrops* stock by increasing the L_∞ distribution to *20%* (that is, $CV_{L\infty}=0.2$) and assuming $L_{50\%}=22$ *mm*, $L_{95\%}=24.5$ *mm* maturity lengths in relation to natural mortality rates *M=0.2* and *M=0.3* with varying estimates of female VBGF coefficients: *K=0.067* yr^{-1}, *K=0.077* yr^{-1}, *K=0.117* yr^{-1} with asymptotic length L_∞=55.2 mm (Haynes et al, 2016) and *K=0.08* yr^{-1} with $L_\infty=56$ *mm* (ICES IBNeph, 2015). Horizontal dashed lines indicate *SPR* ratios of *0.4* (blue) and *0.5* (green) and exploitation rate of *F/M=1* (red).

Table C1: Summary of the available data for Aran grounds stock and attempt to quantify its quality. Data are sorted in potentially poor (grey colour) and good (bold black). Source: ICES WKNeph, 2009.

Fishery dependent data	units	available dates
Landing data	tonnes	1974-1994 **1995 1996 1997** 1998 1999 2000 2001 2002 2003 2004 2005 2006 2007 **2008 2009 2010**
Effort data	Hrs (uncorrected)	1995 1996 1997 1998 1999 2000 2001 2002 2003 2004 2005 2006 2007 2008 2009 2010
Capacity	Number and power of vessels	**1995 1996 1997 1998 1999 2000 2001 2002 2003 2004 2005 2006 2007 2008 2009 2010**
Standardised effort data	Effective effort (Hrs & capacity)	Not available
Commercial LPUE	Kg/Hrs	1995 1996 1997 1998 1999 2000 2001 2002 2003 2004 2005 2006 2007 2008 2009 2010
Commercial CPUE	Kg/Hrs	2002 2003 2004 2005 and 2008 2009 2010
Landings size distributions	(mm)	1995 1996 1997 1998 1999 2000 2001
Catch size distributions	(mm)	2002 2003 **2004 2005** and **2008 2009 2010**
Sex Ratio in landings	%	1995 1996 1997 1998 1999 2000 2001
Sex Ratio in catch	%	**2002** 2003 **2004 2005** and **2008 2009 2010**
Maturity data	%	**2002 2003 2004 2005 2006 2007 2008 2009 2010**

Survey data	units	available dates
IBTS Trawl survey catch size distributions	(mm)	2003 2004 2005 2006 2007 2008 2009 2010
Commercial trawl survey CPUE & size	Kg/Hrs & (mm)	**2001**
UWTV survey abundance	numbers	**2002** 2003 **2004 2005 2006 2007 2008 2009 2010**
UWTV Beam size distributions	(mm)	**2006 2007**

Table C2a: Estimated spawning potential ratio (*SPR*) and relative fishing exploitation rate (*F/M*) of the **GTG-LBSPR** model for Aran grounds stock using 2006, 2007, 2009–2014 beam trawl surveys and according to variable proxy coefficients of the von Bertalanffy growth formula (K and L_∞). Common input parameters of these runs are $M=0.2$, $L_{50\%}=22$ *mm* and $L_{95\%}=24.5$ *mm*. We also assumed coefficient values $\alpha=0.000684$ and $\beta=2.963$ for the carapace length-weight relationship $W=\alpha CL^\beta$ (ICES IBPNeph, 2015) and coefficient value $b=2.566$ for the power curve relationship (aCL^b) between the realised fecundity (*i.e.* the number of eggs extruded) and the carapace length (CL) of female as estimated for the western Irish Sea *Nephrops* stock (Briggs et al., 2002b). Between brackets are indicated the *95%* confidence interval of the estimated *SPR* and *F/M*.

Input parametrs: K=0.077 yr^{-1}, M/K=3.89, L_∞=55.2 mm, $L_{50\%}$=22 mm, $CV_{L\infty}$=0.1								
Year	**2006**	**2007**	**2009**	**2010**	**2011**	**2012**	**2013**	**2014**
SPR	0.573 (0.52–0.62)	0.52 (0.49–0.54)	0.463 (0.44–0.48)	0.476 (0.45–0.50)	0.616 (0.58–0.65)	0.5 (0.46–0.53)	0.679 (0.61–0.74)	0.667 (0.59–0.74)
F/M	0.72 (0.54–0.89)	0.88 (0.76–0.99)	1.25 (1.09–1.4)	1.58 (1.32–1.83)	0.74 (0.59–0.88)	1.05 (0.84–1.25)	0.44 (0.30–0.57)	0.46 (0.29–0.62)
Input parameters: K=0.117 yr^{-1}, M/K=2.56, L_∞=55.2 mm, $L_{50\%}$=22 mm, $CV_{L\infty}$=0.1								
SPR	0.342 (0.31–0.37)	0.307 (0.29–0.32)	0.275 (0.26–0.28)	0.290 (0.27–0.30)	0.382 (0.35–0.40)	0.299 (0.27–0.32)	0.408 (0.37–0.44)	0.400 (0.35–0.44)
F/M	1.57 (1.31–1.82)	1.81 (1.64–1.97)	2.36 (2.13–2.58)	2.86 (2.47–3.24)	1.60 (1.38–1.81)	2.06 (1.74–2.37)	1.15 (0.94–1.35)	1.18 (0.93–1.42)
Input parameters: K=0.067 yr^{-1}, M/K=4.47, L_∞=55.2 mm, $L_{50\%}$=22 mm, $CV_{L\infty}$=0.1								
SPR	0.667 (0.60–0.72)	0.608 (0.57–0.63)	0.540 (0.51–0.56)	0.550 (0.52–0.57)	0.706 (0.66–0.74)	0.583 (0.53–0.62)	0.789 (0.71–0.85)	0.776 (0.69–0.85)
F/M	0.51 (0.35–0.66)	0.65 (0.55–0.74)	0.97 (0.83–1.10)	1.26 (1.03–1.48)	0.53 (0.40–0.65)	0.80 (0.62–.97)	0.26 (0.14–0.37)	0.28 (0.13–0.42)
Input parameters: K=0.08 yr^{-1}, M/K=3.75, L_∞=56 mm, $L_{50\%}$=22 mm, $CV_{L\infty}$=0.1								
SPR	0.530 (0.48–0.57)	0.480 (0.45–0.50)	0.428 (0.40–0.45)	0.442 (0.41–0.46)	0.572 (0.54–0.60)	0.463 (0.42–0.49)	0.629 (0.57–0.68)	0.618 (0.55–0.68)
F/M	0.83 (0.64–1.01)	1.00 (0.88–1.11)	1.40 (1.23–1.56)	1.76 (1.48–2.03)	0.86 (0.70–1.01)	1.18 (0.96–1.39)	0.53 (0.38–0.67)	0.56 (0.38–0.73)

Table C2b: *SPR* and *F/M* estimates of the **GTG-LBSPR** model runs with new common input parameters $M=0.2$, $L_{50\%}=19$ *mm* and $L_{95\%}=24.5$ *mm*. We still assumed coefficient values $\alpha=0.000684$ and $\beta=2.963$ for the carapace length-weight relationship $W=\alpha CL^{\beta}$ (ICES IBNeph, 2015) and coefficient value $b=2.566$ for the power curve relationship (aCL^{b}) between the realised fecundity (*i.e.* the number of eggs extruded) and the carapace length (CL) of female as estimated for the western Irish Sea *Nephrops* stock (Briggs et al., 2002b). Between brackets are indicated the *95%* confidence interval of the estimated *SPR* and *F/M*.

	2006	**2007**	**2009**	**2010**	**2011**	**2012**	**2013**	**2014**
Input parameters: K=0.077 yr^{-1}, M/K=2.59, L_{∞}=55.2 mm, $L_{50\%}$=19 mm, $CV_{L\infty}$=0.1								
SPR	0.389 (0.36–0.41)	0.35 (0.34–0.37)	0.32 (0.31–0.33)	0.34 (0.32–0.35)	0.42 (0.40–0.44)	0.34 (0.32–0.37)	0.45 (0.41–0.48)	0.44 (0.40–0.48)
F/M	1.54 (1.28–1.79)	1.78 (1.61–1.94)	2.32 (2.09–2.54)	2.82 (2.44–3.99)	1.57 (1.35–1.78)	2.03 (1.72–2.33)	1.12 (0.92–1.31)	1.15 (0.90–1.39)
Input parameters: K=0.117 yr^{-1}, M/K=1.7, L_{∞}=55.2 mm, $L_{50\%}$=19 mm, $CV_{L\infty}$=0.1								
SPR	0.222 (0.20–0.24)	0.201 (0.19–0.21)	0.184 (0.17–0.19)	0.202 (-0.17–0.6)	0.249 (0.23–0.26)	0.198 (0.18–0.21)	0.260 (0.23–0.28)	0.255 (0.22–0.28)
F/M	2.82 (2.43–3.20)	3.19 (2.94–3.43)	3.99 (3.65–4.32)	2.78 (2.55–3.0)	2.87 (2.54–3.19)	3.55 (3.09–4.00)	2.19 (1.89–2.48)	2.24 (1.87–2.60)
Input parameters: K=0.067 yr^{-1}, M/K=2.98, L_{∞}=55.2 mm, $L_{50\%}$=19 mm, $CV_{L\infty}$=0.1								
SPR	0.46 (0.42–0.49)	0.42 (0.40–0.44)	0.38 (0.37–0.40)	0.40 (0.38–0.42)	0.50 (0.47–0.52)	0.41 (0.38–0.44)	0.53 (0.49–0.57)	0.52 (0.47–0.57)
F/M	1.22 (0.99–1.44)	1.43 (1.28–1.57)	1.90 (1.70–2.09)	2.33 (1.99–2.66)	1.25 (1.06–1.43)	1.64 (1.37–1.90)	0.85 (0.67–1.02)	0.88 (0.66–1.09)
Input parameters: K=0.08 yr^{-1}, M/K=2.5, L_{∞}=56 mm, $L_{50\%}$=19 mm, $CV_{L\infty}$=0.1								
SPR	0.35 (0.33–0.38)	0.32 (0.31–0.34)	0.29 (0.28–0.31)	0.31 (0.29–0.32)	0.39 (0.37–0.41)	0.32 (0.29–0.34)	0.41 (0.38–0.44)	0.40 (0.36–0.44)
F/M	1.71 (1.44–1.97)	1.96 (1.78–2.13)	2.54 (2.30–2.77)	3.07 (2.66–3.47)	1.75 (1.51–1.98)	2.22 (1.89–2.54)	1.26 (1.04–1.47)	1.30 (1.04–1.55)

References

Abello, P., Abella, A., Adamidou, A., Jukic-Peladic, S., Maiorano, P., Spedicato, M. T. (2002) Geographical patterns in abundance and population structure of *Nephrops norvegicus* and *Parapenaeus logirostris* (Crustacea: Decapoda) along the European Mediterranean coasts. Scientia. Marina. 66, 125–141.

Afonso-Dias, M. (1998) Variability of *Nephrops norvegicus* (L.) populations in Scottish waters in relation to the sediment characteristics of the seabed. PhD thesis, University of Aberdeen, 282 pp.

Agostinelli, C., and Lund, U. (2017) R package circular: Circular Statistics (version 0.4-93). URL https://r-forge.r-project.org/projects/circular/

Aguzzi, J., Sardà, F., Abelló, P., Company, J. B., Rotllant, G. (2003a) Trawls catches rhythmicity of *Nephrops norvegicus* (Decapoda: Nephropidae) in the North-Western Mediterranean: a perspective through depth and season. Mar. Ecol. Prog. Ser. 258, 201–211.

Aguzzi, J., Sarda, F., Abello, P., Company, J.B., Rotllant, G. (2003b) Diel and seasonal patterns of *Nephrops norvegicus* (Decapoda: Nephropidae) catchability in the western Mediterranean. Mar. Ecol. Prog. Ser. 258, 201–211.

Aguzzi, J., Bozzano, A., and Sardà, F. (2004a) First observations on *Nephrops norvegicus* (L.) burrow densities on the continental shelf off the Catalan coast (western Mediterranean). Crustaceana, 77: 299–310.

Aguzzi, J., Company, J. B., Sardà, F. (2004b) Feeding activity rhythm of *Nephrops norvegicus* of the western Mediterranean shelf and slope grounds. Marine Biology 144(3): 463–472.

Aguzzi, J., Sardà, F., Allué, R. (2004c) Seasonal dynamics in *Nephrops norvegicus* (Decapoda: Nephropidae) catches off the Catalan coasts (Western Mediterranean) Fisheries Research 69, 293–300.

Aguzzi, J., Sardà, F. (2008) A history of recent advancements on *Nephrops norvegicus* behavioural and physiological rhythms. Review in Fish Biology and Fisheries 18, 35–48.

Aguzzi, J., Bahamon, N., Marotta, L. (2009a) The influence of light availability and predatory behaviour of the decapod crustacean *Nephrops norvegicus* on the activity rhythms of continental margin prey decapods. Mar. Ecol. 30, 366–375.

Aguzzi, J., Puig, P., Company J. B. (2009b) Hydrodynamic, non-photic modulation of biorhythms in the Norway lobster, *Nephrops norvegicus* (L.) Deep-Sea Research **I 56** 366–373.

Aguzzi, J. and Company, J. B. (2010) Chronobiology of deep-water Decapod crustaceans on continental margins in Advances in Marine Biology, Volume 58: The ecology and biology of *Nephrops norvegicus*. Series Editor: Michael Lesser. Academic Press. Elsevier Ltd. All rights reserved.

Allen C. R., Holling C. S. (2002) Cross-scale morphology Volume 1, pp 450–452 in Encyclopedia of Environmetrics Edited by Abdel H. El-Shaarawi and Walter W. Piegorsch. John Wiley & Sons, Ltd, Chichester, 2002. ISBN 0471 899976.

Allen, C. R., Angeler, D. G., Moulton, M. P., and Holling, C. S. (2015) The Importance of Scaling for Detecting Community Patterns: Success and Failure in Assemblages of Introduced Species. Diversity 2015, 7, 229-241.

Allen, C. R., Angeler, D. G., Cumming, G. S., Folke, C., Twidwell, D., Uden, D. R. (2016) Quantifying spatial resilience. Journal of Applied Ecology 53, 625–635.

Allendorf, F. W., Hard, J. J. (2009) Human-induced evolution caused by unnatural selection through harvest of wild animals. Proceeding of the National Academy of Sciences 16 vol. 106 suppl. 1: 9987–9994.

Angeler, D. G., Allen, C. R., Uden, D. R., Johnson, R. K. (2015) Spatial scaling patterns and functional redundancies in a changing boreal lake landscape. Ecosystems, 18, 889–902.

Ambaum, M. H. P., Brian, J. H., Stephenson, D. B. (2001) Arctic Oscillation or North Atlantic Oscillation?. Journal of Climate, Boston, **vol. 14**, N°16, pages. 3495–3507.

Arnold, L. M., Heppell, S. S. (2014) Testing the robustness of data-poor assessment methods to uncertainty in catch and biology: a retrospective approach ICES Journal of Marine Science.

Atlas, R., Hoffman, R. N., Ardizzone, J., Leidner, S. M., Jusem, J. C., Smith, D. K., Gombos, D. (2011) A cross-calibrated, multiplatform ocean surface wind velocity product for meteorological and oceanographic applications. Bull. Amer. Meteor. Soc., 92, 157–174. doi: 10.1175/2010BAMS2946.1

Auguie, B. (2017) gridExtra: Miscellaneous Functions for "Grid" Graphics. R package version 2.3.

Baho, D. L., Allen, C. R., Garmestani, A. S., Fried-Petersen, H. B., Renes, S. E., Gunderson, L., Angeler, D. G. (2017) A quantitative framework for assessing ecological resilience. Ecology and Society 22(3):17. doi.org/10.5751/ES-09427-220317.

Bailey, N., Chapman, C. J. A (1983) Comparison of density, length composition and growth of two *N. norvegicus* populations off the west coast of Scotland. ICES CM 1983/K: 42, 1–18.

Bailey, N. (1986) Why does the size of Nephrops vary? Scott. Fish. Bull. 49, 31–36.

Bailey, N., Chapman, C. J., Kinnear, J., Bova, D., Weetman, A. (1993) Estimation of *Nephrops* Stock Biomass on the Fladen Ground by TV Survey. ICES CM 1993/K:34 (mimeo).

Bailey, N., Chapman, C. J., Afonso-Dias, M., Turrell, W. (1995) The Influence of Hydrographic Factors on Nephrops Distribution and Biology ICES CM 1995/Q:17 (poster)

Barnston, A. G., and Livezey, R. E. (1987) Classification, seasonality and persistence of low-frequency atmospheric circulation patterns. Monthly. Weather. Review., 115, 1083–1126.

Beaugrand, G., Goberville, E., Luczak, C., Kirby, R. (2014) Marine biological shifts and climate. Proc. R. Soc. B 281: 20133350.

Becker, R. A., Allan R. Wilks, A. R., Brownrigg, R. Minka, T. P. and Deckmyn, A. (2018) maps: Draw Geographical Maps. R package version 3.3.0. https://CRAN.R-project.org/package=maps

Begg, G. A., Friedland, K. D. Pearce, J. B. (1999) Stock identification and its role in stock assessment and fisheries management: an overview. Fisheries Research, 43:1–8.

Bell, M. C., Elson, J. M., Addison, J. T. (2005) The effects of spatial targeting of fishing effort on the distribution of the Norway lobster, Nephrops norvegicus, on the Farn Deeps grounds. New Zealand Journal of Marine and Freshwater Research, 39, 1023–37.

Bell, M. C., Redant, F., Tuck, I. (2006) *Nephrops* species. In: Phillips, B. F. (Ed.), Lobsters Biology, Management, Aquaculture and Fisheries. Blackwell Publishing, Oxford, pp. 412–461.

Bell, E., Clements, A., Dobby, H., Doyle, J., Feekings, J. P., Leocádio, A., Lordan, C., Wieland. K. (2018) Using underwater television surveys to assess and advise on *Nephrops* stocks. International Council for the Exploration of the Sea. ICES Cooperative Research Report; No. 340.

Beverton, R. J. H., Holt, S. J. (1959) A review of the lifespans and mortality of rates of fish in nature, and their relation to growth and other physiological characteristics: 142–180. In CIBA Foundation Colloquia On Ageing Vol. 5 The Lifespan of Animals. Edited by G. E. W. Wolstenholme and Maeve O'Connor. 1959 Ciba Foundation.

Beverton, R. J. H. (1992) Patterns of reproductive strategy parameters in some marine teleost fishes. Journal of Fish Biology 41 (SupplementB), 137–160.

BIM (2017a) Bord Iscaigh Mhara: the Business of Seafood. A Snapshot of Ireland's Seafood Sector. Ireland's Seafood Development Agency (www.bmi.ie).

BIM (2017b) Bord Iascaigh Mhara. Fisheries Conservation Report: *Nephrops* survivability in The Irish demersal trawl fishery. Ireland Seafood Development Agency.

BIM (2018) Bord Iscaigh Mhara. The Business of Seafood. A Snapshot Ireland's Seafood Sector. Ireland's Seafood Development Agency (www.bmi.ie).

Bivand, R. S., Pebesma, E. J., Gomez-Rubio, V. (2013) Applied spatial data analysis with R. Second edition. Springer.

Bivand, R., Lewin-Koh, N. (2018) maptools: Tools for Handling Spatial Objects. R package version 0.9-4. https://CRAN.R-project.org/package=maptools

Bjørkvoll, E., Grøtan, V., Aanes, S., Sæther, B-E., Engen, S., Aanes, R. (2012) Stochastic Population Dynamics and Life-History Variation in Marine Fish Species. The American Naturalist, Vol. 180, No. 3 pp. 372–387.

Björnsson, H. Venegas, S. A. (1997) A manual for EOF and SVD analyses of climate data. McGill University, CCGCR Report No. 97-1, Montréal, Québec, 52pp.
Bolker, B. M. (2007) Ecological models and data in R. Princeton University Press.

Bonjean, F., Lagerloef, G. S. E (2002) Diagnostic model and analysis of the surface currents in the tropical Pacific Ocean. J. Phys. Oceanogr., vol. 32, pg. 2938–954.

Box, G. E. P., Jenkins, G. M. (1970) Time Series Analysis: Forecasting and Control. Holden-Day, San Francisco. 598 pp.

Box, G. E. P., Jenkins, G. M., Reinsel, G. C. (1994) Time series analysis: forecasting and control. 3rd edition, Prentice Hall.

Branch, T. A, Watson, R., Fulton, E. A., Jennings, S., McGilliard, C. R., Pablico, G. T; Ricard, D., Tracey, S. R. (2010) The trophic fingerprint of marine fisheries. Nature, Vol. 468, 431–435.

Branch, T. A., Jensen, O. P., Ricard, D., Ye, Y., Hilborn, R. (2011) Contrasting global trends in marine fishery status obtained from catches and from stock assessments. Conservation Biology, Volume 25, No. 4, 777–786.

Briggs, R. P. (1995) Variability in northwest Irish Sea *Nephrops* populations Fisheries Research 23 (1995) 175–187.

Briggs, R. P. (2000) A preliminary analysis of *Nephrops* survey data from the western Irish Sea. In: Report of the ICES Study Group on Life History of *Nephrops*. ICES CM 2000/G:06 (mimeo). pp. 113–20.

Briggs, R. P., McAliskey, M. (2002a) The prevalence of *Hematodinium* in *Nephrops norvegicus* from the western Irish Sea. J. Mar. Biol. Ass. U.K., 82, 427–433.

Briggs, R. P., Armstrong, M. J., Dickey-Collas, M., Allen, M., McQuaid, N., Whitmore, J. (2002b) The application of fecundity estimates to determine the spawning stock biomass of Irish Sea *Nephrops norvegicus* (L.) using the annual larval production method. ICES Journal of Marine Science, 59: 109–119.

Brooks, S. P., and Gelman, A. (1998) General methods for monitoring convergence of iterative simulations. American Statistical Association, Institute of Mathematical Statistics, and Interface Foundation of North America Journal of Computational and Graphical Statistics, Volume 7, Number 4, Pages 434–455.

Brooks, E. N., Powers, J. E., Cortes, E. (2010) Analytical reference points for age-structured models: application to data-poor fisheries. ICES J. Mar. Sci. 67:165–175.

Brown, E. D., Williams, B. K. (2015) Resilience and Resource Management. Environmental Management 56:1416–1427 doi: 10.1007/s00267-015-0582-1. Creative Commons Attribution 4.0 International License (http://creativecommons.org/licenses/by/4.0/).

Cadrin, S. X., Friedland, K. D., Waldman, J. R. (2005) Stock Identification Methods Applications in Fishery Science. Elsevier. Academic Press.

Campbell, N., Allan, L., Weetman, A., Dobby, H. (2009) Investigating the link between *Nephrops norvegicus* burrow density and sediment composition in Scottish waters. ICES Journal of Marine Science 66, 2052–2059.

Carpenter, S., Walker, B. J., Anderies, M., Abel, N. (2001) From Metaphor to Measurement: Resilience of What to What? Ecosystem 4 765-781.

Carruthers, T. R., Walters, C. J., McAllister, M. K. (2012) Evaluating methods that classify fisheries stock status using only fisheries catch data. Fisheries Research 119-120, 66–79.

Carson Rachel (1962) Silent Spring. Crest book.

Carruthers, T. R., Punt, A. E., Walters, C. J., MacCall, A., McAllister, M. K., Dick, E. J., Cope, J. (2014) Evaluating methods for setting catch limits in data-limited fisheries. Fisheries Research 153: 48–68.

Castro, M., Araujo, A., Monteiro, P., Madeira, A. M., Silvert, W. (2003) The efficacy of releasing caught *Nephrops* as a management measure. Fisheries Research, 65: 475–484.

Catchpole, T. L., Van Keeken, O., Gray, T. S., Piet, G. (2008) The discard problem - A comparative analysis of two fisheries: The English *Nephrops* fishery and the Dutch beam trawl fishery. Ocean & Coastal Management, 51(11), 772–778.

Cavanaugh, J. and Shumway, R. (1997) A bootstrap variant of AIC for state-space model selection. Statistica Sinica 7:473–496.

Chan, K-S., Ripley, B. (2018) TSA: Time Series Analysis. R package version 1.2.

Chapman, C. J., Rice, A. L. (1971) Some direct observations on the ecology and behaviour of the *Norway lobster*, *Nephrops norvegicus*. Marine Biology 10, 321–329.

Chapman, C. J., Priestley, R., Robertson, R. (1972) Observations on the diurnal activity of the Norway lobster, *Nephrops norvegicus* (L.). ICES 20, 254–269.

Chapman, C. J., Johnstone, A. D. F., Rice, A. L. (1975) The behaviour and ecology of the Norway lobster, *Nephrops norvegicus* (L.). In: H. Barnes (Ed.) Proceedings of the 9th European Marine Biological Symposium. Aberdeen University Press, Aberdeen. pp. 59–74.

Chapman, C. J. (1980) Ecology of Juvenile and Adult Nephrops. In: Cobb, J.S., Phillips, (Eds.), The biology and management of lobsters. Ecology and Management, vol. II. Academic Press, London.

Chapman, C. J. (1982) *Nephrops norvegicus* tagging experiments in Scottish waters 1977-1979. ICES CM 1982/K: **22**, 1–7.

Chapman, C. J., Shelton, P. M. J., Shanks, A. M., Gaten, E. (2000) Survival and growth of the Norway lobster *Nephrops norvegicus* in relation to light-induced eye damage. Marine Bioogy 136, 233–241.

Charnov, E. L., Gislason, H., Pope, J. G. (2013) Evolutionary assembly rules for fish life histories. Fish Fish. 14: 213–224.

Charnov, E. L. (2014) Gompertz mortality, natural selection, and the "shape of ageing". Evol. Ecol. Res. 16: 435–439.

Chiesa, J. J., Aguzzi, J., Garcìa, J. A., Sardà, F., De la Iglesia, H. (2010) Light intensity determines temporal niche switching of behavioural activity in deep water *Nephrops norvegicus* (Crustacea: Decapoda). Journal of Biological Rhythms 25, 277–287.

Chiles, J-P., Delfiner, P. (2012) Geostatistics Modeling Spatial Uncertainty. Second Edition by John Wiley & Sons, Inc ISBN: 978-0-470-18315-1.

Clark, Isobel (2001) Practical geostatistics. Elsevier.

Clark W. G (2002) $F_{35\%}$ revisited ten years later. North American Journal of Fisheries Management 22: 251–257. American Fisheries Society.

Clark, Isobel (2010) Statistics or geostatistics? Sampling error or nugget effect? The Journal of The Southern African Institute of Mining and Metallurgy. Volume 110, June 2010. page 307–312.

Coll, M., Palomera, I., Tudela, S., Sardà, F. (2006) Trophic flows, ecosystem structure and fishing impacts in the South Catalan Sea, Northwestern Mediterranean. J. Mar. Syst. 59, 63–96.

COM (2001) 135 Final 20.3.2001. Green Paper On the Future of the Common Fisheries Policy. Commission of the European Communities.

COM (2020) COM 259. final. Report on the implementation of the Marine Strategy Framework Directive on the implementation of the Marine Strategy Framework Directive (Directive 2008/56/EC). SWD(2020) 60 final–SWD(2020) 61 final–SWD(2020) 62 final.

Commandeur, J., Koopman, S. J. (2007) An Introduction to state space time series analysis. Oxford: Oxford University Press.

Cope, J. M. (2013) Implementing a statistical catch-at-age model (Stock Synthesis) as a tool for deriving overfishing limits in data-limited situations.
Fisheries Research 142: 3–14.

Cope, J. M., Dick, E. J., MacCall, A., Monk, M., Soper, B., Wetzel, C. (2013) Data-moderate stock assessments for brown, China, copper, sharpchin, stripetail, and yellowtail rockfishes and English and rex soles in 2013 Pacific Fishery management Council Documents 2013.

Cortes, E. (2016) Perspectives on the intrinsic rate of population growth. Methods in Ecology and Evolution 2016, 7, 1136–1145.

Cosgrove, R., Browne, D., Minto, C., Tyndall, P., Oliver M., Montgomerie M., McHugh, M. (2018) A game of two halves: Bycatch reduction in Nephrops mixed Fisheries. Fisheries Research 210, 31–40.

Cowpertwait P. S. P., Metcalfe A. V. (2009) Introductory Time Series with R. Springer.

Cristo, M. & Cartes, J. E. A (1998) Comparative study of the feeding ecology of *Nephrops norvegicus* (L.), (Decapoda: Nephropidae) in the bathyal Mediterranean and the adjacent Atlantic. Scientia. Marina. 62, 81–90.

Cryer, J. D., Chan, K. S. (2008) Time Series Analysis with Applications in R. 2nd Edition. Springer.

Cumming, G. S. (2011) Spatial Resilience in Social Ecological System. Springer.

Cushing, D. H. (1982) Climate and fisheries. Academic Press, London.

Cushing, D. H. (1990) Plankton production and year-class strength in fish populations: An update of the match/mismatch hypothesis. Advances in Marine Biology, 26, 249–94.

da Silva Santana, C. A., Wieczorek, A. M., Browne, P., Graham, C. T., Power, A. M. (2020) Importance of suspended particulate organic matter in the diet of *Nephrops norvegicus* (Linnaeus,1758). Nature, scientific report 10: 3387.

Daan, N., Gislason, H., Pope, J. G., Rice, J. C. (2011) Apocalypse in world fisheries? The reports of their death are greatly exaggerated. ICES Journal of Marine Science, 68: 1375–1378.

Dakos, V., Carpenter, S. R., Brock, W. A., Ellison, A. M., Guttal, V., Ives, A. R., Kéfi, S., Livina, V., Seekell, D. A., van Nes, E. H., Scheffer, M. (2012) Methods for Detecting Early Warnings of Critical Transitions in Time Series Illustrated Using Simulated Ecological Data. PLOS ONE Volume 7 Issue 7 e41010.

Dakos, V., Carpenter, S. R., van Nes, E. H., Scheffer, M. (2015) Resilience indicators: prospects and limitations for early warnings of regime shifts. Phil. Trans. R. Soc. B 370: 20130263.

Dakos, V., Glaser, S. M., Hsieh, C-h., Sugihara, G. (2017) Elevated nonlinearity as an indicator of shifts in the dynamics of populations under stress. J. R. Soc. Interface 14: 20160845.

Deepayan S., and Andrews, F. (2016) latticeExtra: Extra Graphical Utilities Based on

Lattice. R package version 0.6-28.

Deepayan, S. (2008) Lattice: Multivariate Data Visualization with R. Springer, New York. ISBN 978-0-387-75968-5.

Deser, C. (2000) On the teleconnectivity of the "Arctic oscillation". Geophys. Res. Lett., 27, N°6, 779–782.

Dichmont, M. C., Deng, A. R., Punt, A. E., Brodziak, J., Chang, J. Y, Cope, J. M., Ianelli, J. N., Legault, C. M., Methot, R. D. Jr., Porch, C. E., Prager, H. M., Shertzer, W. K. (2016) A review of stock assessment packages in the United States. Fisheries Research 183: 447–460.

Dick, E. J., MacCall, A. D. (2011) Depletion-based stock reduction analysis: a catch-based method for determining sustainable yields for data-poor fish stocks. Fisheries Research 110, 331–341.

Dickey-Collas, M., Brown, J., Fernanda, L., Hill, A. E., Horsburgh, K. J., Garvine, R. W. (1997) Does the western Irish Sea gyre influence the distribution of pelagic juvenile fish? Journal of Fish Biology 51 (Supplement A), 206–229.

Dickey-Collas, M., McQuaid, N., Armstrong, M. J., Allen, M., Briggs, R. P. (2000a) Temperature-dependent stage durations of Irish Sea *Nephrops* larvae. Journal of Plankton Research Vol.22 no.4 pp.749–760.

Dickey-Collas, M., Briggs, R. P., Armstrong, M. J., Milligan, S. P. (2000b) Production of *Nephrops norvegicus* larvae in the Irish Sea. Marine Biology 137: 973–981.

Dimech M., Kaiser, M. J., Ragonese, S., Schembri, P. J. (2012) Ecosystem effects of fishing on the continental slope in the Central Mediterranean Sea. Marine Ecology Progress Series, Vol. 449: 41–54.

Dolder, J., Thorson, J. T., Minto, C. (2018) Spatial separation of catches in highly mixed fisheries. Scientific Reports, 2018, 8:13886. Nature.
Drewery, J., Bova, D., Kynoch, R. J., Edridge, A., Fryer, R. J., O'Neill, F. G. (2010) The selectivity of the Swedish grid and 120 mm square mesh panels in the Scottish *Nephrops* trawl fishery. Fisheries Research 106, 454–459.

Du Buit, M. H. (1995) Food and feeding of Cod (*Gadus Morhua L.*) in the Celtic sea. Fisheries Research 22: 227–24.

Durbin, J. Koopman, S. J. (2012) Time series analysis by state space methods. 2nd Edition Oxford Statistical Science Series 38. Oxford: Oxford University Press.

Dyson, J. (1977) Business in great waters. The story of British fishermen. Angus and Robertson, London.

Eastwood, P. D., Mills, C. M., Aldridge, J. N., Houghton, C. A., and Rogers, S. I. (2007) Human activities in UK offshore waters: an assessment of direct, physical pressure on the seabed. ICES Journal of Marine Science, 64: 453–463.

EC (2009) Green Paper: Reform of the Common Fisheries Policy COM(2009), 163 final.

EC Regulation 1224/2009. Council Regulation (EC) No 1224/2009of 20 November 2009 in Official Journal of the EuropeanUnion 30.12.2009. L343/1.https://eur-lex.europa.eu/LexUriServ/LexUriServ.douri=OJ:L:2009:343:0001:0050:EN:PDF.

EC Regulation 404/2011. Commission Implementing Regulation (EU) No 404/2011 in Official Journal of the European Union 30.4.2011 L 112/. https://eur-lex.europa.eu/LexUriServ/LexUriServ.do?uri=OJ:L:2011:112:0001:0153:EN:PDF

EEA (2019) European Environment Agency. The european environment, state and outlook 2020. Knowledge for transition to a sustainable Europe. Luxembourg: Publications Office of the European Union, 2019. ISBN 978-92-9480-090-9.

Eiríksson H. (1999) Spatial variabilities of CPUE and mean size as possible criteria for unit stock demarcations in analytical assessments of Nephrops at Iceland. Rit Fiskideildar 16: 239–245.

Eiríksson, H. (2014) Reproductive Biology of Female Norway Lobster, *Nephrops norvegicus* (Linnaeus, 1758) Leach, in Icelandic Waters During the Period 1960–2010: Comparative Overview of Distribution Areas in the Northeast Atlantic and the Mediterranean in Advance in Marine Science Vol 68.

Emsley, S. M., Tarling, G. A., Burrows, M. T. (2005) The effect of vertical migration strategy on retention and dispersion in the Irish Sea during spring-summer. Fisheries Oceanography. 14:3, 161–174.

Engelhard, G. H., Pinnegar, J. K. (2010) *Nephrops*. In: Rijnsdorp, A. D., Peck, M. A., Engelhard, G. H., Möllmann, C., Pinnegar, J. K. (Eds.), Resolving climate impacts on fish stocks. Copenhagen: ICES Cooperative Research Report 301, pp. 203–207.

Engelhard, G. H., Righton, D. A., Pinnegar, J. K. (2014) Climate change and fishing: a century of shifting distribution in North Sea cod. Global Change Biology (2014) 20, 2473–2483.

Eriksson, S. P., Baden, S. P. (1997) Behaviour and tolerance to hypoxia in juvenile Norway lobster (*Nephrops norvegicus*) of different ages. Marine. Biology. 128, 49–54.

Essington, T. E., Beaudreau, A. H., Wiedenmann, J. (2006) Fishing through marine food webs. PNAS vol. 103 no. 9: 3171–3175.

EU (2013) Regulation (EU) No 1380/2013 of the European Parliament and the Council of 11 December 2013 on the Common Fisheries Policy, amending Council Regulations (EC) No 1954/2003 and (EC) No 1224/2009 and repealing Council Regulations (EC) No 2371/2002 and (EC) No 639/2004 and Council Decision 2004/585/EC. O. J. Eur. Union L 354, 22–61.

EU (2016) Commission Delegated Regulation (EU) 2016/2250 of 4 October 2016 Establishing a Discard Plan for Certain Demersal Fisheries in the North Sea and in Union Waters of ICES Division IIa. L 340/2.

FAO (2003) Garcia, S. M., Zerbi, A., Aliaume, C., Do Chi, T., Lasserre, G. The ecosystem approach to fisheries. Issues, terminology, principles, institutional foundations, implementation and outlook. FAO Fisheries Technical Paper. No. 443. Rome, FAO. 2003. 71 pages.

FAO (2010) Landing data for *Nephrops norvegicus* in 1955-2010 using FAO programme and database FishStatJ. http://www.fao.org/fishery/statistics/software/fishstatj/en

FAO FishstatJ (2018) Fishery and Aquaculture Statistics. Global production by production source 1950-2016 (FishstatJ). In: FAO Fisheries and Aquaculture Department, Rome. Updated 2018. (www.fao.org/fishery/statistics/software/fishstatj/en)

FAO (2020) The State of World Fisheries and Aquaculture 2020. Sustainability in action. Rome. (https://doi.org/10.4060/ca9229en.)

Fariña, C., Freire, J., González-Guriarán, E. (1994) *Nephrops norvegicus* in the Galician continental shelf (NW Spain): abundance and distribution. Fish Res., 19: 33–347.

Farmer, A. S. D. (1975) Synopsis of biological data on the Norway lobster *Nephrops norvegicus* (Linnaeus 1758). Food and Agriculture Organisation, Fisheries Synopsis, No. 112: 1–97.

Fernández i Marín, X. (2016) ggmcmc: Analysis of MCMC Samples and Bayesian Inference. Journal of Statistical Software, 70(9), 1-20. doi:10.18637/jss.v070.i09.

Figueiredo, M. J. (1982) The occurrence of resorption in the ovaries Nephrops norvegicus (L.) in Portuguese waters. International Council for the Exploration of the Sea CM 1982/K:28, pp. 1–7.

Finley, A., Banerjee, S., Hjelle, Ø. (2017) MBA: Multilevel B-Spline Approximation. R package version 0.0-9. https://CRAN.R-project.org/package=MBA

Finney, B. P., Gregory-Eaves, I., Sweetman, J., Douglas, M. S. V., Smol, J. P. (2000) Impacts of climatic change and fishing on Pacific salmon abundance over the past 300 years. Science, 290: 795–799.

Fogarty, M. J. (2002) Climate variability and ocean ecosystem dynamics: implications for sustainability. In Challenges of a Changing Earth. Proceedings of the Global Change Open Science Conference, Amsterdam, the Netherlands, 10-13 July 2001, pp. 27–29. Ed. by W. Steffen, J. Jager, D. J. Carson, and C. Bradshaw. Springer, Berlin. 240 pp.

Foley, N. S., Curtin, R., Jackson, E., Keatinge, M., Maloney, D., Nolan, C. and Tyndall, P. (2016) An Economic Survey to Determine the Level of Seafood Activity and Establish its Economic Importance to the Area of Ros an Mhíl. Ros an Mhíl Case Study Report. Fisheries Economics Group, Bord Iascaigh Mhara.

Froese, R., Zeller, D., Kleisner, K., Pauly, D. (2012) What catch data can tell us about the status of global fisheries Marine Biology Volume 159, Issue 6, pp 1283–1292.

Froese, R., Zeller, D., Kleisner, K., Pauly, D. (2013) Worrisome trends in global stock status continue unabated: a response to a comment by R.M. Cook on “What catch data can tell us about the status of global fisheries”. Marine Biology. DOI 10.1007/s00227-013-2185-9.

Froese, R. Pauly, D. (2015) FishBase. World Wide Web electronic publication. www.fishbase.org, version (10/2015), accessed at www.fishbase.org in November/December 2015.

Froese, R., Demirel, N., Coro, G., Kleisner, K., Winker, H. (2016) A simple user guide for CMSY. Published online at http://oceanrep.geomar.de/33076/.

Froese, R., Demirel, N., Coro, G., Kleisner, K. M., Winker, H. (2017) Estimating fisheries reference points from catch and resilience. Fish and Fisheries 18., issue 3: 506–526. John Wiley & Sons Ltd.

Froese, R., Winker, H., Coro, G., Demirel, N., Athanassios, C., Tsikliras, A. C., Dimarchopoulou, D., Scarcella, G., Quaas, M., Matz-Lück, N. (2018) Status and rebuilding of European fisheries. Marine Policy 93 156–170.

Fulton, E. A., Fuller, M., Smith, A. D. M., Punt, A. (2004) Ecological Indicators of the Ecosystem Effects of Fishing: Final Report. Australian Fisheries Management Authority Report, R99/1546.

Fulton, E. A., Smith, A. D. M., Punt, A. E. (2005) Which ecological indicators can robustly detect effects of fishing? ICES Journal of Marine Science, 62: 540–551.

Fulton, E. A., Smith, A. D. M., Smith, D. C. (2007) Alternative Management Strategies for Southeast Australian Commonwealth Fisheries: Stage 2: Quantitative Management Strategy Evaluation. Australian Fisheries Management Authority Report.

Fulton, E. A., Smith, A. D. M., Smith, D. C., Johnson, P. (2014) An Integrated Approach Is Needed for Ecosystem Based Fisheries Management: Insights from Ecosystem-Level Management Strategy Evaluation. PLOS ONE 14 Volume 9 Issue 1 e84242.

Gabriel, W. L., Mace, P. M. (1999) A Review of Biological Reference Points in the Context of the Precautionary Approach. Proceedings, 5th NMFS NSAW. 1999. NOAA Tech. Memo. NMFS-F/SPO-40.

Garrison T. (2009) Essentials of oceanography. 5th Edition. Brooks/Cole. Cengage Learning.

Garstang Walter (1900) The impoverishment of the Sea. a critical summary of the experimental and statistical evidence bearing upon the alleged depletion of the trawling grounds. Journal of the Marine Biological Association 6, pages 1–69. United Kingdom.

Gascuel, D., Merino, G., Döring, R., Druon, J. N., Goti, L., Guénette, S., Macher, C., Soma, K., Travers-Trolet, M., Mackinson, S. (2012) Towards the implementation of an integrated ecosystem fleet-based management of European fisheries. Marine Policy 36: 1022–1032.

Gascuel, D., Coll, M., Fox, C., Guénette, S., Guitton, J., Kenny, A., Knittweis, L., Nielsen, J. R., Piet, G., Raid, T., Travers-Trolet, M., Shephard, S. (2014) Fishing impact and environmental status in European seas: a diagnosis from stock assessments and ecosystem indicators. Fish and Fisheries. Volume 17, issue 1 March 2016 page 31–55.

Gaten, E., Moss, S. Johnson, M. L. (2013) The reniform reflecting superposition compound eyes of *Nephrops norvegicus*: optics, susceptibility to light induced damage, electrophysiology and a ray tracing Mmodel in Advances in Marine Biology, Volume 64: The Ecology and Biology of *Nephrops norvegicus*. Edited by Magnus L. Johnson and Mark P. Johnson. Series Editor: Michael Lesser. Academic Press. Elsevier Ltd. All rights reserved.

Gelman, A., Carlin, J. B., Stern, H. S., Rubin, D. B. (2003) Bayesian Data Analysis. 2nd edition. Chapman & Hall/CRC, Boca Raton.

Gerritsen, H., and Lordan, C. (2011) Integrating vessel monitoring systems (VMS) data with daily catch data from logbooks to explore the spatial distribution of catch and effort at high resolution. ICES Journal of Marine Science, 68: 245–252.

Geweke, J. (1992) Evaluating the accuracy of sampling based approaches to the calculation of posterior moments. In Bayesian statistics 4, (ed. J. O. Bernardo, J. M. Berger, A. P. Dawid, and A. F. M. Smith), pp. 169–94.

González Herraiz, I., Torres, M. A., Farinã A. C., Freire, J., Cancelo, J. R. (2009) The NAO index and the long-term variability of *Nephrops norvegicus* population and fishery off West of Ireland. Fisheries Research 98, 1–7.

González Herraiz, I., Farinã, A. C., Freire, J., Cancelo, J. R. (2015) Exploring long-term variability of *Nephrops norvegicus* population and fishery off North Galicia (NW Spain). Fisheries Reasearch 165: 121–126.

Goodall, Christine Alexandra (1988) The sensory detection of water borne vibrational stimuli and their motor effects in the Norway lobster, *Nephrops norvegicus* (L.). PhD Thesis. University of Glasgow.

Goodyear, C. P. (1980) Compensation in fish populations. In C. H. Hocutt and J. R. Stauffer, eds. Biological monitoring of fish, pp. 253–280. DC Heath, Lexington, KY.

Graham, M. (1935) Modern theory of exploiting a fishery, and application to North Sea trawling. *Journal du Conseil* 10, 264–74.

Graham, M. (1943) The Fish Gate. London: Faber.

Gräler, B., Pebesma, E. J., Heuvelink, G. (2016) Spatio-Temporal Interpolation using gstat. The R Journal 8(1), 204–218.

Gröger, J. P., Fogarty, M. J. (2011) Broad-scale climate influences on cod (*Gadus morhua*) recruitment on Georges Bank. ICES Journal of Marine Science, 68: 592–602.

Gunderson, L. H. (2000) Ecological Resilience in Theory and Application. Annu. Rev. Ecol. Syst. 31:425–39.

Gunderson, L. H and Holling, C. S. (2002) Panarchy: understanding transformations in human and natural systems. Edited by Lance H. Gunderson, C. Holling. Copyright Island Press.

Gunderson, L. H., Allen, C. R., Holling, C. S. (2010) Foundations of ecological resilience. Edited by Gunderson, L. H., Allen, C. R., Holling, C. S. Copyright Island Press.

Haddon Malcom (2011) Modelling and Quantitative Methods in Fisheries. Second Edition. CRC Press Taylor & Francis Group. A Chapman and Hall Book.

Hammond, T. R., Trenkel, V. (2005) Censored catch data in fisheries stock assessment. ICES Journal of Marine Science, 62:1118-1130.

Hannesson, R., Barange, M., Herrick Jr, S. F. (2006) Climate Change and the Economics of the World's Fisheries, Examples of Small Pelagic Stocks Edited by Rögnvaldur Hannesson, Manuel Barange and Samuel F. Herrick Jr. GLOBEC IPO. Published by Edward Elgar Publishing Limited.

Harris, R. R., Adrews, M. B. (2005) Physiological changes in the Norway lobster *Nephrops norvegicus* (L.) escaping and discarded from commercial trawls on the West Coast of Scotland. Journal of Experimental Marine Biology and Ecology, 320: 195–210.

Hare, S. R., Mantua, N. J., Francis, R. C. (1999) Production Regimes: Alaska and West Coast Pacific Salmon. Fisheries Vol 24, No 1.

Hare, J. A., Alexander, M. A., Fogarty, M. J., Williams, E. H., Scott, J. D. (2010) Forecasting the dynamics of a coastal fishery species using a coupled climate-population model. Ecological Applications, Vol 20 issue 2: 452–464.

Harvey, A. C. (1989) Forecasting, structural time series models and the Kalman filter. Cambridge University Press, Cambridge, UK.

Hastings, A, Wysham, D (2010) Regime shifts in ecological systems can occur with no warning. Ecology Letters 13: 464–472.

Haynes, P. S., Browne P., Fullbrook, L., Graham, C. T., Hancox, L., Johnson, M. P., Lauria, V., Power, A. M. (2016) Growth in *Nephrops norvegicus* from a tag-recapture experiment. Nature. Scientific Reports volume 6, Article number: 35143. https://doi.org/10.1038/srep35143.

Hedderich, J., Sachs, L. (2015) Angewandte Statistik, Methodensammlung mit R. Springer Verlag, Berlin, 968 p.

Heino, M., Pauli, B. D., Dieckmann, U. (2015) Fisheries-induced evolution. In D. J. Futuyma (Ed.), Annual review of ecology, evolution, and systematics, Vol. 46. Palo Alto, CA: Annual Reviews Incorporated.

Helske, J (2010) KFAS: Kalman filter and smoothers for exponential family state space models. R package version 0.5.1, http://CRAN.R-project.org/package=KFAS.

Helske, J. (2017) KFAS: Exponential Family State Space Models in R. Journal of Statistical Software, 78(10), 1–39. doi:10.18637/jss.v078.i10.

Hiddink, J. G., Jennings, S., Kaiser, M. J. (2007) Assessing and predicting the relative ecological impacts of disturbance on habitats with different sensitivities Journal of Applied Ecology 44, 405–413.

Hiddink, J. G., Jennings, S., Sciberras, M., Szostek, C. L., Hughes, K. M., Ellis, N., Rijnsdorp, A. D., McConnaughey, R. A., Mazor, T., Hilborn, R., Collie, J. S., Pitcher, C. R., Amoroso, R. O., Parma, A. M., Suuronen P., Kaiser M. J. (2017) Global analysis of depletion and recovery of seabed biota after bottom trawling disturbance. Proceedings of the National Academy of Sciences.

Hilborn, R. (1985) Fleet dynamics and individual variation: why some people catch more fish than others. Can. Journ. Fish. Aquat. Sci. 42: 2–13.

Hilborn, R., Walters, C. J. (1987) A general model for simulation of stock and fleet dynamics in spatially heterogeneous fisheries. Canadian Journal of Fisheries and Aquatic Sciences 44: 1366–1369.

Hilborn, R., Walters, C. J. (1992) Quantitative Fisheries Stock Assessment: Choice, Dynamics and Uncertainty. Springer. Originally published by Routledge, Chapman & Hall.

Hilborn, R. (2002) The dark side of reference points. Bulletin of Marine Science, 70(2): 403–408.

Hilborn, R., Branch, T. (2013) Does catch reflect abundance? No, it is misleading. Nature, Vol 494: page 303–306.

Hill, A. E. (1990a) Pelagic dispersal of Norway lobster *Nephrops norvegicus* larvae examined using an advection–diffusion-mortality model. Marine Ecology Progress Series Vol 64, 217–226.

Hill, A. E. White, R. G. (1990b) The dynamics of Norway lobster (*Nephrops norvegicus, L.*) populations on isolated mud patches. J. Cons. Int. Explor. Mer., 46: 167–174.

Hill, A. E. (1991) Advection-diffusion-mortality solutions for investigating pelagic larval dispersal. Marine Ecology Progress Series Vol 70: 117–128.

Hill, A. E., Brown J., Fernand L. (1996) The western Irish Sea gyre: a retention system for Norway lobster (*Nephrops norvegicus*). Oceanologica Acta. Vol 19, 3–4, 357–368.

Hill, A. E., Brown, J., Fernand L. (1997) The summer gyre in the Western Irish Sea: shelf sea paradigms and management implications. Estuarine Coastal and Shelf Science 44, 83–95.

Hill, J. M. (2007) Structure and flow of carbon and nitrogen to the western Irish Sea. *Nephrops norvegicus* fishery: a stable isotope approach. Thesis-PhD, School of Biological and Chemical Sciences, QueenMary, University of London.

Hillis, J. P. (1974) Field observations on larvae of the Dublin Bay Prawn *Nephrops norvegicus* (L.) in the Western Irish Sea. Irish Fisheries Investigations Series B, Department of Agriculture and Fisheries (Fisheries Division).

Hillis, J. P. (1988) Relation of *Nephrops* catch characteristics to seabed sediment type. ICES CM 1988/K: 37, 13 pp.

Hillis, J. P. (1996) Factors affecting catchability in *Nephrops*: current speed. ICES CM 1996/K: 21, 7 pp.

Hinz, H., Prieto, V., Kaiser, M. J. (2009) Trawl disturbance on benthic communities: chronic effects and experimental predictions. Ecological Applications 19, 761–773.

Hinz, H., Murray, L. G., Lambert, G. I., Hiddink, J. G., Kaiser, M. J. (2012) Confidentiality over fishing effort data threatens science and management progress. Fish and Fisheries doi: 10.1111/j.1467-2979.2012.00475.x.

Hinz, H., Moranta, J., Balestrini, S., Sciberras, M., Pantin, J. R., Monnington, J., Zalewski, A., Kaiser, M. J., Sköld, M., Jonsson, P., Bastardie, F., Hiddink, J. G. (2017) Stable isotopes reveal the effect of trawl sheries on the diet of commercially exploited species. Nature, Scientific Reports, 7: 6334.

Hodgson, D., McDonald, J. L., Hosken, D. J. (2015) What do you mean, "resilient"? Trends in Ecology and Evolution September 2015, Vol. 30, No. 9: pp 503–506.

Holling, C. S. (1992) Cross-scale morphology, geometry and dynamics of ecosystems Ecological Monographs Volume 62 Issue 4: 447–502. The Ecological Society of America.

Holmes, E. E., Ward, E. J., and Wills, K. (2012) MARSS: Multivariate autoregressive state-space models for analyzing time-series data. The R Journal 4:11–19.

Holmes, E. E., Ward, E. J., Scheuerell, M. D. (2018a) Analysis of multivariate time-series using the MARSS package version 3.10.10. November, 1 2018. Northwest Fisheries Science Center, NOAA Seattle, WA, USA.

Holmes E., Ward, E., and Wills, K. (2018b) MARSS: Multivariate Autoregressive State-Space Modeling. R package version 3.10.10.

Holt, S. (2011) Maximum sustainable yield: the worst idea fisheries management. https://breachingblue.files.wordpress.com/2011/tsh_1102452m.jpg.

Hommik, K., Fitzgerald, C. J., Kelly, F., Shephard, S. (2020) Dome-shaped selectivity in LB-SPR: Length-Based assessment of data-limited inland fish stocks sampled with gillnets. Fisheries Research 229, Elseviers publication.

Hordyk, A. R., Ono, K., Sainsbury, K., Loneragan, N., Prince, J. (2014) Some explorations of the life history ratios to describe length composition, spawning-per-recruit, and the spawning potential ratio. ICES J. Mar. Sci. 72: 204–216.

Hordyk, A. R., Loneragan, N. R., Prince, J. D. (2015a) An evaluation of an iterative harvest strategy for data-poor fisheries using the length-based spawning potential ratio assessment methodology. Fish. Res. 171: 20-32.

Hordyk, A. R., Ono, K., Sainsbury, K. J., Loneragan, N., Prince, J. D. (2015b) Some explorations of the life history ratios to describe length composition, spawning-per-recruit, and the spawning potential ratio. ICES J. Mar. Sci. 72: 204–216.

Hordyk, A. R., Ono, K., Valencia, S. R., Loneragan, N. R., Prince, J. D. (2015c) A novel length-based empirical estimation method of spawning potential ratio (SPR), and tests of its performance, for small-scale, data-poor fisheries. ICES J. Mar. Sci. 72: 217–231.

Hordyk, A., Ono, K., Prince, J. D., and Walters, C. J. (2016) A simple length-structured model based on life history ratios and incorporating size-dependent selectivity: application to spawning potential ratios for data-poor stocks. Canadian Journal of Fisheries and Aquatic Sciences 13: 1-13.

Hordyk., H. (2019) LBSPR: Length-Based Spawning Potential Ratio. R package version 0.1.5.

Horsburgh, K. J, Hill, A. E., Brown, J., Fernand, L., Garvine, R. W., Angelico, M. M. P. (2000) Seasonal evolution of the cold pool gyre in the western Irish Sea. Progress in Oceanography 46 1–58.

Howes, E. L., Joos, F., Eakin, C. M., Gattuso, J-P. (2015) An updated synthesis of the observed and projected impacts of climate change on the chemical, physical and biological processes in the ocean. Frontiers in Marine Science. 2:36.

Hurrell, J. W., Deser, C. (2009) North Atlantic climate variability: The role of the North Atlantic Oscillation. Journal of Marine Systems 78: 28–41.

Hurrel, J. (2018) The Climate Data Guide: Hurrell wintertime SLP-based Northern Annular Mode (NAM) Index. Last modified 28 Apr 2018. National Center for Atmospheric Research Staff (Eds). Retrieved from https://climatedataguide.ucar.edu/climate-data/hurrell-wintertime-slp-based-northern-annular-mode-nam-index

Hyndman Rob J. (2001) Box-Jenkins modelling. https://robjhyndman.com/papers/BoxJenkins.pdf

Hyndman RJ, Khandakar Y (2008) Automatic time series forecasting: the forecast package for R. Journal of Statistical Software, 26(3), 1–22.

Hyndman, R., Athanasopoulos, G., Bergmeir, C., Caceres, G., Chhay, L., O'Hara-Wild, M., Petropoulos, F., Razbash, S., Wang, E., Yasmeen, F. (2019) Forecast: forecasting functions for time series and linear models. R package version 8.9.

ICES IBPNeph (2015) Report of the Inter-Benchmark Protocol of *Nephrop*s in FU 17 and 14. International Council for the Exploration of the Sea Advisory Committee. ICES CM 2015/ACOM:38. REF. ACOM, WGCSE.

ICES IBPNeph Annexe (2016) Report of the Inter-Benchmark Protocol of Nephrops in FU17.

ICES WKNephTV (2007) Lordan, C., Doyle, J., Sacchetti, F., O'Driscoll, D., Heir, I., Smith, T., Allsop, C. Report of the UWTV Survey on the Aran, Galway Bay and Slyne Head *Nephrops* Grounds 2006. Working Document to WKNEPTV (2007), 36pp.

ICES WKNeph (2009) Report of the Benchmark Workshop on *Nephrops.* International Council for the Exploration of the Sea (ICES) Advisory Committee. ICES CM 2009/ACOM:33.

ICES WGCSE (2010) Report of the Working Group on the Celtic Seas Region , 13–19 May 2009, Copenhagen, Denmark. ICES CM 2009/ACOM:09. 1430 pp.

ICES WGCSE (2017) Report of the Working Group on Celtic Seas Ecoregion, 9–18 May 2017, Copenhagen, Denmark. ICES CM 2017/ACOM:13. 1464 pp.

ICES WGCSE (2018) Report of the Working Group on Celtic Seas Ecoregion. Norway lobster (*Nephrops norvegicus*) in Division 7.b, Functional Unit 17 (west of Ireland, Aran grounds). ICES CM 2018.

ICES WKIrish5 (2018) Report of the Workshop on an Ecosystem based Approach to Fishery Management for the Irish Sea. International council for the Exploration of the sea, ICES CM 2018/ACOM: 66. Ref: ACOM, SCICOM.

IPCC (2013) Climate Change 2013: The Physical Science Basis. Contribution of Working Group I to the Fifth Assessment Report of the Intergovernmental Panel on Climate Change [Stocker, T. F., Qin, D., Plattner, G.-K., Tignor, M.,. Allen, S. K., Boschung, J., Nauels, A., Xia, Y., Bex, V., Midgley, P. M. (eds.). Cambridge University Press, Cambridge, United Kingdom and New York, NY, USA, 1535 pp.

IPCC (2014) Climate Change 2014: Impacts, Adaptation, and Vulnerability. Contribution of Working Group II to the Fifth Assessment Report of the Intergovernmental Panel on Climate Change [C. B. Field, V. R. Barros, D. J. Dokken, M. D. Mastrandrea, K. J. Mach, T. E. Bilir, M. Chatterjee, K. L. Ebi, Y. O. Estrada, R. C. Genova, B. Girma, E. S. Kissel, A. N. Levy, S., MacCracken, P. R. Mastrandrea, L. L. White (eds.). Cambridge University Press, Cambridge, United Kingdom and New York, NY, USA, 1820 pp.

IPCC (2019) Inter-governmental Panel on Climate Change. Special Report on the Ocean and Cryosphere in a Changing Climate. Pörtner, H.-O., Roberts, D. C., Masson-Delmotte,V., Zhai, P., Tignor, M., Poloczanska, E., Mintenbeck, K., Alegría, A., Nicolai, M., Okem, A., Petzold, J., Rama, B., Weyer, N. M. (eds.).

IPCC SM (2019) Changing Ocean, Marine Ecosystems, and Dependent Communities Supplementary Material. Bindoff, N. L., Cheung, W. W. L., Kairo, J. G., Arístegui, J., Guinder, V. A., Hallberg, R., Hilmi, N., Jiao, N., Karim, M. S., Levin, L., O'Donoghue, S., Purca Cuicapusa, S. R., Rinkevich, B., Suga, T., Tagliabue, A., Williamson, P. In: *IPCC Special Report on the Ocean and Cryosphere in a Changing Climate* [H.-O. Pörtner, D.C. Roberts, V. Masson-Delmotte, P. Zhai, M. Tignor, E. Poloczanska, K. Mintenbeck, A. Alegría, M. Nicolai, A. Okem, J. Petzold, B. Rama, N.M. Weyer (eds.)].

Isaaks, E. H. Srivastava, R. M. (1989) Applied Geostatistics. Oxford University Press.

Jacobson, L. D., De Oliveira, J. A. A., Barange, M., Cisneros-Mata, M. A., Félix-Uraga, R., Hunter, J. R., Kim, Y. J., Matsuura, Y., Ñiquen, M., Porteiro, C., Rothschild, B., Sanchez, R. P., Serra, R., Uriarte, A., Wada, T. (2001) Surplus Production, Variability, and Climate Change in the Great Sardine and Anchovy Fisheries Can. J. Fish. Aquat. Sci. 58: 1891–1903.

Jammalamadaka, S. Rao, SenGupta, A. (2001) Topics in circular statistics. World Scientific.

Jennings, S., Pinnegar, J. K., Polunin, N. V. C., Warr, K. J. (2001a) Impacts of trawling disturbance on the trophic structure of benthic invertebrate communities. Marine Ecology Progress Series Vol. 213: 127–142.

Jennings, S., Kaiser, M. J., Reynolds, J. D. (2001b) Marine fisheries ecology. Blackwell Publishing.

Jennings, S., Kaiser M. J., Reynolds, J. D. (2003) Marine Fishery Ecology. Blackwell.

Jennings, S., Dulvy, N. K. (2005) Reference points and reference directions for size-based indicators of community structure. ICES Journal of Marine Science, 62: 397–404.

Jennings, S., and Dulvy, N. K. (2008) Berverton and Holts's insights into life history theory: influence, application and future in Advances in Fisheries Science 50 years on from Beverton and Holt, page 434–450. Edited by Andy Payne, John Cotter and Ted Potter. Centre for Environment, Fisheries and Aquaculture Science (Cefas) Pakefield Road, Lowestoft, Suffolk.

Jennings, S. (2011) Towards an ecosystem approach to fisheries in Europe: A perspective on existing progress and future directions. Fish and Fisheries 12(2):125–137

Jennings, S. (2012) Towards an ecosystem approach to fisheries in Europe. Oceans of Potential conference: 11–12 September 2012, Plymouth Hoe, Plymouth.

Jennings, S., Lee, J. (2012) Defining fishing grounds with vessel monitoring system data. ICES Journal of Marine Science, 69: 51–63.

Johnson, M. P., Lordan, C., Power, A. M. (2013) Chapter 2: Power Habitat and Ecology of *Nephrops norvegicus* in Advances in Marine Biology. Volume 64, editor Michael Lesser, 2013 Elsevier Ltd

Johnson, M. L., Gaten, E., Shelton, P. M. J. (2002) Spectral sensitivities of five marine decapod crustaceans and a review of spectral sensitivity variation in relation to habitat. Journal of the Marine Biological Association 82, 835–842.

Juan-Jorda, M. J., Mosqueira, I., Freire, J., Dulvy, N. K. (2015) Population declines of tuna and relatives depend on their speed of life. Proc. Biol. Sci. 282 (1811).

Kaiser, M. J., Clarke, K. R., Hinz, H., Austen, M. C. V., Somerfield, P. J., Karakassis, I. (2006) Global analysis and prediction of the response of benthic biota to fishing. Marine Ecology Progress Series, 311, 1–14.

Katoh, E., Sbragaglia, V., Aguzzi, J., Breithaupt, T. (2013) Sensory Biology and Behaviour of *Nephrops norvegicus* in Advances in Marine Biology, Volume 64: The Ecology and Biology of *Nephrops norvegicus*. Edited by Magnus L Johnson and Mark P Johnson. Series Editor: Michael Lesser. Academic Press. Elsevier Ltd. All rights reserved.

Kéfi, S., Guttal, V., Brock, W. A., Carpenter, S. R., Ellison, A. M., Livina, V. N., Seekell, D. A., Scheffer, M., van Nes, E H., Dakos, V. (2014) Early Warning Signals of Ecological Transitions: Methods for Spatial Patterns. volume 9 Issue 3 e92097.

Kimura, D. K., Tagart, J. V. (1982) Stock reduction analysis, an- other solution to the catch equations. Can. J. Fish. Aquat. Sci. **39**: 1467–1472.

Kimura, D. K., Balsiger, J. W., Ito, D. H. (1984) Generalized stock reduction analysis. Can. J. Fish. Aquat. Sci. **41**: 1325–1333.

Kindsvater, H. K., Mangel, M., Reynolds, J. D., Dulvy, N. K. (2016) Ten principles from evolutionary ecology essential for effective marine conservation Ecology and Evolution.

King, M. (2007) Fisheries, Biology, Assessment and Management. Blackwell.

Klinger, T., Chornesky, E. A., Whiteman, E. A., Chan, F., Largier, J. L., Wakefield, W. W. (2017) Using integrated, ecosystem-level management to address intensifying ocean acidification and hypoxia in the California Current large marine ecosystem. Elem Sci Anth. 5:16.

Knezevic, A. (2008) Overlapping confidence intervals and statistical significance. StatNews: Cornell University Statistical Consulting Unit, 73. Available from https://www.cscu.cornell.edu/news/statnews/stnews73.pdf.

Kraak, S. B. M., Reid, D. G., Gerritsen, H. D., Kelly, C. J., Fitzpatrick, M., Codling, E. A., Rogan, E. (2012) 21st century fisheries management: a spatio-temporally explicit tariff-based approach combining multiple drivers and incentivising responsible fishing. ICES J. Mar. Sci. 69 (4), 590–601.

Kraak, S. B. M., Haase, S., Minto, C., and Santos, J. (2019) The Rosa Lee phenomenon and its consequences for fisheries advice on changes in fishing mortality or gear selectivity. ICES Journal of Marine Science, 76: 2179–2192.

Lambert, G. I., Hiddink, J. G., Hintzen, N. T., Hinz, H., Kaiser, M. J., Murray, L. G., Jennings, S. (2012) Implications of using alternative methods of vessel monitoring system (VMS) data analysis to describe fishing activities and impacts. ICES Journal of Marine Science, 69: 682–693.

Lamigueiro, O. P., Hijmans, R. (2018) rasterVis. R package version 0.45.

Larkin, P. A. (1977) An epitaph for the concept of maximum sustained yield. Transaction of the American Fisheries Society, Volume (100) No 1.

Law, R. (2000) Fishing, selection, and phenotypic evolution. ICES Journal of Marine Science, 57: 659–669.

Law, R. (2007) Fisheries induced evolution: present status and future directions. Marine Ecology Progress Series. Vol. 335: 271–277.

Lee, R. M. (1912) An investigation into the methods of growth determination in fishes. Conseil Permanent International pour l'Exploration de la Mer, Publications de Circonstance, 63. 35 pp.

Lin, J., Quinn, T., Hilborn, R., Hauser, L. (2008) Fine-scale differentiation between sockeye salmon ecotypes and the effect of phenotype on straying. Heredity 101, 341–350.

Link, J. S., and Browman, H. I. (2014) Integrating what? Levels of marine ecosystem-based assessment and management. ICES Journal of Marine Science, 71: 1170–1173.

Link, J. S., Watson, R. A. (2019) Global ecosystem overfishing: clear delineation within real limits to production. Science Advances 2019, 5. Applied Ecology.

Lordan, C., Doyle, J., Bunn, R., Fee, D., Allsop, C. (2011) Aran, Galway Bay and Slyne Head *Nephrops* Grounds (FU17) 2011. Marine Institute UWTV Survey report.

Lutchman, I., Grieve, C., des Clers, S., De Santo, E. (2009) Towards a Reform of the Common Fisheries Policy in 2012. A CFP Health Check. Institute for European Environmental Policy.

MacCall, A. D. (2009) Depletion-corrected average catch: a simple formula for estimating sustainable yields in data-poor situations. ICES Journal of Marine Science 66, 2267–2271.

Mace, P. M., Sissenwine, M. P. (1993) How much spawning per recruit is enough? p. 101–118. In S. J. Smith, J. J. Hunt and D. Rivard [ed.] Risk evaluation and biological reference points for fisheries management. Canadian Special. Publication of Fisheries and Aquatic Sciences 120.

Mace, P. M. (1994) Relationships between common biological reference points used as thresholds and target of fisheries management strategies. Canadian Journal of Fisheries and Aquatic Sciences 51: 110–122.

Mangel, M., MacCall, A. D., Brodziak, J., Dick, E. J., Forrest, R. E., Pourzand, R., Ralston, S. (2013) A perspective on steepness, reference points, and stock assessment. Canadian Journal of Fisheries and Aquatic Sciences. 70: 930–940.

Mann, K. H., Lazier, J. R. N. (2006) Dynamic of marine ecosystems biological-physical interactions in the oceans. Blackwell Publishing.

Margalef Ramón (1998) Ecología (9 edición). Barcelona: Omega. ISBN 8428204055.

Marta-Almeida, M., Dubert, J., Peliz, A., dos Santos, A., Queiroga, H. (2008) A modelling study of Norway lobster (*Nephrops norvegicus*) larval dispersal in southern Portugal: predictions of larval wastage and self-recruitment in the Algarve stock. Canadian Journal of Fisheries and Aquatic Sciences 65: 2253−2268.

Martell, S., Froese, R. (2013) A simple method for estimating MSY from catch and resilience. Fish and Fisheries 14, 504–514.

Matheron, G. (1965) Les variables régionalisées et leur estimation. Une application de la théorie des fonctions aléatoires aux Sciences de la Nature. Masson, Paris.

Maynou, F., Conan, G. Y., Cartes, J. E., Company, J. B., Sarda, F. (1996) Spatial structure and seasonality of decapod crustacean populations on the northwestern Mediterranean slope. Limnol. Oceanogr. 41, 113–125.

Maynou, F., and Sardà, F. (1997) *Nephrops norvegicus* population and morphometrical characteristics in relation to substrate heterogeneity. Fisheries Research, 30: 139–149.

Maynou, F., Sarda, F. and Conan, G. Y. (1998a) Assessment of the spatial structure and biomass evaluation of *Nephrops norvegicus* (L.) populations in the northwestern Mediterranean by geostatistics. ICES Journal of Marine Science, 55: 102–120.

Maynou, F. (1998b) The application of geostatistics in mapping and assessment of demersal resources. *Nephrops norvegicus* (L.) in the northwestern Mediterranean: a case study. SCI. MAR., 62 (Supl. 1): 117–133.

Maynou, F., Sardà, F. (2001) Influence of environmental factors on commercial trawl catches of *Nephrops norvegicus* (L.). ICES Journal of Marine Science, 58: 1318–1325.

McAllister, M. K., Pikitch, E. K., Babcock, E. A. (2001) Using demographic methods to construct Bayesian priors for the intrinsic rate of increase in the Schaefer model and implications for stock rebuilding. Canadian Journal of Fisheries and Aquatic Sciences, 58(9), 1871–1890.

McGeady, R., Lordan, C., Power, A. M. (2019) Twilight migrators: factors determining larval vertical distribution in *Nephrops norvegicus* with implications for larval retention. Marine Ecology Progress Series Vol. 631: 141–155.

McGill, B. J., Enquist, B. J., Weiher, E., Westoby, M. (2006) Rebuilding community ecology from functional traits. TRENDS in Ecology and Evolution Vol.21 No. 4. Elsevier.

McQuaid, N., Briggs, R. P., Roberts, D. (2006) Estimation of the size of onset of sexual maturity in *Nephrops norvegicus* (L.). Fisheries Research. 81 (1), 26–36.

Méhault, S., Morandau, F., Fifas, S. (2011) Discarded *Nephrops* survival after trawling. Working document for ICES *Nephrops* working group. *IFREMER Report of project PRESPO*, pp. 15.

Merder, J., Browne, P., Freund, J. A., Fullbrook, L., Graham, C., Johnson, M. P., Wieczorek, A., Power, A. M. (2020) Density-dependent growth in 'catch-and-wait' fisheries has implications for fisheries management and Marine Protected Areas. Ambio. 2020, 49:107–117.

Meredith David (1999) The strategic importance of the fishing sector to rural communities and Ireland: a case study of the Rossaveal Region, Co. Galway.

Mérillet, L., Kopp, D., Robert, M., Pavoine, S., Mouchet, M. (2020) Environment outweighs the effects of fishing in regulating demersal community structure in an exploited marine ecosystem. Glob Change Biol. 26: 2106–2119.

Methot, R. D. Jr., Wetzel, C. R. (2013) Stock synthesis: A biological and statistical framework for fish stock assessment and fishery management. Fisheries Research 142: 86–99.

Meyer, R. Millar, R. B. (1999) BUGS in Bayesian stock assessment. Canadian Journal of Fisheries and Aquatic Sciences 56, 1078–1086.

Microsoft and Steve Weston (2017) foreach: Provides Foreach Looping Construct for R. R package version 1.4.4. https://CRAN.R-project.org/package=foreach.

Milligan, R. J., Albala, A., Atkinson, R. J. A., Neill, D. M. (2009) The effects of trawling on the physical condition of the Norway lobster *N. norvegicus* in relation to seasonal cycles in the Clyde Sea area. ICES J. Mar. Sci. 66, 488–494.

Mills, C. M., Townsend, S. E., Jennings, S., Eastwood, P. D., and Houghton, C. A. (2007) Estimating high resolution trawl fishing effort from satellite-based vessel monitoring system data. – ICES Journal of Marine Science, 64: 248–255.

Morfin, M., Fromentin, J-M., Jadaud, A., Bez, N. (2012) Spatio-Temporal Patterns of Key Exploited Marine Species in the Northwestern Mediterranean Sea. PLoS ONE 7(5): e37907. doi:10.1371/journal.pone.0037907.

Mori, M., Biagi, F., De Ranieri, S. (1998) Fecundity and egg loss during incubation in Norway lobster (*Nephrops norvegicus*) in the North Tyrrhenian Sea. Journal of Natural History, 32, 1641–50.

Murawski, S. A. (2000) Definitions of overfishing from an ecosystem perspective. ICES Journal of Marine Science, 57: 649–658.

Musick, J. A. (1999) Criteria to define extinction risk in marine fishes. Fisheries 24 (12):6–14.

Myers, R. A., Barrowman, N. J. (1996) Is fish recruitment related to spawner abundance? Fish. Bull. 94: 707–724.

Myers, R. A., Bowen, K. G., Barrowman, N. J. (1999) Maximum reproductive rate of fish at low populations sizes. Can. J. Fish. Aquat. Sci. 56: 2404–2419.

Myers, R., Millar, R. B. (1999) BUGS in Bayesian stock assessment. Can. J. Fish. Aquat. Sci. 56, 1078–1086.

Nadon, M. O., Ault, J. S., Williams, I. D., Smith, S. G., DiNardo, G. T. (2015) Length-based assessment of coral reef fish populations in the main and northwestern Hawaiian islands. PLoS ONE 10:e0133960.

Nolan, G. D., Lyons, K. (2006) Ocean climate variability on the western Irish Shelf, an emerging time series., Proceedings of the ICES Annual Science Conference, Theme Session C, C:28.

Nyström, M., Graham, N. A. J., Lokrantz, J., Norström, A. V. (2008) Capturing the cornerstones of coral reef resilience: linking theory to practice. Coral Reefs 27: 795–809.

O'Farrel, M. R., Botsford, W. L. (2005) Estimation of change in lifetime egg production from length frequency data. Can. J. Fish Aquat. Sci. 62:1626–1639.

Ojea, E., Pearlman, I., Gaines, S. D., Lester, S. E. (2017) Fisheries regulatory regimes and resilience to climate change. Ambio 46:399-412.

Ostrom Elinor (1990) Governing the Commons The Evolution of Institutions for Collective Action.

O'Sullivan, D., Lordan, C., Doyle, J., Berry, A., Lyons, K. (2015) Metapopulation connectivity via larval transport of the Norway lobster *Nephrops norvegicus* in waters around Ireland: a modelled approach. Marine Ecology Progress Series, Vol 534, 95–106.

Ottersen, G., Stenseth, N. C., Hurrell, J. W. (2004) Climatic fluctuations and marine systems: a general introduction to the ecological effects In Marine Ecosystems and Climate Variability, pp. 3-15. Ed. by N. Ch. Stenseth, G. Ottersen, J. W. Hurrell, and A. Belgrano. Oxford University Press, Oxford, UK.

Parslow-Williams, P. J., Atkinson, R. J. A., Taylor, A. C. (2001) Nucleic acids as indicators of nutritional condition in the Norway lobster Nephrops norvegicus. Mar. Ecol. Prog. Ser. 211, 235–243.

Parslow-Williams, P., Goodheir, C., Atkinson, R. J. A., Taylor, A. C. (2011) Feeding energetics of the Norway lobster, *Nephrops norvegicus* in the Firth of Clyde, Scotland, Ophelia, 56:2, 101–120.

Pauly, D. (1980) On the interrelationship between mortality, growth parameters and mean temperature in 175 fish stocks. Journal du Conseil Permanent International pour l'Exploration de la Mer, 39: 175–192.

Pauly, D., Christensen, V., Dalsgaard, J., Froese, R., Torres Jr, F. (1998) Fishing Down Marine Food Webs. Science Vol. 279, Issue 5352, pp.

Pauly, D. Maclean, J. (2003) In a perfect ocean: the state of fisheries and ecosystems in the North Atlantic Ocean. Publisher: Island Press.

Pauly, D. (2009) Aquacalypse now-the end of fish. New Republic, 240: 24-27.

Pauly D. (2010) 5 Easy Pieces: How Fishing Impacts Marine Ecosystems. Publisher: Island Press.

Pauly, D. (2013) Does catch reflect abundance? Yes, it is a crucial signal. Nature, Vol 494: p303–306.

Pauly, D., Zeller, D (2016) Catch reconstructions reveal that global marine fisheries catches are higher than reported and declining. Nature Communications, 7, 10244.

Pebesma, E. J. (2004) Multivariable geostatistics in S: the gstat package. Computers & Geosciences, 30: 683–691.

Pebesma, E. J., Duin, R. N. M. (2005) Spatio-temporal mapping of sea floor sediment pollution in the North Sea. In: Geostatistics for Environmental Applications Proceedings of the Fifth European Conference on Geostatistics for Environmental Applications. Philippe Renard, Hélène Demougeot-Renard, Roland Froidevaux (Editors). Springer.

Pebesma, E. J. (2012) spacetime: spatio-temporal data in R. Journal of Statistical Software, 51(7), 1–30. URL http://www.jstatsoft.org/v51/i07/.

Pella, J. J., Tomlinson, P. K. (1969) A generalized stock production model. Bulletin of the Inter- American- Tropical Tuna Commission 13, 419–496.

Petris, G., Petrone, S., Campagnoli, C. (2009) Dynamic linear models with R. Springer.

Pitcher T. J. and Pauly, D. (1998) Rebuilding ecosystems, not sustainability, as the proper goal of fishery management in Reinventing Fisheries Management. Edited by Tony J. Pitcher, Paul J. B. Hart and Daniel Pauly. Published in 1998 by Kluwer Academic Publishers. London.

Pitcher, T. J. (2001) Fisheries Managed to Rebuild Ecosystems? Reconstructing the Past To Salvage the future. Ecological Applications, 11(2), 2001, pp. 601–617.

Pitcher, T. J. (2005) Back-to-the-future: a fresh policy initiative for fisheries and a restoration ecology for ocean ecosystems. Phil. Trans. R. Soc. B (2005) 360, 107–121.

Pochelon, P. N., Calado, R., Dos Santos, A., Queiroga, H. (2009) Feeding Ability of Early Zoeal Stages of the Norway Lobster *Nephrops norvegicus* (L.) *Biol. Bull.* 216: 335–343.

Post, E. (2004) Time lags in terrestrial and marine environments. In Marine Ecosystems and Climate Variability, pp. 165-167. Edited by Stenseth, N. Ch., Ottersen ,G., and collaboration Hurrell, J. W., Belgrano, A. Oxford University Press, Oxford, UK.

Powell, A., Eriksson, S. P. (2013) Reproduction: life cycle, larvae and larviculture in Advances in Marine Biology, Volume 64: The Ecology and Biology of *Nephrops norvegicus*. Edited by Magnus L. Johnson and Mark P. Johnson. Series Editor: Michael Lesser. Academic Press. Elsevier Ltd. All rights reserved.

Plummer, M. (2003) JAGS: a program for analysis of Bayesian graphical models using Gibbs sampling. In: Proceedings of the 3rd International Workshop on Distributed Statistical Computing (DSC 2003) March 20-22, Vienna, 2003. (eds K. Hornik, F. Leisch and A. Zeileis), Vienna Technical University, Vienna pp. 20–22.

Plummer, M., Best, N., Cowles, K., Vines, K. (2006) CODA: Convergence Diagnosis and Output Analysis for MCMC, R News, vol 6, 7–11.

Prince, J. D., Hordyk, A. R., Valencia, S. R., Loneragan, N. R., Sainsbury, K. J. (2015) Revisiting the concept of Beverton-Holt life-history invariants with the aim of informing data-poor fisheries assessment. ICES J. Mar. Sci. 72: 194–203.

Punt, A. E., Campbell, R. A., Smith, A. D. M. (2001) Evaluating empirical indicators and reference points for fisheries management: Application to the broadbill swordfish fishery off eastern Australia. Mar. Freshwater Res., 2001, 52, 819–32.

Quinn, T.P. (2005) The Behavior and Ecology of Pacific Salmon and Trout. University of Washington Press, Seattle, 378 p.

R Core Team (2018) R: A language and environment for statistical computing. R Foundation for Statistical Computing, Vienna, Austria. URL https://www.R-project.org/.

Reiss, J., Bridle, J. R., Montoya, J. M, Woodward, G. (2009) Emerging horizons in biodiversity and ecosystem functioning research. Journal? Volume 24 Issue 9 505–514.

Renard, D., Bez, N., Desassis, N., Beucher, H., Ors, F., Freulon, X. (2018) RGeostats: Geostatistical Package. R package version 11.2.4. http://cg.ensmp.fr/rgeostats

Ribeiro Jr, P. J., and Diggle, P. J. (2018) geoR: Analysis of Geostatistical Data. R package version 1.7-5.2.1. https://CRAN.R-project.org/package=geoR

Rice, A. L., Chapman, C. J. (1971) Observations on the burrows and burrowing behaviour of two mud-dwelling decapod crustaceans, *Nephrops norvegicus* and *Goneplax rhomboides*. Marine Biology, 10, 330–342.

Rijnsdorp, A. D., Buys, A. M., Storbeck, F., Visser, E. G. (1998) Micro-scale distribution of beam trawl effort in the southern North Sea between 1993 and 1996 in relation to the trawling frequency of the sea bed and the impact on benthic organisms. ICES Journal of Marine Science, 55: 403–419.

Rijnsdorp, A. D., Poos, J. J., Quirijns, F. J. (2011) Spatial dimension and exploitation dynamics of local fishing grounds by fishers targeting several flatfish species. Canadian Journal of Fisheries and Aquatic Science, 68(6): 1064–1076.

Rossister, D. G. (2012) Technical Note: Co-kriging with the gstat package of the R environment for statistical computing. University of Twente, Faculty of Geo-Information Science & Earth Observation (ITC) Enschede (NL).

Rothschild, B. J. (2015) On the birth and death of ideas in marine science ICES Journal of Marine Science (2015), 72(5), 1237–1244.

Ruiz-Cuetos, J. C., Felicisimo, A. M., Cuartero, A., Polo, M. E., Rodriguez, P. G., Haut, J. M. (2016) VecStatGraphs2D: Vector analysis using graphical and analytical methods in 2D. R package version 1.8.

Santucci, R. (1926) Lo sviluppo e l'ecologia post-embrionali dello "Scampo" *Nephrops norvegicus* (L.) nel Tirreno e nei mari nordici. Mem. R. Com. Talassogr. Ital. 125, 1–36.

Sardà, Francisco (1995) A review (1967–1990) of some aspects of the life history of *Nephrops norvegicus* ICES Marine. Science. Symposia 199: 78-88.

Sardá Francisco (1998) Symptoms of overexploitation in the stock of the Norway lobster (*Nephrops norvegicus*) on the "Serola Bank" (Western Mediterranean Sea off Barcelona). Scientia Marina 62 (3) pp 295–299.

Sbragaglia, Valerio (2015) Biological rhythms in the Norway Lobster (*Nephrops norvegicus L.*): ecological modulation and genetic basis. Thesis, Institut de Ciències del Mar, Barcelona, Spain.

Sbragaglia, V., Leiva, D., Arias, A., Garcıá J. A., Aguzzi, J., Breithaupt, T. (2017) Fighting over burrows: the emergence of dominance hierarchies in the Norway lobster (*Nephrops norvegicus*). Journal of Experimental Biology (2017) 220, 4624–4633.

Schaefer, M. B. (1954) Some aspects of the dynamics of populations important to the management of the commercial marine fisheries. Bulletin of the Inter-American-Tropical Tuna Commission Vol 1, No 2; pages: 27–56. La Jolla.

Scheffer, M., Carpenter, S. R., Dakos, V., van Nes, E. (2015) Generic Indicators of Ecological Resilience: Inferring the Chance of a Critical Transition. Annu. Rev. Ecol. Evol. Syst. 46:145–67.

Smith, R. S. M. (1987) The biology of larval and juvenile *Nephrops norvegicus* in the Firth of Clyde. Ph. D. Thesis, University of Glasgow.

Schnute, J. T., Richards, L. J. (2002) Surplus production models. p. 105-126 In: Hart. P.J.B. and Reynolds, J.D. (eds.) Handbook of fish biology and fisheries, Volume 2. Blackwell Publishing, Oxford, UK.

Schumacher, M. (1984) Intl Stat Review 52:263–281.

Simon, T. W., Edwards, D. H. (1990) Light-evoked walking in crayfish: behavioural and neuronal responses triggered by the caudal photoreceptor. Journal of Comparative Physiology 166A, 745–755.

Smith, R.S.M. (1987) The biology of larval and juvenile *Nephrops norvegicus* (L.) in the firth of Clyde. PhD. Dissertation, Glasgow University, Glasgow.

Smith, R. W. (1995) Visual Hypothesis Testing with Confidence Intervals. EcoAnalysis Inc., Ojai, CA, 1–6.

Smith, J. C., Papadopoulou, N. K. (2008) The crustacean *Nephrops norvegicus*: growth and reproductive behaviour in Reproductive Biology of Crustaceans: case studies of Decapod crustaceans. Editor: Elena Mente, University of Thessaly Greece. Science Publishers.

Smith, A. D. M., Smith, D. C., Haddon, M., Knuckey, I., Sainsbury, K. J., Sloan, S. (2014) Implementing harvest strategies in Australia: 5 years on. ICES Journal of Marine Science, 71: 195–203.

Spanbauer, T. L., Allen C. R., Angeler, D. G., Eason, T., Fritz, S. C., Garmestani, A. S., Nash, K. L., Stone, J. R. (2014) Prolonged Instability Prior to a Regime Shift. PLOS Volume 9 Issue 10 e108936.

Standish, R. J, Hobbs, R. J., Mayfield, M. M., Bestelmeyer, B. T, Suding, K. N., Battaglia, L. L., Eviner, V., Hawkes, C. V., Temperton, V. M., Cramer, V. A., Harris, J. A., Funk, J. L., Thomas, P. A. (2014) Resilience in ecology: abstraction, distraction, or where the action is? Biological Conservation, Vol 177, pages 43–51.

STECF (2019) Scientific, Technical and Economic Committee for Fisheries: Monitoring the performance of the Common Fisheries Policy (STECF-Adhoc-19-01). Publications Office of the European Union, Luxembourg, 2019, ISBN 978-92-76-02913-7, doi:10.2760/22641, JRC116446.

Stelzenmüller, V., Rogers, S. I., Mills, C. (2008) Spatio-temporal patterns of fishing pressure on UK marine landscapes, and their implications for spatial planning and management. ICES Journal of Marine Science, 65: 1081–1091.

Stenseth N. C., Ottersen, in collaboration with G., Hurrell, J. W., Belgrano, A. (2004) Marine Ecosystems and climate variation. Oxford University Press.

Stentiford, G. D., Neil, D. M., and Atkinson, R. J. A. (2001) The relationship of Hematodinium infection prevalence in a Scottish Nephrops norvegicus population to season, moulting and sex. ICES Journal of Marine Science, 58: 814–823.

Stockbook (2011) Annual Review of Fish Stocks in 2011 with Management Advice for 2012. Marine Institute. Headquarters Rinville, Oranmore, Co. Galway, Ireland.

Stockbook (2018) Annual Review of Fish Stocks in 2018 with Management Advice for 2019. Marine Institute. Headquarters Rinville, Oranmore, Co. Galway, Ireland.

Stoffer, D. S., Wall, K. D. (1991) Bootstrapping state-space models: Gaussian maximum likelihood estimation and the Kalman filter. Journal of the American Statistical Association 86:1024–1033.

Stoffer, D. (2020) astsa: Applied Statistical Time Series Analysis. R package version 1.12.

Streiff, R., Mira, S., Castro, M., and Cancela, M. L. (2004) Multiple paternity in Norway lobster (*Nephrops norvegicus* L.) assessed with microsatellite markers. Marine Biotechnology 6: 60–66.

Styf Hannah (2014) Climate Change and the Norway Lobster. Effects of Multiple Stressors on Early Development. Thesis for the Degree of Doctor of Philosophy. Faculty of Science Department of Biological and Environmental Sciences. Published by the Department of Biological and Environmental Sciences, University of Gothenburg, Sweden. ISBN 978-91-628-9241-8.

Su, Y. S., and Yajima, M. (2015) R2jags: Using R to Run JAGS.
R package version 0.5-7.

Taylor, M. H., Losch, M., Wenzel, M., Schröter J. (2013) On the sensitivity of feld reconstruction and prediction using empirical orthogonal functions derived from gappy data. Journal of Climate, 26, 9194–9205.

Theil, H. (1966) Applied Economic Forecasting, North Holland, Amsterdam.

Then, A. Y., Hoenig, J. M., and Huynh, Q. C. (2017) Estimating fishing and natural mortality rates, and catchability coefficient, from a series ofobservations on mean length and fishing effort. ICES Journal of Marine Science, 75: 610–620.

Thompson, D. W. J. (2016) A Brief Introduction to the Annular Modes and Annular Mode Research http://www.atmos.colostate.edu/~davet/ao/introduction.html.

Timpane-Padgham, B. L., Beechie, T., Klinger, T. (2017) A systematic review of ecological attributes that confer resilience to climate change in environmental restoration. PLoS ONE 12(3): e0173812. https://doi.org/10.1371/journal.Pone.0173812.

Tuck, I. D. (1993) *Nephrops* abundance in relation to environmental factors and fishing pressure. Ph.D. Thesis, University of London. 301 p.

Tuck, I. D., Atkinson, R. J. A., Chapman, C. J. (1994) The structure and seasonal variability in the spatial distribution of *Nephrops norvegicus* burrows. Ophelia 40, 13–25.

Tuck, I. D., Chapman, C. J., Atkinson, R. J. A. (1997a) Population biology of the Norway lobster, *Nephrops norvegicus* (L.) in the Firth of Clyde, Scotland. I. Growth and density. ICES Journal of Marine Science, 54, 125–35.

Tuck, I. D., Chapman, C. J., Atkinson, R. J. A., Bailey, N., Smith, R. S. M. (1997b) A comparison of methods for stock assessment of the Norway lobster, *Nephrops norvegicus*, in the Firth of Clyde. Fisheries Research, 32, 89–100.

Tuck, I. D., Atkinson, R. J. A., Chapman, C. J. (2000) Population biology of the Norway lobster, *Nephrops norvegicus* (L.) in the Firth of Clyde, Scotland II: fecundity and size at onset of sexual maturity. ICES Journal of Marine Science, 57: 1227–1239.

Tully, O., and Hillis, J. P. (1995) Causes and spatial scales of variability in population structure of *Nephrops norvegicus* (L.) in the Irish Sea. Fisheries Research, 21: 329–347.

Ulmestrand, M., Valentinsson, D., Sangster, G. I., Bova, D., Kynoch, R. J., Breen, M., Graham, G. N., Soldal, A. V., Cruickshank, O., Moth-Poulsen, T., Lowry, N. (1998) *Nephrops* survival after escape from commercial fishing gear or discarded from deck. Fishing Technology and Fish Behaviour Working Group, La Coruña, Spain, 20-23 April 1998.

Ungfors, A., Bell, E., Johnson, M. L., Cowing, D., Dobson, N. C, Bublitz, R., Sandell, J. (2013) Chapter 7: *Nephrops* Fisheries in European Waters. In Advances in Marine Biology Volume 64, editor Michael Lesser, Elsevier Ltd.

Anon. (2013) Under water TV survey and catch options for 2014, Aran, Galway Bay and Slyne Head *Nephrops* Grounds (FU17). Lordan, C., Doyle, J., Hehir, I., Allsop, C., Butler, R., Burke, C. Marine Institute.

Anon. (2014a) Under water TV survey and catch options for 2015, Western Irish Sea *Nephrops* Grounds (FU15). Ligas, A., Doyle, J., Lordan, C., Brown, V., Doran, S., McArdle, J., McCausland, I., McCorriston, P., Simpson, S., Schön, P-J. (2014). AFBI and Marine Institute.

Anon. (2014b) Under-Water TV survey and catch options for 2015, Smalls *Nephrops* Grounds (FU22). Lordan, C., Doyle, J., Fitzgerald, R., O'Connor, S., Blaszkowski, M., and Simpson, S. Marine Institute.

Anon. (2014c) Under-Water TV survey and catch options for 2015, Aran, Galway Bay and Slyne Head *Nephrops* Grounds (FU17). Hehir, I., Doyle, J., Lordan, C., O'Cuaig, M., Hannify, O., Fitzgerald, R., O'Connor, S., Keith, M., Murphy, A., Sheridan, M., and Vila, Y. Marine Institute. Marine Institute.

Anon. (2014d) Under-Water TV survey and catch options for 2015, Porcupine Bank *Nephrops* Grounds (FU16). Doyle, J., Lordan, C., O'Cuaig, M., Hannify, O., Murphy, A., Sheridan, M., and Vila, Y.

Anon. (2015) Under Water TV survey and catch options for 2016, Aran, Galway Bay and Slyne Head *Nephrops* Grounds (FU17). Doyle, J., Lordan, C., Fitzgerald, R., O'Connor, S., Fee, D., Butler, R., Stokes, D., Ni Chonchuir, G., Sheridan, M., Simpson, S. Marine Institute.

UWTV (2016) Under Water TV survey and catch options for 2017, Aran, Galway Bay and Slyne Head *Nephrops* Grounds (FU17). Doyle, J., Lordan, C., Stokes, D., O'Brien, S., Kelly, C., Bentley, K., Vacherot, J. P. Marine Institute.

UWTV (2017) Under water TV survey and catch options for 2018, Aran, Galway Bay and Slyne Head *Nephrops* Grounds (FU17). Lordan, C., Doyle, J., Butler, R., Sugrue, S., Allsop, C., O' Connor, S., Vacherot, J. P. Marine Institute UWTV Survey report.

UWTV (2018) Under water TV survey and catch options for 2019, Aran, Galway Bay and Slyne Head *Nephrops* grounds (FU17). Doyle, J., O'Brien, S., Ryan, G., Galligan, S., Hernon, P., Aristegui, M. and Vacherot, J. P. Marine Institute.

Vasilakopoulos, P., Marshall, C. T. (2015) Resilience and tipping points of an exploited fish population over six decades. Global Change Biology.

Vasilakopoulos, P., Raitsos, D. E., Tzanatos, E. Maravelias, C. D. (2017) Resilience and regime shifts in a marine biodiversity hotspot. Scientific Reports, 7: 13647.

Venables, W. N., Ripley, B. D. (2002) Modern Applied Statistics with S. Fourth Edition. Springer, New York. ISBN 0-387-95457-0.

Votier, S. C., Bearhop, S., Attrill, M. J., Oro, D. (2008) Is climate change the most likely driver of range expansion for a critically endangered top predator in northeast Atlantic waters? Biol. Lett. 4, 204–205.

Wallace, J. M. (2000) North Atlantic oscillation/annular mode: Two paradigms-one phenomenon. Quart. J. Roy. Meteor. Soc., 126, 791–805.

Walters, C. J., Hilborn, R., Christensen, V. (2008) Surplus production dynamics in declining and recovering fish populations Canadian Journal of Fisheries and Aquatic Sciences. 65: 2536–2551.

Warnes, G. R., Bolker, B., Bonebakker, L., Gentleman, R., Huber, W., Liaw, A., Lumley, T., Maechler, M., Magnusson, A., Moeller, S., Schwartz, M., Venables, B. (2016) gplots: Various R Programming Tools for Plotting Data. R package version 3.0.1.

Watson, R. and Pauly, D. (2001) Systematic distortions in world fisheries catch trends. Nature 414, 534–536.

Webster, R., Oliver, M. A. (2007) Geostatistics for environmental scientists. Second Edition John Wiley & Sons, Ltd.

Wetzel, C. R., Punt, A. E. (2011) Model performance for the determination of appropriate harvest levels in the case of data-poor stocks. Fisheries Research, 110: 342–355.

White, R. G., Hill, A. E., Jones, D. A (1988) Distribution of *Nephrops norvegicus* (L.) larvae in the western Irish Sea: an example of advective control on recruitment Journal of Plankton Research Vol.10 no.4 pp.735–747.

Wickham, H. (2016) ggplot2: Elegant Graphics for Data Analysis. Springer-Verlag New York.

Wilberg, M. J., Miller, T. J. (2007) Comment on “Impacts of biodiversity loss on ocean ecosystem services”. Science, 316: 1285.

Woillez, M., Rivoirard, J., Petitgas, P. (2009) Notes on survey-based spatial indicators for monitoring fish populations. Aquatic Living Resources 22, 155–164.

Worm, B., Barbier, E. B., Beaumont, N., Duffy, J. E., Folke, C., Halpern, B. S., Jackson, J. B. C., Heike K. Lotze, Fiorenza Micheli, Stephen R. Palumbi, Enric Sala, Kimberley A. Selkoe, John J. Stachowicz, Reg Watson (2006) Impacts of biodiversity loss on ocean ecosystem services. Science, 314: 787–790.

Zeileis, A., Leisch, F., Hornik, K., and Kleiber, C. (2002) strucchange: An R Package for Testing for Structural Change in Linear Regression Models. Journal of Statistical Software, 7(2), 1–38.

Zeileis, A., (2006) Implementing a Class of Structural Change Tests: An Econometric Computing Approach. Computational Statistics & Data Analysis, 50, 2987–3008.

Zeileis, A., Shah A., Patnaik, I. (2010) Testing, monitoring, and dating structural changes in exchange rate regimes. Computational Statistics & Data Analysis, 54(6):1696–1706.

Zeileis, A., Leisch, F., Hornik, K., Kleiber, C. (2012) strucchange: An R Package for testing for structural change in linear regression models.

Zeller, D., Pauly, D. (2005) Good news, bad news: global fisheries discards are declining, but so are total catches. Fish and Fisheries 6, 156–159.

Zeller, D., Cashion, T., Palomares, M., Pauly, D. (2018) Global marine fisheries discards: A synthesis of reconstructed data. Fish and Fisheries 19, 30–39.

Zuur, A. F., Fryer, R. J., Jolliffe, I. T., Dekker, R., Beukema, J. J. (2003) Estimating common trends in multivariate time series using dynamic factor analysis. Environmetrics 14: 665–685.